

**Laboratory Directed  
Research and Development  
Annual Report**

**Fiscal Year 1995**

**February 1996**

**Prepared for  
the U.S. Department of Energy  
under Contract DE-AC06-76RLO 1830**

**Pacific Northwest National Laboratory  
Richland, Washington 99352**

**MASTER**

**DISTRIBUTION OF THIS DOCUMENT IS UNLIMITED**

**DISCLAIMER**

**Portions of this document may be illegible in electronic image products. Images are produced from the best available original document.**



# Contents

## Atmospheric Sciences

A Multidisciplinary Investigation of Heterogeneous Atmospheric Processes .....	3
Beyond Reduced Form Climate Model .....	5
Global Atmospheric Chemistry .....	6

## Biotechnology

750 MHz NMR Determination of the 3D Structure of a Unique Reductive Dehalogenase .....	11
Advanced Biomedical Science and Modeling .....	13
Degradation of Explosives by the Combination of Enzymatic and Microbial Processes .....	15
Dynamics, Modeling and Redesign of Microbial Proteins .....	16
Enzymology of Bacterial Metal Reductase and Dehalogenase .....	19
Fourier Transform EPR Studies of Radiation-Induced Structural Alteration of DNA .....	21
Functional Characterization of Bacterial Plasmids .....	23
Identification, Purification and Characterization of the Reductive Dehalogenase of <i>Desulfomonile tiedjei</i> DCB-1 .....	26
Microbial Gene Expression and Genetic Engineering .....	27
Microbial Genomics .....	28
Microbial Informatics .....	30
NMR Studies of DNA Structure Associated with Chemical Adduction .....	31
Structural Studies of Modified Histone Species .....	34
Vegetable Oil Chlorinated Solvents .....	37
Vegetable Oil-Pilot Scale Test: Transport Analysis .....	38

## Chemical Instrumentation and Analysis

Application of Mass Spectrometry to Life Science and Bioremediation Research .....	43
Development of Laser-Diode Based Sensors for Trace Isotope Assays .....	48
Evaluation of Cellular Response to Insult .....	50

Improved Analytical Ion Trapping Methods .....	52
Size Measurement, Sorting and Chemical Analysis of Nanometer Sized Particles Using an Ion Trap .....	54

## Computer and Information Science

Adaptive Life Simulator .....	57
Advances in Desktop Atmospheric Dispersion Modeling .....	59
Automated Document and Text Processing .....	61
Collaborative Environment Prototype for Molecular Science .....	63
Development of Intuitive User Interfaces .....	65
Direct Numerical Simulation of Turbulence .....	67
Fourier Transform Ion Cyclotron Resonance Mass Spectroscopy Data Acquisition and Modeling .....	69
Heterogeneous Information Systems .....	71
Human Factors Evaluation of Immersive Virtual Environments Technology .....	73
Information Systems Meta Data Investigation .....	77
Medical Imaging Three-Dimensional Reconstruction and Visualization .....	79
Molecular Visualization on Parallel Computers .....	80
Neural Network Data Processing for Sensor Applications .....	81
Parallel TEMPEST .....	83
Subsurface Transport in Heterogeneous Materials .....	84

## Design and Manufacturing Engineering

Industrial Modeling Expert .....	87
Microscale Freeform Fabrication Using Electron-Beam Curing .....	88
Solid Freeform Fabrication of Ceramic Membranes .....	90

## Ecological Science

Ecological Modeling of Regional Responses to Global Change .....	93
Optimal Decision-Making for Water Resource Management .....	95
Phytomechanics: Using Plants as Physiological Transducers .....	96
Prototype Map-Based Information Management System .....	97

## Electronics and Sensors

A Real-Time Adaptive Intelligent System for Sensor Validation .....	101
Cylinder Design for Reduced Emission Origins .....	102
Development of Two-Dimensional Electrochemistry for Sensor Applications .....	104
Low Cost Sensing Technology for Operations and Maintenance Applications .....	105
Materials Evaluation .....	107
Process Control System Development .....	109
Remote Automobile Performance and Emission Monitor .....	111
Ultrasonic Measurement of Elastic Properties of Bone .....	112

## Health Protection and Dosimetry

Capillary Neutron Focusing for Boron Neutron Capture Therapy Adsorbates and Their Surfaces .....	117
Detection of <i>H. Pylori</i> Infection Using Laser Breath Analysis Instrumentation .....	118
Development of High-Sensitivity Detection Techniques for the Measurement of Ionizing and Non-ionizing Radiation .....	120
Optical In Vivo Blood Characterization and Multivariant Analysis .....	121
PBPK-Based Breath Analysis Instrumentation .....	123
Physiologically Based Pharmacokinetic Modeling of Organic Waste Site Chemicals .....	125
Quantitation of Hypoxic Cells .....	127
Real-Time Dosimetry for Therapeutic Radiation Delivery .....	129
Testing of Noise and ELF Instruments for RF/MW Interference .....	131

## Human Systems Performance

Interactive Technologies for Adaptive Training .....	135
Translating Work Environment Research into Design .....	137

## Hydrologic and Geologic Sciences

Dual-Gas Tracer Characterization of Diffusion Limitations in Enhanced In Situ Remediation .....	141
Formation of a Contaminant Barrier by Injecting Metallic Iron Colloids into the Subsurface Environment .....	143
Integrated Environmental Monitoring .....	145

Interpretation of Single-Well Tracer Tests .....	147
Microbiological Controls on Contaminant Behavior .....	149
Monitoring Technology for Water Control Facilities .....	151

## **Integrated Technology Policy and Regulatory Analysis**

Development of Meso-Level Perspectives for Modeling the Global Environmental Consequences of Human Behavior .....	155
Integrated Climate Change Analyses: A Pilot Study .....	158
North American 3E Model .....	160
Technology Adoption Study .....	163

## **Marine Sciences**

Development of Lagrangian Particle-Tracking Method for Quantifying Fluxes in the Near-Shore Marine Environment .....	167
Semipermeable Membrane Devices for Sampling Non-Polar Organic Compounds in Air, Water, and Soil .....	170

## **Materials Science and Engineering**

Bioactive Coatings and Composites for Orthopedic Devices .....	175
Catalytic Materials Synthesis .....	177
Coatings Characterization .....	179
Development of Ultracapacitor Materials .....	180
Glass Structure, Chemistry, and Stability .....	182
High Temperature Catalytic Materials .....	183
Industrial Applications of High Surface Area Supported Metal Catalysts .....	185
Matrix Crack Insensitive Composite Materials .....	186
Mesoporous Materials .....	188
Nanoparticle Processing .....	190
Nanoparticle Science .....	192
Novel Electrosynthesis of Organic/Inorganic Electroactive Polymers Based on Co-Polymerization of Organic Molecules with Cyclic Chlorophosphazenes .....	193
Ordered Mesoporous Membranes .....	196

Selective Oxidation in Membrane Reactors . . . . .	198
Solution Chemistry . . . . .	199
Supported Metal Catalysts . . . . .	201
Surface Modification . . . . .	202
Synthesis of Model Inorganic Ion Exchange Materials . . . . .	204

## Molecular Science

Adsorption on Fe-(hydr)oxides Under Nonequilibrium Conditions . . . . .	209
Bonding and Structure of Organic Ligands at Oxide/Water Interfaces . . . . .	210
Catalytic Chemistry of Metal Oxides . . . . .	213
Characterization of Structure and Dynamics of Surface Adsorbates and Their Surfaces . . . . .	215
Colloid-Colloid Interactions: Forces and Dynamics . . . . .	217
Effects of Surface Complexation and Structure on the Dissolution Precipitation Kinetics of Carbonate Minerals . . . . .	219
Elastic Properties, Solution Chemistry and Electronic Structures of Oxides, Silicates and Environmental Catalysis . . . . .	221
Environmental Catalysis . . . . .	223
Flow Injection Analysis . . . . .	224
High Field NMR and NMR Imaging . . . . .	226
High Resolution and Solid State NMR Studies of Proteins and DNA-Adducts . . . . .	228
Identification and Structural Determination of Paramagnetic Species Using Pulsed EPR . . . . .	230
Magnetic Resonance Spectroscopy . . . . .	233
Magnetic Resonance Spectroscopy Studies of Glasses, Minerals and Catalysts . . . . .	234
Materials Surface and Interface Chemistry . . . . .	237
Mechanisms of Radiolytic Decomposition of Complex Nuclear Waste Forms . . . . .	239
Multinuclear Solid State NMR Characterization of Early Forms of Mineralization . . . . .	241
NMR Studies of Altered-DNA/Protein Complexes . . . . .	243
NMR Studies of Proteins . . . . .	245
Novel Synthesis of Metal Cluster/Polymer Composites . . . . .	246
Numerical Solution of the Schrödinger Equation . . . . .	249

Protein-DNA Complexes: Dynamics and Design .....	250
Solid State Multisensor Array .....	253
Spectroelectrochemistry .....	254
Structural and Kinetic Studies at Model Oxide Surfaces .....	256
Theoretical and Computational Molecular Science Research .....	259
Tumor Formation in Cells and Tissues Studied by Means of Liquid-State and Solid-State NMR .....	260
X-Ray Absorption Fine Structure .....	263

## **Nuclear Science and Engineering**

Boiling Water Reactor Advanced Fuels .....	267
--	-----

## **Process Science and Engineering**

Advanced Instrumentation Real-Time Acoustic Planar Imaging of Dense Slurries - RAPIDS .....	271
Analytical and Reaction Chemistry .....	273
Catalyst Development and Testing .....	275
Ceramic Permeation Membranes .....	276
Characterization of Rapid Dechlorinators: Remediation of DNAPL .....	277
Colloidal Waste Science .....	280
Development of Carbonate Barriers for In Situ Containment .....	282
Electric Field and Current Modeling of Electrical Discharge Processing .....	284
Electroactive Materials .....	286
Electroconversion .....	288
Enhanced Mixing for Supercritical Fluid Oxidation—Phase Separations .....	290
Evaluation and Selection of In Well Separations .....	291
Experimental Investigation of Pipe Flows of Complex Fluids .....	294
Fundamental Reaction Diagnostics/Kinetics .....	296
Homogeneous Isotopic Turbulence .....	298
Hydrogen Separation Technology Using the CHASP Process .....	299
In Situ Containment Using Heat-Enhanced and Carbonate Barriers .....	300

Ionizing Radiation Assisted Processing of Hazardous Wastes .....	302
Isolation and Use of Extremophilic Bacteria for the Treatment of High Nitrate and Sulfate Containing Wastes .....	304
Kinetics, Scale-up and Demonstration of Uranium Bioprecipitation Technology .....	306
Membrane Materials .....	308
Membrane Separations .....	309
Microplasma Reactor .....	310
Modeling of Colloidal Systems .....	312
Plasma Engineering and Prototype Development .....	313
Reaction Engineering .....	315
Structure Function Analysis .....	317
Supercritical Fluid Separations .....	319
Synthesis Reaction in a High Energy Corona .....	321
Ultra High Rate Sputter Deposition of Highly Reflective Metal Films .....	322
Vacuum Extruded Polymer Films .....	326
Vining Plant Control .....	328

## **Risk and Safety Analysis**

A Tribal Risk Model .....	333
Cell and Tumor Growth Kinetics .....	335
Cell Signaling Mechanisms .....	338
Comparative Metabolism and Pharmacokinetics .....	341
Development of Environmental Dosimetry Modeling Parameter Database Editor .....	343
Direct and Indirect Genotoxic Mechanisms .....	344
Ethical, Legal, and Social Implications of the Human Genome Project for Screening, Monitoring and Health Surveillance of Department of Energy Workers .....	346
Health Protection and Standards for Hazardous Chemicals .....	347
Light at Night .....	348
Technical Analysis and Integration of Health Effects Data .....	353

## **Statistics and Applied Mathematics**

The Development of Adjoint Sensitivity Methods for Complex Physical and Chemical Simulation Models . . . . .	359
Uncertainty Analysis for Computer Models . . . . .	360

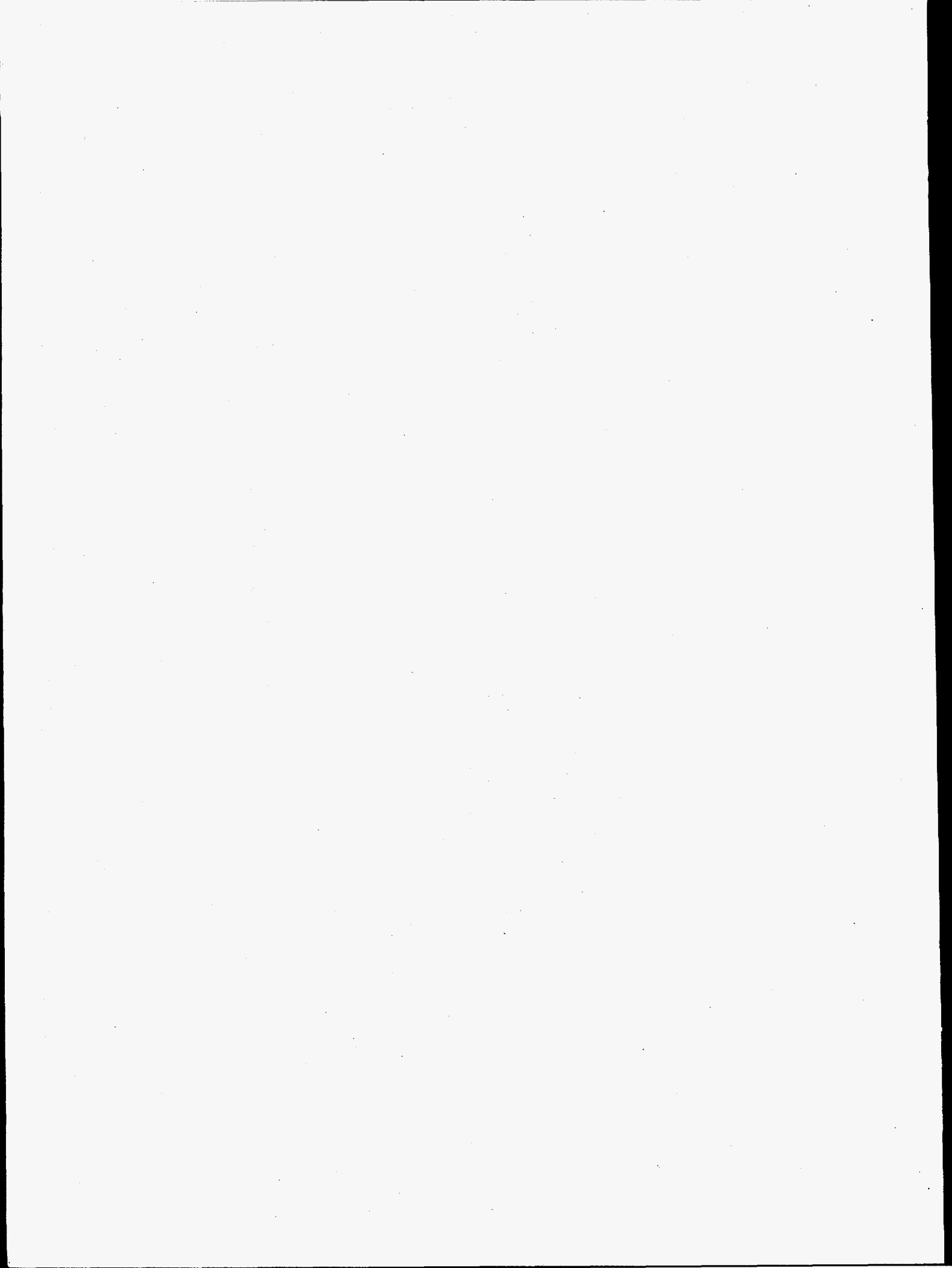
## **Thermal and Energy Systems**

Advanced Numerics and Visualization for Power Systems . . . . .	365
Advanced Power System Dynamic Stability Assessment . . . . .	367
Artificial Intelligence for Power System Control . . . . .	368
Biodegradable Electrostatic Filter Development . . . . .	372
Compact Spiral Composite Evaporative Cooler . . . . .	373
Exhaust System Thermal Management . . . . .	374
Heating Plant Maintenance Training System . . . . .	375
High Performance Micro Heat Engine Development . . . . .	376
Micro Heat Exchanger Development . . . . .	377
Microcompressor Development . . . . .	379
Microscale Sheet Architecture Prototype Development . . . . .	381
Off-Peak Cooling by Direct-Contact, Open- or Closed-Cycle Ice-Making . . . . .	382
Portable Dynamic Analysis and Design System . . . . .	383
Pulsed Amplitude Synthesis and Control Development Converter System . . . . .	385

<b>Acronyms and Abbreviations . . . . .</b>	<b>389</b>
---	------------



## **Atmospheric Sciences**



# *A Multidisciplinary Investigation of Heterogeneous Atmospheric Processes*

Douglas Ray (Chemical Structure and Dynamics)

Bruce C. Garrett (Theory, Modeling, and Simulation)

Yang Zhang and Richard C. Easter (Atmospheric Sciences)

---

## **Project Description**

The goal of this project was to understand, at a molecular level, the uptake of gas-phase atmospheric pollutant species into aqueous droplets. This was accomplished through a multidisciplinary effort involving macroscale atmospheric chemistry modeling, molecular-scale theoretical modeling, and surface second harmonic generation spectroscopy.

The project was divided into three tasks: 1) the development, testing, and application of a detailed, mixed-phase atmospheric chemistry box model; 2) the simulation of molecular-scale processes at gas-liquid interface; and 3) the uptake of gases by aqueous solutions probed by surface nonlinear optical spectroscopy. The long-term result of this project will be an improved scientific and technological capability to study the importance of heterogeneous chemical processes in the context of global environmental change.

## **Technical Accomplishment**

### *Development, Testing, and Application of a Detailed, Mixed-Phase Atmospheric Chemistry Box Model*

Appropriate gas- and aqueous-phase chemical mechanisms and an appropriate parameterization of interphase mass transfer processes have been selected to construct a multiphase box model. Assumptions associated with the gas and liquid interfacial mass transfer have been justified. Comparisons between different chemical integration techniques have been made. An advanced computational algorithm (LSODE) for chemical integration has been selected and implemented in the box model.

The development of the multiphase box model has been completed. The box model was tested under a variety of atmospheric conditions and compared against the results from other established models. In addition, more detailed literature searches were conducted to locate available information on the laboratory measurement of accommodation coefficients on liquid-phase surfaces. An informal report of the findings of that survey was completed. The accommodation coefficients and their variation ranges for various chemical species included in

the box model have been determined based on the values from the literature survey. These values are directly used in the box model for the base case study and the sensitivity studies. This information is invaluable to the molecular scale simulations and the laboratory experiments.

We have begun to use the box model to explore the effects of heterogeneous processes and aqueous-phase chemistry on tropospheric ozone formation. Some preliminary results have been obtained under typical atmospheric conditions. A significant reduction in gas-phase concentrations (9 to 34 percent) have been found in the presence of heterogeneous processes and aqueous-phase chemistry. These preliminary results show that heterogeneous processes and aqueous-phase chemistry can significantly influence the photochemical oxidant cycle by changing concentrations of many important gas-phase species. These results also demonstrate a need to further explore the interactions among ozone, its precursor gases, and heterogeneous surfaces. Sensitivity studies of the model to variations in the mass accommodation coefficients are in progress. These sensitivity runs will quantify the effect of the mass accommodation on gas-phase photochemistry. The results will also guide future laboratory measurements and molecular-scale calculations.

### *Simulation of Molecular-Scale Processes at Gas-Liquid Interface*

One of the first steps in this task was the evaluation of interaction potentials for water. Simulations were run using a pairwise additive interaction potential, the extended single point charge (SPC/E) model, and an interaction potential that includes many-body effects using a polarization model (POL1). The reliability of these models was assessed by comparing experimental observables (such as surface tension, structural information, etc.) against the computed results. For example, the computed values of the surface tension for the SPC/E model agrees with the experimental values to within about 20 percent over a temperature range from 270K to 370K.

Recently, a model for the mass accommodation process has been postulated that assumes the surface of water is a

dense gas-like state, composed of clusters of various sizes that continually undergo nucleation and evaporation. As a test of this model, molecular dynamics simulations have been used to directly examine the structure of the water surface. The density of the water near the surface decreases, falling off smoothly to zero in the vacuum. This is not the result of the clustering near the surface as predicted by the phenomenological model of Davidovits et al. Instead, there is the tendency to form transient cavities in the surface which, averaged over time and distance, give a lowered density compared to the bulk.

Potentials for the interaction of solute molecules, such as simple alcohols and ethylene glycol, have been developed and tested by comparing computed bulk phase properties with experimental ones. For example, interaction potentials for ethanol and ethylene glycol accurately reproduce experimental solvation energetics. These potentials have been used to study the orientation of the solute molecules at the interface. Figure 1 shows the distributions of angles of the C-O and C-C bonds in ethanol with the surface normal. The C-O bond prefers to be oriented parallel to the surface normal allowing the OH group to be inserted into the liquid for better solvation. The methyl groups are hydrophobic and tend to stick out of the surface at a preferred angle of about 60 degrees.

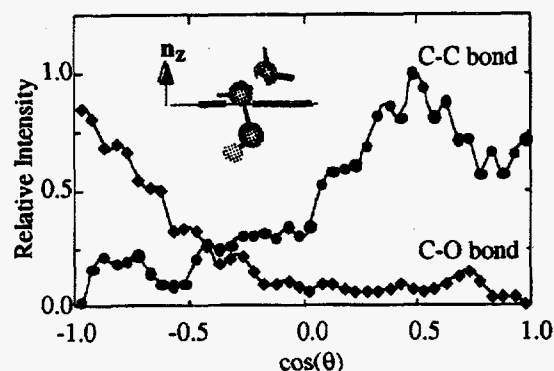


Figure 1. Orientation of ethanol at the liquid/vapor interface of water. The distribution of angles between the surface normal ( $n_z$ ) and the C-C bond and C-O bond are shown as triangles and circles, respectively. Results are averaged over 50 psec of a molecular dynamics simulation at 298K.

A direct knowledge of the potential of mean force for insertion of a solute molecule from the gas phase, through the surface and into bulk water is needed as input into calculations of the mass accommodation coefficient. As a first test of the methodology, the potential of mean force has been calculated for insertion of a single water molecule. Preliminary results show that the energy in the

bulk is lower than for the single water molecule in the gas phase, but the potential of mean force shows no evidence of a bound surface state as is expected for alcohols. Efforts are now in progress to calculate the potentials of mean force for insertion of ethanol and ethylene glycol into water.

#### *Uptake of Gases by Aqueous Solutions Probed by Surface Nonlinear Optical Spectroscopy*

Measurement of the adsorption isotherm for dimethyl sulfoxide (DMSO) on dimethyl sulfoxide/water solutions by surface second harmonic generation spectroscopy and determination of  $\Delta G^\circ_{\text{ads}}$  at 298K have been accomplished. Dimethyl sulfoxide was selected for these experiments because of its role in tropospheric chemistry and because accurate values for the mass accommodation coefficient and Henry's Law constant of dimethyl sulfoxide in water are available. Our determination of  $\Delta G^\circ_{\text{ads}}$ , in conjunction with data obtained from the literature, provides the first complete set of thermodynamic data for the mechanism proposed for the uptake of nonreactive solutes by dilute aqueous solutions (see Figure 2).

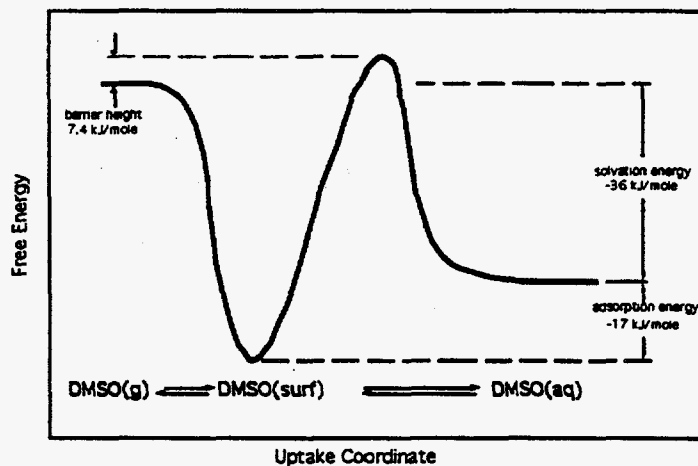


Figure 2. Schematic Potential Energy Surface for the Uptake of DMSO by Liquid Water

#### **Publication**

R. Doolen and D. Ray. 1995. "Uptake of Gases by Aqueous Solutions Probed by Surface Nonlinear Optical Spectroscopy." *Laser Techniques for Surface Science II*, vol. 2547, pg. 364.

# *Beyond Reduced Form Climate Model*

David C. Bader and Ruby Leung (Earth Sciences)

---

## **Project Description**

One definition of climate is the statistical distribution of meteorological events over a given time period. The time scale for weather phenomena ranges from a few hours to a few weeks, with the phenomena that largely determines climate (precipitation events, transport of air masses, long-lived clouds, etc.) at the longer end of this spectrum. The annual cycle still provides the largest climatic variation for any subcontinental region that can be defined. Given a long enough record (10 to 40 years), it can be assumed that a sufficient number of events will have been observed to define the climate ensemble. It is assumed that properties of the general circulation, such as Hadley cell intensity, the phase and amplitude of the extratropical wave train, equatorial Kelvin wave frequency, and others that are both defined and undefined, determine the probability density function for different types of weather events within a region. It is believed that these characteristics can be captured in monthly mean analyses of the general circulation. The goal of this project was to find empirical relationships between monthly mean atmospheric general circulation statistics and surface weather data for a subcontinental region.

These relationships can then be used to predict regional climate, including a measure of weather uncertainty, from the general circulation structure that will be predicted by climate prediction models.

## **Technical Accomplishments**

The four-state region of Missouri, Iowa, Nebraska, and Kansas was selected for the study because it was the subject of an earlier project describing the effect of climate change on the region's agriculture and economy. Surface meteorological data were obtained and data analysis software routines were developed to work with the data sets. Preliminary statistical analysis of the temperature and precipitation was performed to look at spatial correlations among stations in the region.

Acquisition of the general circulation fields were delayed because of the unavailability of the data. The National Meteorological Center's reanalysis project is behind schedule and there is an insufficient record length to perform robust statistical analyses. The project has been suspended until the data are available.

# Global Atmospheric Chemistry<sup>(a)</sup>

Richard C. Easter and Rick D. Saylor (Atmospheric Sciences)

---

## Project Description

The overall objective of this project was to enhance our capabilities in global atmospheric chemistry modeling by implementing Pacific Northwest National Laboratory's Global Chemistry Model (GChM) on a high-performance parallel computing platform and using the model to study global tropospheric carbon monoxide. Specific objectives included

- developing an efficient parallelized version of GChM
- adapting the chemistry and physics of GChM for simulating tropospheric carbon monoxide, perform simulations to interpret CO measurements obtained from the space shuttle in October 1984, and publish and present the results.

## Technical Accomplishments

In the past few decades, air pollution problems associated with energy usage and industrial activities have grown from local scale (photochemical smog) to regional scale (acid rain) to fully global scale problems (stratospheric ozone depletion). Numerical models of atmospheric chemistry are key tools for assessing our overall understanding of the chemical and physical processes involved and for estimating the effects of changing human activities on global air quality. The numerical models themselves have grown in complexity as our understanding of the atmospheric processes that affect air pollution have evolved. The computational performance of parallel processing platforms allows us to address global air pollution problems with current generation atmospheric chemistry models.

The Laboratory's Global Chemistry Model was developed over the past several years to address global scale atmospheric chemistry problems. GChM simulates the effects of emissions, transport (advection by mean winds, vertical turbulent mixing, vertical mixing by subgrid convective clouds), chemical reactions (clear air and in-cloud), and removal processes (precipitation scavenging and dry deposition) on atmospheric trace species. Early versions of GChM were used to investigate the role of fair-weather cumulus clouds in the long-range transport

and oxidation of carbon monoxide and methane, and the trans-Atlantic transport of soluble sulfur species.

Carbon monoxide was selected for the GChM applications of this project for several reasons. On a global basis, CO plays a significant role in the troposphere's overall oxidative capacity through its reaction with OH. Furthermore, depending on the local abundance of nitrogen oxides, CO can participate in reactions that either increase or decrease the formation of tropospheric ozone. Finally, mid-tropospheric CO measurements that were obtained from the October 1984 measurement of air pollution from satellites (MAPS) space shuttle flight have a unique near-global coverage for a tropospheric trace species, and thus provide an excellent opportunity for comparison with model results.

The CO version of GChM was implemented on the Intel Touchstone DELTA supercomputer using domain decomposition. The model operates on a regular, three-dimensional grid (latitude, longitude, and a normalized pressure coordinate), and the parallel implementation used decomposition of the horizontal domain, with each processor responsible for a certain rectangular block of vertical columns. With this implementation, interprocessor communication was only required during horizontal transport calculations. This decomposition provides good load-balancing among processors for calculations involving horizontal and vertical transport. However, the inclusion of nonlinear chemistry and cloud processes introduces serious imbalances in the code's computational load. Calculations involving photochemical reactions require much more time on the daytime than the nighttime side of the globe, and calculations for cloud processes are only required where clouds are present. These factors limited the code efficiency to about 50 percent on the DELTA. To improve efficiency, a dynamic load-balancing approach was designed in which computational tasks are passed from one processor to another based on the processors' individual computational loads.

The parallel implementation was also ported to a cluster of IBM RS-6000 high performance workstations. Because of the fewer number of processors in the cluster, a latitude only domain decomposition was possible here, with each processor having one latitude band in the

---

(a) Project was a task under the project formerly entitled "Computational Modeling of Complex Physical Systems."

northern hemisphere and one in the southern hemisphere. This eliminated load balancing problems associated with daytime/nighttime and also shorter/longer days near the poles. Also, differences in cloud frequency were reduced because each processor was responsible for more grid points, and better computational efficiency was achieved.

Modification of GChM's chemistry and physics was required for the CO simulations. A photochemical mechanism for CO, methane, nitrogen oxides, and ozone was implemented using a pseudo steady-state numerical technique. CO emissions sources and a treatment for vertical eddy diffusivity were adapted from earlier work by Saylor. Observed meteorological fields for autumn 1984 were obtained from the European Centre for Medium Range Weather Forecasting (ECMWF), and model was modified to use these data.

An initial set of simulations was performed at 3.75° horizontal resolution. Based on the results of the first simulations, a number of improvements to the model's chemistry and physics were undertaken. More recent estimates of anthropogenic, biomass burning, and biogenic emissions of CO were acquired to replace the values used initially. The nitrogen oxides fields used in the model were revised downwards in light of recent measurements. Simulated mid-tropospheric CO was particularly sensitive to convective cloud vertical transport, and the ECMWF data for 1984 contained very little information on convective clouds, so an alternate convective cloud treatment was developed using monthly climatological convective precipitation data.

Final simulations were performed at 1.875° and 3.75° horizontal resolution. The simulated distribution of CO agreed relatively well with the MAPS mid-tropospheric measurements and with available aircraft and surface measurements. Emissions sensitivity simulations and comparisons with available measurements indicated that

actual emissions during the October 1984 MAPS experiment may have differed substantially from the emissions estimates used in this study, particularly in southern Africa and the high northern latitudes. Further sensitivity simulations showed that the greatest contributions to uncertainties in simulated CO were from the convective cloud vertical transport and the CO emissions.

#### Publications

R.D. Saylor, R.C. Easter, E.G. Chapman, and M.K. Brown. 1995. "Simulation of the Tropospheric Distribution of Carbon Monoxide During the 1984 MAPS Experiment." *J. Geophys. Res.* (in preparation).

R.D. Saylor, R.C. Easter, and E.G. Chapman. 1994. "Analysis of Mid-Tropospheric Carbon Monoxide Data Using a Three-Dimensional Global Atmospheric Chemistry Numerical Model." In *Air Pollution Modeling and Its Application X*, eds. S.-E. Gryning and M. Millan, Plenum Publishing Corp., New York.

#### Presentations

R.D. Saylor, R.C. Easter, E.G. Chapman, and M.K. Brown. 1995. "Estimates of Emissions Inferred from Satellite Measurements of Mid-Tropospheric Carbon Monoxide." American Geophysical Union Chapman Conference on Biomass Burning and Global Change, March 13-17, Williamsburg, Virginia.

R.C. Easter, R.D. Saylor, and E.G. Chapman. 1994. "Analysis of Mid-Tropospheric Carbon Monoxide Data Using a Three-Dimensional Global Atmospheric Chemistry Model." Conference on Atmospheric Chemistry, American Meteorological Society Annual Meeting, January 23-28, Nashville, Tennessee.

1. The first part of the document discusses the importance of maintaining accurate records of all transactions and activities. It emphasizes that proper record-keeping is essential for transparency and accountability, particularly in financial matters. The text outlines various methods for organizing and storing data, including digital databases and physical filing systems.

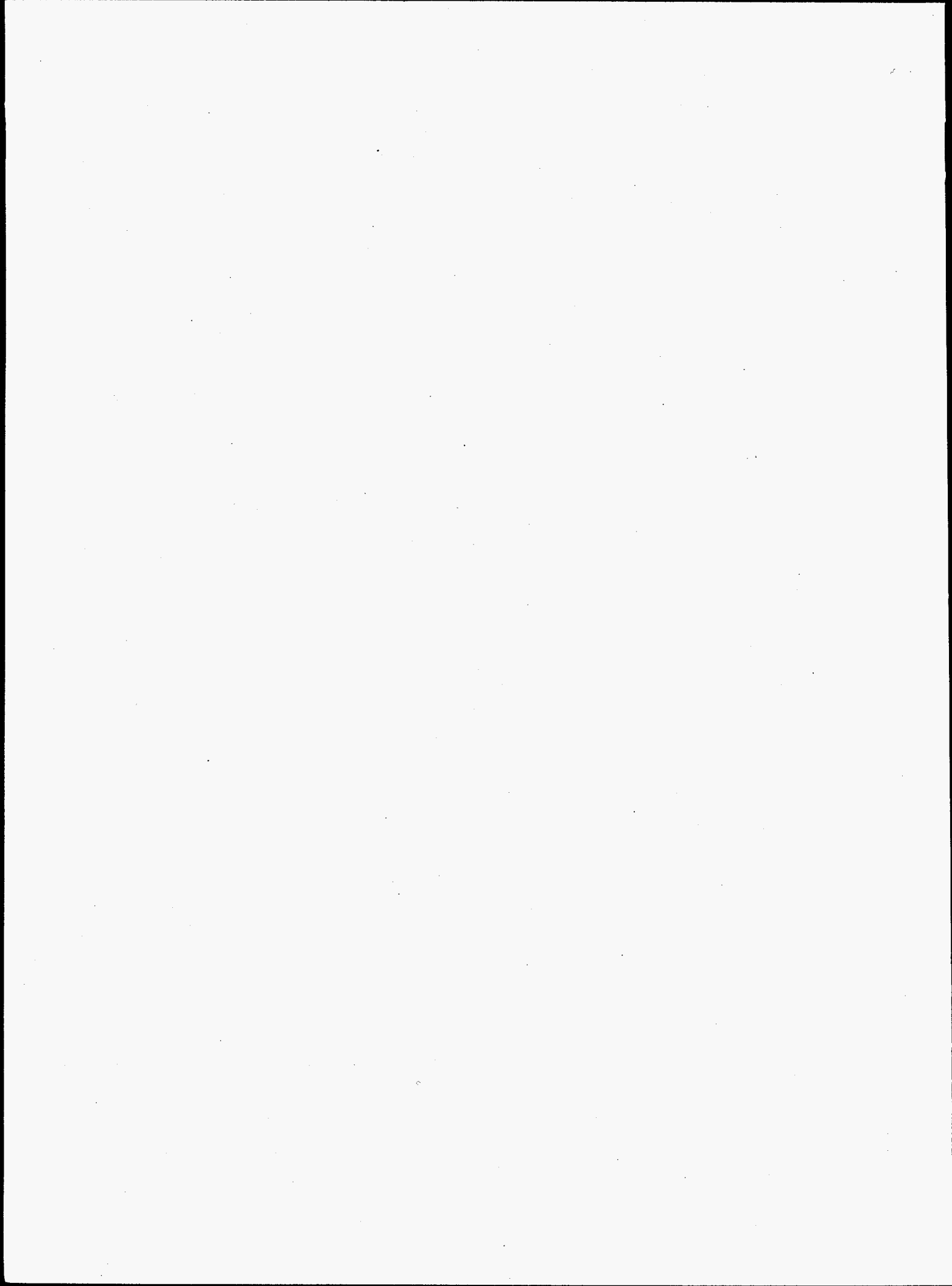
2. The second section focuses on the role of technology in modern record management. It highlights how software solutions can streamline processes, reduce errors, and improve accessibility. Examples of specific tools and platforms are provided, along with a discussion on the security measures necessary to protect sensitive information.

3. The third part of the document addresses the challenges associated with long-term data retention. It explores the legal requirements for archiving records and the importance of regular audits to ensure compliance. The text also discusses the impact of technological advancements on the longevity of digital data and offers strategies for mitigating risks.

4. The final section provides a summary of key findings and recommendations. It reiterates the importance of a proactive approach to record management and encourages the adoption of best practices. The document concludes with a call to action, urging stakeholders to take immediate steps to enhance their record-keeping systems.



## **Biotechnology**



# 750 MHz NMR Determination of the 3D Structure of a Unique Reductive Dehalogenase

Michael A. Kennedy (Macromolecular Structure and Dynamics)

## Project Description

Tetrahydroquinone reductive dehalogenase (TeCH-RD) is a bacterial enzyme that has been isolated from *Flavobacterium* sp. strain ATCC 39723. It has been shown to be involved in the degradative pathway of pentachlorophenol. Specifically, TeCH-RD carries out the reductive dechlorination of tetrachlorohydroquinone to dichlorohydroquinone. TeCH-RD is 247 amino acids in length with a corresponding molecular weight of 28.1 kD. The goal of this project was to use nuclear magnetic resonance spectroscopy to determine the three-dimensional solution-state structure of the enzyme. An integrated biophysical, biochemical, analytical, and modeling approach is being used to identify the three-dimensional structure of TeCH-RD.

## Technical Accomplishments

Tetrachloro-*p*-hydroquinone reductive dehalogenase (TeCH-RD) was recently purified from a pentachlorophenol-degrading *Flavobacterium* sp. strain ATCC 39723 by a Pacific Northwest National Laboratory/Washington State University team. The enzyme is thought to first catalyze the formation of a hydroquinone-glutathione adduct between a tetrachloro-*p*-hydroquinone (TeCH) and a glutathione and then to split the adduct at the expense of another glutathione (GSH) to produce 2,3,6-trichloro-*p*-hydroquinone and the oxidized form of glutathione (GS-SG). The deduced amino acid sequence shows strong similarity with two previously reported plant glutathione transferases (GSTs). TeCH-RD is the only reductive dehalogenase that has been characterized to date. The enzyme's ability in splitting hydroquinone-glutathione adducts may represent a new type of activity catalyzed by glutathione transferases, which is very important to prevent building up multiple substituted hydroquinone-glutathione adducts. Hydroquinones, metabolites of many xenobiotics, react with glutathione to form multiple substituted (more than one glutathione per quinone hydroquinone-glutathione) adducts. The conjugates have recently been shown to be more toxic than the original quinone metabolites in animal studies.

Nuclear magnetic resonance spectroscopy is the leading method for determination of solution-state protein structure. Secondary structure of proteins up to 31.4 kD have been determined at 600 MHz with 0.7 mM solutions

of uniformly  $^{15}\text{N}$  and  $^{13}\text{C}$ -labeled materials. The current estimate of the molecular weight range for complete three-dimensional nuclear magnetic resonance structure determination of proteins, employing the latest innovations in fractional deuteration of protein side chains and using up to 750 MHz field strengths, is between 30 and 60 kD. We have been able to show that under buffer conditions being used for nuclear magnetic resonance studies, TeCH-RD exists as a monomer in solution. Therefore, the TeCH-RD subunit is well within the molecular weight range for structural studies.

Strain JD01, an *E. coli* JM105 harboring the TeCH-RD expression vector, pJD01 has been used to produce large quantities of TeCH-RD. Overproduction of TeCH-RD is induced by the addition of isopropylthio- $\beta$ -D-galactoside. For  $^{15}\text{N}$ -labeled and  $^{15}\text{N}$ ,  $^{13}\text{C}$ -TeCH-RD production, JD01 is cultured in Isogro (Isotec, Inc.) labeled protein hydrolysate. Triple-labeled protein including  $^2\text{H}$ ,  $^{13}\text{C}$ , and  $^{15}\text{N}$  is being prepared from cultures grown in media based on deuterated algae grown in heavy water and with labeled carbon and nitrogen sources.

Mass measurements and tandem mass spectrometry experiments have permitted the verification of the sequence of the overexpressed proteins on the basis of precisely determined relative molecular mass ( $< \pm 0.01$  percent employing linear quadrupole instrumentation), product ion mass spectra and peptide mapping. Additionally, the nature, extent, and residue location of post-translational modifications can be determined using the same approach. Where improved resolving power and tandem mass spectrometric capabilities are required, ion trap and Fourier transform ion cyclotron instrumentation can be employed. As an example, Figure 1 shows that the  $^{15}\text{N}$  labeled material contained isotopic enrichment to 98.6 percent completion.

Preliminary nuclear magnetic resonance studies have been initiated and the data indicate that TeCH-RD is a good candidate for nuclear magnetic resonance investigation. Determination of secondary- and tertiary-protein structure is a five-step process. First, preliminary studies are performed with unlabeled material to determine if the protein is "well behaved" for nuclear magnetic resonance studies (i.e., protein aggregation, purity). Second, assignment of the  $^{15}\text{N}$  chemical shift spectrum are initiated using the uniformly  $^{15}\text{N}$  labeled protein for heteronuclear

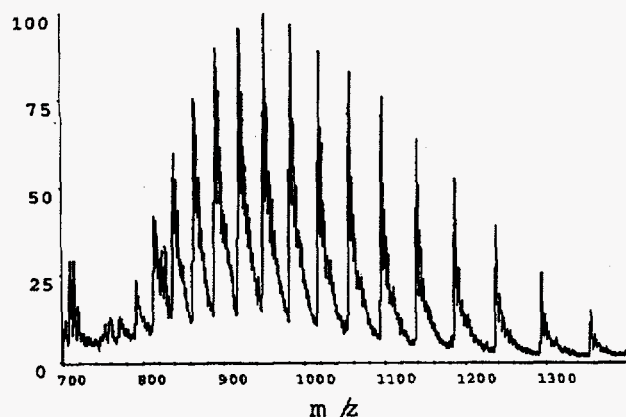


Figure 1. Electrospray ionization mass spectrum of purified recombinant,  $^{15}\text{N}$ -labeled TeCH-RD.

multiple quantum coherence (HMQC)- $\{^{15}\text{N}-^1\text{H}\}$ ,  $^{15}\text{N}$ -separated NOESY and  $^{15}\text{N}$ -separated TOCSY experiments. Resonance assignments are completed using coherence transfer between  $^1\text{H}$ ,  $^{15}\text{N}$ , and  $^{13}\text{C}$  nuclei. Proton-proton distance determination are performed using  $^{15}\text{N}$ - and  $^{13}\text{C}$ -separated NOESY experiments. Finally, structure refinements are generated using nuclear magnetic resonance data and distance geometry methods in conjunction with, in this case, homology modeling comparisons. Figure 2 shows preliminary nuclear magnetic resonance data collected at 750 MHz. The  $^1\text{H}$ - $^{15}\text{N}$ -heteronuclear multiple quantum coherence spectrum shows excellent resolution at 750 MHz.

The ability to determine three-dimensional structure either by x-ray crystallography or nuclear magnetic resonance spectroscopy has lagged behind sequence determination. As a result there has been ongoing interest in solving the

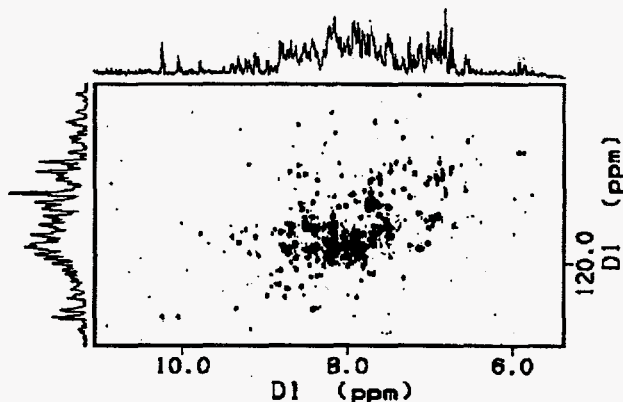


Figure 2. 750 MHz  $^1\text{H}$ - $^{15}\text{N}$  HMQC of TeCH-RD

protein folding problem via determination of three-dimensional structure based on amino acid sequence data. In the case of TeCH reductive dehalogenase, based on a comparison of amino acid sequence and enzymatic mechanism, it is likely that the protein is functionally (and structurally) related to the family of glutathione transferases. Multiple sequence alignments are being used to determine which segments of TeCH correspond to the secondary structure elements in rat and human glutathione transferase. Secondary structure prediction algorithms such as Chou-Fasman and GOR are being used to assess the reasonableness of the initial secondary structure assignments for TeCH. All of this information is then being used in conjunction with a distance geometry approach to obtain a family of potential structures for TeCH. This family of structures is then evaluated on the basis of a number of structural and functional tests of the reasonableness of the model structures and their consistency with available experimental data. Figure 3 shows the distance geometry based structure of TeCH-RD using constraints from homology modeling based on the x-ray structures of related mammalian glutathione transferase proteins.

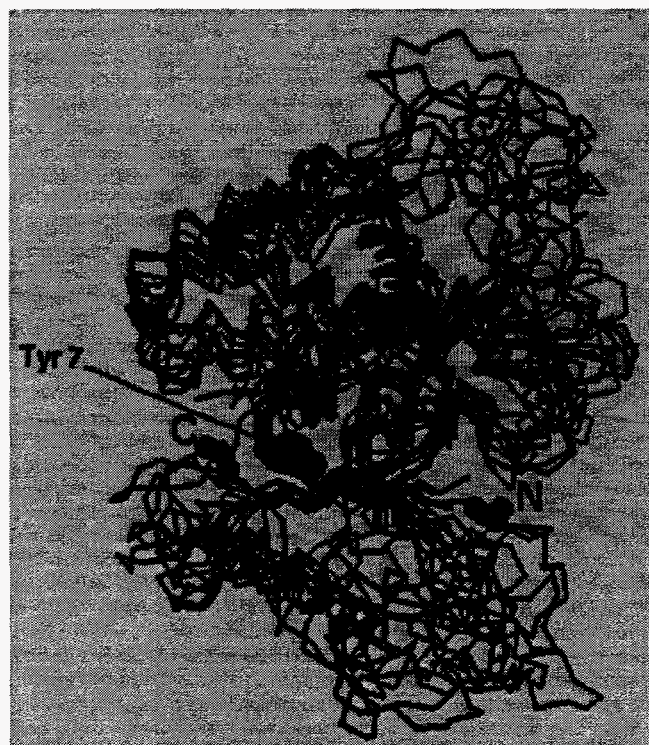


Figure 3. Distance geometry based structure of TeCH-RD using constraints generated from homology modeling using x-ray structures of related mammalian glutathione S-transferases.

# *Advanced Biomedical Science and Modeling*

Richard E. Weller and Melvin R. Sikov (Biology and Chemistry)

---

## **Project Description**

Advanced technologies that emphasize molecular approaches to complex biomedical problems are being emphasized in federally funded research. This project was proposed to develop advanced research concepts and systems in the biomedical sciences through multidisciplinary collaborative research. Work performed during the course of this project has identified a number of emerging, innovative approaches and concepts to enhance human health.

## **Technical Accomplishments**

### *Imaging to Detect and Diagnose Disease*

Work in FY 1994 using a prototypic cell line, HL-60, suggested a novel approach for identifying tumor cells based on their metabolic activity and ability to synthesize a unique polymer. In FY 1995, the technology was evaluated both ex vivo and in vivo using a rat mammary tumor cell line. For the in vivo studies, the tumor cell line was grown ex vivo and then transferred to female Wistar rats by the subcutaneous inoculation of approximately 106 cells into the inguinal fat pad. Tumors were palpable by 5 to 7 days post inoculation at which time the animals were dosed with 1 mg/kg of the essential substrate given intraperitoneal once daily for 5 days. The tumors were then harvested, the cells dispersed, and excited at 355 nm. Increased emission in the spectral region with a modal 500 to 520 nm peak was again observed in treated cells. The in vivo studies were repeated in older, retired, female breeder Wistar rats to see if reproductive status had any effect on the ability of the tumor cells to synthesize the polymer compared to surrounding normal mammary tissue. Results of that study are still pending.

### *Thermal Imaging*

In FY 1994 a preliminary set of images of transplanted rat mammary tumors was obtained using an Inframetrics thermal imaging camera that employs a mercury-cadmium telluride detector with an 8 to 12 micron response range. Tumor images were recorded on lesions as small as 2 to 3 mm in diameter at depths of 1.5 to 2 cm below the surface of the skin. Analyses of the thermal readings

disclosed that the measured temperatures associated with the two-dimensional projections of the developing tumors were lower than those of surrounding areas. In FY 1995, a series of "blinded" studies were conducted in both young and old female Wistar rats. Rat mammary tumors were transplanted using the protocol previously described. Thermal images were then obtained every other day on each rat beginning 48 hours after inoculation with the tumor cell line and continuing until 30 days post inoculation at which time tumor growth was evident both palpably and visually. Each animal was sedated and positioned according to a standard operating procedure prior to each imaging session to assure reproducibility. The operator who obtained the images was "blinded" to which rats had been inoculated with the tumor cell line or "sham" inoculated with sterile physiologic saline to serve as control animals.

Random noise, typical of the class of imaging system employed in this project, rendered texture analysis or segmentation ineffective. The use of a frame grabber system with frame averaging functions would help considerably. Gradient filters were also hampered by the pixel-to-pixel variation in what should be a smooth background. Median filtering was very effective in correcting that problem. Tumors appeared as dark regions on the abdomen. In the early stages of tumor development the tumor signature is usually crescent shaped with a brighter region in the concavity. Using these methods we were able to recognize tumor growth as early as 13 days post-inoculation when the growth was approximately 1 mm in diameter.

### *Enhanced Interpretation of Diagnostic Images*

The focus of this work in FY 1995 was to examine the use of fractals in digital analysis of mammograms for detection of microcalcifications. A literature search was done to determine the state-of-the-art of the role of fractals in the enhancement and analysis of digitized mammograms to detect microcalcifications. Fractal analysis has been tested as a measure for many mammographic properties: fibrosity, density, tumor identification, and detection of microcalcifications. Substantial work has been done to evaluate the use of fractals in textural analysis of biological tissue, but little specifically with regard to microcalcifications.

Although fractals have received considerable attention as texture descriptors, their success alone has been marginal. As with most texture methods, segmentation of microcalcifications in a digital mammogram has only been found to be 80 to 85 percent accurate. Alone, these methods are not sufficient to be incorporated into an

automated mammo graphy screening system. It was concluded that combining texture segmentation techniques, possibly with neural networks to aid the classification on nonlinear relationships, will prove more effective than one method by itself.

# *Degradation of Explosives by the Combination of Enzymatic and Microbial Processes*

Manish M. Shah and Rodney Skeen (Environmental Technologies)  
James A. Campbell (Materials and Chemical Sciences)

---

## **Project Description**

More than 25 Department of Defense and Department of Energy sites contaminated with explosives need to be remediated. Ongoing military operations are producing explosive-contaminated waste streams on a continuous basis and there is currently no cost-effective technology to degrade explosives in soil and water. Certain bioremediation technologies have the potential to remediate these sites in a cost-effective manner, however, current microbial processes are limited by technical problems such as toxicities of explosives, slow rates, and incomplete mineralization. The incomplete mineralization has been attributed to formation of polymeric products of TNT. We proposed to overcome these limitations by enhancing microbial processes using enzymatic catalysis of the explosives.

## **Technical Accomplishments**

The overall goal of this research was to develop a cost-effective treatment technology for biodegrading explosives by combining enzymatic and microbial processes. A simplified reaction scheme for the proposed process is shown below:

### **Step 1:**

Explosives + material  $\rightarrow$  Reduced Explosives + Oxidized material

### **Step 2 (Microbial):**

Reduced Explosives  $\rightarrow$  (Aerobic Microbial Processes)  
( $\text{CO}_2 + \text{H}_2\text{O} + \text{NO}_2^-$ )

or

Reduced Explosives  $\rightarrow$  (Anaerobic Microbial Processes)  
( $\text{CH}_4 + \text{CO}_2 + \text{H}_2\text{O} + \text{NH}_4^+ + \text{N}_2$ )

We discovered a process that can reduce 2,4,6-trinitrotoluene (TNT). We also found that the materials used in the process can be recycled with inexpensive ethanol dehydrogenase enzyme. An estimated treatment time for 1 liter of waste stream containing 440  $\mu\text{M}$  (100 ppm) of explosive could be as low as 4 seconds for the process using 1 gram of the material. This is a significant improvement over traditional microbial processes which would require anywhere from 1 day to weeks or months. The transformation products were reduced and are expected to be more easily and rapidly biodegraded than TNT. Hence, the next steps in these proof-of-principle studies are to identify the metabolites of TNT and investigate their biodegradability. The products of TNT degradation are very polar organic compounds.

# *Dynamics, Modeling and Redesign of Microbial Proteins*

Rick L. Ornstein (Theory, Modeling, and Simulation)

---

## **Project Description**

The objective of this project was to compare the underlying structure-function-dynamics relationships of bacterial proteins/enzymes under biologically moderate physiological conditions and under extreme conditions, such as in aqueous versus nonaqueous solvents. Nonaqueous enzymology is of great importance both from the mechanistic point of view and from the practical application point of view. Developing enzymes that are functional in highly concentrated halocarbon solutions, such as carbon tetrachloride, may prove useful in the development of new strategies for environmental remediation and monitoring of pollutant plumes, as well in developing "green" processes. Doing so will require gaining an understanding of the underlying structural and dynamic effects to enzymes induced by such solvents. State-of-the-art computational molecular dynamics simulations, starting with an experimental aqueous three-dimensional protein structure, allows one to directly compare structure-function-dynamics relationships of a protein in solvents for which experimental structural data is not available.

## **Technical Accomplishments**

Recent studies by Klibanov and coworkers have demonstrated that subtilisin (and other enzymes) maintains considerable activity in certain nonaqueous solvents. Klibanov, Ringe, and coworkers have recently determined the x-ray crystal structure of subtilisin in water and in water with acetonitrile. In FY 1995, we performed molecular dynamics simulations on this bacterial enzyme in four different solvent systems: water, water and acetonitrile, water and carbon tetrachloride, and water and dimethyl sulfoxide. The effect of carbon tetrachloride on enzyme properties is of particular interest in view of its propensity at the Hanford Site.

Starting coordinates for all heavy atoms of subtilisin and crystal waters were obtained from the crystal structure from aqueous solution. For the simulation in water, subtilisin and crystallographically located solvent molecules were solvated by an additional 35 Å sphere of water (over 4300 water molecules in total). For the simulation in carbon tetrachloride the protein, together with crystal waters, was immersed in a box of carbon tetrachloride containing 1275 carbon tetrachloride

molecules. The molecular dynamics simulations were carried out using the AMBER 4.0 program and force field. Overall the calculated time-averaged structure in water and in carbon tetrachloride are very similar to each other and to the aqueous x-ray structure, except for significant differences in loop (or turn) regions, resulting in many extra intra-protein hydrogen bonding interactions.

Unlike water, carbon tetrachloride is a nonpolar solvent and has very low dielectric constant, with no hydrogen bonding capability. In a solvent with little or no hydrogen bonding capability, the hydrogen bonding contribution to the free energy of protein folding will be an even more important determinant than in aqueous solution. Normally, removing protein-solvent hydrogen bonds would increase the free energies of both folded and unfolded states. In aqueous solution a properly folded protein is believed to have more internal hydrogen bonds than the unfolded form. In nonaqueous solution, an increase in the total number of intra-protein hydrogen bonds could stabilize either an active or inactive conformation. Thus, understanding intra-protein hydrogen bonding is an important factor in designing an enzyme for a particular nonaqueous environment. The number of intra-protein hydrogen bonds in each solvent over the time course of the simulations are shown in Figure 1. The total number of hydrogen bonds increased during the initial part of the simulation in carbon tetrachloride from 241 hydrogen bonds in the initial structure and then stabilized at 265. This is opposite to that normally observed for proteins in aqueous simulation. In the water simulation, the total number of hydrogen bonds decreased and generally ranges between 210 and 220. In a nonpolar solvent such as  $\text{CCl}_4$ , it is energetically very unfavorable to have protein hydrogen bond donor and acceptor groups not participating in hydrogen bonding. The inability of the protein to form strong hydrogen bonds with a nonpolar hydrophobic solvent may lead to structural changes if additional internal hydrogen bonds can be formed. Thus some of the protein surface loops rearranged leading to additional hydrogen bonds which are not present in the x-ray structure or the aqueous simulation. The catalytically relevant hydrogen bond between Asp 32 and His 64, however, is present throughout the simulation, as seen in our simulations of subtilisin in water, acetonitrile, and dimethyl sulfoxide. The increase in total number of intra-protein hydrogen bonds and the formation of water-mediated hydrogen bonding networks in carbon



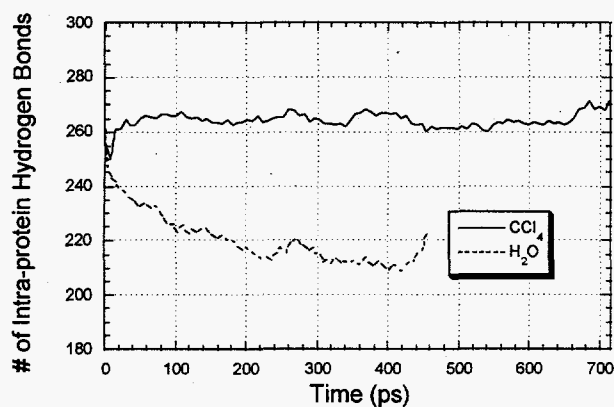


Figure 1. The Calculated Total Number of Intra-protein Hydrogen Bonds in Different Solvents

tetrachloride is consistent with the generally observed increase in thermostability and reduced flexibility of proteins in nonaqueous solutions.

The increase in total number of intramolecular protein hydrogen bonds in carbon tetrachloride is expected to affect protein flexibility. The flexibility (or rigidity) of an enzyme can be measured by the root mean square (RMS) fluctuation about the time-averaged simulated structure. The calculated root mean square fluctuation for subtilisin in  $\text{CCl}_4$  and water are plotted in Figure 2. Some of the residues of subtilisin in the water simulation show larger root mean square fluctuation than the same residues in the  $\text{CCl}_4$  simulation, while some show smaller root mean square fluctuation. The amino acid residues that show larger than 1.0 Å root mean square fluctuation in the water simulation are involved in surface turns and in the C-terminus. However, the root mean square fluctuations of residues in the  $\text{CCl}_4$  simulation are more uniformly distributed. This is consistent with the recent molecular dynamics simulations of BPTI in chloroform by Hartsough and Merz. The increase in the total number of intramolecular hydrogen bonds and the formation of networked, water-mediated hydrogen bonds are probably responsible for the reduced flexibility at solvent accessible surfaces of the enzyme in  $\text{CCl}_4$ .

To further assess the interaction between protein and solvents, we investigated the solvent dynamics at the protein surface. One way to look at this is to check the root mean square fluctuation of each solvent molecule.

We calculated a time-averaged structure for the last 500 ps of the trajectory and examined the root mean square fluctuation about the time-averaged structure. For simplicity only the oxygen atoms of waters and carbon atoms of the carbon tetrachlorides were monitored. As expected most of the carbon tetrachloride molecules are very mobile and display very large root mean square

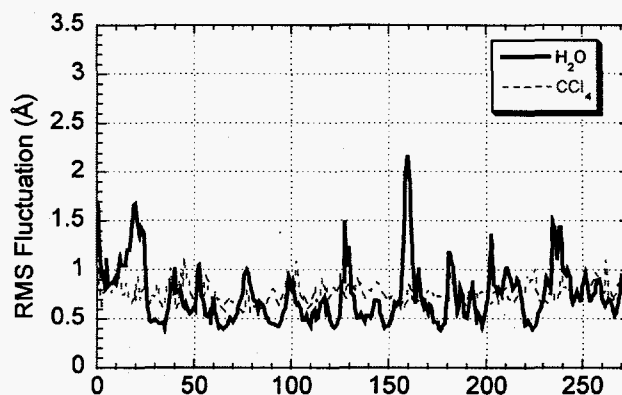


Figure 2. Comparison of Calculated RMS Fluctuation

fluctuation, while on the other hand, all of the water molecules show comparatively small root mean square fluctuation during this 500 ps period. The low mobility of water results from the inability of  $\text{CCl}_4$  to interact strongly with water; thus water molecules cluster to each other or hydrogen bond to protein. The largest root mean square fluctuation for water molecules is only about 7 Å compared with a high value of 45 Å for  $\text{CCl}_4$ . To illustrate this point further, we traced the movements of three representative water molecules. One of the water molecules is tightly bound with an root mean square fluctuation of 0.9 Å. It is very interesting to note that the water with the largest root mean square fluctuation slides along the protein surface. In nonpolar solvents such as  $\text{CCl}_4$ , the energetic cost of water leaving the protein surface and moving into bulk solvent would be very high. Therefore, water molecules tend to stay on the surface and only move laterally along the surface of protein. For similar reasons, chloride ions also stay close to protein and waters; they are either hydrogen bonded to water or hydrogen bonded to polar hydrogens of the protein.

## Publications

Y.-J. Zheng and R.L. Ornstein. "Molecular Dynamics of Subtilisin Carlsberg in Aqueous and Nonaqueous Solutions." *Biopolymers* (in press).

Y.-J. Zheng and R.L. Ornstein. "A Molecular Dynamics Study of the Effect of Carbon Tetrachloride on Enzyme Structure and Dynamics: Subtilisin." *Prot. Eng.* (in press).

Y.-J. Zheng and R.L. Ornstein. "A Molecular Dynamics Analysis of the Effect of DMSO on Enzyme Structure and Dynamics: Subtilisin." *Proteins* (accepted pending revision).

## **Presentations**

Y.-J. Zheng and R.L. Ornstein. 1995. "Structure and Dynamics of Enzymes in Organic Solvents." Ninth Conversation in the Discipline Biomolecular Stereodynamics, June 20-24, Albany, New York.

Y.-J. Zheng and R.L. Ornstein. 1995. "Protein Dynamics of Subtilisin Carlsberg in Aqueous and Nonaqueous Environments." Ninth Symposium of the Protein Society, July 8-12, Boston, Massachusetts. (Abstract # 133-S).

Y.-J. Zheng and R.L. Ornstein. 1995. "Protein Dynamics of Subtilisin Carlsberg in Aqueous and Nonaqueous Environments." High Performance Computational Chemistry Workshop, August 13-16, Pleasanton, California.

# Enzymology of Bacterial Metal Reductase and Dehalogenase

Yuri A. Gorby and Luying Xun (Environmental Microbiology)

## Project Description

The objective of this project was to purify, sequence, and develop a molecular probe for the enzyme responsible for reduction of multivalent metals in the dissimilatory metal reducing bacterium *Shewanella alga*, strain BrY. This enzyme catalyzes the reduction of metals such as iron, manganese, cobalt, uranium, and chromium. This activity is important for directing the fate and transport of these multivalent radionuclides and heavy metals in natural and contaminated surface and ground waters. Understanding the mechanisms by which this important enzyme functions is vital for predicting the fate of these metals in the environment and for exploiting metal reducing bacteria in engineered bioreactor systems designed to remove heavy metals and radionuclides from aqueous waste streams.

## Technical Accomplishments

We have purified a protein complex from *S. alga*, strain BrY, that expresses metal reductase activity. The complex contains a hydrogenase, menaquinone, and a c-type cytochrome. Metal reductase activity was lost when any of these components were removed from the complex. Circumstantial evidence suggested that the cytochrome c serves as the terminal reductase. This component receives electrons from another component within the electron transport chain and passes those electrons to an oxidized metal. We focused our efforts on describing this novel enzyme as part of the purified complex.

Oxidized and reduced absorption spectra of the c-type cytochrome in BrY were similar to c-type cytochromes found in a wide variety of microorganisms that are unable to reduce metals (Figure 1). However, the midpoint potential of this cytochrome (-205 mV) was much lower than other c-type hemes (Figure 1 inset).

With this midpoint potential it is thermodynamically impossible for BrY to reduce any multivalent electron acceptor with a midpoint potential below about -200 mV. We previously determined that BrY can reduce a wide range of metals with midpoint potentials above, but not below, -200 mV.

We further investigated the cytochrome c in BrY by electron paramagnetic resonance (EPR) spectroscopy to gain a better understanding of the structure of this

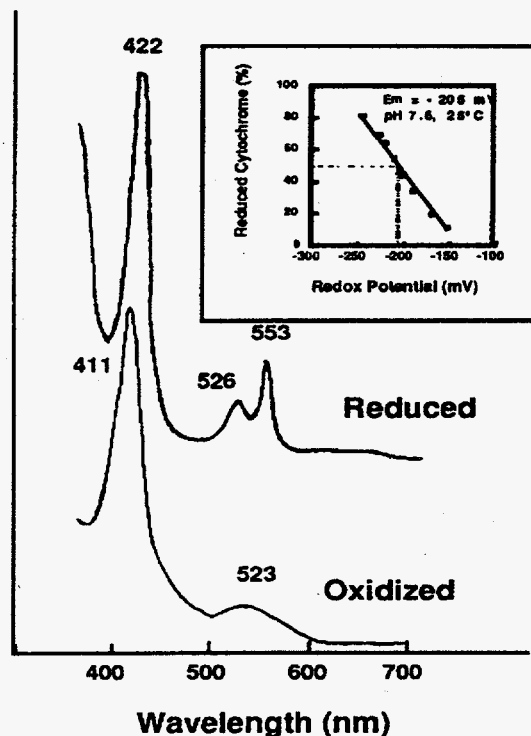


Figure 1. Visible absorption spectra of oxidized and reduced cytochrome c from BrY. Inset indicates the midpoint potential of this cytochrome c.

enzyme. Figure 2 represents electron paramagnetic resonance spectra generated at two temperatures.

Differences in the relative intensities of the resonance peaks indicate that many components of the protein complex contribute to the electron paramagnetic resonance signal.

To determine which peaks represent the c-type heme, electron paramagnetic resonance spectra were generated at various redox potentials (see Figure 3).

The complex became electron paramagnetic resonance silent when it was first completely reduced by the addition of sodium dithionite (Figure 3A). To determine what peaks represented the c-type cytochrome, the redox state of the system was adjusted to -210 mV, just below the midpoint potential of the cytochrome. Loss of resonance peaks at  $g=2.9$ , 2.26, and 1.58 is typical of the low spin

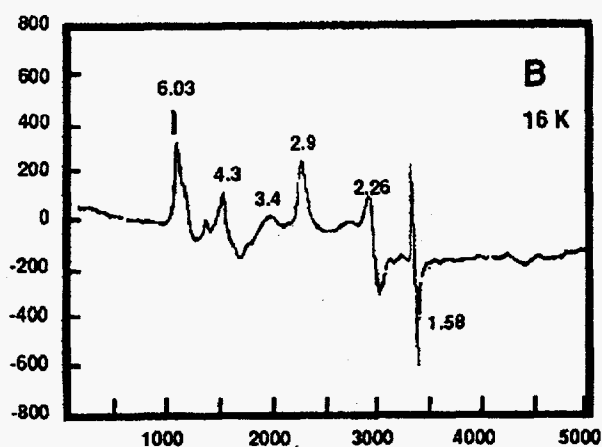
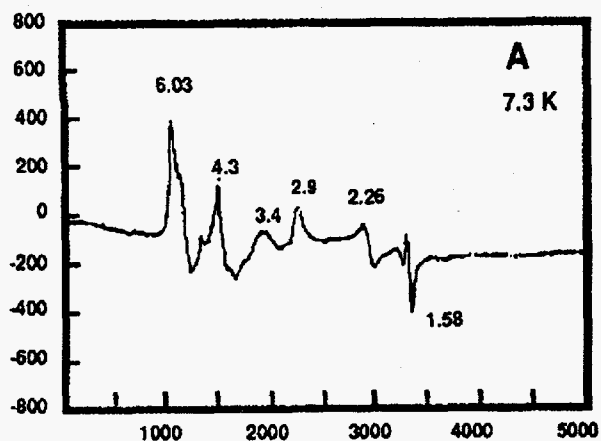


Figure 2. EPR spectra of metal reductase complex at two temperatures. Note the change in relative intensities of resonance peaks between the two spectra. Magnetic field strength is represented on the x axis.

( $S=1/2$ ) ferric heme species of c-type cytochromes. The  $g$ -values also indicate that this cytochrome is similar to the imidazole complex of heme octapeptide in mammalian cytochrome c.

Results obtained from research conducted in FY 1995 were important for understanding the mechanisms of enzymatic reduction of metals by bacteria and possibly for describing how this unique metabolism evolved among diverse and distinct groups of microorganisms.

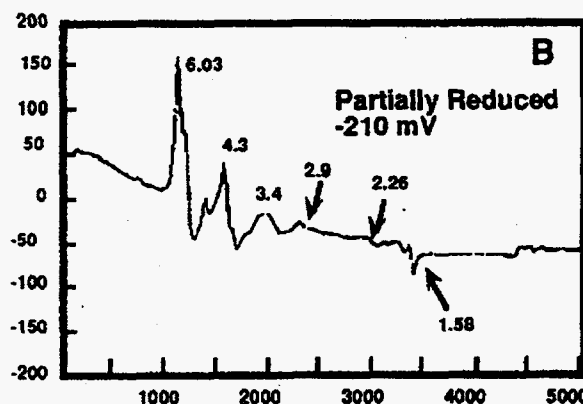
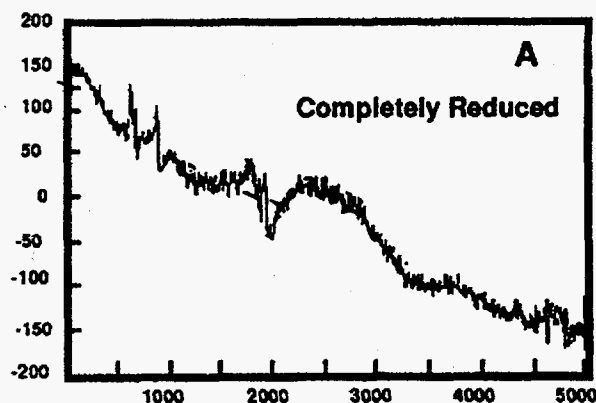


Figure 3. EPR spectra of (A) completely reduced and (B) partially reduced reductase protein complex from BrY.

Determining the midpoint potential of the active redox center of the heme defines not only the limit of metals that can be reduced, but also provides a sensitive tool for selectively controlling the valence of the iron center. This control allows for interrogation of the heme center using a variety of molecular analytical techniques. Through increasing our understanding of the molecular processes involved in enzymatic reduction of metal comes the ability to exploit this activity to its fullest potential as a remediation tool.

#### Publication

R. Caccavo, Jr., Y.A. Gorby, and M.J. McKinerney. "Purification of the Metal Reductase Complex in the Dissimilatory Metal-Reducing Bacterium *Shewanella alga*, Strain BrY" *Applied Environmental Microbiology*, (submitted).

# Fourier Transform EPR Studies of Radiation-Induced Structural Alteration of DNA

Michael K. Bowman (Macromolecular Structure and Dynamics)

## Project Description

This project seeks to help develop a program for the characterization of free radicals and altered forms of DNA and the enzymes that deal with damaged DNA. This included characterization of the spatial pattern of damage to DNA, the characteristics of DNA containing damage, and the enzymes involved in the repair of damaged DNA.

## Technical Accomplishments

Damage to DNA is very serious because it can lead to permanent changes in the genome. However, cells have a very efficient mechanism for the recognition and repair of damage to DNA. Yet, this highly evolved mechanism for the repair of DNA is sometimes defeated by radiation induced damage. The reason for this is thought to involve the presence of local clusters of damage that are much more difficult to repair than isolated damage sites. We have used the phenomenon of instantaneous spectral diffusion to measure the size of damage clusters in DNA at various states of hydration. We find that the level of hydration seems to modulate the spatial extent of the clusters to a similar extent as it does to the limiting yield of damage.

We collaborated with Professor Bruce Robinson from the University of Washington to characterize the mobility and surroundings of a spin label incorporated rigidly into a synthetic oligomer of DNA (see Figure 1). We directly measured  $T_1$  and  $T_2$  in liquid solutions of the oligomers at room temperature and found that the oligomer was strongly immobilized and locked into the DNA structure. In addition, we began to measure the ENDOR spectra of the spin-labeled DNA. ENDOR signals from nearby protons were observed (Figure 2), and we searched for signals from phosphorus in the backbone of the DNA. The phosphorus provided a means of measuring the local structure of the DNA relative to the altered site. We anticipated that some of the DNA damage recognition proteins would recognize this altered site and allow us a bird's eye view of the recognition complex.

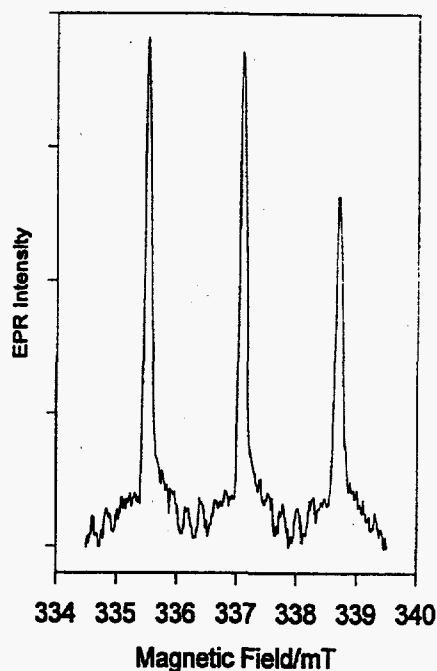


Figure 1. Echo-induced EPR spectrum of a DNA oligomer spin labeled with a base analog containing a nitroxide group. The spectrum is taken in water and the unequal peak heights show anisotropic rotational motion of the oligomer in solution.

We also studied the active site and models of ribonucleotide reductase, which is a damage-induced enzyme involved in DNA synthesis and repair. It contained a mixed-valent pair of metal ions. We succeeded in preparing models in the mixed-valent state.

We found a correlation in them between the electron paramagnetic resonance spectral properties and state of protonation of an oxygen bridging the metal ions. This allowed us to assign some of the structures observed in ribonucleotide reductase and several similar enzymes. We also examined the common electron paramagnetic resonance model of oxovanadium-histidine complexes involved in the active sites of enzymes. We found that VO-histidine actually contains coordination of both the imine and amine nitrogens of histidine. A much better model is that of the VO-imidazole complex where a single type of nitrogen is involved.

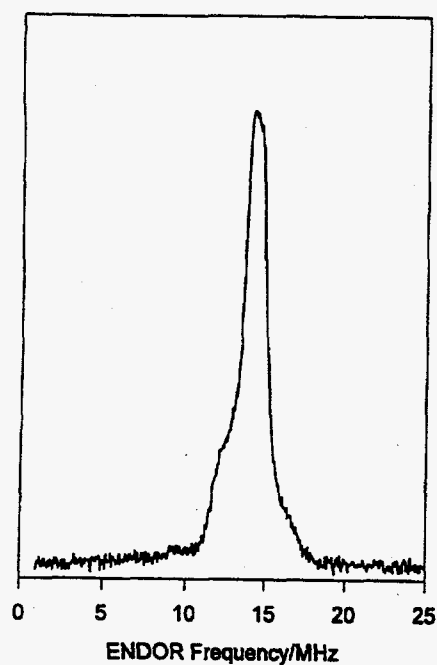


Figure 2. The ENDOR spectrum of a DNA oligomer incorporating a base analog with a nitroxide spin label group attached. The intense line at 14 MHz is from weakly interacting protons in the DNA and water in the solvent. It overlaps the peaks from more strongly interacting protons which appear as shoulders split by hyperfine interactions of about 5 MHz.

#### Publication

S.A. Dikanov, R.I. Samoilova, J.A. Smieja, and M.K. Bowman. 1995. "Two-Dimensional ESEEM Study of  $\text{VO}^{2+}$  Complexes with Imidazole and Histidine: Histidine is a Bidentate Ligand." *Journal of the American Chemical Society*, 117, 10579-10580.

## Functional Characterization of Bacterial Plasmids

**James K. Fredrickson and Margaret F. Romine (Environmental Microbiology)**

## Project Description

The objective of this project was to identify biodegradative functions associated with large plasmids in the subsurface bacterium *Sphingomonas* sp. strain F199. F199 is able to degrade single ring aromatics including *p*-cresol, toluene, benzoate, salicylate, and all isomers of xylene, as well as multiple ring aromatics including biphenyl, dibenzothiophene, and naphthalene. Results from FY 1994 demonstrated that the ring cleavage activity is encoded in two separate regions on the F199 plasmid pNL1. The fact that genes encoding this activity in other biodegrading bacteria are found adjacent to other genes necessary for biodegradation, suggests that the pNL1 plasmid will contain additional genes of this class. It was also found that four related subsurface aromatic-degrading *Sphingomonads* also harbored large plasmids. Determination of similarity in sequence and location of the biodegradative genes in these strains to F199 was also pursued.

## Technical Accomplishments

Partial sequence analysis of the two regions on pNL1 encoding catechol ring cleavage activity revealed that the genes encoding this activity were not identical. In degradation of multiple ring compounds, cleavage of aromatic rings occurs at more than one step and is commonly carried out by different enzymes. In order to determine which gene encoded the enzymes necessary at each of these steps, extracts from *E. coli* cells harboring a subclone from one or the other gene were tested for their ability to degrade the single ring aromatics catechol, 3-methyl catechol, and 4-methyl catechol and the multiple ring aromatics 2,3 dihydroxybiphenyl and 1,2 dihydroxynaphthalene (1,2 DHN). The latter two compounds are intermediates in the degradation of biphenyl and naphthalene, respectively. These compounds, as well as single ring aromatics such as toluene and xylene, lead to production of catechols. Cleavage of each of the compounds, except 1,2 DHN, to the corresponding yellow colored cleavage product was monitored spectrophotometrically. 1,2 DHN cleavage was monitored by measuring oxygen consumption. The results demonstrated that the gene encoded on clone 6 preferentially degraded multiple ring compounds, while that on clone 6 preferred single ring aromatics.

Alignment of the protein sequences to other known catechol dioxygenases demonstrated that the *xylE* gene from *S. yanoikuyae* B1 and *Sphingomonas* sp. HV3 as the two most closely related genes to the clone 18 gene, while that of the clone 6 gene was most closely related to the *bphC* genes in *S. yanoikuyae* B1 and *S. paucimobilis* Q1 (see Figure 1). The function of the enzymes in the related bacteria supports our functional data on clones 6 and 18. In adherence to the nomenclature in the literature, the genes in F199 will be called *bphC* and *xylE*. The finding that all the *Sphingomonas* sequences fall in families that are distinct from the other catechol dioxygenases suggests that these three *Sphingomonas* strains share target substrates and the range and/or specificities for these substrates will be unique from other well characterized enzymes that are included in the dendrogram.

During FY 1995, we collaborated with Dr. Gerben Zylstra of Rutgers University to determine if there was homology between sequences encoding biphenyl/*m*-xylene degradative genes in *S. yanoikuyae* B1 and *S. paucimobilis* Q1 and each of the subsurface strains.

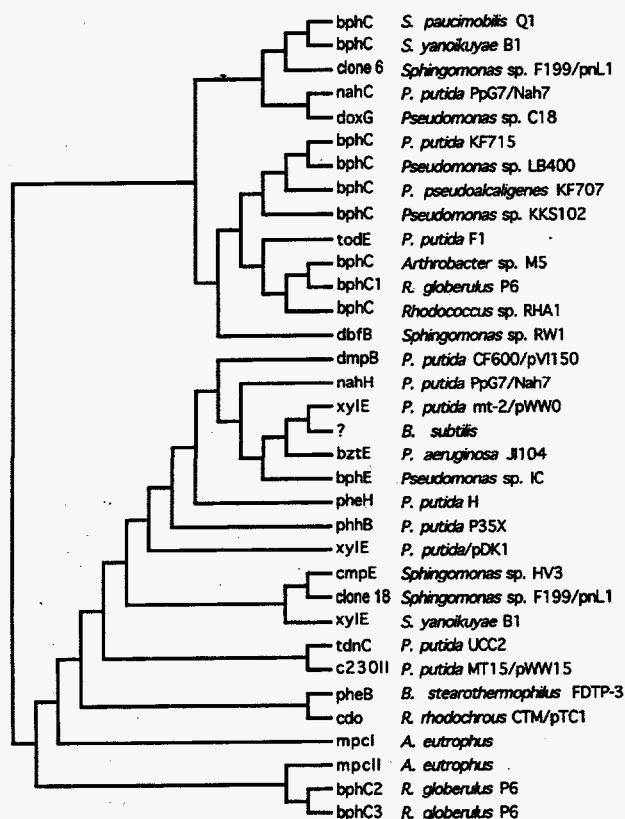


**Figure 1. Dendrogram of Ring Cleavage Dioxygenases**



Probes containing sequences with 1) the *xylE* gene, 2) the *bphC* gene, and 3) the entire degradative region from *S. yanoikuyae* B1 were hybridized to blots of *Bam*HI digested genomic DNA or blots of uncut plasmid DNA. The results from the genomic blots demonstrated that the sequences of these genes in each of these strains were similar. The *bphC* probe allowed detection of a single fragment of 4.2 kilobase in all strains except the nondegrading *Sphingomonas* strains B0477, ATCC 29837, and ATCC 14666. Using the *xylE* probe, a fragment of 9.8 kilobase was detected in F199, B0695, and B0712, of 12 kilobase in B0478 and B0522, and of 4.9 kilobase in both *S. yanoikuyae* B1 and *S. paucimobilis* Q1. Using the entire degradative region as a probe, several additional fragments were detected that differed among the subsurface strains and between *S. yanoikuyae* B1 and *S. paucimobilis* Q1, which displayed an identical hybridization profile (Figure 2). These results suggest that there is extensive homology of the biodegradative genes in the subsurface strains and the two nonsurface strains.

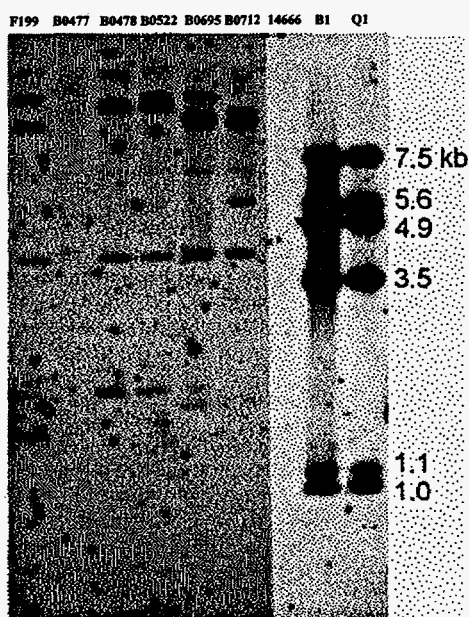


Figure 2. Hybridization profile of *Sphingomonas* genomic DNA digested with *Bam*HI and probed with the *Sphingomonas yanoikuyae* B1 *m-xyl/bph* probe.

Hybridization with undigested DNA localized the genes on plasmids in all the subsurface strains and on the chromosome in *S. yanoikuyae* B1 and *S. paucimobilis* Q1. The sizes of the hybridizing plasmids in the subsurface strains are 150 kilobase (B0478), 180 kilobase (B0522), 270 kilobase (B0712), and 180 kilobase (F199 pNL1). In strain B0695, two plasmids of 180 and 750 kilobase

hybridized with the probe. The occurrence of two hybridizing plasmids in B0695 was not accompanied by an increasingly complex hybridization pattern with genomic DNA (i.e., the number and sizes of fragments was similar to that of other subsurface strains). This finding would suggest that the sequences are on similar size restriction fragments on both plasmids or that only a small portion of homology exists on one of the plasmids.

Partial sequencing in the regions adjacent to *bphC* revealed six additional genes homologous to known biodegradative genes. The genes are arranged on at least two operons, which permits differential regulation of the enzymes. Three of the identified genes encode proteins that are homologous to protein components of dioxygenases that catalyze the first step in degradation of aromatic compounds. These enzymes are composed of three to four different protein subcomponents. They include the electron transfer components, ferredoxin and ferredoxin reductase, and a substrate binding portion. The substrate binding portion exists as either four identical protein subunits or as a mixture of two large subunit proteins and two small subunit proteins. Two of the genes are homologous to the large subunit of the dioxygenase family, but have sequences that are unique from each other. These genes appear to be transcribed in the same direction and possibly expressed at the same time. The gene homologous to the small subunit, however, is transcribed in a different direction, suggesting that its expression is not coupled to that of the large subunit proteins.

The occurrence of two unique genes homologous to the large subunit dioxygenase family suggests the possibility of shuffling large subunit proteins in vitro, resulting in three different holoenzymes (Figure 3). Since these components are involved in substrate binding, it would further suggest that assembly of these three enzymes would allow the F199 to attack a much broader range of aromatics than that of other well characterized bacteria that only encode one large subunit gene. Additionally, the sequences of the two dioxygenase large subunit genes are quite different than published sequences from other dioxygenase large subunits, suggesting that the substrate range for the F199 dioxygenases will be unique.

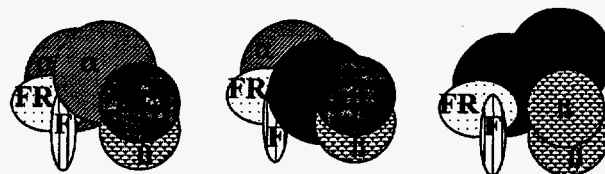


Figure 3. Model of how different enzymes with different substrate ranges might be generated by mixing slightly different protein subunits.



We have also successfully transferred the pNL1 plasmid to another *Sphingomonas* host using a mutant F199 which carries a transposon marker on pNL1 that knocked out activity for multiple ring aromatics only. When transferred, the plasmid conferred ability to degrade the single ring aromatics, such as toluene and m-xylene on the new host. Ability to degrade p-cresol and benzoate were not transferred with the plasmid. Since the latter degradative functions were not affected by the transposon insertion in F199, the data suggests that these functions lie either on the chromosome or on the other F199 plasmid. The successful transfer of pNL1 to another host demonstrates that the genes necessary for bacterial conjugation are present in F199.

### **Publications**

L.C. Stillwell, S.J. Thurston, R.P. Schneider, M.F. Romine, J.K. Fredrickson, and J.D. Saffer. "Physical Mapping and Characterization of a Catabolic Plasmid from the Deep-Subsurface Bacterium *Sphingomonas* sp. Strain F199." *Journal of Bacteriology* 177(15), 4537-4539.

E. Kim, P.J. Aversano, M.F. Romine, R.P. Schneider, and G.J. Zylstra. "Evolution of Aromatic Degradative Pathways Evidenced by Homology Studies Between Surface and Deep Subsurface *Sphingomonas* Strains." *Applied and Environmental Microbiology* (submitted).

### **Presentation**

M. Romine, J. Fredrickson, L. Stillwell, R. Schneider, J. Saffer, E. Kim, P. Aversano, G. Zylstra. 1995. "Identification of Plasmid-Encoded Biodegradative Activities in Five *Sphingomonas* Bacteria Isolated from the Deep Subsurface." Society of Industrial Microbiology: Annual Meeting, August 6-11, San Jose, California.

# *Identification, Purification and Characterization of the Reductive Dehalogenase of Desulfomonile tiedjei DCB-1*

Luying Xun and Shuisong Ni (Washington State University, Tri-Cities)

---

## **Project Description**

Reductive dehalogenation is one of the promising anaerobic bioremediation techniques in the removal of halogenated compounds from the environment. The key enzyme involved in this process is the reductive dehalogenase. *Desulfomonile tiedjei* is the only anaerobic bacterium in pure culture capable of reductive dehalogenation of halogenated aromatic compounds. The dehalogenase system in this organism is believed to be linked to its energy metabolism.

The overall objectives of this project were to identify, purify, and characterize the reductive dehalogenase system of *Desulfomonile tiedjei* DCB-1 and to clone and sequence the corresponding genes. Both biochemical and molecular biological techniques will be used to characterize the reductive dehalogenase system of *Desulfomonile tiedjei* DCB-1, and the knowledge gained from this study will enable us to develop a model system of reductive dehalogenation by anaerobic microorganisms and facilitate designing effective bioremediation methods for halocarbon removal.

## **Technical Accomplishments**

The dehalogenase that converted 3-chlorobenzoate to benzoate was identified and purified from the cytoplasmic membrane of DCB-1. Although the enzyme consisted of two subunits of 64 kDa and 37 kDa, it was purified as a single unit by passing through several chromatographic columns. The enzyme was yellow and had an absorption peak at 409 nm. Its ultraviolet-visible spectra indicated that it is a heme protein. The yellow chromophore has been demonstrated to be covalently linked to the 37 kDa subunit by reverse phase HPLC analysis.

The N-terminal amino acid sequence of the small subunit was determined. The sequence, 24 amino acids in length, was used to design degenerate nucleotide primers for

polymerase chain reaction. Agarose gel electrophoresis revealed a DNA band of about 71 base pair which corresponded to the expected size encoding the N-terminal sequence. This 71 base pair band was eluted from the agarose gel and later cloned into a TA vector for DNA sequencing. One of those clones showed DNA sequences which completely matched those of the N-terminal region of the small peptide (37,000). Based on the DNA sequence, a 30 base pair end-labeled nucleotide was synthesized to screen the genomic library for the dehalogenase gene(s).

This is the first time a reductive dehalogenase has been purified from an anaerobic bacterium. It offers new possibilities for us to understand the nature of reductive dehalogenation by anaerobic microorganisms.

Apparently, such organisms use chlorinated compounds as terminal electron acceptors, and the process is reductive dehalogenation. In addition, we will be able to design gene probes to monitor the dehalogenase genes for bioremediation.

## **Publication**

S. Ni, J.K. Fredrickson, and L. Xun. 1995. "Purification and Characterization of a 3-Chlorobenzoate-Reductive Dehalogenase from the Cytoplasmic Membrane of *Desulfomonile tiedjei* DCB-1." *J. Bacteriol.* 177 (17):5135-5139.

## **Presentation**

S. Ni and L. Xun. 1995. "Purification and Partial Characterization of a 3-Chlorobenzoate-Reductive Dehalogenase from *Desulfomonile tiedjei* DCB-1." General Meeting of American Society for Microbiology, Washington, D.C. (poster presentation).

# *Microbial Gene Expression and Genetic Engineering*

Jeffrey D. Saffer and Kwong-Kwok Wong (Biology and Chemistry)

---

## **Project Description**

Gene expression and genetic engineering studies are an integral part of microbial biotechnology. For fundamental research, specific proteins and enzymes need to be expressed to provide materials for structural biology studies. Frequently this requires constructing over-expression vectors and developing suitable purification schemes. Engineering of the target enzyme or protein through site-specific mutagenesis prior to expression is a necessary component of structure/function studies.

For applications, overexpression of enzymes is usually needed for large-scale production and bioprocessing. Specific alterations in the enzyme's primary structure may be required to achieve desired properties. Engineering of host bacterial functions may also be altered to enhance either protein production or cell function required for industrial applications.

## **Technical Accomplishments**

The identification of enzymes and functional proteins has great value for basic and applied research. Characterization of those proteins can be carried out to some extent with the (usually) minute quantities that can be isolated from their original source. However, many structural determinations require substantial amounts of protein. In addition, bioprocessing, either with purified protein or with microbes expressing the protein, generally requires substantially more protein than normally expressed. Several approaches have been developed for producing large amounts of proteins. In each case, it was found optimal to increase expression in the selected organism to the highest level possible, thereby saving considerable cost in subsequent purification.

The approaches for overexpression in general use fall into two categories. The first is overexpression of native products. This is required for some proteins whose activity is especially sensitive to sequence variations and whose folding requires specific pathways. The second is the creation of a fusion protein, which allows rapid purification of the overexpressed protein by affinity chromatography specific for the tag region. The cost and time savings of this approach, however, can be negated by difficulties in removing the tag. Nonetheless, this method is of great value.

We have now conducted an evaluation of various overexpression schemes and established the required methods. These capabilities are being applied to specific problems in microbial biotechnology.

Starvation-inducible promoters are desirable for several microbial biotechnological applications, such as in situ bioremediation and bioreactors. Bacteria in nature are often in famine or low nutrient environments. Thus, starvation and dormancy are the normal physiology for bacteria in nature. Enhanced expression of desired proteins in these starved and almost non-growth bacteria will be extremely useful for in situ bioremediation. Starvation-inducible promoters are likely to be the best choice for doing this task for in situ bioremediation. For bioreactors, high cell density or biomass is usually necessary to achieve high catalytic activity and to minimize operational cost. At such a high cell density, it is hard to keep the microbes growing rapidly because of nutrient delivery limitations. As a result, the level of desirable biochemical activity is limited. With the use of starvation-inducible promoters, we might be able to achieve a high cell density bioreactor, a highly desirable biochemical activity, but with minimal nutrient supply.

The RNA fingerprinting technology (RAP-PCR) will be adopted to identify and clone starvation-inducible genes. The RAP-PCR technology (or differential display) allows simultaneous comparison of RNA transcripts from bacteria grown under different environmental conditions. RNA is prepared from bacteria grown under starvation condition and nutrient prevalent condition. An arbitrarily chosen primer can initiate cDNA synthesis from many RNA transcripts, and the subsequent cDNA molecules will be amplified by arbitrarily primed PCR. About 20 to 40 PCR products will be displayed either on agarose gel or sequencing gel. PCR products, which are only amplified from the cDNA derived from RNA transcripts of starved cells, are likely to be starvation inducible gene candidates. Subsequently, identification of starvation promoters and construction of starvation expression vectors can be achieved.

# Microbial Genomics

Jeffrey D. Saffer (Biology and Chemistry)

---

## Project Description

The use of microbes in biotechnology is rapidly increasing. These diverse organisms represent the majority of organisms in the world and provide a limitless resource of genetic coding information. To exploit microorganisms fully, considerable information needs to be learned about their function and genetic coding capacity. This project uses genomic studies to provide a genetic basis for bioremediation and other biotechnological applications. The microbial genome research program has focused on the subsurface *Sphingomonas* species F199, which has capability for aromatic hydrocarbon degradation. The majority of the genes responsible for this activity have been identified using genomic approaches and have been found to be localized on a 180 kilobase pair (kb) megaplasmid. The genomic arrangement of other subsurface *Sphingomonas* species has now been determined and the relationship among DNA sequences on the various plasmids elucidated. Each subsurface strain capable of aromatic degradation contains a megaplasmid with homology to the 180 kilobase megaplasmid from F199.

## Technical Accomplishments

Most enzymatic activities of use in bioremediation are plasmid-borne. In addition, biodegradative genes on plasmids are usually organized into polycistronic units; this organization facilitates identification of other genes in the pathway of interest. Therefore, these studies focus on plasmids within bacteria of interest. Through physical mapping and sequencing, progress can be made in fundamental areas such as plasmid genetics, gene organization, element mobilization, and plasmid transfer.

Pacific Northwest National Laboratory scientists have isolated a *Pseudomonas*-like bacterium from the deep (400 m) subsurface [*Appl Env Microbiol* 57:796, 1991]. This bacterium, F199, is uniquely able to biodegrade an array of aromatic hydrocarbons including toluene and naphthalene. Furthermore, F199 can function under microaerophilic conditions making it especially suitable for bioremediation.

We have determined that F199 contains three genetic elements of 2 Mb, 480 kilobase, and 180 kilobase. To characterize the 180 kilobase plasmid, termed pNL1, a cosmid library of the plasmid sequences was constructed to provide easy access to different regions of the large

plasmid and to facilitate generation of a physical map. Digestion of the cosmid clones with restriction endonucleases was used to determine which cosmid clones overlapped each other and to define the order of all the clones. This information also led to a restriction map of the entire plasmid. In addition, pulsed field electrophoresis was used to locate the cleavage sites for restriction enzymes that cut the plasmid infrequently. The cosmid clones were analyzed to determine which ones contained dioxygenase gene capable of meta cleavage of catechol. Several cosmids were identified and the regions of each that overlapped were used to localize these genes of interest. DNA sequence was derived from these regions and has led to the discovery of several genes involved in the degradative pathway.

The genome structure of five other subsurface *Sphingomonas* strains as well as two typed strains, *S. capsulata* and *S. paucimobilis* was determined. The results show that all of these *Sphingomonas* strains have large plasmids with the size distribution being unique for each strain. The subsurface strain B0478 has the most plasmids with four, and five of the eight strains have plasmids of 480 kilobase or larger.

The considerable variability in plasmid content raised the issue of whether the total genome size was consistent among the strains. To estimate the total genome size for each *Sphingomonas* strain we analyzed appropriate restriction enzyme digests of total genomic DNA. The resulting data showed that the genome sizes within this closely related group were surprisingly different, ranging from about 2600 to 4200 kilobase.

To determine whether certain DNA sequences were common among the plasmids in each strain, the plasmids of F199 were used as probes against the other strains. The 180 kilobase pNL1 plasmid revealed strong hybridization to the 150 kilobase plasmid of strain B0478, the 180 kilobase plasmid in B0522, the 180 kilobase and 750 kilobase plasmids B0695, the 110 kilobase and 270 kilobase plasmids in B0712. In addition, a weak signal was found associated with some, but not all, of the other plasmids in these same strains. There was no detectable hybridization to the plasmids in B0477, *S. capsulata* or *S. paucimobilis*. Interestingly, plasmids with homology to pNL1 were contained only in strains that catabolize aromatic compounds. This suggested that the primary hybridization may be to catabolic genes. To clarify this, we then used a probe that was generated by

PCR-amplification of the 2,3-catechol dioxygenase (*Xy/E*) gene on pNL1. The resulting pattern of hybridization was similar to that resulting from hybridization to the entire pNL1 plasmid, except that the 110 kilobase plasmid in B0712 did not hybridize nor was there any signal for those plasmids that showed only weak hybridization to pNL1.

A similar analysis was carried out using total DNA from the 480 kilobase F199 plasmid pNL2. In general, hybridization was observed for the larger plasmids in strains with aromatic catabolic activity; signal was detected for the 630 kilobase, 650 kilobase, and 750 kilobase plasmids from B0478, B0522, and B0695, respectively.

Weak hybridization was observed to the 450 kilobase plasmid from B0478, but none was found for the large 600 kilobase plasmid in the catabolic strain B0712.

#### **Publication**

L.C. Stillwell, R.P. Schneider, S.J. Thurston, M.F. Romine, J.K. Fredrickson, J.D. Saffer. 1995. "Physical Mapping and Characterization of a Catabolic Plasmid from the Deep Subsurface Bacterium *Sphingomonas* sp. F199." *J Bacteriol* 177:4537-4539.

# Microbial Informatics

Richard D. Douthart (Biology and Chemistry)  
Margaret F. Romine (Environmental Microbiology)

---

## Project Description

The technical objectives of this project were to provide access for staff at the Laboratory to sequence analysis tools through linkage to the Center for Visualization, Analysis, and Design in the Molecular Sciences (VADMS) at Washington State University; establish Pacific Northwest National Laboratory as the primary database curator and server to the larger community for small genomes; and create a flexible small genome graphical user interface (GUI) tool using the conceptual basis developed on the CAGE/GEM and GnomeView projects.

## Technical Accomplishments

Over the past year, the technical objectives and expected results for this project have been altered to reflect a rapid increase in interest and research in bioinformatics by the scientific community, largely due to the recent release of the first complete bacterial genome.

In order to support analysis of data generated from the internal sequencing of F199 plasmid pNL1 and assorted genes from other bacteria, an agreement was developed with the Washington State University, Center for Visualization, Analysis, and Design in the Molecular Sciences (VADMS) that provides individuals at the Laboratory unlimited access to a collection of sequence analysis tools that are maintained at this site.

A workshop was held in June 1995, to establish the state of technology in analyzing genomic size sequences. It was concluded from this meeting that recent extensive progress by other organizations in database development offers us effective collaborative appointments, minimizing the need to develop our internal database.

Dr. R. Overbeek demonstrated a web site that he was in the process of developing, called PUMA: An Integration of Biological Data to Support the Interpretation of Genomes. The site is intended as an environment to support the presentation of the *Methanococcus jannaschii* genome that will be released later this year. At the time, the site included links to a collection of metabolic pathways (EMP) created by Evgeni Selkov and sequence alignments generated by Randy Smith at the Baylor College of Medicine. More recently, links to the phylogeny have also been added.

A collaboration was established with Dr. Overbeek to help in organization of information relevant to microbial bioremediation. Dr. L. Wackett, at the University of Minnesota, has since joined in this collaboration, offering to help in linking his biocatalysis web site currently under construction. The biocatalysis site currently depicts five degradative pathways with links to sequence and toxicological information. The linkage between the two sites will allow direct access to alignment of sequences for enzymes in biodegradative pathways, which are important in designing probes for monitoring presence and/or expression of the corresponding genes. Additionally, the existing sites will be enhanced by adding more biodegradative pathways, updating the relevant alignments, and generating a graphical representation of biodegradative operons.

Linkage between these two sites will be key in organization of information for modeling flow of energy through core metabolic pathways that lead into specific biodegradative pathways. It will also give us a better understanding of what phylogenetic groups optimally carry out these reactions and how the existing pathways can be manipulated to degrade new compounds or generate new products.

# NMR Studies of DNA Structure Associated with Chemical Adduction

Michael A. Kennedy (Macromolecular Structure and Dynamics)

## Project Description

This project seeks to understand how sequence context affects local DNA structure and how this, in turn, influences the chemistry that takes place at the surface of the DNA molecule. Two specific questions were addressed. First, the unusual structure and dynamics found at TpA steps in DNA were investigated. Second, the minor groove structure was investigated in sequences that contain guanidine nucleotides either inserted into adenine tracts, or in tracts of guanines.

## Technical Accomplishments

In the area of TpA sites, we first probed the local structure surrounding a TpA site in two hexadecamer sequences,  $[d(CGAGGTTTAAACCTCG)_2]$  and its A9-methylated derivative. These sequences were selected for study because of their strikingly different patterns of migration during polyacrilamide gel electrophoresis, indicating a distinct difference between the structure of AAATTT and TTTAAA containing DNA fragments. The methylated derivative was studied to help understand the underlying structural features at TpA steps which give rise to the detected base dynamics. The structure of each sequence was determined using nuclear magnetic resonance (NMR) data collected at 750 MHz. In the unmethylated sequence, the structure local to the TpA step was found to be distinct compared to normal B-type DNA. Unusual structural parameters included an increased propeller twist, large rise, and large angle between the planes of adjacent intrastrand bases. Collectively, it appears that poor base stacking is a feature of TpA steps that either is responsible for, or a result of, the large amplitude slow motions detected at TpA steps in DNA.

In order to determine how widespread the unusual structure and base dynamics are in DNA, we investigated the sequence context effects on the TpA base dynamics. Immediate sequence context was first probed by preparing sequences which preserved either the thymine preceding the TpA step or the adenine following the TpA step. In all four possible sequences, the nuclear magnetic

resonance parameters which have been found to be sensitive to base dynamics, i.e., broadening of non-exchangeable adenine-H2 and adenine-H8 proton resonances and temperature dependence of these same resonances, was observed. For example, Figure 1 shows how the linewidth of adenine-H2 resonances varies with sequence in this series of DNA fragments. This provided an initial indication that the base dynamics may occur at all TpA steps in DNA. In order to confirm this observation, we investigated the 16 possible variations in immediate sequence context. Once again, in all sequence environments, we observed evidence for the unusual base dynamics, albeit the magnitude of the line-broadening varied with sequence as shown in Figure 2. Furthermore, the temperature of the linewidth maximum also varied with sequence and is moderately correlated with the magnitude of the excess linewidth as shown in Figure 3.

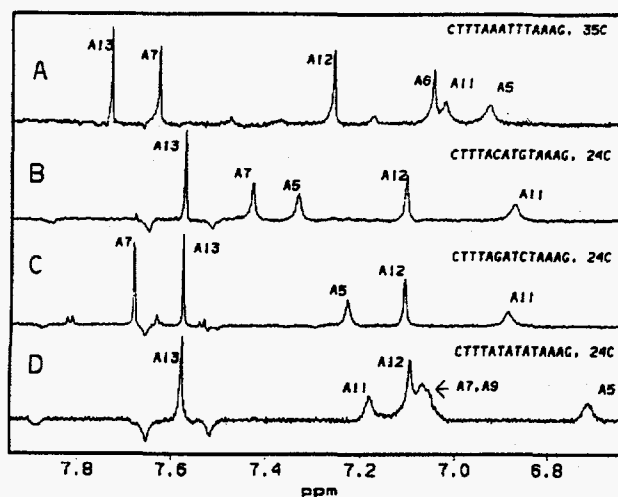


Figure 1. One-dimensional 750 MHz  $^1\text{H}$  NMR partially relaxed inversion spectra phased upright for the DNA sequences (A)  $[d(\text{CTTTAAATTTAAAG})_2]$  at 35°C, (B)  $[d(\text{CTTTACATGTAAAG})_2]$  at 24°C, (C)  $[d(\text{CTTTAGATCTAAAG})_2]$  at 24°C, and (D)  $[d(\text{CTTTATATATAAG})_2]$  at 24°C.

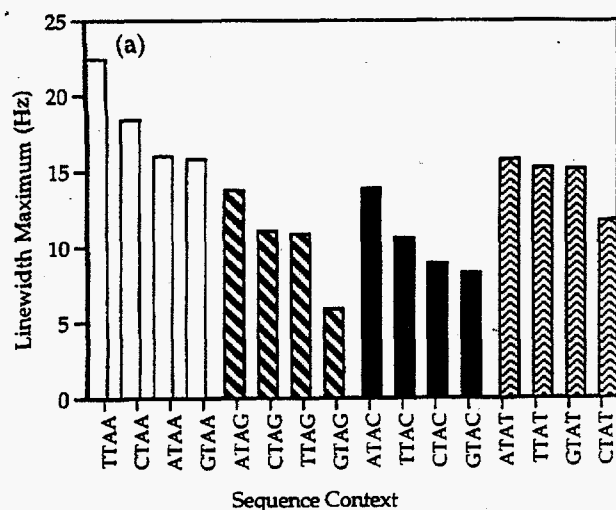


Figure 2. Maximum linewidth values of the adenine H2 resonance at the TpA step plotted as a function of sequence context. Columns 1-4 have an adenine following the TpA step; 5-8 have a guanine; 9-12 have a cytosine, and 13-16 have a thymine.

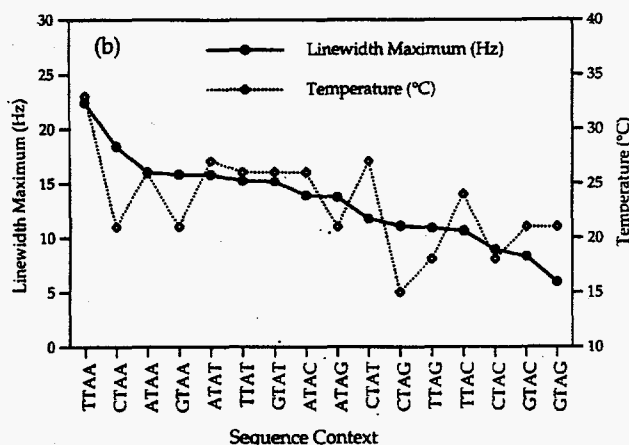


Figure 3. Maximum linewidth values of the adenine H2 resonance at the TpA steps (on the left axis) and the corresponding temperature at which these maxima occur (on the right axis) plotted as a function of sequence context.

These results indicate that the unusual structure and dynamics observed at TpA steps in DNA can be expected in all sequence contexts. Moreover, the magnitude and rate of dynamics and the local structure may also depend on the local sequence environment. These observations point to the TpA step in DNA as being a distinct structural building block. When considering the variety of molecular interactions and chemistry that is localized at TpA steps in DNA, it is now necessary to consider what role the structure and dynamics of the helix topology plays

in regulating intermolecular interactions at the surface of the DNA molecule. Some of the important molecular interactions localized at TpA steps in DNA include the binding of restriction enzymes to restriction sites containing TpA steps and the subsequent cleavage of the DNA backbone at the TpA step, the reduced base pair lifetime and three- to fivefold more rapid imino exchange at TpA steps in DNA, the lack of protection from hydroxy radical cleavage at TpA steps in comparison to ApT steps in DNA, the binding of transcription factors to TpA-rich sites such as the TATA binding protein, and specific binding of drugs to TpA sites in DNA.

## Publications

K. McAteer, P.D. Ellis, and M.A. Kennedy. "The Effects of Sequence Context on Base Dynamics at TpA Steps in DNA Studied By NMR." *Nucleic Acids Res.* (in press).

J.M. Lingbeck, M.G. Kubinec, J. Miller, B.R. Reid, G.P. Drobny, and M.A. Kennedy. "The Effect of Adenine Methylation on the Structure and Base Dynamics of TpA Steps in DNA: NMR Structure Determination of [d(CGAGGTTTAAACCTCG)<sub>2</sub>]: and its Methylated Derivative at 750 MHz." *Biochemistry* (in press).

K. McAteer, P.D. Ellis, and M.A. Kennedy. "NMR Evidence for Base Dynamics at All TpA Steps in DNA." *J. Am. Chem. Soc.* (submitted).

M.A. Kennedy, M.G. Kubinec, J.M. Lingbeck, K. McAteer, B.D. Thrall, and P.D. Ellis. "750 MHz NMR Studies of Chemically Modified DNA Structure/Dynamics: Sequence Context Effects and Protein Recognition." *Bulletin of Magnetic Resonance* (in press).

M.A. Kennedy, M.G. Kubinec, J.M. Lingbeck, K. McAteer, B.D. Thrall, and P.D. Ellis. "Sequence Context Effects on DNA Structure and Dynamics." *Proceedings of the 34th Hanford Symposium on Health and Environment* (in press).

## Presentations

M.A. Kennedy, M.G. Kubinec, J.M. Lingbeck, K. McAteer, B.D. Thrall, and P.D. Ellis. 1995. "750 MHz NMR Studies of Chemically Modified DNA Structure/Dynamics: Sequence Context Effects and Protein Recognition." The 12th Conference of the International Society of Magnetic Resonance, July 16-21, Sydney, Australia.



J.M. Lingbeck, M.G. Kubinec, K. McAteer, and M.A. Kennedy. 1995. "750 MHz NMR Studies of DNA Structure/Dynamics: Correlations with Observed Molecular Interactions." The 19th Annual Meeting of the Australian Society for Biophysics held in Conjunction with the British Biophysical Society, July 21-23, Sydney Australia.

J.M. Lingbeck, M.G. Kubinec, K. McAteer, and M.A. Kennedy. 1995. "Effect of Methylation on Base Dynamics at the TpA Step in [d(CGAGGTTTAAACCTCG)]<sub>2</sub>." The 36th Experimental Nuclear Magnetic Resonance Conference, March 26-30, Boston, Maine.

J.M. Lingbeck, M.G. Kubinec, K. McAteer, and M.A. Kennedy. 1995. "Effect of Methylation on Base Dynamics at the TpA Step in [d(CGAGGTTTAAACCTCG)]<sub>2</sub>." The 24th Keystone Symposia on Molecular and Cellular Biology, April 3-9, Keystone, Colorado.

M.A. Kennedy. 1995. "NMR Studies of DNA Structure Associated with DNA Modifications." DOE/PNL workshop on Nuclear Magnetic Resonance and the Environment April 27-28, Richland, Washington.

# *Structural Studies of Modified Histone Species*

David L. Springer (Biology and Chemistry)  
Charles G. Edmonds (Chemical Sciences)

---

## **Project Description**

In response to insult, cells are known to adjust their chromatin structure and alter their cell cycle to permit the repair of DNA damage. This research evaluated post-translationally modified histones during the cell cycle and identified perturbations of this profile of modifications due to insult from chemical agents, radiation, or their combination.

These experiments were mounted on populations of cell cycle synchronized cells, as well as fractions separated by flow cytometry. Histones were isolated and purified by high performance liquid chromatography (HPLC) and polyacrylamide gel electrophoresis and the extent and types of modifications determined by electrospray ionization mass spectrometry and tandem mass spectrometry. Final results of this work provide, for the first time, information on the multiple histone modifications as they simultaneously vary during the normal and perturbed cell cycle. These experiments explore the relationship between events in which DNA was damaged and the processes that are prerequisite for successful repair. This contributes to an improved understanding of regulatory processes governing cellular replication and the processes that constitute the cellular response to insult. These studies are closely allied to biochemical and molecular studies of DNA damage using nuclear magnetic resonance and other techniques.

It is our premise that a fundamental understanding of the relationship of histone modification to chromatin structure and its alteration throughout cell cycle and during cell damage and repair can only be obtained by consideration of the full range of type, extent, and site of modifications. We hypothesized that the normal time dependent profile of histone modifications through the cell cycle is non-random and predictable. Furthermore, this consistency will also pertain to modifications arising in response to chemical or radiation insult. During our effort, we evaluated the similarities and differences in profile that arise in the normal cycle in cultured K562 human lymphoblastoma and HeLa cells and also the changes that arise in the response to chemical insult using electrospray ionization mass spectrometry and tandem mass spectrometry. These experiments demonstrated the feasibility of our ultimate goal to elucidate the full details of these processes. We hypothesized that predictive changes in histone modifications occurs in response to DNA damage and that the profile of changes will vary with end damaging agents

and that these changes are distinguishable by distinct proteins of histone modification. It is likely that these chemical or radiation induced alterations in chromatin structure play a roll in cell cycle and repair processes.

## **Technical Accomplishments**

It has been known for some time that ionizing radiation causes a division delay in mammalian cells which is dominated by a period of G<sub>2</sub>-phase arrest. The magnitude of the delay depends upon the type of cell, the position of the cell in the replication cycle at the time of irradiation, the dose, and the linear energy transfer of the radiation. The length of G<sub>2</sub>-phase arrest increases linearly with dose. It has been postulated that radiation-induced division delay could be a mechanism that affords cells time to repair damage. In an effort to gain insight into the events that govern this delay mechanism, we have studied histone post-translational modifications in cells naturally traversing G<sub>2</sub> in comparison to those which are undergoing check point control in G<sub>2</sub> arrest.

To obtain populations of cells in unperturbed G<sub>2</sub> and those arrested in G<sub>2</sub>, HeLa S3 cell cultures were synchronized and cells were harvested at several time points. HeLa cell cultures were synchronized at the G<sub>1</sub>/S phase border by the double thymidine block method. Synchronized control and irradiated cultures were released at 0 hours and examined at times over the succeeding 15 hours. Cells were harvested and nuclei isolated. From these nuclei, histones were extracted and characterized by ESI-MS.

These studies are allied with work ongoing at Pacific Northwest National Laboratory by Dr. Noelle F. Metting and the cell populations from which the cdc2-cyclin B complexes are isolated are the same cell populations from which the histone proteins will be isolated. These studies allow us to correlate the post-translational modifications to histones throughout the cell cycle with the activity and phosphorylation states of proteins in the signal transduction pathway, and lead to new and interesting insights into the mechanisms that regulate the cell cycle.

Preliminary studies on histone H4, isolated from untreated cycling HeLa cells harvested at 2 and 8 hours after release, showed a marked difference in post-translational modifications of the two proteins. At each of these two time points, the majority of the cells should exist at the G<sub>1</sub>/S border and the G<sub>2</sub>/M border, respectively. These

histones were analyzed by directly infusing the proteins into a Finnigan TSQ 7000 mass spectrometer. The ESI-MS spectrum of the 15+ charge state of both H4 proteins is shown in Figure 1, containing, among others, a peak at  $m/z$  754.8.

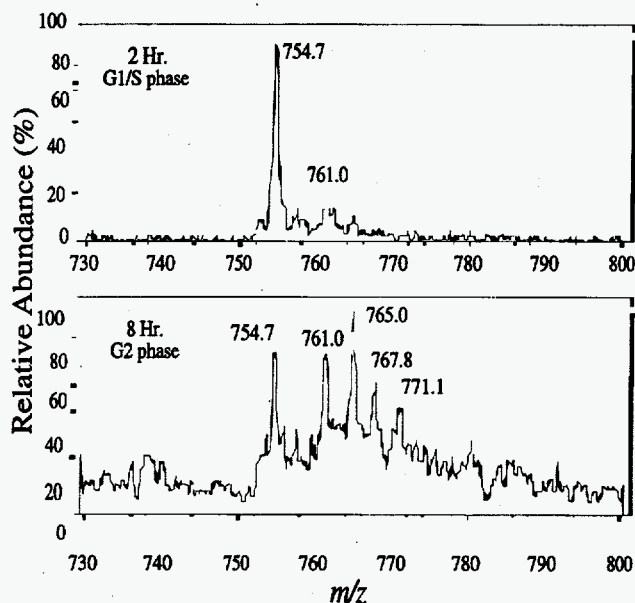


Figure 1. Region of the mass spectrum containing the  $(M+15H)^{15+}$  molecular ion of histone H4 isolated from free cycling HeLa cells harvested at the  $G_1/S$  and  $G_2/M$  borders.

This form of histone H4, predominant at 2 hours after release from the double thymidine block, has a mass of 11305 Da, and differs from the predicted mass for the principle species by 70 Da. This is putatively assigned to the addition of one acetyl and two methyl modifications ( $42.04 + 14.03 + 14.03 = 70.1$ ). However, at 8 hours after release, other forms of the histone appear. A peak at  $m/z$  761.3 corresponds to a protein with a mass increment of 98 Da. This increment can correspond to either a covalent addition of two acetyl groups and one methyl group, or the non-covalent association of a  $PO_4^{2-}$  or  $SO_4^{2-}$  group. The predominant form of the histone is represented by a peak at  $m/z$  765.0 and has a mass increment from the peak at  $m/z$  761.3 of 56 Da which corresponds to the addition of one acetyl group and one methyl group. A third peak at  $m/z$  767.8 corresponds to a protein whose mass is increased by 42 Da over the previous peak. This corresponds to the addition of an acetyl group. Although the biological function of methylation is unknown, it has been thought for some time that histones are not reversibly methylated. Annunziato and colleagues have recently found that histones H3 and H4 isolated from cycling HeLa cells were multiply methylated. The methylation of H3 was dependent on the

state of acetylation while the methylation of H4 was independent of the state of acetylation. These researchers also found that H4 methylation decreased dramatically at cells arrested in the  $G_1/S$  border, though states of methylation increased as cells progressed through the cell cycle. This observation is in agreement with our observations.

The treatment of the cycling HeLa cells with 1.75 Gy of  $\gamma$ -irradiation 2 hours after the release from the  $G_1/S$  border, should result in the arrest of the cells in the  $G_2/M$  border. Cells were harvested at the 0 hour and 8 hour time points, which corresponded to the cells existing predominantly on the  $G_1/S$  and  $G_2/M$  borders, respectively. Histone H4 was isolated from each of these cell populations and characterized by ESI-MS on a Finnigan TSQ 7000 mass spectrometer (Figure 2).

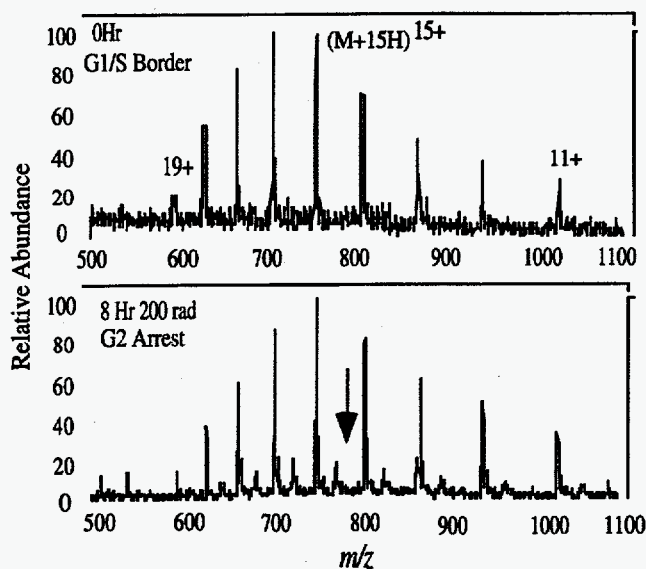


Figure 2. Electrospray ionization mass spectra histone H4 isolated from HeLa cells arrested at the  $G_1/S$  and the  $G_2/M$  borders. Additional proteins in the  $G_2/M$  cells correspond to multiply phosphorylated and acetylated H4.

The ESI mass spectrum of histone H4 isolated from the 0-hour time point (top panel) shows a number of peaks which correspond to a protein with a mass of 11305 Da, which, similar to the uncycling cell, corresponds to histone H4 with two methyl and one acetyl group attached. However, in cells arrested in  $G_2$ , the predominant form of the histone still has a mass of 11305 Da, although there is an additional species whose mass is increased by 304.5 Da. This increment corresponds to the addition of five acetyl, one methyl, and one phosphoryl group; or four acetyl, four methyl, and one phosphoryl group to the histone.

The results presented here indicate that the study of the variation in post-translational modifications to histone proteins through the cell cycle, in either freely cycling cells or those perturbed by damage into G<sub>2</sub> arrest, the mechanisms involved in cell cycle check point control.

Our unique collaborative interaction with Dr. Metting in which the cdc2 kinase experiments are performed on the same cell populations allows direct correlation of other cell cycle events with the modification of the histones.

# Vegetable Oil Chlorinated Solvents

Jim K. Fredrickson and Fred J. Brockman (Environmental Microbiology)

---

## Project Description

Vegetable oil has been suggested to promote the in situ bioremediation of groundwater and sediment contaminated with nitrate and/or chlorinated solvents. As microorganisms generally do not gain energy directly from the oxidation of these compounds, an electron donor must be supplied as an energy source to drive the desired metabolic reactions, namely denitrification or dechlorination. In addition to providing a source of carbon and energy for growth and metabolism, vegetable oil has the added benefits of having desirable chemical and physical properties. Vegetable oil is nontoxic and therefore safe for in situ and most highly chlorinated solvents such as tetrachloromethane, trichloroethylene (TCE), and perchloroethylene (PCE) are poorly soluble in water but quite soluble in vegetable oil. Therefore, the vegetable oil can act to concentrate solvents that are dissolved in groundwater and even reduce the toxicity to microorganisms of non-aqueous phase liquids. Also, the relative viscosity of vegetable oil aids in its retention in water saturated sediments. A companion project, Vegetable Oil-Pilot Scale Test: Transport Analysis, is focused on optimizing and modeling the emplacement and metabolism of vegetable oil in the subsurface. The use of vegetable oil for promoting denitrification in subsurface sediments was recently demonstrated by Jim Hunter and Ron Follett of the USDA-ARS in Ft. Collins, Colorado. Field demonstrations of this technology are being planned in a collaboration between Pacific Northwest National Laboratory, USDA, and Shannon-Wilson.

The goal of this task was to develop supporting scientific data through proof-of-principle batch experiments with anaerobic sediment, chlorinated solvents including tetrachloromethane, trichloroethylene and perchloroethylene vegetable oil, and supplemental nutrients including nitrogen, phosphorous, and electron acceptors.

## Technical Accomplishments

The potential for vegetable oil to promote microbiological degradation of chlorinated solvent was assessed in microcosm experiments with anaerobic sediments obtained from the Yakima River delta, vegetable oil, chlorinated solvent, and supplemental nutrients. An additional treatment included the dechlorinating bacterium *Desulfomonile tiedjei*. These replicated treatments along with a variety of controls were incubated and sacrificed at various time points to measure the concentration of the chlorinated solvents and chlorinated metabolites and residual vegetable oil.

The results from these experiments indicate that the ability of vegetable oil to enhance the anaerobic biodegradation of chlorinated organic compounds is both contaminant and electron acceptor specific. For example, the addition of vegetable oil to anaerobic sediments with nitrate added as the terminal electron acceptor significantly enhanced the biodegradation of carbon tetrachloride, did not impact the degradation of trichloroethylene, and inhibited the biodegradation of perchloroethylene. With sulfate as the terminal electron acceptor, similar results were observed except that the addition of vegetable oil had relatively little impact on the amount of carbon tetrachloride that was degraded. It is currently unclear why perchloroethylene degradation was inhibited in the presence of vegetable oil. One possibility is that the enzymes involved in the oxidation of vegetable oil are the same ones involved in perchloroethylene degradation. If this is true, then the presence of the oil would have resulted in a substrate level inhibition of perchloroethylene degradation. In summary, it appears that vegetable oil has considerable potential for enhancing the in situ biodegradation of carbon tetrachloride.

# Vegetable Oil-Pilot Scale Test: Transport Analysis

Glendon W. Gee, Gary P. Streile, and Ashokkumar Chilakapati (Water and Land Resources)

---

## Project Description

The objective of this project was to estimate transport parameters and provide a preliminary analysis for the in situ treatment of high nitrate waters in groundwater wells using vegetable oil. A scoping study will be initiated to determine the feasibility of injecting soybean oil into a groundwater well and subsequently recovering water from the well and assessing the efficiency of the process under the constraints of the known hydrology and biochemistry. Two codes will be used: 1) STOMP, a two-phase flow and transport code will be used to analyze the distribution of the oil in the groundwater zone and estimate the flow fields; and 2) RAFT, a biochemical and transport simulator will be used to estimate the efficiency of nitrate reduction and water concentrations in the recovered waters. Output from the STOMP code in the form of flow fields and oil distributions will be used in connection with expected pumping rates as input to the RAFT code to generate the final groundwater nitrate concentrations in the recovered well water. The expected outcome for the research is an increased understanding of the types of contaminants and environments where use of vegetable oil could stimulate subsurface bioremediation.

## Technical Accomplishments

We have reviewed the literature on the use of innocuous oil as a carbon source for microbial enhancement. We are currently collaborating with the Agricultural Research Service (ARS) staff at Ft. Collins, Colorado, who have conducted a series of tests using vegetable (soy bean) oil as a carbon source for denitrifying bacteria (Hunter and Follett 1995). Batch reactor and column tests run by the Agricultural Research Service (designed as small-scale proof-of-principle tests for the overall concept) provide us with preliminary information regarding rates of microbial growth, nitrate removal, and oil consumption. We have extensively reviewed and analyzed data from these tests (Hunter and Follett 1995, as well as other unpublished data) for the purpose of

- determining appropriate mathematical forms for microbe, oil, and nitrate rate laws
- estimating the values of characteristic parameters contained in those rate laws

- determining the need for and design of supplementary experiments (to be conducted by Agricultural Research Service) to improve quantification of the rate law parameters.

Based on our work with the Agricultural Research Service data, we have refined our strategy for designing the pilot-scale field test based on laboratory data and computer simulation. Two computer codes, RAFT (Chilakapati 1995) and STOMP (White and Oostrom 1995a,b; Nichols et al. 1995), are being used as part of this design strategy to evaluate the use of vegetable oil to enhance bioremediation of aquifer waters containing elevated levels of nitrates.

First we used the Agricultural Research Service batch and column data to determine appropriate conceptual and mathematical models for the overall denitrification process (i.e., the mathematical forms of rate laws for microbial growth, nitrate removal, and oil consumption that will be accommodated in the RAFT computer code for reactive solute transport). We then used the Agricultural Research Service data (preferable batch data) to estimate values for as many of the rate law parameters as possible. We also calculated theoretical values for as many of the rate law parameters as possible for comparison with the experimental values, and then used the parameter estimation algorithms in the RAFT code to test goodness-of-fit of the model to the Agricultural Research Service batch data, and adjusted the rate law parameters (within reasonable limits) if warranted.

One-dimensional RAFT simulations of the conditions of one or more Agricultural Research Service column experiments were done to see if we could validate our reaction rate models and parameter values by generally reproducing the breakthrough results of these experiments. Once we were comfortable with the appropriateness of the reaction model and parameter values, we did RAFT simulations of an idealized field scenario consisting of steady one-dimensional water flow (at a rate representative of the expected rate of flow to an extraction well) containing nitrate (at a concentration representative of the expected concentration in the field) through a system with an initially uniform distribution of immobile oil throughout a given length. These simulations produce a ballpark estimate of what oil saturations and oil zone thicknesses would be needed to

ensure that the nitrate concentration in the groundwater would be reduced below the 10 ppm regulatory limit by the time the water is extracted from the well, and that the process would be effective for a specified length of time.

Next, once we know estimates of what oil saturations and oil zone thicknesses we should shoot for, we conduct simulations with the STOMP computer code (for multiphase flow) to determine the oil injection protocols needed to establish such a zone around a well. These simulations are three-dimensional, in radial coordinates. Then, once we have determined how to establish an oil zone with the desired characteristics, we use the results from the STOMP simulations (i.e., the oil saturation distribution and the water flow velocity distribution) as inputs to additional RAFT simulations. These RAFT simulations indicate if the denitrification process will produce the desired concentration lowering in the extracted water for the desired length of time in the pilot-scale field experiment scenario. Iterations between STOMP and RAFT simulations may be necessary to determine with the ultimate design for the field test.

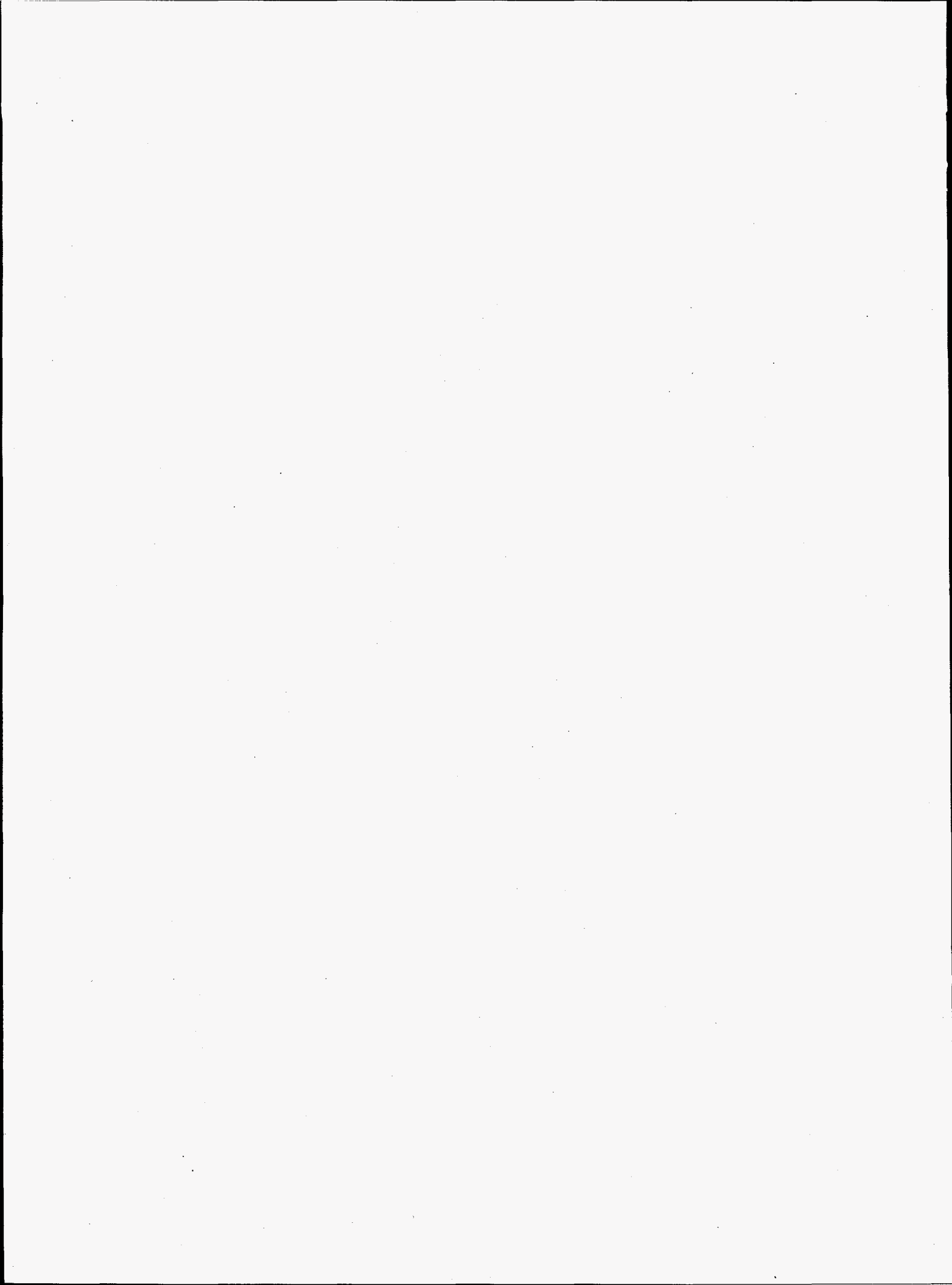
Because the work was initiated in September 1995, only preliminary results with the computer codes have been obtained to date. The batch and column data from Agricultural Research Service led us to choose a dual-Monod model for the three rate laws describing the time-rate of change of microbe, oil, and nitrate concentration. This set of expressions contains five characteristic parameters: the maximum rate of microbial growth, the yield coefficient (for microbial biomass produced per amount of oil), the stoichiometric coefficient (for the amount of nitrate utilized per amount of oil), and the half-saturation constants for oil and nitrate. Theoretical values for the yield coefficient and the stoichiometric coefficient were calculated. Batch and column data were used to calculate experimental estimates of the yield coefficient, stoichiometric coefficient, and maximum microbial growth rate. Because the batch data set available for use in the rate-law validation exercise corresponds to nitrate concentrations above the nitrate-limitation regime, the half-saturation constant for nitrate was fixed at zero, thus simplifying the goodness-of-fit calculations. Several RAFT simulations were run where different parameters were fixed at estimated values while allowing others (especially the half-saturation constant for oil) to be fitted

by the code. A set of parameters was ultimately determined by this procedure that balanced goodness-of-fit to the batch data with consistency with the theoretical and experimental estimates of these parameters.

Based on these estimates of rate law parameters, we are continuing the use of RAFT to simulate column-experiment scenarios and to scale-up the reactions to an aquifer-scale scenario that will provide us with the oil-zone characteristics needed for subsequent STOMP simulations. Based on work to date, we are satisfied that the available computer codes are adequate to assist in the engineering design of a pilot-scale test to remove elevated nitrates in situ.

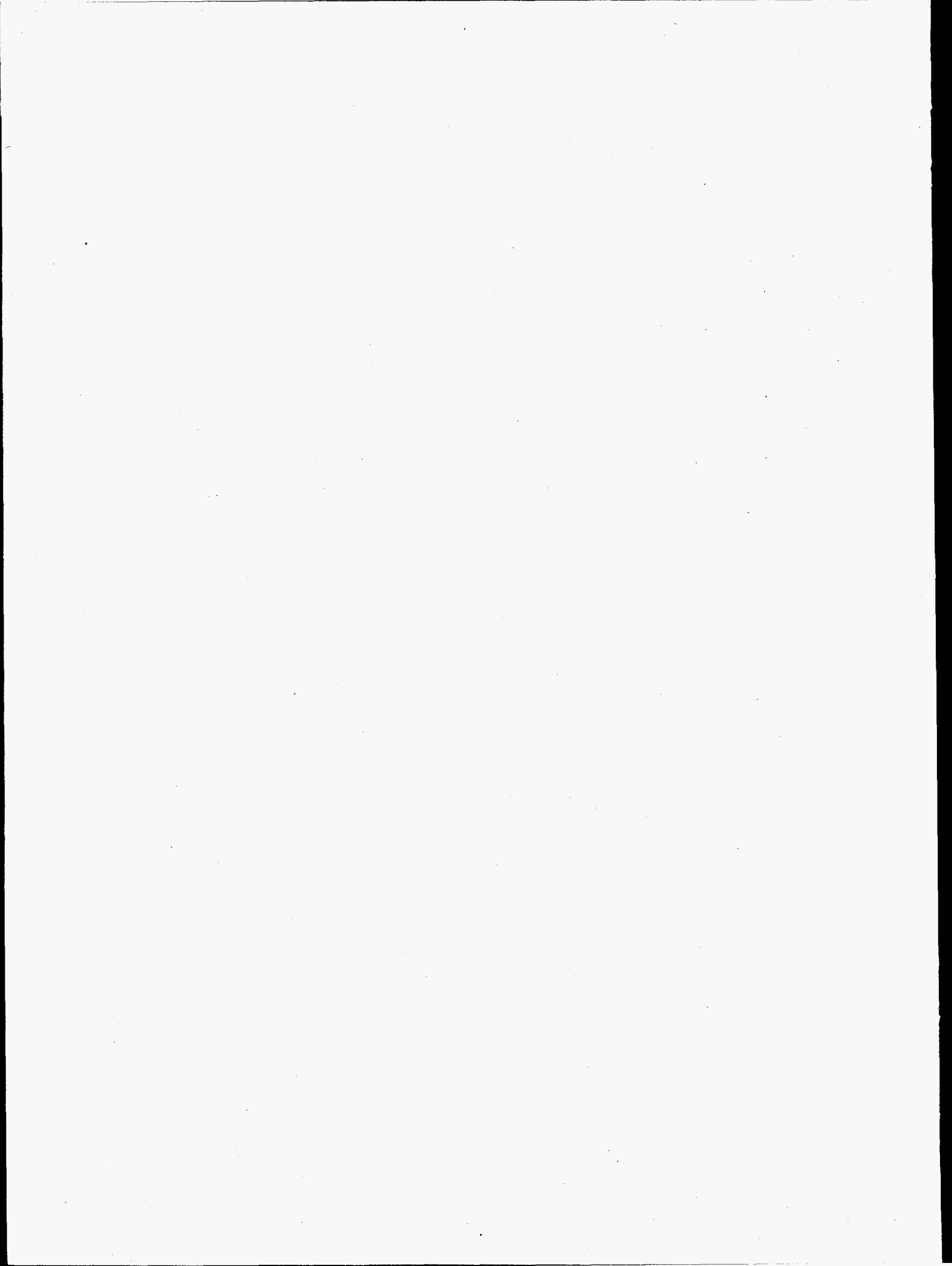
## References

- A. Chilakapati. 1995. *RAFT: A simulator for ReActive Flow and Transport of groundwater contaminants*. PNL-10636. Pacific Northwest National Laboratory, Richland, Washington.
- J.K. Fredrickson, F.J. Brockman, G.P. Streile, J.W. Cary, and J.F. McBride. "Enhancement of In Situ Microbial Remediation of Aquifers." U.S. Patent #5,265,674.
- W.J. Hunter and R.F. Follett. 1995. "Use of vegetable oil to bioremediate high nitrate well water." pp 79-82. In *Clean Water-Clean Environment-21st Century*, Vol. II. American Soc. Agr. Engrs. St. Joseph, Missouri.
- W.E. Nichols, N.J. Aimo, M. Oostrom, and M.D. White. 1995. *STOMP: Subsurface Transport Over Multiple Phases: Application Guide*. Pacific Northwest National Laboratory, Richland, Washington (in press).
- M.D. White and M. Oostrom. 1995a. *STOMP: Subsurface Transport Over Multiple Phases: Theory Guide*. Pacific Northwest National Laboratory, Richland, Washington (in press).
- W.D. White and M. Oostrom. 1995b. *STOMP: Subsurface Transport Over Multiple Phases: User's Guide*. Pacific Northwest National Laboratory, Richland, Washington (in press).





## **Chemical Instrumentation and Analysis**



# *Application of Mass Spectrometry to Life Science and Bioremediation Research*

Richard D. Smith (Macromolecular Structure and Dynamics)

---

## **Project Description**

Recent developments in the area of mass spectrometry provide the basis for significant and new contributions to biochemical and microbiological research. This new role is derived from advances in sensitivity, applicability to large molecules, the ability to address complex biological mixtures, and the extent of structural detail obtainable (sequence, location, and chemical nature of structural modifications and adductions, etc.).

## **Technical Accomplishments**

### *Characterization of Trace Level Biopolymers*

Identification and structural characterization of very low (ultra-trace) levels of a structurally modified or chemically adducted component in a large excess of unaltered material is an essential capability. An example is the environmental levels of DNA damage induced by exposure to environmental levels of chemicals or ionizing radiation. Recent improvements in sensitivity derived from improved ion manipulation techniques have recently enabled preliminary experiments at the single cell level. Studies utilizing mammalian erythrocytes demonstrate single cell sensitivity for select cell components and, using tandem mass spectrometric techniques, partial amino acid sequences have also been obtained from select proteins directly from small cell populations (i.e.,  $\geq 75$  cells). Capillary isotachopheresis with Fourier transform mass spectrometry was also employed to analyze low-level DNA damage products of oligomeric DNA. The use of isoelectric focusing is currently being investigated due to its attractive properties for cellular proteins. Finally, a dynamic range enhancement technique based on quadrupolar axialization and "colored noise" waveforms was developed which provides enhanced sensitivity toward low-level damage products in the presence of a large excess of undamaged material.

### *Development and Application of Bioaffinity Characterization Mass Spectrometry*

During FY 1995, we showed that electrospray ionization with Fourier transform ion cyclotron resonance (FTICR) can be used broadly for the study of noncovalent interactions and complexes of biopolymers. In particular, we showed the application to the study of protein-DNA

interactions and the study of enzyme-inhibitor complexes. Initial studies were conducted on both single and double stranded DNA in noncovalent complexes with proteins, using well characterized model systems to demonstrate that our electrospray ionization-Fourier transform ESI-FTICR methods can be used to examine intact protein-DNA complexes from solution, and that strong binding oligonucleotides can be readily distinguished from others displaying weak binding.

Our studies have now demonstrated that the complexes observed by ESI-mass spectrometry in properly conducted experiments reflect known solution behavior, and that highly specific protein-DNA associations (and noncovalent associations in general) can be detected intact. In particular, protein-DNA complexes can be examined in competitive binding experiments without adverse effects due to weaker nonspecific interactions. Figure 1 shows a series of FTICR mass spectra for complexes of the eukaryotic transcription factor, PU.1, with double-stranded oligonucleotides. PU.1 is known to bind with high selectivity to the recognition sequence GGA(A/T). The top panel shows that a solution of the PU.1 protein with an excess of a 17 base pair duplex having the recognition sequence results in an FTICR mass spectrum in which the protein-duplex DNA complex dominates (top). The complex is clearly quite stable in the FTICR ion trap, and there is no evidence of protein without DNA or evidence of random 2:1 or 1:2 complexes. Upon adding PU.1 protein to a mixture of double-stranded oligonucleotides in a competitive binding study, with one having the recognition sequence (wild type) and one not (mutant), showed binding with only the wild type (Figure 1, middle panel). Repeating the same experiment with a 20-fold excess of the mutant duplex again shows only complex formation with the wild type (bottom panel). Gel shift assays confirmed that the mass spectrometric method correctly reflected solution behavior. The advantage of the ESI-FTICR approach over the conventional gel shift assay is that large libraries of damaged species can be examined simultaneously and also identified.

The generation and searching of large combinatorial libraries has become popular for certain classes of compounds for the purposes of drug discovery. In the combinatorial approach, mixtures are synthesized and subsequently examined for their affinity to a targeted

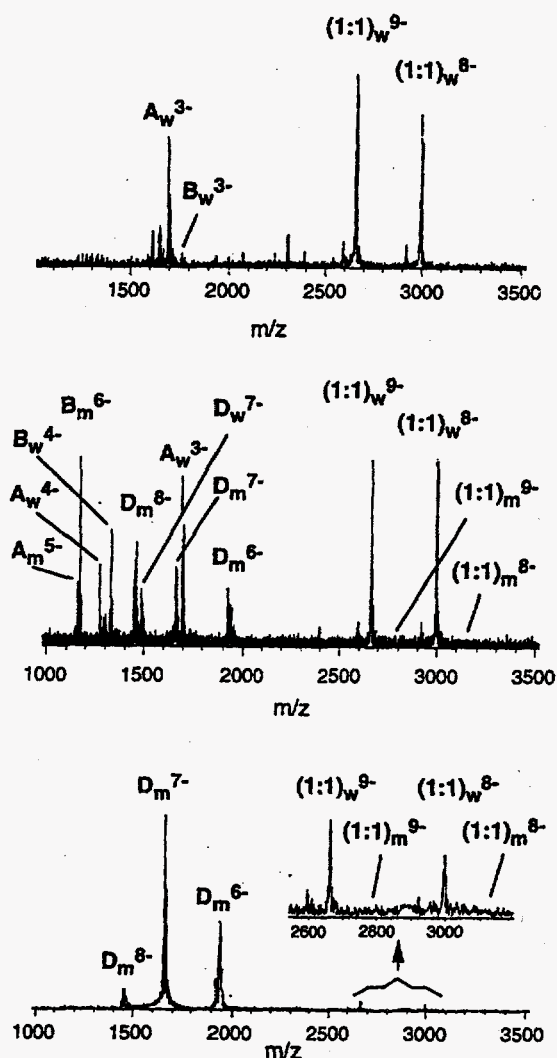


Figure 1. FTICR mass spectra of the PU.1 protein with a double stranded 17 bp oligonucleotide having the GGA(A/T) recognition sequence (top), and in competitive binding experiments with (middle) a 1.3-fold and (bottom) a 20-fold excess of a 19 bp oligonucleotide without the recognition sequence. The experiments show the expected 1:1 complexes, and excess DNA duplex is evident at low  $m/z$ . Gel mobility shift assays confirmed that these results correctly reflected solution behavior.

biopolymer, typically by partitioning subsets of the library in various fashions (often involving binding to solid supports) so as to facilitate the identification of the most active components. This concept has proven attractive since it allows much larger numbers of compounds to be screened, and has provided the basis for many new drug discovery companies. An essential aspect of screening large libraries of compounds is the ability to identify the active components on the basis of their strong binding to the selected target.

Initial studies demonstrating our approach for the identification of species from combinatorial libraries have been conducted in collaboration with Professor George Whitesides (Harvard University), who has developed

bovine carbonic anhydrase (BCA) inhibitor systems based on a benzenesulfonamide core structure with a variety of substituent groups attached. They have characterized the interactions and determined the binding constants of the inhibitors. We have studied several inhibitor mixtures and found the relative abundance ratios of the various complexes observed by ESI-FTICR were consistent with their relative affinities toward bovine carbonic anhydrase in solution. An important aspect of our approach involves the identification of the individual binding species by the dissociation of the complexes in the FTICR ion trap followed by their further characterization in the same experiment by high resolution and multi-stage methods. To demonstrate the use of larger combinatorial libraries, a mixture of para-substituted benzene sulfonamide inhibitors was synthesized (using solid phase chemistries) in which all combinations of 17 amino acid residues were incorporated into two positions ( $17 \times 17 = 289$  components). Low concentration solutions of the bovine carbonic anhydrase and the inhibitor library were electrosprayed and the 9-charge state for the bovine carbonic anhydrase-inhibitor complexes were isolated in the FTICR trap. Next, the complexes in the ion trap were dissociated, and the resulting spectra showed only the intact enzymes and the singly charged inhibitors. Based upon these results, we can then project relative binding of the inhibitors to bovine carbonic anhydrase based upon the relative intensities of the inhibitors obtained from the mass spectrometric experiment. Figure 2 shows a significant variation in binding affinity for the inhibitors indicated by this experiment. Synthesis and affinity measurements for a number of individual components have confirmed the ranking of binding affinities established by this approach.

#### Relative Binding Affinity to BCAll for 289-Component Inhibitors from Mass Spectrometry

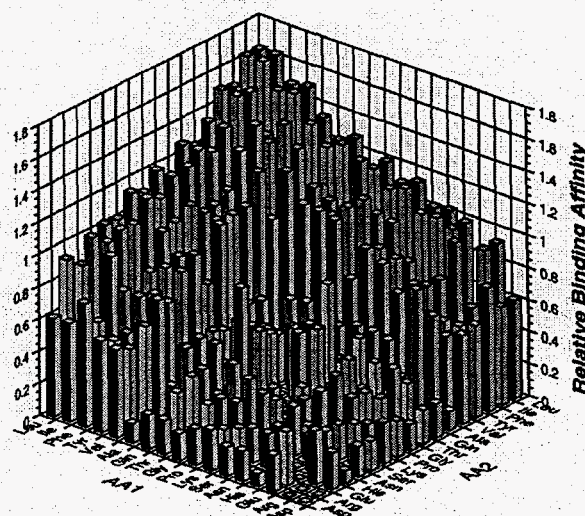


Figure 2. Preliminary results showing the relative binding affinities with BCA for the components of the 289-component combinatorial library of inhibitors obtained from a single BACMS experiment.

We have shown that individual species selected from a library can then be analyzed by collisional dissociation methods so that the selected component can be identified. In a broader context, the advanced capabilities we are currently developing have potential applications in the next phase of the Human Genome program, where the interactions and functions of the 100,000 or so proteins coded and potentially expressed, by the human genome are explored to understand the basis of specific disease states.

## Publications

- S.A. Hofstadler, F.D. Swanek, D.C. Gale, A.G. Ewing, and R.D. Smith. 1995. "Capillary Electrophoresis-Electrospray Ionization Fourier Transform Ion Cyclotron Resonance Mass Spectrometry for the Direct Analysis of Cellular Proteins." *Anal. Chem.*, 67, 1477-1480.
- B.L. Schwartz, J.E. Bruce, G.A. Anderson, S.A. Hofstadler, A.L. Rockwood, R.D. Smith, A. Chilokti, and P.S. Stayton. 1995. "Dissociation of Tetrameric Ions of Noncovalent Streptavidin Complexes Formed by Electrospray Ionization." *J. Amer. Soc. Mass Spectrom.*, 6, 459-465.
- R.D. Smith, J.E. Bruce, Q. Wu, X. Cheng, S.A. Hofstadler, G.A. Anderson, R. Chen, R. Bakhtiar, S.O. Van Orden, D.C. Gale, M.G. Sherman, A.L. Rockwood, and H.R. Udseth. 1996. "The Role of Fourier Transform Ion Cyclotron Resonance Mass Spectrometry in Biological Research-New Developments and Applications." *Mass Spectrometry in the Biological Sciences*, A. Burlingame, S. Carr, Eds., Elsevier, New York, 25-68.
- Q. Wu, S.O. Van Orden, X. Cheng, R. Bakhtiar, and R.D. Smith. 1995. "Characterization of Cytochrome c Variants with High-Resolution FTICR Mass Spectrometry: The Correlation of Fragmentation and Structure." *Anal. Chem.*, 67, 2498-2509.
- J.E. Bruce, S.L. Van Orden, G.A. Anderson, S.A. Hofstadler, M.G. Sherman, A.L. Rockwood, and R.D. Smith. 1995. "Selected Ion Accumulation of Noncovalent Complexes in a Fourier Transform Ion Cyclotron Resonance Mass Spectrometer." *J. Mass Spectrom.*, 30, 124-133.
- Z. Zhao, J.H. Wahl, H.R. Udseth, S.A. Hofstadler, A.F. Fuciarelli, and R.D. Smith. 1995. "On-line Capillary Electrophoresis-Electrospray Ionization Mass Spectrometry of Nucleotides." *Electrophoresis*, 16, 389-395.
- D.C. Gale and R.D. Smith. 1995. "Characterization of Noncovalent Complexes Formed between Minor Groove Binding Molecules and Duplex DNA by Electrospray Ionization-Mass Spectrometry." *J. Amer. Soc. Mass Spectrom.*, 6, 1154-1164.
- X. Cheng, Q. Gao, R.D. Smith, E.E. Simanek, M. Mammen, and G.M. Whitesides. 1995. "Detection of Hydrogen-Bonded Supramolecular Aggregates Using Electrospray Ionization from Chloroform." *Rapid Commun. Mass Spectrom.*, 9, 312-316.
- X. Cheng, R. Chen, J.E. Bruce, B.L. Schwartz, G.A. Anderson, S.A. Hofstadler, D.C. Gale, R.D. Smith, J. Gao, G.B. Sigal, M. Mammen, and G.M. Whitesides. 1995. "Using Electrospray Ionization Mass Spectrometry to Study Competitive Binding of Inhibitors to Carbonic Anhydrase." *J. Amer. Chem. Soc.*, 117, 8859-8860.
- Z. Zhao, H.R. Udseth, and R.D. Smith. "Characterization of Metastable Intermediates of Enzymatic Peroxidation of NAD<sup>+</sup> by On-line Capillary Electrophoresis-Electrospray Ionization Mass Spectrometry." *J. Mass Spectrom.* (in press).
- B.L. Schwartz, D.C. Gale, R.D. Smith, A. Chilkoti, and P.S. Stayton. 1995. "Investigation of Noncovalent Ligand Binding to the Intact Streptavidin Tetramer by Electrospray Ionization Mass Spectrometry." *J. Mass Spectrom.*, 30, 1095-1102.
- J.E. Bruce, G.A. Anderson, R. Chen, X. Cheng, D.C. Gale, S.A. Hofstadler, B.L. Schwartz, and R.D. Smith. 1995. "Bio-Affinity Characterization Mass Spectrometry." *Rapid Comm. Mass Spectrom.*, 9, 644-650.
- Q. Gao, X. Cheng, R.D. Smith, C.F. Yang, and I.H. Goldberg. 1996. "Binding Specificity of Post-Activated Neocarzinostatin Chromophore Drug-Bulged DNA Complex Studied Using Electrospray Ionization-Mass Spectrometry." *J. Mass Spectrom.*, 31, 31-36.
- R.D. Smith, X. Cheng, B.L. Schwartz, R. Chen, and S.A. Hofstadler. 1995. "Noncovalent Complexes of Nucleic Acids and Proteins Studied by Electrospray Ionization-Mass Spectrometry." *ACS Symposium Volume*, A.P. Snyder, Ed.
- X. Cheng, A.C. Harms, P.N. Goudreau, T.C. Terwilliger, and R.D. Smith. "Direct Measurement of Oligonucleotide Binding Stoichiometry of Gene V Protein by Mass Spectrometry." *Proc. Nat'l Acad. Sci.* (in press).

X. Cheng, S.A. Hofstadler, J.E. Bruce, A.C. Harms, R. Chen, R.D. Smith, P.N. Goudreau, and T.C. Terwilliger. 1995. "Electrospray Ionization with High Performance Fourier Transform Ion Cyclotron Resonance Mass Spectrometry for the Study of Noncovalent Biomolecular Complexes." *Techniques in Protein Chemistry VI*, R.H. Angeletti, Ed., Academic Press.

#### Presentations

X. Cheng, Q. Gao, R.D. Smith, E.E. Simanek, M. Mammen, and G.M. Whitesides. 1995. "Electrospray Ionization of Neutral Complexes from Non-Polar Solvents." 42nd American Society for Mass Spectrometry Conference on Mass Spectrometry and Allied Topics, May 21-26, Atlanta, Georgia.

X. Cheng, Q. Wu, Q. Gao, S.A. Hofstadler, and R.D. Smith. 1995. "Structural Aspects of Metal-Oligonucleotide Binding Studied by ESI-CID-MS." 42nd American Society for Mass Spectrometry Conference on Mass Spectrometry and Allied Topics, May 21-26, Atlanta, Georgia.

X. Cheng, A.C. Harms, R.D. Smith, P.E. Morin, P.N. Goudreau, and T.C. Terwilliger. 1995. "Characterization of Protein-DNA Complexes using ESI-MS." 42nd American Society for Mass Spectrometry Conference on Mass Spectrometry and Allied Topics, May 21-26, Atlanta, Georgia.

X. Cheng, R. Chen, J.E. Bruce, B.L. Schwartz, G.A. Anderson, S.A. Hofstadler, D.C. Gale, and R.D. Smith. 1995. "Characterization of Carbonic Anhydrase-Inhibitor Noncovalent Complexes." 42nd American Society for Mass Spectrometry Conference on Mass Spectrometry and Allied Topics, May 21-26, Atlanta, Georgia.

R.D. Smith, J.E. Bruce, R. Chen, X. Cheng, B.L. Schwartz, G.A. Anderson, S.A. Hofstadler, and D.C. Gale. 1995. "Searching Chemical Diversity for Molecular Recognition by ESI-MS." 42nd ASMS Conference on Mass Spectrometry and Allied Topics, May 21-26, Atlanta, Georgia.

R. Chen, J.E. Bruce, X. Cheng, S.A. Hofstadler, G.A. Anderson, A.L. Rockwood, H.R. Udseth, and R.D. Smith. 1995. "A New Dual Cell for Selective Ion Accumulation and Separation in FTICR/MS." 42nd ASMS Conference on Mass Spectrometry and Allied Topics, May 21-26, Atlanta, Georgia.

R. Chen, J.E. Bruce, X. Cheng, D.W. Mitchell, S.A. Hofstadler, G.A. Anderson, and R.D. Smith. 1995. "Studies of Large Individual Ions by FTICR Mass Spectrometry." 42nd ASMS Conference on Mass Spectrometry and Allied Topics, May 21-26, Atlanta, Georgia.

D.C. Gale, D.G. Camp, and R.D. Smith. 1995. "Selectivity and Binding Mode of DNA Interacting Molecules Studied by ESI-MS." 42nd ASMS Conference on Mass Spectrometry and Allied Topics, May 21-26, Atlanta, Georgia.

A.C. Harms, R.D. Smith, Y. Jenkins, and J.K. Barton. 1995. "Non-Covalent Associations of Metal Complexes with DNA Duplexes by ESI-MS." 42nd ASMS Conference on Mass Spectrometry and Allied Topics, May 21-26, Atlanta, Georgia.

S.A. Hofstadler, F.D. Swanek, D.C. Gale, Z. Zhao, J.E. Bruce, A. Ewing, and R.D. Smith. 1995. "Direct Analysis of Cellular Proteins by Capillary Electrophoresis FTICR-MS." 42nd ASMS Conference on Mass Spectrometry and Allied Topics, May 21-26, Atlanta, Georgia.

D.C. Gale, A.K. Morris, A.C. Harms, D.G. Camp, E.C. Sisk, A.F. Fuciarelli, H.R. Udseth, and R.D. Smith. 1995. "Correlation Between ESI-MS, CID Data, and DNA Duplex Melting Temperatures." 42nd ASMS Conference on Mass Spectrometry and Allied Topics, May 21-26, Atlanta, Georgia.

Z. Zhao, H.R. Udseth, and R.D. Smith. 1995. "On-Line Characterization of Peroxidation Intermediates of NAD<sup>+</sup> by CE-ESI-MS." 42nd ASMS Conference on Mass Spectrometry and Allied Topics, May 21-26, Atlanta, Georgia.

Q. Wu, S. Van Orden, X. Cheng, R. Bakhtiar, and R.D. Smith. 1995. "The Correlation of Fragmentation and Structure of a Protein." 42nd ASMS Conference on Mass Spectrometry and Allied Topics, May 21-26, Atlanta, Georgia.

G.A. Anderson, J.E. Bruce, S.A. Hofstadler, A.L. Rockwood, and R.D. Smith. 1995. "Low Noise FTICR Detection Electronics." 42nd ASMS Conference on Mass Spectrometry and Allied Topics, May 21-26, Atlanta, Georgia.



X. Cheng, A. Harms, R.D. Smith, P.E. Morin, P.N. Goudreau, and T.C. Terwilliger. 1995. "Characterization of Protein-DNA Complexes Using Mass Spectrometry." 11th Int. Symposium on Affinity Chromatography Biological Recognition, May 25-31, San Antonio, Texas.

X. Cheng, R. Chen, J.E. Bruce, B.L. Schwartz, G.A. Anderson, S.A. Hofstadler, D.C. Gale, R.D. Smith, J. Gao, G.B. Sigal, M. Mammen, and G.M. Whitesides. 1995. "Direct Bio-Affinity Characterization of Mixtures by Mass Spectrometry." 11th Int. Symposium on Affinity Chromatography Biological Recognition, May 25-31, San Antonio, Texas.

S.A. Hofstadler, X. Cheng, R. Chen, J.E. Bruce, and R.D. Smith. 1995. "Electrospray Ionization with High Performance Fourier Transform Ion Cyclotron Resonance Mass Spectrometry for the Study of Noncovalent Biomolecular Complexes." The Ninth Symposium of the Protein Society, July 8-12, Boston, Massachusetts.

S.A. Hofstadler. 1995. "Advanced Mass Spectrometric Methods for the Analysis of Complex Biomolecules." Brigham Young University invited seminar, March 31, Salt Lake City, Utah.

R.D. Smith, J.E. Bruce, X. Cheng, R. Chen, D.C. Gale, B.L. Schwartz, and G.A. Anderson. 1995. "High Performance Electrospray Ionization Mass Spectrometry in the Study of the Noncovalent Associations of Proteins and DNA." Spring ACS Meeting, April 2-6, Anaheim, California.

# *Development of Laser-Diode Based Sensors for Trace Isotope Assays*

Bret D. Cannon and James F. Kelly (Chemical Sciences)

---

## **Project Description**

This project demonstrated the feasibility of portable isotopic assay instruments based on laser-diode light sources combined with graphite-furnace atomic absorption that are capable of quantifying subnanogram amounts of particular isotopes of metallic elements. Individual isotopes can be optically resolved and measured using Doppler-free saturated absorption with laser-diodes developed for communications, consumer electronics, and other mass markets. Portable saturated absorption systems can be designed that require limited technical expertise to operate using laser-diodes. Such instruments will be particularly suitable for detecting proliferation effluents and could be used in the field to support onsite inspections for treaty verification. A much broader application for such isotopic assay instruments is use of isotope dilution to provide absolute quantification for graphite-furnace atomic absorption without the exacting work of preparing calibration standards that are exactly matched to the samples to be measured.

## **Technical Accomplishments**

Organizations monitoring proliferation or waste remediation would benefit from portable assay equipment that gives accurate elemental and isotopic abundance information in the field. Such instruments need to provide subnanogram sensitivity, good isotopic selectivity, simple sample preparation, and for many applications, reliable measurement of absolute concentrations. Conventional atomic absorption in a graphite furnace or other atomization sources has the needed sensitivity but lacks isotopic selectivity and requires extensive sample preparation and calibration to make accurate absolute concentration measurements. Replacing conventional atomic absorption with Doppler-free saturated absorption using laser-diodes provides isotopic selectivity, which in turn allows easy and accurate determination of absolute concentrations by isotope dilution.

We investigated Doppler-free saturated atomic absorption with radio-frequency modulated laser-diodes and heterodyne detection to ascertain if this approach can provide the isotopic selectivity and sensitivity for such instruments. Heterodyne detection of radio-frequency modulated laser light improves the minimum detectable absorption by factors of 100 to 10,000 over conventional

absorption techniques and shot noise limited absorption measurements have been achieved by many researchers using this technique. Laser-diodes are small, rugged, and reliable light sources that are suitable for atomic absorption measurements with many elements including U, Ba, Cs, Rb, Li, K, Pu, and many lanthanides. The recent commercial introduction of a laser-diode-based source emitting near 430 nm adds Ca, Tc, and Cr to this list of elements. Either frequency doubling other commercially available laser-diodes or additional progress in developing blue and blue-green laser-diodes would permit micro-assays of most other metals.

In FY 1994, setting up and characterizing the apparatus was accomplished. A vacuum system containing a commercial graphite furnace and windows to allow laser beams to pass through the center of the furnace was assembled and tested. Radio-frequency modulation of a single frequency laser-diode was characterized using both an external electrooptic modulator direct modulation of the current through the laser-diode. While both modulation techniques have significant limitations, direct modulation demonstrated the potential for minimum detectable absorbances of  $10^{-6}$ .

In FY 1995, based on the characterization done the previous year, we revised the laser-diode electronics and obtained laser line widths comparable to the lifetime broadening of strong atomic transitions (less than 10 MHz), which is more than five times narrower than in FY 1994 and greatly improves the selectivity. In addition, less than 1 mW of radio-frequency power is now required to use any modulation frequency between 10 MHz and 500 MHz rather than being restricted to a single narrow resonance at 140 MHz as in FY 1994. Optimal choice of modulation frequency increases the magnitude of the Doppler-free signal and suppresses the Doppler background signal thus improving sensitivity and selectivity. With these improved laser-diode electronics, we characterized Doppler-free saturated absorption of an atomic uranium transition at 860.795 nm with a radio-frequency modulated laser-diode. We established that operating pressures must be below 2 mbar of argon as collisions broaden and strongly suppress the Doppler-free signal. At 1.3 mbar (1 torr) of argon and with 5 mW of laser light entering the cell (light intensity of  $80 \text{ mW/cm}^2$ ), the Doppler-free line width is 10 to 20 MHz and its amplitude is about 10 percent of the amplitude of the Doppler-broadened absorption. Using radio-frequency



modulation and heterodyne detection for these conditions makes the Doppler-free signal amplitude comparable to that of the Doppler-broadened signal and improves the minimum measurable absorbance to between  $10^{-5}$  to  $10^{-6}$ ; an improvement by a factor of between  $10^2$  and  $10^3$  over conventional atomic absorption.

The laser-diodes used for this work are totally unsuited for routine analytical use because the lasing wavelength is not reproducible from day to day or morning to afternoon and only the high accuracy wavelength measuring instrument

in our laboratory made this work possible. We have found some laser-diode models from other manufacturers to be more reproducible in their lasing wavelength but finding laser-diodes that can be reproducibly tuned to a desired transition wavelength is the biggest problem is using laser-diodes for spectroscopy. Several different approaches to this problem exist but they all involve a combination of increased cost, decreased ruggedness, and increased size.

# *Evaluation of Cellular Response to Insult*

Charles G. Edmonds (Macromolecular Structure and Dynamics)

---

## **Project Description**

Methods for the evaluation of cellular response to physical and/or chemical insult were developed and applied to questions of adverse effects of environmental contamination. The co-regulation of gene expression resulting in the modulation of chromatin structure, perturbation of cell cycle, repair of DNA damage, and the control of programmed cell death were evaluated by state-of-the-art methods based on two-dimensional gel electrophoresis (2D-PAGE), in combination with advanced mass spectrometric techniques.

The molecular details of the outcome of environmentally induced cellular damage revealed sensitive and specific markers of these events. These details also provide important insight into the underlying scientific questions bearing on health effects of energy production which include individual variations in susceptibility and risk to workers and the population at large arising from the remediation and restoration of the Hanford Site.

## **Technical Accomplishments**

Our focus during FY 1995 was the foundation of the infrastructure for the 2D-PAGE experiment in our laboratory. In addition, we demonstrated the methodological capability for the recognition of previously sequenced proteins from two-dimensional gels using matrix assisted laser desorption ionization (MALDI) mass spectrometry. In initial experiments, protein was detected on micro-preparative two-dimensional gels by Coomassie Blue staining. Following excision of the protein spot from the gel, protein was digested *in situ* and peptides were subsequently eluted. MALDI mass spectrometry analysis was done via the thin film technique using alpha-cyano-sinapinic acid as ultraviolet absorbing matrix. Peptide masses observed were presented to the reformatted PIR sequence database using "PeptideSearch" software developed by Mann and coworkers at EMBL.

In additional experiments, four protein spots of "archival" origin (gel plugs stored for more than 5 years at -70°C) were examined. Three of these yielded MALDI spectra which were useful for subsequent correct identification in the database. In two cases, useful spectra were obtained from manipulation of a single gel plug. The ability to concentrate protein from multiple two-dimensional gels into a single spot/band has been demonstrated. Using this

technique, nine proteins tested and six yielded a single band on the concentration gel. The three unsuccessful experiments showed multiple bands of lower  $M_r$  of degradation of these "archival" samples. Subsequent MALDI spectra of digests have been obtained for two of the proteins. Early results revealed the presence of peptide masses 71 amu greater than expected; suggestive of acrylamine monomer adduction during the concentration gel electrophoresis. Suitable adjustment of electrophoretic conditions has eliminated this artifactual adduction.

Our tactic in the initial phase of this project has been to proceed to applied questions as soon as methodological tools are available. To this end, we have proceeded with the use of silver-staining to visualize on two-dimensional gels newly synthesized polypeptides having induced expression in response to x-ray exposure of U1-Mel cells (the positive control for subsequent radon exposure studies). The choice of silver staining simplifies our initial effort since this detects polypeptide "steady-state" levels and is a simpler and more practical alternative to metabolic labeling with  $^{35}\text{S}$ -methionine to detect induced *de novo* synthesis. Prior studies with human lymphoid cells (J.R. Strahler, personal communication) have shown that >90 percent of the polypeptides detected with  $^{35}\text{S}$ -methionine labeling corresponded to silver-stained spots detected on the same two-dimensional gel. We have proceeded in the confidence that we could detect the x-ray inducible proteins (XIPs) described by Boothman by silver-staining and have observed three high  $M_r$  (> 150 kDa) polypeptides whose expression is increased in response to x-irradiation. The expression changes were observable on silver-stained gels of total cell lysates 4 to 6 hours after irradiation. From the position on the two-dimensional gels (pI and apparent  $M_r$ ), these polypeptides may correspond to some of the x-ray inducible proteins observed by Boothman using  $^{35}\text{S}$ -methionine labeling. Additionally, several lower mass polypeptides were observed with altered expression levels. In particular, some instances of down regulation were observed. It is reasonable that early signal transduction events such as phosphorylation of existing proteins may occur in response to ionizing radiation. Several of the changes observed in our x-ray exposure experiments involve Panel A proteins having a pI more or less acidic than a nearby protein of similar  $M_r$  and spot morphology (color, shape, resolution). This suggests that the new spot represents a phosphorylation or dephosphorylation of the nearby protein. We will extend our studies of x-ray inducible

changes to include incorporation of  $^{32}\text{P}$  into protein to confirm whether "charge shift" spots are in fact phosphoproteins in altered levels of modification. Our first radon exposure experiment has been performed. Analysis of radon treated (50 cGy) and control U1-Mel cells revealed three proteins as candidates for having increased expression with irradiations. Relocation of the radon treatment to the 331 Building will allow the repetition of these crucial preliminary experiments using U1-Mel cells.

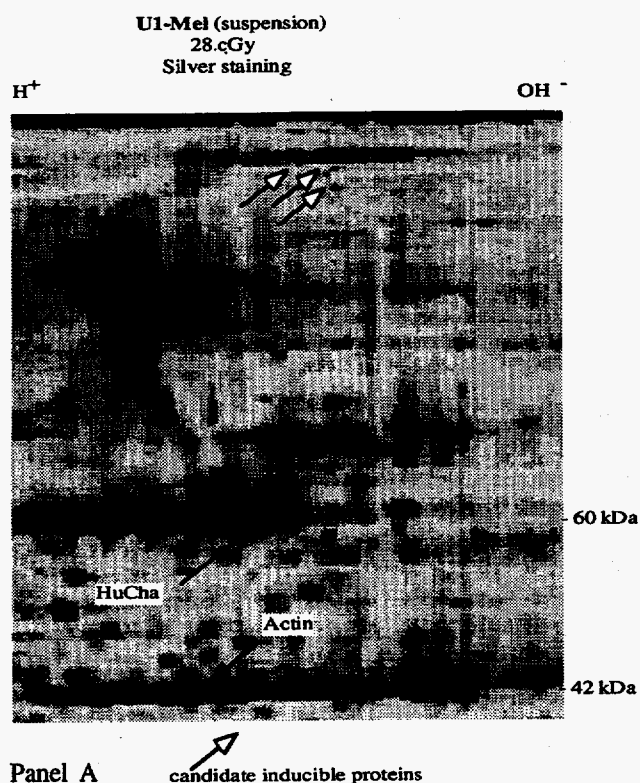
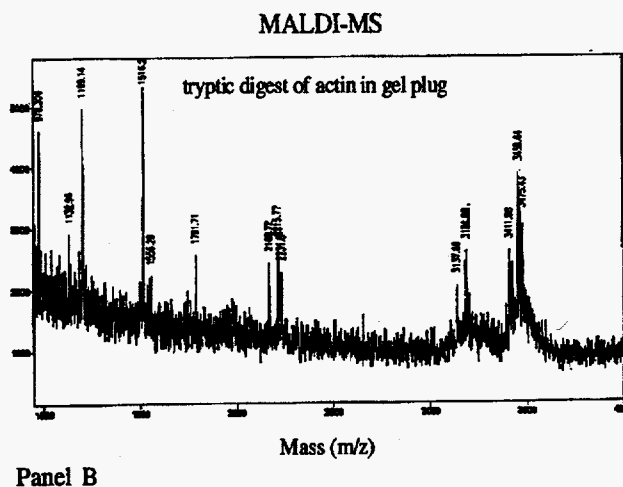


**Figure 1.** Altered protein expression in human melanoma cells following exposure to radon (28 cGy). Panel A shows the 2D-PAGE separation of melanoma cellular proteins with known proteins actin and human chaparonen (HuCha) indicated and candidate radon inducible proteins marked by open arrows.

In preparation for looking for protein expression changes between Bl6 and A/J mice in response to urethane treatment, we have observed three instances of genetic variation between these two strains in both untreated lung and liver. The differences are seen as isoelectric variants on two-dimensional gels, indicating homozygosity for one of two alleles at the three loci. Additionally, at least six other proteins are expressed at different levels in the two strains, most notable at reduced levels in Bl6 compared to A/J. With the limited results thus far, it is uncertain whether these differences in level of expression are under genetic control or represent individual physiological variation.



Panel B shows the MALDI mass spectrum actin prepared in the gel plug by trypsin digestion.

# Improved Analytical Ion Trapping Methods

Steven A. Hofstadler, Michael G. Sherman, and Richard D. Smith (Chemical Sciences)

---

## Project Description

This research was directed at methods aimed at increasing the utility and range of applications of ion trapping methods for analytical mass spectrometry for use in a broad range of applications at Pacific Northwest National Laboratory and Hanford. The research has emphasized use of computational and experimental studies to define improved trapped ion cell geometries for mass spectrometry, methods for more efficient trapping of externally generated ions, and the use of new electromagnetic field combinations to enhance performance. A new approach for large molecule, small particle, and possibly single cell characterization has been developed and is being explored for possible application to virus identification, the study of nanoparticle reactions, and potentially as a broadly useful method for "real-time" detection or characterization of larger submicron and micron size particles. On a broader level, this effort will provide an initial step toward a program aimed at implementing advanced mass spectrometric methods in support of DOE environmental, waste, remediation, and health effects research.

## Technical Accomplishments

The need for improved analytical and characterization capabilities at Hanford is enormous, including in situ tank characterization, groundwater monitoring, atmospheric sampling, in situ remediation support, bioremediation studies, broad laboratory-based analysis capabilities, the monitoring of waste processing, transport and disposal, as well as health effects research. It has been demonstrated that improved analysis/characterization methods, and their increased utilization, can substantially decrease the cost of cleanup activities. However, current support in development of advanced methods is fragmented, and is primarily driven by near-term demands.

In one phase of this effort we determined appropriate conditions, based upon computer modeling studies, for effective trapping and measurement of individual particles. This provided the basis for a greatly improved analytical methodology for characterization of a broad range of "particles," spanning the spectrum from those of biological interest (i.e., individual cells, chromosomes, viruses, etc.) to those relevant to the development of new materials. As a demonstration of this approach we

initially observed, over the course of numerous remeasurements, shifts to higher  $m/z$  for individual (i.e., single) poly[ethylene glycol] (PEG) ions reacting with added neutrals (crown ethers) or residual background gas constituents. We also observed multiple reaction steps for single ion charge transfer during the transient decay from a single time-domain FTICR transient. This stimulated the development of a novel approach for examining such data that we refer to as "time resolved ion correlation" (TRIC). The TRIC technique was developed to more effectively examine the time dependence individual ion signals and to establish a time-resolved link between reactant and product ion. The TRIC technique relies on the production of individual time-domain signals to follow reaction processes for each ion observed.

Comparison of several individual ion time-domain signals extracted from a single transient generally allows a correlation between the appearance and disappearance of individual ions to be constructed. This is possible even when numerous ions are simultaneously present due to differences in  $m/z$  (since large ion transitions are generally restricted to a relatively small  $m/z$  region of the spectrum) and the temporal signature provided by the TRIC analysis. By transforming discrete portions of the transient, it is apparent that each species is observed at different times during the transient and, most importantly, the disappearance of one species coincides exactly with the appearance of another species. The step-wise shifts allow the charge to be determined. Thus, we can observe the step-wise reaction of the ion, and in separate experiments have been able to observe the reactions of individual trapped ions for periods in excess of several hours. Single ions of bovine albumin having as few as 30 charges have been detected with signal-to-noise levels of  $\approx 2$ . Such measurements could also be substantially speeded by the ability to measure a number of individual ions simultaneously by observing the time resolved reaction steps in the course of a single transient.

In an alternative, yet complementary scheme, we have employed a direct charge measurement method suitable for very large ( $> > 1$  MDa) ions. Preliminary direct charge measurements obtained from individual ions from a (nominal)  $1.1 \times 10^8$  Da Coliphage T4 DNA sample derived from *Escherichia coli* B host strain ATCC, are in the molecular weight range expected, indicating that the ions are substantially intact. The masses determined for the largest peaks were all determined to be in the range of

~100 MDa. These preliminary results show that even extremely large ions can be effectively transferred to the gas phase and be studied by the ESI-FTICR process.

The analysis of very large ions by FTICR affords unique opportunities to study fundamental interactions of charged particles in the trapped ion cell, as well as ion molecule and ion-ion interactions. For example, under pressure-limited conditions, the transient from a highly charged individual ion will be longer than from an ensemble of smaller ions since loss of phase coherence is not possible for an individual ion. Signal from Coliphage T4 DNA individual ions at a pressure of  $\leq 1.0 \times 10^{-9}$  torr has been detected >90 minutes after initial excitation. These results also suggest that the dephasing effect (loss of coherency) is of greater importance than damping of cyclotron motion in signal decay of an ion cloud for larger molecules. Because larger ions produce such long-lived time domain signals, their reactions with other species (background neutrals, reactive gases, etc.) can be closely monitored during a single transient by using the TRIC techniques. While the physical size of these ions is uncertain, the extensive charging (and relatively low  $m/z$ ) suggests that they undergo Coulombic extension during the electrospray process, and may have lengths on the order of 100  $\mu\text{m}$ ! The large number of charges carried by each of these ions also creates a unique situation for the study of ion-ion interactions and Coulombic effects.

Other potential applications of individual ion analysis methods include the characterization of synthetic polymers, large structural proteins, and DNA restriction fragments, for which mass determinations should be at least  $10^2$  more precise than by electrophoresis. DNA sequencing may be possible if a method can be developed to induce the stepwise degradation of a trapped oligonucleotide ion. It should also be possible to investigate selective noncovalent associations of small molecules with large molecules in solution by trapping such complexes and inducing their dissociation in the FTICR cell. The upper MASS range is uncertain, but the initial electrospray droplet charging ( $\sim 10^5$ ) and the  $m/z$  range available by FTICR ( $> 200,000$ ) suggest molecules in excess of  $10^9$  Da may be amenable to study.

## Publications

R. Chen, X. Cheng, D.W. Mitchell, S.A. Hofstadler, A.L. Rockwood, Q. Wu, M.G. Sherman, and R.D. Smith. 1995. "Trapping, Detection, and Mass Determination of Coliphage T4 DNA Ions of  $10^8$  Da by Electrospray Ionization Fourier Transform Ion Cyclotron Resonance Mass Spectrometry." *Anal. Chem.*, 67, 1159-1163.

S.A. Hofstadler, Q. Wu, J.E. Bruce and R.D. Smith. 1995. "Enhanced Accumulated Trapping Efficiency Using an Auxiliary Trapping Electrode in an External Source Fourier Transform Ion Cyclotron Resonance Mass Spectrometer." *Int. J. Mass Spectrom. Ion Proc.*, 142, 143-150.

D.W. Mitchell, A.L. Rockwood, R. Chen and R.D. Smith. "Trapping Field-Induced Frequency Shifts for Orthorhombic and Cylindrical FT-ICR Ion Traps." *J. Chem. Phys.* (in press).

D.W. Mitchell, A.L. Rockwood, and R.D. Smith. 1995. "Frequency Shifts and Modulation Effects Due to Solenoidal Magnetic Field Inhomogeneities in Ion Cyclotron Mass Spectrometry." *Int. J. Mass Spec. and Ion Proc.*, 141, 101-116.

D.S. Wunschel, K.F. Fox, A. Fox, J.E. Bruce, D.C. Muddiman, and R.D. Smith. 1996. "Analysis of Double Stranded Polymerase Chain Reaction Products from the *Bacillus cereus* Group by Electrospray Ionization Fourier Transform Ion Cyclotron Resonance Mass Spectrometry." *Rapid Commun. Mass Spectrom.*, 10, 29-35.

B.L. Schwartz, A.L. Rockwood, R.D. Smith, D.A. Tomalia, and R. Spindle. 1995. "Detection of High Molecular Weight Starburst Dendrimers by Electrospray Ionization Mass Spectrometry." *Rapid. Commun. Mass Spectrom.*, 9, 1552-1555.

J.E. Bruce, G.A. Anderson, and R.D. Smith. "Colored Noise Waveforms and Quadrupole Excitation for Dynamic Range Expansion in Fourier Transform Ion Cyclotron Resonance Mass Spectrometry." *Anal. Chem.* (in press).

D.W. Mitchell and R.D. Smith. 1995. "The Cyclotron Motion of Two Coulombically Interacting Ion Clouds with Implications to Fourier Transform Ion Cyclotron Resonance Mass Spectrometry." *Phys. Rev. E*, 52, 4366-4386.

X. Cheng, D.G. Camp II, Q. Wu, R. Bakhtiar, D.L. Springer, B.J. Morris, J.E. Bruce, G.A. Anderson, C.G. Edmonds, and R.D. Smith. "Accurate Molecular Weight Determination of Plasmid DNA Using Mass Spectrometry." (submitted).

D.W. Mitchell and R.D. Smith. "Prediction of a Space Charge Induced Upper Molecular Weight Limit Towards Achieving Unit Mass Resolution in FT-Ion Cyclotron Resonance Mass Spectrometry." *J. Mass Spectrom.* (in press).

# Size Measurement, Sorting and Chemical Analysis of Nanometer Sized Particles Using an Ion Trap

Michael L. Alexander (Automation and Measurement Sciences)

## Project Description

The objective of this project was to develop a device for measurement of the size and number of particles in a (dry) sample with diameters of 10 to 1000 nm. The apparatus under development traps particles according to their mass-to-charge ratio ( $m/z$ ) and uses laser light scattering to independently measure the size of the trapped particles. Ions with a specific  $m/z$  can then be ejected, counted, and transported to other instrumentation for chemical analysis. The device will provide complete on-line characterization of nanometer sized particles currently unavailable.

## Technical Accomplishments

The first task in this project was to evaluate several possible ion trap designs for adaptation to particle trapping, counting, and size measurement. These included the bi-hyperboloidal (Paul type) ion trap, flat plates, and parallel ring electrodes. Computer simulations were used to determine the stable regimes for the various trap designs when used to hold charged particles. Parameters for stable trapping and selective excitation of particles with a given  $m/z$  were determined from these simulations. These parameters include radio-frequency trapping frequency, amplitude, and resonant excitation frequency, amplitude and duration. Although the Paul trap exhibits a somewhat larger stability region in this parameter space, the dual ring design was chosen because of the easy access for laser light scattering measurements to determine the size and number of particles in the trap. The parameters for the particles of interest were found to be: trapping frequency = 50 to 1000 Hz at 50 to 500 volts and excitation frequency = 5 to 100 Hz at 20 to 250 volts.

The second task was the design and construction of the device using the ring electrodes. A schematic diagram is shown in Figure 1. The rings had to be custom machined and mounted to high tolerance. Particles are introduced to the trap through a hypodermic needle floated at a high

potential. This ensures that the particles have the uniform charge necessary for trapping according to size. The particles are held in an AC field generated by the trapping power supply. Only those particles with the correct  $m/z$  are modulated at the excitation frequency. This frequency is used as the reference signal into a lock-in amplifier that is also monitoring the scattered laser light. The resulting signal has greatly reduced signal-to-noise. Initial measurements using uniform 0.5 micron latex spheres showed at least a two orders of magnitude improvement using the lock-in detection over conventional light scattering techniques. Work in the next year will include extension of this technique to smaller particles ( $< 20$  nm). Signal-to-noise improvements using a higher power laser at a shorter wavelength will make this detection size limit possible based on the results from this first year. Additionally, experiments will be carried out using the ion trap to sort particles according to their size for chemical analysis.

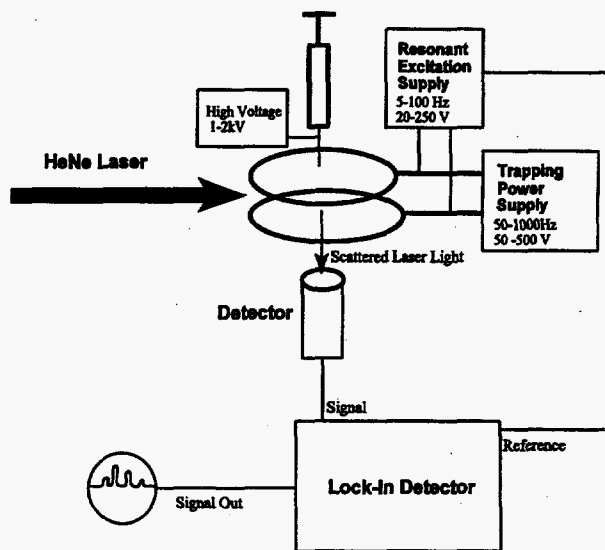
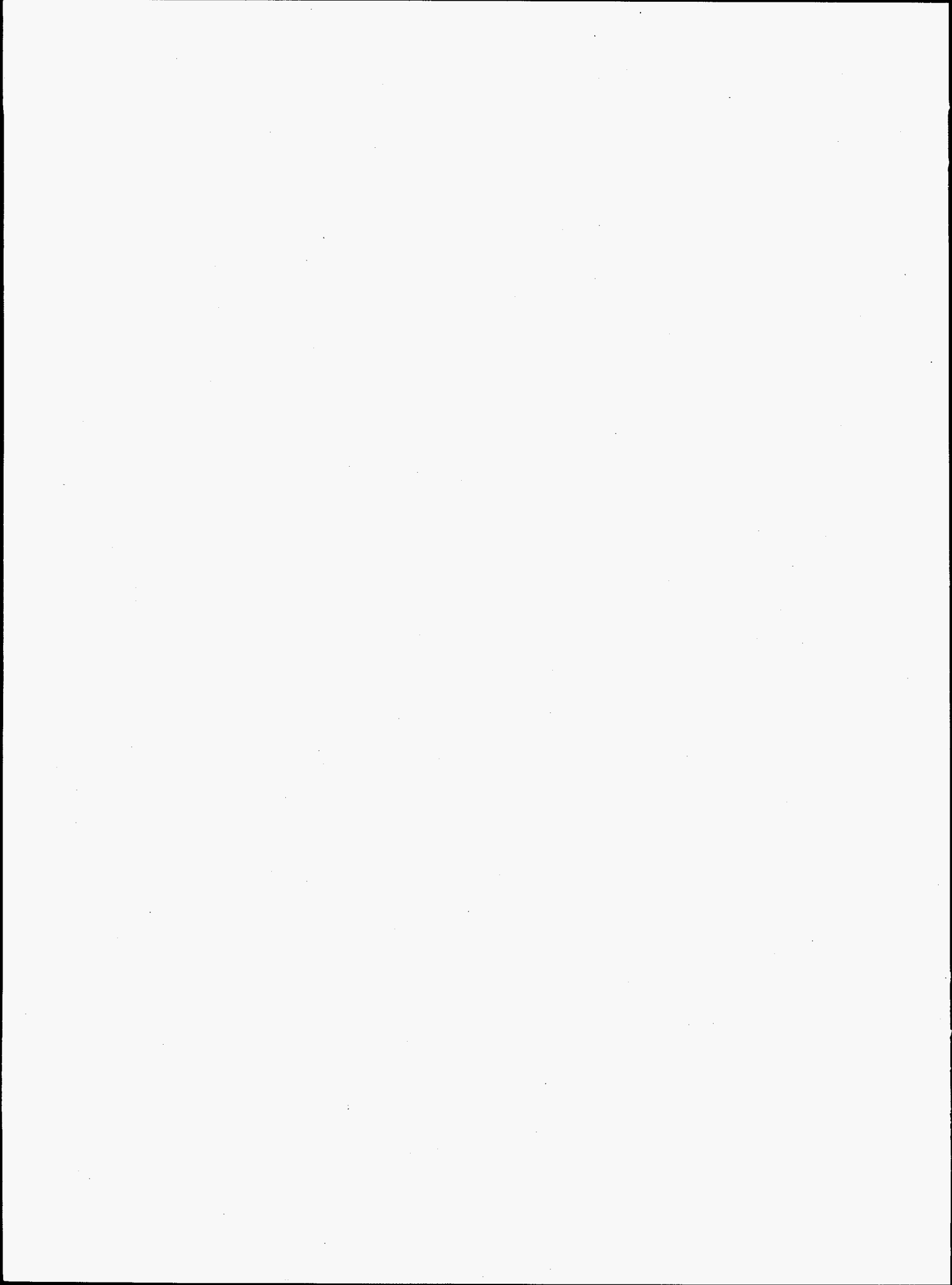


Figure 1. Schematic Diagram of Particle Sizing Apparatus

## **Computer and Information Science**





# *Adaptive Life Simulator*

Lars J. Kangas (Information Technologies)

---

## **Project Description**

The objective of this project was to explore a novel approach to modeling and diagnosing the cardiovascular system. The models used exhibited subsets of the dynamics of the cardiovascular behavior of an individual or a group of individuals and were incorporated into a compared cardiovascular diagnostic system. The diagnostic system compared modeled physiological variables with the current variables of an individual and diagnosed medical conditions from any deviations that existed between the two sets of variables.

This approach is unique in that each cardiovascular model is developed from physiological measurements of an individual. Any differences between the modeled variables and the variables of an individual at a given time are used for diagnosis. This approach also exploits sensor fusion to optimize the use of biomedical sensors. The advantage of sensor fusion has been demonstrated in applications including control and diagnostics of mechanical and chemical processes.

## **Technical Accomplishments**

A novel approach to modeling and diagnosing the cardiovascular system was developed. The models exhibit subsets of the dynamics of the cardiovascular behavior of an individual or a group of individuals. These models are incorporated into cardiovascular diagnostic systems. A diagnostic system compares modeled physiological variables with the current variables of an individual and diagnoses medical conditions from any deviations that exist between the two sets of variables.

One approach to cardiovascular modeling is to build a model representative of a group of individuals with similar characteristics (i.e., sex, age, physical condition, medical condition, etc.). However, cardiovascular behavior is unique to each individual, thus a generic cardiovascular model used in a medical diagnostic system would not be as sensitive as a system based on a model that is adapted to the patient being diagnosed.

The described approach incorporates models based on groups of individuals, such as women and men in different age groups, and models specific to each individual. The latter models are possible if the individuals have previously been evaluated in a clinical test, such as graded

exercise test or cardiovascular stress test, from which a model can be developed. These models, besides age and sex, are also using parameters describing the heights and weights of the individuals to further simulate them to the individuals.

The artificial neural network (ANN) technology was selected for the cardiovascular modeling because of its many capabilities including sensor fusion, which is the combining of values from several different sensors. Sensor fusion enables the artificial neural networks to learn complex relationships among the individual sensor values, which would otherwise be lost if the values were individually analyzed. In medical modeling and diagnosis, this implies that even though each sensor in a set may be sensitive only to a specific physiological variable, artificial neural networks are capable of detecting complex medical conditions by fusing the data from the individual biomedical sensors.

Recurrent feed-forward artificial neural networks were selected for the cardiovascular modeling to capture the temporal information in physiological variables. These variables are time-series data from which both the absolute values and the rates of change need to be modeled. Recurrent artificial neural networks recycle a small portion of information from time  $t-1$  at time  $t$ . Indirectly, decreasing portions of information from time  $t-2$ ,  $t-3$ ,  $t-4$ , etc., are also captured, thus enabling recurrent ANNs to model the temporal dynamics in data.

The development of a model takes one or more sequences of physiological variables collected with biomedical sensors during graded exercise tests and learns the temporal dynamics of these variables to produce artificial neural network-based cardiovascular models. An example of such a model for a male individual is developed from all available healthy male exercise test data.

The modeling artificial neural network system has five inputs to take the workload, age, weight, height, and sex as input. These artificial neural networks has seven outputs, corresponding to heart rate, breathing rate, systolic blood pressure, diastolic blood pressure, metabolic oxygen requirement, oxygen uptake, and oxygen saturation, were clamped to the "actual" values during the training phase. After training, the model can generate the appropriate physiological responses for simulations of varying values of workload, age, height, weight, and sex.

The cardiovascular modeling system was developed to be used in a diagnostic system to identify several medical conditions such as those listed in Table 1. These models will also increase the sensitivity of detecting or excluding several other conditions that cannot be uniquely diagnosed in an exercise test alone such as those listed in Table 2. Additional medical conditions can be added to the system as example data becomes available and when additional physiological variables are recorded that enable identification of other conditions.

---

**Table 1. Conditions Detectable with Exercise Testing**

Myocardial Ischemia  
 Peripheral Vascular Disease  
 Exercise-Induced Asthma  
 Vasoregulatory Asthenia  
 Unfitness  
 Vasoregulatory Asthenia  
 Psychogenic Dyspnea  
 Muscle Phosphorylase Deficiency

---



---

**Table 2. Conditions Not Directly Detectable with Exercise Testing Alone**

Chronic Bronchitis  
 Pulmonary Emphysema  
 Pulmonary Infiltration, Alveolitis, and Fibrosis  
 Pulmonary Thromboelism and Hypertension  
 Congenital Cardiac Abnormalities  
 Cardiac Valvular Obstruction or Incompetence  
 Primary Myocardial Disease  
 Generalized Neuromuscular Disorders

---

## Publications

L.J. Kangas, P.E. Keller, S. Hashem, R.T. Kouzes, and P.A. Allen. 1995. "Adaptive Life Simulator: A Novel Approach to Modeling the Cardiovascular System." Presented at and In *Proceedings of the American Control Conference '95*. June 21-23, Seattle, Washington.

P.E. Keller, L.J. Kangas, S. Hashem, R.T. Kouzes, and P.A. Allen. 1995. "Artificial Neural Networks to Model and Diagnose Cardiovascular Systems." Presented at and In *Proceedings of the World Congress on Neural Networks '95*. July 17-21, Washington, D.C.

L.J. Kangas, P.E. Keller, S. Hashem, R.T. Kouzes, and P.A. Allen. 1995. "A Novel Approach to Modeling and Diagnosing the Cardiovascular System." Presented at and In *Proceedings of the Workshop on Environmental and Energy Applications of Neural Networks '95*. March 30-31, Richland, Washington.

L.J. Kangas, P.E. Keller, P.A. Allen, and R. Wright. 1995. "Artificial Neural Networks to Model and Diagnose Cardiovascular Systems." Presented at and In *Proceedings of the IEEE TAC/Northcon '95*. October 10-12, Portland, Oregon.

## Presentation

L.J. Kangas, P.E. Keller, S. Hashem, R.T. Kouzes, and P.A. Allen. 1995. "Cardiovascular Modeling and Diagnosis in Real-Time." Presented at the 2nd Advanced Combat Casualty Care Workshop. May 16-17, Silver Springs, Maryland.

# *Advances in Desktop Atmospheric Dispersion Modeling*

Jerome D. Fast and K. Jerry Allwine (Atmospheric Sciences)

---

## **Project Description**

A demonstrable capability of applying coarse-grained parallel computer technology to desktop atmospheric dispersion modeling has been accomplished. Parallel computer technology was applied to PGEMS, an atmospheric dispersion model, to address the critical issues facing future requirements of this class of dispersion models. This research forms a basis for future work with DOE addressing emergency response requirements of site cleanup and production operations, and routine air quality assessments and analysis to meet regulatory and safety requirements. Existing coarse-grained parallel computers can reduce the execution time required by desktop atmospheric dispersion models without a significant increase in hardware cost. This reduction in execution time will permit improvements to be made in the scientific foundations of these applied models, in the form of more advanced diffusion schemes and better representation of the wind and turbulence fields (both historical and forecast). This is especially attractive for emergency response applications where speed and accuracy are of utmost importance. Since desktop atmospheric dispersion models must also be robust, well documented, have minimal and well controlled user inputs, and have clear outputs, the development of a graphical user interface for PGEMS was also initiated.

## **Technical Accomplishments**

Over the past decade, staff at the Laboratory have developed desktop dispersion models for several clients (e.g., Nuclear Regulatory Commission, Environmental Protection Agency, DOE, U.S. Forest Service, and Pacific Gas and Electric Co.). One model, PGEMS, was initially developed several years ago for PG&E. It is based on the MELSAR model (developed for EPA), and the MESOI model (developed for NRC). PGEMS is highly modular and the basic scientific components of the model can be ported to a wide range of computers. However, the original user interface and input and output modules were designed for a VAX computer with a Tektronix 4107 terminal, which, given the current advances in desktop computers, rendered these interface modules sorely outdated. Revisions were made to the meteorological processing and transport modules of PGEMS for installation on a DOS-based desktop computer as the emergency response model at PG&E's Diablo Canyon nuclear power plant. These improvements, in

addition to the general-use features of PGEMS, made it the preferred candidate model for implementation on a parallel processing computer as part of this research.

The PGEMS code was adapted to and benchmarked on several computer systems, including a Gateway 486/66, a Power Macintosh, a Macintosh Quadra 700, a Sun Sparc 5, an IBM RISC 6000 model 590, and an IBM RISC 6000 model 41T.

Various vendors were contacted in FY 1993 about upgrading their desktop computers to coarse-grained parallel machines. After these discussions, it was decided in FY 1994 that the IBM PowerPC was the best candidate for testing coarse-grained parallel codes. IBM appeared to be the only vendor with definite plans to release a desktop symmetric multiprocessing (SMP) computer; they announced the release of a two- to four-processor symmetric multiprocessing computer in December 1995. Two single-processor IBM RISC 6000 model 41T computers, the predecessor to the IBM symmetric multiprocessing computer, were purchased (one in FY 1994 and one in FY 1995) and PGEMS was tested within the UNIX operating system. The IBM 41T computers are currently networked with several IBM RISC 6000 model 590 computers capable of running the Parallel Virtual Machine (PVM) software for parallel processing. A parallel-processing version of PGEMS has been successfully tested on this network using Parallel Virtual Machine. It was anticipated that Parallel Virtual Machine would also be used on the new symmetric multiprocessing computer, thus minimizing revisions to the parallel-processing version of PGEMS for installation and operation on the symmetric multiprocessing computer. It became apparent in FY 1995 that IBM would not release their symmetric multiprocessing machine as planned so this objective could not be achieved; therefore, the parallel version of PGEMS was evaluated on the existing cluster of IBM computers so that it would be ready when symmetric multiprocessing computers eventually do become available.

While models such as PGEMS can be run on existing networks of computers, the total computational time will also be highly dependent upon the time required to exchange data among the computers. A symmetric multiprocessing machine would not have this limitation. It can be shown that to optimize the total run time  $t_{total}$ , one can obtain a relationship between the total

computational time on  $n$  processors and the total computational time for one processor given by

$$\text{Ratio} = \frac{t_{\text{total}}}{t_c} = \frac{1}{n} + \frac{n}{\sqrt{r}}, \text{ where } r = \frac{t_c}{t_d}$$

$t_{\text{total}}$  = total run time =  $t_1 + t_2$

$n$  = number of processors

$t_c$  = total CPU time for 1 chip to run whole model

$t_d$  = data exchange time

$t_1$  = total CPU time among multiprocessors =  $t_c / n$

$t_2$  = data exchange time among multiprocessors =  $nt_d$

In Figure 1, this ratio has been determined as a function of data exchange rate. The total computational time will be reduced when more processors are used on a network of computers only if  $r$  is large (time required to exchange data is relatively small).

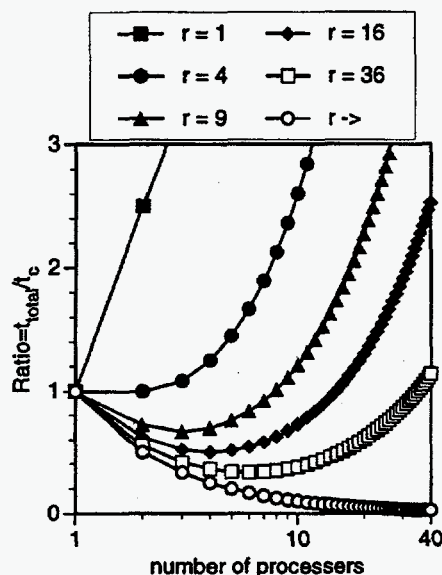


Figure 1. Total Computational Time as a Function of Number of Processors and Data Exchange Time

Also in FY 1994, a new diffusion module was developed based on a simple puff diffusion scheme and a more physically realistic particle diffusion parameterization.

Parallel computer technology makes this treatment of diffusion feasible for real-time emergency response applications.

The specific accomplishments of this project include

- completed the transfer and testing of PGEMS on a wide range of desktop computers (IBM PC compatible, Macintosh, UNIX workstations)
- developed and tested a new diffusion module for PGEMS that is a combination of a simple puff diffusion scheme and a more physically realistic particle diffusion parameterization
- tested successfully an advanced parallel computational technology (Parallel Virtual Machine) that allows networks of homogeneous and heterogeneous computers/processors to be used as a single large parallel computer
- determined performance characteristics of the parallel-processing version of PGEMS and compared these performance characteristics with the single-processor version of PGEMS
- solved the parallel computational problems of PGEMS using Parallel Virtual Machine to harness the aggregate power of homogeneous and heterogeneous networks.

The result of work completed through FY 1995 is a version of PGEMS with an advanced particle diffusion scheme operating on a coarse-grained parallel computer that is available for demonstrations. In addition, the development of a new graphical user interface, based on Visual Basic, for running PGEMS on Microsoft Windows has been initiated. Since PGEMS itself has been ported to a variety of computer platforms, the final version of the graphical user interface should be designed for a variety of computer platforms as well.

## Presentation

X. Bian and J.D. Fast. 1995. "New Developments and Research in an Advanced Atmospheric Dispersion Model." Pacific Northwest National Laboratory Atmospheric Department seminar, Richland, Washington.

# *Automated Document and Text Processing*

Kelly A. Pennock (Information Technologies)

---

## **Project Description**

This project is an attempt to extend the state of the art in information retrieval technology and tune its use specifically to information discovery through visualization and advanced information displays. Information retrieval is defined by the basic operations of text information storage and access. Advances in communication and networking have encouraged rapid growth in the volume of available information, making more information available than can be used. The vast majority of this information (95 percent by National Institute of Standards and Technology estimates) is in the form of written natural language. Written natural language is flexible, descriptive, and comprehensive; it is also complex, difficult to structure, and time-consuming to process. To bridge the gulf between usable information in textual form and used information, significant advances in information retrieval systems are required.

The next generation of text processing systems must support extensive user interaction, exploration, and analysis of extremely large databases. Among the features that will be included in future systems are topic extraction, content-based retrieval, enhanced querying including natural language queries and query-by-example, automated summarization, and information visualization. The goal of this project is the identification and implementation of a basic set of algorithms and techniques that will support these text processing system enhancements. A variety of processing approaches ranging from statistical to natural language was studied, abstracted, combined, and enriched.

## **Technical Accomplishments**

The primary contribution of the Document Understanding Project was the conception, construction, and experimental use of a prototype information retrieval with a number of superior characteristics. The System for Information Discovery (SID) includes a variety of features which separate it from current academic and industrial systems. The following describes the major components

and capacities of the system, which considered individually and as a whole, reflect the major accomplishments of the project.

### *Topic Identification*

A method of statistically identifying topics from within natural-language-based documents was successfully implemented. The method, relying on serial clustering algorithms and adapted from basic work on text compression, provides a database-specific, non-heuristic based method for identifying the appropriate topic of each word. This measure allows the important ideas of a document to be identified quickly and without prior knowledge. This information can be used for indexing, categorization, or a number of other uses.

### *Text Compression*

A unique method for text compression was identified, extrapolating from the work on topic measures. Basically, word lists are filtered first by frequency and then by topic value (as described). The amount of compression for the test data sets run was typically 90 percent, which indicates that only 10 percent of the vocabulary for a given data set was necessary to characterize and retrieve documents. This reduction in the magnitude of the requisite vocabulary for characterization offers the opportunity to enhance the speed of the system and the magnitude of the document collections that can be processed.

### *Topic/Document Representation*

A novel method for representing topics was also derived during FY 1995. The method relies on describing each topic in a distributed fashion, so that topics are described in terms of their relationships to other topics. The method used to represent topics was also be used to represent documents, so that documents are also defined in terms of their relationship to topics. The signature representation provides a flexible method for representation and somewhat of an automated summary of the document.

### *Document Illustration*

Presentation of specific document contents was explored and a strategy for adjusting the retrieval system for topic identification and topic and subdocument representation for an individual document (as opposed to the entire document collection) was developed. Adjusting the retrieval system to multiple levels of scale is an important feature for information presentation.

### *Information Threads*

One of the most interesting ideas generated in this project was a concept entitled "information threads." Information threads offer a unique method for navigating through information by selecting a major topic, keyword, or combination of keywords and then following different information paths identified by the system. Information threads will expand the traditional query method of user interaction with information systems.



# *Collaborative Environment Prototype for Molecular Science*

Richard T. Kouzes and James D. Myers (Computing and Information Sciences)

---

## **Project Description**

In this LDRD project, we are developing a Collaboratory Prototype Environment for Molecular Research as the means to share molecular science data and its processing with external collaborators, and to enable more effective science to be carried out with advanced instrumentation. We work with researchers in nuclear magnetic resonance (NMR) spectroscopy and molecular beam reaction dynamics (MBRD) to identify their needs and will design the collaboratory environment to support them.

The major objectives of this work were to

- design and integrate a prototype collaboratory software environment (CSE)
- develop a dynamic cross platform shared screen viewer application for the collaboratory software environment
- implement a system for desktop video conferencing within the Laboratory and with external collaborators
- develop the mechanisms to move data directly from acquisition programs in the Laboratory to an analysis program on a remote collaborator's desktop via a World Wide Web based "electronic notebook"
- demonstrate the utility of such collaborative tools for molecular science researchers
- evaluate the technical and social issues of the collaborative environment
- plan future research based on this evaluation.

## **Technical Accomplishments**

During the first full fiscal year of this project, the following were completed: an initial prototype, development of a cross platform screen sharing tool, deployment of the environment and several tools to internal and external groups, and the design and partial implementation of second generation tools based on user feedback. In addition, the project has taken the lead in developing a Laboratory-wide capability for low-cost desktop videoconferencing.

The initial collaboratory software environment prototype developed in FY 1994 was improved and modified to work with the televiewer developed in early FY 1995. The televiewer software allows dynamic sharing of the contents of a rectangle, window, or entire screen between UNIX and Microsoft Windows machines. Based on the use of the initial televiewer implementation, a second version providing compression and individual data streams to workstations of varying capabilities has been designed and is being implemented.

The project staff gained considerable experience with electronic notebooks through the use of the Virtual Notebook System (VNS) from The Forefront Group. Experimentalists and theorists in three different groups at the University of Utah and the Laboratory have been connected over the Internet and can now make use of the Virtual Notebook System to exchange and store text, graphics, and other information on UNIX, PC, and Macintosh computer platforms. The theorists on the project at the Laboratory can store images of molecular structures and diagrams of vibrational motions they have calculated to be used by the experimentalists at the University of Utah in their modeling efforts of collisionally induced dissociation reactions. We have worked closely with this group to learn the strengths and weaknesses of the notebook system. We have and continue to work closely with The Forefront Group to propose improvements to the product, participating in two revision beta tests and testing a gateway tool that allows browsing the notebook from the World Wide Web (WWW). We have recently been invited to join a Virtual Notebook System consortium to guide it toward use as a scientific laboratory notebook.

CU-SeeMe, a video conferencing application for the Macintosh and PC (from Cornell University), and the UNIX-based Multicast Backbone (MBONE) tools were brought in and evaluated. The collaboratory project has performed tests to provide external videoconferencing across the Laboratory firewall, and supports a pilot system to provide CU-SeeMe capabilities internally and, via a reflector bridge, between Laboratory molecular science researchers and their external collaborators. Connection to UNIX Multicast tools will also be provided, allowing true cross platform videoconferencing between Macintosh, PC, and UNIX workstations. Security and administrative plans have been developed to

minimize the impact of video traffic on other network communications. During the next year, software to manage connections, conference scheduling, and bandwidth limits via the World Wide Web will be created and integrated with the collaboratory environment.

Modules for handling network communication and the interactive display of graphical scientific data have been built and may be "dropped in" to future applications. Using these tools, a program has been developed for the simulation of the results from a molecular beam experiment. A collaborator running this program on his/her desktop machine may enter the relevant parameters for the computationally intensive calculation and run it from anywhere on the Internet using a machine at Pacific Northwest National Laboratory. Once the calculation is finished, the results are sent back and displayed on a resizable, zoomable graph on the user's desktop. When the program is running, all of the network communication is taking place in the background, essentially invisible to the user, and the results appear within seconds rather than the many minutes that would be required if the calculation were taking place locally. A World Wide Web interface was created for this program to further simplify use by external collaborators.

The collaboratory project also participated in several beta tests and evaluations of collaborative software and collaborative development environments, including IBM's Person to Person and Lotus Notes. Based on feedback on the collaboratory software environment and associated tools, and an assessment of new technologies, the collaboratory project designed a second generation environment around World Wide Web capabilities, adding the ability to manage an array of interactive collaborative tools. Through the use of Common Gateway Interface (CGI) processes and specialized MIME file types, we can

use the World Wide Web to launch our collaborative processes on both the server machine and client computers. Our existing socket based messaging communications will be integrated with the new code giving us bi-directional communications (not possible through the World Wide Web alone). Combining the technologies developed for the first collaboratory software environment prototype and the capabilities of the World Wide Web will enable the development of a simpler, more user friendly interface to the collaborative tools in the environment, while decreasing the development effort required. Technical feasibility has been demonstrated and implementation will occur in FY 1996.

We have also given numerous talks and a short course on the collaboratory concept at chemistry, physics, and information technology conferences. Four presentations were made in sessions at the August 1995 American Chemical Society National Meeting in Chicago. The project has also received recognition in several magazines and on the local television news.

#### **Presentations**

R.T. Kouzes and J.D. Myers. 1995. "Collaboratories: Scientists Working Together Apart." DOE Office Information Technology Workshop, July 18-20, Augusta, Georgia.

R.T. Kouzes and J.D. Myers. 1995. "Electronic Collaborative Tools Workshop." 1995 IEEE Conference on Real-Time Computer Applications in Nuclear Particle and Plasma Physics, May 24-28, Michigan State University National Superconducting Cyclotron Laboratory, East Lansing, Michigan.



# *Development of Intuitive User Interfaces*

James A. Wise (Information Technologies)

---

## **Project Description**

The objective of this project was to perform the necessary background research and technology development to create a software, hardware, and physical environment for an analyst's workstation that demonstrates the potential of advanced interaction techniques and uses a next generation metaphor in human-computer communications. The metaphor is "an information space you walk into," and provides the user with the capability of interacting with information much in the way one interacts with the physical world. The intuitive user interface is both an environmental setting with large screen displays and directional sound, as well as the means to interact with these informational representations in ways that are analogous to interacting with spatial objects in the natural world.

## **Technical Accomplishments**

During FY 1995, work concentrated on research in the following areas that needed to be reviewed, assessed, and combined to bring the elements of advanced human computer interface design to the state of the art:

- cognitive schema underlying information visualizations
- sonification of the intuitive user interface as an adjunct to information visualization
- spatio-temporal representation in an intuitive user interface through development of an animated query language
- touch and gesture as input and control means to an intuitive user interface
- design of physical environment for intuitive user interface.

### *Cognitive Schema*

Review of research located publications that substantiated the spatial metaphors underlying formation and use of language. Spatial primitives were extracted from this research and used to form requirements for intuitive user interface perceptualizations of information. This research

provided the basis for requirements definitions in the specific ways that an interface is to be made more intuitive through the different sensory and control strategies that are employed.

### *Sonification*

The sonification research created a proof-of-principle demonstration of the usefulness of a sonic display component in the intuitive user interface. Both symbolic and analogic uses of sonification were demonstrated. These included alerting to data change and conveying qualitative information about the data. It was discovered through this demonstration of sonification that verbal terms can be located and recognized by a human user faster through sonification than through visualization, and that the audification in an analogic way assists and encourages "gisting" of a visual display, wherein the user gains a rapid understanding of data content or meaning without having to attentively inspect the data. These demonstrations will enable the inclusion of sonification into the SPIRE visualization system during FY 1996.

### *Animated Query Language Development*

An Animated Query Language (AQL) is a means to make spatio-temporal information more accessible to the user and analyst. Animation is time made visible, and an animated query language enables a user to rapidly and easily browse continuous numerical data, test results from dynamic systems models, find rhythms or cycles in data, and improve the current generation of link analysis displays. Current animation methods are very slow and cumbersome to set up and use, and do not lend themselves to ad hoc queries and data exploration.

The intuitive user interface research created a new query language and tested it in a proof-of-principle demonstration with an environmental data file. The grammar of the animated query language allows animations to be constructed as easily as users currently make Boolean queries on text retrieval systems. With this animated query language, a user can type in a sentence in an English type structure and receive an animation in reply. The animated query language will be used to provide the basis for animation of Themescapes, a SPIRE visualization, in FY 1996.

### *Touch and Gesture Control of an Intuitive User Interface*

This research investigated the state of the art of gestural interfaces and touch exploration of visualizations as a means of getting away from the traditional keyboard and mouse controls of current WIMP interfaces. The results showed that currently available hardware do not adequately utilize the differential touch mechanisms available to people for exploration, and that there is significant potential here for combining visualizations with touch as a means of inquiry.

Dataglove technology is just becoming sensitive enough to recognize the finger movements inherent in the eight basic touch movements, but wearing a glove has inherent limitations. Glove technology is most feasible in terms of functionality and cost for exploration of gestural control of interfaces.

There is also a continuing need for text inputs to an interface that is distinctive from function inputs. The best current alternative to a QWERTY keyboard for text input is a "chord" keypad, but this requires specialized training. Chord keypads, however, offer portability if one wishes to be able to walk around in an extensible information space and still make text inputs without returning to a fixed keyboard.

Conclusions from this research were to investigate the use of a chord keypad as the intuitive user interface is built next year and wait for better glove technology in the first quarter of FY 1996 to better assess its usefulness as a gestural input means.

### *Design of a Physical Environment for an Intuitive User Interface*

This component of the intuitive user interface task sought the means to construct a working prototype intuitive user interface for technology integration and demonstrations in FY 1996. Steelcase Inc. has agreed to provide new office furnishings components it is developing that incorporate visual projection and sound technology which could be used to build the intuitive user interface. FY 1996 work will combine the Laboratory's SW visualizations with Steelcase furnishings in creating a prototype.

### **Conclusion**

This year's work on the intuitive user interface has completed background research that provided a theoretical basis and justification for the intuitive user interface, along with necessary technology investigation to include sonification, animation, and gestural interaction with large-scale information visualizations. These are all means to increasing an analyst's productivity in an advanced information technology environment. A conceptual design of the physical characteristics of the intuitive user interface was completed, and a furnishings system to support the displays and interaction devices will be supplied.

### **Presentation**

R. Bruce. 1995. "Animated Query Language for Spatio Temporal Information Systems." Presented at the NCGIA National Summer Study Institute, July 24-29, Woods Hole, Maine.

# *Direct Numerical Simulation of Turbulence<sup>(a)</sup>*

Jon R. Phillips (Fluid Dynamics)

---

## **Project Description**

The flow between parallel plates that are at different temperatures is a problem that has received the attention of many investigators. There are still aspects that have not been considered. The three-dimensional laminar transitional and low Grashof number turbulent flow states of the unstratified vertical slot flow geometry—the double-pane window flow have been computed. This geometry occurs in very large aspect ratio insulating windows such as those found on commercial buildings. The spectral computational methods used in this project emphasized accuracy and speed on the Intel Delta architecture so that large problems are effectively and efficiently simulated.

Much is known about the linear stability of the unstratified double pane window flow. One-dimensional laminar unicellular flow persists in the window until a Grashof number of about 1005 is reached at the Prandtl number of air. At that point the flow becomes susceptible to small disturbances such that multiple stationary transverse vortices form. The Grashof number is a dimensionless ratio of the buoyancy and viscous forces while the Prandtl number is the dimensionless ratio of viscous and thermal diffusivities. Beyond the Grashof number of the initial instability there are a large variety of laminar two and three-dimensional convection states until aperiodic turbulent motion begins.

Direct turbulence simulations with 2.4 and 14 million degrees of freedom were computed on up to 128 processors. Tens of thousands of time steps are required for a simulation to “spin-up” so that stationary statistics of the turbulent flow can be tallied. Larger simulations require up to 100 machine hours to compute stationary statistics.

The code computes the instantaneous temperature and velocity vector fields and the important temporal statistical correlations such as the Reynolds stresses. Through these numerical “experiments” time-averaged turbulence quantities that are difficult to measure can be computed.

In particular, it is difficult to measure the velocity temperature correlation that is necessary to model the turbulent heat transport through the double-pane window.

Since these simulations involve no turbulence models, it is required that all physical motions of the fluid at the continuum scale be adequately modeled to determine the statistical effects of the motions on the averaged flow variables. The complexity of the flow solution and the required resolution of the simulation increases rapidly as the Grashof number increases. This rapid increase in the number of flow “scales” makes this a problem that requires the very large computational resources of massively parallel computers such as the Intel Delta.

## **Technical Accomplishments**

Technical accomplishments during FY 1995 include the following:

- many transitional laminar flow states have been computed
- turbulent calculations with Grashof numbers of 8,100 and 22,500 are complete
- high-performance graphics hardware and software were used as a tool to interpret data fields often using stereographic imaging.

Examples of statistical data for two different Grashof numbers are shown in Figures 1 and 2. Figure 1 shows the time averaged velocity that is a function of the distance across the slot between the heated and cooled planes. Figure 2 shows the time averaged temperature distribution. On average, the heated fluid rises and the cooled fluid falls although turbulent unsteady motions of the fluid cause heat and momentum to transfer more readily across the slot as is evidenced by the flattening of the profiles near the center of the slot.

---

(a) Project was a task under the project formerly entitled, “Computational Modeling of Complex Physical Systems.”

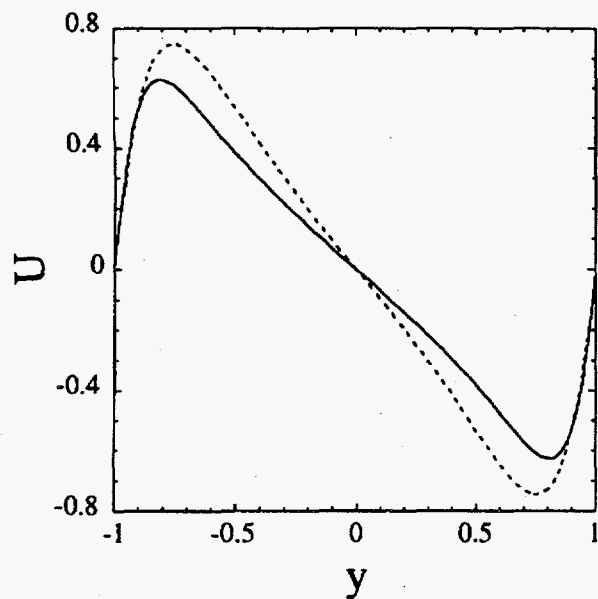


Figure 1. Time-averaged velocity profiles: dashed,  $Gr = 8,100$ ; solid,  $Gr = 22,500$ .

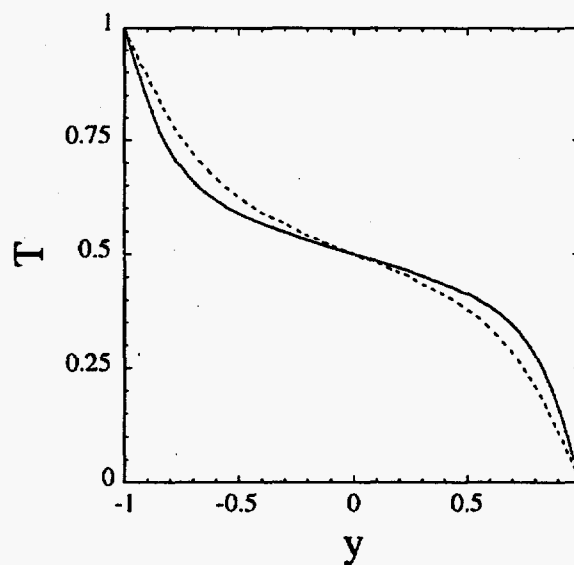


Figure 2. Time-averaged temperature profiles: dashed,  $Gr = 8,100$ ; solid,  $Gr = 22,500$ .

#### Publication

J.R. Phillips. "Direct simulations of turbulent unstratified natural convection in a vertical slot for  $Pr = 0.71$ ." *International Journal of Heat and Mass Transfer* (in press).

# *Fourier Transform Ion Cyclotron Resonance Mass Spectroscopy Data Acquisition and Modeling*

Richard T. Kouzes and Michael Gorshkov (Computing and Information Sciences)

---

## **Project Description**

The objective of this project was to develop advanced computerized analysis techniques for Fourier transform ion cyclotron resonance mass spectrometry (FTICR-MS). Instruments are under development that are capable of making measurements on selected ions at a level of precision an order of magnitude better than given in the atomic mass table, as well as high-resolution measurements of mass spectra from heavy biologically important ions followed by their structure identification. Development of new methods of data acquisition, and ion manipulation in FTICR were carried out to increase performance of these instruments. The target goals of the project were to increase the mass-spectral characteristics of the FTICR instruments such as mass resolution, signal-to-noise ratio, efficiency of ion trapping, and dynamic range.

## **Technical Accomplishments**

Ion cyclotron resonance mass spectrometry (ICR-MS) has been exploited for many years to perform precision mass measurements and ion structure analysis. Most recent efforts in the area of FTICR-MS have concentrated on developments for measuring organic compounds or specific masses. Improvements in magnet and computer technology have allowed these broad range instruments to obtain resolutions in selected cases to better than 10 ppb (one part per billion). The objective of this research is to develop computer and electronic methods that allow FTICR-MS instruments to perform measurements at highest achievable mass resolution and mass determination accuracy.

We have previously carried out a number of studies of FTICR ion traps devices using computer models of the ion motion, in order to look at the effects of magnetic field inhomogeneities and non-ideal electric fields on the ion motion, pursuing Monte Carlo techniques and integration of the particle motion. Also, the development has been carried out to provide very long FTICR transients acquired at high frequency. In order to improve vacuum quality and ion transmission into the FTICR trap from external ion sources a novel shutter design was invented and implemented in the Laboratory's FTICR-MS instruments.

During FY 1995, we concentrated on design of new electronic schemes to improve trapping efficiency of an FTICR ion trap, as well as development of new computer algorithms for FTICR signal processing to increase mass resolution and signal-to-noise ratio in acquired FTICR mass spectra. Another aspect of the project was to develop, through intensive computer modeling, a new approach to designing FTICR-MS systems. Computer modeling of the ion cyclotron resonance system is a crucial aspect of this work in order to fully understand parameters to modify for improved performance. Such modeling included numerical simulations of ion motion in magnetic and electric fields in an ion cyclotron resonance ion trap, calculation of the three-dimensional magnetic field created to radially confine the ions in the FTICR trap, and FTICR signal simulations to find the optimal processing procedure of obtaining spectral information.

The resolution of an FTICR-MS instrument is limited by the time that the transient is observed. This time applies a fundamental restriction on the obtainable peak width in Fourier transform mass spectra. We developed a new method of pre-Fourier transform signal processing which is based upon the data-filling of the recorded time-domain spectra by means of data reflection at zero time (Data Reflection Algorithm). This method gives improved resolution of FTICR mass spectra by a factor 1.7, and increases the signal-to-noise ratio by a factor of 2 compared with conventional techniques. The algorithm has been successfully tested for FTICR spectra obtained from electrospray ionization (ESI) of biological molecules (bovine insulin) on a 7-tesla FTICR instrument and nuclear magnetic resonance spectra from Cd-111.

A new ion cooling technique has been developed in order to effectively cool the multiply-charged ions obtained from electrospray ionization of heavy biological molecules. The conventional methods are based upon the ion cooling via their collisions with neutral buffer gas molecules, that requires additional time in getting FTICR mass spectra because of the necessity to pump the trap down before acquiring the time-domain spectrum. Moreover, collisional cooling becomes ineffective when the masses of ions increases as in the case of electrospray ionization of biomolecules. We developed and built new electronics in which the crucial element is a circuit tuned into the resonance with the ions being trapped and cooled in the FTICR trap. Computer simulations show that ions

of practical interest can be cooled effectively for a time an order of magnitude less than that of collisional cooling. This scheme will be evaluated for implementation in other Laboratory FTICR-MS instruments.

The resolution and sensitivity of the FTICR-MS instrument depends on the radius of ion cyclotron rotation and cyclotron frequency (measured in FTICR-MS). Because of non-ideal electric and magnetic fields in the FTICR ion trap, relativistic mass increases effects of the trap's wall and presence of space charges, the ion's cyclotron frequency depends upon the radius. This presents a problem for ion excitation and detection in FTICR-MS with strong magnetic fields, especially when the masses of physically important light atomic ion are to be measured. A new technique based upon the use of a multielectrode FTICR trap configuration providing ion feedback excitation and multifrequency detection was invented. The novel concept of ion excitation involves the use of a feedback electronic loop to capture the instantaneous ion cyclotron frequency followed by return of this frequency back into the excitation circuit.

#### Publications

M.V. Gorshkov and R.T. Kouzes. 1995. "Possible Applications of an External Resonant Circuit in Fourier Transform Ion Cyclotron Resonance." *Rapid Communications in Mass Spectrometry*, v.9, 317-321.

M.V. Gorshkov and R.T. Kouzes. 1995. "Data Reflection Algorithm for Spectral Enhancement in Fourier Transform ICR and NMR Spectroscopies." *Analytical Chemistry*, v.67, 3412-3420.

A.J. Peurrung and R.T. Kouzes. 1995. "Analysis of Space-Charge Effects in Cyclotron Resonance Mass Spectrometry as Coupled Gyrator Phenomena." *International Journal of Mass Spectrometry and Ion Processes*, v.145, 139-153.

M.V. Gorshkov and R.T. Kouzes. 1995. "A Scheme for Feedback Excitation in FTICR-MS based on multielectrode trap." Presented at and In *Proceedings of the 43rd ASMS Conference on Mass Spectrometry and Allied Topics*, May 21-26, Atlanta, Georgia, p.1096.

M.V. Gorshkov and R.T. Kouzes. 1995. "Possible Use of Time Domain Signal Inverse Algorithm in FTICR-MS." Presented at and In *Proceedings of the 43rd ASMS Conference on Mass Spectrometry and Allied Topics*, May 21-26, Atlanta, Georgia, p.720.

#### Presentation

M.V. Gorshkov and R.T. Kouzes. 1995. "Possible Applications of External Resonant Circuit for Cooling the Multiply Charged Heavy Ions in FTICR-MS With Electrospray Ionization." Presented at the 7th Sanibel Conference on Mass Spectrometry, January 21-24, Sanibel Island.

# *Heterogeneous Information Systems*

James C. Brown (Information Technologies)

---

## **Project Description**

Technology today requires a tedious manual process for the development and capture of a data integration scheme that is domain specific. This process identifies what can be linked by manually specifying the semantic relationship. Automation of this process has not been addressed. To be more widely used, automated methods for discovering, building, and maintaining these relationships must be developed. Additional research in the optimal method for computer representation and storage of these rules is also required.

## **Technical Accomplishments**

Specific objectives outlined for this research effort included the following:

- investigation into the current state of the practice and the state of the research in the area of meta-data management.
- define and develop intelligent agent processes to assist with the meta-data process. These agents will be classified in three categories 1) those that gather (or seek out) the meta-data from multiple distributed heterogeneous information sources; 2) agents to analyze, classify, and cluster contents of the meta-data; and 3) agents to populate the meta-data repository.

To date, we have succeeded in meeting these objectives in varying degrees. The following is a breakdown of the technical accomplishments by category along with the projected efforts still required to fully prove the concepts and viability of this work.

### *Investigation of Current Practice*

There are few formal groups working on meta-data in the same context that we are discussing it. Most of the work being done by others falls into two categories: 1) physical meta-data, and 2) data pedigree and quality.

The first category, physical meta-data, is an overlap with the physical aspects that we are concerned with. The focus of others has been on what is the minimal set of information required to define a data object. This has primarily been for the purpose of providing a mechanism

for accessing the information at a later time by some application. We, also, are interested in this type of meta-data. By reviewing what has been done in this area, and combining that work with our own specific needs, we have been able to create an initial definition for a meta-data repository structure to store and manage meta-data.

One of the most prestigious groups paying attention to the issues of meta-data is the IEEE. They are organizing a conference on meta-data to be co-sponsored by the IEEE Mass Storage Systems and Technology Technical Committee (IEEE MSS&TC) and the National Oceanic and Atmospheric Administration (NOAA). The issues to be addressed in this conference forum include:

1. What is meta-data
  - 1.1 Meta-data and semantics
2. Meta-data modeling: techniques and representation
  - 2.1 Application-specific meta-data models
  - 2.2 Multimedia representation
3. Meta-data management
  - 3.1 Creation
  - 3.2 Updating
  - 3.3 Maintaining/Consistency
  - 3.4 Policies
4. Meta-data generation/extraction
  - 4.1 Automatic techniques
  - 4.2 Data Mining
  - 4.3 Extraction from multimedia databases
  - 4.4 Meta-data repositories
5. Meta-data usage
  - 5.1 Query
  - 5.2 Application development
  - 5.3 Search
  - 5.4 Information system integration
6. Standards
  - 6.1 What exists
  - 6.2 What's needed

As a result of the Pacific Northwest National Laboratory LDRD effort, we will be participating as part of the program committee for this conference. The conference is tentatively scheduled to take place in April 1996.



## *Intelligent Agent Processes*

We also investigated the work being done in intelligent agent definition and development. We found that the term "intelligent agents" means different things to different groups. On one hand, these agents may simply be processes that run in the background to search and collect information. To another group, they may be self-modifying modules of code that can execute on and migrate from/to multiple systems. In this case, the agents take on an almost "living" nature.

We also found several search and collection 'systems' that have been created as an intermediary filtering mechanism for finding and searching for information. Included in this category are systems like Harvest, Web Crawler, and Glimpse. Rather than replicate work that has already been done, we elected to adopt some of this work and to customize the environment to fit our specific needs.

There are six primary categories of information agents identified for this research effort. Each of the agents are fundamental to the success of this effort. They include the following:

- Search - To be able to cruise through information cyber-space to locate potential items of interest based on high-level user input words/phrases. There are several agents in this category that will be developed.
- Collect - To gather meta-data from potential items of interest and to bring it back to the meta-data repository system.

- Extract - To gather meta-data from structured databases.
- Populate - To insert the collected and extracted meta-data into the meta-data repository for subsequent analysis and browsing by users and other agents. Several agents of this category will be developed based on the different collection and extraction agents required.
- Analyze - To determine both physical and semantic linkages among information sources that have been registered in the meta-data repository entries. There will be several analysis agents developed.
- Maintain - To periodically scan meta-data repository entries to review and verify/restore existence/accuracy of the sources for the meta-data. Several agents of this category will be developed based on the variety of information sources and types that are registered in the meta-data repository.

## **Presentation**

We are participating in the upcoming IEEE Metadata Conference sponsored by the IEEE Mass Storage Systems and Technology Technical Committee. This conference will be held on 16 - 18 April 1996 at the NOAA Auditorium in Silver Spring, Maryland. We are submitting a paper on our research to date to this conference and already have one staff member on the program committee.



# *Human Factors Evaluation of Immersive Virtual Environments Technology*

Richard A. May (Information Technologies)

John S. Risch (International Environmental and Technology Assessments)

Daniel T. Donohoo (Medical Technologies)

---

## **Project Description**

This project was initiated to study the potential of emerging immersive virtual environments (also known as virtual reality) technology for improving the understanding of multidimensional scientific data. The goals of this effort were threefold:

1. A critical analysis of the value-added of individual components of immersive virtual environments systems (e.g., six degree-of-freedom input devices and wide field-of-view stereoscopic displays) for facilitating a number of common data visualization, processing, and analysis tasks.
2. The identification of areas of applicability of immersive virtual environments technology for scientific data analysis.
3. The development of human factors guidelines for creating effective immersive interfaces for scientific applications.

## **Technical Accomplishments**

### *Technology Evaluation*

This research represented the first project by the Pacific Northwest National Laboratory immersive virtual environments lab. The first priority was to integrate and understand the immersive hardware to be used for this project. This included the six-degree-of-freedom trackers, input devices, and head-coupled visual displays. It became obvious early on that the six-degree-of-freedom input device supplied by the vendor would not meet our needs. An input device was created using some off-the-shelf technology, and staff augmented the device. This new input device was then incorporated with the rest of the equipment.

Because this was the first immersive project at the Laboratory, significant effort was spent on consideration of navigation, orientation, and interaction paradigms. Initial investigations showed a severe weakness in existing head tracking methodologies. Head tracking is the mapping of head motion (position and orientation) into the

virtual environment. The simple approach used by most immersive virtual environments researchers was not satisfactory. Our solution was the development of a head tracking model. This model has proved very effective and is now incorporated in many of the other immersive virtual environments projects under development in the Laboratory.

Both the stratigraphic editor and earth visualization system required importing geographic data from several sources. Some of the more common data formats were selected for use and data loaders were created. Different cartographic projections were used by the various data formats. A public domain cartographic projection software package from USGS was used to convert the projects. Once the data was loaded, routines were developed for registration of the data. Both the earth visualization system and the stratigraphic editor are meant as tools for scientific research. This required us to retain a high degree of accuracy. Care was taken to develop algorithms that would ensure proper geographic referencing between the topological and raster data.

For the stratigraphic editor, a non-uniform rational b-splines (NURBS) library from the University of Manchester was used. This provided the ability to mathematically manipulate the NURBS equations used to represent the strata. Our main task was the development of methods to provide an immersive interface to the NURBS library. Routines were developed to allow the user to select, edit, and manipulate the NURBS surface. To support usability tests of different interface paradigms, several input and interaction modalities were created. A significant amount of effort was spent on developing well controlled and repeatable experiments for immersive environment usability tests.

The earth visualization system was a more complex problem. The sheer volume of data required for this system eliminated any possibility of using a brut force approach. The first step was to reduce the amount of data being processed. Simple subsampling of the terrain data was not acceptable because it would not preserve geographic structures. To get around this limitation we implemented existing algorithms that would preserve geographic structures. We chose an algorithm that focused on eliminating low frequency data. This method

proved to be quite effective at reducing the volume of data. Still this was not sufficient to maintain sufficient frame rates.

Level-of-detail management was implemented to reduce the number of polygons having to be rendered. Level of detail is a technique for selecting areas of the display to show at much lower detail. For a system such as this, distant terrain was represented with much fewer polygons than data near the user's point of view. This, combined with efficient data management schemes, helped to keep system response time at an acceptable level.

#### *Application of Immersive Visual Environments to Scientific Data Analysis*

A number of tests were conducted in collaboration with Pacific Northwest National Laboratory geoscientists to develop effective techniques for interactively manipulating surface models. Based upon these studies, it was concluded that an editing approach utilizing NURBS for surface modeling held the most promise.

Subsequent work concentrated on the development and evaluation of a rudimentary NURBS-based geologic surface editing tool. The prototype software is capable of loading surface models generated using commercial geostatistical software, editing them by direct manipulation, and writing out the modified models in their original file format for subsequent processing. Editing of models is accomplished by selecting subregions of the model for modification, then interpolating a NURBS surface through the data points within the selected region. The NURBS surfaces can then be modified by interactively repositioning the NURBS control points in three-dimension using a six degree-of-freedom mouse. On completion of editing, the height of the original surface data postings in the region of interest is replaced with the height of the NURBS surface at those locations.

The NURBS-based surface editor was evaluated by EESC structural modeling experts using a number of representative geologic data sets. Feedback from the participating geoscientists led to a number of modifications and enhancements to the original system.

#### *Human Factors Analysis*

In collaboration with Drs. Chris Wickens and Polly Baker of the University of Illinois, a summary of the human factors research literature as it relates to scientific visualization in virtual environments was prepared. This work built upon a review completed for the National Science Foundation and provided preliminary guidance for the development of the prototype applications for our own empirical work. As was expected from our prior search of this literature, there has not been sufficient research to

develop a comprehensive set of guidelines to develop effective user interfaces in these environments. The current research base does, however, provide suggestions for the value of some of the salient features of virtual environments. Among the more important conclusions that can be drawn from the summary of the literature are

- stereographic display is only effective where there is a paucity of other depth data
- integrative decisions are enhanced by three-dimensional data display
- egocentric viewpoints lead to more accurate data comparisons
- exocentric viewpoints generally result in better global data interpretation and improved data search
- direct manipulation for data exploration is supported
- system responsiveness significantly affects user performance; six to ten frames per second are recommended at a minimum
- tools in virtual environments should be self-disclosing, provide implicit control, and limit the number of choices.

An unfortunate result of the current research base is that it offers little specific guidance for the developer of immersive virtual environmental applications.

To augment the available data and acquire human performance data that were more directly applicable to the scientific data analysis, several usability tests were designed and conducted. These studies were designed specifically to provide data to guide the development of the prototype geological surface editor that was developed in this research. Three experiments or usability tests were conducted: two at Pacific Northwest National Laboratory and one at the University of Illinois.

University of Illinois researchers conducted an experiment to investigate the features of frame of reference, display dimensionality, and stereopsis on user performance in a scientific visualization task. The effects of immersion or nonimmersion, the presence or absence of stereopsis in the data display, and two- or three-dimensional data presentation on selected scientific visualization tasks were evaluated. Performance was measured across separate scientific visualization tasks: search, travel, local judgment support, and global judgment support.

The results of the experiment demonstrated several tradeoffs related to the user's frame of reference. The first is that immersion disrupts a search for objects or data

in a three-dimensional environment. The data further suggested that this search decrement is due to a key-hole phenomena resulting from an inability to view the entire data set. Travel in the environment, however, benefits from immersion. This is partially due to a correspondence between the axis of control and the viewpoint leading to an ecological compatibility and partially to salient motion cues in the environment. Lastly it was found that local judgments are slightly faster when the user was immersed in the environment, but recall of the overall data configuration is much worse. These data indicate that immersive virtual environments applications require both immersive and nonimmersive views dependent on the scientific visualization task that is being performed.

The most prominent effect in the experiment was found in the dimensionality variable. The three-dimensional representation of the data always leads to superior task performance. This is an especially important result in that it shows that immersive virtual environments has the potential to reduce the cognitive burden involved in integrating data observed in traditional display environments and can lead to more effective searches of scientific data.

Finally, the inclusion of stereopsis in the data display resulted in only marginal improvement in task performance. This result suggests that added computational costs of stereographic display may not be warranted in many situations.

The usability tests conducted in the Laboratory's immersive virtual environments lab focused on the basic user interaction tasks that are required for a geoscientist to effectively navigate and manipulate the data expected in a geological surface editor. These human factors studies investigated the input/output characteristics of the six-degree-of-freedom input device used in our immersive virtual environments laboratory, methods of interacting with control points that can be used to interactively manipulate three-dimensional surfaces, and the value of providing stereopsis for the surface editing task.

Results of the first usability test assisted in optimizing the input device used in the immersive virtual environments lab and suggested the value of utilizing more dynamic transfer functions for input devices in future applications.

The second usability test employed a synthetic surface editing environment that was prototyped to test differences in user performance in three-dimensional surface editing. The test varied three different surface selection techniques and two different display modes: monographic and stereographic. In this test, these aspects of immersive virtual environments were manipulated to understand their effect on a user's ability to directly manipulate a three-

dimensional data surface. Performance was measured in terms of the task completion time and accuracy in changing the shape of a test surface to match a reference surface. This task was chosen because of its direct applicability to the geosciences applications.

Results of this usability test demonstrated the value of stereographic display to the three-dimensional surface editing task. Surface matching performance was both more accurate and faster with stereo when compared to the monographic display. Additionally, proximity methods of grasping objects in the environment resulted in faster, but no less accurate surface manipulation when compared to contact methods of object acquisition.

## Conclusions

### *Technology Evaluation*

There is significant promise for using immersive technologies to analyze three-dimensional geological data. Our initial efforts at a stratigraphic editor has drawn interest from several geologists. NURBS proved to be an effective prototyping tool for a stratigraphic editor but lacks for overall usability in three-dimensional geological structure editing. The forces at work in nature are not properly represented by NURBS equations. The creation of a mathematical model for representing the forces that shape the earth's crust need to be researched.

Usability testing is an important tool for understanding immersive interfaces. The development of immersive interfaces is a new research area and is complicated by the fact that it attempts to make interactions with the computer more "natural." What may be natural to one person may be not be natural to another. Usability testing allows the developer to understand how a general representation of users will interact with the system. However, the creation of robust usability tests for immersive interfaces can be difficult and time-consuming. Sufficient time and resources must be allocated to the task.

### *Application to Immersive Visual Environments*

Investigation of the application of immersive visual environments to scientific data analysis provided the following conclusions

- Increasing interactivity through the use of head-coupled display systems and six degree-of-freedom hand controllers, "mice" significantly improves understanding of the forms of, and spatial interrelationships among, the elements of three-dimension geologic structural models.

- Stereopsis (stereo viewing) alone provided limited value-added for improving understanding of multidimensional phenomena, however, the use of stereoscopic displays significantly improved the performance of multidimensional manipulation tasks.
- While the NURBS approach to geologic structural model editing proved considerably more efficient than existing techniques, it was less effective than expected. A simpler approach involving direct manipulation of model vertices via virtual "sculpting" tools is expected to prove more efficient.
- Immersive virtual environments systems are currently far from a "plug and play" technology; considerable work needs to be done before immersive virtual environments technology can be used on a routine basis for scientific applications.

- The expense of immersive virtual environments systems (\$300K+) is currently only marginally justified by their utility. System prices are expected to decline by an order of magnitude within the next year, however, enabling widespread application of the technology in the near future.

#### *Human Factors Analysis*

The human factors research performed in this study demonstrated that the manner in which the user interface is developed can have a major impact on the effectiveness and acceptability of applications developed using immersive virtual environments. The research has provided us with an understanding of the complexities in developing immersive virtual environment applications, methods for testing design alternatives, and some initial guidance for the developer of immersive virtual environments.

# *Information Systems Meta Data Investigation*

James C. Brown (Information Technologies)

---

## **Project Description**

During FY 1995, we developed a computerized meta-data model that would adequately store and manage the meta-data information necessary to provide the ability to store the knowledge about information objects and to automatically analyze, classify, and cluster contents of multiple distributed heterogeneous information sources. This research effort also defined the requirements for an automated agent that would be able to examine data within the source database tables and information files, as well as the meta-data stored in the information system catalogs to discover potential linkages. Data with similar domains were also considered likely candidates for linkage and integration. The agent's discoveries were stored in the meta-data storage mechanism for other computer applications to access. Alternative structures of this meta-data design were evaluated through a series of prototypes.

## **Technical Accomplishments**

The specific objective outlined for this research effort included the following: define a meta-data storage/repository (MDR) structure to actively manage meta-data associated with distributed heterogeneous databases and information sources.

Most of the work being done by others falls into two categories: 1) physical meta-data, and 2) data pedigree and quality. The first category, physical meta-data, is an overlap with the physical aspects that we are concerned with. The focus of others has been on what is the minimal set of information required to define a data object. The primary purpose for this is to provide a mechanism for accessing the information at a later time by

some application. We, also, are interested in this type of meta-data. By reviewing what has been done in this area, and combining that work with our own specific needs, we have been able to create an initial definition for a meta-data repository structure to store and manage meta-data.

We were able to locate few significant (or more mature) efforts being done in the realm of semantic meta-data management. Most of what has been done comes out of the Microelectronics and Computer Technology Corporation (MCC) Cyc efforts. The approach taken there has been to feed information "facts" into the Cyc system and to have it categorize and associate these facts with others that have been previously ingested. The Cyc effort has been a multiyear multimillion dollar effort that has resulted in the definition of information categories and methodologies for associating information facts amongst themselves.

In our efforts, we are interested in using large structured and unstructured information objects as the inputs for developing semantic (content-based) linkages. Our objective is to associate the information sources to each other based on physical and semantic meta-data. This is to enable users to search and retrieve more information than what appears to be available when searching with more limited capability tools. We do not intend for the meta-data repository to be able to fill in gaps in information or to infer additional information based its "knowledge" of what is available.

In the work performed in FY 1995, we prototyped a version of the meta-data object model. We populated the model prototype with representative data to be able to test its viability as a functioning component of a multi-tiered information architecture.



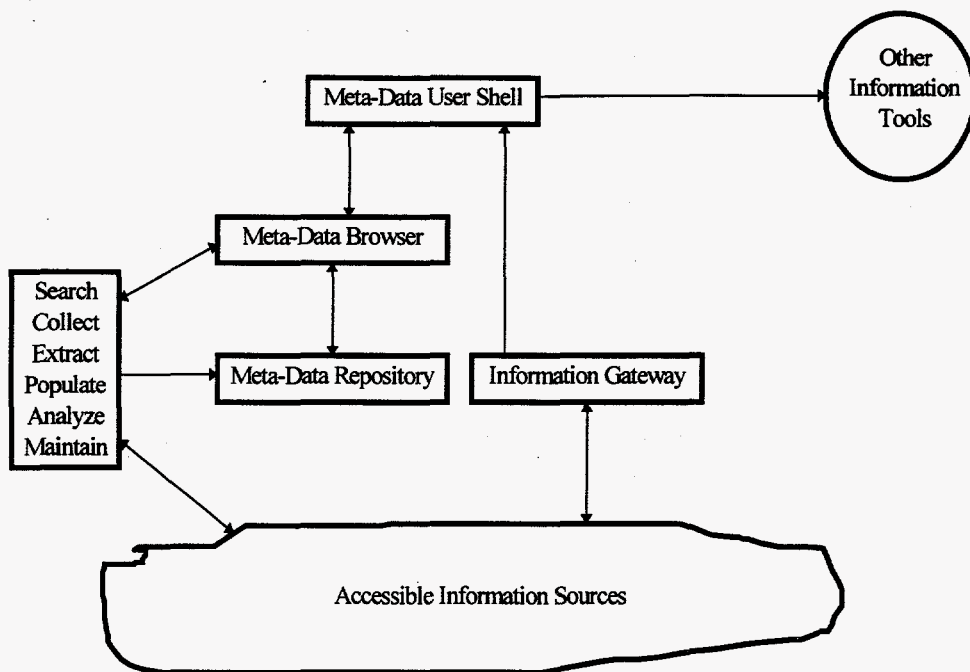


**Figure 1. The initial MDR design and process interconnectivity. In the work performed during FY 1995, we were able to prototype and demonstrate the viability of the meta-data user shell, meta-data browser, meta-data repository, information gateway, and hand-off of information to another tool. We were also able to develop search, collect, extract, and populate agent processes.**

# *Medical Imaging Three-Dimensional Reconstruction and Visualization*

Richard A. May (Information Technologies)  
Randy W. Heiland (Computer and Information Sciences)

---

## **Project Description**

The objective of this project was to develop proof-of-concept techniques and algorithms for real-time, immersive visualization and interaction with volumetric data. Goals for this project include

- develop new capability in medical data visualization
- build on Pacific Northwest National Laboratory's core capability of scientific visualization
- create more intuitive interfaces for medical data analysis.

## **Technical Accomplishments**

The original approach was to develop editing techniques for both polygonal data and volumetric data. These techniques would be developed in a three-dimensional immersive environment to investigate the usability and effectiveness of immersive technologies for this application. An SGI Onyx computer was used for the research but we wanted to focus on developing a system that could run on a desktop system.

An initial investigation into data segmentation and registration showed that incorporating polygonal data was beyond the scope of this project. Furthermore, discussions with medical professionals brought into question the usefulness of this approach. Our focus then turned to solving the problem of developing a real-time editing system for volumetric data only. We identified two potential public domain volume renderers, Volren from Silicon Graphics Inc. and the VolPack library from Stanford University. Volren was significantly faster but suffered from two serious drawbacks: 1) it is an end user application and extracting the volume rendering-specific code would have been an involved task; and 2) more importantly, the Volren algorithms are dependent on the SGI Reality Engine II hardware. Porting a system generated from the Volren routines would be quite difficult. The VolPack library, on the other hand, does not suffer from either of these problems. It is a more general-purpose volume rendering software library and, with minor modifications, was well-suited for our project.

The final key aspect of our approach was researching innovative immersive interfaces. The problem of real-time three-dimensional volumetric editing is inherently complex. Immersive technologies hold the potential to provide a more intuitive and natural interface.

There were several accomplishments made during the development of these techniques and algorithms.

Volumetric data was collected from several sources for testing. Dr. Chris Macedonia, an OB/GYN at Madigan Army Medical Center, provided us with fetal ultrasound datasets. Ultrasonic data from a breast phantom was obtained from a Battelle project. CT and magnetic resonance imaging data were obtained from the Visible Human project, a high-resolution digital dataset of the entire human body, available on the Internet through the National Institutes of Health National Library of Medicine.

The initial immersive interface design incorporates head tracking to control data orientation and uses a three-dimensional mouse for data selection. This interface represents the first effort at the Laboratory to design an effective immersive interface for a specific application. With the end goal of using these techniques on a desktop system, cost of the immersive technology was an important issue. We used low-cost displays and input devices for development where possible.

Due to the complexity of volumetric medical data, it was important to incorporate stereoscopic imaging. The proof-of-concept system uses the Virtual I/O I-glasses! as the display device. The I-glasses! support stereoscopic imaging by taking advantage of NTSC interlacing. We utilize this capability by generating a stereo pair, interlacing the images, and sending this combined image to the display. This represents a new visualization technique.

Deletion of user selected subvolumes of the volumetric data set was implemented. This initial functionality demonstrates the ability to interactively edit volumetric data in an immersive environment. Interactive editing of volumetric data is a new area of research. As general computer processor power increases, volumetric rendering will play a much more prominent role in scientific visualization. This research is allowing us to gain expertise in this emerging field.

# *Molecular Visualization on Parallel Computers*

Randy W. Heiland (Computer and Information Sciences)

---

## **Project Description**

Scientific visualization plays a key discovery and analysis role in many scientific application domains. This work targets those applications that require visualization performance beyond the capabilities of standard tools. For example, for a computer simulation, one might want to visually verify that an iterative calculation of a particular three-dimensional scalar field is progressing normally. Often, one may need such visualizations to be quickly computed so that interactive viewing is possible.

The objective of this project was to develop parallel visualization software, i.e., software that will run concurrently on multiple processors, for the display of a range of three-dimensional molecular datasets. The primary reason for writing such software is to speed up computationally intensive rendering (display) algorithms.

## **Technical Accomplishments**

There are two classes of rendering algorithms associated with three-dimensional scalar data: surface-rendering and volume-rendering. A common example of a surface-rendering algorithm is one that displays an isosurface, i.e., a surface of constant value, within the three-dimensional data. This technique generates (potentially) hundreds of thousands of polygonal facets that need to be rendered as two-dimensional pixels onto the computer screen. A parallel algorithm using the Global Arrays toolkit was implemented in 1994 to display such a polygonal dataset.

The focus of this project during FY 1995 was on volume-rendering a three-dimensional dataset. A volume-renderer, unlike a surface-renderer, attempts to display the entire three-dimensional field. It does this by generating a translucent image that combines certain user-specified structure(s) within the data as opaque and surrounding structure(s) as semitransparent. Such an algorithm is computationally intensive and, thus, a good candidate for parallelization.

The primary progress made this year is summarized as follows:

- developed project direction with colleagues in parallel rendering
- obtained prototype parallel volume-rendering software
- developed advanced prototype using an emerging "standard" parallel message-passing language (MPI)
- defined and developed molecular orbital visualization application.

## **Publication**

R.J. Littlefield, R.W. Heiland, and C. Macedonia. "Virtual Reality Volumetric Display Techniques for Three-Dimensional Medical Ultrasound." This paper (published on the World Wide Web) demonstrates the use of volume rendering for three-dimensional medical datasets.



# *Neural Network Data Processing for Sensor Applications*

Richard T. Kouzes and Paul E. Keller (Computing and Information Sciences)

---

## **Project Description**

The objective of this project was to demonstrate the potential data processing capabilities of artificial neural networks in sensing applications. This effort concentrated on the problem of identifying objects (e.g., contaminants) in the environment from their sensor signatures. This work involved the development of neural network techniques for automated sensing applications and an evaluation of whether the neural network approach is beneficial to these applications.

## **Technical Accomplishments**

The Laboratory is actively engaged in chemical sensing technology (sensors, spectrometers, etc.). The quantity and complexity of the data collected by these sensing systems can make conventional analysis of the data difficult. Artificial neural network (ANN) techniques can be used to automate analysis and to analyze data in real-time, significantly reducing the amount of human intervention required with many sensor and spectroscopic analysis methods. Improving sensor and spectroscopic analysis techniques could benefit several programs at the Laboratory. In addition, development of artificial neural network techniques for sensing systems complements our current work in environmental sensing technology.

While most areas in sensing technology are mature, the application of artificial neural network technology to real-world problems is relatively new. An artificial neural network is a computing architecture derived from a rudimentary model of the brain. It is basically an information processing paradigm composed of a large number of highly interconnected processing elements (neurons) working in unison to solve specific problems and can be implemented in either hardware or software. Artificial neural networks are generally used in pattern recognition, prediction, modeling, decision making, and optimization. One application of this technology is the recognition and identification of the chemical composition of a vapor. Sensor arrays coupled with artificial neural networks that perform automated chemical classification are often referred to as artificial or electronic noses. Several applications of this kind include food quality control, environmental monitoring, and medical diagnostic aides. The artificial neural network models we have used

in this project include the backpropagation algorithm, fuzzy ARTMAP, optimal linear associative memory, and linear perceptron.

Evaluation of these techniques consists of collecting data from sensor systems presented with known analytes (i.e., chemical vapors, chemical dyes, isotopes) and mixtures of analytes, training the artificial neural networks to identify these analytes, and then testing the artificial neural networks on additional data sets of analytes and mixtures with known compositions.

During FY 1994, we designed and built a prototype electronic nose from an array of 10 tin-oxide sensors, data acquisition system, computer, and artificial neural network software. This prototype was trained for chemical vapor recognition and was tested on eight common household and office supply chemicals. Also, the application of artificial neural network techniques to radioactive isotope identification was explored. In this application, the artificial neural network was trained to identify the isotopic composition of radiological contaminants. We implemented the optimal linear associative memory artificial neural network in software and trained it with gamma-ray spectral data provided by Westinghouse Hanford Company. The artificial neural network was successfully tested with gamma-ray spectra of eight radioactive isotopes along with mixtures of these isotopes.

In FY 1995, we concentrated on the development of artificial neural network techniques for analyzing chemical sensor data. Techniques were developed for simultaneously identifying multiple analytes with the prototype electronic nose by using both the backpropagation artificial neural network algorithm and the fuzzy ARTMAP ANN algorithm. As part of this effort, we developed a tool for building and testing fuzzy ARTMAP ANNs. Both artificial neural network techniques were used with the electronic nose and were tested on mixtures of chemical vapors with very similar results. In most cases, both artificial neural network techniques were able to correctly identify the components in the mixture. When applying artificial neural networks to sensor analysis, one must stress that artificial neural networks produce a qualitative result. In the case of mixture identification, the artificial neural networks were trained to identify the presence or absence of known analytes, not their concentrations.

In early FY 1995, we extended our FY 1994 work on the application of artificial neural networks in nuclear spectroscopy. We implemented the linear perceptron artificial neural network and compared it to the FY 1994 work with the optimal linear associative memory (OLAM). We concluded that the OLAM approach was superior over the linear perceptron for this application.

One of the objectives of this project was to identify and evaluate applications of artificial neural network technology to DOE missions. As part of this effort, we hosted the Workshop on Environmental and Energy Applications of Neural Networks at the Laboratory on March 29-31, 1995, which was cosponsored by this LDRD project. Approximately 75 participants from DOE national labs (Pacific Northwest National Laboratory, Idaho National Engineering Laboratory, Sandia National Laboratory), DOE Hanford Site contractors, universities involved with DOE projects and laboratories, industry involved in DOE related mission areas, and other Battelle facilities (Columbus, Ft. Lewis) attended and discussed applications of artificial neural networks to environmental, energy, and medical technology.

As part of our effort to develop collaborative efforts with the outside world and to provide an informal level of peer review, we continued to maintain a World Wide Web (WWW) server on the field of artificial neural networks. This server contains descriptions of our work, associated papers, tutorial information about artificial neural network technology, and hypertext links to other groups performing similar research around the world. This site can be viewed by any individual on the internet through a World Wide Web client such as Netscape, Mosaic, or Lynx and has been visited by 400 to 600 people a week. It appears to be the most comprehensive World Wide Web site on the field of neural networks. From this World Wide Web site, we have established many contacts and have had several interactions with the people browsing our site.

## Publications

P.E. Keller, L.J. Kangas, G.L. Troyer, R.T. Kouzes, and S. Hashem. 1995. "Nuclear Spectral Analysis via Artificial Neural Networks for Waste Handling Applications." *IEEE Transactions on Nuclear Science* 42, 709-715.

P.E. Keller, R.T. Kouzes, L.J. Kangas, and S. Hashem. 1995. "Transmission of Olfactory Information for Telemedicine." *Interactive Technology and the New Paradigm for Healthcare*, K. Morgan, R.M. Satava, H.B. Sieburg, R. Matteus, and J.P. Christensen (Eds), IOS Press and Ohmsha, Amsterdam, chapter 27, pp. 168-172.

## Presentations

P.E. Keller, R.T. Kouzes, L.J. Kangas, and S. Hashem. 1995. "Electronic Noses for TeleMedicine." Advanced Technology Applications to Combat Casualty Care Workshop, May 17-18, Silver Spring, Maryland.

S. Hashem, P.E. Keller, R.T. Kouzes, and L.J. Kangas. 1995. "Neural Network Based Data Analysis for Chemical Sensor Analysis." SPIE AeroSense '95 Conference, April 17-21, Orlando, Florida.

P.E. Keller, L.J. Kangas, G.L. Troyer, S. Hashem, and R.T. Kouzes. 1995. "Neural Networks for Nuclear Spectroscopy." Workshop on Environmental and Energy Applications of Neural Networks, March 30-31, Richland, Washington.

S. Hashem, P.E. Keller, R.T. Kouzes, and L.J. Kangas. 1995. "Electronic Noses and Their Applications in Environmental Monitoring." Workshop on Environmental and Energy Applications of Neural Networks, March 30-31, Richland, Washington.

P.E. Keller, R.T. Kouzes, L.J. Kangas, and S. Hashem. 1995. "Transmission of Olfactory Information for Telemedicine." *Medicine Meets Virtual Reality III*, January 19-22, San Diego, California.

P.E. Keller and R.T. Kouzes. 1994. "Gamma Spectral Analysis via Neural Networks." IEEE Nuclear Science Symposium (NSS'94), October 30 - November 5, Norfolk, Virginia.

# Parallel TEMPEST<sup>(a)</sup>

Donald S. Trent (Information Technologies)

## Project Description

The objective of this project was to produce a usable parallel version of the TEMPEST code. We debugged, documented, optimized, and verified the parallel version of TEMPEST using a number of three-dimensional test problems. A parallel TEMPEST code would improve the accuracy of the computational models by allowing the user to increase the resolution of the simulations, as well as decrease the time needed to solve problems by allowing more processors to work on different parts of the problem simultaneously.

## Technical Accomplishments

Numerical predictions of complex three-dimensional thermal-hydraulics processes are now a standard tool for mechanical and process design engineers. Although computational simulations are far less expensive than full-scale testing, the costs remain substantial to develop fast and robust numerical solutions methods. With the appearance of commercially available and affordable massively parallel computers, network of workstations and modest size symmetric multiprocessors, there is a need to develop scalable parallel algorithms to simulate large and complex problems and to take advantage of parallel processors with non-uniform memory access patterns and relatively large communication latencies.

Parallel TEMPEST was developed in 1993-1995 using the message passing model of parallel programming. Communication packages TCGMSG or MPI are used for interprocessor communication. A non-symmetric iterative linear equation solver, BiCGStab, and a hybrid iterative Krylov solver were implemented to speed up the solution of the pressure equation and the heat equation on problems using more than one processor. Using one processor, the original TEMPEST solution algorithm was more than 50 percent faster than the new algorithm. The new algorithm is more scalable. Using Argonne National Laboratory's 128 processor SP-1, we were able to achieve a speedup of more than 68 using the new algorithm on a three-dimensional thermal convection problem with 702,000 grid points.

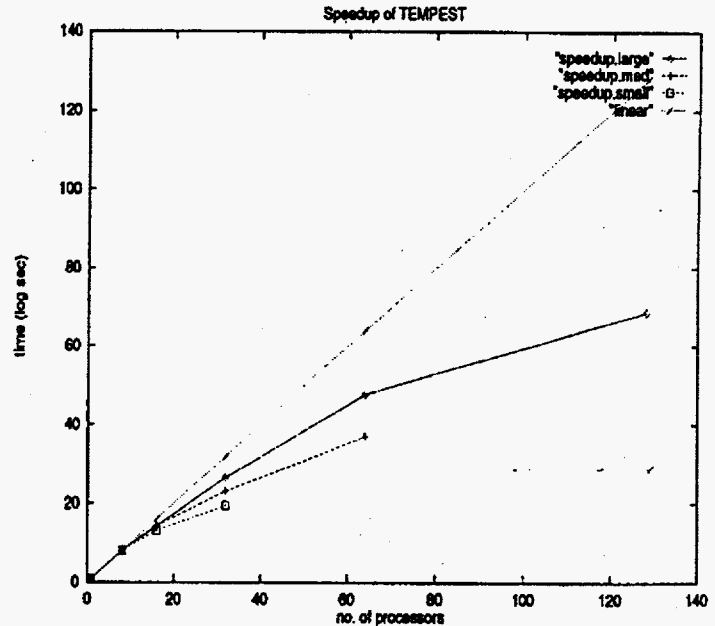


Figure 1. Speedup for thermal convection simulation of a horizontal cylindrical tank using 200,000, 500,000 and 702,000 grid points.

In real terms this means that we can solve this problem 38 times faster than is currently possible using the fastest serial version on an IBM RS6000/370 workstation. On the Laboratory's eight-processor SGI Power Challenge, we were able to achieve a speedup of 3.8 over the fastest serial version on that machine.

Problems using less than 50,000 grid points cannot achieve the same rate of performance because the latency of interprocessor communication quickly diminishes any advantage of performing arithmetic in parallel. More work is required to improve this situation.

## Publication

G. Fann and D.S. Trent. "Performance of a Parallel CFD Code TEMPEST." Accepted for *Proceedings of High Performance Computing 1996*.

(a) This project was a task under the project formerly entitled, "Computational Modeling of Complex Physical Systems."

# *Subsurface Transport in Heterogeneous Materials<sup>(a)</sup>*

Steven B. Yabusaki (Hydrology)

---

## **Project Description**

The objective of this project was to use the large memory and high performance of massively parallel processing computers to investigate new theories defining the relationship between spatial heterogeneity of physical properties and solute transport. High performance computational tools and advanced visualization techniques were developed to model ultrahigh resolution fluid behavior in saturated, heterogeneous porous media. Efficient parallel algorithms for fluid flow and transport were developed to perform numerical experiments on a realistically complex synthesized geologic data set from the Aquifer Heterogeneity Identification project. This numerical testbed allowed us to evaluate a variety of upscaling techniques and determine the conditions for useful application.

This project consisted of the following activities:

- Algorithms were developed for a massively parallel processing computer to simulate flow and advective transport through saturated, heterogeneous (discontinuous and anisotropic), three-dimensional, porous media. These algorithms accounted for the specification of unique, fully three-dimensional, second rank tensors for the conductivity at each grid cell; and advective transport of particles released into the system.
- These algorithms were applied to ultrahigh resolution (millions of grid cells) synthetic data sets.
- Visualization techniques were developed to resolve the fine details of the flow through complex, high-contrast material properties in three-dimensions.

## **Technical Accomplishments**

### *Scientific Results*

- Identified permeability scaling behavior in geologically complex groundwater systems
- identified shortcomings of standard modeling approaches
- identified the sensitivity of scaling index to the particular metric being observed (i.e., flow, velocity, travel time, transport, early and late arrivals).

- the flow and transport algorithms were incorporated into an evaluation of a stochastic convective reactive transport method.

### *Codes*

- Massively parallel flow model uses 16,777,216 grid cells of resolution
- semianalytical particle advection code accurately tracks massless particles.

## **Publications**

S.B. Yabusaki. 1995. First Pacific Northwest National Laboratory technical article placed on a public web server (<http://etd.pnl.gov:2080>), World Wide Web.

S.B. Yabusaki. "Scaling of Flow and Transport Behavior in Groundwater Systems." Research results compiled for publication in a special visualization edition of the journal, *Advances in Water Resources*.

S.B. Yabusaki. "Multidimensional, Multicomponent, Subsurface Reactive Transport in Nonuniform Velocity Fields: Code Verification Using an Advective Reactive Streamtube Approach," *Water Resources Research* (submitted).

## **Presentations**

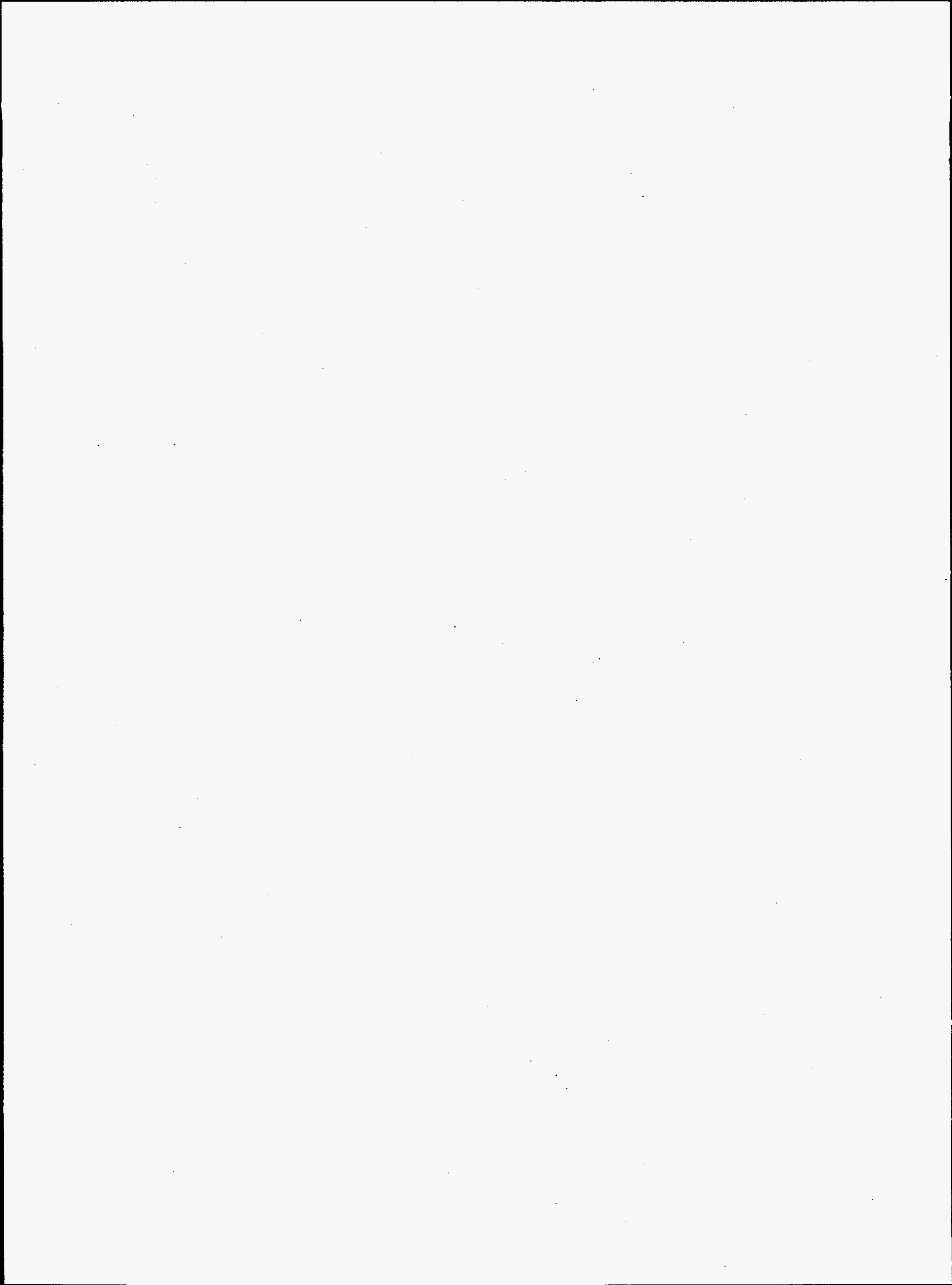
S.B. Yabusaki, C.I. Steefel, and B.D. Wood. 1995. "Assessing the Accuracy of Multicomponent Reactive Transport Models in Nonuniform Flow Fields with an Advective Reactive Streamtube Approach." Geological Society of America Annual Meeting, November 6-9, New Orleans, Louisiana.

S.B. Yabusaki, C.I. Steefel, and B.D. Wood. 1995. "Multicomponent Geochemical Transport in Complex Groundwater Systems: Verification using Stochastic-Convective Reactive Transport." 3rd SIAM Conference on Mathematical and Computational Issues in the Geosciences on February 8-10, San Antonio, Texas.

---

(a) Project was a task under the project formerly entitled, "Computational Modeling of Complex Physical Systems."

## **Design and Manufacturing Engineering**



# Industrial Modeling Expert

Joseph M. Roop (Technology Systems and Analysis)

---

## Project Description

The objective of this project was to acquire, refine, and calibrate an energy demand/environmental emissions model of the U.S. industrial sector. We proposed to acquire the Canadian Industrial Model (the Industrial Sector Technology Use Model [ISTUM-II]) from researchers at Simon Fraser University in British Columbia, who have been working with the model for a decade. The refinements proposed were modest: to organize the industries along U.S. industry lines and to make such improvements as necessary to reflect the current status of domestic industry. We renamed the model the Industrial Technology and Energy Modeling System (ITEMS), to differentiate this model from several variations of ISTUM.

## Technical Accomplishments

This project was organized to provide the Pacific Northwest National Laboratory with an operational energy end-use model of the industrial sector. Having such a model would allow the Laboratory to perform the technology analysis that would employ an operational model that allows for the investigation of alternative technological substitutions. Moreover, this tool will come at modest expense because it borrows from substantial work already done.

Over the past several years, the need for a model, such as ITEMS, has become apparent to those working in the area of industrial energy. Efforts to reinvent government suggest that metrics of performance be defined for work ongoing at the Department of Energy and other federal agencies. These efforts require tools to analyze how industry may adopt more efficient technologies developed by joint efforts of government and industry. Especially important was the need for a tool to investigate how firms purchase more energy-efficient equipment or retrofit to make energy more productive. And, there is also a need for a tool that can explore these implications for their policy consequences.

With these needs in mind, work on the six steps of the project began in October 1994, with a visit to Simon Fraser University in Burnaby, British Columbia. For nearly a week, John Nyboer trained three Laboratory staff members and a temporary staff member from the University of Washington.

The model was organized into 11 modules, one for each of the following eight industries: food processing; wood products; pulp and paper; chemicals; petroleum refining; stone, clay and glass; iron and steel; and other primary metals; and three modules that combined industries; fabricated metals and equipment (SICs 34-37), other manufacturing, and nonmanufacturing industry. ITEMS modules were constructed for food processing and the three combined industries. The other seven modules were modified (quite extensively) from Canadian modules. Then each of these modules was calibrated to Model Energy Code data.

The technology demonstration cases were selected based on conversations with staff working to provide technical information about projects under way at DOE's Office of Industrial Technologies. Three technologies were selected that are currently under development for the pulp and paper industry. AQ pulping catalysts, black liquor gasification, and impulse drying of paper. The characterization of these technologies was used to embed them into the pulp and paper module of ITEMS. Then the model was simulated to determine the penetration of these technologies and what effect their adoption might have on energy use. Of these three cases, the model suggested that one technology would penetrate rapidly; one would capture a share of the market under very favorable payback assumptions, but much higher operations and maintenance costs precluded it dominating the market. The third technology, based on the limited characterization, could not overcome much higher capital costs unless very long payback periods were assumed.

## Presentations

J.M. Roop. 1995. "ITEMS: Introduction and Overview." Presented to OIT and Invited Guests, May, Washington, D.C.

S.L. Freeman. 1995. "ITEMS: Industrial Technology and Energy Modeling System." Presented as a Poster Session, ACEEE Summer Study on Industrial Energy Efficiency, August, Grand Island, New York.

J.M. Roop. 1995. "ITEMS: Industrial Technology and Energy Modeling System." Seminar presentation at the Surrey Energy Economics Centre, October, Gilford, U.K.

# *Microscale Freeform Fabrication Using Electron-Beam Curing*

Brian K. Paul (Technology, Planning and Analysis)

---

## **Project Description**

Current competitive trends in the manufacturing industry point to future requirements for rapid product development. Manufacturing rapid prototyping technology is positioned as an enabling technology for rapid product development involving the physical fabrication of prototypes (first built models) directly from computer-aided design files. The most revolutionary of these technologies are solid freeform fabrication technologies which are additive processes that build up mechanical part prototypes one thin layer at a time.

The goal of this project was to develop a capability in solid freeform fabrication research and development to meet needs for rapid, highly flexible manufacturing technologies. The low-cost, no setup time, one of a kind, ability of solid freeform fabrication to generate parts directly from CAD/CALS files with no tooling is transformational technology. Present solid freeform fabrication techniques are based in simple laser scan polymertization techniques. Research was developed to extend the concept to more practical engineering materials and more precise technologies.

This technology base is the next generation of what the defense industrial base and industry have been trying to develop for low volume weapons systems, spares, and maintenance. The ability to take a CALS file and produce a part to order rapidly can have tremendous cost savings impacts in the defense industrial and logistics infrastructure where low volume, long lead spare parts and tooling are a problem.

One of the greatest impacts on cycle time in most production operations in discrete manufacturing is the creation of tooling for short runs of limited life cycle products, especially those based on high technology and/or rapidly evolving technologies. If the materials usable for the solid freeform fabrication technique are extendable to metals, ceramics, and other materials capable of being used as forming, molding, or casting tooling, solid freeform fabrication could become a national competitive advantage for the next century.

## **Technical Accomplishments**

Results from a survey of solid freeform fabrication literature revealed that solid freeform fabrication industrial applications are flourishing. Combined, revenues generated by the industries currently served by solid freeform fabrication technology exceed a trillion dollars per year. And, the future looks even brighter. Current wisdom sees solid freeform fabrication applications evolving from rapid prototyping to rapid fabrication in part due to the rapid progression of virtual reality-based product development technology. Applications such as rapid fabrication of stamping, forming, and molding dies; rapid development and market testing of new products; and microfabrication of three-dimensional parts each have the potential to transform industry and society.

While the future of solid freeform fabrication technology looks promising, fewer than 70 outlets exist in the United States for accessing this technology and only one exists in the Pacific Northwest. A survey of over 20 solid freeform fabrication technologies shows that the technology is currently capital intensive lacking the dimensional accuracy, build speed, surface finish, and mechanical properties to satisfy these future expectations. As a result, technology development is needed to overcome these limitations and speed the proliferation of solid freeform fabrication applications in industry.

In this project, efforts were first made to study current solid freeform fabrication processes in order to determine the causes of current limitations. Several new process concepts were identified each with large market potentials. In particular, process development was initiated for developing the freeform fabrication of high-density ceramic parts. This technology was based on a drop-gelation method of binding ceramic powder for sintering and densification. Continued effort has sought to verify the existence of new markets, develop this concept, and facilitate the deployment of new rapid prototyping process concepts.



## **Publications**

B.K. Paul and C.O. Ruud. 1995. "Rapid Prototyping and Freeform Fabrication." in (Ed.) B. Wang, *Integrated Product, Process and Enterprise Design*, Chapman & Hall.

L.O. Levine and B.K. Paul. 1995. "Implementing Technology to Enhance Your Agility." in (Eds.)

L.O. Levine and J. Montgomery, *Transition to Agile Manufacturing: A Handbook for Small to Medium-Sized Manufacturing Firms*, American Society for Quality Control.

B.K. Paul and S. Baskaran. "A Review of Particulate Materials Processing in Additive Freeform Fabrication." *Reviews in Particulate Materials*. (in process).

## **Presentation**

B.K. Paul and S. Baskara. "A Review of Additive Freeform Fabrication Techniques for the Production of Metal and Ceramic Tooling." *Twelfth International Conference on Computer-Aided Production Engineering*, August 5-7, 1995, Cookeville, Tennessee.

# *Solid Freeform Fabrication of Ceramic Membranes*

Suresh Baskaran and Gordon L. Graff (Materials Sciences)

---

## **Project Description**

Solid freeform fabrication is the machine capability to convert virtual objects, such as in a computer-aided design file, to solid objects without part-specific tooling. In solid freeform fabrication, a computer-aided design model is electronically sectioned into layers and the data transmitted to a solid freeform fabrication machine which then builds the component using a sequential, layered, or lithographic approach. Solid freeform fabrication technology is currently used for rapid prototyping, for short-run production, for mold/die making, and has the potential to significantly impact manufacturing. Some solid freeform fabrication technologies can also be used to create unique single-component designs, such as parts with internal holes or unmachineable slots.

## **Introduction**

There are many solid freeform fabrication processes, but only a few are suitable for fabricating dense structural ceramics. From an assessment of ceramic solid freeform fabrication processes in September 1994, the following needs were identified. A new or improved solid freeform fabrication process 1) must be able to fabricate components with important structural ceramic materials including alumina, zirconia, and silicon nitride (silicon nitride, in particular, is commercially important and strategically significant); 2) requires no secondary pressing or lamination operation which limits shape complexity; 3) must have the capability to form inaccessible holes/unmachineable slots; and 4) should be environmentally benign without any binder handling and removal issues.

Based on these needs, Pacific Northwest National Laboratory initiated this project to investigate the use of chemical drop-gelation on slurry layers to fabricate ceramic components.

Ceramic powder slurries containing polysaccharide alginate binders were gelled by interaction with multivalent cations, particularly calcium. Ceramic slurries were then prepared with high solids (powder) loading. In a manner similar to three-dimensional ink jet printing of binder droplets on a dry powder bed, localized

gelation in selected areas of a slurry layer was caused by impact of droplets of a salt solution. Samples were fabricated by repeatedly applying and gelling layers of the slurry. The gelled part was finally removed from the slurry, washed to remove impurity ions, dried, and sintered.

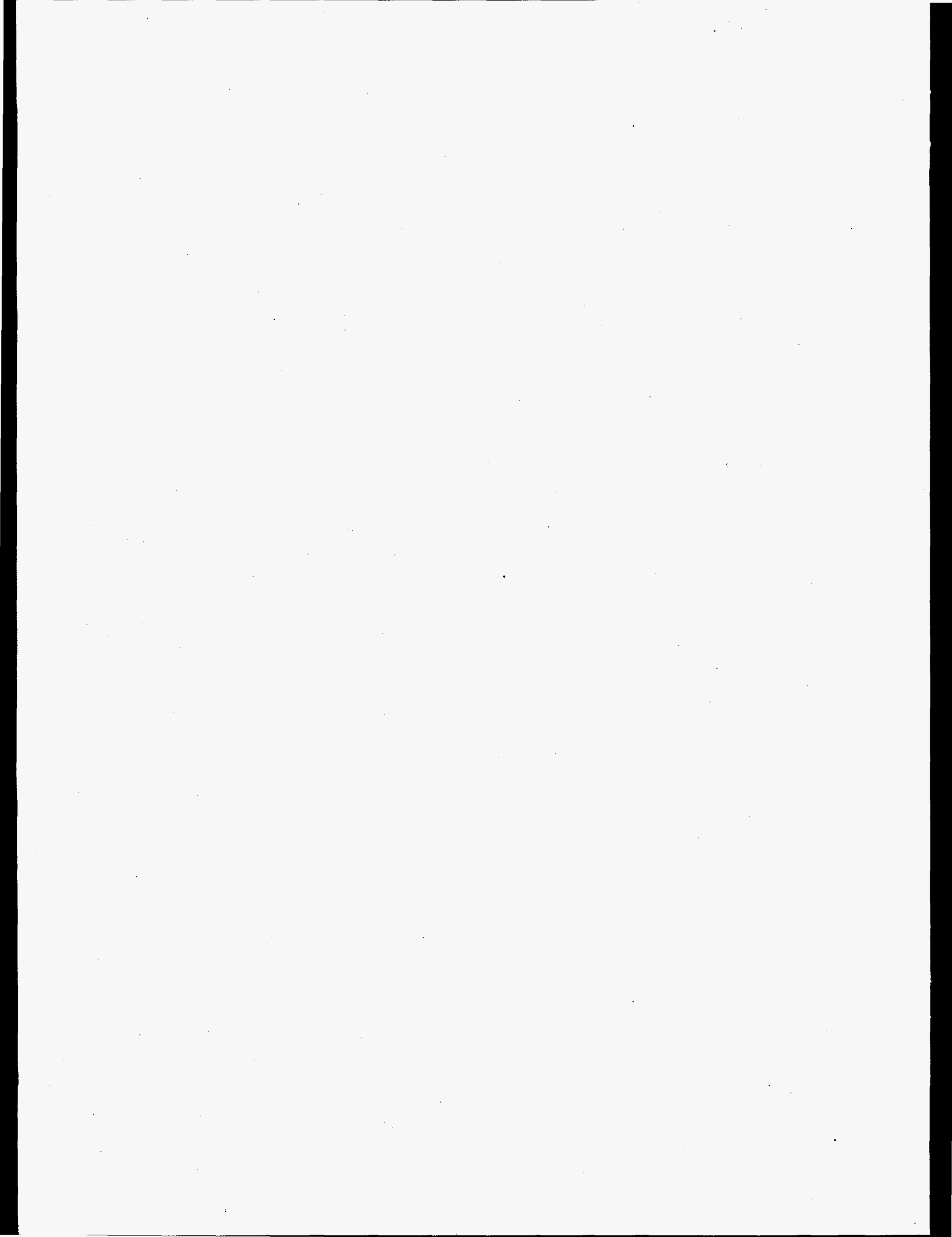
## **Technical Accomplishments**

The aqueous chemistry of alumina suspensions has been well studied, so the slurry-gelation approach was investigated with the alumina system. After initial alumina slurry development, the process approach was demonstrated using simple equipment. The slurry was leveled with a metal straight-edge to form thin layers, and calcium salt solution sprayed from an airbrush through a square stencil. Layer-to-layer bonding, and coalescence of gelled regions in the horizontal plane were demonstrated. High density alumina slabs were fabricated by sintering. Sintered layer thicknesses down to 80  $\mu\text{m}$  ( $\approx 0.003$  inch) were formed. In sections up to 8 mm thickness, no impurity contamination from the gelling process was detectable by the SEM/EDS analytical technique. The ability to form an unmachineable slot in a dense ceramic was also shown. A sintered three-walled alumina structure with an inaccessible hole in the center wall was fabricated using three different stencils.

The results indicate that, with appropriate slurry development, the process could be extended to zirconia, silicon nitride, and other ceramic powders. The wet strength of gelled slurries appears to be adequate, with further improvements possible by optimizing the binder molecular weight and amount and concentration of gelling agent. With advanced machine development, this solid freeform fabrication method can potentially be used to fabricate useful engineering ceramic components with the necessary dimensional control, surface finish, and mechanical properties.

Experiments were also conducted to investigate extrusion freeform fabrication of ceramics using a thermally gelling polysaccharide (agar) binder. Dense alumina was demonstrated by thermal drop-gelation of concentrated alumina slurries containing agar.

## **Ecological Science**



# *Ecological Modeling of Regional Responses to Global Change*

Edward J. Rykiel, Jr. (Global Environmental Change)

---

## **Project Description**

The objective of this project was to develop a strategy for building a unifying perspective at Pacific Northwest National Laboratory for understanding biogeophysical processes governing earth systems. Such an understanding is essential for evaluating questions of ecosystem vulnerability to land use and climate changes, and of sustainability of ecosystem stability, productivity, and diversity. The principal motivation is the need to link ecological, hydrological, and climate change research because 1) ecological processes determine the biosphere response to and interaction with the hydrologic and atmospheric systems; 2) current models do not simulate responses to global change that involve ecological state changes such as shifts from grassland to desert (i.e., ecological phase transition models), nor do they simulate the dynamics of change from one ecosystem type to another; 3) new species mixes are likely to come into existence as a consequence of both alien species introductions and climate change; 4) in current models, no feedbacks occur among the atmospheric, hydrologic, and ecosystem components (e.g., changes in ecosystem type do not affect streamflow or climate); and 5) national energy policies will inevitably create the need for evaluations at the ecosystem, regional, national, and global scales.

The project has three basic components

1. Research into new theoretical approaches for understanding and predicting ecological responses to global change.
2. Development of one or more process-level models that integrate ecological, hydrological, atmospheric, and human systems to simulate regional responses to global change.
3. Development of reduced-form models and their application to hypothetical policy decision making related to ecosystem vulnerability and sustainability.

The model integration research will be conducted in the context of developing a prototype global change workstation (information system) to visualize simulation of local, regional, and global dynamics. It is expected that this work will result in the development of ecological process modules and integration within the set of earth

systems models being developed and linked for global change studies at the Laboratory; a strategy to deal with spatial and temporal linkages to other modules in the earth systems model set for scaling up or down; and obtaining or accessing the necessary databases for model parameterization. Our focus areas were the Pacific Northwest region and the Yakima River watershed.

## **Technical Accomplishments**

Initial work focused on linking the Pacific Northwest National Laboratory regional climate model to the Laboratory's watershed model. This linkage was successfully accomplished, but revealed several areas where compatibilities between the two models could be improved. These areas included inconsistencies in vegetation parameterizations between the two models and lack of a subgrid parameterization for vegetation with respect to elevation in the climate model.

The problem of simulating earth system behavior at multiple spatial and temporal scales remains intractable because of computational constraints. Consequently, we have focused on developing a strategy for integrating models at scales appropriate to a particular problem domain. The computational system must, therefore, contain a model base as well as a database. The difficulty with this approach is that model inputs and outputs must be matched with a minimum of user intervention. We are examining automated systems to facilitate this development.

The problem of multiple spatial and temporal scales in global change research has been recognized as a significant stumbling block in forecasting ecosystem responses. We set out to develop a visualization system with the capability of displaying data and simulation results at any spatial scale from global to local. This work has focused on a terrain modeling scheme which is now operational and ready to accept geographic data. Although the visualization system is still in a prototype development stage, the U.S. Army has funded additional development work on a specific application to port the terrain modeling software to specially equipped personal computers to assist in field training activities. This application is an unanticipated spin-off of the terrain modeling activity and demonstrates that the uses of basic research are often impossible to predict.

Although sophisticated simulation models are useful tools for assessing the implications of global climate change, theoretical advances may also provide significant insights into ecosystem behavior. We are examining the theory of ecological phase transitions to determine if it can provide clues to ecosystem responses to land use and climate changes. We have developed examples of ecosystem behavior that can be characterized as phase transitions, and we are examining the relationship of phase transitions to ecosystem vulnerability to change and the resulting implications for ecosystem sustainability and management.

#### **Publications**

E.J. Rykiel Jr. "Testing Ecological Models: The Meaning of Validation." *Ecological Modelling* (in press).

M.S. Wigmosta, L.R. Leung, and E.J. Rykiel. "Regional Modeling of Climate-Terrestrial Ecosystem Interactions." *J. Biogeography* (in press).

W.C. Forsythe, E.J. Rykiel, Jr., R.S. Stahl, H. Wu, and R.M. Schoolfield. 1995. "A Model for Daylength as a Function of Latitude and Day of Year." *Ecological Modelling* 80:87-95.

#### **Presentations**

J.S. Risch and E.J. Rykiel. 1995. "Multiresolution Terrain Modelling for Coupled Simulation, Data Integration, and Visualization." First International Conference, Global Analysis, Interpretation and Modelling (GAIM) Core Project, International Geosphere-Biosphere Program, September 25-29, Garmisch-Partenkirchen, Germany.

E.J. Rykiel, Jr. and J.S. Risch. 1995. "Multiscale Visualization of Terrestrial Landscapes for Ecological Modelling." Annual American Institute of Biological Sciences and International Society for Ecological Modeling-North American Chapter, August 6-10, San Diego, California.

# *Optimal Decision-Making for Water Resource Management*

Lance W. Vail (Hydrology)

---

## **Project Description**

The objective of this project was to develop and demonstrate an integrated framework for management of water resources. The framework was to provide a mechanism whereby a set of existing numerical models could be linked in a manner to provide a thorough understanding of the tradeoffs involved in managing water resource systems for multiple objectives. Such objectives might include improving fish habitat, increasing hydropower production, increasing the likelihood that irrigation demands are satisfied, and reducing the likelihood of flooding. The output from such a framework was to provide both decision makers and stakeholders with adequate information for making informed decisions regarding managing water resources.

## **Technical Accomplishments**

Reservoir operating rules define the magnitude and schedule of reservoir releases under a variety of different conditions (e.g., a high-water year versus a low-water year; full reservoirs versus empty reservoirs). Water resource managers attempt to define reservoir operating rules that balance the conflicting objectives of the water system. Additionally, the lack of reliable long-term weather predictions requires the water resource manager must select operating rules that are likely to perform satisfactorily under a variety of climate conditions.

During FY 1995, we developed a framework that can be used to define the noninferior (optimal in a multiple objective sense) set of tradeoffs between multiple objectives and the reservoir operating rules that are associated with specific tradeoff decisions. A numerical search procedure based on the mechanics of natural selection and natural genetics called 'genetic algorithms' was extended from considering only a single objective to a 'Pareto genetic algorithm' that can consider multiple objectives simultaneously. A Pareto genetic algorithm can further capitalize on the parallel nature of genetic algorithms for improved computational efficiency.

Within this new integrated framework, the Pareto genetic algorithm defines the reservoir operating rules and a system response module composed of a variety of numerical models of physical and biological systems and evaluates the performance of the selected operating rules for an extended record of unregulated inflows. This extended inflow record provides a long enough period (often hundreds of years) to develop an adequate sample on which to estimate statistical performance measures for each of the objectives. The extended inflow record is developed by synthetically extending historical records employing time-series analysis methods frequently used in hydrologic sciences. The extended inflow records are translated via the reservoir operating rules into reservoir elevations and stream flows. The reservoir elevations and stream flows provide the input required to drive the models of the physical and biological systems.

To demonstrate this framework, the Shasta-Trinity system in the Central Valley of California was considered. Hydropower production, stream temperature, and flood control were the three objectives considered. Cooler water from the Trinity River is transferred into the Sacramento River through a series of tunnels. This cooler water improves the habitat for endangered anadromous fish species in the Sacramento River. Water diverted from the Trinity also represents considerably greater power generation per acre-foot than the generally warmer water released from Shasta Dam on the upper Sacramento River. Conflicting with these objectives that tend to favor increased Trinity River diversions is the need to ensure adequate flows in the Trinity River to protect endangered fish species in that river. Flood control is also an important objective of the reservoir operation.

This demonstration successfully illustrated the ability to define resource management tradeoffs for multiple conflicting objectives. The Pareto genetic algorithm's computational efficiency for such reservoir management problems can be further increased by capitalizing on the parallel nature of the algorithm. This framework is also adaptable to a variety of other resource management problems that require assessing the tradeoffs between multiple objectives.

# *Phytomechanics: Using Plants as Physiological Transducers*

Raymond J. Shippell (Environmental Technologies)

---

## **Project Description**

The objective of this study was to identify some of the missing components that currently exist in development of sensor arrays that are useful in monitoring plant transpiration, strain, health, and growth as influenced by external factors of temperature, light, humidity, irrigation, pollution, toxins, and chemicals such as insecticides and fertilizers. Ultimately, these sensor arrays may be beneficial to environmental monitoring and cleanup/restoration, and useful in national security applications.

## **Technical Accomplishments**

A plant responds to its environment in several ways. One is through alteration in the rate of transfer of water through the stems of the plant as it transpires. These changes induce extremely small variations in internal water stress and, therefore, in the size of the capillaries through which the water moves. The overall effect is minute changes in the diameter of the stems. By monitoring these changes, it is possible to observe an immediate response of a plant to its environment. The change in diameter will be related to stem-sap flow, soil water conditions, root anoxia, and oxidant stress. Utility of the long-term sap stem flow, stem strain measurements,

and soil water availability information needs to be correlated by means of time series analyses or data dependant systems (DDS) methodology.

During FY 1994, a 2-day workshop was held that brought together staff from Michigan Technological University and Pacific Northwest National Laboratory to discuss the application of plants as physiological transducers. It provided an opportunity for technical staff with common backgrounds and interests to introduce themselves and discuss mutual organizational capabilities and experiences and to identify the next step(s) in pursuing joint research.

The first steps in developing the time series analysis or data dependant systems capability were taken during FY 1995 with focus on using and analyzing existing Pacific Northwest National Laboratory collection data. Five-year data provided by the Laboratory was analyzed for growth trends and plant dynamics using a daily average for the 5-year period, annual averaged data for individual years, monthly averages, and an hourly decomposition that related growth changes with temperature and time. The analysis indicated that the data obtained under field conditions and analyzed with data dependant systems, illustrated the same trends as those generated under controlled laboratory conditions.



# *Prototype Map-Based Information Management System*

Katherine B. Miller, Charles W. Purcell, and Cynthia W. Abrams (Systems and Risk Management)

---

## **Project Description**

The objective of this research was to develop a platform-independent, modified GAP analysis template that can be successfully used to identify resources and ecosystems on federal lands without requiring extensive and expensive surveys. If successful, this could result in significant savings to DOE and other federal agencies in the conduct of analyses to determine whether ecosystems will be impacted by remedial activities. The tangible results of this project will be a proof-of-concept Geographical Information System that contains natural resource and ecosystem information for the DOE Savannah River site.

## **Technical Accomplishments**

Accomplishments during FY 1995 included the following:

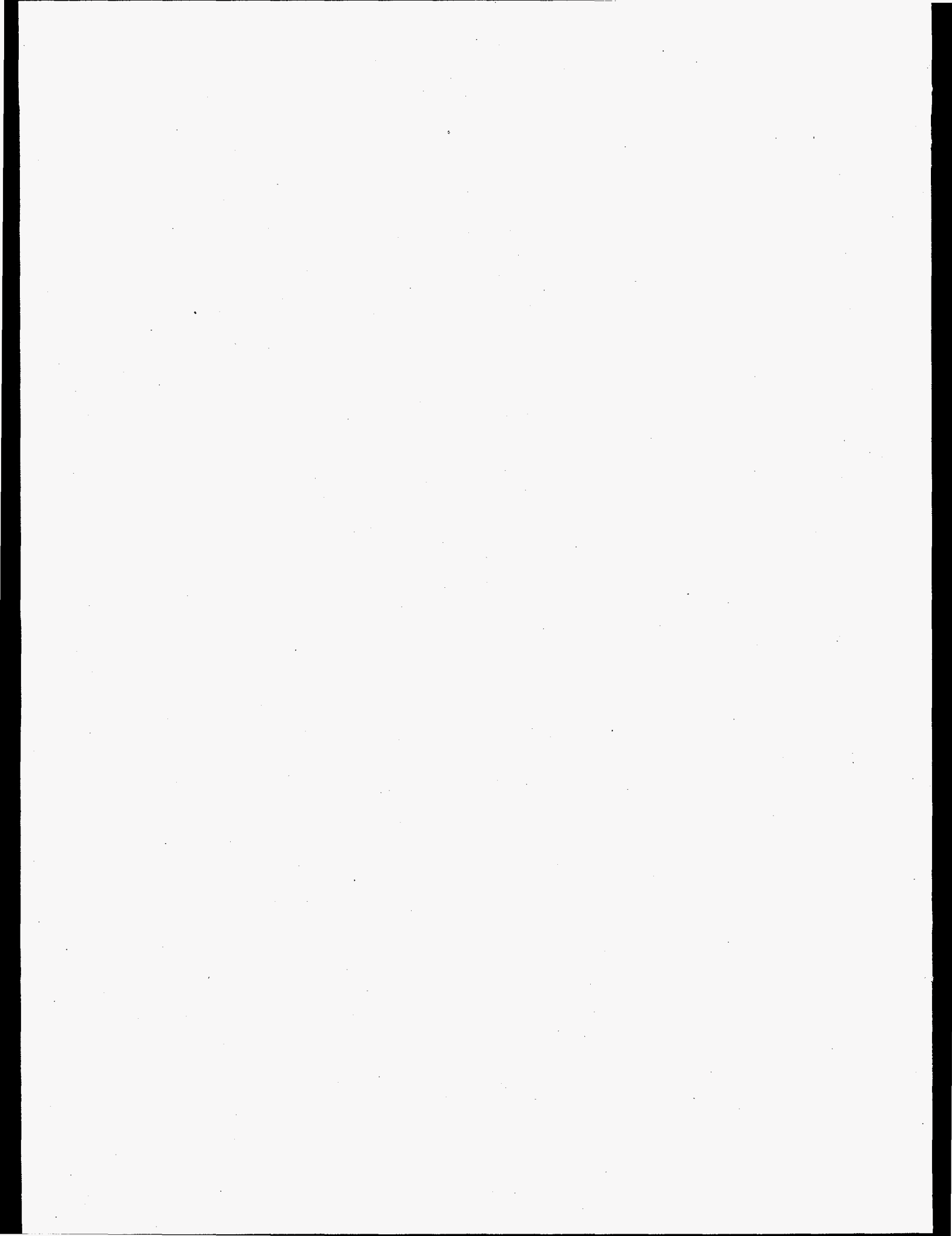
- extensive research into the modification and application of the GAP analysis concept
- identification and acquisition of geographical information software (IDRISI)
- identification and acquisition of data for the Savannah River Site which is of sufficient content to test the theory and provide some initial "ground-proofing" of the accuracy of the data.

This approach will allow DOE and other federal agencies to comply with the requirements of the national Contingency Plan, the Clean Water Act, and other regulations which require management of natural resources on an ecosystem basis. The template could also be used for facilities, such as some DOD sites that are facing closure where land use decisions may impact resources on lands currently withheld from public use.

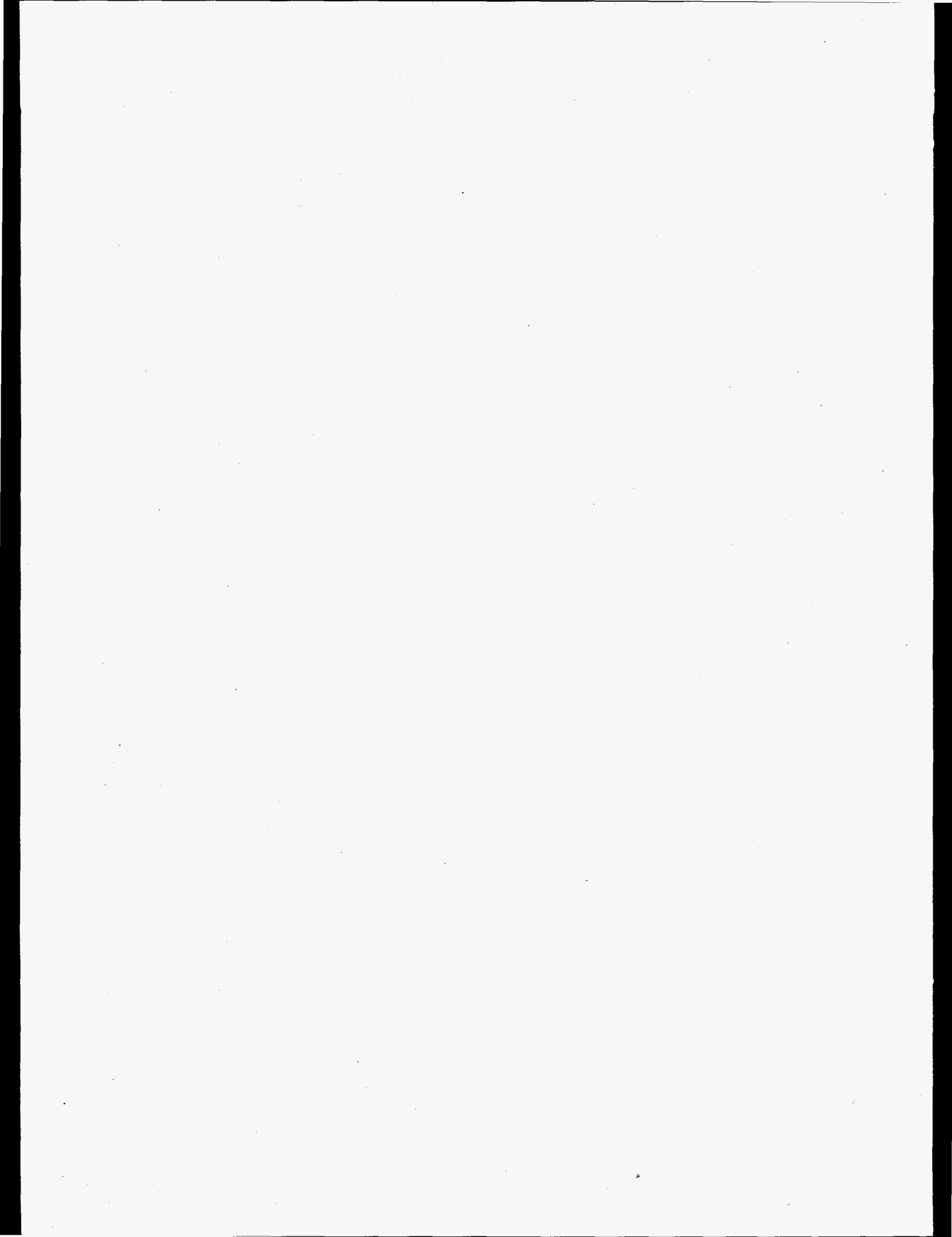
This system linkage allows decision makers and analysts to have realistic knowledge of the location and existence of natural resources and ecosystems on their facilities. In combination with other models, this template can identify potential changes to these resources over time and as a result of remedial and land use decisions being undertaken.

## **Presentation**

K.B. Miller. 1995. "Prototype Map-Based Information Management System," National Association of Environmental Professionals Conference, June 10-13, Washington, D.C.



## **Electronics and Sensors**



# *A Real-Time Adaptive Intelligent System for Sensor Validation*

Francis G. Buck and Richard J. Meador (Environmental Technologies)  
Kevin J. Adams (Information Technologies)  
Daniel R. Sisk (Health)

---

## **Project Description**

This effort was focused on developing an internal systemic approach to sensor validation that could be coupled to other system level models to demonstrate the potential for automated, real-time, condition monitoring; operational optimization; integrated degradation; and fault diagnosis. This will provide the capability for on-line engineering and operational support for reducing both the risks and the cost of operations and maintenance for industrial plants, utilities, and other process applications.

## **Technical Accomplishments**

Sensors are used to measure process variables for control, monitoring, and data collection systems. The accuracy and validity of the sensor input greatly affects the product result that uses the sensor input data. To ensure that reliable input is used, a mechanism for validating the input and flagging incorrect data is required. A sensor validation process can be developed at the system level—a group of individual components with sensor inputs—such that the energy balance (i.e., mechanical, hydraulic, electrical, etc.) of the process is used to monitor, compare, evaluate, and determine acceptability of sensor inputs.

An example of this is a typical closed loop fluid system used for heat transfer. As with an electrical circuit, an energy balance around the “loop” can be used to verify if the flow out of a node point is equal to flow into the node. Using this simple approach with a combination of direct measured values (sensor input) and derived values (calculated values from sensor inputs and design constants) a process can be developed to evaluate the multiple resultant flow determinations to authenticate the validity of the flow sensor for flow through a pipe.

Advantages to this approach include 1) the process is independent of the type of sensor used; 2) systemic level “automatic” redundancy of sensor input; and 3) can be modular based on the component building blocks that make up both mechanical and electrical process systems.

The result of this project was to complete a functional prototype for a closed loop system. During the development process, however, it was found that computational similarities due to system components was predominant rather than system type. Thus, it was determined that we would proceed in developing the two system validator types in parallel. To date, we have accomplished the following:

- The software runs on personal computers using LabWindows and runs on Sun machines using DataViews.
- The graphical user interface is drawn using a platform specific tool.
- Each component and displayed sensor value is tagged with a unique name using the graphical user interface.
- Platform specific code is written to hook into the graphical user interface.
- All other code is platform independent.
- System configuration is determined from data files describing each sensor and each component.
- The software links sensors and components to the graphical user interface based on sensor or component name as specified in the configuration files.
- The software uses the sensor configuration file to map the input data (file or Data Acquisition System) to the internal software variables.
- The software determines the operating state of each component based on the sensor values associated with that component.
- The software performs some sensor validation based on component operating states and values of related sensor.

# Cylinder Design for Reduced Emission Origins

Gregory J. Exarhos and Charles F. Windisch Jr. (Materials Sciences)

## Project Description

The objective of this project was to develop real-time optical sensors for the evaluation of oil film viscosity in the combustion chamber of a spark ignition engine. Spatial characterization of oil film viscosity in the combustion chamber will provide insight to the interactions between oil films and hydrocarbon fuel mixtures which are known to influence engine emissions, wear, and performance. Laser-induced fluorescence was targeted as a potential real-time optical sensing method because of the high intensity optical signal that results under laser excitation and the ability to excite and collect the fluorescence signals using optical fibers that facilitate coupling to an engine under operating conditions.

## Technical Accomplishments

Fluorescence depolarization measurements on a number of dye molecules introduced into lubricating oil have been conducted with a polarized laser beam. The dye molecules examined in this study include BTBP dye (*N,N-bis(2,5-di-tert-butylphenyl)-3-4-9-10-perylenedicarboximide*) and DDCI dye (*diethyldicarbocyanine iodide*). The few parts per million concentration of dye molecules are introduced to the lubricating oil as probe molecules. Fluorescence depolarization measurements are performed using vertically polarized laser light to excite an oriented population of probe molecules. The fluorescence depolarization is characterized by the anisotropy of the fluorescence intensity through measurements of the vertical and horizontal polarization intensity ratio. The depolarization ratio is dependent upon both the rotational diffusion time of the probe molecules which depends strongly on viscosity and by the fluorescence lifetime which can reflect solvent effects of the host fluid. Thus, each dye molecule candidate must be calibrated for use in each fluid host before meaningful viscosity measurements can be made.

During FY 1995, we demonstrated that the viscosity of lubricating oil can clearly be related to the fluorescence depolarization ratio of probe molecules by measuring the depolarization ratio and comparing the optically derived viscosity with independent viscosity measurements acquired using kinematic viscometer tubes. In these preliminary experiments 1 ppm DDCI was introduced into ethylene glycol, ethylene glycol:water mixtures and acetone. The viscosity of the resulting mixtures was also

measured at 21°C using a kinematic viscometer. The viscosity of the resulting fluids varied from 21 to 1.2 cP and the measured depolarization ratio varied from 0.047 to 0.436 exhibiting nearly an order of magnitude variation over this viscosity range.

To understand how dye molecules performed in the viscosity range characteristic of automotive oil, the dye molecule BTBP was introduced to Red Line base stock, fully formulated Penzoil 5-30W, and Castrol 30W oil. The depolarization ratio was measured for a bulk sample as well as an oil film on a metal substrate. Differences both in the measured depolarization ratio and the total intensity were observed between the bulk sample and the oil film where the films were less than 125 microns thick. This result suggests that surface tension of films can affect the rotational diffusion time of the probe molecules when the films are sufficiently thin thereby perturbing the depolarization ratio. The decreased total intensity results from the reduced number of probe molecules that are excited by the laser in a thin film. The doped oil was then mixed with between 0 and 100 wt% heptane and the resulting viscosity of a deposited oil film was determined using the depolarization ratio measurements described above. The results for the Red Line base stock-heptane mixtures are displayed in Figure 1. The measured viscosity exhibits a cubic decrease with increasing weight percent of heptane.

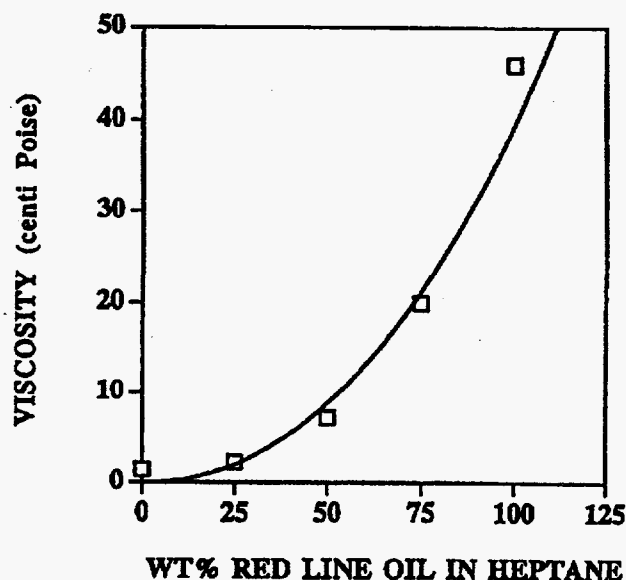


Figure 1. Optical viscosity measurements versus Heptane concentration in Red Line base oil.

The temperature dependence of the depolarization ratio of an oil film doped with the BTBP probe molecule was measured from 21°C to 135°C. Fluorescence emission spectra measured in vertical and horizontal polarizations at several temperatures are shown in Figure 2. Unexpectedly, the intensity of the fluorescence emission of BTBP increases with temperature. There are several possible explanations for this behavior. One possibility is that the observed transition is a "hot" band meaning that the population of this excited state electronic level increases with temperature. Other possibilities can be tested using fluorescence lifetime measurements. As

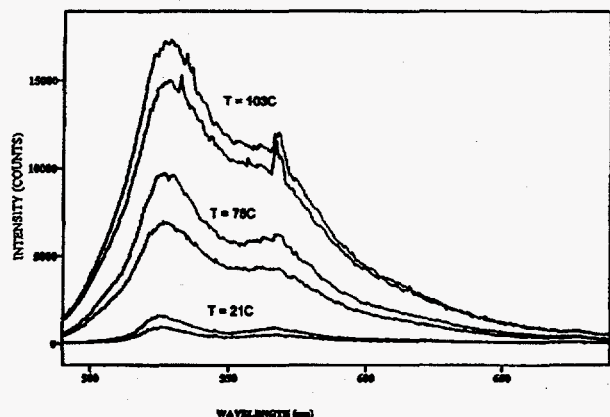


Figure 2. Laser-induced fluorescence spectra of BTBP dye in Red Line Oil. Of each temperature set, the lower trace is measured with horizontal polarization and the upper trace with vertical polarization.

expected, the depolarization ratio decreases with increasing temperature as result of the lower oil film viscosity.

Figure 3 displays the expected linear relationship between the natural log of the calculated viscosity and  $1/T$ .

The prospect of using fluorescence emission spectra as a real-time optical sensor of oil film viscosity, and perhaps temperature and film thickness, in a combustion chamber is promising.

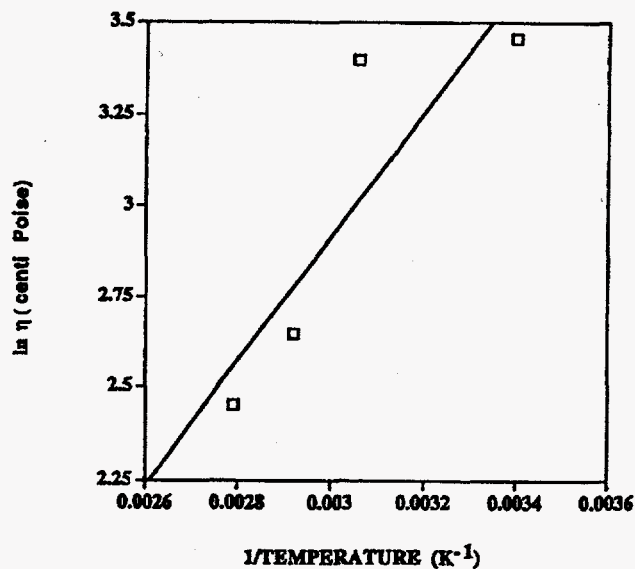


Figure 3. Temperature Dependence of Viscosity

# *Development of Two-Dimensional Electrochemistry for Sensor Applications*

Peter C. Rieke (Materials and Chemical Sciences)

---

## **Project Description**

We proposed to develop a potential sensor based on a unique two-dimensional electrochemical system. Self-assembled monolayers terminated in sulfonic acid groups can be formed on silica substrates containing interdigitated electrodes. Preliminary electrochemical experiments have demonstrated that the sulfonic acid groups act as a two-dimensional electrolyte, and that ionic conduction occurs via proton transfer between the fixed sulfonic acid groups. We have also demonstrated that redox reactions may be performed at the electrodes. Unlike conventional electrochemical systems, the system contains no bulk electrolytes and the self-assembled monolayers layer can be in direct contact with a gas phase. This system has considerable promise as a new type of sensor and for miniature batteries or fuel cells. Based on these preliminary experiments, we propose to optimize the construction and performance of the self-assembled monolayers/interdigitated electrodes array and to demonstrate their use as a sensor for gas phase analytes with emphasis on hydrogen and amines.

## **Technical Accomplishments**

Initial work focused on depositing self-assembled monolayers on the interdigitated electrodes and successfully sulfonating these. The major problem is that the quartz substrates do not support self-assembled monolayers formation as well as the more commonly used silica substrates. Despite this, with some manipulation of the deposition condition we were able to obtain reasonable self-assembled monolayers coverage as determined by advancing contact angles.

Some deposition conditions resulted in destruction of the interdigitated electrodes fingers and hence made the devices useless. There was quite a bit a variability between batches of devices. On some of the batches, it was virtually impossible to deposit a good self-assembled

monolayer without destroying the interdigitated electrodes. By working with the manufacturer we were able to obtain interdigitated electrodes that would withstand the self-assembled monolayers deposition conditions. This was very discouraging work and occupied a great deal of time before resolution.

Initial conductivity experiments focused on eliminating measurement artifacts from the impedance analyzer. The impedance of the interdigitated electrode devices is sufficiently high that the impedance of the instrument makes a significant contribution to the signal. Some time was spent determining the frequency range and experimental conditions which were appropriate and gave believable results. The Laboratory recently acquired a new alternating current impedance apparatus with much higher input impedance, and this should extend the reliable range of our measurements. Unfortunately, these effects are an occupational hazard of alternating current impedance.

The above problems prevented us from making the progress we expected; however, we were able to extend the initial work with some preliminary experiments. The initial experiments results concerning the effect of percentage sulfonate on mixed self-assembled monolayers was repeated and the influence of humidity was confirmed. This assured us that the new electrodes were functioning in the same manner as the old electrodes.

We also converted some of the 100 percent self-assembled monolayers to the sodium form by immersion in NaCl solution and washing with water. X-ray photoelectron spectroscopy indicated the presence of sodium in appreciable amounts but we were not able to obtain quantitatively accurate results. Alternating current impedance measurements showed that these devices were substantially more resistive than the acid form and that higher levels of humidity were required to obtain sufficient conductivity. Impedance was again high enough that obtaining reliable measurements was difficult.



# *Low Cost Sensing Technology for Operations and Maintenance Applications*

Chester L. Shepard and Norman C. Anheier (Energy)

---

## **Project Description**

In order to make any industrial process as efficient as possible, real-time control with the correct number of sensors to measure the needed process parameters is required. While sensors exist today that can measure almost any physical parameter desired, high cost per sensing point often precludes integrating these sensors in the quantities that are required for process control. Installation, maintenance, and calibration, as well as the cost of the actual sensor are major factors in determining the cost per sensor point. This project addresses several key aspects that can significantly reduce the cost per sensor point.

## **Background**

The primary goals of this project were the identification and subsequent development of technologies which are applicable in industrial facilities. We were seeking not necessarily new measurement methods, but more cost-effective measurement methods. To this end the entire process of performing measurements in industrial plants was examined and barriers to the use of sensors were identified. The costs of measurements involve not only the initial instrumentation costs but also installation costs, maintenance costs, and utilization costs. Fiber optic sensors are attractive because their use can greatly reduce installation costs (fewer wires). Process powered sensors which derive the necessary power for their operation from some process which occurs in their operating environment are also attractive for the same reason. Two technologies were identified which conformed to our selection criteria.

The first technology we developed was the gas composition instrument. If successful this instrument will provide a significant cost reduction in measurement of, for example, the concentration of various molecular constituents in a natural gas stream. While our efforts have been and will continue to be in demonstrating the feasibility of this measurement method, which is quite novel, in the long term this device can be deployed in situ in the field and can be powered by natural gas combustion in a miniature fuel cell, and instrument communication with a distant data processing center could be wireless. Presently the gas industry verifies the content of their product by collecting gas samples either at field sites or at

distribution points and then analyzing these samples in a laboratory by standard means such as mass spectroscopy, a highly reliable and very accurate method. However, the entire measurement process is quite costly and there is strong interest on the part of the gas industry in reducing the costs.

The second technology which we are developing is a sensor platform. Our efforts have been in the direction of including wider dynamic range and improved "smart" operation capability in existing devices. The platform provides electric power to any of several sensors connected to it and reads and digitizes the analog outputs from the sensors. In addition, isolation from high voltages is provided as well as immunity from electromagnetic noise. A very good application for this technology is in the electric power industry where current and voltage in high tension transmission lines must be measured. Bulky and expensive transformers can be replaced with these devices, resulting in lower equipment, installation, and maintenance costs; and improved safety.

## **Technical Accomplishments**

Significant progress was made in laboratory studies with the gas composition instrument. We first performed initial feasibility experiments using existing components and spare parts in order to show promise for the idea. Calculations were performed to simulate an experiment and determine the measurement accuracy required for the pressure transducer. It turns out that exceptional accuracy is required. We then procured the best commercial pressure transducer available and built a prototype instrument. Limited testing with pure gases and air were performed in order to determine the performance characteristics of the instrument. Components of air were determined to within about 1 percent (of total gas) accuracy. Argon and water vapor in air are presently just barely resolvable. Testing with this prototype will continue in FY 1996 in order to further develop the analytical model and investigate other mathematical methods for data analysis.

Technical progress on the sensor platform was not as great due to the late start of this task (June 1995). We attended a conference where the needs of the electric power industry for sensor development were widely

discussed. We met several times with Bonneville Power Administration representatives and a commercial supplier in order to plan the project and determine performance requirements for the sensor platform. We purchased a commercial unit and components, such as a low-power 16-bit analog-to-digital converter, for modifying the unit. Testing of the commercial unit has been completed. Plans for field tests with prototype units have been completed and arrangements with Bonneville Power Administration

for use of their site are nearly finalized. We will apply the sensor platform for measurement of current in high voltage transmission lines and compare its performance with standard measurement methods. Two prototype sensor platforms will be fabricated in FY 1996 and tested at Bonneville Power Administration field sites. The second prototype will be built after evaluation of field tests with the first prototype. This final prototype will also undergo field testing.

# Materials Evaluation

Margaret S. Greenwood, Robert V. Harris, and George J. Schuster  
(Automation and Measurement Sciences)

---

## Project Description

The United States infrastructure is in rapid decline due to neglect and a lack of understanding of material behavior in the harsh environments they are subjected to. The primitive state of nondestructive material characterization methods prevent timely detection and measurement of material degradation, which may subsequently lead to catastrophic failure. The intent of this research is to initiate a systematic scientific investigation of the interaction of a variety of probing modalities with the material, in order to extract material parameters useful in predicting failure and estimating remaining life of the structure under test.

## Technical Accomplishments

The first step was a selection of the material property to be investigated. Toward that end, a literature search was undertaken to determine the current state of research on the following properties: residual stress, applied stress, texture, grain size, precipitation hardening, Young's modulus, density, yield strength, tensile strength, and Poisson's ratio. As a result of this literature search, the property selected was residual stress.

While there are several techniques for measuring the stress near the surface of a component, there are no nondestructive methods for measuring the stress within that component. One method had been suggested by the theoretical studies of Wallace Anderson. He suggested that a pulse of heat applied to the end of a rod, with an applied stress at a certain distance from one end, could indicate the location of the stress. The measurement would be a velocity change due to the change in temperature. This method was analyzed using numerical techniques and we found that the resulting velocity change would be extremely small. The conclusion was that this method would not be appropriate for our research on stress. A report of the complete analysis was prepared.

It was decided to use surface waves to measure residual stress at or near a surface. It is well known that the velocity of ultrasonic surface waves changes slightly with the stress. The objective was to use this property to determine stress on the surface as well as several millimeters below the surface by using waves of different frequency. The penetration depth of the surface waves is

approximately equal to 1.5 wavelengths. The plan of the experiment was to use EMATs (electromagnetic acoustic transducer) that required no liquid couplant to the surface (as piezoelectric transducers do). The frequencies of 0.5 MHz, 1.0 MHz, and 2.0 MHz would penetrate to depths of 9 mm, 4 mm, and 2 mm, respectively. Thus, stress as a function of depth could be obtained. The EMATs were specially designed for our experiment.

The measurements were obtained by placing three EMATs in a straight line on the surface of the test piece. The transmitting EMAT produced the ultrasonic surface wave in the form of an eight-cycle sine wave that traveled to the two receiving EMATs. The signal from each receiving EMAT was captured on a digital oscilloscope. A cross-correlation program was written to give the time difference between the signals, where the increment in time was 0.25 nanoseconds. This program was checked out using signals from piezoelectric transducers. Two test specimens of stainless steel 304 were designed and fabricated. The first was a calibration standard that was designed for use with a tensile testing machine that could apply a force up to 70,000 pounds. The objective was to determine the velocity change due to a known uniform stress and to determine a calibration curve. Then, the second piece would be stressed in a way to produce a distribution of stresses. This stress at a point would be determined by measuring the velocity, and from the known calibration, the stress at that point. In this way the stress distribution of the part could be determined.

In June 1995, the experimental setup was moved from 2400 Stevens to Bldg 326 and set up on the tensile testing machine. After one month of testing, using various methods to try to reduce the noise, the analysis of the data showed that it was not possible by this method to see the small changes in time required. This was attributed to the noise that accompanied the random-interleaved sampling method of the digital oscilloscope and the fact that many averages had to be taken to reduce the noise inherent in EMAT measurements with stainless steel. The measurements were just "too washed out" to show the small time differences necessary.

The remaining funds were used to develop another experimental technique and to fabricate an aluminum specimen. The EMATs were set up using a Matec system that measures the time difference by measuring changes in phase. The computer was programmed to record the

values and take averages of a large number of readings. The system is currently working and we are planning to take experimental data to test whether this system will measure the time change with sufficient accuracy for stainless steel. If, however, the experimental error is too large with stainless steel, then we shall make measurements using the aluminum specimen. The signal-to-noise ratio is much larger for aluminum than for

stainless steel. The aluminum, however, has residual stresses in order to increase the yield strength. The feasibility of this second method will be tested. Since funding is not now available, the plan is to supervise a Science and Engineering Research Semester student in taking many more sets of measurements and to write a paper on these results.

# Process Control System Development

Ronald L. Hockey (Energy)

## Project Description

A series of experiments were conducted in testing a new concept, based on electromagnetic induction, for nondestructive detection of flaws in sheet metal moving at high speed. Ultrasonic methods, developed for this purpose in the past, have had only limited success at low speeds and very little success at high speed.

Sheet metal is known to contain various amounts of nonmetallic inclusions, ranging from trace amounts to significant concentrations. If inclusion content becomes large enough, the end product can be adversely affected. Some of the more common types of nonmetallic inclusion materials are silicon dioxide and aluminum oxides. Inclusions are not found uniformly distributed throughout sheet stock. They tend to appear in clusters, usually elongated strings due to the rolling processes involved in making sheet stock.

This project was limited to proof-of-concept experimentation using synthetic inclusions (drill holes and saw cuts) in aluminum and steel plus a limited number of tests using steel with inclusions at the surface. Testing included sheet metal moving past a magnet and sense coil in the 5,000 to 10,000 feet per minute speed range.

## Technical Accomplishments

A feasibility study completed by the authors a few years ago showed that an eddy current technique could detect some nonmetallic inclusions in low-carbon steel moving at low (below 200 feet per minute) speed. The speed limitation resulted from the eddy current instrument not responding fast enough to inspect sheet metal moving at normal processing speeds. Rather than inducing currents into the metal while measuring coil impedance, the motion of the metal sheet was used to induce current as it passes over a fixed magnetic field. The voltage developed across a sense coil is monitored to detect changes in the induced current caused by resistivity changes in the metal.

Voltage measured across the coil remained zero until a flaw (or resistivity change) moved into the magnetic field and altered the induced current distribution. When the current distribution was distorted by a simulated, nonmetallic inclusion, voltage was found to develop across the sense coil, in proportion to the volume of nonconductive material.

As a starting point to establishing sensitivity, 25 cm diameter metal disks were made from 2 to 3 mm thick aluminum and steel sheet stock. Each disk had a center hole for mounting to the table saw arbor. Flaws, consisting of drill holes and notches, of various sizes were also machined into each disk to simulate large nonmetallic inclusions. With the disk rotating at about 3,000 rpm, the magnet was slowly moved into position causing disk rotation to decrease by about 500 to 800 rpm, due to the opposing torque that develops on the saw motor from the applied magnetic field.

The z-axis of the precision scanner was stepped in increments of about 0.5 mm, after the magnet and sense coil were held on one radial location long enough to record one complete revolution of the rotating disk. The raster pattern that was recorded made it possible to image the flaw pattern and adjust the coil position relative to the magnet field for improved performance.

Figure 1 shows the sense coil voltage when a 2.2 mm thick aluminum disk, with a series of radial slots and holes, was tested. This voltage versus position data is unfiltered and has a signal-to-noise ratio large enough to detect a 0.5 mm diameter through-hole. The smallest drill hole detected to date with this technique is 0.38 mm in diameter and 20 percent through-wall. Smaller holes were not examined in this limited proof-of-principle test but are expected to be detectable once the instrumentation is optimized for smaller defects. Several sheets of steel with inclusions breaking the surface were tested, but no destructive testing was performed for verification.

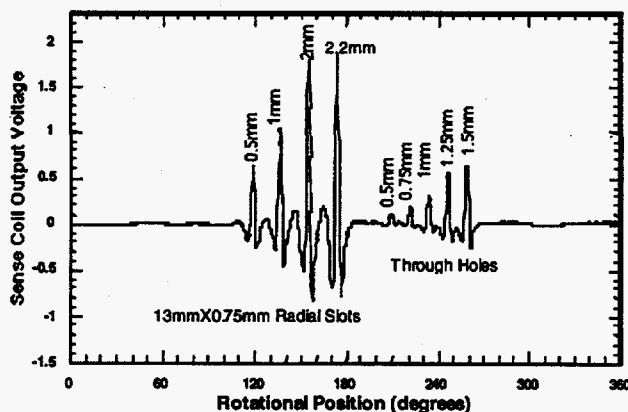


Figure 1. Sense coil voltage versus angular position on aluminum disk containing holes and saw cuts.

A similar test was conducted using a steel disk. Unfiltered raster images of the sense coil voltage were recorded when scanned radially over a 2.2 mm thick steel disk. The flaws are four through-holes with diameters ranging from 1.5 mm down to 0.5 mm and five 0.5 mm diameter holes drilled to depths of 50 to 25 percent through-disk. The partial through-disk holes were drilled from both sides showing this method to be more sensitive to flaw volume than flaw depth. One of the saw cut slots was oriented along a radius and the other perpendicular.

As mentioned above, two pieces of steel sheet (0.25 mm thick), one with inclusions seen breaking the surface and another without surface-breaking inclusions, were inspected by this method. Results in the form of a gray-scale image are shown in Figures 2a and 2b. The large indication appearing near the 330 degree position is a drill hole, used as reference in both cases. Only about one half of the inclusions seen breaking the surface align with light gray indications whereas the other half did not correlate with any particular portion of the gray-scale voltage spectrum. Relatively few light gray (higher voltage) regions were found in the steel sheet without surface-breaking inclusion.

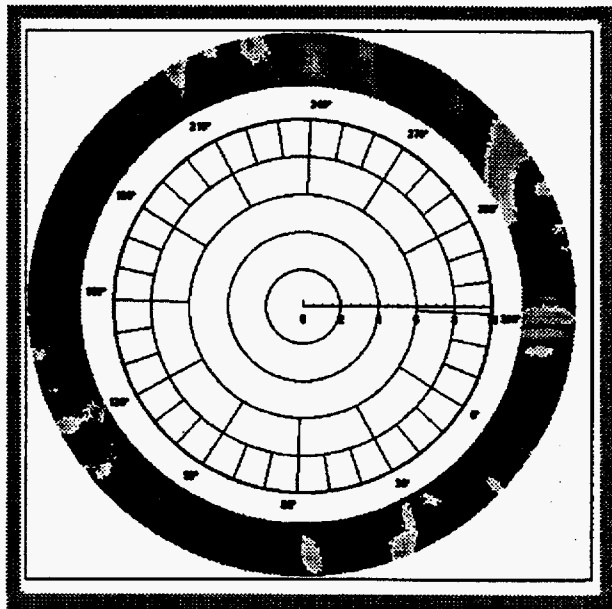


Figure 2a. Radial scan of thin steel disk with inclusions seen at surface.

This technique shows promise for detecting small nonmetallic inclusions in sheet metal moving at high speed; but without metallographic comparison, it is difficult to quantify its effectiveness in measuring inclusion content or sizing capabilities. The images in Figure 2 imply that this method can detect more inclusions in the steel with inclusions seen breaking the surface than a sheet without surface-breaking inclusions. However, Figure 2b does not prove there are no inclusions present; and the sheet tested to obtain Figure 2a could have had inclusions beneath the surface. Therefore, until destructive testing (like an acid etching) is completed, few conclusions can be derived regarding this technique's capability unless results from another method (like x-ray) become available.

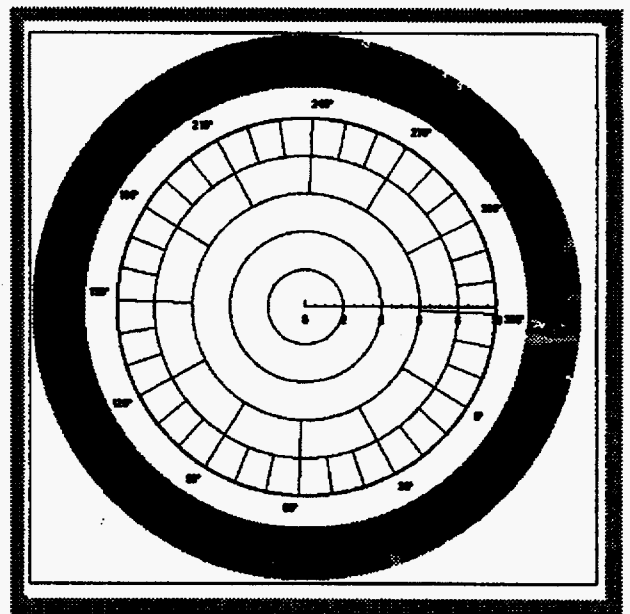


Figure 2b. Radial scan of thin steel disk without inclusions seen at surface.

#### Publication and Presentation

R. Hockey, D. Riechers, R. Ferris, and R. Kelly. 1995. "Passive Pulsed Eddy Current Inspection of Sheet Metal." Presented at and In *Proceedings of the Review of Progress in Quantitative Nondestructive Evaluation*; Annual Conference, University of Washington, July 30-August 4, Seattle, Washington.

# *Remote Automobile Performance and Emission Monitor*

Kevin B. Widener and Ronald W. Gilbert (Electronic Systems)

---

## **Project Description**

The objective of this project was to demonstrate the successful integration of currently available automobile sensing technology, provide a means of analyzing the data from these sensors, and remotely telemeter the data to a collection system. We believe such a system could eventually be incorporated in DOE's fleet of government vehicles (beginning with Hanford) to identify automobiles that are not performing up to specifications with regards to gas mileage and emissions.

## **Technical Accomplishments**

As part of this project, a microcontroller-based data acquisition system was designed and prototyped that directly interfaced to the diagnostic computer of a automobile. Software was written to read the asynchronous data and decode the diagnostic messages. These diagnostic messages were then serially communicated to an active radio-frequency transponder. The transponder was read by the interrogator unit. The

data read by the interrogator were then read by a personal computer. Software was developed to communicate with the radio-frequency interrogator and display the data as output by the automobile's diagnostic computer.

Once the hardware and software were integrated and debugged in the laboratory, the developed systems were installed in a late model vehicle. Testing and verification of the system was accomplished by driving the vehicle at highway speeds. The system worked well.

The demonstration was documented with videotape and is available for viewing.

Throughout the development of this project, we found several companies that made instruments that read diagnostic port information but none that radio-frequency telemetered the data to a central collection point. We also found that data formats from current vehicles are proprietary. However, there are Society of Automotive Engineers standards that are to be implemented by U.S. car manufacturers in the near future.

# *Ultrasonic Measurement of Elastic Properties of Bone*

Gerald J. Posakony and Robert V. Harris (Imaging and Nondestructive Evaluation)

---

## **Project Description**

The objective of this project was to evaluate ultrasonic techniques and procedures that might be used to determine the density and/or structure of cancellous bones in the human body. The present accepted method for establishing bone density is through the use of radiographic densitometers. While effective, the equipment required and the procedures followed are relatively expensive. The goal of this project was to develop an inexpensive, non-invasive, alternate procedure that could be used by a physician to screen individuals for low-density bone mass that could indicate conditions such as osteoporosis.

## **Technical Accomplishments**

In the FY 1994 phase of this project, laboratory studies showed a direct relationship between ultrasonic attenuation and test frequency for a small group of 12 cadaver calcanei (heel bones). This indicated that different cancellous structures had different attenuation coefficients. Ultrasonic attenuation in the calcaneus can be attributed principally to scatter of the ultrasonic energy in the cancellous structure of the bone. Tests were made at ultrasonic frequencies from 140 kHz to 1250 kHz. Other parameters such as ultrasonic velocity and backscatter were found to be ineffective indicators of bone structure. Velocity varied little among the cancellous bone structures. Backscatter data, while present, was highly variable as it depended on the location at which the measurements were made. The importance of these initial studies was the observation that test frequencies between 500 and 1000 kHz gave a much wider range of attenuation values than frequencies below 500 kHz which implied that more quantitative information could be gained through measurements in the higher frequency range. In all measurements a through-transmission technique was used and the transmitting transducers were designed to ensure that measurements were made in the far-field of the sound-field pattern. Further, a small diameter (1 mm) receiving transducer was used to minimize the influence of phase interference of the received signal.

During FY 1995, the study was expanded to include an additional 100 calcaneus bones and new test procedures that could be used for ultrasonically defining the attenuation versus density response. Further, studies were made to determine the most effective frequency range for

making density and/or bone structure measurements. A frequency range from 600 to 800 kHz was found to be the best compromise for frequency related measurements of cancellous structure. In this frequency range the attenuation differences in the values that were obtained ranged from a low of about 10 dB to a high of over 40 dB. Above 800 kHz the increased scatter from the cancellous structures in some bones resulted in ambiguous attenuation data. Below 600 kHz the attenuation differences between the bones in the study group decreased and at a frequency of 140 kHz the total range was only about 5 dB.

The initial study showed a relationship between ultrasonic attenuation and test frequency. While these parameters were of technical interest, using these values for diagnostic purposes would require extensive clinical studies to establish the value of the relationship.

During the second phase of the study, a decision was reached to establish a relationship between ultrasonic attenuation and bone density. Test frequencies from 250 kHz and 1000 kHz were repeated. Again it was determined that the frequency range between 600 kHz and 800 kHz would be the most valuable and tests were performed on 100 bones at these frequencies. Density measurement of each of the bones was determined using a precision balance to measure weight and the water displacement method to determine volume. In the first instance, the entire bone density of the entire bone was used and these values were plotted against the attenuation measurements. A plot of these results showed no apparent relationship between attenuation and density. This resulted in a re-evaluation of the focus of the project to establish whether the concept was applicable.

Destructive correlation of several of the bones established a very substantial difference in the cancellous structure between the bottom and top of the bone. Since the location at which the measurements were made varied from bone to bone, it was felt that this was the uncontrolled variable that caused the lack of relationship between the ultrasonic attenuation and density measurements. To resolve the problem, a 2-cm diamond core drill was used to core 50 of the bones. The cores were taken at a center distance of approximately 2 cm from the base or bottom of the bone. Attenuation measurements were made of the cored bones at frequencies of 600 and 800 kHz. The Figure 1 plot shows ultrasonic attenuation versus density of the cored bones



using a test frequency of 800 kHz. Since the ultrasonic beam propagated thorough the center of the cored section of bone, the measurement should reflect the cancellous structure in this region. The bone density of the cored sections ranged from a low of about 0.19 to a high of 0.39. Attenuation, vertical axis, varied from a low of 14 dB to a high of 40 dB. The higher attenuation related to the higher density. The least-squares correlation coefficient for the data was calculated at 0.87 which is considered very good for these initial tests.

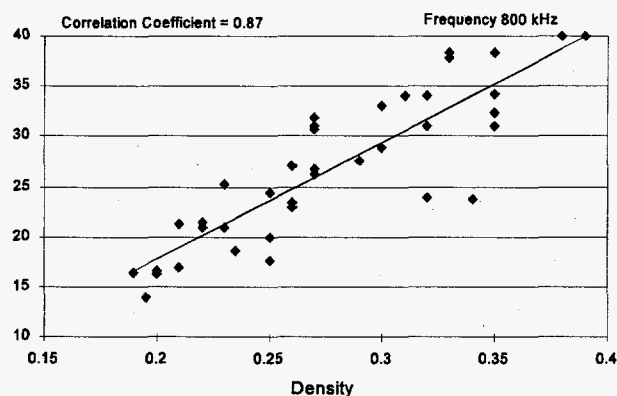
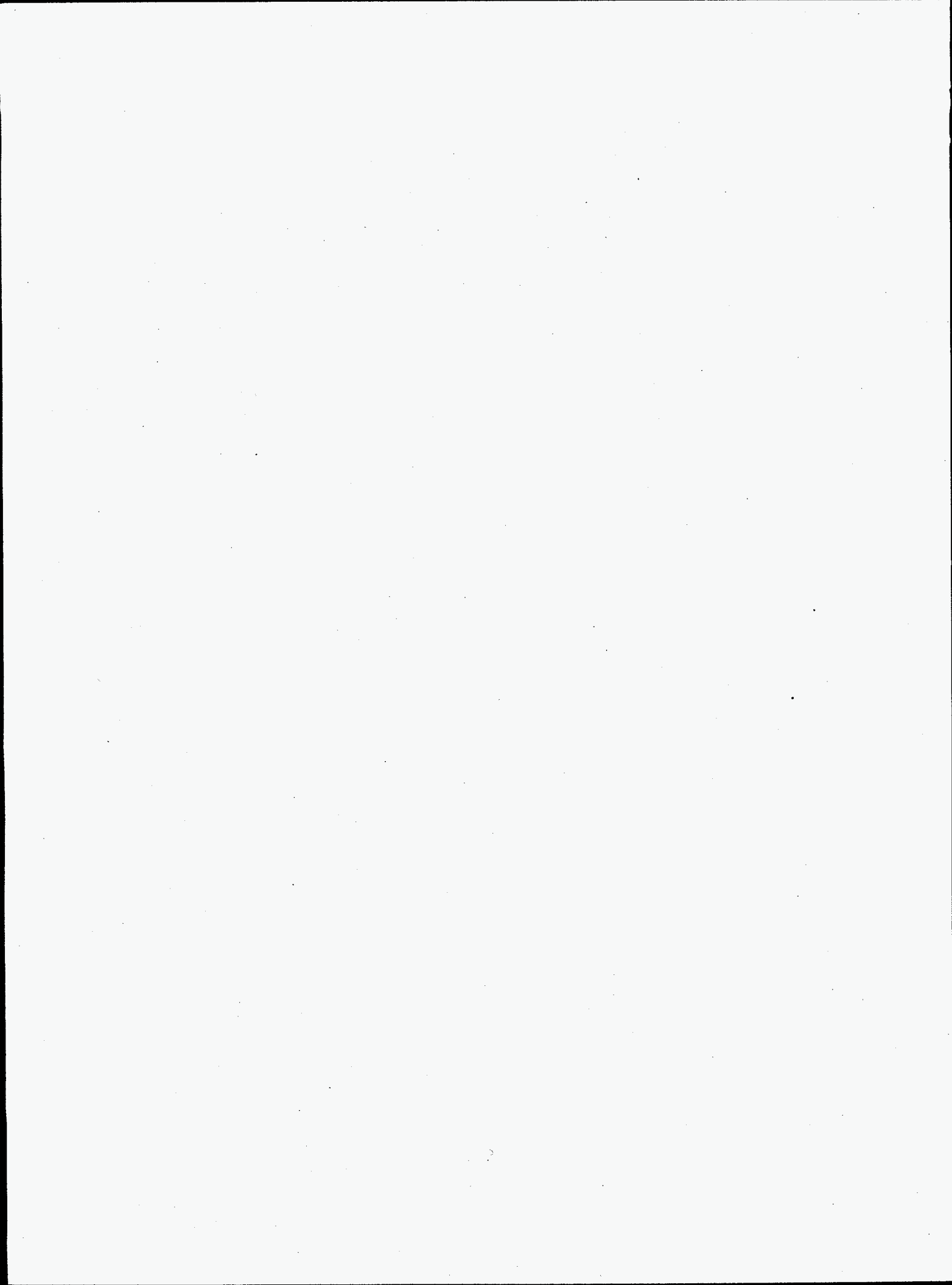


Figure 1. Plot of Attenuation versus Density

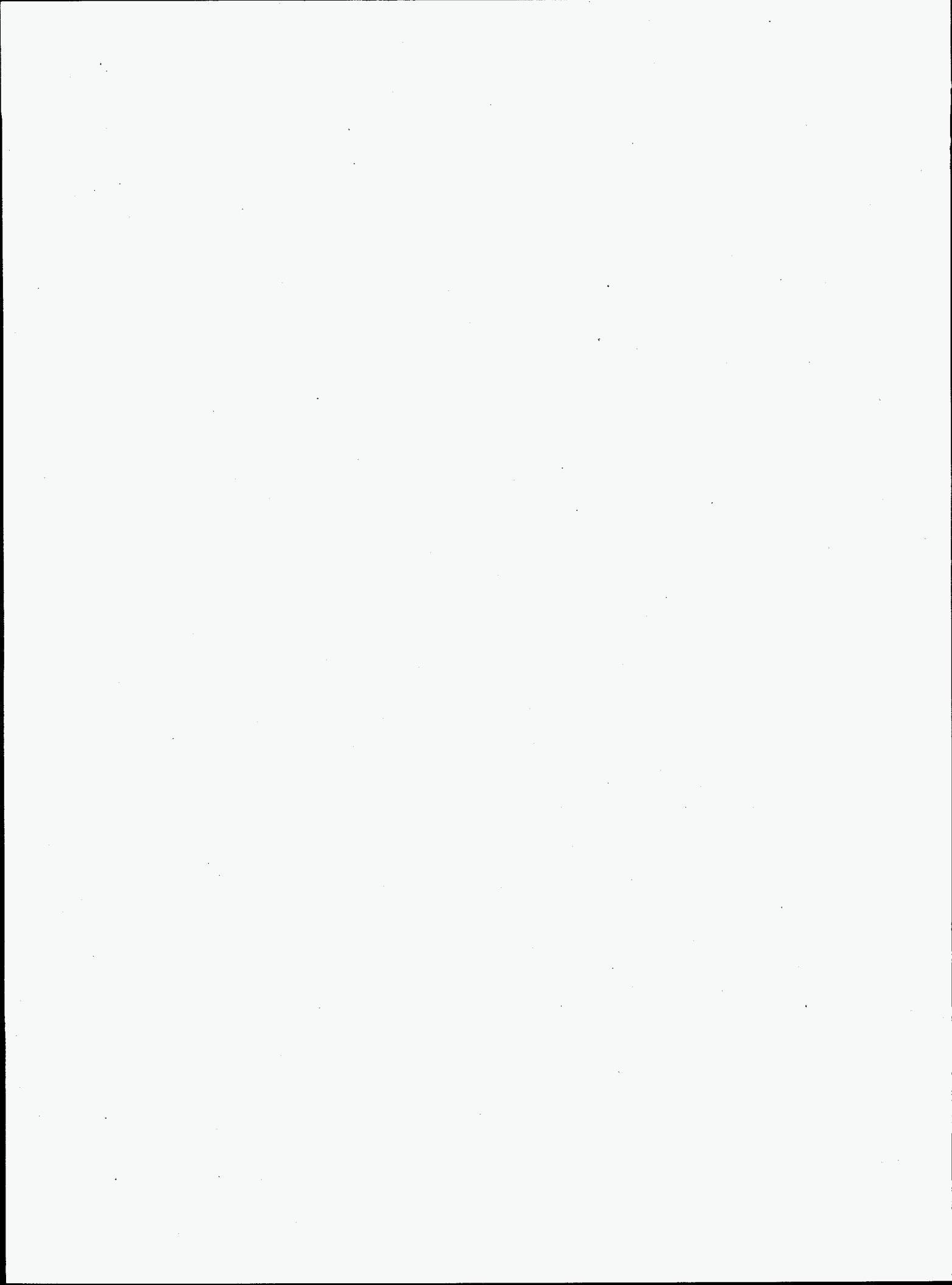
The results of these measurements are very encouraging. At the ultrasonic frequency used for the measurement, there is an apparent direct relationship between the attenuation and density. There are several "outliers" which may have been the result of cored bones which had a varied cancellous structure through the area measured. Further studies need to be made to determine the exact causes of the outliers and to further enhance the value of the correlation coefficient.

Questions have been posed regarding differences that might be anticipated between living bones and the cadaver bones used for the study. In the laboratory experiments, the cadaver bones were water filled and a vacuum was pulled to remove all air. In living bone, the cancellous structure is filled with blood, marrow, and other constituents, however, at the low frequencies used for the measurements it is felt that little attenuation difference will occur between living and fluid filled cadaver bones.

Initial tests performed in vivo showed that the attenuation in the calcaneum fell in an approximate range of above average density. In future studies, it is felt that a more important parameter will be measurement of bone structure rather than density. Relating bone structure with attenuation could provide a reliable means for defining in vivo bone mass.



## **Health Protection and Dosimetry**



# Capillary Neutron Focusing for Boron Neutron Capture Therapy Adsorbates and Their Surfaces

Anthony J. Peurrung (Materials and Chemical Sciences)

## Project Description

The objective of this work was a demonstration of the utility of capillary-based neutron optics for the treatment of deep-seated brain tumors. Theoretical and numerical calculations were used to show that this technology allows the timely destruction of cancerous tissue with a selectivity that exceeds that of current technology for a significant class of tumors.

## Technical Accomplishments

The development of capillary neutron optics permits a new technology for neutron radiotherapy involving the application of a focused thermal neutron beam at the medically optimal location within the patient. A subthermal neutron beam begins to converge as it travels through a neutron "lens," reaching a narrow focus within a tube that allows it to pass directly to the treatment region. Figure 1 contains a side view of the proposed treatment technique.

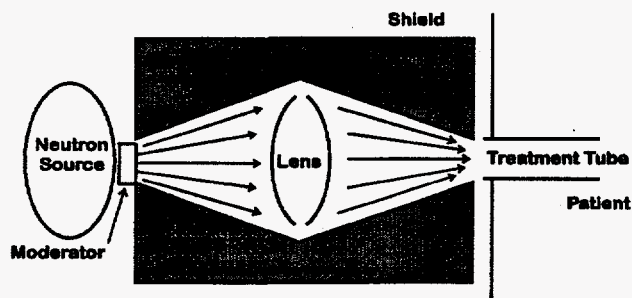


Figure 1. Side View of the Proposed Treatment Technique

The technology developed during the course of this project holds several important advantages for boron neutron capture therapy (BNCT) of deep-seated brain tumors. Previously, deep-seated tumors could not be effectively treated using thermal neutron beams because of the limited penetration of slow neutrons in hydrogenous human tissue. Any attempt to irradiate a deep-seated tumor would necessarily inflict substantial damage to healthy tissue near the brain's surface. Recently, epithermal (medium

energy) neutron beams have been investigated for treatment of deep-seated tumors. Although able to penetrate sufficiently deep in human tissue, epithermal beams are difficult to generate and control. It is unclear whether economically viable BNCT therapy on a national level is feasible using epithermal neutron beams.

This project has thoroughly investigated the possibility of using capillary neutron optics to focus a thermal neutron beam in such a way that it can be guided directly to the site of a tumor through a hollow "treatment tube." In addition to a theoretical analysis of the required neutron optics, numerical Monte Carlo modeling of neutron transport within the treated brain was performed to allow a demonstration of overall treatment feasibility.

The results of this project have indicated that current capillary lens technology allows effective and localized treatment of brain tumors in a time that is comparable to that possible using epithermal beams. Although the proposed technology requires an invasive surgery during treatment, the more effective utilization of limited neutron source resources possible with this technique may conceivably make its use essential to the more widespread implementation of BNCT therapy. In addition, several other types of cancers may react well to the localized neutron radiotherapy possible with this system.

## Publication

A.J. Peurrung. "Capillary Optics for Neutron Radiotherapy." *Medical Physics* (submitted).

## Presentations

A.J. Peurrung. 1995. "Capillary Optics for Neutron Radiotherapy." Idaho National Engineering Laboratory, March 16, Idaho Falls, Idaho.

A.J. Peurrung. 1995. "Capillary Neutron Optics for Boron Neutron Capture Therapy." Pacifichem '95, December 19, Honolulu, Hawaii (abstract accepted).

# Detection of *H. Pylori* Infection Using Laser Breath Analysis Instrumentation

James J. Toth (Systems and Risk Management)  
Steven W. Sharpe (Environmental Molecular Sciences)  
Karla D. Thrall (Health Protection)

## Project Description

The objective of this project was to identify disease-specific biomarkers in expired breath through the use of highly sensitive infrared laser detection. Breath analysis is an advancing technique that can help the physician diagnose disease at its earliest and most treatable stages. Spectroscopic interrogation of biomarkers in the breath using near-infrared lasers provides new measurement capability for simple, noninvasive testing. Near-infrared lasers were used for the identification and speciation of breath ammonia. The kinetic fate of ingested urea excreted in the urine was modeled with good agreement to findings reported in the literature.

## Background

Analysis of exhaled breath for the presence of chemical species indicative of specific diseases or as a means of following metabolic processes can be accomplished in several ways including 1) measuring absolute concentrations, 2) measuring altered ratios, or 3) measuring tagged species due to the introduction of specific chemicals. In the third approach, the biomarker should ideally be non-radioactive with a small natural abundance such as  $^{15}\text{N}$ . A case in point is the measurement of exhaled ammonia for the diagnoses of *Helicobacter Pylori* infection. The ammonia biomarker may potentially be used to identify other disease states, such as the increased metabolism of certain amino acids, perhaps as an indicator for physical or chemical trauma. The *H. Pylori* infection has been shown to be a major cause of gastritis and is implicated in gastric ulcers.

Since the *H. Pylori* bacterium is known to break urea down into  $\text{CO}_2$  and  $\text{NH}_3$ , a large change in the ratio of  $^{15}\text{NH}_3$  to  $^{14}\text{NH}_3$  post-dosing is indicative of the presence of the *H. Pylori* infection. To examine the possibility of the efficacy of an optically based ammonia breath test, the project focused on using the near-infrared laser spectroscopic regions to monitor a patient for  $\text{NH}_3$  before and after introduction of an oral dose of urea ( $^{15}\text{N}$  tagged).

To understand the fate of the introduced oral dose of urea, we began to develop a physiologically based pharmacokinetic (PBPK) model to characterize the fate of urea in the body.

## Technical Accomplishments

During FY 1995, a real-time bench-top apparatus for mid-infrared breath analysis was developed, and many of the preliminary issues concerning laser-based breath analysis resolved.

A preliminary physiologically based pharmacokinetic (PBPK) model was developed to characterize the uptake and tissue retention of urea and ammonia in the rat and in man. Data found in the scientific literature describing the oral administration of urea and the elimination of ammonia was used to develop kinetic parameters for the human PBPK model. An example of the model prediction in comparison to actual observed human data is illustrated in Figure 1. Further development of the preliminary PBPK model is dependent upon experimental studies to measure ammonia elimination kinetics via the lung following introduction into the blood stream.

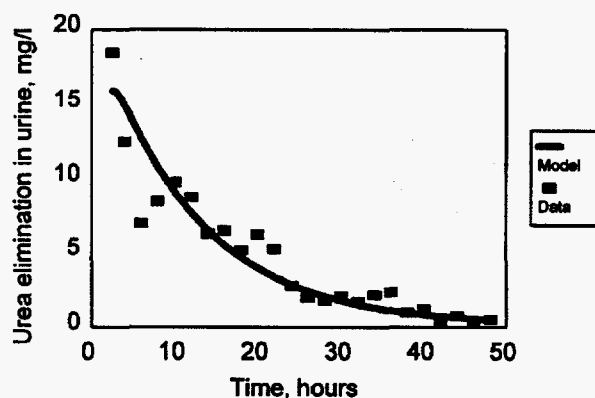


Figure 1. Comparison of human experimental data from Jackson et al. with the PBPK model prediction of urinary urea excretion following administration of urea.

For the laser-based breath analysis, quantitative measurements and spectral maps associated with the near-infrared spectral region (ca., 1550 nm) for both  $^{15}\text{NH}_3$  and  $^{14}\text{NH}_3$  have been obtained, as shown on Figure 2. Based on this data and our mid-infrared results, we were able to perform a sensitivity analysis comparing the mid-infrared and the proposed near-infrared instrument. The results indicate that a near-infrared instrument will be capable of low parts-per-billion detection of ammonia with complete resolution of  $^{15}\text{NH}_3$  and  $^{14}\text{NH}_3$ . Major spectral interferents such as water and carbon dioxide do not appear to present a problem. The data suggest that a real-time apparatus for ammonia breath analysis is technically feasible.

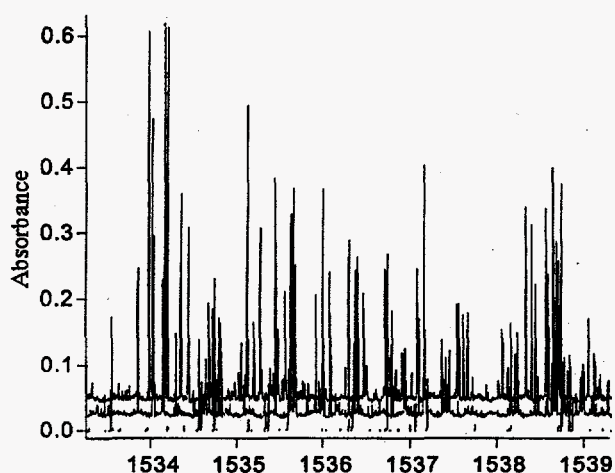


Figure 2. Spectral response of ammonia compared to air at 50 percent relative humidity (RH). The top spectra is ammonia as  $^{15}\text{NH}_3$ . The middle spectra is ammonia  $^{14}\text{NH}_3$ , and the bottom spectra is air, 50 percent RH.

# *Development of High-Sensitivity Detection Techniques for the Measurement of Ionizing and Non-ionizing Radiation*

Joseph C. McDonald (Health Protection)

---

## **Project Description**

The most direct and the most accurate way of measuring the quantity of energy deposited by either ionizing or non-ionizing radiation in matter makes use of the detection of the temperature rise induced in a known mass of the material under study. Radiometric calorimetry has been employed for such measurements for many years. Recently, however, cryogenic techniques have become commonly available and this low temperature regime offers significant advantages over conventional room temperature measurement techniques. Detectors are generally more sensitive at lower temperatures and heat capacities of most substances decrease, making the temperature rise induced by the deposition of radiant energy larger and easier to measure. This research will develop the technique for use in the calibration of instruments used to measure both ionizing and non-ionizing radiations. Using the same calibration technique for both types of radiation will help to increase the degree of uniformity in the assessment of hazards to workers.

## **Technical Accomplishments**

The goal of this research was to improve the accuracy of measurements performed for radiation protection purposes. This was achieved by using techniques that are now employed by nuclear physicists and astrophysicists to measure the quantity of energy deposited by elementary particles in solids. These techniques will be applied to the practical problem of measuring the energy deposited by ionizing and non-ionizing radiation in the human body.

The first step was to determine the feasibility of using the proposed approach. Although the technique of cryogenic calorimetry had been demonstrated to be successful in elementary particle research, it had not been used for the measurement of ionizing and non-ionizing radiation. The principal investigator consulted with two researchers: Dr. Alan Cummings from the University of California at Berkeley, and Dr. Dan McCammon from the University of Wisconsin. Both researchers suggested that the proposed technique would be feasible and they were both very helpful in providing technical information regarding instruments, equipment, and methodology.

The calorimetric technique relies on the measurement of the energy deposited by ionizing (or non-ionizing)

radiation in the form of heat. The temperature rise in conventional calorimeter absorbers, such as tissue-equivalent plastic, is quite small even for large doses. For instance, a dose of 0.01 Gy would produce a temperature rise of approximately  $5 \times 10^{-6}$ K. The measurement equipment currently in use at Pacific Northwest National Laboratory can discern this level of temperature increase, but the signal to noise ratio will be approximately 10:1.

Research into the cryogenic calorimetric technique demonstrated that the decrease in specific heat capacity and increase in sensitivity of thermistor thermometers at low temperatures result in a temperature rise per unit absorbed dose of approximately a factor of 1000 as compared with room temperature measurements. The temperature rise for 0.01 Gy will then be approximately  $5 \times 10^{-3}$ K with a signal to noise ratio of better than 10,000:1.

Available samples of tissue equivalent plastics and miniature thermistors were cooled to liquid nitrogen temperature (77K) in order to verify their ability to survive low temperatures. No damage to these devices was observed. The technique proposed in this work was shown to be feasible with little modification of existing recording equipment. The Quantum Designs multi-function controller could still be used with input to a computer for display and data storage. The largest area of work remaining is in the design and construction of a cryostat to house the calorimeter absorber and temperature control and measuring devices.

As a first step, it was anticipated that a commercially available cryostat could be used for evaluation. Unfortunately, time and money ran out before this task could be accomplished. The cryostat to be used was designed for optical measurements, but could have been modified for use with ionizing and non-ionizing radiations.

## **Presentation**

J.C. McDonald. 1995. "Radiation Metrology Research at the Pacific Northwest Laboratory." Seminar presented at the University of Wisconsin, May 12, Wisconsin.



# *Optical In Vivo Blood Characterization and Multivariant Analysis*

Norman C. Anheier (Sensors and Measurement Systems)

---

## **Project Description**

The development of optical biomedical sensing techniques is currently an area of increasing interest and activity. A particular category of optical sensing applications that has been receiving a great deal of attention of late is blood chemistry sensing. Frequently, the ultimate goal of optical blood chemistry sensing research and development is a noninvasive miniature sensor. Some blood chemistry parameters being targeted are concentrations of  $O_2$ ,  $CO_2$ , and glucose. However, achieving the necessary accuracy and utility in noninvasive sensors for these and other chemical parameters requires knowledge of viable, robust blood optical signatures associated with the target blood chemistry parameter. The situation is made considerably more difficult by the severely limiting optical characteristics of intervening tissue. There are many commercially available noninvasive sensors for  $O_2$ , pulse, and other blood parameters. Some of these sensors have proven value due to accuracy, ease of operation, and simple calibration. The success of these sensors drives the interest for complementary sensors that detect other blood chemistry parameters.

The objective of this project was to develop a methodology that allows identification of near infrared (NIR) spectroscopic signatures of blood chemistry parameters. Once useful signatures are identified, data can be used to predict analyte concentrations in the blood stream. An initial study (Case I) focused on three common anti-cancer drugs. These included methotrexate (MTX), cis-platinum (CIS), and doxorubicin (ADR). The spectral data analysis for these compounds was performed using multivariate statistical analysis techniques. Noninvasive, in vivo, or implantable blood chemistry sensing devices and methods may be possible if the statistical techniques successfully correlate absorption to analyte concentration.

## **Technical Accomplishments**

The preliminary literature search was extended to identify blood chemistry target parameters, existing blood chemistry spectroscopic research, and applications of multivariate statistical analysis for determination of blood analyte concentration. The literature search found no reports of using optical spectroscopy to sense anti-cancer drug concentrations in blood.

To screen analytes for useful spectroscopic signatures, three methodologies were developed. These included spectroscopy, sample preparation and handling, and data analysis. The baseline spectrophotometry methodology established spectral data acquisition procedures. The sample preparation and handling task established a safe chemical handling and dilution protocol. Multivariate statistical analysis served as the data analysis tool. Variations of full-spectrum multivariate statistical methods were developed that will allow calibration equations to be produced from a subset of the spectral features.

Sterile saline was used to dilute the Case I anti-cancer drugs in concentrations ranging from 1000 down to 0.1 ppm. These dilutions bound the bloodstream concentrations of typical therapeutic treatments. Dose rates were calculated for a typical patient 77-kg weight, 1.7-m height, and with 2-m<sup>2</sup> surface area.

A Varian Cary 5 spectrophotometer, operated in the double beam mode, was used to measure absorbance features of the Case I compounds in the wavelength range from 400 to 2500 nm. Absorbance features were measured with a spectral bandpass of 5 nm at 1-nm intervals. A 0.1-mm path length sample cell was held in a custom temperature controlled cell holder, since temperature variations can cause large variations in the spectrum of water.

In Case I we looked at methotrexate and cis-platinum at concentrations of 1000 and 700 ppm and doxorubicin at a concentration of 2000 ppm. No absorbance features were detected in the methotrexate and cis-platinum samples. Figure 1 shows a typical absorption spectra of saline (below) and 20 mg of doxorubicin in 10 ml of saline (overlaid above). The dip in the spectra near 800 nm is a measurement artifact. The saline spectra shows the expected  $H_2O$  first overtone at 1450 nm and the  $H_2O$  combination band at 1940 nm. Evident in the doxorubicin spectra is an absorption peak centered on 500 nm.

Unfortunately this peak is the only absorption feature found in the anti-cancer drugs used in the Case I study. In addition, this feature falls below the tissue transmission window, therefore it cannot be detected using noninvasive detection methods.

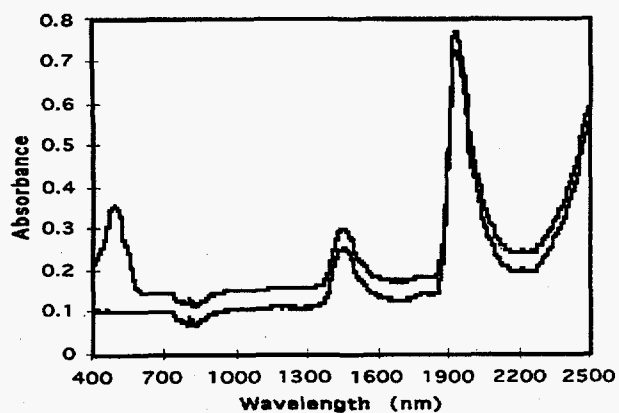


Figure 1. Although the FY 1995 study showed a null result for the Case I analytes, the instrument measurement procedures, sample preparation and handling protocols, and data analysis are now in place to enable the efficient performance of additional case studies of other analytes of importance.

# ***PBPK-Based Breath Analysis Instrumentation***

Karla D. Thrall (Health Protection)

---

## **Project Description**

The goal of this project was to continue research leading to the development of a semi-portable real-time monitoring instrument capable of estimating levels of volatile chemicals in tissues of waste-site cleanup workers within the DOE complex. Research was directed toward theoretical development and validation of physiologically based pharmacokinetic (PBPK) models to extrapolate an experimental animal system to predict internal dose following occupational exposure in humans; and continuing activities to improve technologies for the detection and characterization of compounds present in exhaled breath.

## **Technical Accomplishments**

### ***Breath-Analysis Instrumentation***

Development of the PBPK-based breath-analysis instrumentation for field use was significantly moved forward during this fiscal year through acquisition of a field portable mass spectrometer developed (with non-LDRD funds) by Teledyne Electronic Technologies. The glow discharge ion source is currently in the process of being optimized for sensitivity and selectivity for a wide variety of volatile organic compounds.

### ***PBPK Modeling***

The principal objectives of this project during FY 1995 were to 1) design a series of laboratory tests to demonstrate the capabilities of a system that combines sensitive new breath-analysis instrumentation with PBPK models using carbon tetrachloride as the example chemical, and 2) expand the PBPK modeling toward an additional chemical commonly encountered at DOE facilities that could be used in conjunction with the breath-analysis instrumentation.

Experimental data on exhaled breath collected during the previous fiscal year from laboratory rats exposed to varying levels of carbon tetrachloride in a corn oil vehicle were used to develop a preliminary PBPK model to describe the oral uptake of carbon tetrachloride. The model uptake parameters were optimized against this data in order to more fully understand the role dose and vehicle volume levels play in the compartmentalization of an oral gavage dose of carbon tetrachloride.

As a direct result of these experiments and the PBPK modeling, a series of additional studies have been planned to further enhance the general scientific understanding of carbon tetrachloride biokinetics, particularly in relation to the evolution of volatile markers of lipid peroxidation (ethane, pentane, and acetone).

Additional modeling efforts were directed toward development of a preliminary PBPK model to describe the uptake, tissue distribution, metabolism, and elimination of benzene. Our initial PBPK model is the cross-product of two different benzene PBPK models available in the literature. At the current time, the benzene PBPK model is being used to predict the levels of benzene in exhaled breath and benzene metabolites in the urine that should be measurable in humans exposed to various levels of benzene occupationally. In the future, this information will aid in the development of occupational exposure assessment demonstrations using the real-time breath-analysis instrumentation.

## **Publication**

K.D. Thrall, D.V. Kenny. "Evaluation of a Carbon Tetrachloride Physiologically Based Pharmacokinetic Model Using Real-Time Breath-Analysis Monitoring of the Rat." *Inhalation Toxicology* (in press).

## **Presentations**

K.D. Thrall, D.V. Kenny. 1995. "Validation of a Carbon Tetrachloride PBPK Model Using Real-Time Kinetic Data." Presented at the 34th Annual Meeting of the Society of Toxicology, March 5-9, Baltimore, Maryland.

K.D. Thrall. 1994. "PBPK-Based Breath Analysis Instrumentation." Presented at the 1994 Northwest Occupational Health Conference, October 13-14, Bellevue, Washington.

K.D. Thrall, G.W. Endres, and D.V. Kenny. 1994. "Instrumentation to Improve Worker Health Protection." Presented at the Third Annual Occupational Safety and Health Conference, October 25-28, San Diego, California.

K.D. Thrall, and D.V. Kenny. 1994. "Real-Time Breath-Analysis Instrumentation and Physiologically Based Pharmacokinetic Modeling: A New Opportunity in Chemical Mixtures Research." Presented at the U.S. EPA HERL Symposium on Chemical Mixtures and Quantitative Risk Assessment, November 7-10, Research Triangle Park, North Carolina.

# Physiologically Based Pharmacokinetic Modeling of Organic Waste Site Chemicals

Karla D. Thrall and Kyeonghee M. Lee (Health Protection)

## Project Description

A physiologically based pharmacokinetic (PBPK) model has been developed for the organic solvent 2-butoxyethanol. The model has been validated against the available published kinetic data. Additional experimental studies are required to improve model predictions, especially across age, species, and gender.

## Background

2-Butoxyethanol (2-BE; ethylene glycol n-butyl ether) is a cleaning solvent found in more than 700 consumer products at concentrations ranging from 2.8 to 20 percent. Thus, there is a high potential for accidental human exposure to this solvent. It has been consistently shown that 2-butoxyethanol causes both dose- and time-dependent hemolysis of red blood cells in laboratory animals. However, it is not the parent compound but its major metabolite, 2-butoxyacetic acid (BAA), that is primarily responsible for the observed hematotoxicity.

A fundamental problem in human health risk assessment is in the extrapolation of experimental results from laboratory animals to the human population. Most of the toxicity and pharmacokinetic information on 2-butoxyethanol and 2-butoxyacetic acid has been gathered from rodent studies, and only limited and qualitative information is available on human exposure situation. To provide a physiological basis to extrapolate toxicokinetic findings from laboratory animals to humans, a PBPK model for 2-butoxyethanol and 2-butoxyacetic acid has been developed. This model incorporates quantitative descriptions of physiological and biochemical processes of animals and physicochemical properties of test compounds so that, by employing the appropriate input parameters, the same model can be utilized to describe the in vivo dynamics of chemical disposition in any species under a variety of exposure scenarios.

## Technical Accomplishments

In this project, a recently published 2-butoxyethanol PBPK model (Corley et al. 1994. *Toxicol. Appl. Pharmacol.* 129:61-79) was extended to simulate the disposition of 2-butoxyethanol and 2-butoxyacetic acid under various

exposure conditions including chronic exposure of 2-butoxyethanol. The chronic model simulation is intended to quantitatively describe and evaluate kinetic data derived from a 2-year bioassay study on 2-butoxyethanol when it becomes available. Most PBPK models reported to date have been developed and validated only against kinetic data following acute exposures. However, the kinetic behavior of a chemical is likely to change with an extensive exposure period. Chronic exposure is also likely to bring about time-dependent physiological changes in the animal which gradually affect the disposition and elimination of a chemical. These age-related changes were incorporated into the 2-butoxyethanol PBPK model to simulate the time-dependent blood kinetics of 2-butoxyethanol and 2-butoxyacetic acid and urinary accumulation of 2-butoxyacetic acid in both rats and mice following a chronic inhalation exposure (Figure 1). Biochemical and physiological input parameters were allometrically scaled based on time-dependent changes in animal body weight. By comparing model simulation predictions and actual data, we were able to identify where more quantitative information is required in order to better simulate the chronic behavior of these chemicals. This suggests that differences in the kinetics of 2-butoxyethanol and 2-butoxyacetic acid depend strongly on the age, species,

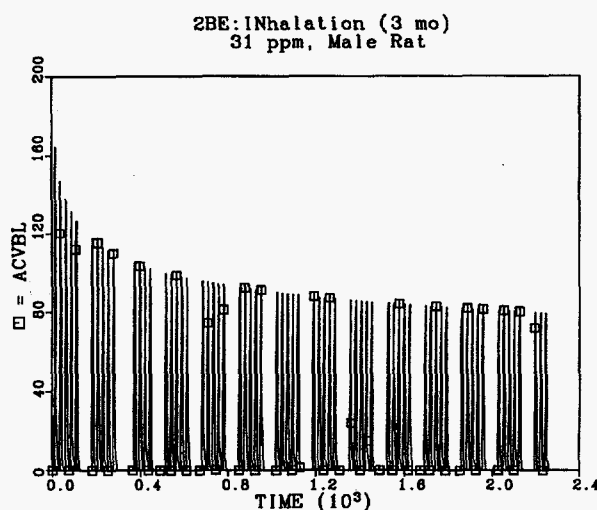


Figure 1. PBPK model prediction of the blood concentration of BAA simulated using male F344 rats exposed to 2-BE (31.25 ppm) by a whole body inhalation for 6 hours, 5 days per week for 3 months.

and gender of the animal. Thus, an integral part of this modeling exercise was to identify the data gaps needed to further improve our understanding of chemical biokinetics under a variety of exposure scenarios.

Due to the complexity of the PBPK model structure and the number of parameters involved, it is important to have an understanding of how the model predictions vary with respect to parameter uncertainty. These estimates of variability in PBPK modeling are used to identify input parameters that make a significant contribution to the overall model error, and thus improve health risk estimates. Thus, sensitivity analysis of the model was performed focusing on biochemical and metabolic parameters associated with 2-butoxyacetic acid disposition (Figure 2).

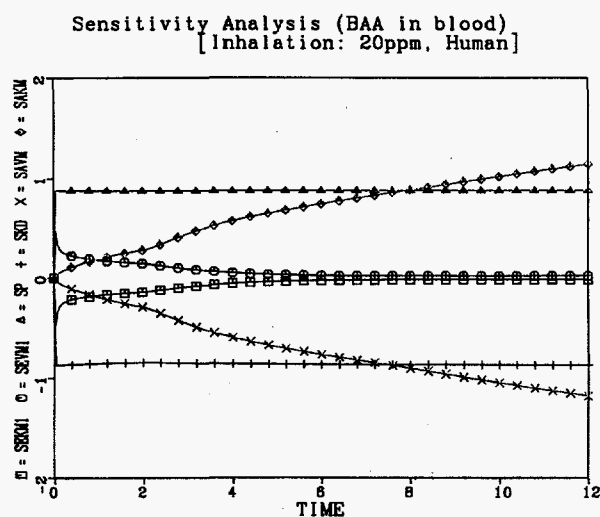


Figure 2. Sensitivity plot for the biochemical parameters related to the disposition of BAA. A positive sensitivity coefficient indicates a positive influence on the blood concentration of BAA. This plot is generated for human inhalation exposure (20 ppm for 2 hours under mild exercise condition).  $S_{EKm1}$ , affinity constant of 2-BE metabolism to BAA;  $S_{EVmax1}$ , maximum rate of the 2-BE metabolism into BAA;  $S_p$ , plasma protein-BAA binding sites;  $S_{Kd}$ , plasma protein-BAA dissociation constant;  $S_{AKm}$ , affinity constant of BAA renal transport;  $S_{AVmax}$ , maximum rate of BAA renal transport.

## Publications

K.M. Lee, R.D. Stenner, R.A. Corley, and K.D. Thrall. 1995. "A Physiologically Based Pharmacokinetic (pbpk) Model for 2-Butoxyethanol and its Hemolytic Metabolite, 2-Butoxyacetic Acid." *International Toxicologist* 7:63-PF2.

## Presentations

K.M. Lee and K.D. Thrall. 1995. "Validation and Sensitivity Analysis of the Physiologically Based Pharmacokinetic (PBPK) Model for 2-Butoxyethanol." To be presented at the Third Annual Symposium of Health Effects and Research Laboratory (HERL), Raleigh, North Carolina.

K.M. Lee, R.D. Stenner, R.A. Corley, and K.D. Thrall. 1995. "A Physiologically Based Pharmacokinetic (PBPK) Model for 2-Butoxyethanol and its Hemolytic Metabolite, 2-Butoxyacetic Acid." Presented at the meeting of the International Congress of Toxicology (ICT-VII), Seattle, Washington.

# Quantitation of Hypoxic Cells

Alfred F. Fuciarelli (Biology and Chemistry)

## Project Description

Rapid, noninvasive techniques are being developed for the detection, quantitation, and clinical assessment of hypoxic cells in solid tumors. Re-population of inoperable solid tumors by previously hypoxic cells in patients treated with radio- or chemotherapy is thought to be a major reason for treatment failure. However, this hypothesis has not been rigorously tested due to the inability to selectively label, quantitate, and monitor this subpopulation of cells in an appropriate *in vitro/in vivo* model tumor system and, particularly, during the course of therapy. Our experimental approach developed techniques that will facilitate a rigorous test of this hypothesis and addressed the potential for hypoxic cells to limit curability. Fluorescence activated cell sorting techniques were developed to isolate hypoxic cells from tumors with the aid of compounds that are selectively metabolized by hypoxic cells. Our work exemplifies technology that can significantly impact cancer detection and treatment and will provide the scientific basis for establishing the importance of hypoxic cells associated with the clinical management of inoperable solid tumors.

## Technical Accomplishments

Human tumors contain regions of well-oxygenated viable cells that proliferate at an uncontrolled rate relative to surrounding normal tissue. As solid tumors grow, proliferating cells can become too distant from the vascular supply and regions of necrosis occur within the tumor cell mass. However, at the interface between the area of necrotic tissue and the area of actively proliferating cells is an area of poorly oxygenated cells which are more radio- and chemoresistant (Figure 1). Following cancer therapy, regrowth of solid tumors by these hypoxic cells is suggested to be a major reason for treatment failure. However, this hypothesis has not been rigorously tested due to the inability to selectively label, quantitate, and monitor this subpopulation of cells in an appropriate *in vitro/in vivo* model tumor system and, particularly, during the course of therapy.

Several methods were proposed for determining the fraction of hypoxic cells in solid tumors. These included polarographic needle electrode measurements, quantification of 2-nitroimidazole binding, and phosphorus magnetic resonance spectroscopy. Advantages and disadvantages exist with all techniques. However,

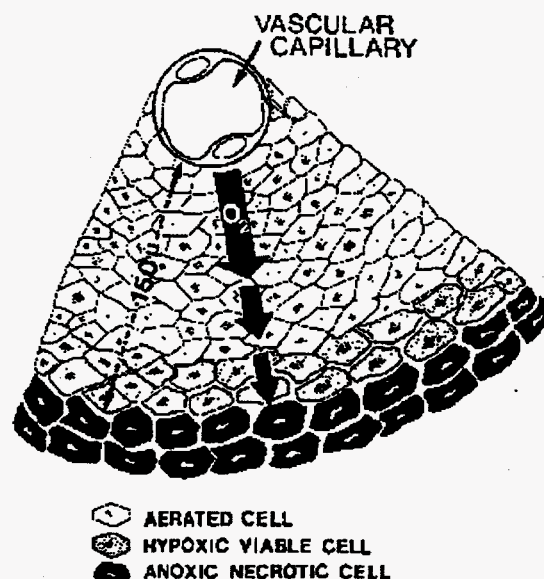


Figure 1. Diffusion of oxygen from a capillary through tumor tissue is limited by the rapid rate of metabolism by respiring tumor cells. At distances exceeding 150  $\mu\text{m}$  from the capillary, cells become hypoxic and are more radio- and chemoresistant. (E.J. Hall, *Radiobiology, for the Radiobiologist*, 3rd Edition, JB Lippincott Co., Philadelphia, 1988.)

hypoxia-dependent bioreductive metabolism of 2-nitroaromatic markers is attractive because bioreduction and binding of the marker to cellular macromolecules will be limited primarily to metabolically active hypoxic cells thereby minimizing error introduced by measurement of hypoxia in regions of necrosis. Although several methods are possible to detect the 2-nitroimidazole markers, immunochemistry-based approaches offer exciting experimental opportunities. An example of the development of immunohistochemical probes for detection of hypoxic cell markers has been described in our early work (J.A. Raleigh, G.G. Miller, A.J. Franko, C.J. Koch, A.F. Fuciarelli, D.A. Kelly. *British Journal of Cancer* 56:395-400, 1987). In combination with fluorescence activated cell sorting capabilities available at the Laboratory, immunochemical detection and separation of hypoxic cells enables unprecedented studies with this cell population.

Through a collaboration with Dr. James A. Raleigh from the University of North Carolina Medical School at Chapel Hill, pimonidazole (1 gm) was synthesized,



monoclonal antibodies were raised to the cellular adduct of pimonidazole, and the antibodies were labeled with fluorescein isothiocyanate (FITC). Techniques were developed at the Laboratory to

1. control and maintain low oxygen status in cells grown in tissue culture
2. treat and label hypoxic human lymphoid (K562) cells with the monoclonal antibody-FITC conjugate in tissue culture
3. optimize conditions for flow cytometric detection and sorting.

An example of our progress to date is represented by flow cytometric analysis of human lymphoid cells treated with pimonidazole and labeled with a monoclonal antibody tagged with FITC (see Figure 2). The hypoxic cell population is well separated from the subpopulation of well-oxygenated cells. This work represents a crucial foundation for our second year studies which involve experiments using an in vitro/in vivo rodent mammary tumor model system.

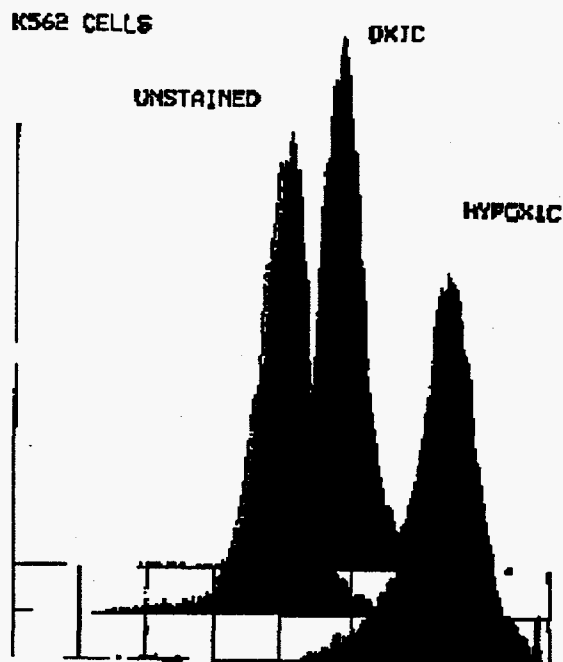


Figure 2. Flow cytometric analysis of human lymphoid cells (K562) treated with pimonidazole and labeled with a monoclonal antibody tagged with fluorescein isothiocyanate demonstrating the ability to discriminate between hypoxic and well-oxygenated cells.



# Real-Time Dosimetry for Therapeutic Radiation Delivery

Richard A. Craig (Automation and Measurement Sciences)  
Mary Bliss, Paul L. Reader, and Debra S. Sunbery (Chemical Sciences)

## Project Description

The overall objective of this work was the development of devices which offer greatly improved accuracy and precision for the delivery of therapeutic radiation.

## Technical Accomplishments

The project was structured into five tasks

1. in situ, real-time thermal neutron dosimeter for boron-capture neutron therapy
2. flat-plate, real-time device for dose measurements and beam imaging for thermal neutron therapy
3. flat-plate, real-time dosimeter for measurement of total delivered dose in x-ray/gamma therapy
4. in situ, real-time photon dosimeter for x-ray/gamma therapy
5. in situ, real-time dosimeter for fast-neutron therapy.

The products of Tasks 1 and 2 were designed for an experimental cancer treatment known as boron neutron capture therapy (BNCT). The treatment is based on the fission of a boron-loaded pharmaceutical under a high neutron flux. The fission releases a large amount of energy, killing cancerous cells. The dosimeter would provide immediate information on the neutron flux, data that are currently not available. The beam-imaging device would give information on neutron-beam location and flux.

As a result of the collaboration established with Idaho National Engineering Laboratory's BNCT team, it was determined that a collection of 7 to 10 single-fiber real-time neutron-sensing detectors was preferable to a single sensor plus a flat-plate detector. Accordingly, the efforts of Tasks 1 and 2 were collapsed into a single task, the goal of which was to develop an effective single-point sensor plus the appropriate electronics.

The BNCT dosimeter consists of a segment of scintillating fiber bonded to the end of a passive fiber that is, in turn, attached to a counting system. The scintillating fiber was developed at the Laboratory. The original purpose for producing the fiber was for large-area, low-count-rate,

environmental sensors. Only recently have the fibers been utilized for high-count-rate applications.

The smallest dosimeter tested consisted of a fiber sensor 120  $\mu\text{m}$  in diameter and 2 cm long. The dosimeter was inserted into a dry tube directly below the reactor core, and the count rate compared to reactor power (see Figure 1 - reactor power is proportional to the neutron flux). Thermal neutron fluxes up to  $10^{10}$  neutrons/cm<sup>2</sup>/sec were used. The sensor performance did not degrade after several hours of testing; although, radioactive activation of the sensor components occurred as expected.

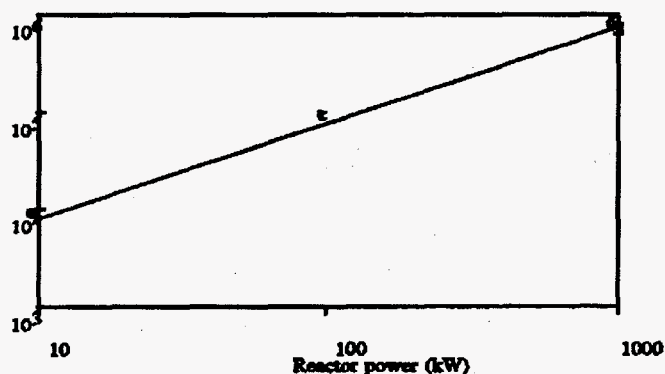


Figure 1. Response of Thermal-Neutron, Real-Time Dosimeter to Variation in Reactor Power

The product of Task 3 was designed to produce real-time information to the physician about the intensity and location of the beam during delivery of gamma/x-ray therapeutic radiation. This radiation mode is one of the most common type of radiation therapy in current practice. A prototype panel for testing was constructed using commercially fabricated plastic scintillating fiber.

The product of Task 4 is designed to be an in situ sensor to provide the gamma ray/x-ray radiologist with real-time information about the dose rate at the desired delivery site. Work on this task was unfunded.

The product of Task 5 is designed to be an in situ device to provide real-time information about the dose being delivered to the tumor site during fast-neutron therapy. Fast-neutron therapy is an experimental technique in which high-energy neutron beams are directed at the treatment site; in order to reduce the damage to normal tissue, the beam is directed through the patient in a variety

of directions crossing at the desired treatment site. This complicated exposure geometry makes it very difficult to calculate doses to the normal tissue and to the treatment site. Thus, a real-time dosimeter that can be located at the tumor site is a genuine need. A complication for fast-neutron therapy is that the delivered dose arises from several sources: recoil of nuclei from impact with the fast neutron, ionization produced by the recoil nuclei, capture of thermalized neutrons, and associated gamma radiation.

Collaboration with University of Washington Radiological Science Faculty has resulted in the identification of another treatment mode for which real-time dosimetry would fill a need. Radiation implants are sources which are temporarily or permanently inserted at a treatment site. Although doses are relatively easy to calculate for these, verification of the dose delivered is highly desirable.

## **Publications and Presentations**

M. Bliss, R.A. Craig, P.L. Reeder, and D.S. Sunberg. 1995. "Development of a Real-Time Dosimeter for Therapeutic Neutron Radiation." *IEEE Trans on Nuc. Sci* 42,639.

M. Bliss, R.A. Craig, P.L. Reeder, and D.S. Sunberg. 1995. "Development of a Real-Time Dosimeter for Therapeutic Neutron Radiation." Presented at and in Proceedings *IEEE Nuclear Science Symposium and Medical Imaging Conference Record*, V2, 935, November 1994, Norfolk, Virginia.

M. Bliss, R.A. Craig, P.L. Reeder, and D.S. Sunberg. 1995. "A Real-Time Dosimeter for Boron-Capture Neutron Radiation." In *Proceedings of the Accelerator-Based Neutron Sources Workshop*.

# Testing of Noise and ELF Instruments for RF/MW Interference

Matthew H. Smith (Health Protection)

## Project Description

Industrial hygiene instruments are used to assess health hazards in the workplace. In many cases, they are used in environments that can interfere with their operation. Environmental exposure to radio-frequency and microwave (RF/MW) fields has been shown in our study to interfere with the operation of noise dosimeters and instruments used to measure extremely low frequency magnetic fields.

Instruments were tested in accordance with American National Standard: Performance Specifications for Health Physics Instrumentation (ANSI N42.17A-1989). The results of this work could lead to specific recommendations for testing different types of industrial hygiene instruments.

## Technical Accomplishments

During FY 1995, testing for susceptibility to RF/MW fields continued on several types of instruments. These instruments included a noise dosimeter (instrument A), an extremely low frequency magnetic field meter using an induction coil (instrument B), an extremely low frequency magnetic field meter using a three-axis hall effect probe (instrument C), and an extremely low frequency meter using orthogonal loops (instrument D).

The instruments were tested for microwave susceptibility by exposing them at a power density of 10 mW/cm<sup>2</sup> (frequency = 2450 MHz). Radio-frequency susceptibility was tested in the frequency range 0.3 to 35 MHz. The field strength in this range was held at 100 V/m.

Instruments A, B, and C were all found to be susceptible (i.e., exposure reading differed by greater than 15 percent when compared to reference reading) to microwave exposure. Figure 1 illustrates the response of the noise dosimeter to microwave exposure. Figures 2 and 3 show the microwave test results for instruments B and C respectively. Instruments B and C were also susceptible to radiofrequency exposure. The results of these tests are shown in Figure 4.

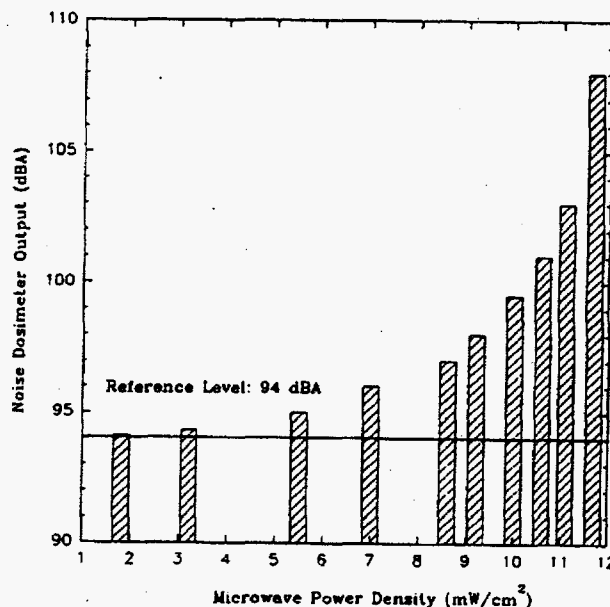


Figure 1. Response of Noise Dosimeter to Microwave Field

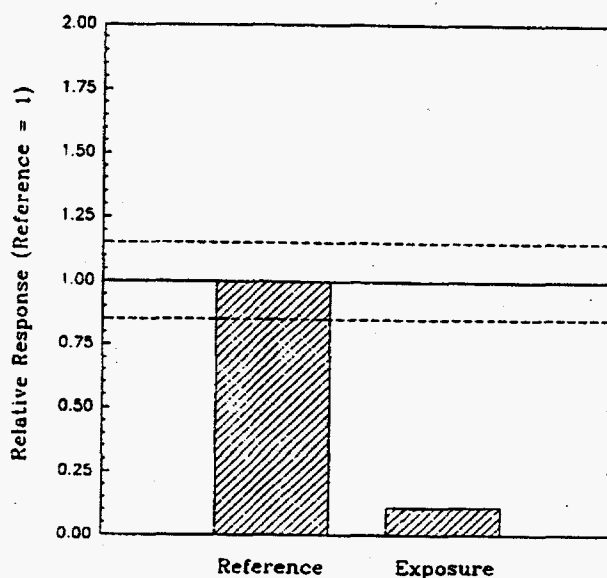


Figure 2. Response of Instrument B to Microwave Field

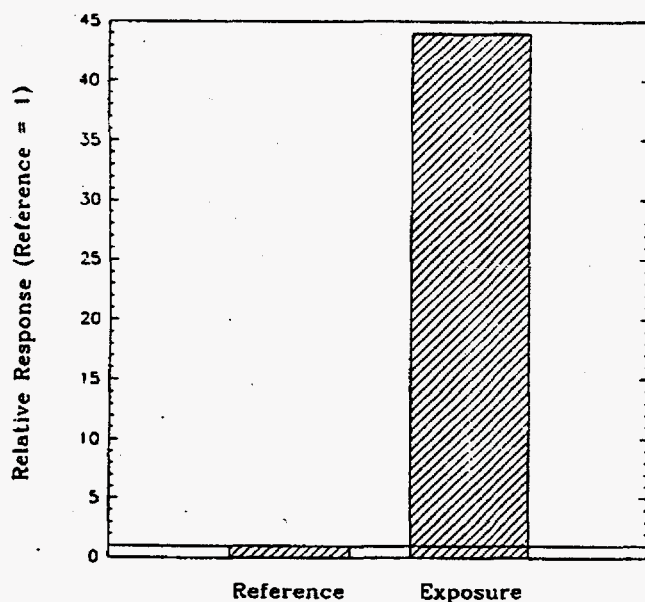


Figure 3. Response of Instrument C to Microwave Field

Instrument C also demonstrated a lack of selectivity regarding fields it was designed to measure (both alternating current and direct current magnetic fields). When set up to measure static (direct current) magnetic fields it was found that adding exposure from an alternating current magnetic field source would alter the instrument's reading. The same problem occurred when measuring alternating current fields and a interfering direct current field was added. Instrument B was designed to measure alternating current fields exclusively. No susceptibility from interfering direct current fields was found.

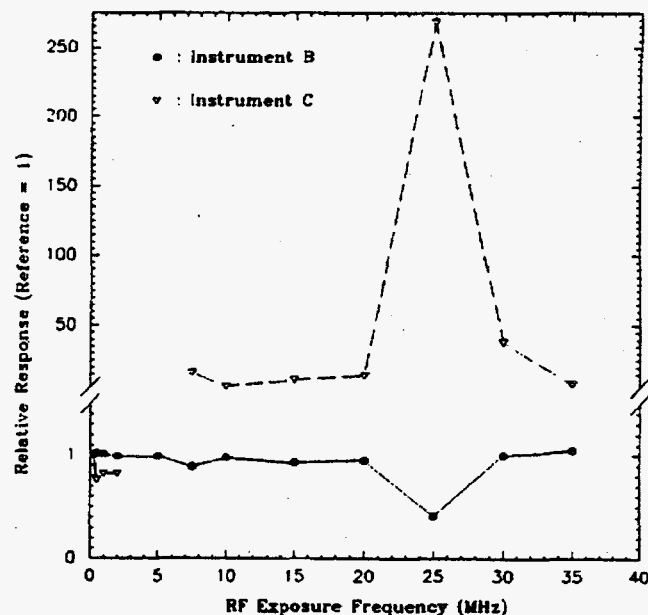


Figure 4. Relative Response of Instruments B and C to RF Exposure

Instrument D passed all the RF/MW interference tests administered during this project. The positive attributes of this instrument included good shielding and electronic design. Those instruments that failed were often housed in plastic cases with little or no RF/MW shielding.

## **Human Systems Performance**



# Interactive Technologies for Adaptive Training

Frank L. Greitzer and Bill W. Brown (Technology Management and Social Sciences)  
Brian A. Gladstone (Health)

## Project Description

Inspectors, auditors, and other oversight staff in a variety of contexts frequently conduct inspections without a thorough familiarity with the targeted items or the facility to be examined. As a result, ill-prepared individuals may either commit too many "false-positives" or fail to detect the targets. An interactive, computer-based training system can be a valuable tool to improve observational skills and help familiarize inspectors with a variety of examples and situations that would be difficult or impossible to provide in a "real" setting.

The objectives of this research were to explore innovative concepts for improving the development process for computer-based training (CBT) systems, as well as their training effectiveness. The research focused on

- development of a foundation for tailoring the computer-based training delivery to alternative training objectives or scenarios
- incorporation of interactive video to provide more realistic interactions and reduce costs and risks associated with onsite training.

## Technical Accomplishments

The approach to this project was based on the creative application of interactive technologies—effectively incorporating multimedia (photos, video, and sound), hypertext, graphical user-computer interfaces—and an interactive approach to training that emphasizes student participation rather than more conventional, passive "page turning." To facilitate this type of computer-based training development, a framework was designed and developed to help an instructor or course designer tailor material to diverse training objectives, instructional approaches, training scenarios, or student backgrounds.

To illustrate the concepts, a prototype system was developed for a portion of an observational skills training course. An interactive course map is shown in Figure 1. The fully developed observational skills training course will have sections on human perception and recognition, attention, memory, mental imaging, and judgment, as well as an integrated, interactive exercise employing a video "walk-through" of a facility in which the student may control the path through the facility and the detail

provided on objects encountered along the path. The course content includes two levels of instruction: 1) basic instruction on human observational skills that applies to general domains of interest, and 2) supplementary material comprising specific examples relevant to the selected domain of international safeguards inspections. The basic instruction material is presented as the main core of the course, with quiz items following each of the sections. The supplementary material was implemented as a separate module, so that domain-specific material may be substituted easily for a different observational skills training application context.

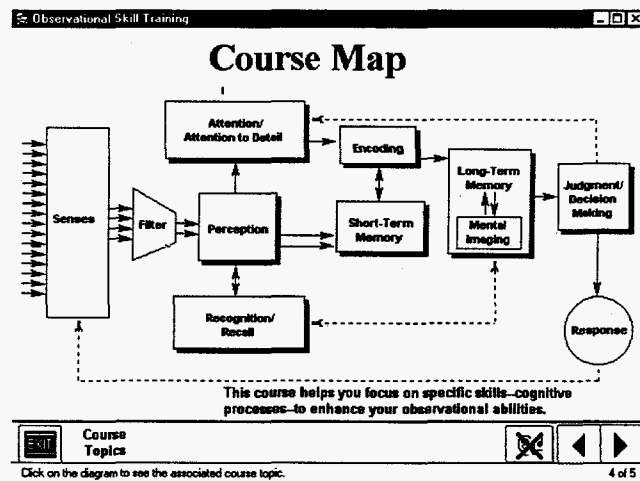
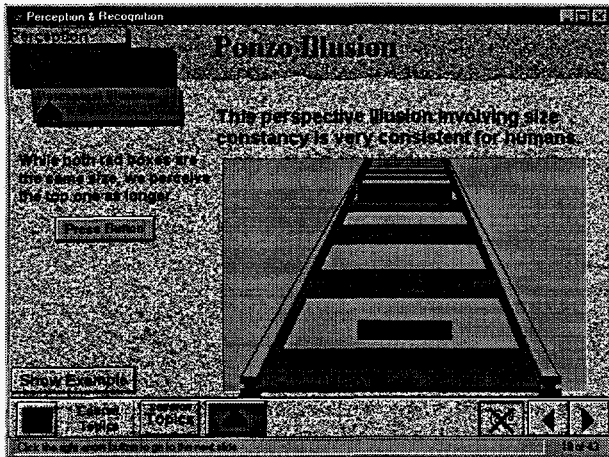


Figure 1. An Interactive Course Map for the Observational Skills Training Course

The prototype contains a basic instruction section on perception and recognition skills, as well as an illustrative interactive exercise incorporating a video walk-through of a facility. The basic instruction section provides dynamic demonstrations of perceptual phenomena to help raise the student's awareness of human capabilities, limitations, and biases. Figure 2 exhibits a representative example of an interactive screen, demonstrating a perceptual illusion.

The illustrative interactive exercise provides a video-based "walk-through" of a facility in a safeguards inspection scenario. Using a facility map for reference, the student tours the facility by moving down corridors, turning left or right, clicking on objects to obtain more information, and reporting on what is observed.



**Figure 2. A Sample Screen from the Observational Skills Training Course**

While this portion of the training was not fully implemented in the prototype, plans for further development are to provide feedback to the student about what features were missed during the walk-through, and to provide brief "replays" of selected portions of the tour as part of the debriefing/feedback for the student.

In addition to serving as a stand-alone computer-based training system, the course material and approach taken in this work may be used for other purposes: a) the material may be used as visual aids for a lecture presentation; and b) the interactive walk-through approach may be used to help prepare inspectors for planned facility inspections by helping to familiarize them with the facility prior to the visit.

The system runs in Microsoft-Windows on a 486-class personal computer.

## Conclusions

This research demonstrated concepts of interactive, flexible, and tailorable multimedia-based computer-based training systems. The prototype system developed for observational skills training is being applied to international nonproliferation inspection training for possible use as a lecture aid in the classroom or as stand-alone computer-based training. The computer-based training and video-based walk-through approach demonstrated in this project offers effective means of lowering the cost of training and preparation for inspections. The system design concepts exhibited in the prototype help demonstrate innovative approaches to interactive computer-based training that will be necessary to meet the needs of modern training applications.



# Translating Work Environment Research into Design

Janet G. Heubach (Technology Planning and Analysis)

---

## Project Description

The purpose of this project was to implement the first step toward developing an electronic prototype tool to translate data and theory from environmental research into the architectural design process. The project was conceived to bridge the broad gap between research and applications in architecture, particularly research related to the design of work environments. There is growing evidence that two major problems exist that inhibit the transfer of knowledge from human-environment research to the architectural design profession. First, designers are generally not aware of the large body of research on human-environment relationships that could be used as a basis for designing buildings that are comfortable, functional, and enhance the productivity and health of building occupants. Second, even if they are aware of the research findings, research is often presented in ways that are not very useful to designers. That is, it tends to be data dominant and verbal rather than image dominant and visual. Since designers tend to draw heavily upon personal "image banks," research findings that are communicated in a manner that more adequately taps into the visual mode are likely to be better utilized and integrated into building design.

## Technical Accomplishments

The project originally focused on the design of work environments for two reasons: 1) there is increasing interest in worker productivity in the building design field, and 2) the work environment focus clearly built upon the team's previous experience. A Laboratory report summarizing this work (*Work Environments and Organizational Effectiveness: A Call for Integration*) was published in June 1994.

The project was broken down into several stages. In the first stage, the team focused on identifying themes and issues from work environment research and organizational effectiveness studies. Once a key list of issues were identified; they were further developed using a hierarchical process. The steps included the following:

- review literature to identify key environmental needs
- characterize major subcomponents or dimensions of each need

- describe environmental attributes and properties associated with the dimensions
- suggest images or metaphors that capture the psychological and experiential aspects of the environment.

The needs and environmental attributes were identified through a literature review. The review focused on empirical studies, however, since the environmental design research field is relatively young, we had to also draw upon theoretical work.

The first step in the process was to identify important organizational goals and needs that are related to the physical environment (such as communications processes, employee well-being, organizational attachment). The second step involved identification of environmental features and attributes that affect the attainment of the particular goal or need. For instance, the goal "worker well-being" was broken down into eight dimensions associated with well-being (control, belonging, participation, stimulation, stress reduction, self-esteem, organizational attachment, and personalization). In the third step, we identified the environmental features associated with each dimension. For "sense of belonging," the following environmental attributes were identified: presence of pleasing and comfortable gathering places, places for group events and celebrations, visual access to coworkers, coworkers located close by, group identity markers, and artifacts that provide a sense of place and organizational image.

Once the physical attributes and properties were described, the fourth step was to identify metaphors and images to convey the psychological and experiential sense of environment. For example the "belonging" need suggested the following images: the commons, a friendly neighborhood street, the hearth, the country kitchen.

The preliminary version of the communications prototype was tested with the work environments group of the Environmental Design Research Association (EDRA) at its annual meeting in Boston in March 1995. This group consists of environmental psychologists, organizational psychologists, and designers. They raised several concerns: 1) although the overall goal of the tool was an excellent idea, there was probably not sufficient research to make a valid connection between the organizational goals and the workplace features that contribute to or

inhibit the attainment of those goals; 2) a more useful approach would be to develop a general tool (built upon identification of a basic or core set of human needs) that could be adapted for numerous environmental settings and not just work environments; 3) the tool should be developed not only with designers in mind, but for a wide range of other stakeholders who would have an interest in the physical environment.

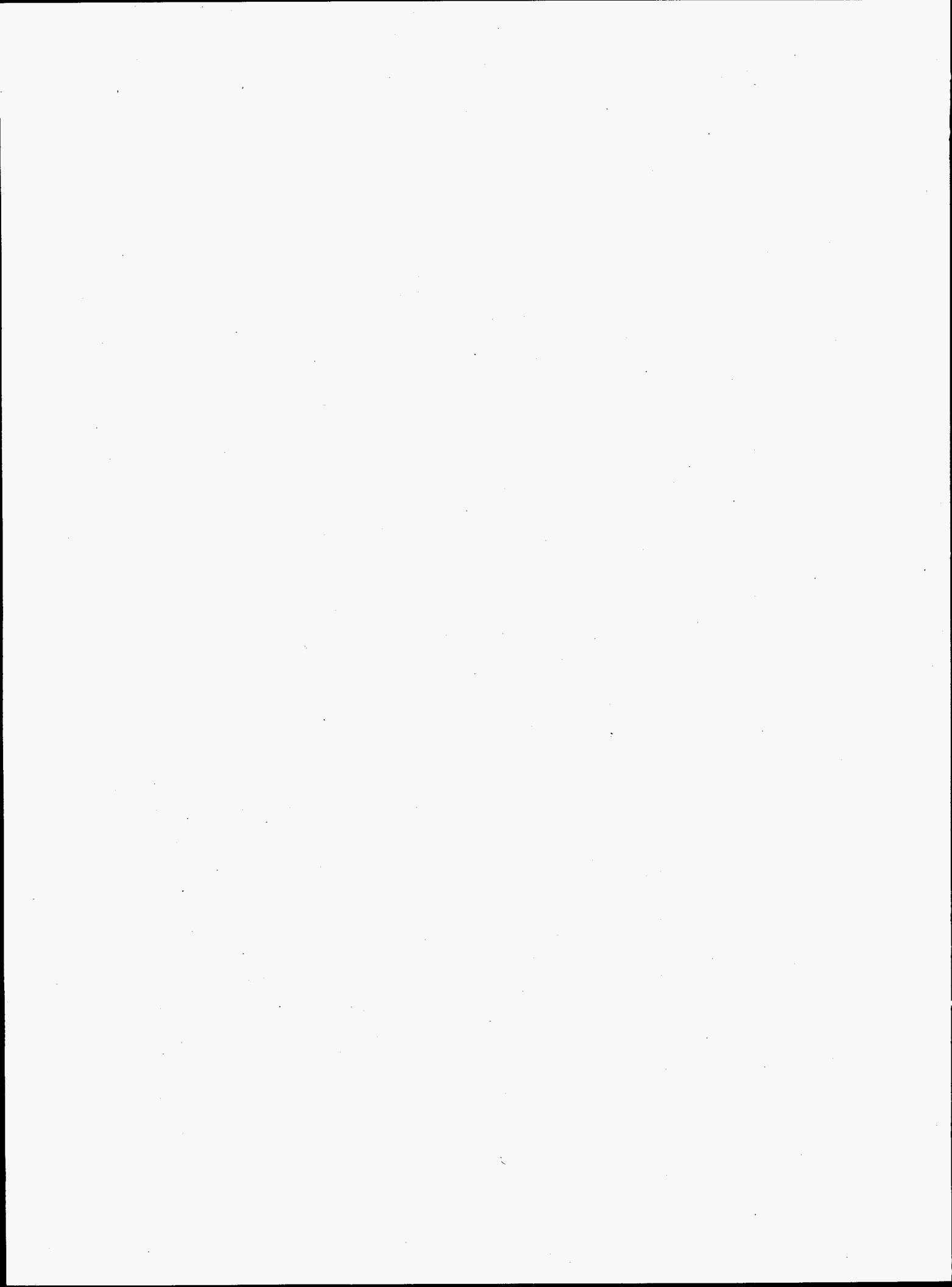
With this critique in mind, we identified a number of researchers who have written on the topic of "basic needs" and the environment and from this body of literature identified common themes and elements that formed a new set of basic needs. At this point, we followed a similar hierarchical process of going from the general need to the attributes and features of the environment that affect the specific need. The final product of this effort is a matrix of core human environmental needs and the spatial attributes and properties that contribute to meeting these needs.

The primary accomplishment of the project was the development of the environmental needs matrix and the initial testing of the prototype at the Environmental Design Research Association conference. The tool, if it were to be developed further, might be more effectively done as a hypertext document that could connect to other sources of information and which could be developed in such a way that users could modify it through their own use and experiences (e.g., it would be a "living" tool). In this way, the accumulated experiences of the design and research communities could be integrated in one document. At the present time, designers, users, and researchers have different sources of information and communication.

### **Presentation**

J. Heubach and J. Heerwagen. 1995. "Research Data and Visual Images." Presented at the Environmental Design Research Association Conference, March, Boston, Massachusetts.

## **Hydrologic and Geologic Sciences**



# Dual-Gas Tracer Characterization of Diffusion Limitations in Enhanced In Situ Remediation

Phillip A. Gauglitz, Loni M. Peurrung, and Gautum Pillay (Process Technology and Engineered Systems)

## Project Description

Effective design of in situ remediation technologies often requires an understanding of the mass transfer limitations that control the removal of contaminants from the soil. In addition, the presence of nonaqueous phase liquids (NAPLs) in soils will affect the ultimate success or failure of remediation processes. Knowing the location of NAPLs within the subsurface is critical to designing the most effective remediation approach. This work focuses on developing a technique that uses gas tracers to detect the location of NAPLs in the subsurface and to elucidate the mass transfer limitations associated with the removal of contaminants from soils.

To detect NAPL/DNAPLs (dense nonaqueous phase liquids), two tracer gases, which are identical except for their solubility in the NAPL/DNAPL, are injected into the soil. By analyzing the difference between the two tracers as they leave the soil, the existence and amount of the NAPL/DNAPL can be determined. Understanding the location and amount of NAPL/DNAPLs within soils will allow for an optimal placement of wells for remediating the contaminated soil or, equivalently, will allow for the minimum number of wells for effective remediation. In both cases, determining the location and amount of NAPL/DNAPLs within soils will greatly reduce the cost for remediation. For advance remediation processes, the success and cost effectiveness often hinge on whether the rate of removal of underground contaminants will be limited by the contaminants' volatility or by slow diffusion processes. The difference in the elution of the two tracer gases from the soil also highlights the critical diffusion limitations within the soil. This information can then be used to select and properly design the most cost-effective remediation method.

We have chosen a suite of fluorinated gases, including  $\text{SF}_6$ ,  $\text{CH}_2\text{F}_2$ ,  $\text{C}_4\text{F}_{10}$ ,  $\text{C}_6\text{F}_{14}$ , and  $\text{CHF}_3$ , with a wide range of solubilities to inject as tracers. These tracers are detectable at very low concentrations (as low as parts per billion) using a gas chromatograph with an electron capture detector. The solubility of the tracers in both the NAPL/DNAPL and the water phases within the soil directly affects the retention of the tracers. In addition, the retention of a NAPL/DNAPL soluble tracer increases monotonically with the amount of the NAPL/DNAPL phase. Methods based on the relative solubility of tracers, such as the proposed method, are commonly referred to

as partitioning tracer methods. This project will first test the selected gas tracers for their ability to detect NAPL/DNAPLs in soils, and will then seek to perfect a mixture of tracers that gives the best data for NAPL/DNAPL detection. Tracers that may be superior to the fluorinated gases listed above will be sought and tested.

The proposed method of partitioning gas tracers for detecting NAPL/DNAPLs offers a cost-effective technique for sampling a large volume of soil. In addition, because tracers are generally confined to the region between the injection withdrawal wells, the proposed method will only give a positive detection if the NAPL/DNAPLs occur between these two wells. Accordingly, by injecting the partitioning tracers in multiple wells surrounding the region of NAPL/DNAPL contamination, the spatial location of the NAPL/DNAPLs can be determined.

## Technical Accomplishments

The first objective of this work was to relate the retention of gas tracers to both the amount of NAPL/DNAPL present in a soil sample and to the solubility of the different gas tracers in the NAPL/DNAPL, water, and vapor phases. For these experiments,  $\text{C}_4\text{F}_{10}$  and  $\text{C}_6\text{F}_{14}$  were tested as tracer gases by injecting them into columns packed with soil and a known amount of a NAPL.

Experimental results show that  $\text{C}_6\text{F}_{14}$  is a suitable tracer for partitioning into a NAPL phase within soil. Tracer retention results for  $\text{C}_4\text{F}_{10}$  show that this tracer has too little partitioning into the NAPL, for most applications. In the experiments conducted, a mixture of  $\text{SF}_6$ ,  $\text{C}_4\text{F}_{10}$ , and  $\text{C}_6\text{F}_{14}$  tracers was injected into soils columns containing 0, 8,500, and 17,000 ppm mineral oil. As expected, the retention of the partitioning tracer increased with the amount of NAPL contaminant. To assess the effect of mass transfer on tracer retention, a series of experiments were conducted at different flow rates. At sufficiently low flow rates, the tracer retention should be unaffected by mass transfer. For the flows tested (30, 15, 6, 3, and 1.5 cm/hr Darcy velocity), the data showed essentially no effect of mass transfer resistances.

Tracer tests were also conducted in a large container of fine sand containing a NAPL. While the tracers were detected, substantial leaking of gas did not allow us to

demonstrate detection of the NAPL with this test. Retention experiments with a water soluble perfluorocarbon tracer,  $\text{CH}_2\text{F}_2$ , were also conducted. While this tracer is twice as soluble in water as  $\text{CO}_2$ , and simple theory suggests it should have a small retention, the retention of  $\text{CH}_2\text{F}_2$  was not delayed within the accuracy of these experiments. A substantially more water soluble tracer, trifluoroacetone, was obtained and will be tested in future experiments.

#### Publication and Presentation

P.A. Gauglitz, L.M. Peurrung, D.P. Mendoza, and G. Pillay. 1995. "Dual-Gas Tracers for Subsurface Characterization and NAPL Detection." Presented at and In *Proceedings of the Second Tracer Workshop*, University of Texas, November 14-15, 1994, Austin, Texas.

# Formation of a Contaminant Barrier by Injecting Metallic Iron Colloids into the Subsurface Environment

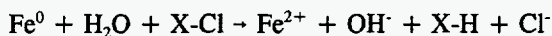
Kirk J. Cantrell and Daniel I. Kaplan (Systems Engineering and Project Management)

## Project Description

Chemically reactive barriers to contaminant migration is an active area of research and development. This in situ technique for remediation of contaminated groundwater offers many advantages over more conventional approaches such as pump-and-treat, excavate-and-treat, or impermeable confinement barriers.

Great interest has recently developed in the use of zero-valent metals (iron in particular) for remediation of groundwater. An entire session with 40 presentations and posters was devoted to this topic at an American Chemical Society meeting in Anaheim, California, April 2-6, 1995. A number of pilot and field demonstrations have been initiated using zero-valent iron ( $\text{Fe}^0$ ) and one full-scale remediation has been in use since 1987.

Many studies have shown that  $\text{Fe}^0$  is a highly reductive material capable of dehalogenating many halogenated hydrocarbons. Zero-valent iron can also chemically reduce several highly mobile oxidized oxyanions (e.g.,  $\text{CrO}_4^{2-}$ ,  $\text{MoO}_4^{2-}$ , and  $\text{TcO}_4^-$ ) and oxyanions (e.g.,  $\text{UO}_2^{2+}$ ) into their insoluble forms. The degradation of halogenated-hydrocarbon compounds (X-Cl) by  $\text{Fe}^0$  has been proposed to occur as follows.



The reaction has been shown to be abiotic, surface area dependent, pH dependent (slower at higher pH levels), and generally unaffected by the ionic strength levels found in most groundwater. Reduction of other contaminants such as halogenated pesticides, nitro aromatic compounds, and other metals  $\text{Cu}^{2+}$ ,  $\text{Ag}^+$ , and  $\text{Hg}^+$ .

Work has been conducted recently at the Laboratory to determine if  $\text{Fe}^0$  colloids could be injected into groundwater aquifer media (represented by sand) with the ultimate objective of forming a barrier in situ through the coordinated use of injection and extraction wells (Figure 1). This approach has considerable advantages over the trench-and-fill methods currently being employed. The primary advantages are accessibility to deep aquifers, and minimal waste disposal and health and safety requirements, because excavation of a trench is not required.

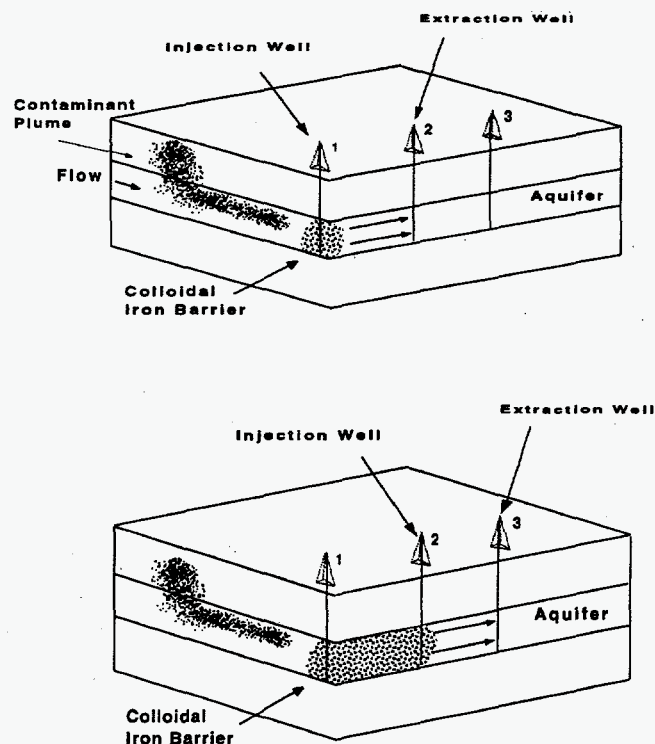


Figure 1. A chemically reactive barrier for the in situ remediation of contaminated groundwater formed through the coordinated use of injection and extraction wells.

Previous publications on the formation of a chemically reactive barrier with  $\text{Fe}^0$  colloids have reported on the effectiveness of various commercially available  $\text{Fe}^0$  colloidal particles to reduce contaminants, the effects of colloid concentration, ionic strength, and surfactant type and concentration on  $\text{Fe}^0$  colloid suspension stability, the breakthrough behavior of zero-valent iron colloids in sand column experiments, and various attempts to model this behavior.

## Technical Accomplishments

Work conducted in FY 1995 included the emplacement of zero-valent iron colloid in sand columns as a function of the following experimental variables: 1) injection rate, 2) colloid concentration, and 3) volume of colloidal suspension injected. The results of this work were fit to a

semiempirical model developed to describe the filtration of dilute, well-flocculated suspensions of particles in deep porous beds. Eleven one-meter-long column experiments and one 3-meter-long column experiment were conducted.

It has been determined that it is possible to inject suspensions of colloidal zero-valent (metallic) iron into sand columns at concentrations which would be effective as an in situ reactive barrier. The quantity of iron injected into the columns does not significantly reduce porosity, which is an important factor in the construction of a permeable reactive barrier intended to allow groundwater to flow freely through the barrier. It was also determined that it is possible to inject the iron colloids to form a relatively flat concentration profile with distance. This indicates that it will be possible to form a permeable reactive barrier through the coordinated use of injection and extraction wells and that the iron can be distributed relatively evenly between the wells as opposed to having the majority of the iron colloids filtered out near the injection point and having relatively low concentration of iron between the wells. The best results were obtained at relatively high flow rates and low to moderate concentrations of iron colloids in the injected suspensions.

A semiempirical model developed to describe the filtration of dilute, well-flocculated suspensions of particles in deep porous beds was used in an attempt to model the data. The utility of the model was limited. In most cases, the model was able to fit the data; however, at the highest colloid concentrations and at low flow rates the model failed to adequately describe the experimental data. The reasons for the failure of the model to adequately describe all of the data determined in this study is not clear at this

time; however, the model does not explicitly account for gravitational settling, and blocking or cake filtration. These phenomenon may have occurred during some of the experiments conducted in this study.

It was determined that it is possible to form a chemically reactive barrier by injection of metallic iron colloids to a distance of at least 3.0 m: greater distances were not attempted during this study. This barrier would be effective under typical groundwater conditions for more than 30 years, at which time the barrier could be easily replenished. Future work is being aimed at injecting the metallic iron colloids to much greater distances which will allow for a significant increase in cost effectiveness of this in situ remediation technique and improving the modeling of  $\text{Fe}^0$  colloid removal within porous media.

#### Publication

D.I. Kaplan, K.J. Cantrell, T.W. Wietsma, and M.A. Potter. "Formation of a Chemical Barrier with Zero-Valent Iron Colloids for Groundwater Remediation." *J. Environ. Qual.* (submitted).

#### Presentation

D.I. Kaplan, K.J. Cantrell, and T.W. Wietsma. 1995. "Formation of a zero-valent iron colloid barrier for the in situ remediation of reducible groundwater contaminants." American Society of Agronomy Annual Meeting, St. Louis, Missouri.



# *Integrated Environmental Monitoring*

Thomas J. Carlson (Systems Engineering and Project Management)

---

## **Project Description**

The objective of this project was to develop a set of analytical procedures and software tools that could be used to improve monitoring network design decisions. Such decisions include the choice of monitoring locations, sampling frequencies, sensor technologies, and monitored constituents. Integrated environmental monitoring is being designed to provide a set of monitoring alternatives that balance the tradeoffs between competing monitoring objectives, such as the minimization of cost and the minimization of uncertainty. The alternatives provided are the best available with respect to the monitoring objectives, consistent with the physical and chemical characteristics of the site, and consistent with applicable regulatory requirements. The selection of the best monitoring alternative to implement is made by the decision maker after reviewing the alternatives and tradeoffs produced by this process.

## **Technical Accomplishments**

During FY 1993, the framework for the network design process was conceptualized, development of a numerical testbed for the approach was initiated, and approaches were developed to target user needs. During FY 1994, the framework was refined, a prototype tool set was assembled, a demonstration problem was defined with the help of potential customers, and work on the demonstration was initiated. During FY 1995, the framework was successfully demonstrated.

### *Refinement of a Decision Framework*

A framework for monitoring decision making was developed during FY 1993. This framework was refined during FY 1994 to focus on critical tools for network planning. The process began with the identification of the monitoring objectives. The next step was to generate the monitoring alternatives that represent the tradeoffs that must be made between competing objectives. Several components are required to generate optimal monitoring network design alternatives. A conceptual model that represents the current understanding of the site ensures that the monitoring alternatives are consistent with the physical and chemical characteristics of the site. An

uncertainty assessment quantifies what is uncertain about site characteristics. The conceptual model, the uncertainty analysis, and the objective statements are combined in a decision model that provides the actual mechanism for the generation of optimal monitoring alternatives. The outcome of the decision model is a tradeoff diagram that will allow the decision makers to choose between monitoring alternatives in a more quantitative way than is currently available.

### *Prototype Tool Set*

Where possible, existing tools were selected for use in demonstrating the design framework. Tools include a groundwater flow model (MODFLOW), a contaminant transport model (FCT), a geostatistical package (GSLIB), and a simulated annealing optimization algorithm (SA).

### *Framework Demonstration*

A demonstration problem was chosen that has relevance and applicability to current Hanford monitoring needs

- good prospects of stakeholder (DOE, users, regulatory agencies, public) acceptance
- achieves results with available resources.

Technical staff and project managers involved in groundwater monitoring onsite were interviewed to identify relevant monitoring issues for the Hanford Site and determine if the demonstration's theme would have stakeholder acceptance.

The demonstration problem consists of a waste disposal facility discharging a contaminant to an unconfined aquifer. Groundwater flow moves from the disposal facility toward a river. A compliance boundary is located between the river and the disposal facility. Remedial action will be required if the contaminant concentration at any point along the compliance boundary exceeds a regulatory limit. The precise path taken by the contaminant as it flows toward the river and the future concentration of contaminant at the compliance boundary are uncertain due to the spatial variability of the unconfined aquifer.

The monitoring objectives on which the demonstration of the design of a network were based included the following:

- Minimize cost, assumed to be proportional to the number of monitoring locations. This objective will be to reduce the total number of monitoring wells.
- Maximize the probability of detecting a contaminant concentration at the compliance boundary in excess of the regulatory limit. This objective was to increase the number of wells located along the compliance boundary and those wells were placed where the contaminant has the greatest probability of exceeding the regulatory limit.
- Maximize the probability of correctly predicting whether the contaminant will exceed the regulatory limit at the compliance boundary. This objective was to increase the number of monitoring wells at locations other than the compliance boundary. Wells were placed in those locations where monitoring is expected to result in the greatest reduction in the uncertainty of contaminant concentration at the compliance boundary.

The objectives conflict with each other both in the total number of monitoring wells (objective 1 argues for as few wells as possible while objectives 2 and 3 argue for many wells) and in the locations of those wells (compare objectives 2 and 3). Objectives 2 and 3 also have an element of time in them. The probability of detecting a contaminant that reaches the compliance boundary (objective 2) will depend on the frequency of sampling. The probability of correctly predicting whether a contaminant will reach the compliance boundary (objective 3) is a function of what is known about the groundwater flowfield and the current location of the contaminant. As the contaminant moves, the uncertainty in its location tends to increase unless new information (through additional monitoring) is obtained.

The network design incorporates uncertainty in the contaminant location through a Monte Carlo simulation of groundwater flow and transport. This simulation provides an estimate of the expected concentration of the contaminant at any location and time, as well as the variability (or uncertainty) of the contaminant concentration. In an informal way, this information can be used to guide the location of additional monitoring wells since it may be most valuable to monitor at those locations where the uncertainty is greatest. For the demonstration problem, the Monte Carlo simulation results were used in a much more quantitative way.

The network design method requires that a set of potential monitoring locations be defined. The stochastic simulation results were used to limit these locations to the region where the contaminant concentration had a reasonable probability of exceeding the detection limit. The simulated annealing code was used with the Monte Carlo simulation results to find monitoring well locations that balanced the three objectives listed above.

The network design method provides a quantitative measure of the probability of the contaminant exceeding the regulatory threshold at the compliance boundary. This probability can be used to decide between various options

- intervene/remediate immediately (if the probability of exceeding the threshold is high, e.g.,  $> 0.90$ )
- perform routine monitoring at the compliance boundary with no intervention (if the probability of exceeding the threshold is low, e.g.,  $< 0.10$ )
- carry out additional monitoring to better characterize the contaminant distribution (if the probability of exceeding the threshold is neither high nor low).

For the demonstration problem, the maximum contaminant concentration at the compliance boundary did not fit either a normal or lognormal model, but was positively skewed with a very long tail. The probability of the contaminant concentration at the compliance boundary exceeding the regulatory threshold was found to be 16 percent. This value is relatively small, but not insignificant. The optimization model suggested that this probability could be reduced by sampling the contaminant concentration along the boundary of the plume. The best locations and times to sample were specified by the model.

In the event that the contaminant concentration at the compliance boundary exceeds the regulatory threshold, the optimization model estimated that a single well located on the compliance boundary had a 38 percent chance of detecting it. Two wells being monitored increased the probability of detection to 69 percent, three wells increased it to 94 percent, and four wells offered approximately 100 percent detection. The optimization model determined the best locations along the compliance boundary to monitor.

# Interpretation of Single-Well Tracer Tests

Timothy D. Scheibe and Stephen H. Hall (Systems Engineering and Project Management)

## Project Description

Tracer tests which employ a single well to characterize subsurface flow and transport properties include the drift-and-pumpback and "point dilution" methods. These tests, which can be conducted simultaneously, employ a downhole probe that measures in situ solute concentrations within a borehole at various depths and times. Although the tests have been applied to field sites and have yielded useful information regarding these sites' characteristics, these field projects have also indicated the need to develop greater insight regarding their interpretation. For example, while aquifer transmissivity can easily be estimated by the drift-and-pumpback method, the results may also contain important information regarding the aquifer dispersivity, natural heterogeneity, and (for nonconservative tracers) retardation coefficients or other measures of sorptivity.

To enhance the interpretability of the results of these tests, and thereby extend their usefulness, we have undertaken a series of numerical simulations based on the field data collected from two sites. A simple two-dimensional analytical model of radial flow, combined with a particle-tracking model of transport, was developed and successfully applied to provide estimates of field-scale dispersivity by fitting to the field data. More detailed, numerical, three-dimensional, heterogeneous aquifer models were applied to examine the effects of complex aquifer heterogeneity. With the interpretive tools and insight being developed, these single-well tracer tests will become powerful methods for rapid and relatively inexpensive field characterization of aquifers.

## Technical Accomplishments

Three model approaches to simulating and interpreting the drift-and-pumpback single-well tracer test were developed and evaluated

1. fully analytical
2. analytical flow/numerical transport
3. fully numerical.

Each model approach has advantages and disadvantages relative to its ease of use and general applicability. The utility of each was evaluated through application to a number of test cases. Models 1 and 2 were developed and

coded as part of this project; approach three employed a pre-existing numerical code written at the Laboratory, called RAFT.

The first test case evaluated was data collected at an aquifer thermal energy storage (ATES) site in Alabama (UASRC site). This site exhibited a simple tracer recovery curve, and all necessary model parameters had been measured other than aquifer dispersivity. The single-well tracer test results had previously been interpreted to estimate pore velocity, but had not been analyzed with regard to dispersion. Using the relatively simple models (class 1 and 2 above), the dispersivity parameters (longitudinal and transverse dispersivity) were adjusted by trial-and-error or by numerical optimization to develop a "best-fit" estimate of the dispersivity. Figure 1 shows the close match between the tracer recovery curve predicted by the model and that observed in the field. The second test case was data collected at another ATES site (GM site). The observed response at this site was more complex, showing possible effects of layered heterogeneity within the aquifer. The models were employed to attempt to fit this behavior using a two-layer heterogeneous aquifer conceptualization. The resulting model predictions are compared with the observed data in Figure 2. Note that, while the fit shown is not as good

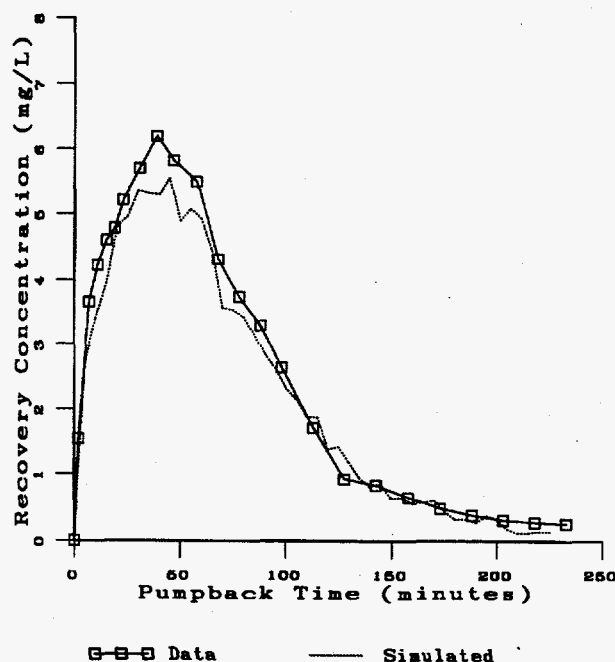


Figure 1. Comparison between model response and measured response, for UASRC site.

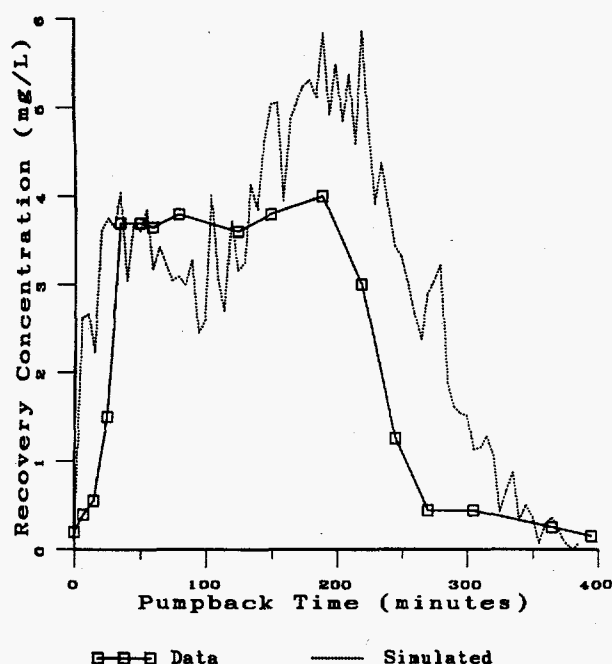


Figure 2. Comparison between model response and measured response, for the GM site.

Figure 2. Note that, while the fit shown is not as good as that in Figure 1, the use of a two-layer aquifer conceptualization introduces additional parameters that are not constrained by available information. Therefore, it would be possible to improve the fit in Figure 2 to an arbitrary degree, but the results would not necessarily be physically meaningful. The important conclusion drawn from this exercise is that a multi-layer model can lead to a bimodal or flattened response curve, and that modeling of such a response would require prior characterization of the relative thicknesses and hydraulic conductivities of the layers to obtain physically meaningful results. Such characterization could be performed using the point-dilution method, which can be implemented simultaneously with the drift-and-pumpback test.

These results indicate that relatively simple model simulations can provide estimates of dispersivity parameters based on the results of the drift-and-pumpback and point dilution tests, in either macroscopically homogeneous or simply layered aquifer systems.

In more complex heterogeneous systems, the expected response of the drift-and-pumpback test was unknown. Therefore, in the final stage of this study, the third model approach (fully numerical) was used in conjunction with synthetic heterogeneous aquifers to simulate the response. Two heterogeneous systems were analyzed. The first was a perfectly layered system with multiple layers of differing thicknesses and hydraulic properties. This synthetic aquifer was generated as part of another project using a simple Markov transition probabilistic method. The second synthetic aquifer contained complex heterogeneity at two scales, and was generated using geostatistical simulation techniques (also as part of another project). These two synthetic data sets were input to the fully numerical flow and transport simulator to determine the estimated response to a simulated drift-and-pumpback test. The resulting simulated response curves were interesting in that they exhibited similar behavior to the two actual datasets discussed above (UASRC and GM sites). In the case of the layered system, the simulated response was multimodal; in the case of the complex heterogeneity, the response was unimodal and had similar form to the UASRC site. These results indicate that the form of heterogeneity can be determined to some degree from the test response, and that certain heterogeneous systems will behave as macroscopically homogeneous.

#### Acknowledgment

Simulated aquifer systems based on the Oyster, Virginia, site were developed under the Bacterial Transport Subprogram within the U.S. Department of Energy's Subsurface Science Program, Dr. Frank Wobber, Program Manager.

#### Presentation

T.D Scheibe, S.H. Hall, and A. Chilakapati. 1995. "Interpretation of Single-Well Tracer Tests," Geological Society of America Annual Meeting, November 6-9, New Orleans, Louisiana.

# Microbiological Controls on Contaminant Behavior

Raymond E. Wildung (Environmental Science Research Center)

---

## Project Description

The primary objective of this investigation was to provide the advanced, long-term capabilities in organic geochemistry, microbial physiology, and biochemistry needed to link molecular-scale investigations in chemistry and microbiology to solution of problems in environmental restoration.

## Technical Accomplishments

Rapidly developing capabilities in molecular sciences need to be linked to resolution of problems being faced by DOE in environmental restoration. Environmental processes that must be addressed include enzyme-level phenomena governing microbial biodegradation/sequestration and geochemical reactions occurring at mineral-solution interfaces. In conjunction with hydrologic transport, these phenomena govern contaminant mobility in the subsurface and form the basis for development of new remediation concepts.

### Microbial Physiology and Biochemistry

In FY 1995, the task in microbiology played a key role in developing advanced capabilities for use in bioremediation. In order to understand the reaction mechanisms and to improve the activities of a reductive dehalogenase, tetrachloro-*p*-hydroquinone (TeCH-RD) important in degradation of contaminants, a collaboration with molecular sciences research staff was established to determine the three-dimensional structure and reaction mechanisms by nuclear magnetic resonance. Since TeCH-RD is a 29 kDa protein, determining its structure requires nuclear magnetic resonance spectrometer capabilities on the cutting edge of science, such as the 750 MHz nuclear magnetic resonance spectrometer at the Laboratory. Significant progress has been made in stabilizing the protein, maintaining a monomer status, labeling it with N<sup>15</sup>, and analyzing labeled and unlabeled products by two-dimensional nuclear magnetic resonance.

Focus has also been on the molecular biology of nitrilotriacetate (NTA) degradation by *Chelatobacter* strain ATCC 29600. Nitrilotriacetate is a chelating agent, and its degradation is thought to decrease the mobility of heavy metals and radionuclides in the environment. A

nitrilotriacetate monooxygenase (NTA-Mo) has been purified that catalyzes the oxidation of nitrilotriacetate to iminodiacetate and glyoxylate and its N-terminal amino acid sequence determined. The gene responsible for expression of this enzyme was cloned using an oligonucleotide probe developed on this project. The genes were then sequenced.

The biochemistry of 2,4,5-trichlorophenoxyacetate (2,4,5-T) degradation by *Pseudomonas cepacia* AC1100 has also been under study. The compound 2,4,5-T is a chlorinated aromatic herbicide. This study focuses on understanding its biodegradation pathway and has provided much needed information on dehalogenation mechanisms. The 2,4,5-T oxygenase has been purified and characterized. Investigations are now directed toward defining a second enzyme in the 2,4,5-T degradation pathway.

The biochemistry of 3-chlorobenzoate degradation by *Desulfomonile tiedjei* is another exciting new avenue of research under way on this project. Reductive dehalogenation is the only known mechanism for remediation of many chlorinated compounds and this research is challenging because *D. tiedjei* grows very slowly and requires strictly anaerobe conditions. In addition, the enzyme is a membrane protein. However, this research has successfully purified and characterized the enzyme, and has placed the Washington State University-Pacific Northwest National Laboratory team in the leading position to understand the reductive dehalogenation by anaerobic microorganisms. Current effort is focused on cloning the corresponding genes.

A new research effort, initiated in FY 1995, defines the biochemistry of ethylenediaminetetraacetic acid (EDTA) degradation by a newly isolated bacterium. This project broadens the research on other chelating agents and focuses it on a chelate known to be responsible for mobilization of radionuclides in subsurface systems beneath DOE waste sites and which complicates separation of radionuclides in tank wastes. This research has identified a monooxygenase that breaks down EDTA. The purification of the enzyme is in progress. Understanding the degradation of this chelate will provide the basis for technology to markedly reduce the likelihood of radionuclide exposure in the environment and during waste processing.



## Organic Geochemistry

New investigations in geochemistry are expected to develop joint capability in subsurface solute and colloid transport processes at multiple scales. Close consideration is being given to the linkage with microbial processes governing solute behavior in subsurface systems. The focus is on 1) determining the mechanisms controlling subsurface transport in physically heterogeneous porous media, and 2) developing kinetics models of sorption and deterministic modeling of experimental results. The mineralogy, surface chemistry, and physical properties of the porous medium is being determined using (e.g., atomic force microscopy and x-ray photoelectron spectroscopy). Laboratory column experiments will be designed to determine the rates of sorption to aluminosilicates (quartz and montmorillonite) and ferric oxide-coated quartz. Porous medium hydraulic properties, surface structures, and the kinetic rates of attachment will be incorporated in deterministic reactive chemical transport models to aid in design of pilot-scale experiments to test the effects of hydraulic property variation on solute transport.

A preliminary study on the biodegradation of naphthalene in multiphase systems containing nonaqueous phase liquids (NAPLs) has been completed. The results indicated that relative to aqueous systems, conversion of naphthalene to CO<sub>2</sub> increased in the presence of decane, dodecane, and hexadecane. Biodegradation was apparent, but decreased in the presence of octane, and was negligible in the presence of hexane. Thus biodegradation was sustained in systems where log K<sub>ow</sub> of the NAPL was greater than 5 and inhibited when log K<sub>ow</sub> of the NAPL was less than 4. Additional research is proposed to elucidate the mechanisms controlling biodegradation in systems with residual NAPLs that are nontoxic to the bacteria.

The initial findings summarized here and results from other work suggest that some bacteria are able to use the substrate directly from the NAPL phase and other strains cannot. This may be the factor which determines whether NAPLs enhance or inhibit the extent of biodegradation and is the subject of further study. Related research that

addresses contaminant partitioning, mass transfer, and bacterial attachment at the NAPL-water interface will continue to explore the mechanisms governing biodegradation in systems that contain residual NAPLs.

A related project also addresses the bioavailability of organic substrates in soil and groundwater systems; this research is directed toward developing simple methods for independently approximating biodegradation kinetics in soil-water systems. An approach to accomplish this combines measured sorption parameters with the biodegradation rate constant that is measured in aqueous solution. The models provide a means for estimating biodegradation kinetics in systems where bioavailability is decreased due to sorption of the substrate to the soil.

## Publications

- S. Ni, J.K. Fredrickson, and L. Xun. 1995. "Purification and Characterization of a Novel 3-chlorobenzoate Dehalogenase from the Cytoplasmic Membrane of *Desulfomonile tiedjei* DCB-1." *J. Bacteriol.* 177:5135-5139.
- Y. Xu, and K. Wagnon. 1995. "Purification and Properties of 2,4,5-trichlorophenoxyacetate Oxygenase from *Pseudomonas cepacia* AC1100." *Appl. Environ. Microbiol.* 61:3499-3502.
- A.P. Gamerdinger, R.S. Achin, and R.W. Traxler. *Journal of Environmental Quality* 24:1150-1156 (in press).
- L. Xun. "Purification and Characterization of Chlorophenol 4-monooxygenase from *Pseudomonas cepacia* AC1100." *J. Bacteriol.* (submitted).
- Y. Xu, M.W. Mortimer, M.L. Kahn, F.J. Brockman, and L. Xun. "Cloning and Sequencing of a Gene Cluster Encoding Nitrilotriacetate Monooxygenase of *Chelatobacter heintzii* ATCC 29600." *Appl. Environ. Microbiol.* (submitted).

# *Monitoring Technology for Water Control Facilities*

Thomas J. Carlson (Systems Engineering and Project Management)

---

## **Project Description**

The objective of this project was to develop new light emitting tag and photogrammetric technology that would help to reduce the environmental costs of hydropower operations and other uses of surface water. It will provide a means to obtain essential biological criteria and to integrate these criteria into the design and operation of water control and power production facilities.

This technology is directed at monitoring and evaluation of the behavioral responses of fish to engineered structures and feeding back to the engineering design process information critical to the design and operation of such structures. The lack of biological design criteria or the means to obtain those criteria for hydropower and water control facilities is currently one of the major impediments to recovery of fish stocks in the Columbia River basin and elsewhere.

## **Technical Accomplishments**

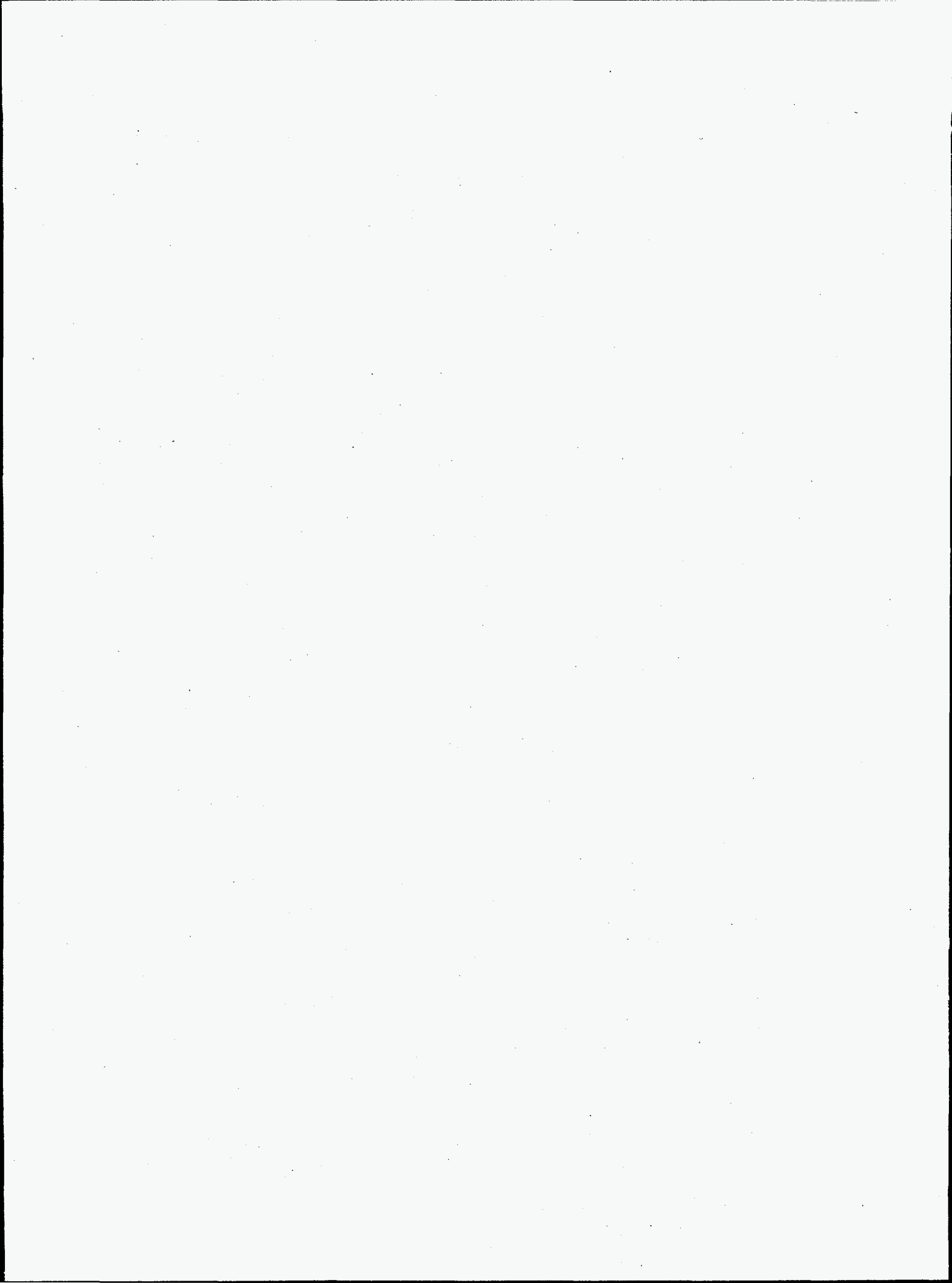
The project was divided into two interrelated parts

1. Laboratory evaluation of the absorption of light at wavelengths of 500, 700, and 880 nm during passage through water under clear, low, and high turbidity conditions.
2. Estimation of parallax using a stereo pair of standard CCD array video cameras in deployments where the image paths would include three media of different refractive index.

Standard light emitting diodes were used as the light sources for the laboratory tests of absorption. Power was provided by 3-V micro batteries. The relative level of transmitted light was measured using image processing techniques. Test conditions included measuring the light transmitted through water of varying levels of turbidity

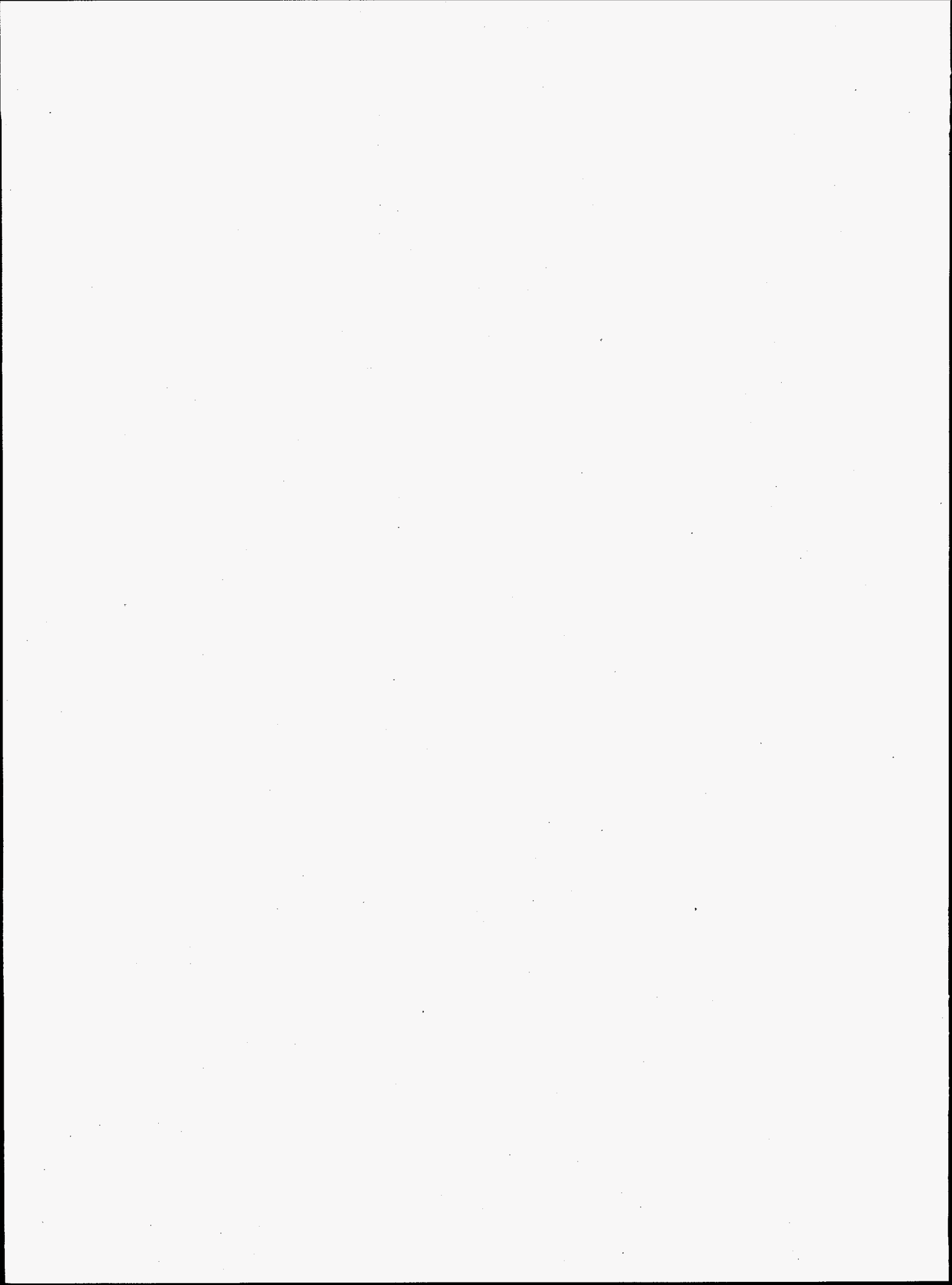
over light paths through water ranging from 0.1 to 0.5 m in 0.1-m increments. All measurements were made under conditions of darkness with the only light source being the light emitting diode under test. Absorption was as expected with the longer wavelengths of light experiencing significantly higher levels of absorption at all levels of turbidity. Under clear water conditions, all of the light emitting diodes tested produced light that was readily detected over the maximum light path through water, 0.5 m. Under low turbidity conditions, 19 to 24.5 NTU, light at all wavelengths was also detectable over the maximum path length. However, under high turbidity conditions, 64 to 76 NTU, no light was detectable at any wavelength at path lengths greater than 0.3 m. Analysis of data continues to derive turbidity dependent extinction coefficients as a function of wavelengths and source intensity. This information is essential for the design of experiments using light emitting tags at water control facilities.

The imaging geometry for the case of an image path through three media of different refractive index, air, glass, and water, was determined. The parallax equations resulting from this geometry were solved using a computer program written in FORTRAN, as well as a spreadsheet program written using a macro language internal to the spreadsheet program. The programs permit evaluation, in terms of parallax within a user selected volume, of different imaging geometry, including the location and separation of cameras and the configuration of individual camera CCD arrays and lenses. The programs will be used to design experiments, including selection of cameras and lenses, to observe fish behavior and the dynamics of other particles in flowing water in a variety of underwater experimental settings. The initial use of the programs will be to evaluate the feasibility of observing the trajectories of fish with light emitting tags moving through hydroturbines. The trajectory of fish through hydroturbines is a major uncertainty in design of a new generation of hydroturbines that are less harmful to fish.





## **Integrated Technology Policy and Regulatory Analysis**



# *Development of Meso-Level Perspectives for Modeling the Global Environmental Consequences of Human Behavior*

Steven F. Rayner (Global Climate Change)

---

## **Project Description**

The objective of this research was to develop meso-level perspectives for the study of human behavior in relation to global climate change and its impacts. The meso-level of human behavior is that lying between the micro-level of human individuals and the macro- or global-level. At the meso-level, institutional frameworks shape the collective behavior of individuals, organizations, and markets.

## **Background**

Economic models such as the Edmonds-Reilly-Barns (ERB) model, the Second Generation Model (SGM), and the Global Change Assessment Model (GCAM) predict the individual behavior of human beings with the assumption that each will attempt to maximize his or her personal gain. This assumption has frequently been questioned by other social sciences (e.g., political science and anthropology), which focus empirically on the behavior of human institutions rather than that of idealized individuals in idealized markets. However, modelers have been concerned that abandoning the single metric of rationality assumed in the utility maximizing individual at the center of microeconomic theory would leave them with the impossible task of modeling a potentially infinite number of real individual utility functions. Until recently, qualitative social science has offered no consistent basis on which a smaller, more tractable number of utility functions could be based.

A convergence of factors offers an opportunity for macro-models to better represent realistic human behavior while preserving some degree of parsimony. The emergence of Cultural Theory in the 1980s provides a basis for modeling three to five utility functions that are universally, but unevenly, distributed among human populations, including social decision makers. These utility functions are maintained not by individual human preferences, but by meso-level institutions. Cultural Theory also provides consistent criteria to measure these factors mathematically, while accessible computing power has increased sufficiently to handle the increased complexity that such modeling would require.

## **Technical Accomplishments**

FY 1995 research was focused on the following five areas:

1. representing cultural factors in macroeconomic models
2. cultural shaping of climate change damage functions
3. investigation of household fertility decisions
4. meso-modeling approaches to agricultural decision making
5. diversity in discounting behavior.

### *Representing Cultural Factors in Macroeconomic Models*

Most macroeconomic models assume that nations will select the least expensive action among options. This assumption is acceptable when the choice is between familiar and low-cost, low-risk options. However, when choice involves technologies that are high-cost, high-risk, or novel, non-price factors, such as political considerations, play a much greater role. The Edmonds-Reilly-Barnes model, for example, used a price surrogate for public acceptance of nuclear power, consequently overpredicting penetration of nuclear power in the U.S. and underpredicting it for Japan and Europe, based on International Energy Agency projections for the year 2000. The current work investigated whether using cultural theory can help account for differences in political behavior and whether these differences can be reflected in a model at the level of the nation-state.

This study used an index developed by Geert Hofstede as a proxy for cultural theory in quantifying public acceptance of nuclear power. The index enables us to translate relative degrees of acceptance into an equation that will help determine rates of penetration of nuclear technology in three countries: Japan (hierarchy), Sweden (egalitarian), and the United States (individualist). Hierarchies such as Japan are distinguished by their preference for bureaucratic procedures and control. Egalitarians such as Swedes are characterized by their

emphasis on equality, cooperation, and consensus. Individualist cultures such as the United States encourage competition and entrepreneurial activity, with emphasis on maximizing benefits to the individual.

The study demonstrates the possibility of incorporating cultural factors into macroeconomic models. Including such intangibles in modeling efforts may enhance the predictive power of models and ultimately assist policy-makers in formulating appropriate responses to questions of future energy and technology choices. The results were presented to the International Institute for Applied Systems Analysis (IIASA) Risk, Policy, and Complexity (RPC) planning meeting, and a paper is currently being revised for publication.

#### *Cultural Shaping of Climate Change Damage Functions*

A vast spectrum of differing viewpoints currently exists about the impacts of climate change issue in both policy and scientific communities. We explored the use of cultural theoretic concepts as a method for interpreting these differences in assumptions and conclusions about the climate change issue. Using our MiniCAM integrated assessment modeling system, we constructed scenarios to illustrate both climate change abatement costs and climate change damage functions for each of three cultural archetypes: the individualist, the egalitarian, and the hierarchist.

In brief, we presented the individualist culture viewpoint as believing in the ability of human systems and economies to adapt well to climate change; therefore, intervention is both unnecessary and costly, since it interferes with the workings of the market system. In contrast, the egalitarian cultural viewpoint sees climate change as catastrophic, but also tends to believe that climate change prevention costs would be small or negative if we introduced appropriate technologies. Finally, the hierarchist cultural viewpoint is agnostic about climate change or markets, but believes strongly in our ability to manage systems to deal with the change.

The results from the MiniCAM scenarios illustrate the magnitude of the gap in viewpoints numerically. Under all scenarios, global temperature increased by about 2.5°C by 2100. In the Individualist scenario, this temperature increase resulted in a net benefit to the global economy of about half a percent of global gross national product. In stark contrast, the Egalitarian scenario showed damages reaching 10 percent of global gross national product from climate change. The Hierarchist scenario showed smaller damages from warming, about 2 to 3 percent of gross national product.

Our analysis demonstrated that conflicting views about dealing with climate change arise not just from

disagreements or uncertainties about technology and physical science, but also from the latent cultural beliefs of the people performing the analysis.

#### *Investigation of Household Fertility Decisions*

The goal of this work was to identify those factors that determine the fertility rate and hence family size and to explore how family size decisions have been modeled in the past. We carried out an extensive literature search and synthesized the material into five products: 1) an annotated bibliography, 2) a review of the factors that have appeared in empirical analyses as having a significant influence on fertility, 3) a discussion of the model developed by Gary Becker that employs the "dynastic utility function" to explain intergenerational interactions, 4) a short discussion piece that speculates about the relation between family size choice and sustainable development and how both could use the dynastic utility function, and 5) a discussion regarding how the second through the fourth items might be used in a meso-modeling exercise.

The results suggest that meso-models might build on the fertility and family economics literature in two ways. Most importantly, the general equilibrium model itself should incorporate lagged feedback from three factors to the population growth parameter. Meso-models could also be improved by reorienting the utility function (assuming the model is an optimization exercise) away from a simple maximization of discounted flows of consumption goods, and toward a dynastic utility function that captures motives for families to postpone consumption or to favor more sustainable paths of development and resource use.

#### *Meso-Modeling Approaches to Agricultural Decision Making*

The Laboratory's GCAM systematically links human activities responsible for emissions of greenhouse gases and land use change to their effects on atmospheric processes, consequent change in climate, and impacts on natural and managed ecosystems. GCAM deals with processes at the global scale, so broad simplifications are made in many of the assumptions underlying the component models. For example, human activity is treated in GCAM as driven by population growth and rational economic behaviors. Social and cultural factors are not modeled directly in GCAM or in other approaches to the problem.

Agricultural productivity and decision making are currently simulated in GCAM with the Erosion Productivity Impact Calculator (EPIC) developed at Texas A&M University and modified at the Laboratory. Mexican farms provide a good opportunity to adapt and

test EPIC across a range of agricultural systems from the most advanced to the subsistence level.

Information was assembled on the geography, farm characteristics, and land management practices employed in the three agricultural sectors in 10 northern Mexican states. Drawing on a variety of U.S. and Mexican sources, we collected data on the amount of land under cultivation in each state, as well as the number, size, and type of farms (e.g., subsistence; medium-tech, semi-collective *ejidos*; commercial). With respect to land management techniques, we gathered information on annual crop yields and rotations, agricultural technologies, and the amount of land subject to irrigation. Further research provided population and income statistics as well as information on social trends in the agriculture sector. A final component of the research consisted of background data describing the contribution of agriculture to Mexico's overall economy and various environmental problems associated with farming.

Based on this information, appropriate changes can now be made in the EPIC model to permit its application to the variety of decision makers in Mexican agriculture. More generally, this project enhances our ability to analyze the current situation of agricultural systems in developing countries and their sensitivity to change due to environmental and sociopolitical factors.

#### *Diversity in Discounting Behavior*

Cultural theory, as a tool for understanding and evaluating behavior in an institutional framework, can shed light on discounting behavior and potential alternatives to the single-behavior approach that is used in most models. This investigation sought to determine whether the predictions that cultural theory makes about discounting behavior can be observed in the literature. Various literature was examined to see if a diversity of viewpoints about discounting exist and whether these differences in viewpoint were related to the predictions made by cultural theory. The results of the review corresponded with the predictions made by cultural theory.

A review of the literature indicated that a diversity of viewpoints exist, but that five themes can be discerned: 1) the discount rate should vary based on risk, 2) discounting methods need to be adjusted to balance efficiency with equity, 3) discounting is bad, 4) the appropriate discount rate can be determined through the use of a new procedure (particulars may vary), and 5) institutions discount differently depending on whether they are acting as an institution or as an individual. Therefore, arguments for varying the discount rate, calculating an "appropriate rate," and not discounting at all can be found in the literature.

## Conclusions

These five projects represent the first steps toward more realistic representation of institutional variation in integrated assessment models for climate change research and policy. We confirmed that there is poor understanding throughout the social sciences of the articulation of human behavior at the local level to the behavior of the global social and economic system. Furthermore, knowledge of local behaviors that is available has not penetrated very deeply into the global descriptive agendas of the IPCC or the Human Dimensions Program of the International Social Science Council.

However, we have identified what may be the most significant obstacle to developing modeling perspectives linking the local and the global. The desired integration cannot be achieved simply by increasing the scale and quantifiability of interpretive analysis to meet a more thickly textured descriptive analysis as it attempts to accommodate lower levels of aggregation. The gap between the two approaches is not merely spatial but raises fundamental issues of what kinds and sources of knowledge we value as analysts.

One scholar argues that the difference between the local and global perspectives is not one of hierarchical degree, in scale or comprehensiveness, but one of kind. In other words, the local is not a more limited or narrowly focused apprehension than the global, it is one that rests on an altogether different mode of apprehension - one based on an active perceptual engagement with components of the dwelt-in world, in the practical business of life, rather than on the detached, disinterested observation of a world apart (Tim Ingold, "Globes and Spheres," in K. Milton [ed], *Environmentalism*, London, 1993:40-41).

The scholar experiencing the world from within is displaced (for example, in satellite imagery) by an observer viewing the world from without. Nothing is intrinsically objectionable in this standpoint; except when we privilege observation over experience. Local knowledge, originating in experience, is downgraded as partial, parochial, and ultimately unreliable whereas global knowledge is treated as universal, total, and real. Ultimately this difference in standpoint may represent a greater obstacle to developing meso-scale perspectives than any of the technical obstacles encountered in our research.

## Publication and Presentation

S.F. Rayner. 1995. International Institute for Applied Systems Analysis (IIASA) Risk Policy, and Complexity, IIASA, August 7-9, Laxenburg, Austria.

# *Integrated Climate Change Analyses: A Pilot Study*

Marilyn J. Quadrel (Environmental Management)  
Denise Lach (Battelle Seattle Research Center)

---

## **Project Description**

The purpose of this project was to develop a set of analytic tools that could be used to maximize the effectiveness of Global Change Research Project (GCRP) information in long-term decision making. Originally, the project was designed as a proof-of-principle study to develop, test, and recommend methods for assessing the context within which policy issues relevant to global change are defined, decisions are identified, and choices are made. It was envisioned that these tools could be applied at the beginning of integrated assessment programs to guide information exchange between the science and policy communities in order to better focus research and integration efforts on those topics that are most likely to benefit from information about global change. After a debriefing session on the results obtained in FY 1994, the FY 1995 analyses were refocused through an institutional analytic method that resulted in recommendations for techniques for analyzing the "readiness" of organizations to use external information and the "usefulness" of such information in organizational decision processes.

## **Technical Accomplishments**

The analysis work in FY 1995 began with a qualitative examination of all four organizations in which interviews were conducted during FY 1994—Northwest Power Planning Council, Bonneville Power Administration, Oregon Department of Fish and Wildlife, and a public power utility. Four preliminary findings emerged from the analysis.

1. Organizational members consistently described a model for organizational decision making that explained how decisions are framed, whose participation is valued (and whose isn't), what information is valued, and what processes must take place for a decision to be understood as "made."
2. In the public sector organizations we examined, respondents did not describe a traditional type of decision making (i.e., a single decision maker making unilateral choices between alternatives). Instead, they described a building of normative consensus among relevant organizational and extra-organizational actors. This iterative, interactive process is similar to negotiation that we classically describe as decision making.

3. Scientific information is not privileged in organizational decision making. It competes with local knowledge, political mandates and pressures, stakeholder pressures, and internal organizational needs in making contributions to decision processes. In those organizations that successfully integrate scientific information, a "bridge" exists to translate the external data into organizationally useful information.
4. In public sector organizations, decision processes are severely limited by political circumstances or regulatory mandate(s). Many decisions, in fact, are dictated by mandates that constitute strict boundaries or limits to the organization decision framework. The use of external information in these decisions is often limited because it is organizationally expensive to collect and integrate into routine decision processes.

The results were then interpreted through an institutional perspective that identified organizational barriers to information use in decision making

- Existing decision routines in the organizations do not include the use of external information (e.g., global change research results).
- Bridges (individuals or organizations) that could be used to link external information sources and internal decisions processes are often in positions peripheral to the decision-making structure.
- Organizational constraints on highly embedded problems devalue wide searches for innovative solutions.

It appears that isomorphic institutional constraints are not currently strong enough to compel organizations in this policy arena to find global change research results "useful" in their decision processes. The 1995 analyses suggests that organizations find information useful for a wide variety of reasons beyond economic utilization including coercive, normative, and mimetic pressures from outside organizations and institutions. The analysis also suggests that structures internal to the organization make it more or less amenable to using external information in decision processes including the presence of "bridges" who act to facilitate the transfer of information, semipermeable boundaries that encourage the elicitation of outside information, and routine decision processes in flux.

These findings suggest that we can develop effective analytic techniques or tools that can assess whether external institutional pressures are strong enough to compel organizations to find global change information "useful," and whether internal organizational structures are available to create a state of "readiness" for

information use. In combinations, these two techniques for assessing "usefulness" and "readiness" states may provide a method for rapidly assessing the likelihood that global change research results will be or can be used in organizational decision processes.

# North American 3E Model

James A. Edmonds and Norman J. Rosenberg (Global Environmental Management)

---

## Project Description

The goal of this research was to develop and test an integrated and quantitative model of the North American economic-energy-environmental system, termed the NA3E Model. This model will stand on its own as an independent computational tool and be directly useful in continued development of the Pacific Northwest National Laboratory Second Generation Model (SGM). The NA3E model will integrate the United States, Mexican, and Canadian Modules of the Second Generation Model. The overall Second Generation Model architecture is designed so that models can be integrated without any changes in either system boundary definitions or computer code.

The NA3E model will be used to project future features of the North American economic-energy-environmental system in sufficient detail to permit evaluation of various aggregate policies and practices relevant to sustainable development trajectories. Attention will be focused on how near-term energy, environmental, and economic decisions will affect the evolution of the increasingly integrated North American energy system, which is the focus of significant current attention due to developments such as the North American Free Trade Agreement (NAFTA).

The specific knowledge developed from each of the five project tasks will also be integrated into the expanded version of the Second Generation Model tailored to the current situation in North America. The resulting modeling capability will be unique among global environmental analysis tools and could have major application in supporting U.S. government and private sector decisions related to competitiveness, trade, energy, and environmental policy issues.

## Technical Accomplishments

A key element of this project has been to develop specific research collaborations with organizations in the U.S., Canada, and Mexico using existing contacts with North American energy and environmental experts. Organizations involved in developing the Mexican and Canadian modules of the Second Generation Model are the Institute for Integrated Energy Systems, University of Victoria, and Centro de Economia, Colegio de Postgraduados, Montecillo, Edo de Mexico.

The NA3E project involved the conduct of five interrelated tasks:

1. Integrated near-term technological changes and policy decisions that will shape the future U.S. energy system.
2. Developed the basis for an integrated model of the Mexican energy system.
3. Developed the basis for an integrated model of the Canadian energy system.
4. Developed an ecological baseline and responses to the growth of a North American energy system.
5. Developed a quantitative understanding of the interrelationships and coupling of the future U.S., Canadian, and Mexican energy systems.

The NA3E project was successful in accomplishing the goals of Tasks 1 through 3 by attracting talented collaborators in Canada and Mexico to the tasks of developing modules of the Second Generation Model for these nations. The Mexican team was led by Dr. Jaime Matus of the Centro de Economia, Colegio de Postgraduados at Montecillo, Edo de Mexico. The Canadian team was led by Dr. Hans-Hölger Rogner of the Institute for Integrated Energy Systems at the University of Victoria. Both teams developed and delivered to Pacific Northwest National Laboratory the requisite databases for their regions. The Canadian team went beyond to develop baseline cases of future economic, energy activities, and atmospheric emissions.

Efforts during FY 1995 were concentrated primarily on Task 4. Because funding for the NA3E project was less than had been planned for in FY 1995 and no funds have been provided for FY 1996, Task 4 has not been fully completed.

While many of the goals of the NA3E project were achieved, the ultimate goal of linking and running an integrated North American Model (Task 5) has not been accomplished. Problems associated with assembling the Mexican database consumed more resources than had been anticipated.



The "environment E" component, addressed in Task 4, contributes to the NA3E project through two linked activities:

- development of a continentally coherent and GIS-mappable information base on soils, climate, water resources, land use, physical infrastructure, and other relevant factors to facilitate identification of specific regions, localities, and enterprises that may be affected by the implementation of NAFTA, climate extremes and natural interannual climate variability, as well as potential climate changes forced by greenhouse warming
- development of a capability for process simulation modeling of North American agriculture (water resources, forestry, and unmanaged ecosystems) that will make use of, and contribute to, the information base.

#### *Progress on the GIS*

High resolution Digital Elevation Mapping (DEM) data of 3 arcsec resolution were acquired and processed for all of Mexico. Digital soils data at multiple scales were provided for Mexico by our partner institution, INIFAP. However, data were incomplete in some cases, and of poor quality in others, and must be augmented with information from data sets of coarser resolution. This work has not yet been done.

We have obtained hard-copy maps of land use and vegetation in three of the states of northern Mexico—Monterrey, Chihuahua, and Tijuana—at several scales ranging from 1:24,000 to 1:1,000,000. These data must be digitized, compared to more recent satellite imagery, and processed for use in natural resource simulation models.

A limited amount of climatic and hydrologic data has also been obtained in Mexico. One important task remaining with respect to all the data described above is to ensure consistency of definition and mapping units across the U.S./Mexico border.

Detailed data on Canadian soils and agriculture, obtained with the help of our partner institutions, has been processed into the NA3E continental GIS. Additional effort is required to process this data into scales and forms usable in modeling efforts. Of significant importance in creating a coherent continental scale database is ensuring consistent and reliable data across borders. This is not a simple matter because of the differences that exist between countries in data collection practices, taxonomy, data quality, and availability.

Thus far, we have been unable to obtain detailed digital elevation data for Canada. We have also run into an issue with respect to climatic data because of a new policy requiring that climatic data be purchased (at rather high prices) from Environment Canada. Our colleagues in that agency are attempting to resolve this problem. Satellite data on land use and vegetation cover in Canada has been accessed, but has not yet been processed.

#### *Progress on Modeling North American Agriculture*

During 1995, we began to model agriculture across portions of the U.S./Canada and U.S./Mexico borders. The regions selected for study are of considerable importance to the overall agricultural economy of the involved nations. Professor Cesar Isuarralde of the University of Alberta and Dr. Hector Quinones of the Instituto Mexicano de Tecnologia del Agua (IMTA) collaborated in this work. Spring wheat is the crop of interest in the U.S./Canada effort covering the Dakotas and Montana in the Northern Great Plains and the Prairie Provinces of Alberta, Manitoba, and Saskatchewan. A capability has also been developed to model canola, barley, and forage crop production in this region. The production of maize, wheat, and soybean under irrigation is to be modeled for the Rio Grande-Rio Conchos basin on the U.S./Mexico border.

Representative farms on the U.S. side of the Rio Grande Basin have been developed for application of the EPIC model. Hector Quinones of IMTA has defined the primary agricultural regions on the Mexican side of the basin. Most of the data needed to develop the Mexican representative farms have been obtained. Major soils of the region (according to the Mexican soil taxonomy system) have been identified. We still lack needed data on physical and chemical characteristics of these soils. Our colleagues at Texas A&M are working to draw this information from FAO sources. EPIC and other sophisticated simulators are usually applied to high tech, energy- and information-intensive agriculture such as is practiced in the developed countries. The model has yet to be applied to low-tech, low-input agriculture practiced in less developed countries. Through this LDRD project, we have begun an effort to rectify this situation using Mexico as our test case. Mexico provides a good opportunity to adapt and test EPIC across a range of agricultural systems from the most advanced to the subsistence level. "Medium-tech," semi-collective farms (known as ejidos) are also important, both in number of farmers and in contributions to Mexico's total agricultural production. Information has been assembled on the geography, farm characteristics, and land management practices employed in the three agricultural sectors in 10 northern Mexican states. For example, drawing on a

variety of U.S. and Mexican sources, we have collected data on the amount of land under cultivation in each state, as well as the number, size, and type of farms (e.g., subsistence, ejido, commercial) in each state. With respect to land management techniques, we have gathered information on annual crop yields and rotations, agricultural technologies (e.g., use of agricultural

chemicals and machinery), and the amount of land subject to irrigation. Information has been gathered on the demographics of the states, income statistics, and social trends in the agricultural sector. Data has also been assembled on the contribution of agriculture to Mexico's overall economy and on various environmental problems associated with farming in Mexico.

# Technology Adoption Study

Mark J. Niefer (Energy Technologies)

## Project Description

The objective of this project was the development of a microeconomic-based theoretical and empirical framework for forecasting aggregate energy demand and the demand for alternative fuels within an industry incorporating information on the use of production technologies.

## Technical Accomplishments

A microeconomic-based theoretical and empirical framework for forecasting aggregate energy demand and the demand for fossil fuels and electricity in the cement industry incorporating information on the use of three specific production technologies was developed. The framework was used to estimate the impact of each of these technologies on energy demand within particular plants. Table 1 presents a brief summary of the impact of the three technologies on average plant energy intensity in the cement industry.

Table 1. Energy Intensity Estimates (Million Btu Per Ton)

Technologies Used	Average Fossil Fuel Intensity	Average Electric Intensity	Average Energy Intensity
None	4.90	0.452	5.35
High-Efficiency Classifiers Only	4.41	0.461	4.87
Dry-Preheater Kilns Only	3.80	0.549	4.35
Dry-Precalciner Kilns Only	3.74	0.460	4.20
Dry-Preheater Kilns and High Efficiency Classifiers	3.39	0.454	3.84
Dry-Precalciner Kilns and High Efficiency Classifiers	3.32	0.445	3.77

Source: Niefer (1995)

In addition, the productivity impacts of each of these technologies on plant productivity was examined. It was found that plants using both dry-precaciner kilns and high-efficiency classifiers were between 35 and 49 percent more productive than plants using neither of these technologies.

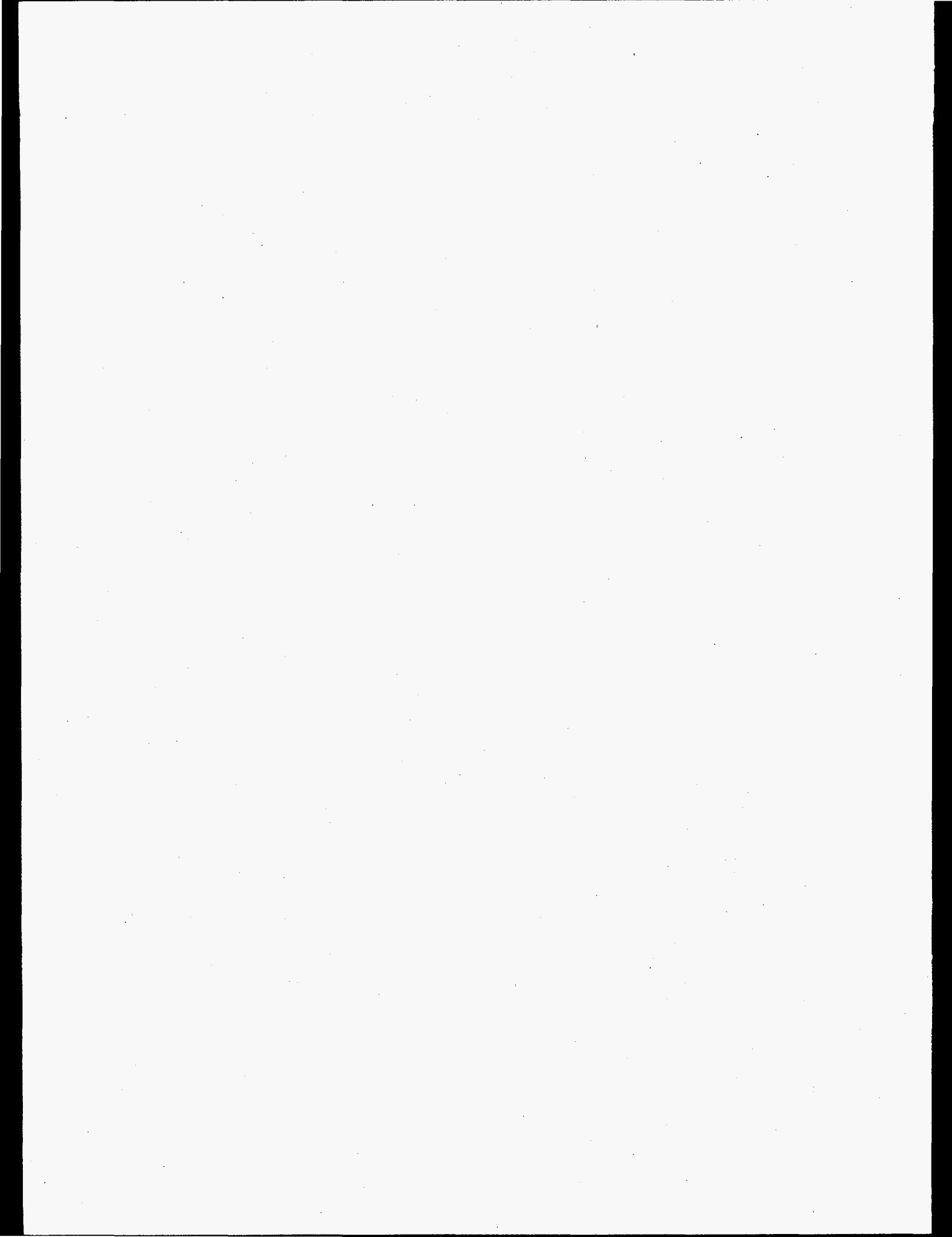
The use of the framework for forecasting was limited by the fact that an empirical model of energy demand based on plant-level data requires plant-level forecasts of energy prices and output demand. These were issues that were not carefully considered in the writing of the original proposal. Further work is required to produce a plant-based forecast of cement industry energy demand.

## Publication and Presentation

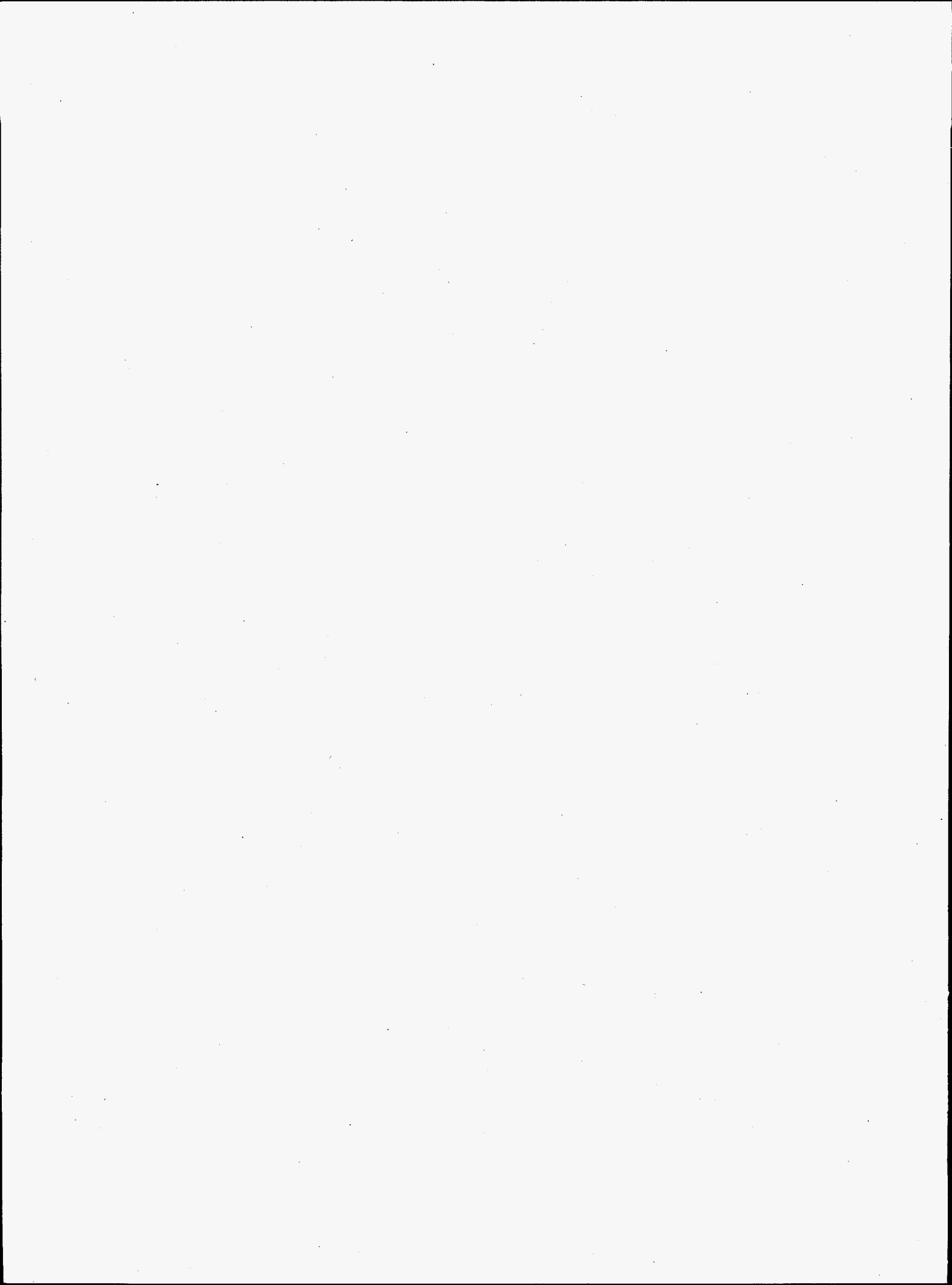
M.J. Niefer. 1995. "Technology, Energy Intensity, and Productivity in the Cement Industry: A Plant-Level Analysis." *Proceedings of ACEEE 1995 Summer Study on Energy Efficiency in Industry*, Volume II, 227-235. Presented at ACEEE 1995 Summer Study, August, Buffalo, New York.

## Presentation

M.J. Niefer. 1995. "Modeling Industrial Energy Demand: A Microeconometric Approach." Presented at IGT Symposium on Industrial Energy Modeling, April, Atlanta, Georgia.



## **Marine Sciences**



# Development of Lagrangian Particle-Tracking Method for Quantifying Fluxes in the Near-Shore Marine Environment

Lyle F. Hibler and Paul J. Farley (Marine Chemistry and Ocean Processes)  
Marshall Richmond (Hydrologic Processes)

## Project Description

The objective of this project was to couple oceanic dispersion modeling with Lagrangian drifter field programs. This coupling would provide a method for more accurate representation of oceanic dispersion and contaminant transport. The drifter design was tailored to coastal environments; that is, to follow surface currents and to be tracked by differential global positioning system (DGPS). We began modifications of candidate ocean models to take advantage of drifter statistics together with dispersion algorithms in order to provide better simulations of coastal contaminant dispersion.

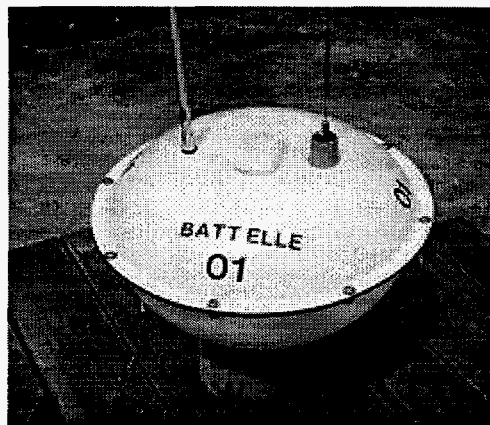


Figure 1. Prototype DGPS Drifter

## Technical Accomplishments

The following three tasks were undertaken during FY 1995:

1. development of DGPS-tracked drifters
2. implementation of a particle-tracking algorithm into a three-dimensional circulation model (Princeton Ocean Model)
3. implementation of a particle-tracking algorithm into a two-dimensional vertically averaged circulation model (RMA2).

## The Development of DGPS-Tracked Drifters

The initial drifter design was adapted from the work of our collaborators at the Naval Post-Graduate School. Modifications were made to simplify the design and to allow DGPS-tracking, which is more accurate than GPS or ARGOS satellite-tracking. This design change improved position accuracy from 100 m to 10 m. The redesign of the circuitry permits greater use of off-the-shelf components, which lowers the unit cost and improves reliability. A programmable interface is used to configure position fixing frequency. This interface also allows additional sensors and data-logging capabilities to be custom designed for various applications. The prototype drifter and a schematic of its electronics are shown in Figures 1 and 2, respectively.

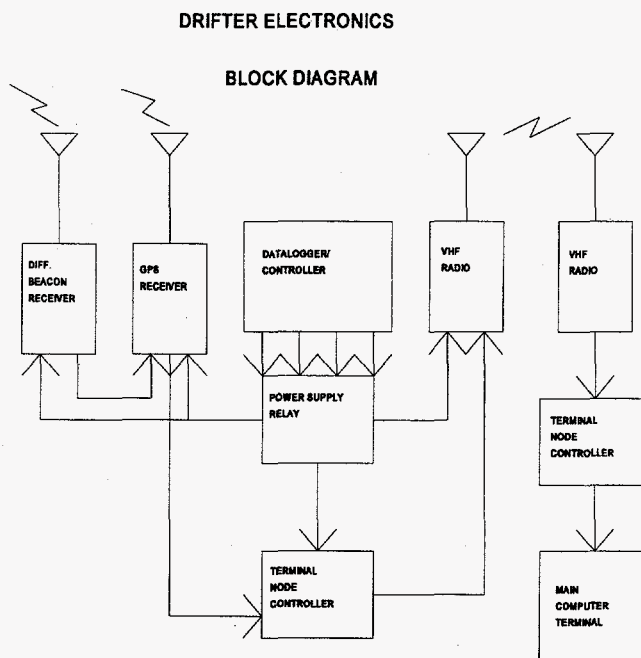


Figure 2. DGPS Drifter Component Schematic

### Three-Dimensional Circulation Modeling Using Princeton Ocean Model

During FY 1995, we acquired Princeton Ocean Model (made available for research use by its author, Dr. Mellor, Princeton University), and began testing the model code. The main FORTRAN program modules were compiled, evaluated, and configured for test systems. The parameterizations governing the horizontal and vertical mixing and dispersion were evaluated specifically with the goal of eventually modifying the algorithms to incorporate true Lagrangian particle tracking.

#### Particle Tracking with Princeton Ocean Model

The particle tracking method that will be incorporated into the Princeton Ocean Model was tested for a simple case of a uniform velocity field. The evolution of the particle position is computed from

$$x_p(t+\Delta t) = x_p(t) + u' \Delta t + Z \sqrt{2\nu_T \Delta t}$$

where  $\Delta t$  is the time step,  $Z$  is a random number with zero mean and unit variance, and  $\nu_T$  is the turbulent eddy viscosity. A total of 100 particles was released into a constant velocity of 1 m/s with a constant eddy viscosity of 0.20 m<sup>2</sup>/s. The mean position and width of the dispersing clusters of particles after 10 seconds and 30 seconds agree well with the theoretical estimates given in Fischer et al. (1979). This particle evolution algorithm will be incorporated into the model for use with the Mellor-Yamada 2.5-degree closure scheme.

#### Two-Dimensional Circulation Modeling Using RMA2

We have also investigated the RMA2 model for use in coastal dispersion studies. This finite-element model produces spatially continuous estimations of the vertically averaged circulation (Norton et al. 1973; Thomas and McAnally 1990). A drifter field program designed to quantify the dispersion characteristics within the estuaries, together with applications of the model, could make valuable contributions to contaminant transport studies, such as the Ocean Margins Program of the U.S. Department of Energy, or the assessment of the contamination of the Kara Sea from radionuclide transport through the Ob and Yenisei River systems, as part of the Office of Naval Research Arctic Nuclear Waste Assessment Program (ONR-ANWAP).

In the example shown in Figure 3, the modeled hydrodynamics are driven by tides, freshwater discharges, and boundary shear forces (wind and bottom friction). In this case, 10 hypothetical drifters were placed into the flow field at the head of the Ob estuary, and a random

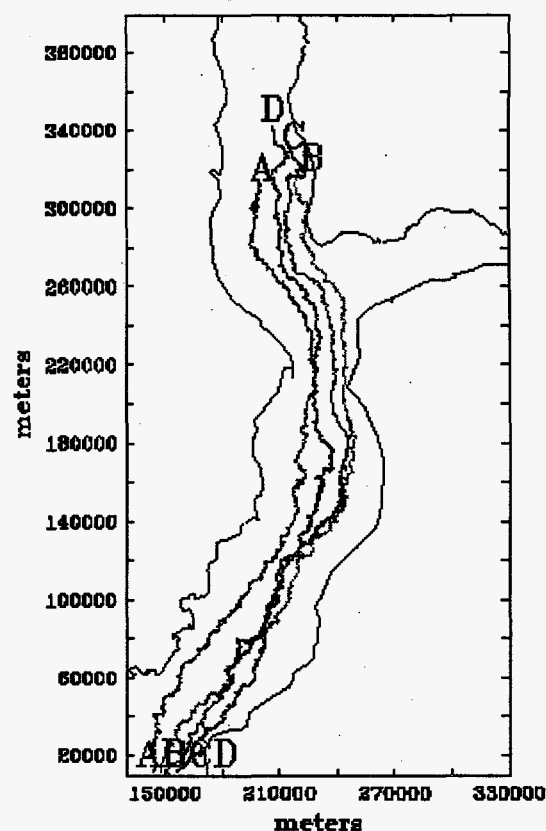


Figure 3. Modeled Drifter Trajectories in the Ob Estuary

walk algorithm was used to modify the trajectories that the drifters would take if driven by mean advective transport alone. The random walk parameters are velocity-scaled perturbations designed to characterize deviations from currents estimated from the RMA2 model. The estimated paths of four drifters during a 2-month simulation are shown in Figure 3. Trajectories derived in this manner would be compared with those derived from the Lagrangian drifter deployment. Appropriate statistical comparisons would be made to guide model parameter (mixing coefficients) selection.

#### References

- A.F. Blumberg and G.L. Mellor. 1983. "Diagnostic and Prognostic Numerical Circulation Studies of the South Atlantic Bight." *J. Geophys. Res.* 88:4579-4592.
- A.F. Blumberg and G.L. Mellor. 1987. "A Description of a Three-Dimensional Coastal Ocean Circulation Model." In *Three-dimensional coastal ocean models*, N. Heaps (ed.), American Geophysical Union, 208 pp.
- H.B. Fischer, E.J. List, R.C.Y. Koh, J. Imberger, and N.H. Brooks. 1979. *Mixing in Inland and Coastal Waters*. Academic Press, New York.



H.B. Fischer, E.J. List, R.C.Y. Koh, J. Imberger, and N.H. Brooks. 1979. *Mixing in Inland and Coastal Waters*. Academic Press, New York.

W.R. Norton, I.P. King, and G.T. Orlog. 1973. *A Finite Element Model for Lower Granite Reservoir*. Water Resources Engineers, Inc., Walnut Creek, California.

W.A. Thomas and W.H. McAnally, Jr. 1990. *User's Manual for the Generalized Computer Program System: Open-Channel Flow and Sedimentation, TABS-2*. U.S. Army Engineer Waterways Experiment Station, Vicksburg, Mississippi.

## **Presentations**

T. Paluszkievicz. 1995. Presentation to the Recent Advances in Oil Spill Modeling of Transport Workshop, Dartmouth, Massachusetts.

T. Paluszkievicz. 1995. Presentation of Marine Sciences Capabilities, NUWC, Keyport, Washington.

M.C. Richmond. 1995. Presentation to USACE, Walla Walla District, Walla Walla, Washington.

# *Semipermeable Membrane Devices for Sampling Non-Polar Organic Compounds in Air, Water, and Soil*

Eric A. Crecelius and Lisa F. Lefkowitz (Marine Sciences Laboratory)

---

## **Project Description**

Semipermeable membrane devices (SPMDs) have the potential for use as passive samplers in both the environment and in waste systems. Semipermeable membrane devices have the ability to passively concentrate hydrophobic organic chemicals (HOCs) from air and water, thus providing a time-integrated sampler for chemicals that may be below detectable levels by conventional sampling techniques. The selectivity and concentration factor depend upon the chemical, the type of membrane and the type of material inside the membrane. For example a polyethylene membrane coated inside with a layer of lipid material will concentrate hydrophobic organic chemicals, such as polycyclic aromatic hydrocarbons (PAHs) and polychlorinated biphenyls (PCBs), from air and water.

The purpose of this study was to demonstrate the application of semipermeable membrane devices for monitoring contaminants in water, soil, and sediment in the environment. In addition, the semipermeable membrane device was used as a surrogate for estimating bioaccumulation of chemicals in organisms. This approach is attractive because it reduces time, money, and animal handling issues as compared to traditional bioaccumulation studies.

## **Technical Accomplishments**

We have been actively investigating the use of these devices for predicting bioaccumulation of non-polar organic compounds by aquatic organisms, such as clams from contaminated aquatic environments, and have had very promising results. A number of studies were initiated and completed during 1995 including field deployments at multiple locations around the country to assess the in situ approach to determine the presence and concentration of hydrophobic organic chemicals in an aquatic environment. These semipermeable membrane devices could be attached to the tracer and recovered after a brief period in the open ocean. Results could be used to monitor trace levels of hydrophobic organic chemicals in remote ocean regions.

A brief description of some of the studies that we have performed in the last year include the following:

- A laboratory study was performed to assess the uptake rates of various nonpolar organics, including polychlorinated biphenyls, pesticides, and polycyclic aromatic hydrocarbons from two contaminated sediments. Both polyethylene sheets and semipermeable membrane devices filled with lipid were placed in contact with a sediment water slurry and rolled for a period of up to 2 months. Bags and poly sheets were removed at regular intervals over this period and the rate of release from the sediments and the subsequent uptake by the semipermeable membrane devices and poly sheets were evaluated. Equilibrium appeared to be reached more quickly in the poly sheets. For some of the larger polycyclic aromatic hydrocarbons compound, equilibrium did not appear to be achieved even after 60 days. This makes comparison to actual tissue bioaccumulation results questionable, as the standard bioaccumulation tests only last 28 days. Uptake into the semipermeable membrane devices and poly sheets were compared to actual bioaccumulation results associated with previous tests performed on these sediments. Bioaccumulated concentrations of hydrophobic organic chemicals in both the tissue and the semipermeable membrane devices agreed well, when expressed on a lipid basis, encouraging further investigation into this application.
- A laboratory study was performed to establish the partition coefficients and uptake rates for a wide range of hydrophobic organic chemicals (including polychlorinated biphenyl congeners and polycyclic aromatic hydrocarbons) from water into the polyethylene film. This study was initiated to determine if polyethylene alone would be a suitable semipermeable membrane device for determining dissolved concentrations in water. An extensive database of partition coefficients ( $K_p$ ) between polyethylene and water was established.
- A field survey was conducted with both semipermeable membrane devices filled with lipid and with polyethylene film samples in Elliot Bay, near Seattle, to demonstrate the application of this device for identifying sources and transport of chemicals in natural waters. Results show a definite trend in levels of contaminants near the Duwamish River, which has been shown to be a source of contamination to Puget Sound. Dissolved concentrations of polycyclic aromatic hydrocarbons were calculated using partition

coefficients for the polyethylene films generated by Battelle Marine Sciences Laboratory. These polyfilm concentrations agreed well with established water concentrations of these compounds determined by conventional methods.

- Over 30 sets of semipermeable membrane devices, including both polyfilled and polyethylene sheet devices, were deployed along a 100 mile stretch of the Columbia River. Both semipermeable membrane devices from each device were analyzed for a list of polycyclic aromatic hydrocarbons, polychlorinated biphenyl congeners, and chlorinated pesticides. Because of a concern over the source of chlorinated compounds observed in birds and fish along various stretches of this river, this data should be useful for governmental parties involved in the management of the Columbia River watershed.
- A number of semipermeable membrane devices were deployed in conjunction with NOAA in the Miami River in Florida. This river is considered one of the most polluted rivers in Florida. Shellfish samples were also collected to correspond to deployment sites along the river and in some of the tributaries. Preliminary results show specific point sources of hydrophobic organic chemicals along the river and coming from some of the tributaries. This data will be shared with NOAA.

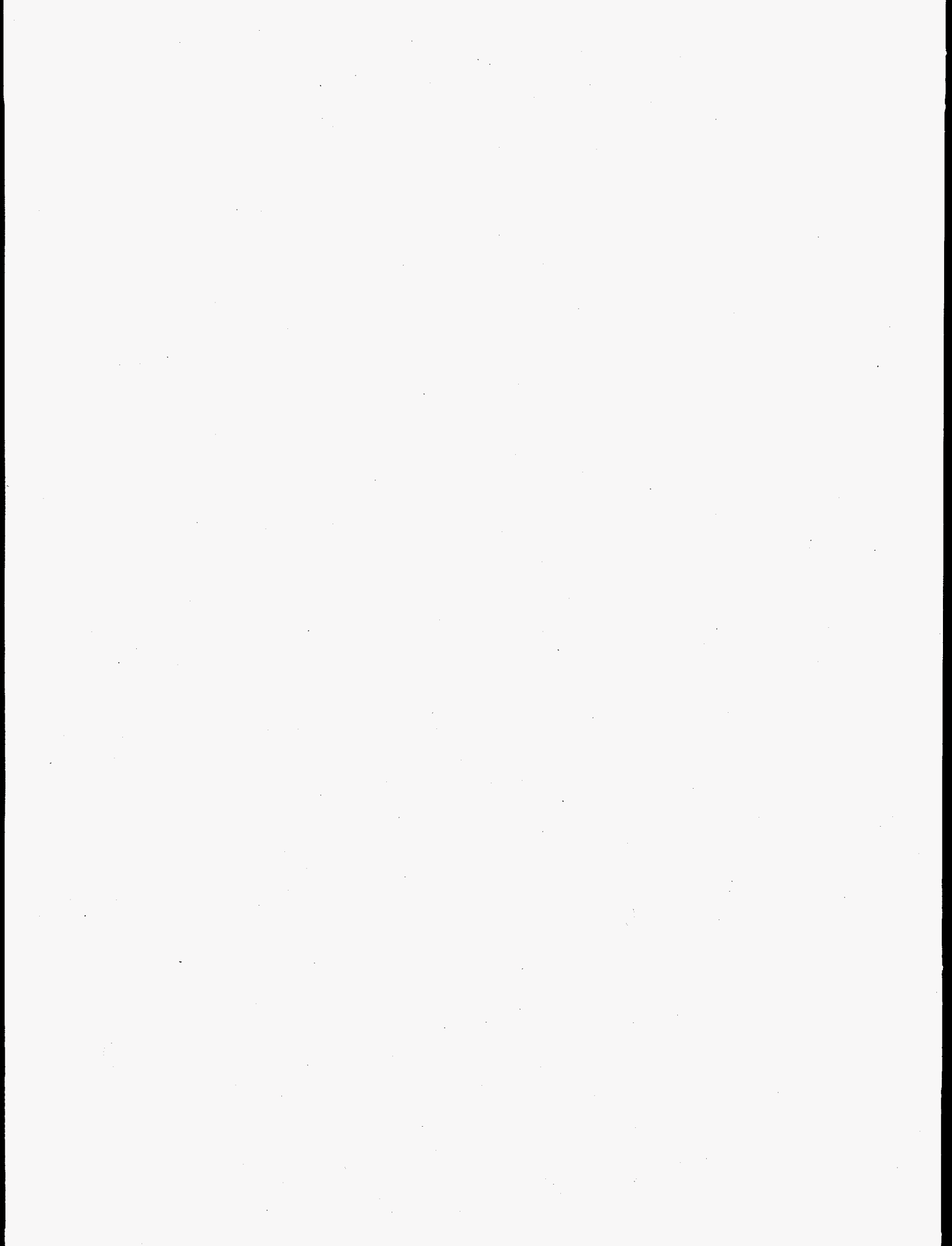
## **Presentations**

L.F. Lefkovitz and E.A. Crecelius. 1995. "Use of Semipermeable Membrane Devices (SPMDs) to Monitor PAHs in Elliot Bay." Presented at the Puget Sound Research, '95, Bellevue, Washington.

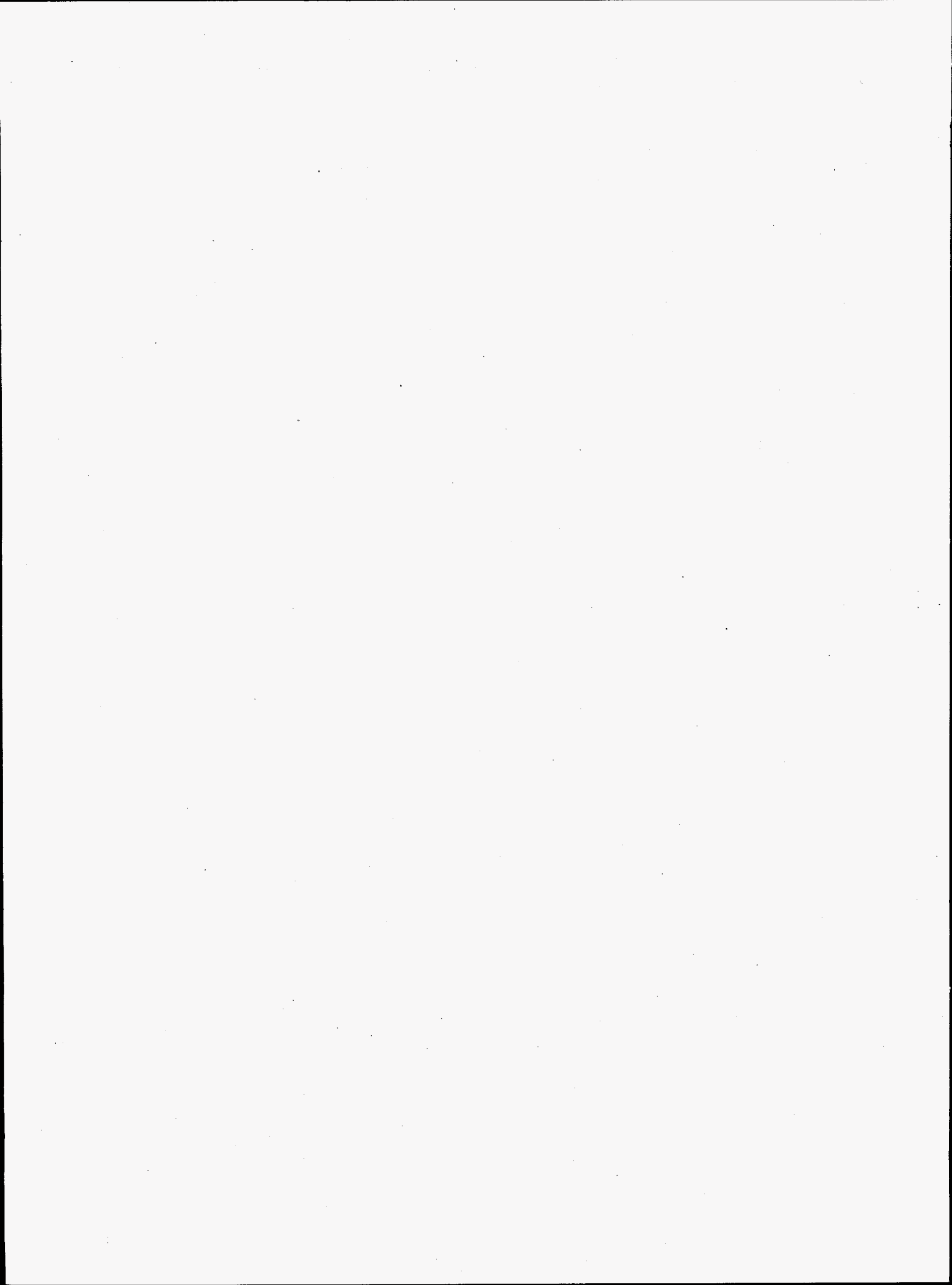
L.F. Lefkovitz and E.A. Crecelius. 1995. "Applications of Semipermeable Membrane Devices." AOAC Northwest Regional Meeting, June, Olympia, Washington.

L.F. Lefkovitz and E.A. Crecelius. 1995. "The Use of SPMDs to Predict Bioaccumulation of PAHs and PCBs from Sediment." Presented at SPMD Workshop and Symposium, 3rd Annual Meeting, Columbia, Missouri.

L.F. Lefkovitz and E.A. Crecelius. 1995. "The Effect of Turbulence on the Release Rate of Phenanthrene from and SPMD." Presented at SPMD Workshop and Symposium, 3rd Annual Meeting, Columbia, Missouri.



## **Materials Science and Engineering**



# Bioactive Coatings and Composites for Orthopedic Devices

Allison A. Campbell and Gordon L. Graff (Materials and Chemical Sciences)

---

## Project Description

Historically, large bone defects (due to accident, illness, or age) have been repaired by autografting bone from another part of the body. However, autografts have several disadvantages including morbidity, increased operative times, and in some cases, insignificant amounts of healthy bone to fill larger defects. Complications associated with this procedure have been reported to be as high as 20 percent.

Recent interest has focused on the use of composites composed of either tricalcium phosphate (TCP) or hydroxyapatite (HAP) and thermoplastics, collagen, and other polymeric materials as bone scaffolds, fillers, and reconstructive agents and/or devices. The composite matrix can be used as a delivery system for bone growth factors and produce a biomaterial that is osteoinductive, as well as osteoconductive.

The objective of this work was to produce a synthetic coating or composite material for bone replacement applications. The composite materials were composed of polymer and calcium phosphate minerals. The use of natural polymers, such as collagen, was explored as the scaffold material. Both a resorbable material, tricalcium phosphate, as well as other non-resorbable calcium phosphates (including octacalcium phosphate and hydroxyapatite) were investigated as fillers in composites or as coatings. Research focused on using a solution deposition method to produce bioactive coatings and/or composites on or within polymeric medical materials. The aqueous mineralization process offers a unique method to produce these new bioactive composites and coatings. This process is advantageous in that it is possible to produce specific calcium phosphate coatings on a variety of materials.

## Technical Accomplishments

This work involved the development of modification schemes for scaffold material. With the natural polymer collagen, polymer was used in its native state, or after

exposure to 0.01 M  $\text{HNO}_3$  or 0.01 M  $\text{NaOH}$  for 10 minutes. In addition, collagen coatings were investigated, as well as three-dimensional sponges as the template for subsequent mineral formation.

Once modification schemes were developed, work focused on the mineralization of these surfaces and scaffolds. In this step, the collagen material was placed into an aqueous solution containing soluble precursors of the desired calcium phosphate material. Solution pH, ionic concentration, and temperature were maintained in a regime where the solutions are supersaturated with respect to the desired mineral phase, thereby creating the driving force for nucleation and growth.

Results to date include the mineralization of collagen films with both hydroxyapatite and octacalcium phosphate (Figures 1 and 2 respectively). Dense and porous mineral coatings have been produced.

We have also mineralized three-dimensional collagen sponges with HAP and OCP (Figure 3).

In addition, we have modified the collagen sponge with an acid or base exposure in order to determine the effect, if any, on the amount and/or rate of mineral deposition. It was found that both the acid and base wash reduced the ability of the collagen sponge to mineralize calcium phosphate from solution.

The ability to form calcium phosphate/collagen composite materials via solution deposition routes provides an advantageous method for producing materials that may be used as bone fillers. The solution deposition provides that flexibility to tailor the resulting materials by controlling the amount of mineral deposited, as well as the phase of the material. The low temperature process may be further adapted to other biodegradable polymers, as well as other mineral phases.

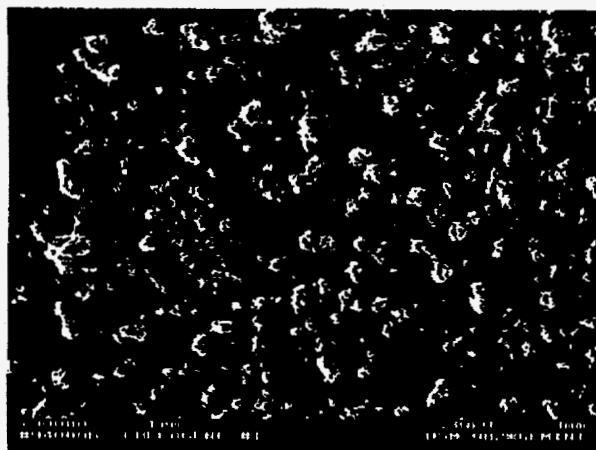


**Figure 1. Hydroxyapatite Mineralized on Collagen**

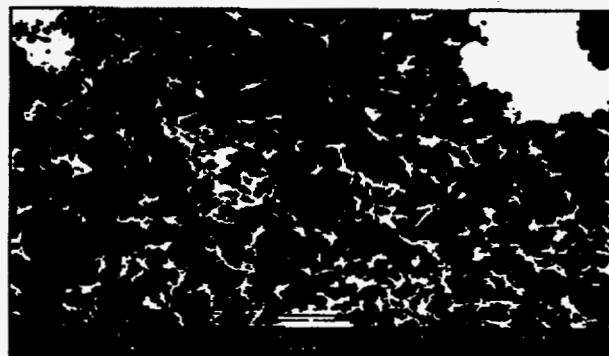


**Figure 2. Octacalcium Phosphate Mineralized on Collagen**

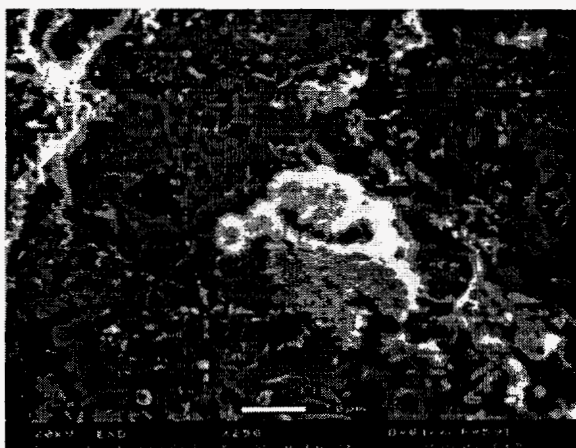


**Figure 3. Calcium Phosphate Mineralized Within a Collagen Sponge**



# Catalytic Materials Synthesis

Dean W. Matson (Materials and Chemical Sciences)

---

## Project Description

The objective of this project was to evaluate the Rapid Thermal Decomposition of precursors in Solution (RTDS) flow-through hydrothermal process as a method for generating nanocrystalline solid superacid catalysts. RTDS processing conditions required to synthesize catalytically active sulfated zirconia powders were investigated. Once optimum synthesis conditions were established, quantities of the active RTDS powder product were synthesized for consolidation into bulk products for use in catalytic applications.

The RTDS method involves the production of nanocrystalline powders from aqueous feedstock solutions as they are forced through a pressurized and heated linear reactor. Precursor species dissolved in the feed solutions react with other solute species and the solvent under the hydrothermal conditions in the RTDS reactor to form nanocrystalline powders. RTDS products are removed from the hydrothermal region by passing the reacted solution through a small orifice at the downstream end of the reactor. Products are collected as aqueous suspensions from which the solid component is separated by centrifugation or by spray drying.

Using a bench-scale RTDS reactor, a series of experimental studies were undertaken to evaluate the effects of various processing parameters on the physical, crystallographic, and catalytic properties of RTDS-generated sulfated zirconia powders. Among the variables evaluated were the effects of precursor concentration, the source of zirconium ions (precursor species), the source of sulfate, and the RTDS reactor temperature. Other post-RTDS processing variables, such as the method of separating the solid powder from the RTDS-generated suspension and the temperature required for catalyst activation were also studied. Catalytic activities of the sulfated zirconia powders were evaluated using a butane isomerization reaction under a set of standardized test conditions.

## Technical Accomplishments

Several processing variables were identified that either directly or indirectly affected the catalytic activity of RTDS-generated sulfated zirconia powders. Active catalyst powders were demonstrated to be produced using

a number of different water soluble zirconium-containing precursors and sulfate sources. Various combinations of zirconium sulfate, zirconyl nitrate, a zirconium citrate ammonium complex, sulfuric acid, ammonium sulfate, and sodium sulfate were investigated as precursor species, both with and without the presence of added urea in the feed solution. However, the best combination of RTDS system operation, powder product purity, and catalytic activity were obtained using a zirconium sulfate/urea precursor combination. The use of zirconium sulfate reduced the effects of extraneous dissolved salts that were present in the product suspension when other precursor species such as zirconyl nitrate were used. By adding urea to the feedstock solution, ammonium ions were generated under the hydrothermal conditions in the RTDS reactor, yielding a basic product suspension. Solid particulate products could be produced under either acidic (without urea) or basic conditions at sufficiently high RTDS temperatures ( $\geq 300^\circ\text{C}$ ). However, the yield of collectable solids was much higher, and powder separation more efficient, in product suspensions generated from feedstock solutions containing urea.

The RTDS reactor temperature was found to affect both the powder product crystallinity in the as-collected powder products and catalytic activities of the activated (calcined) powders. Below a  $300^\circ\text{C}$  RTDS reaction temperature, product yields were low, suggesting incomplete reaction at the residence times used (1 to 5 seconds). With a zirconium sulfate/urea precursor solution and a  $300^\circ\text{C}$  RTDS processing temperature, powder x-ray diffraction analysis of the solid product indicated that it was amorphous. However, crystallinity of powder products increased systematically with RTDS processing temperatures up to  $400^\circ\text{C}$ . After calcination at  $500^\circ\text{C}$  and  $600^\circ\text{C}$  for 1 hour in air, crystallinity of the zirconia powders generally increased, and became more pronounced at the higher calcination temperature. Variations in post-calcination crystallinity persisted among the samples originally processed at different RTDS reaction temperatures, suggesting structural variations related to processing history. These effects were also observed in the vibrational spectra (Raman and FTIR) of the as-generated and calcined powders. Activities of the RTDS-generated sulfated zirconia powders toward catalysis of the butane isomerization reaction were also found to vary as functions of both RTDS processing temperature and catalyst activation (calcination) temperatures.

An additional processing variable found to affect the catalytic activity of RTDS generated sulfated zirconia powders was the method of solid separation from the RTDS product suspension. Both sedimentation/centrifugation and spray drying were evaluated as solid separation methods. The powder flow characteristics of spray dried RTDS products were attractive relative to those of centrifuged solids from the same suspension. However, the spray drying process tended to incorporate other water soluble species present in the RTDS product suspension into the dried powder and reduced the measured catalytic activity.

#### **Publications**

D.W. Matson, J.C. Linehan, J.G. Darab, M.F. Buehler, M.R. Phelps, and G.G. Neuenschwander. 1995. "RTDS: A Continuous, Rapid, Thermal Synthesis Method." Preprints, Div. of Petroleum Chem., American Chemical Society 40: 95-98.

D.W. Matson, J.C. Linehan, J.G. Darab, M.F. Buehler, M.R. Phelps, and G.G. Neuenschwander. "A Flow-Through Hydrothermal Method for the Synthesis of Active Nanocrystalline Catalysts." Chapter in *Advanced Techniques in Catalyst Preparation*, W.R. Moser, ed. (submitted).

#### **Presentation**

D.W. Matson, J.C. Linehan, J.G. Darab, M.F. Buehler, M.R. Phelps, and G.G. Neuenschwander. 1995. "RTDS: A Continuous, Rapid, Thermal Synthesis Method." Presented at the 1995 Spring National Meeting of the American Chemical Society, April 1-6, Anaheim, California.

# Coatings Characterization

Gordon L. Graff, Jun Liu, and Suresh Baskaran (Materials Sciences)

## Project Description

The primary objective of this research was to use state-of-the-art SEM, TEM, NMR, and Raman characterization to investigate fundamental mechanisms controlling thin film growth. Detailed characterization was performed on deposited films, on deposition solutions, and on precipitates (particles) forming in the bulk solution.

## Technical Accomplishments

Since slow deposition rates remains a technical limitation to our solution derived coatings, detailed solution, substrate, and thin film characterization are required to understand fundamental mechanisms and rate limiting processes controlling film growth. Previous work indicated that the extremely rapid hydrolysis and condensation reactions that occur in aqueous solutions of  $\text{Sn}^{4+}$ ,  $\text{Zr}^{4+}$ , and  $\text{Ti}^{4+}$  cations may limit film growth since solution conditions favor a burst of nucleation with little subsequent growth. In addition, detailed tunneling electron microscopy studies showed that thin film growth mechanisms are fundamentally different on polymeric substrates than on SAM-containing metal substrates.

During FY 1995, exciting results were obtained using high resolution tunneling electron microscopy (lattice imaging) performed on the "as deposited"  $\text{TiO}_2$  and  $\text{ZrO}_2$  thin films. Previously reported results in the literature have stated that the initial precipitates formed in aqueous solutions are amorphous, hydrated oxides, or hydroxides. Using sectioning techniques developed by Jun Liu, we were able to collect lattice images of the  $\text{TiO}_2$  and  $\text{ZrO}_2$  thin films directly precipitated on Si substrates ( $70^\circ\text{C}$ ). Figure 1 is a high resolution tunneling electron microscopy image of the "as deposited"  $\text{ZrO}_2$  thin

film showing crystalline, tetragonal  $\text{ZrO}_2$  with an average crystallite size of approximately  $50\text{\AA}$ . Similar microstructures were observed for the  $\text{TiO}_2$  films deposited at low temperature. This represents a unique and simple method for producing dense nanocrystalline materials.

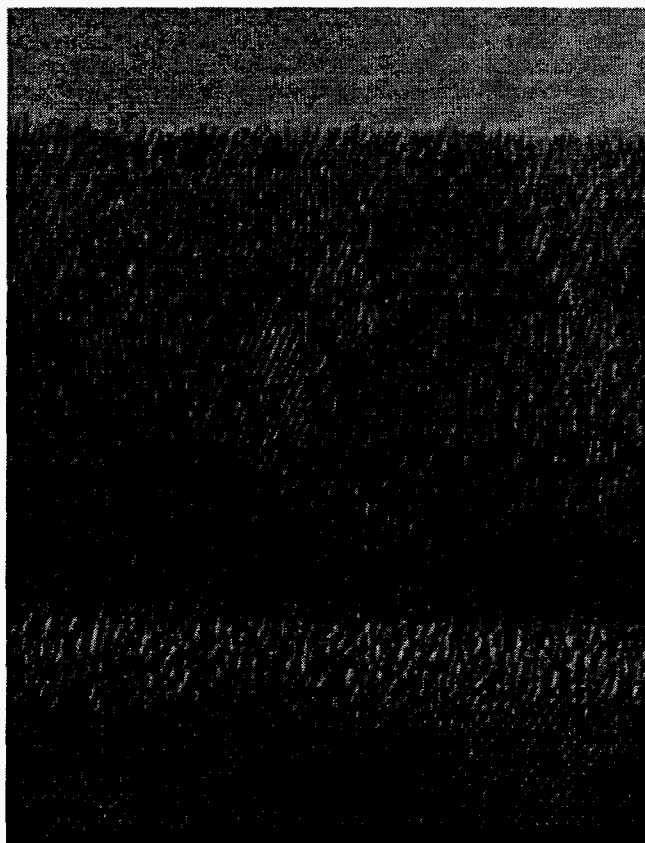


Figure 1. High Resolution TEM Image of the "as Deposited"  $\text{ZrO}_2$  Thin Film

# Development of Ultracapacitor Materials

Peter C. Rieke (Materials and Chemical Sciences)

## Project Description

Ultracapacitors are being considered as load leveling devices in future electric and hybrid automobiles. Current technology suffers from either very high expense (e.g., RuO<sub>2</sub> based ultracapacitors), or inadequate materials properties resulting in poor longevity and performance. After examination of the existing devices and materials we decided to abandon conventional materials (metal oxides and organic materials) and seek a new and novel approach to the problem. The new materials must meet the following objectives:

- multiple oxidation states
- electronic conductivity
- insolubility in electrolytes.

A literature search revealed a number of materials that apparently met all of the above criteria and had not been investigated for battery and ultracapacitor applications. Cyclicvoltametric studies were conducted on electrodes made of four materials. These experiments showed that a whole new class of materials met the above criteria and could be considered for use in ultracapacitors. From this, it is quite likely we can break away from the limited suitability of oxides and the high expense of RuO<sub>2</sub> in particular. While these tests were very preliminary, these materials show promise as a new and novel solution to the current materials problems of ultracapacitors.

## Technical Accomplishments

Initially, the main objective of this work was to improve a RuO<sub>2</sub> based ultracapacitor. During this initial phase, a literature search focused on RuO<sub>2</sub> was conducted. The area of interest and the literature search was expanded to other types of ultracapacitors including the polymer carbon based ultracapacitors. For various reasons, it was decided that none of the current materials were suitable for automotive applications.

In summary, it was decided to abandon all traditional materials and start anew with novel materials. A list of criteria was developed that would define the suitability of potential materials. These included the following:

- Multiple Oxidation States - This criteria ensures that the material is capable of undergoing the necessary redox chemistry needed for use as an ultracapacitor.

- Electronic Conductivity - Moderate to high conductivities are needed to act as a suitable electrode material. Many materials can be eliminated from consideration simply due to their insulating properties.
- Insolubility in Electrolytes - 4M sulfuric acid is the electrolyte of choice due to operating temperature constraints. This severely limits the choice of suitable materials as many will be soluble under these conditions. Other electrolytes such as KOH or organics may also be considered.

Metal oxides are a prime candidate as evidenced by the success of RuO<sub>2</sub>. This material meets all the above criteria except it is too expensive for large-scale application. A literature survey on the electrochemistry of metal oxides revealed a large body of work; much of it directed at ultracapacitors and batteries. Further examination of oxides was conducted using information from Pourbaix diagrams. After reviewing the periodic table of oxides, it became obvious that RuO<sub>2</sub> was the only real candidate and that all other oxides were seriously deficient in one of the above criteria. In most cases, high solubility in various electrolytes was the limiting problem. Given these sobering observations and the existing large body of work on the subject, we decided to abandon a detailed investigation of metal oxides.

The search was expanded to other metal compounds. The literature search revealed a number of materials that apparently met all of the above criteria. Very little information on their electrochemical characteristics was available, suggesting that these materials had not seriously been investigated for battery and ultracapacitor applications.

Samples of four materials were purchased for in-house evaluation. Powders of these were mixed with epoxy and spread over a platinum grid. Cyclicvoltametric studies in 4M H<sub>2</sub>SO<sub>4</sub> were conducted on these electrodes. All the materials showed some electrochemical activity, thus, showing that these materials can indeed be used as ultracapacitors. However, the method of making the electrodes and the crudity of these tests does not really allow us to make quantitative choices based on these cyclicvoltametric curves. None of the electrodes underwent any significant deterioration after soaking for 1 hour in 4M sulfuric acid. All had sufficient electrical

conductivity that cyclicvoltametric curves could be obtained. Thus, all these materials meet the above three criteria.

These experiments have shown that a whole new class of materials can be considered for use in ultracapacitors. It is quite likely we can break away from the limited suitability of oxides and the high expense of  $\text{RuO}_2$  in particular. Much still needs to be done, and we need to find ways to prepare these materials as high-surface-area thin films for further testing.

We also need to expand the list of tested materials. A wide variety of electrochemical, surface analytical techniques, and materials properties tests need be conducted on the thin films.

### *Composite Metal Oxide - Polymer Ultracapacitors*

Conductive polymers have been considered for ultracapacitors but have generally been found lacking in total capacitance and have inadequate discharge rates. One solution to this problem is to incorporate metal/metal oxide clusters into the polymer to boost conductivity and charge storage capacity. A number of metal (ruthenium, nickel, and iron) polymer composite films were prepared and characterized by cyclic voltammetry and x-ray photoelectron spectroscopy. Nickel was found to have a specific capacitance of about 1000 F/g of material. This is better than that reported for the Pinnacle Research  $\text{RuO}_2$  electrode of 720 C/g. These results suggest that the metal/polymer composites do allow an increased capacitance. It remains to be shown that the charge discharge rates are sufficiently high for ultracapacitor application.

# *Glass Structure, Chemistry, and Stability*

Keith D. Keefer (Environmental Technologies)

---

## **Project Description**

Although there have been many structural models and thermodynamic theories developed to describe silicate melts, they are rarely used in the analysis of experimental data and virtually never relied upon for engineering estimates. Although most of the thermodynamic treatments may adequately describe melt behavior over a known compositional range, they are poor at predicting behavior outside of that range. They typically do not reflect the true polymeric structure of silicate liquids. The structural models, too, have little predictive power because they are usually used to rationalize observed behavior rather than reflect the underlying chemistry and its relationship to the polymeric nature of silicate species. In this project, we are developing an accurate chemical description of silicate species and using that chemical description as the basis for a rigorous statistical thermodynamic treatment of silicate liquids that fully accounts for their polymeric nature. The silicate speciation that comes out of the structural model is compared with spectroscopic and thermodynamic data to validate the model. The objective is to account for both sets of observations with one comprehensive theory.

The significance of this approach is that it will provide a rigorous thermodynamic treatment of silicate liquids in terms of the Lewis acidity of each of five silicate species that are categorized by only the number of bridging oxygens on each tetrahedron. This Lewis acidity should be essentially the same for all silicate melts and independent of the type of network modifying oxides in the system. What will change, however, is the Lewis basicity of the network modifier oxides that are dissolved in the melt. The predictive power comes from the fact that the Lewis acid/base behavior, once established in one system or compositional range, should not differ much over a large quantitative and qualitative range of melt compositions.

The one of the most important features of this theory is that while the thermodynamic aspects describe the liquidus behavior, the local chemical speciation provides a description of the short-range structure and chemical behavior at the molecular level, the longer range polymeric structure can be treated with percolation theory

and used to understand larger scale melt behavior. For example, it appears that Q3 groups are much more likely to be hydrated than other species and so a large concentration of Q3 in a glass is likely an indicator of low chemical durability. But it is very likely that ease of glass formation is due to the percolation of oxygen bridges and systems with large amounts of Q3 are also going to have the largest percolation threshold and be the easiest to quench to a glass. Using a lattice treatment of the statistical thermodynamics allows the percolation threshold of the silicate polymer and therefore glass formation to be predicted. The knowledge that would be obtained in this proposed study could be used to predict formulations that would have good glass forming qualities and still exhibit good chemical durability.

## **Technical Accomplishments**

We have developed two major theoretical treatments of the speciation theory and developed computer codes to implement them. One treatment is a Monte Carlo calculation in which individual reaction enthalpies are calculated and used to model a set of ten chemical reactions that have the property of moving bonds on a lattice. The system is allowed to relax and the speciation is then measured. Correlation functions are calculated to determine the onset of phase separation. We have also derived an analytical treatment of the energetics of the system that allows a direct calculation of the free energy of the system and of the solvus.

Raman scattering measurements have been made of series of glasses quenched from the binary silicate systems  $\text{Na}_2\text{O-SiO}_2$ ,  $\text{K}_2\text{O-SiO}_2$ , and  $\text{Li}_2\text{O-SiO}_2$ . A total of eight glasses were prepared in the former two systems and four in the latter. The results show that although there are differences in the speciation in three systems as predicted by the theory, the differences are smaller than calculated. The reason is believed to be due to the fact that the liquidus temperatures from which the glasses were quenched were different and so the degree of thermal randomization is different in each. This observation may indicate that the model has the potential to describe liquidus curves, as well as solvi.



# High Temperature Catalytic Materials

Kalahasti S. Rame and John G. Darab (Materials and Chemical Sciences)  
John L. Cox and Timothy L. Hubler (Environmental Technologies)

---

## Project Description

This project focused on developing catalytic materials for high temperature applications. The class of metal oxides referred to as hexa-aluminates has been targeted for investigation. During FY 1995, the work focused on the synthesis, chemistry, and catalytic properties of these materials.

At present, improved catalysts that can withstand high-temperatures are the roadblock to improved efficiency, economics, and environmental impact of a number of energy and chemical processes. Improved catalysts are needed for methane conversion which is of considerable interest; representing as it does, an important fuel for combustion devices, a source of hydrogen for the petrochemical industry, and a source of synthesis gas for the chemical process industry. New and improved catalysts that can perform economically are highly desired. Catalytic combustion of methane is an area of interest for the development of stationary gas turbines, which is the technology of choice for new electricity loads. Catalysts are being sought with low light-off temperature, low NO<sub>x</sub> emission and high temperature stability. Japanese industry is currently far ahead of the U.S. in this area of catalysis research and development. Fuel cells are another important area for high temperature (> 1000°C) catalyst research. Catalyst stability and durability at these high temperatures are of paramount importance to these advanced energy devices, particularly for high temperature fuel cells where catalyst stability is an issue.

Recently, Japanese scientists found that hexa-aluminates and some structurally related compounds show substantial catalytic activity in methane combustion, as well as high sintering resistance, so that a large surface area (8 to 15 m<sup>2</sup>/g at 1400°C) is retained at high temperature. Members of this class of hexa-aluminates are known to have the magnetoplumbite type structure belonging to the hexagonal "layered" aluminates structural family, which comprises spinel-like blocks separated by mirror planes containing large cations. This structural characteristic permits them to perform as high temperature catalyst materials utilized in the catalytic combustion, and other high temperature applications, e.g., steam reforming, and high-temperature membranes for selective gas permeation (National Research Council Panel 1993).

## Technical Accomplishments

Conventional methods for preparing high-surface area, single phase, hexa-aluminates, including by solid-state reaction of the component oxides at elevated temperature, and wet chemical co-precipitation have not been entirely satisfactory. As the number of metal components in the hexa-aluminate increases, these methods of synthesis become even less satisfactory. This problem has been circumvented by using a sol-gel method of synthesis, specially tailored for the multicomponent hexa-aluminates targeted for investigation. In the sol-gel process, metal alkoxides are dissolved in a common or like solvent and hydrolyzed by the slow addition of H<sub>2</sub>O-solvent solution. The hydrolyzed species produce gels with metals bonded through -O and -OH species. These gels upon calcination produce homogeneous and single phase materials at usually lower calcination temperatures than conventional solid state reaction. The factors that influence the homogeneity and phase purity of the materials produced by sol-gel process are alkoxides solubility, hydrolysis and condensation rates, pH, and temperature to mention a few. This sol-gel process has been used to produce homogeneous single-phase hexa-aluminates with high surface area at temperatures above 1200°C.

The Sr-Al-O system was chosen to standardize the sol-gel synthesis method. Initially, use of isopropoxide precursors of both Sr and Al precursors was attempted. The process had serious difficulties in producing compositionally homogeneous gels due to the poor solubility of aluminum isopropoxide in most of the common solvents. Alternatively, aluminum tri-sec-butoxide was used along with strontium methoxy propoxide in methoxy ethanol. In this system, the precursors tend to hydrolyze at different rates upon the addition of H<sub>2</sub>O. This was overcome by pretreating the metal alkoxides with small quantities of glacial acetic acid. The modified alkoxides produced homogeneous gels upon hydrolysis. These gels were calcined and the phase developments were studied using x-ray diffraction.

The study also focused on the development of the single-phase material from precursors and its thermal stability. The precursor powders were x-ray amorphous and no crystalline peaks were present. These precursors upon calcination at different temperatures 800°C, 850°C,

900°C, and 950°C for 1 hour produced crystalline phase similar to delta aluminum oxide. When calcined for longer duration at these temperatures, the delta aluminum oxide x-ray diffraction pattern appeared diffused due to the onset of diffusion reaction. Between 900°C and 1000°C various Sr-Al-O phases such as  $\text{SrAl}_2\text{O}_4$ ,  $\text{SrAl}_4\text{O}_7$  were produced along with the hexa-aluminate  $\text{SrAl}_{12}\text{O}_{19}$  phase in major proportions (> 50 percent). On heating to 1000°C for 12 hours, the gel produced nearly single phase  $\text{SrAl}_{12}\text{O}_{19}$ .

Thermal stability studies utilized BET surface area measurements in conjunction with high-temperature treatment and the results are shown in Table 1. The indicator of thermal stability of a catalyst is its sintering resistance at high temperatures as revealed by a decrease in surface area. The surface area of  $\text{SrAl}_{12}\text{O}_{19}$  at 1300°C for 6 and 1400°C for 2 hours was found to be 7.5 m<sup>2</sup>/g and 6.9 m<sup>2</sup>/g respectively. Hexa-aluminate powders with novel compositions  $\text{SrPrAl}_{12}\text{O}_{19}$ ,  $\text{SrCeAl}_{12}\text{O}_{19}$ ,  $\text{CaCeAl}_{12}\text{O}_{19}$ , and  $\text{CaPrAl}_{12}\text{O}_{19}$  were also synthesized

and evaluated for surface area and catalytic properties. High surface area of 9.5 m<sup>2</sup>/g and 8.6 m<sup>2</sup>/g at 1300°C for 6 hours and 1400°C for 2 hours was found for the Ca-Ce-Al-O hexa-aluminate.

The catalytic activity of the prepared hexa-aluminates were also studied and the results are shown Figure 1. The activity measurements were made under conditions of 4 percent CH<sub>4</sub>, 8 percent O<sub>2</sub>, 88 percent He, 50,000<sup>-1</sup> space velocity with 0.1 ML of the listed catalyst calcined approximately 4 hours at 1200°C. The T<sub>10%</sub> is the temperature at which 10% methane combustion occurs. The rates were micromole of CH<sub>4</sub>/s-m<sup>2</sup> at 800°C; T<sub>90%</sub> is the temperature at which 90% methane conversion occurs.

## Reference

National Research Council Panel Views. 1993.  
New Directions in Catalytic Science and Technology.

## Presentations

K.S. Ramesh, J.J. Kingsley, J.L. Cox. 1995. "Synthesis and Properties of Hexa-aluminates for Catalytic Combustion." Presented at the Annual Session of the American Ceramic Society, Cincinnati, Ohio.

K.S. Ramesh. 1995. "Catalyst Materials for High Temperature Processes." Presented at the Center for Advanced Ceramic Technology, Alfred University, August, Alfred, New York.

Table 1. Thermal Stability

Composition	Surface Area m <sup>2</sup> /g	
	@ 1300°C for 6 Hours	@ 1400°C for 2 Hours
$\text{SrAl}_{12}\text{O}_{19}$	7.3	6.9
$\text{Sr}_{0.8}\text{Pr}_{0.2}\text{Al}_{12}\text{O}_{19}$	6.0	3.4
$\text{Sr}_{0.8}\text{Ce}_{0.2}\text{Al}_{12}\text{O}_{19}$	1.4	1.2
$\text{Ca}_{0.8}\text{Ce}_{0.2}\text{Al}_{12}\text{O}_{19}$	9.5	8.7
$\text{Ca}_{0.8}\text{Pr}_{0.2}\text{Al}_{12}\text{O}_{19}$	6.0	4.8

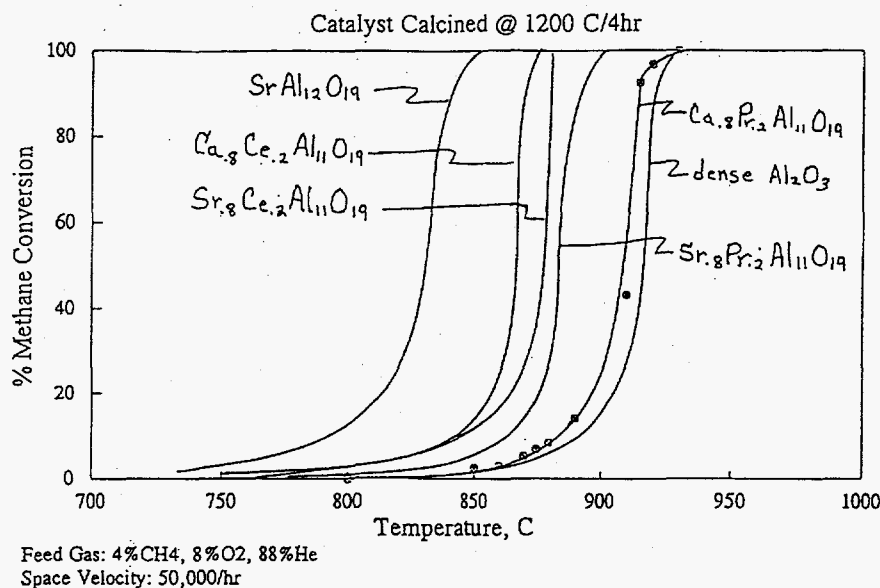


Figure 1. Combustion Catalyst Activity



# *Industrial Applications of High Surface Area Supported Metal Catalysts*

Todd A. Werpy (Chemical Technology)

---

## **Project Description**

This project was intended to find applications for high surface area inorganic support materials. The initial focus was upon high surface area mesoporous materials that could be used for catalyst supports. The interest in these materials comes from the need to find more suitable support materials that possess not only high relative surface areas, but also a largely mesoporous structure that could be beneficially used in a number of different mass transport limited, liquid phase reactions. Mass transport limitations have been identified in many chemical processes that use more traditional types of supported catalysts. Surface areas of existing supports have either been low, or much of the surface areas are within small diameter micropores which substrate molecules have difficulty accessing. Catalytic metals supported on such materials are therefore underutilized, ultimately driving up process costs. In the first phase of this work, mesoporous silica supports will be compared to various other high surface area support materials. A liquid phase hydrogenation reaction of interest to a potential industrial client will be used as the test reaction. In addition to the performance of the catalysts prepared on the special mesoporous supports, the complete characterization of the catalysts with respect to the surface areas, pore diameter distributions, and metals dispersion also need to be done to ascertain the benefits afforded by the special supports.

## **Technical Accomplishments**

Initially, only small batches (5 to 10 g each) of the mesoporous silica materials were available for testing as catalyst supports. In the initial phase of testing, catalysts prepared by impregnating prospective support materials with Pd and Re containing compounds (5 wt% each) were tested for their activity in an ester hydrogenation reaction. A mesoporous silica, prepared such that it possessed an average pore diameter of 30 Å, was compared to an Engelhard "premium grade" carbon support. Neither the details of preparation, nor the average pore diameter distribution for the Engelhard support were fully disclosed. The activities of the catalysts prepared on their respective supports were very comparable. In order to have sufficient amounts of material to do additional testing, it was decided to increase the batch size of the mesoporous silica preparation. The catalysts prepared from the larger sized batches failed to perform as well as those prepared from the smaller batches that had been tested. Microscopic analyses of the resulting materials revealed that the materials prepared in the larger batch had a disordered structure and possessed considerable closed porosity. Apparently, additional scale-up details need to be worked out in order to insure a uniform quality mesoporous silica.

Laboratory staff have also been successful in synthesizing mesoporous silicas that have larger average pore diameter distributions (up to about 100 Å average pore diameters). None of these materials have been obtained in sufficient quantity to manufacture into catalysts, at this time.

# Matrix Crack Insensitive Composite Materials

Charles H. Henager and Russell H. Jones (Materials and Chemical Sciences)

## Project Description

Ceramic matrix composites offer the possibility of high-strength, corrosion-resistant, high-temperature materials with a fracture resistance adequate for use as structural materials in a variety of systems. Reinforcement of a brittle ceramic matrix material by brittle fibers or whiskers separated from the matrix by a weak interface contributes to fracture resistance through reinforcement pull-out, crack bridging, crack deflection, and matrix micro-cracking. Previous work by Henager and Jones using fiber-reinforced composites showed that the transition from stage II cracking to stage III occurred at a higher stress intensity ( $K$ ) than expected from four-point-bend fracture tests when the loading rate was very slow. This pointed to the possible increase in the toughness of a ceramic matrix composite at high temperatures under slow crack growth conditions. It was suggested that high temperature plasticity of fibers in the crack-wake bridging zone controls the velocity of cracks in ceramic matrix composites. In ceramic matrix composites, the zone exhibiting this bridging is increased during slow crack growth because the fibers relax by high-temperature creep. This study explores the effect of the bridging on resultant toughness after slow crack growth by comparing the toughness of a variety of materials under slow crack growth conditions. A model is developed to understand this phenomenon.

## Technical Accomplishments

Materials for testing were selected and purchased this year. A new postdoctoral fellow, Dr. Charles Lewinsohn, was brought into the project. Experimental results will be generated this year with the new materials.

The main result was the development of a computer model to describe crack bridging in composites. The model computes the shape of a bridged crack using a mathematical approach known as Green's function method. Each bridging fiber is treated as the superposition of unit bridging forces and the net effect of many bridges is computed using convolution integrals and superposition. A computed bridged crack profile is shown in Figure 1. The calculation of the crack shape using this approach allows us to compute the stress intensity at the tip of the crack and to apply a simple rule-based decision on whether the crack extends (exceeds the matrix toughness value) or arrests. The model is dynamic

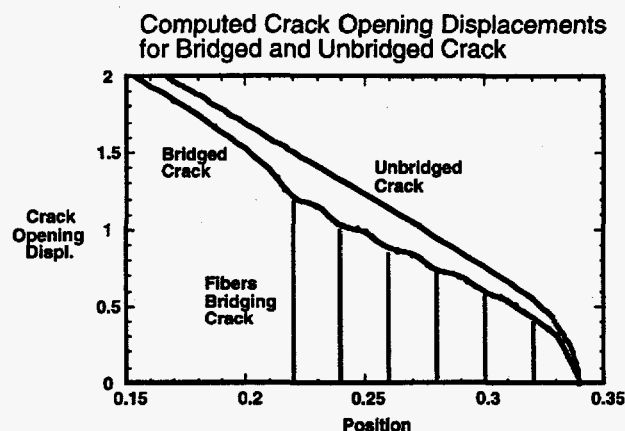


Figure 1. The computed crack opening displacement for a bridged and unbridged crack from the computer model developed here.

because the bridging fibers are allowed to relax with time following experimental fiber creep laws. This brings in the element of time and allows the model to compute how long it takes a given bridged crack to grow across an array of fibers.

The results of the model verified our initial guess that the creep rate of the fibers does control the velocity of the bridged crack in the composite. However, a surprising result, shown in Figure 2, was that the model also indicated that there may exist a fiber creep rate that optimizes the time-dependent toughness of the composite material. This is a useful and important result, at which the experimental data will be directed this year.

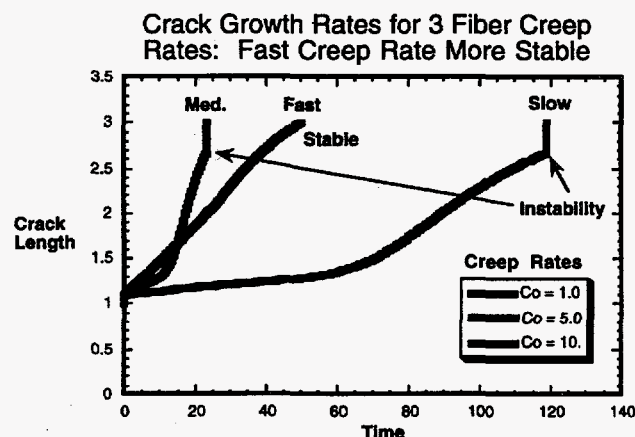


Figure 2. The computed crack length as a function of time curves for three different creep rates. The fastest creep rate is seen to be more stable than the medium creep rate fiber.

The experimental materials include ceramic-based composites having fibers of differing creep strengths, as well as an aluminum-based laminar composite that will allow us to study crack bridging over a wide temperature range to search for these optimal creep rates.

#### Publication

C.R. Jones, C.H. Henager, Jr., and R.H. Jones. 1995. "Crack Bridging by SiC Fibers During Slow Crack Growth and the Resultant Fracture Toughness of SiC/SiC<sub>f</sub> Composites." *Scripta Met. et. Mater.* (in press).

# Mesoporous Materials

Jun Liu (Materials Science)

## Project Description

The objective of this research was to explore the synthesis of ordered mesoporous materials and nanoscale structures based on self-assembly of ordered structures in surfactant solutions. These materials can be used as ion exchangers for environmental cleanup, catalysts, and catalyst supports. This research also forms the basis of a new class of ordered nanocomposite materials.

## Technical Accomplishments

Many organic systems, such as surfactant solutions, can form a variety of well-ordered structures (liquid crystals) with hexagonal, lamella, and cubic symmetry. If these structures can be used as a template to synthesize ceramic materials, it will generate a new class of materials that can be used in industrial processes based on size and shape selectivity of porous structures, such as catalysis, separation, and chemical sensing.

In 1992, ultralarge pore zeolite-like materials were discovered. The new materials are characterized by the pore diameters that can be adjusted between 18 Å and 200 Å through the synthesis conditions, and by the monodispersity and ordering of the pores. It is believed that these molecular sieves are formed on ordered surfactant liquid crystalline structures, which act as templates to control and stabilize the ultralarge porous structures.

However, currently, only aluminosilicates and a few other materials can be prepared. The objective of this study was to uncover the underlying principles that govern the formation of the mesoporous materials and to develop a methodology that can be used to prepare nonsilicate materials for ion exchangers, catalysts, and other applications.

This project involved

- the characterization of structures formed in surfactant
- an investigation into the stability and modification of the template structures by the inorganic precursor materials and the interactions between the inorganic and organic phases

- growing and stabilizing of the inorganic materials within the template structures under hydrothermal conditions
- studying the hydrolysis and condensation of the ceramic precursors during the ordering process.

## Synthesis of Ordered Mesophase Zirconia Materials

Because of the low solubility of the zirconia precursor at high pH, an acid synthesis route was developed. For the positively charged zirconia precursor at low pH, amphoteric surfactants were used. Sodium dodecyl sulfate only produced lamellar phases because the head group size is too small when the charge on the head group was neutralized by the oppositely charged ceramic precursor. Three-dimensional mesophase zirconia was synthesized using coco betaine that has a large head group size. The mesophase zirconia formed as rod-like (noodle-like) crystals. X-ray diffraction showed a sharp peak at 4 nm, and multiple broad peaks at high angles, which suggested that the ceramic material is also weakly crystalline. This is the first time we observed crystalline structure in mesophase material. It is believed that the ordered mesophase zirconia was formed through a cooperative intercalation mechanism of the surfactant micelles and the lamellar ceramic precursors.

## Stabilization of Non-Silicate Mesoporous Materials

Most nonsilicate mesoporous materials are not expected to be thermally stable due to the tendency to crystallize. Various techniques have been explored to stabilize the high surface area materials, including pretreatment of the ceramic precursors and post-treatment of the as prepared mesophase materials. The purpose of the treatment is to reduce the water content, to increase the degree of cross-linking, to dope the materials to prevent crystallization, and to increase the wall thickness. Preliminary results showed that the thermal stability is increased, and the weight loss is considerably reduced.

## Mesoporous Silicates as Support for Metallic Catalysts (collaborating with Dr. Yong Wang)

Tunneling electron microscopy and high resolution tunneling electron microscopy shows that the metals are dispersed in the matrix as ordered particles. The catalytic

activity of the 5%Pd5%Re/SiO<sub>2</sub> composite is used in the hydrogenation of butyrolactone to 1,4-butanediol. The main use of 1,4-butanediol is in the production of engineering plastics (polyurethanes and polybutylene terephthalates). The performance of such catalysts is much more active than the commercial CuCr catalyst and is similar to the performances of our best in-house made catalysts on oxidized carbon support for the hydrogenation.

#### *Ordered Ceramic Composites as Magnetic Materials*

Similar methods were used to infiltrate nickel into the silica support. The magnetic phase is well dispersed in the matrix as rod-like particles. All the magnetic particles have the same diameter. The composite materials have been thoroughly characterized by high resolution tunneling electron microscopy and electron energy loss spectroscopy. The materials consist of a nickel oxide core, and 5 Å amorphous nickel silicate interfacial region. This provides an ideal composite to investigate the size effect on the magnetic properties. Measurement of the magnetic hysteresis loop suggests that all the magnetic domains are well aligned and a high magnetic permeability has been obtained.

#### **Publications**

J. Liu, A.Y. Kim, and J.W. Virden. 1995. "Synthesis of Mesoporous Silicate Spherulite in Surfactant Solutions." *J. Porous Materials* (in press).

B.J. Palmer and J. Liu. 1995. "Simulation of Self-Assembly of Surfactant Micelle." *Langmuir* (in press).

L.Q. Wang, J. Liu, G.J. Exarhos, and B.C. Bunker. 1995. "Investigation of Structure and Dynamics Surfactant Molecules in the Mesophase Silicates Using Solid-State <sup>13</sup>C NMR." *Langmuir* (submitted).

J. Liu, Y. Wang, Y.L. Chen, A.Y. Kim, J.W. Virden, L.A. Chick, and M. Qian. 1995. "Ordered Nanomagnets Based on Mesoporous Silica." *Nature* (submitted).

#### **Presentations**

J. Liu, L. Wang, A.Y. Kim, B.J. Palmer, and J.W. Virden. 1995. "Nucleation of Mesoporous Materials Studied by Magnetic Resonance." Workshop on Access in Nanoporous Materials Symposium, Michigan State University, June, East Lansing, Michigan.

J. Liu, A.Y. Kim, M. Qian, W. Yong, and Y.L. Chen. 1995. "Self-Assembly of Mesoporous Ceramic Materials." 1995 Pacific Regional Meeting of the Ceramic Society, November, Seattle, Washington.

# Nanoparticle Processing

Beth L. Armstrong (Materials Sciences)

## Project Description

The overall goal of this project was to investigate material fabrication processes of nanoparticles into pellets, thin films, membranes, and bulk ceramics. Until the development of the RTDS process, attaining nanoparticulate materials in large quantities was difficult and very expensive. Competing technologies are now only just beginning to provide nanoparticulate materials in pound quantities. Thus, processing nanoparticulates into large, bulk components was simply not feasible due to a lack of material with reproducible characteristics. Even if the materials were available, processing of nanoparticulates into bulk components is extremely difficult due to the high surface area of the powders, typically  $>200 \text{ m}^2/\text{gm}$ , and the hygroscopic nature of the powders themselves. These powders do not flow or pack well due to the high surface areas and excess water.

During FY 1994, consolidation of RTDS products was investigated for structural ceramic applications. With such applications being judged inappropriate for the RTDS powders, FY 1995 efforts focused on using RTDS and mesoporous powders for catalytic applications. The issues of processing ultrafine powders were still similar to the objectives set in FY 1994—overcoming problems of consolidating powders with highly hydrated surfaces, maintaining high surface activity, and fabricating mechanically robust components. These components must retain their high pore volume after processing to facilitate high reactivity and mass transport.

## Technical Accomplishments

The project was separated into two sections:

- 1) characterization and processing of RTDS produced sulfated zirconia nanoparticulate powders, and
- 2) characterization and processing of mesoporous silica.

### *Characterization and Processing of RTDS Sulfated Zirconia Nanoparticulate Powders*

Work completed by Thomas D. Brewer, Charles H.F. Peden, and William J. Thomson during FY 1994 on the project "Catalyst Development and Testing" showed that sulfated zirconia catalytic activity results for n-butane isomerization were superior to the five other sulfated metal oxide catalysts that were tested. In addition, these investigators and the RTDS project team adapted the

RTDS process to produce superacidic sulfated nanoparticulate zirconia. These preliminary results were the basis of the focus of the processing effort outlined for this project in FY 1995.

The RTDS superacidic sulfated zirconias were provided by Dean W. Matson. The focus of the effort was to coat or infiltrate porous supports with a thin, active layer of the sulfated zirconia using slurry coating techniques. The direct product of the RTDS technique was sulfated zirconia suspended in an aqueous solvent. Because of the residual nitrates present in the suspension, the powders were separated by centrifugation, dried, sieved, and resuspended in an aqueous solvent for coating purposes. A variety of porous supports including partially magnesia stabilized zirconia with varying pore structures and amorphous silica were evaluated. Catalytic activity was used as a measure to weigh the success of the processing techniques. Due to limitations in the design of the reactor with respect to the size of the supported zirconias and improper loadings, catalytic activities for a n-butane isomerization reaction (reported as conversion at  $600^\circ\text{C}$  over 1 hour) were significantly lower than that reported for the powder equivalent. Typically, initial powder conversion ranged on average from 60 percent conversion at 1 minute to 15 percent at 60 minutes. Supported material values ranged on average to 2 percent conversion at 1 minute to 1.2 percent at 60 minutes.

### *Characterization and Processing of Mesoporous Silica*

Mesoporous silicas were provided by Jun Liu and Anthony Y. Kim using the aqueous synthesis technique evaluated on the "Catalyst Development and Testing" project during FY 1994. Since the effect of processing during consolidation on the porous mesostructure was unknown, the focus of this section was to consolidate the mesoporous silica into a pelletized form, heat treat the pellets and evaluate the resulting properties including surface area, phase, microstructure, pore volume, and pore size distribution.

The pellets were exposed to three temperatures:  $800^\circ\text{C}$ ,  $1000^\circ\text{C}$ , and  $1200^\circ\text{C}$ . With increasing temperatures, surface area decreased from over  $1000 \text{ m}^2/\text{gm}$  to 886.5, 196.6, and  $2.1 \text{ m}^2/\text{gm}$ , respectively. Likewise, total pore volume also decreased with increasing temperatures. The mesoporous structure was maintained up to  $1000^\circ\text{C}$ . At  $1200^\circ\text{C}$ , the mesoporous silica became crystalline, and the mesoporous structure was lost.

## Publication and Presentation

B.L. Armstrong. 1995. "Synthesis and Processing of Nanocrystalline  $\text{ZrO}_2$ ." Presented at and in *Proceedings from the NIST Nanomaterials Processing Workshop*, Gaithersburg, Maryland.

# Nanoparticle Science

Larry A. Chick (Materials Sciences)

---

## Project Description

The nanoparticle science project is directed at developing combustion synthesis methods to produce nanoparticle titanates and ferrites, ceramic materials that are useful in electrochemical devices such as batteries, in membrane reactors and separators, as electronic ceramics, as piezoelectric ceramics, and as mixed oxide catalysts. For cost-effective fabrication and retention of desirable properties, it is necessary that these complex oxide ceramics be synthesized with high surface area and high chemical homogeneity, characteristics that are typical of combustion synthesized ceramic powders.

Combustion synthesis has been developed and used to make a wide variety of single, binary, and ternary oxides such as  $\text{Al}_2\text{O}_3$ ,  $\text{CeO}_2$ ,  $\text{Y}_3\text{Al}_5\text{O}_{12}$ ,  $\text{LaCrO}_3$ , and  $\text{LaSrFeCoO}_3$ . However, titanates have not been synthesized due to the lack of a stable aqueous precursor. A method for preparing titanates using a combustion process has been reported in the literature, however, the material chosen for the titanium precursor is not stable in water and decomposes rapidly. Therefore, it would be difficult to make large quantities of high-purity, controlled stoichiometry powder with this precursor.

In this project, the titanates will be synthesized using a combustion synthesis process similar to the glycine nitrate process. This new process has been developed using a novel water soluble titanium material. This material, trade named TYZOR LA, is a dihydroxy bis(ammonium lactato) titanium aqueous solution. The barium precursors used will include the nitrate and the acetate. Spray drying of the precursor, followed by furnace reaction will be compared to direct combustion of the precursors. Final

surface area and phases detected by x-ray diffraction will be used to choose between and optimize the synthesis techniques. Sintering behavior and electrical properties will be investigated and compared to those of commercial barium titanates.

Ferrites will be synthesized using the glycine-nitrate process, with nitrates as the primary precursors. Combustion redox and calcination conditions will be adjusted to optimize phases and surface area.

## Technical Accomplishments

During FY 1995, a variety of titanates including  $\text{BaTiO}_3$ ,  $\text{PbTiO}_3$ ,  $\text{SrTiO}_3$ ,  $\text{Al}_2\text{TiO}_3$  and  $\text{Pb}(\text{ZrTi})\text{O}_3$  ( $\text{PbLa}(\text{ZrTi})\text{O}_3$ ) were synthesized using the TYZOR precursor. Most of the effort this year went into optimizing the process for synthesizing  $\text{BaTiO}_3$ . Best results were obtained by spray drying the TYZOR with barium acetate, followed by calcining in air. Powders having BET surface areas between 9 and 11  $\text{m}^2/\text{g}$  were produced. Neodymium was incorporated as a sintering aid. Sintered densities slightly higher than those for a commercial  $\text{BaTiO}_3$  powder (Tam Corp.) were obtained. Samples were provided to Ferro Corp. Electrical properties are currently being tested at University of Cincinnati.

Several ferrite materials were synthesized using the glycine-nitrate process.  $\text{NiO-NiFe}_2\text{O}_4$  was produced at 25  $\text{m}^2/\text{g}$ . This material is a replacement for the Ti-supported CuO catalyst currently used in the Dow process for vapor phase oxidation of benzoic acid to phenol. Initial tests showed that the glycine-nitrate process material produces higher yield than the Ti-supported CuO.



# *Novel Electrosynthesis of Organic/Inorganic Electroactive Polymers Based on Co-Polymerization of Organic Molecules with Cyclic Chlorophosphazenes*

Mira A. Josowicz (Materials Sciences)

---

## **Project Description**

The objectives of this project were to carry out additional studies on the electrochemical-chemical polymerization process used to

- deposit composite organic-inorganic films
- evaluate the film composition and microstructure
- characterize toward the ability to enhance chemical reactivity (diffusivity) of specific molecules.

The molecular-level understanding of interactions between the species in a solution or vapor phase was planned. Knowledge of the interaction is needed to realize the potential application of the material as a sensitive layer for chemical sensors, separator membranes, or as protective or biomimetic coating.

## **Technical Accomplishments**

The synthetic route for in situ polymerization of cyclomatrix inorganic-organic material on conducting substrate involves electrogeneration of a reactive quinone radical anion at the cathode that then reacts via nucleophilic substitution with the hexachlorocyclophosphazene precursor. The electrolytic synthesis and characterization of the novel material are a complex matter. To maximize the attractive feature of the electrolytic step to initiate the electrochemical-chemical-electrochemical (ECE) reaction mechanisms, experiments were carried out to obtain a more complete understanding of the effects of the solvent, electrolytes, and precursors.

The study concentrated on aprotic solvents, such as acetonitrile (AcCN), dimethylformamide (DMF), propylene carbonate (PC), tetrahydrofuran (THF) and on electrolytic salts, such as tetrabutylammonium tetrafluoroborate ( $\text{Bu}_4\text{NBF}_4$ ), tetrabutylammonium iodide ( $\text{Bu}_4\text{NI}$ ), potassium iodide (KI), sodium perchlorate ( $\text{NaClO}_4$ ). The effect of factors such as proton activity, usable potential range, dielectric constant, and solubility of the precursors limits the selected solvents only to AcCN or AcCN:THF mixture in the ratio of 1:4. This solvent limits the use of the a priori selected electrolytic

salts only to  $\text{Bu}_4\text{NBF}_4$  and  $\text{Bu}_4\text{NI}$ . The resulting selection of these electrolytes has been to control activity of various quinone radicals through a facilitated electron transfer within a potential range from 0 up to -2.5 V versus the  $\text{Ag}/\text{Ag}^+$  reference electrode.

Considerable progress in characterizing physicochemical properties of the novel material resulted from experimental efforts that concentrated on structural architecture, electrochemical, and electrical properties. In our FY 1994 report, we reported that the structural architecture of the film can be controlled through selection of different quinone type molecules. From the optical micrographs it was actually possible to see differences in the gross morphological structure of these films. Scanning electron microscopy (SEM) was applied to map out phosphorus atoms. It was found in the poly(cyclophosphazene-benzoquinone), the phosphorous atoms could be identified in repetitive units, which would suggest a pore size of approximately 10 Å. The use of that technique for the analysis of the polycyclo(phosphazene-antraquinone) film was not so straightforward. Consequently, further investigations will be necessary if that technique is to be used in the future.

In order to gain further insight into the pore size of the "as made" material, a permeation method was used. In this method, a size indicator redox couple, such as potassium ferrocyanide/potassium ferricyanide, was used. It has been observed that poly(cyclophosphazene-benzoquinone) film deposited at a constant potential of -1.0 V versus  $\text{Ag}/\text{Ag}^+$  electrode is acting as an electronic barrier layer for this redox couple. However, during the synthesis of the material, when the applied potential to the working electrode was -2.0 V versus  $\text{Ag}/\text{Ag}^+$  electrode, the resulting coating is as a porous material. To maximize the possibility to detect the pores, a comparison between the peak height of the recorded redox peak on bare platinum electrode and on the electrode covered with the phosphazene was conducted. The results show that approximately 30 percent of the original surface remains open. This finding opened the possibility to use the poly(cyclophosphazene-benzoquinone) film as the separator in a battery or a supercapacitor.

Combined electrochemical and quartz crystal microbalance experiments have been carried out in order

to determine the density of the poly(cyclophosphazene-benzoquinone) film. From the frequency responses of the quartz crystals before and after the synthesis of the film and from the thickness of the deposited films (which was in the range between 1 and 2  $\mu\text{m}$ ) the density of  $1.35 \pm 0.15 \text{ g/ccm}$  has been determined.

In order to examine the possibility of introducing an additional functionality to the novel film, rodizonic acid dihydrate which contains four -OH groups in the benzoquinone molecule has been selected. The -OH groups can be seen as sites capable of forming a hydrogen bonds. That interaction capability can facilitate the use of the novel material in chemical sensors or as polyelectrolyte in battery or ultracapacitor applications. The replacement of the benzoquinone precursor by the rodizonic acid dihydrate resulted in a formation of a thin yellow film on the substrate. This material is currently under investigation for application in chemical sensors.

The aim of the present work, to present some catalytic activity of the phosphazene film was investigated by studying the electrochemical activity of sulfuric acid. The strength of the sulfuric acid as an oxidant agent depends on the its concentration. Since the change in the oxidizing properties depend on the concentration of  $\text{SO}_2$  it was interesting to investigate if reduction of sulfuric acid may result in  $\text{SO}_2$  production. The electrolysis of 4.5 M sulfuric acid has been investigated using a cyclic voltammetry. A platinum electrode modified with the poly(cyclophosphazene-benzoquinone) film, synthesized at -1.0 V or -2.0 V, respectively, was used. The electrolysis was carried out by scanning the potential of the working electrode from 0.1 V up to 1.2 V (20 cycles) versus the standard saturated calomel electrode (SSCE). The x-ray photoelectron spectroscopy analysis proved, that accommodation of S-atoms and oxygen atoms into the poly(cyclophosphazene-benzoquinone) film takes place. For the polycyclophosphazene film synthesized at -1.0 V up to 2.9 percent of S-atoms and up to 12 percent oxygen atoms were found. This atomic-ratio accounts for the  $\text{SO}_2$  molecule. When the poly(cyclophosphazene-benzoquinone) film was synthesized at -2.0 V, up to 6 percent of S-atoms and 24 percent of oxygen atoms were produced.

The results will suggest an interaction of sulfite ions with the quinone oxygen which act as an oxidant. At present there is no evidence how the concentration of the sulfate-sulfite is changing in solution.

The poly(cyclophosphazene-quinone) films, as deposited, are electrical insulators. Their resistance is in the megaohm range. In order to enhance the conductivity of the synthesized films, iodine doping has been investigated. For this purpose three types of doping procedures have been used and compared: 1) from the vapor phase, 2) electrochemical doping, and 3) from the solution. All

the doping procedures led to an enhancement of the electronic conductivity of the polycyclophosphazene films. The difference between these three procedures was monitored by testing the initial work function of the film by using a Kelvin probe. In all cases, the iodine was acting as an electron donor and the phosphazene film as an electron acceptor. The most stable doping was obtained when the electrochemical procedure was used. In that case the electrolyte solution contained 10 mM potassium iodide in 0.1 M sulfuric acid. The doping was carried out at constant potential of +0.8 V for 1.5 hours. During that time the iodide was oxidized at the platinum electrode surface to iodine which was retained in the matrix. The optical micrograph shows that iodine is incorporated into the polymer matrix in a crystalline form. The inhomogeneity of the poly(cyclophosphazene-benzoquinone) actually facilitates the nucleation of the iodine in the polymer matrix. The measured electronic conductivity of the films after that type of doping increased to a kilohm range.

The application of the iodine-doped poly(cyclophosphazene-benzoquinone) in chemical sensors has been proved. It has been found that poly(cyclophosphazene-benzoquinone) film doped with iodine forms a charge transfer complex with tributylphosphate (TBP). This interaction allows a detection of TBP in the range from 8.8 ppm up to 4.0 ppb level.

Furthermore, it was found that the poly(cyclophosphazene-benzoquinone) film can be deposited on electrochemically or chemically prepared polyaniline film. This may lead to an application to construct devices based on organic semiconductor/insulator or organic semiconductor/organic metal if the poly(cyclophosphazene-benzoquinone) film is doped with iodine. The preliminary investigations of these structures indicate a diode behavior. However, further investigations will be necessary in order to provide more information about the charge transfer interactions taking place at such a junction.

## Publications

J. Li, M.A. Josowicz, and J. Janata. 1995. "Potentiometric Detection of Tributylphosphate Vapor Based on Charge-Transfer Complex Formation." *Electroanalysis* (submitted).

M.A. Josowicz, J. Li, and J. Janata. 1995. "Application of Poly(cyclophosphazene) Film for Potentiometric Detection of Tributylphosphate (TBP)." Abstract in *Proceedings of the International Chemical Congress of the Pacific Basin Societies*, Honolulu, Hawaii.

## **Presentation**

M.A. Josowicz, J. Li, and J. Janata. "Potentiometric Detection of Tributylphosphate (TBP) Vapor."  
Electrochemical Society Meeting, October 1994, Chicago, Illinois.

# Ordered Mesoporous Membranes

Jun Liu (Materials and Chemical Sciences)

## Project Description

This work aims to produce ceramic membranes and thin films with uniform porosity adjustable in the nanometer size range based on nucleation and self-assembly of surfactant liquid crystalline structures on functionalized surfaces or at liquid-liquid interfaces. In 1995, formation of free-standing thin films on a liquid-liquid interface was demonstrated. Nanoporous membranes on porous supports were prepared using a diffusion reactor. Growth of ordered structures on functionalized surfaces was also investigated.

## Technical Accomplishments

The discovery of ultralarge porous zeolite-like materials is considered a landmark in the history of synthesis of molecular sieve type materials. The new materials are characterized by the pore diameters that can be adjusted between 1.5 nm and 20 nm through the synthesis conditions, and by the monodispersity and ordering of the pores. Unfortunately, these materials can be only prepared in the powder form. One of the most important applications of such materials will be membranes and films. In 1994, Laboratory scientists proposed a new synthesis route to make membranes and films based on the discovery of a heterogeneous nucleation mechanism. This process uses functionalized surfaces and liquid-liquid interfaces to induce in situ growth of the ordered films at low temperature ( $< 150^{\circ}\text{C}$ ). The novel synthesis process consists of one step, low temperature ( $< 150^{\circ}\text{C}$ ) reaction and calcination ( $< 600^{\circ}\text{C}$ ), and can be easily applied to complicated shapes. Potential applications of the new membrane material include catalysis, separation, and fluid cleanup, and exchange media.

This work is based on surface induced growth of three-dimensional ordered structures. This is an important area for scientific research because it is a common phenomenon in physical chemistry, materials science, and biological science. This research involved nucleation and growth on functionalized surfaces to grow thin films, reaction at liquid-liquid interface to grow membranes supported by porous support, structural and chemical characterization, and performance testing.

## Demonstration of Free-Standing Thin Films on a Liquid-Liquid Interface

Surfactant and silicate solutions were placed side-by-side to form a stable liquid-liquid interface in a sealed reactor. The whole solution was then reacted at  $105^{\circ}\text{C}$ . A continuous uniform thin film was formed on the interface. It contains a macro-porous layer and a nanoporous layer. This principle can be adapted to prepare films on porous support.

## Preparation of Nanoporous Membranes on Porous Supports

A diffusion cell reactor was designed to prepare membrane materials on porous support. A porous support was sandwiched and sealed by O-rings between two glass tubes, which contain silicate and surfactant solutions respectively. The reaction occurred at the interface between the silicate and the surfactant solutions within the porous support (illustrated by Figure 1). A very uniform membrane ( $> 100\ \mu\text{m}$ ) was formed within the porous support, which was clearly visible to the naked eye as a shiny transparent layer on the surface of the silica support. No defects, such as cracking and macroporosity in the film were observed. X-ray diffraction proved that the membrane consists of hexagonally ordered porosity.

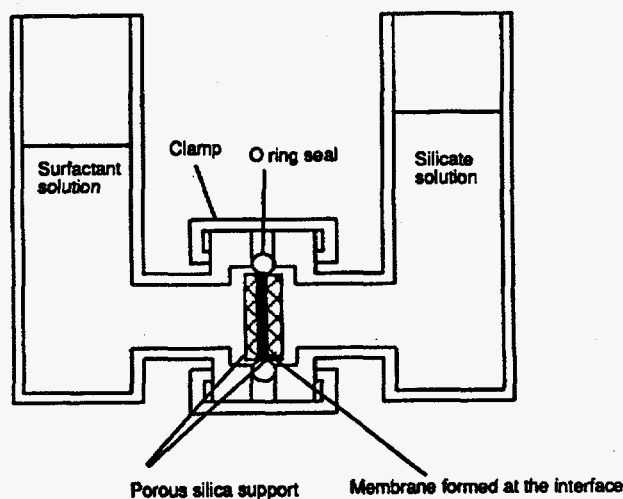


Figure 1. Diffusion cell reactor for the preparation of mesoporous membranes.

#### *Preliminary Permeability Test of the Membranes*

The porous support and the membrane materials have reasonable mechanical strength. A preliminary permeability test was performed by passing a solution containing 6 nm colloidal gold particles. The gold particles were red in the solution and blue when dried. Although the membrane was hydrophilic and absorbed a large amount of water, the gold particles, which were slightly larger than the pore diameter, could not penetrate the membrane and stopped at the interfaces.

#### *Preparation of Mesostructures on Functionalized Surfaces*

Self-assembled monolayers on silicon were used as the substrates. Surfaces with high sulfonate concentrations were prepared by exposing the substrate to sulfur trioxide vapor in a two-stage reactor. The vinyl groups were converted to sulfonate groups by this reaction. Other functional groups, such as dimethyl amine, and trimethyl amine, are also being tested. Uniform films and ordered structures have been grown on the functionalized surface.

# Selective Oxidation in Membrane Reactors

Larry R. Pederson and Jeffrey W. Stevenson (Materials and Chemical Sciences)  
William J. Thomson (Washington State University/Tri-Cities)

---

## Project Description

The purpose of this project was to investigate mixed ion and electron-conducting metal oxides as semipermeable membranes in the oxidative coupling of methane into  $C_2$  hydrocarbons (ethane and ethylene). In addition to providing high purity oxygen from an air source, these mixed conductors are also catalytically active in converting methane to higher hydrocarbons. Membrane materials were synthesized, fabricated into fully dense tubes and flat plates, and permeation and catalytic properties evaluated.

## Technical Accomplishments

Mixed conducting metal oxides in the compositional series  $La_{1-x}Sr_xCo_{1-y}Fe_yO_3$  were prepared by combustion synthesis methods. These perovskite compositions are predominantly electron conductors. Although the transference number for oxygen ions is  $\approx 10^{-3}$ , the oxygen ion conductivity in this series exceeds that of yttria-stabilized zirconia, a ceramic that conducts only oxygen ions. Flat plates and tubes were fabricated by cold-isostatic pressing; these were sintered to full density at 1200°C to 1300°C.

Passive oxygen fluxes were evaluated as a function of temperature. Oxygen permeation rates were favored by high strontium substitution for lanthanum and by high cobalt substitution for iron. Oxygen fluxes up to approximately 1 standard cubic centimeter oxygen per square centimeter membrane surface area were obtained for samples approximately 2 mm in thickness from an air source at ambient pressures. These permeation rates are sufficiently high to be of value in membrane reactor applications.

In collaboration with Professor W.J. Thomson, Washington State University, oxidative coupling reactions of methane to yield ethane and ethylene were studied as a function of temperature, methane partial pressure, and membrane composition. Both the selectivity and the overall reaction rate rose with increased strontium substitution for lanthanum in the membrane. A selectivity of 50 percent was found for  $La_{0.4}Sr_{0.6}Co_{0.2}Fe_{0.8}O_{3-\delta}$  at 700°C and a methane partial pressure of 1 atm. The selectivity for  $La_{0.6}Sr_{0.4}Co_{0.2}Fe_{0.8}O_{3-\delta}$  was 30 percent under otherwise identical conditions. Selectivity increased with increases in the methane partial pressure. Selectivities were further enhanced by the addition of doped magnesium oxide catalysts.

# Solution Chemistry

Gordon L. Graff, Bruce C. Bunker, Suresh Baskaran, and Lin Song (Materials Sciences)

## Project Description

New coating materials and techniques are important to industry not only to extend the useful life of components but also to allow the substitution of lighter-weight materials. Research efforts are focused on the development of corrosion resistant, chemically resistant, catalytic, and/or ultraviolet-blocking coatings that can be deposited from inexpensive, aqueous salt solutions.

## Technical Accomplishments

### $\text{TiO}_2$

Significant advances have been made in the development of aqueous solution routes for the deposition of  $\text{TiO}_2$  films on polymeric substrates. Careful control of solution chemistry using the inexpensive Ti-precursor solution has resulted in film deposition rates as high as 400 Å/min at 70°C with good film adhesion on polycarbonate. Figure 1 shows the deposition rates for  $\text{TiO}_2$  films as a function of starting Ti concentration. In addition, Figure 2 shows a typical ultraviolet-visible transmission spectra for the  $\text{TiO}_2$  coatings on a fused quartz coupon. At film thicknesses of approximately 900 Å, ultraviolet radiation is strongly absorbed, while the films retain acceptable transmission in the visible region. Recent experiments conducted on coated PC have shown that transmission in the visible spectrum remains above 75 percent after application of 1000 Å to 2000 Å of  $\text{TiO}_2$ . In addition, uniform coatings have been deposited on highly convoluted polycarbonate test samples. To date, no other coatings process has outperformed the biomimetic technique in coating the complex shaped coupons.

### $\text{ZrO}_2$

Solution routes for the deposition of  $\text{ZrO}_2$  precursor films were also successfully developed in FY 1995. Initial attempts at film growth from zirconyl nitrate proved fruitless, so  $\text{Zr}(\text{SO}_4)_2$  was used as a starting soluble salt. The sulfate salt was effective in depositing zirconium hydroxide sulfate films at 70°C. The as-deposited films convert to crystalline  $\text{ZrO}_2$  at temperatures as low as 400°C. Yttria has also been incorporated into the Zr hydroxide films using coprecipitation and/or sequential layering techniques. The production of  $\text{Y}_2\text{O}_3$ -stabilized  $\text{ZrO}_2$  films seem possible, though further work in this area

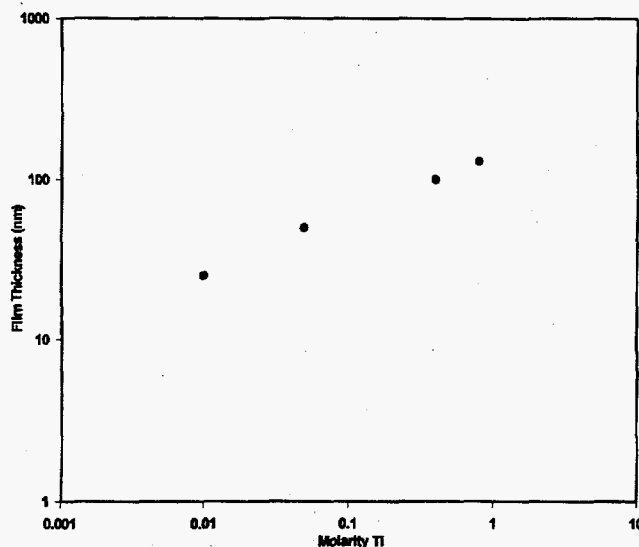


Figure 1. Deposition Rates for  $\text{TiO}_2$  Films as a Function of Starting Ti Concentration

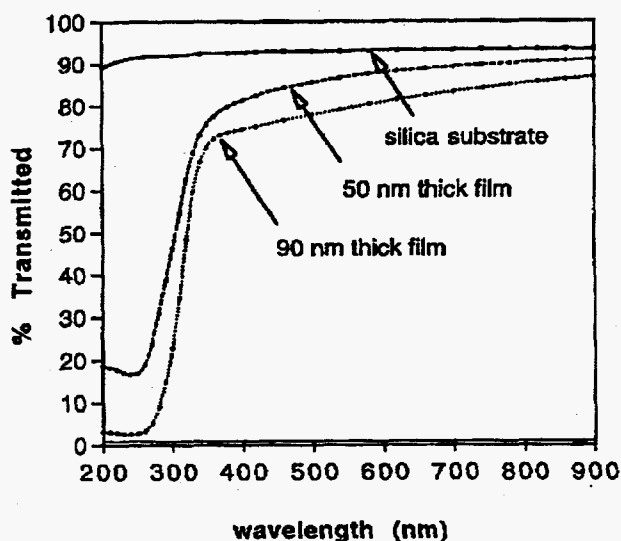


Figure 2. A Typical Ultraviolet-visible Transmission Spectra for the  $\text{TiO}_2$  Coatings on a Fused Quartz Coupon

is required. One potential drawback to the use of the sulfate salt is the presence of residual sulfur in the final calcined film. This problem has been circumvented by the addition of oxalate anion to our deposition solutions. The presence of oxalate has eliminated residual sulfur from the films and, as an unexpected bonus, increased film deposition rates.

## ZnO

Exhaustive experiments have been completed using Zn acetate, nitrate, and chloride as starting salts, but none have proven useful in making films. XRD analysis have shown that ZnO particles can be formed in the aqueous solutions under a number of conditions, but uniform film

growth has not been observed. Experiments are under way using urea and HMTA as complexing agents to control cation hydrolysis and solution pH. Though not complete, deposition solutions containing urea and/or HMTA have not generated ZnO films. All experiments conducted to date have been in acidic solutions where the solubility of  $\text{Zn}^{2+}$  is high.



# *Supported Metal Catalysts*

Thomas D. Brewer (Chemical Sciences)

---

## **Project Description**

This project focused on developing highly dispersed metal catalysts using materials developed at Pacific Northwest National Laboratory for producing high surface area inorganic oxides. A number of specific chemical reactions based on hydrogenation, dehydrogenation, and polymerization was employed to evaluate conversion, selectivity, catalyst lifetime, and regenerability of the catalysts. Initially, the focus of this project was on the development of non-acidic, mesoporous, supported metal catalysts for the dehydrogenation of C4 alkanes to C4 alkenes, with future catalytic applications including hydrogenation of aqueous maleic anhydride to 1,4-butanediol and ethylene polymerization.

The objective of this work was to develop novel metal supported catalysts for industrially important reactions that complement technologies developed at Pacific Northwest National Laboratory for producing high surface area inorganic materials. Processes which offer the desired materials properties are the glycine-nitrate combustion synthesis process, rapid thermal decomposition of solutes in solution process, and the process under development for producing mesoporous materials. These processes can produce either nanoscale particle size or ultrahigh surface area silica, zirconia, and aluminosilicate materials which offer a unique opportunity for application as supports for metal catalysts. These supports are unique because the high surface area and the large pore volume to surface area ratio inherent in these materials afford the potential

for highly dispersed metal deposition. A highly dispersed supported metal catalyst results in greater catalytic efficiency and the need for smaller catalyst volumes, thus reducing the cost of the overall catalytic process. Chemical reactions based on hydrogenation, dehydrogenation, and polymerization will be employed to evaluate conversion, selectivity, catalyst lifetime, and regenerability of the supported metal catalysts.

## **Technical Accomplishments**

The approach to this research was based on developing catalysts to replace currently used catalysts, such as platinum supported on alumina. Silica catalyst supports for the first half of FY 1995 were synthesized in cooperation with other staff members involved in mesoporous materials research. The mesoporous silica to support platinum by employing standard impregnation technology was used. The catalysts were characterized for metal dispersion, metal loading, surface area, pore size distribution, and pore volumes using a RXM-100 catalyst characterization system. The catalysts were tested for conversion, selectivity, lifetime, and regenerability based on the dehydrogenation reaction of C4 alkanes to C4 alkenes.

The principal investigator left the Laboratory before the project was complete. The results of this project are unavailable.

# Surface Modification

Suresh Baskaran and Gordon L. Graff (Materials and Chemical Sciences)

## Project Description

Previous research at Pacific Northwest National Laboratory has demonstrated that carefully tailored organic interfaces will catalyze the nucleation and growth of ceramic thin films from aqueous solutions. Thus, if the surfaces of target substrate materials can be correctly modified, low temperature, ambient pressure, and deposition of ceramic coatings can be directly achieved on complex shaped and/or temperature sensitive substrates.

## Technical Accomplishments

To date, the most commonly used surface modification technique used in biomimetic mineralization has been the self-assembled monolayer - a short alkyl silane coupling agent which can be covalently attached to the surfaces of metal oxides. This technique is not industrially acceptable since it requires multiple synthesis steps in high purity organic solvents and the self-assembled monolayer is mechanically fragile (readily scratches off). Further, self-assembled monolayer techniques are not readily applicable to polymeric substrates. Currently, only one surface modification technique (sulfonation of polystyrene) has been developed for plastics that successfully induces ceramic film formation. Similar surface modification schemes must be devised for other industrially useful polymers such as polycarbonate, acrylic, acetal, PVC, nylon, polyethylene, and polypropylene. The modification schemes must also be kept simple, inexpensive, and environmentally benign.

Three modification pathways were investigated to synthesize polymeric surfaces that induce thin film formation

1. direct chemical modification of substrate surfaces
2. interpenetrating polymer networks
3. low energy plasma treatments.

### *Direct Chemical Modification*

Previous work on polystyrene had shown that highly hydrophilic surfaces could be synthesized by treatment of native polystyrene with  $\text{SO}_3$  vapor. This aggressive reaction resulted in direct attachment of sulfonate groups on the aromatic rings of the polystyrene and generated surfaces that readily induced heterogeneous precipitation of  $\text{FeOOH}$ , and  $\text{SnO}_2$  films. Unfortunately, the reaction

also damaged the surface of the polystyrene, causing surface crazing or even spalling under extreme conditions. Experiments were conducted using less aggressive fuming and concentrated sulfuric acid solutions. By using vapors collected over mildly heated fuming sulfuric, we have produced sulfonated polystyrene with minimal surface damage. Since polycarbonate is highly aromatic, we also attempted direct sulfonation of this polymer. The fuming sulfuric technique, developed for polystyrene, worked ideally for polycarbonate and resulted in highly wetting (contact angle  $< 5^\circ$  with water) surfaces on polycarbonate. The sulfonated polycarbonate promoted  $\text{FeOOH}$ ,  $\text{SnO}_2$ , and  $\text{TiO}_2$  film growth from aqueous salt solutions.

Similar sulfonation reactions were attempted on acetal but without success. For this reason a more aggressive chemical approach was attempted in which the acetal surface was first etched with gaseous  $\text{HCl}$ , followed by gaseous  $\text{SO}_3$ . X-ray photoelectron spectroscopy spectra and surface contact angle measurements verified that the two-step reaction resulted in the attachment of sulfonate groups to the polymer surface. Unfortunately, the substrate surface sustained extensive damage, and this surface modification scheme has been abandoned.

### *Interpenetrating Polymer Networks*

An initial survey of the most promising, commercially available surface primers and resin coating formulations for incorporation of poly(sodium 4-styrenesulfonate) into the surface of polycarbonate has been completed. Since we had shown that the presence of surface sulfonate sites on polystyrene and polycarbonate could favorably promote film growth, we first attempted to incorporate a similar molecule (styrenesulfonate) using an interpenetrating networks strategy. Systematic combinations of 12 top coat resins and four surface primers were evaluated, and several produced highly transparent, adherent coatings containing the sulfonate polymers. Six of the most promising top coats (based on optical clarity and adhesion) were further evaluated in deposition solutions. Two of the six surfaces were effective in promoting  $\text{FeOOH}$  deposits on the substrate, but neither generated uniform surface coatings. These findings were promising, and a focused effort is currently under way to sulfonate polycarbonate using simple spray or dipping methods. The basic reaction scheme is to first chloro- or bromomethylate the aromatic rings in polycarbonate, followed by reaction with dimethyl sulfide to produce a

sulfonium salt. Finally, the sulfonium salt can be easily displaced with sodium bisulfite to form the sulfonate surface group.

#### *Low Energy Plasma*

Extensive experiments were conducted on acetal and polyethylene using air, O<sub>2</sub>, N<sub>2</sub>, and Ar plasmas. In several cases, the low energy plasma treatments resulted in substantial changes in surface properties (contact

wetting angle), but the changes were short lived. Within minutes after removal from the plasma chamber, contact wetting angles were significantly reduced (particularly for acetal), but after storing for 24 hours in dry N<sub>2</sub>, the measured contact angles were near the values measured on native substrates. Several samples (freshly reacted) were immediately placed in deposition solutions (Fe) but no film growth was observed.

# Synthesis of Model Inorganic Ion Exchange Materials

James E. Amonette (Environmental Dynamics and Simulation)

## Project Description

The objective of this project was to develop and demonstrate the capability to synthesize mineral and inorganic compounds in sufficient purity and quantity to be used as model compounds for experimental verification of theoretical predictions. The initial focus is on two classes of environmentally relevant materials:

1. The layered aluminosilicates that dominate the cationic chemistry of soils and sediments and can be designed with high specificity for Cs and Sr cations.
2. The layered double hydroxide (LDH) compounds that exhibit anionic exchange behavior (i.e., hydrotalcite-like materials) and may be suitable for removal of phosphate, sulfate, and pertechnetate anions.

These two classes of materials were selected because of their abundance in soils and sediments and/or their possible use as ion-exchange materials in processing of high-level wastes and remediation of contaminated groundwater. In FY 1995, the primary experimental effort was focused on the layered double hydroxide compounds, since these may serve as templates for synthesis of the layered aluminosilicates.

## Technical Accomplishments

### Layered Double Hydroxides

Layered double hydroxides consist of positively charged, brucite-like,  $\text{Mg}(\text{OH})_2$  layers where partial isomorphous substitution of smaller M(III) cations for M(II) cations has occurred. As a result, anions and water molecules are incorporated into the space between these layers (i.e., the interlayer region) to balance the positive charge developed in the layer. Four different hydrotalcite-like layered double hydroxides having a range in Mg/Al ratios (2.25 to 1.33) and either  $\text{CO}_3^{2-}$  or terephthalate [ $p\text{-C}_6\text{H}_4(\text{COO})_2^{2-}$ ] as their interlayer anions were synthesized by coprecipitation/digestion methods under ambient conditions.

Samples A-C were synthesized according to different procedures reported in the literature. Sample D was prepared using a modification of the sample C method (lower pH of crystallization), but had the same initial Mg/Al ratio in the mother liquor as samples B and C

(i.e., 2). The initial Mg/Al ratio in sample A was 3. Samples A and B have  $\text{CO}_3^{2-}$  as the interlayer charge-balancing anions; terephthalate anions serve this function in samples C and D. To determine the phase-purity and crystallinity of the layered double hydroxides, specimens were characterized by x-ray diffraction (using zero-background slides),  $^{27}\text{Al}$  magic-angle spinning nuclear magnetic resonance (MAS-NMR), and scanning electron microscopy. Elemental analyses of the samples were obtained by energy-dispersive x-ray spectrometry (EDX) of the scanning electron microscopy samples and inductively-coupled plasma atomic emission spectroscopy (ICP-AES) of acid-digested specimens.

The powder x-ray diffraction patterns and  $^{27}\text{Al}$  MAS-NMR spectra obtained for these layered double hydroxides are shown in Figure 1. Samples A-C exhibit x-ray diffraction patterns similar to those reported in the literature. Assuming a layer thickness of 0.48 nm, the  $d$  spacings shown correspond to interlayer spacings of 0.28 to 0.29 nm for samples A and B ( $\text{CO}_3^{2-}$  interlayer anion), and 0.90 to 0.92 nm for samples C and D (terephthalate interlayer anion). Each sample exhibited at least three x-ray diffraction reflections from the  $00l$  planes indicating a well-ordered layered structure. Samples C and D also seemed to contain some amorphous material as shown by

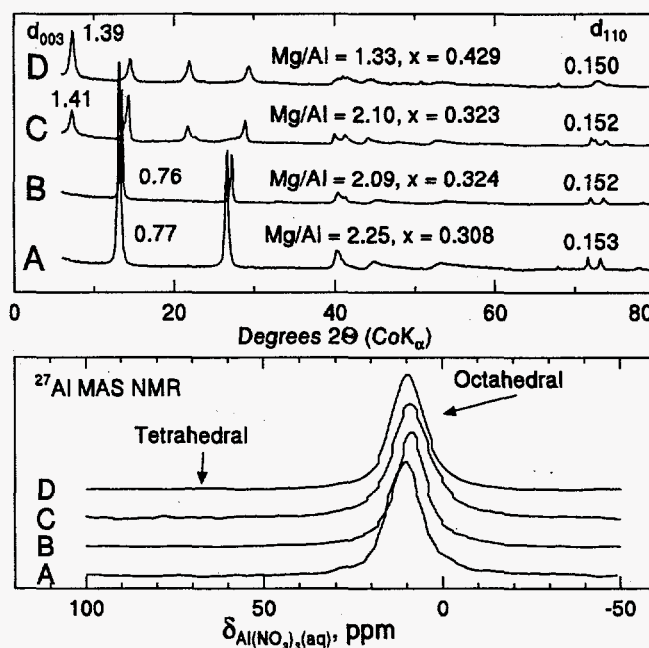


Figure 1. X-ray diffraction patterns (top) and  $^{27}\text{Al}$  MAS-NMR spectra (bottom) for four LDHs synthesized by different methods.

the presence of a small hump in the background between 20 and 40 °2 $\theta$ . Samples A and D contained a small amount of a second phase [probably Mg<sub>3</sub>(OH)<sub>4</sub>(NO<sub>3</sub>)<sub>2</sub>] as shown by the small peaks near 51 and 68 °2 $\theta$ . Broader peaks and lower overall intensities were seen for the samples synthesized with terephthalate (i.e., C and D) than those in the carbonate form (A and B). Replacement of the terephthalate ion by carbonate to see what impact the interlayer anion has on the x-ray diffraction patterns is planned for next year.

Analysis by scanning electron microscopy showed larger particles and a platy morphology for sample D suggesting that this material was more crystalline than the others. Evidently, the size of the coherently diffracting domains for sample D was very much smaller than the particle size, whereas these dimensions were much closer for the other samples. The samples were compositionally homogeneous on a 5-nm scale, based on several energy-dispersive x-ray analyses at random locations on each specimen. The results of the energy-dispersive x-ray analyses agreed well with the ICP-AES data, further indicating compositional homogeneity of the samples. The <sup>27</sup>Al MAS-NMR spectra of the samples showed that all Al in the samples was octahedrally coordinated, as expected for the layered double hydroxide structures (Figure 1, bottom).

Because the Mg<sup>2+</sup> and Al<sup>3+</sup> cations have different ionic radii (72 and 53.5 pm, respectively), the *a* dimension [*a* = 2*d*<sub>110</sub>] is controlled by the Mg/Al ratio or *x* value. Other work in the literature has shown that the *a*-dimension value decreases linearly from 0.314 nm for brucite [Mg(OH)<sub>2</sub>, *x* = 0] to 0.304 nm for layered double hydroxides with *x* = 0.33. Beyond *x* = 0.33 (for layered double hydroxides synthesized under hydrothermal conditions) the value of *a* remains constant at 0.304 nm. Samples A-C demonstrate this trend, with *a*-dimensions ranging from 0.306 for sample A to 0.304 for samples B and C. Sample D has an *a*-dimension of 0.301, a value clearly below the limit suggested in the literature. Although the measurement is tempered by the apparent overlap of the 110 and 113 reflections for sample D (these reflections [peaks at about 71.7 and 73.2 °2 $\theta$ ] are clearly resolved in samples A-C and indicate a relatively well-ordered crystalline structure), the *a*-dimension agrees well with the value predicted by extrapolating the relationship between *x* and *a* observed at lower values of *x*. Thus, even though the scanning electron microscopy photographs suggest that sample D is the most crystalline, the x-ray diffraction data show that a significant degree of structural disorder exists in this sample.

Apart from crystallinity, the most striking differences between samples A-C and sample D is the Mg/Al ratio. The Mg/Al ratio of 1.33 for sample D corresponds to an Al/(Al+Mg) ratio, *x*, of 0.43. This is much higher than

the *x* = 0.33 (Mg/Al = 2) ratio thought to be the upper limit for Al substitution in layered double hydroxides synthesized under ambient conditions and with CO<sub>3</sub><sup>2-</sup> in the interlayers, and represents, to our knowledge, the highest Mg/Al ratio reported for a layered double hydroxide synthesized under ambient conditions. Apparently the terephthalate anion helps stabilize the layered double hydroxide structure to allow high degrees of substitution.

Comparable levels of Al substitution can be achieved in carbonatic layered double hydroxides, however, when hydrothermal conditions are employed (e.g., *P*<sub>H<sub>2</sub>O</sub> = 100 MPa and *T* = 100°C to 350°C).

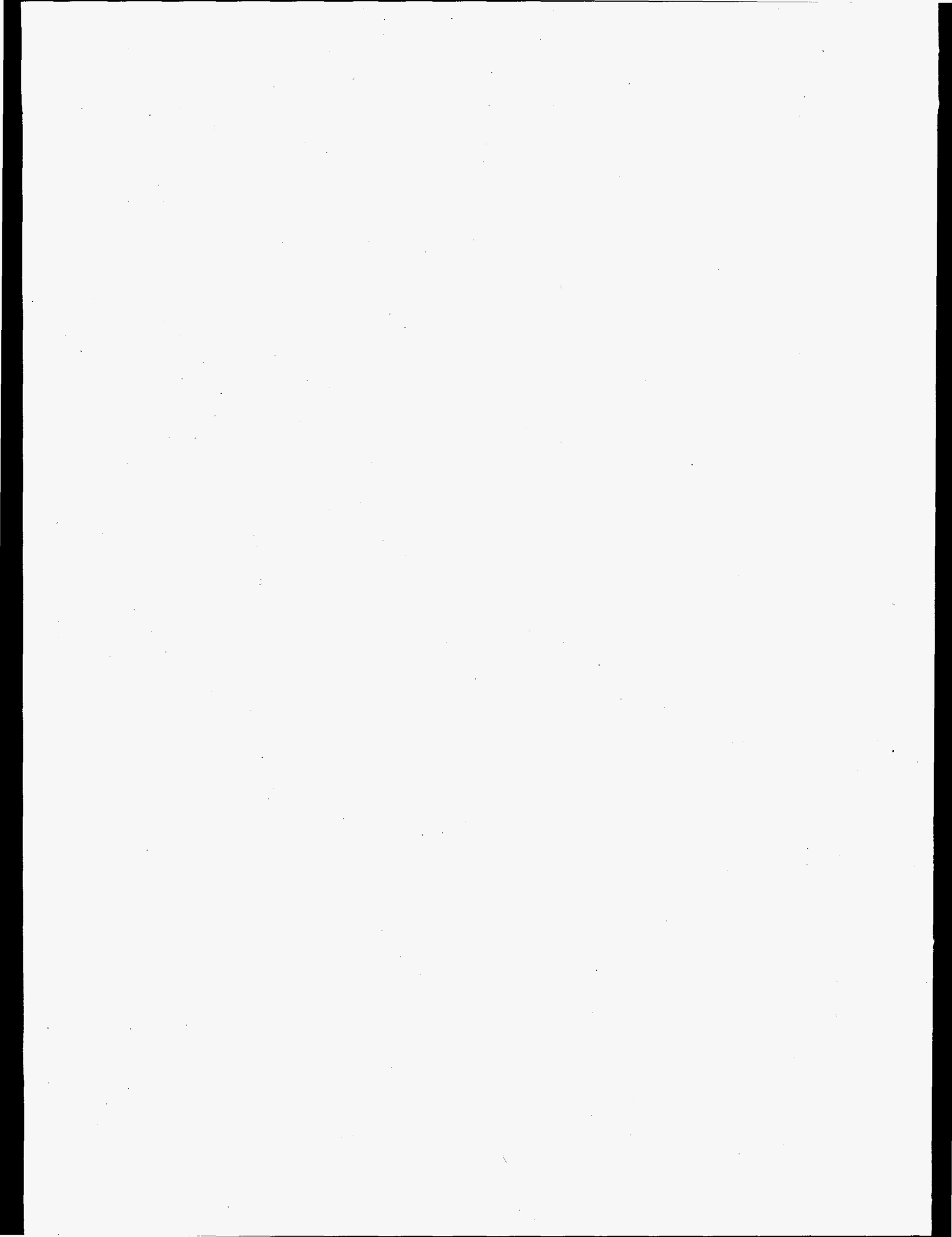
This preliminary work with the layered double hydroxides has shown that the solution pH, as well as the type of counter anion, can have a significant effect on the composition and crystallinity of the final product. Samples A and D, for example, had large differences between the initial Mg/Al ratio and that in the final product. These two samples also exhibited trace amounts of a Mg-rich second phase, and a lower Mg/Al ratio than the starting solution. These results suggest that with the binary layered hydroxides, the highest phase purity is achieved when the solubilities of the two end-members are similar. At lower pHs, the solubility of the Al end-member was substantially less than that of the Mg end-member, causing the product to have a higher Al content than expected from the Mg/Al ratio of the starting solution. In the coming year, our work will focus on clarifying this principle to achieve the highest phase purity and crystallinity in the LDHs and allow us to proceed to synthesis of the more complex layered aluminosilicates.

#### *Layered Aluminosilicates*

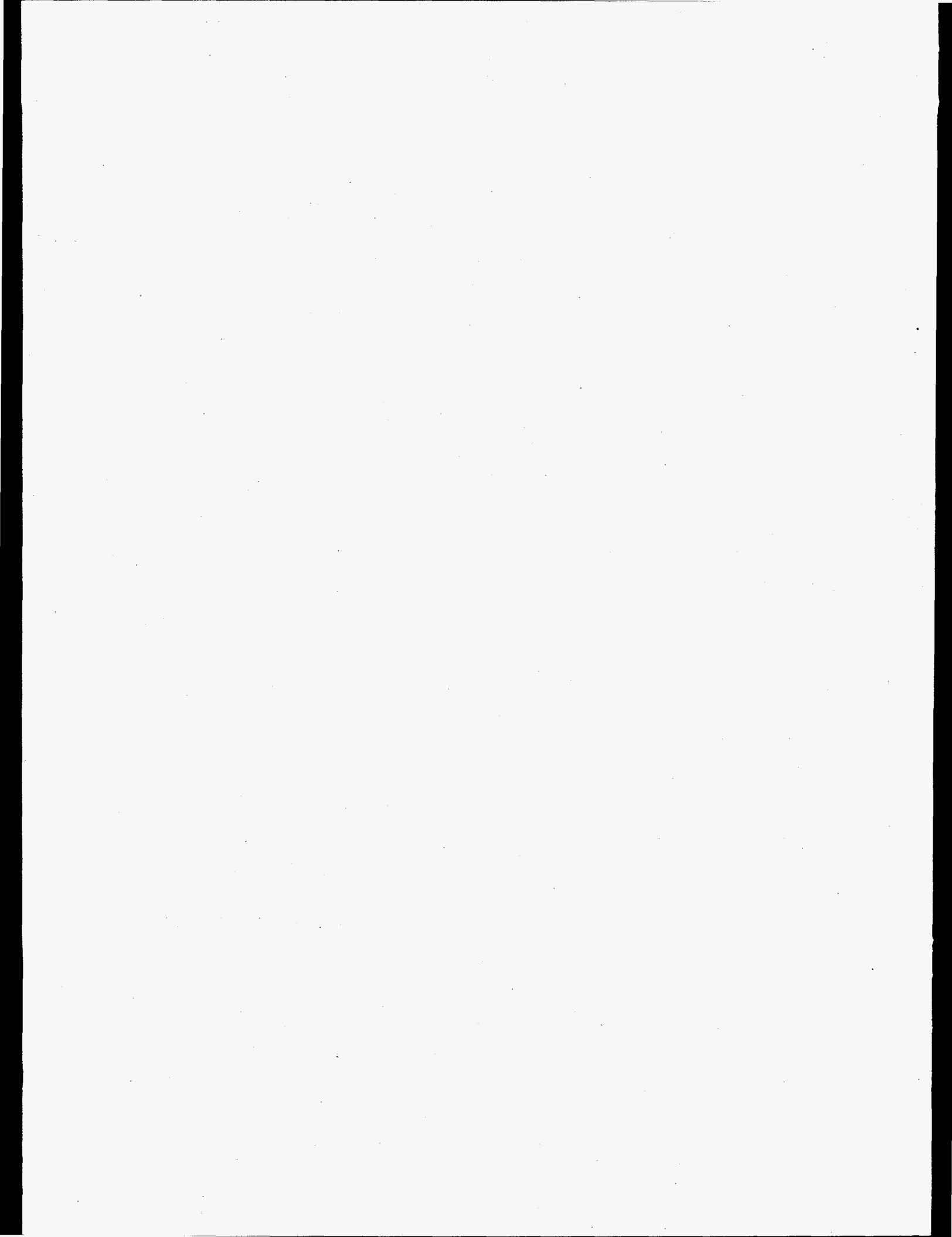
Aside from the experience gained from the layered double hydroxide synthesis work and the eventual use of layered double hydroxides as templates for layered aluminosilicate synthesis, our work toward developing a synthesis capability for the layered aluminosilicate minerals was confined to preparation of a thorough review of the synthesis procedures published for smectites, perhaps the most common of these minerals. This review, prepared in collaboration with Drs. T. Klopogge and S. Komarneni, is mostly finished, and will be submitted for publication.

#### **Publication**

J.T. Klopogge, S. Komarneni, and J.E. Amonette.  
"Synthesis of Smectite Minerals: A Critical Review."  
*Clays and Clay Minerals* (to be submitted).



## **Molecular Science**





# *Adsorption on Fe-(hydr)oxides Under Nonequilibrium Conditions*

Carl I. Steefel (Environmental Dynamics)

---

## **Project Description**

A flow-through reactor was used to determine adsorption on Fe-(hydr)oxide surfaces under nonequilibrium conditions, at a variety of saturation states. These results were compared to adsorption data collected under complete equilibrium conditions. It has long been assumed that adsorption data collected under equilibrium conditions can adequately describe the nonequilibrium adsorption behavior of contaminant plumes in porous media. These experiments provided the data needed to determine the validity of this important assumption. In addition, the macroscopic adsorption experiments yielded unique insights into the nature of the mineral-water interface as a function of the bulk equilibrium state of the solution. Macroscopic experiments of this kind have not previously been carried out and would provide data which can be compared with detailed microscopic and spectroscopic observations of the mineral-water interface.

The experimental approach was designed to provide data on the adsorption of various subsurface contaminants under geochemical conditions when the sorbent itself is not at equilibrium. Since equilibrium adsorption data, eventually cast in the form of surface complexation constants was to be derived, the method is only applicable to adsorption reactions which are much more rapid than the dissolution reaction involving the sorbent. The focus was on the hydrous ferric oxides and goethite in particular since there is a wealth of adsorption data for the hydrous ferric oxides determined under complete equilibrium conditions.

The experimental apparatus consisted of a well-stirred flow-through reactor. These devices are ideal for measuring mineral reaction rates under steady-state conditions, since a constant flow of reactive fluid is circulated through the reaction chamber holding the sorbent. The influent was a fluid which is undersaturated with respect to the Fe-(hydr)oxide. By maintaining a sufficiently rapid flow rate, it is possible to pass the fluid through the well-stirred reactor without coming to

equilibrium. By adjusting the flow rate for a given mineral reaction rate, one can obtain a range of steady-state solution compositions all the way from equilibrium to far from equilibrium conditions. If the residence time of the fluid in the reactor is greater than the equilibration time for the adsorption reactions, one can achieve equilibrium adsorption despite the fact that the Fe-(hydr)oxide itself is undersaturated.

## **Technical Accomplishments**

Results of laboratory experiments carried out in FY 1995 indicate that flow-through reactors can be used to measure absorption accurately under nonequilibrium conditions. A series of experiments were carried out at different pH values and different concentrations of the absorbing ligands, CoEDTA and EDTA, on both the Fe-hydroxide goethite and on the Al-hydroxide goethite and on the Al-hydroxide gibbsite. The experiments were primarily carried out far from equilibrium. All experiments used dual-labeled CoEDTA ( $^{60}\text{Co}$  and  $^{14}\text{C}$ ) or labeled EDTA which was pumped through stainless steel reactors containing the hydroxide phase.

A series of modeled and measured flow-through experiments were carried out with goethite. The model values were calculated using surface complexation equilibrium constants obtained by using FITEQL to analyze a typical pH edge determined in a batch (i.e., non flow-through) system. The results indicate a fairly good agreement between the computed and the measured values. Discrepancies do exist, however, between the flow-through reactor determined values and the values obtained in the batch. Further work is required to determine if these minor discrepancies are analytical artifacts or whether they in fact represent differences in the character of the mineral surface as a function of saturation state. To do this, it will be necessary to carry out a systematic series of experiments at a variety of saturation states.

# *Bonding and Structure of Organic Ligands at Oxide/Water Interfaces*

Calvin C. Ainsworth (Earth and Environmental Sciences)  
Donald M Friedrich (Chemical Structure and Dynamics)

---

## **Project Description**

The objective of this research was to examine the sorption chemistry of organic ligands at the solid-water interface by application of state-of-the-art optical spectroscopic methods. In support of this objective, research was performed to develop state-of-the-art sensitive spectroscopic methods using laser induced fluorescence and high-sensitivity infrared spectrometry (FTIR) in novel ways that will allow spectroscopic interrogation of organic ligands at the solid-water interface at low sorbate surface coverage ( $\leq 1$  percent), and to identify and characterize the nature (bonding, structure, and dynamics) of interfacial organic species.

## **Technical Accomplishments**

Interactions between organic ligands and minerals at the solid-water interface are integral to many processes occurring in soils and subsurface materials. These processes include contaminant transport, soil formation, and diagenesis. Often, these interactions are characterized as surface complexation reactions and are assigned a structure based on inadequate data. Under these conditions, modeling efforts are little more than exercises in curve fitting. In order to better understand and simulate important aqueous-mineral interfacial phenomena, it is crucial to obtain spectroscopic data concerning speciation, structures, and dynamics of organic ligands at the aqueous-mineral interface under controlled conditions that are still relevant to the natural environment.

The current investigations are performed using salicylic and phthalic acids (mono- and dicarboxylic acids, respectively) as probes and  $\text{Al}_2\text{O}_3$  as the mineral interface. The two acids were chosen because they are both fluorophores and are reported in the literature as model compounds for the study of organic ligand-surface speciation (bonding, structure) as a function of important geochemical variables (pH, ionic strength, surface loading).  $\text{Al}_2\text{O}_3$  was chosen because of its spectroscopically benign nature (infrared and ultraviolet transmittance, weak Raman interference). Most experiments are performed in constant temperature, dilute suspensions (1 g/L) of  $\text{Al}_2\text{O}_3$ , and geochemically relevant low concentrations of organic ligand ( $10^{-7}$  M).

In FY 1994 fluorescence spectra of sodium salicylate was detected at levels of less than one salicylate molecule per alumina particle ( $10^{-8}$  M) in 1 g/L  $\text{Al}_2\text{O}_3$  suspensions using polarized ultraviolet laser excitation. Two types of surface complexes were identified, an ester-like ligand-exchange complex and an ion-associated surface complex. Fluorescence polarization anisotropy indicated orientational diffusion of both types of surface complex was hindered.

In FY 1995 preparation methods were developed for producing reproducible, stable suspensions of narrow size distribution consisting of small particles (mean diameter  $\approx 70$  nm). Solution-phase complexes of salicylate- $\text{Al}^{3+}$  were prepared and their fluorescence emission, fluorescence excitation, and absorption spectra were measured over a wide range of ionic strength and pH. Emission lifetimes and orientational diffusion of free and sorbed salicylate were measured.

Two distinct salicylate- $\text{Al}^{3+}$  species are seen in the excitation and absorption spectra of aqueous suspensions, aqueous solution at room-temperature and cryogenic ethanol solution are similar. From polarization anisotropy measurements of free salicylate, salicylate- $\text{Al}^{3+}$  complexes, and sorbed salicylate, the emission and excitation transition moments in each species are nearly parallel. The large Stokes gap between emission and excitation bands and the vibrational structure seen in emission and excitation at cryogenic temperatures are consistent with a model of rapid conformational relaxation in the lowest excited singlet state prior to emission. One of the well-known excited state conformers is the proton-transfer tautomer of salicylate. This tautomer is clearly seen as a minor component in the emission spectrum of salicylate- $\text{Al}^{3+}$  in ethanol solution. Proton transfer can only occur if the phenolic hydroxyl is protonated and H-bonded to one of the salicylate carboxyl oxygens. The characteristic excitation of this tautomer-forming species may therefore be identified with the monodentate form of the aluminum complex. This is the first direct spectroscopic evidence that salicylate- $\text{Al}^{3+}$  exists in equilibrium between monodentate and bidentate complexes and demonstrates the utility of polarized emission spectroscopy for speciation.

Time-resolved measurements of the rotational diffusion of salicylate in solution and suspensions have been initiated using a new ultrafast streak camera. Time-resolved measurements of emission anisotropies of free and sorbed salicylate prove that sorbed salicylate ions do not diffuse orientationally on the time scale of the fluorescence (Figure 1). In these suspensions containing  $10^{-6}$  M total salicylate, no fast component of the anisotropy decay is observed, indicating that the majority of salicylate is bound to the alumina particles. This is consistent with previous radiolabel measurements that placed an upper limit on the concentration of free, solution-phase species of less than 10 percent of the  $10^{-7}$  M total salicylate in suspension. This upper limit increases with increasing bulk salicylate concentration in the suspension (e.g., <20 percent at  $10^{-5}$  M). Direct optical absorbance measurements indicate less than 2 percent of  $10^{-6}$  M total salicylate is free. Improvements in signal-to-noise ratio of time-resolved and steady-state anisotropy measurements will enable direct resolution of free salicylate species expected at concentrations higher than  $10^{-7}$  M total salicylate.

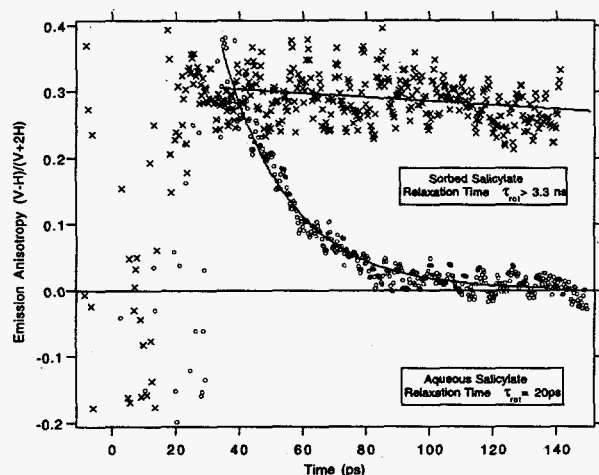


Figure 1. Decay of fluorescence anisotropy vs time for aqueous salicylate (o) and salicylate-alumina aqueous suspension (x) consisting of  $10^{-6}$  M sodium salicylate and 1 g/L alumina colloid (70 nm average diameter). Free salicylate rotational diffusion time (20 ps) is consistent with a solute diameter of 0.6 nm in the Stokes-Einstein model of rotational diffusion.

The effect of suspension turbidity on depolarization of the fluorescence anisotropy was experimentally determined (Figure 2). A simple phenomenological model of extinction by scattering was used to fit the data. It was shown that small sample loadings of narrow size distribution (<1 g/L) result in a small degree of depolarization caused by light scattering. This gives confidence that the measured anisotropies can be extrapolated to the zero-scattering limit and can be

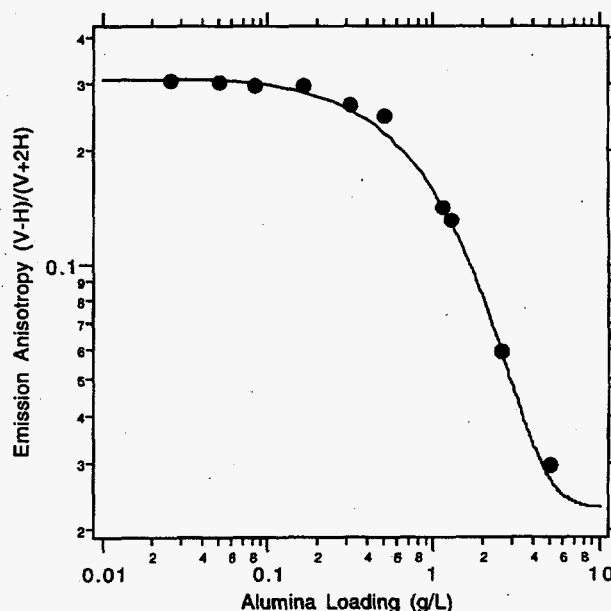


Figure 2. Effect of alumina suspension loading on observed emission polarization anisotropy. Observed anisotropy values (dots) are fit to a simple phenomenological scattering model (solid line) in which turbidity  $\tau$  randomizes a fraction of the intrinsically polarized fluorescence components  $V_0$  (vertical) and  $H_0$  (horizontal)

$$V = V_0 \exp(-\tau) + \kappa(V_0 + H_0)[1 - \exp(-\tau)]$$

$$H = H_0 \exp(-\tau) + \kappa(V_0 + H_0)[1 - \exp(-\tau)]$$

In this fit to the data, the randomization coefficient  $\kappa$  is 0.4, indicating that approximately 20% of the scattered light is not redirected into the detected unpolarized component (second term in each equation).

interpreted in terms of sorbate/solute distribution and rotational mobility of sorbed species. From the low-scattering, upper-limit anisotropy of 0.3, it is found that 95 percent of the excitation transition dipole moment is parallel to the molecular emission transition moment in the salicylate-alumina complex.

## Publication

C.C. Ainsworth, D.M. Friedrich, and P.L. Gassman. 1994. "Fluorescence Spectroscopy of Salicylate- $\text{Al}_2\text{O}_3$  Surface Complexes." *Agronomy Abstracts*.

## Presentations

C.C. Ainsworth, D.M. Friedrich, and P.L. Gassman. 1994. "Fluorescence Spectroscopy of Salicylate- $\text{Al}_2\text{O}_3$  Surface Complexes." Presented at the 1994 Soil Science Society Annual Meetings, November 13-18, Seattle, Washington.

C.C. Ainsworth, D.M. Friedrich, P.L. Gassman. 1995. "Fluorescence Spectroscopy of Salicylate-Aluminum Oxide Surface Complexes." Presented at the 1995 Western Spectroscopy Association Meeting, February 1-3, Pacific Grove, California.

C.C. Ainsworth, D.M. Friedrich, P.L. Gassman, Z. Wang. 1995. "Fluorescence Spectroscopy of Salicylate- $\delta$ -Al<sub>2</sub>O<sub>3</sub> Surface Complexes." Presented at the 1995 Clay and Clay Minerals Annual Meeting, June 3-8, Baltimore, Maryland.

C.C. Ainsworth, D.M. Friedrich, P.L. Gassman, Z. Wang. 1995. "Speciation of Al(III)-Salicylate Surface Complexes in Aqueous Colloidal Alumina Suspensions." Presented at the 1995 Pacific Northwest AVS Symposium, Geochemical Surface Science Technical Session, September 18-21, Troutdale, Oregon.

# Catalytic Chemistry of Metal Oxides

Charles H.F. Peden (Materials and Interfaces)

## Project Description

The objective of this project is to study the chemistry and catalytic properties of metal-oxide materials. While the surface chemical properties of metal-oxides impact an enormous number of environmental and energy problems and potential technological solutions, a general absence of detailed studies on well-characterized systems has prevented progress in developing a fundamental understanding in this area.

Transition metal oxides have found numerous applications as heterogeneous catalysts for other industrially important processes, such as the selective oxidation, isomerization, and metathesis of hydrocarbons, and the selective catalytic reduction (SCR) of  $\text{NO}_x$ . In spite of their importance, oxide catalytic materials and processes have received much less attention from a fundamental science point of view than have catalysis by metals. For this reason, we have initiated this project, which includes fundamental studies of the catalytic properties of oxide materials.

## Technical Accomplishments

During FY 1995, we have completed construction of a unique high-pressure catalytic reactor/ultrahigh vacuum (UHV) surface science apparatus capable of conducting kinetic and mechanistic studies of catalytic reactions on well-defined single crystal oxide surfaces. We also performed interim experiments in collaboration with Dr. David Belton of General Motors Research Labs in order to develop an understanding of NO reduction over supported metal catalysts to contrast with the behavior of oxide catalysts, as well as to provide design improvements to the apparatus presently under construction at Pacific Northwest National Laboratory.

In these studies, we examined the effect of surface structure on the NO-CO activity and selectivity by comparing the reactivity of Rh(110) and Rh(111) single crystal catalysts. These studies are motivated by many reports demonstrating that the selectivity for the two possible nitrogen containing products from NO reduction,  $\text{N}_2\text{O}$  and  $\text{N}_2$ , are dependent on Rh loading in supported catalysts. In last year's LDRD report, we described studies of the effects of temperature, NO conversion, and NO-CO ratio on the activity and selectivity of the NO-CO reaction at high ( $1 \text{ torr} < P < 100 \text{ torr}$ ) pressures over the two Rh single crystal surfaces. We used the results to

rationalize the behavior of realistically supported Rh catalysts for this important automobile exhaust catalytic reaction. While we found relatively small differences in the NO-CO activity over Rh(110) and Rh(111), large differences were evident between these surfaces with regard to their selectivities for the two competitive nitrogen-containing products,  $\text{N}_2\text{O}$  versus  $\text{N}_2$ . The more open Rh(110) surface tends to make significantly less  $\text{N}_2\text{O}$  than Rh(111) under virtually all conditions that we probed with these experiments. These results can be understood in terms of the relative surface coverages of adsorbed NO and N-atoms on the two surfaces under steady-state reaction conditions in that higher N coverages on the (110) surface favor N-atom recombination ( $\text{N}_2$  formation) more than the  $\text{NO} + \text{N}$  reaction ( $\text{N}_2\text{O}$  formation) on Rh(110) relative to Rh(111). We tested these conclusions by making an indirect assessment of the state of the reactive surface with x-ray photoelectron spectroscopy. This technique can clearly distinguish between adsorbed nitrogen present as either molecular NO or as N-atoms formed by NO dissociation during reaction. For Rh(111), the spectrum shows only a single N(1s) feature with a binding energy near 400.3 eV due to adsorbed NO. In contrast, the NO N(1s) feature on Rh(110), while present, is significantly smaller than another N(1s) feature at lower binding energy, 397.6 eV, due to adsorbed N-atoms.

Some of the highlights for work this year include the extension of the kinetic experiments on Rh(111) to much lower NO partial pressures. In our previous work, we found the reaction to be insensitive to NO pressure above a partial pressure of 1 torr. With a new reactor design, we have performed model single crystal catalyst studies under continuous flow conditions for the first time. This has allowed us to access a much wider range of reaction conditions (temperature and reactant partial pressures). At lower NO pressures, the reaction was quite sensitive to NO concentrations. An example of this behavior is shown in Figure 1 and is described in more detail in Permana et al. (see Publications). In the figure is plotted the effect of NO pressure on the specific rates for  $\text{CO}_2$ ,  $\text{N}_2\text{O}$ , and  $\text{N}_2$  formation for the NO-CO reaction over Rh(111) using: (A) 4 torr of CO at 598K; and (B) 8 torr of CO at 623K. We are using this additional kinetic data to verify our kinetic model of the overall process. In addition, we were now able to rationalize seemingly contradictory data in the literature obtained on realistically supported Rh catalysts that were performed under slightly different reaction conditions.



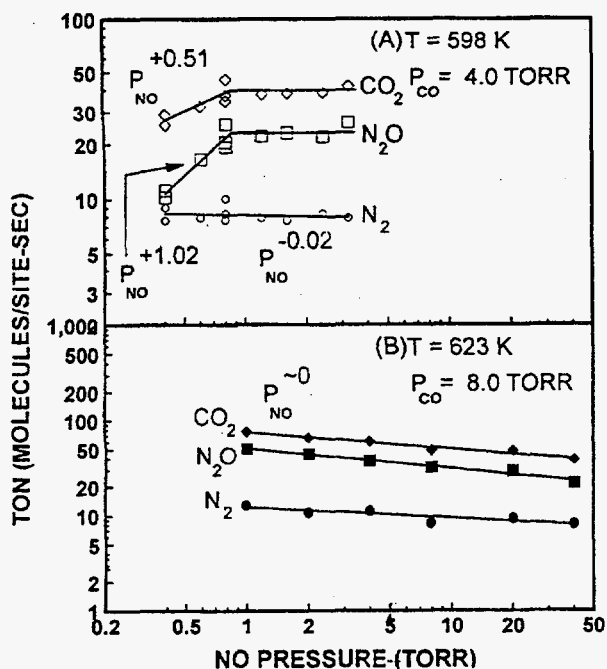


Figure 1. Effect of NO pressure on the specific rates for  $\text{CO}_2$ ,  $\text{N}_2\text{O}$ , and  $\text{N}_2$  formation for the NO-CO reaction over Rh(111).

## Publications

C.H.F. Peden, D.N. Belton, and S.J. Schmeig. 1995. "Structure-Sensitive Selectivity of the NO-CO Reaction over Rh(110) and Rh(111)." *J. Catal.* 155, 204.

H. Permana, K.Y.S. Ng, C.H.F. Peden, S.J. Schmeig, and D.N. Belton. "Effect of NO Pressure on the Reaction of NO and CO over Rh(111)." *J. Catal.* (in press).

## Presentations

D.N. Belton, S.J. Schmeig, H. Permana, K.Y.S. Ng, and C.H.F. Peden. 1995. "Mechanistic Kinetics of the  $\text{NO} + \text{CO} + \text{O}_2$  Reaction: Combined Infrared, Kinetic, and Surface Science Study." Invited talk presented at the 14th North American Meeting of the Catalysis Society, June, Snowbird, Utah.

Y.-J. Kim, S. Thevuthasan, G.S. Herman, C.H.F. Peden, S.A. Chambers, D.N. Belton, and H. Permana. 1995. "X-Ray Photoelectron Diffraction Studies of NO Adsorption on the Rh(111) Surface." Presented at the Pacific Northwest Chapter of the American Vacuum Society Meeting, September, Troutdale, Oregon.

# Characterization of Structure and Dynamics of Surface Adsorbates and Their Surfaces

Paul D. Ellis (Macromolecular Structure and Dynamics)

## Project Description

Supported silver on alumina is used extensively in the ethylene oxide (EO) process. Although this system represents a prototypical promoted catalyst, which is relatively well characterized, the promotional effects of cesium salts are not fully understood. When this work was initiated the following was understood about the ethylene oxide process:

- cesium on the silver surface is in the form of an oxide
- there is anion dependence to the selectivity of the promotion by cesium.

Currently, there is no clear explanation of these two points. Furthermore, there appears to be a mutual contradiction between the two observations, (i.e., how can cesium be an oxide and still have an anion dependence to the promotion effects?). We have examined, by low temperature (70K) solid-state nuclear magnetic resonance how the interaction of the ethylene molecule with the ethylene oxide catalyst changes with increasing promoter concentration. We have determined that the role of the promoter is more diverse than previously suspected.

## Technical Accomplishments

During FY 1995, we have attempted to correlate the spectroscopic changes with the state and function of the cesium in the ethylene oxide catalyst systems. We have investigated the carbon-carbon bond length ( $r_{CC}$ ) dependence in ethylene as a function of added promoter salt using a spin echo experiment. In the absence of cesium salts,  $r_{CC}$  was determined to be  $1.342 \pm 0.009$  Å—a result which is close to the value of  $r_{CC}$  of 1.335 to 1.340 Å for ethylene in the gas phase, reflecting the weak interaction between silver and adsorbed ethylene. On the other hand, in the presence of 26 percent  $CsNO_3$  (based on the weight of silver metal) the C-C bond distance increases to  $1.368 \pm 0.009$  Å, which indicated an increase in the binding affinity of silver for ethylene. Figure 1 summarizes the spin echo measurements of the carbon-carbon bond distance. Ab initio Gaussian-92 calculations suggest that in the gas phase a cesium cation would have negligible effects on the length of the C-C bond in ethylene. Hence, it appears that the change in bond distance is due to a surface mediated

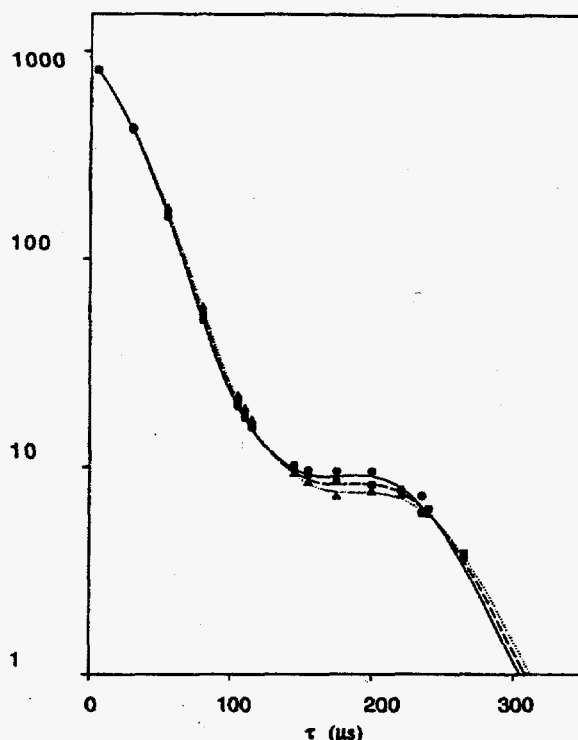


Figure 1. Spin echo and best fit from (■) 0%, (●) 14%, and (▲) 26% cesium promoted silver catalysts.

interaction caused from the direct contact between the cesium center and the silver surface. Furthermore, a SEDOR (spin echo double resonance) experiment was performed to determine the distance between ethylene and cesium centers. The SEDOR experiment provides a means to determine distances between spins which are coupled "through space" by dipolar processes. At present, we have demonstrated that two ethylene molecules are associated with a single cesium center. The best fit to the data indicated that two ethylene molecules flanked the cesium in a side-by-side configuration with the closest ethylene proton-cesium distance at 4.40 Å. From this result, and the fact that the cesium salt must make direct contact with the silver surface to increase the C-C bond length in our model, we have determined that the interaction of ethylene and silver is not mediated through an intervening oxide anion. Given this observation, it is difficult to describe the interaction of cesium with the silver surface by anything other than a direct interaction between cesium salt with the silver, as opposed, to cesium interacting with the silver as an oxide.

These data facilitate the following hypothesis: The cesium acts to promote the ethylene oxide process by acting as a polarizable ion pair on the surface and not as an oxide. Further, the polarizability of the cation anion pair can be monitored via the modulation of the C-C bond length of absorbed ethylene. These now provide a rationale for the anion dependence of the promotion of cesium salts in the ethylene oxide process.

The silver alumina catalysts were studied by infrared spectroscopy for use as a possible dechlorination catalyst in the presence of methane. Although methane was observed in product mixture indicating the reduction of carbon tetrachloride, conditions where the reaction could be sustained were never found.

In all the experiments, CO<sub>2</sub> was observed, and above 200°C HCl was observed. This led us to investigate the reaction of CCl<sub>4</sub> with the γ-alumina support. By adding water to the CCl<sub>4</sub> and using N<sub>2</sub> as the carrier we were able to sustain the following reaction at a temperature of 300°C



Figure 2 shows the results of a typical experiment under the following conditions: temperature 300°C, CCl<sub>4</sub>, H<sub>2</sub>O, N<sub>2</sub> carrier gas.

The reaction produced a constant turnover of HCl and CO<sub>2</sub> for over 6 hours. The dip in all three profiles indicates where the CCl<sub>4</sub> was switched off and on to show the response of CO<sub>2</sub> and HCl.

## Publications

J.M. Koons, E. Hughes, H.M. Cho, and P.D. Ellis. 1995. *J. Magn. Reson.*, Series A 114, 12.

J.M. Koons. 1995. "Extracting Parameters from Solid-State NMR Lineshapes." PH.D. Thesis, University of South Carolina.

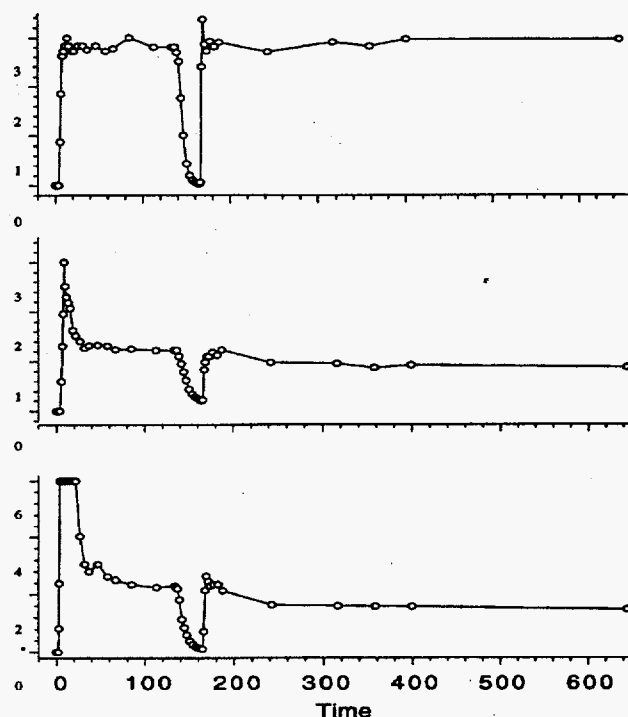


Figure 2. Reaction of CCl<sub>4</sub>/H<sub>2</sub>O over γ-Alumina at 300°C

E. Hughes. 1995. "The Investigation of Silver Alumina Catalysts by Infrared and Solid-State NMR Spectroscopy." PH.D. Thesis, University of South Carolina.

## Presentations

E. Hughes, J.M. Koons and P.D. Ellis. 1995. "Investigation of Cesium Promoted Silver Catalysts by Low Temperature Solid State NMR." March, ENC, Boston, Massachusetts.

P.D. Ellis, E. Hughes, and J.M. Koons. 1995. "Investigation of Cesium Promoted Silver Catalysts by Low Temperature Solid State NMR." A.C.S. meeting Hawaii.



# Colloid-Colloid Interactions: Forces and Dynamics

Donald R. Baer (Materials and Interfaces)

## Project Description

The objective of this project was to measure forces between colloids in solution under conditions similar to those expected during the processing of waste tanks. Interparticle forces have a direct impact on the stability of colloids in solution and hence determine whether colloids flocculate or remain suspended and the degree of compaction of solids. We are measuring these forces using two different techniques: 1) a force microscope for direct force measurements on single colloids; and 2) an optical waveguide to determine the dynamic interaction fluorescently tagged colloids have with the surface of the waveguide.

## Technical Accomplishments

### Force Measurement II

Rapid progress was made during FY 1995 as initial experiments on silica as a model system showed viability of the experiments. These studies were followed by measurements and analysis of more relevant alumina surfaces. The most recent efforts have been on quantifying information from the data and learning the limitations of the method.

One of the goals set for this project was to use a force microscope to measure forces between model surfaces in solution in order to establish this technique as being reliable. We used silica as the model surface since it has been the surface whose forces have been measured most thoroughly by the surface force apparatus. Silica also is readily available in suitable forms for investigation here. We have successfully immobilized single silica colloids, 2.6  $\mu\text{m}$  in diameter, to one end of the force sensor (cantilever) of the instrument. Force measurements between the silica colloid and a polished silica wafer were made in sodium chloride solutions whose ionic strength varied from  $10^{-4}\text{M}$  to  $1\text{M}$  and whose pH varied from 5.0 to 9.0. Figure 1 shows how the force (normalized to the radius of the colloid) as a function of separation distance varies with ionic strength. Under these conditions, one expects to observe repulsive electrostatic and attractive van der Waals DLVO forces. In actuality, only repulsive forces are observed indicating the presence of another force that counteracts the attractive van der Waals force, which dominates the electrostatic forces at short separation distances. In water, the surface of silica

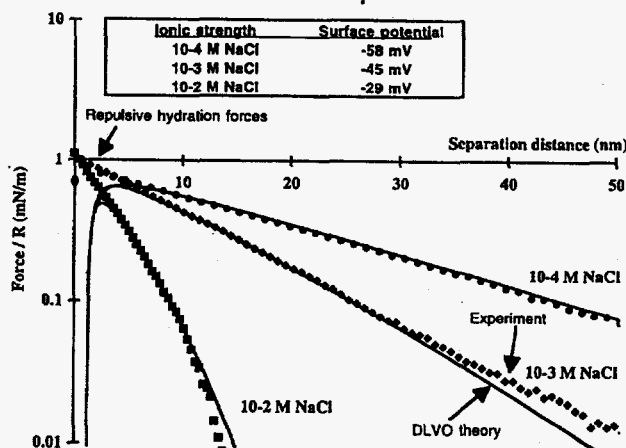


Figure 1. How the force (normalized to the radius of the colloid) as a function of separation distance varies with ionic strength.

becomes hydrated and forms a gel-like layer. It is the compression of these gel-like layers that contributes to this repulsive hydration force. The presence of only repulsive forces indicate that a suspension of silica particles under all conditions observed is stable. One can also fit the data to a numerical solution to the Poisson-Boltzmann equation to determine the surface charge of silica and the Debye length (a measure of the decay rate of the electrostatic repulsion) of the solution.

We have also extended our studies to aluminum oxide surfaces, since a significant fraction of the solid material in waste tanks is comprised of boehmite or gibbsite. Aluminum oxide surfaces do not hydrate like silica and would not be expected to exhibit hydration forces. Force measurements indicate that under mild basic conditions, aluminum oxide surfaces no longer have a repulsive interaction due to reduced surface charge and a suspension under these conditions would be unstable in the absence of any surface adsorbates. The isoelectric point of the aluminum oxide surface occurs at a pH near 9.0. As the pH of the solution decreases, the repulsive electrostatic begins to dominate at large separation distances. The typical force curve exhibits a repulsive maximum at short separation distances. A numerical integration of the force-distance curve yields a plot of the potential energy between alumina colloids as a function of separation distance. Figure 2 shows an example of the result of numerical integration of the interparticle force. The potential shows a repulsive maximum which must be overcome if the colloids are to flocculate in  $10^{-4}\text{M}$  NaCl

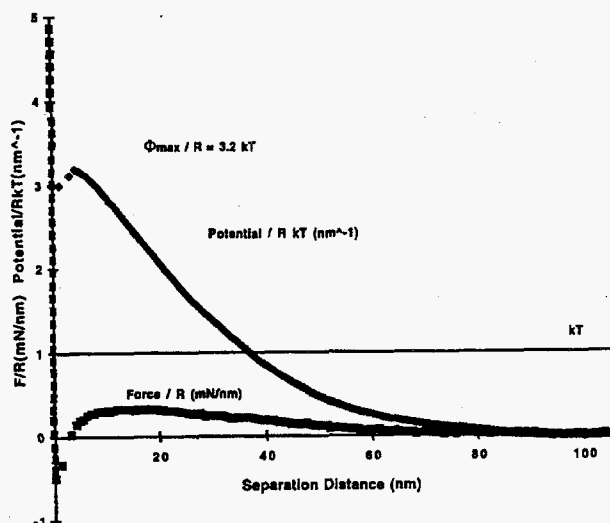


Figure 2. An example of the result of numerical integration of the interparticle force.

at pH 5.9. In terms of thermal energy units (kT), this maximum,  $\Phi_{\max}$ , is 3.2 times the radius (in nm) of the colloid.

Colloid stability can be determined for systems having a potential energy maximum. The stability,  $W$ , is a ratio of slow flocculation rate to rapid flocculation rate (which is the rate of flocculation if no repulsive energy potential is present). When  $W=1$ , the suspension is unstable, but becomes more stable as  $W$  increases. Specifically,  $W \sim \exp(\Phi_{\max}/kT)$ . To be a stable suspension (> 120 day flocculation rate),  $W > 10^6$  or  $\Phi_{\max} > 14kT$ . The primary boehmite particle in many of the tanks has a size of 3 to 10 nm. Using a typical particle size of 5 nm, the flocculation rate would be 8 hours in  $10^{-4}M$  NaCl at pH 5.9.

Currently, under some solution conditions, the full range of forces cannot be measured. We are currently considering methods to expand the force range. The studies will also be extended to situations where impurities or surface adsorbates are present.

### *Dynamical Interactions II*

The dynamical studies have demonstrated the ability of the optical measurement to produce the data. However, the results show a combination of fundamental and experimental limitations to the information that can be obtained from the data.

For the dynamic aspects, we have used an optical technique to study the interaction of the colloids with the surface of an optical fiber. Light which excites the fluorescently tagged colloids is coupled into the optical fiber which is placed in a solution containing the colloids. This light penetrates into the solution evanescently to a depth of approximately 100 nm. Any colloids which enter this evanescent field, will fluoresce and some of the light will couple back into the fiber. The frequency dependence of the fluorescent light is a function of colloid interaction with the fiber. If there is a strong interaction, the colloid will reside in the evanescent field longer and the fluorescent signal will have a different time signature than a colloid which moves in and out of the field rapidly due to negligible interaction with the fiber surface.

Our goal for the year was to be able to detect fluorescent light emitted from colloids in the vicinity of an optical fiber and begin analyzing its spectrum as a function of solution conditions. We have been successful at detecting this fluorescence. The time signature, however, does not vary appreciably with changing solution conditions. We suspect that some of the excitation light extends beyond the evanescent field due to imperfections of the fiber surface and perhaps somewhat due to light scattered omnidirectionally by the colloids within the evanescent field. As a result, fluorescence from distant colloids is being scattered back into the fiber to an extent that it dominates any local signal. As such, local interactions between colloid and fiber surface will play a diminished role in the time signature of the fluorescence signal. We expected to remedy this situation by employing a prism rather than an optical fiber in work commencing this year.

### **Presentation**

A.S. Lea and D.R. Baer. 1995. "Forces Measured Between Silica Surfaces in Solution Using a Scanning Force Microscope." American Geophysical Union: Spring Meeting, May 30 - June 2, Baltimore, Maryland.

# *Effects of Surface Complexation and Structure on the Dissolution Precipitation Kinetics of Carbonate Minerals*

Carl I. Steefel (Environmental Dynamics)

---

## **Project Description**

This project describes an interdisciplinary experimental and spectroscopic study of the effects of surface complexation and surface structure on the macroscopic rates of dissolution and precipitation of carbonate minerals under geochemical conditions. The dissolution and precipitation kinetics will be studied both far from and close to equilibrium using mineral suspensions in well-stirred flow-through reactors. The application of surface complexation models will be extended from surface-controlled dissolution taking place far from equilibrium to both near-equilibrium dissolution and to precipitation. The macroscopically measured dissolution and precipitation rates will be systematically related to structural and chemical information about the interfacial species. The proposed research will significantly increase our ability to determine surface complexation effects on mineral reactivity close to equilibrium. In addition, the research was to advance our ability to integrate "chemical effect" on mineral reactivity (e.g., solution chemistry, surface complexation) with "physical effects" associated with the microtopography of the carbonate mineral surface. It is essential to have a sound understanding of carbonate mineral reactivity since carbonate minerals are important phases in the subsurface and can have a significant effect on contaminant mobilities.

The project included the following specific tasks:

### **1. Near-Equilibrium Dissolution Experiments**

The key aspect of this part of the project was to extend and test the application of surface complexation theory to surface-controlled dissolution reactions occurring close to equilibrium. A change in the mineral surface as a function of saturation (thus producing a change in the relative abundances of the various kinds of sites on the surface) likely modifies the relative contributions of different surface complexes to the overall dissolution rate. Experimentally, this effect was investigated by systematically carrying out dissolution experiments through the entire range of saturation state (far from equilibrium up to equilibrium). The experiments to determine the macroscopic rates of reaction were carried out in a well-stirred flow-through system using mineral suspensions.

Mineral-solution interfaces were imaged with scanning force microscopy using single crystals in a flow cell. Spectroscopy was used to determine if changes in local bonding environments could be detected at mineral surfaces that have reacted in different regimes of undersaturation.

### **2. Precipitation Experiments**

Precipitation experiments were carried out in the same apparatus as in the dissolution experiments using well-characterized mineral seed particles. Surface complexation were systematically varied by running experiments at different values of  $P_{CO_2}$  and over a range of pH.

### **3. Microtopography and Surface Complexation Using Microscopic and Spectroscopic Methods**

By imaging the carbonate mineral surface under the geochemical conditions which characterize the dissolution and precipitation experiments, the role of surface structure on the macroscopic dissolution and precipitation rates of carbonate should be confirmed.

## **Technical Accomplishments**

A series of flow-through experiments using suspensions of coarse calcite were carried out at Pacific Northwest National Laboratory and in the laboratory of Dr. P. Van Cappellen at Georgia Institute of Technology. Because of the rapid rate of dissolution of calcite in even mildly acidic solutions (an influent pH of 5 was used), it was necessary to use suspensions consisting of about 400  $\mu\text{m}$  calcite. In order to produce steady-state results, it was also found to be necessary to carefully acid wash and age the calcite to eliminate fines which otherwise dominate the dissolution kinetics. Flow-through experiments were carried out over a wide range of flow rates in order to vary the residence time of the fluid in the reactor and thus to examine rates both some distance from equilibrium and close to equilibrium. The results indicate that it is possible to obtain reproducible results with relatively coarsely crystalline calcite suspensions even very close to equilibrium. We were able to duplicate the pH dependence of calcite dissolution as determined in the

study by Chou and Wollast (1990). The pH dependence observed in this study and in the study by Chou and Wollast contrasts with the lack of a pH dependence found by Plummer et al. (1978). This can probably be attributed to the fact that a flow-through reactor was used in which  $P_{CO_2}$  was not held constant as in the batch experiments of

Plummer et al. (1978) but rather evolved as the reaction progressed. It is likely, therefore, that the lower rate of dissolution at higher pH observed in this study is due to the lower  $P_{CO_2}$  which affected the formation of  $CO_2$ -bearing surface complexes on the calcite surface and not directly to a pH effect (Van Cappellen et al. 1993).

# *Elastic Properties, Solution Chemistry and Electronic Structures of Oxides, Silicates and Environmental Catalysis*

Anthony C. Hess (Theory, Modeling, and Simulation)

---

## **Project Description**

In general, geochemically important materials are typified by a level of structurally and stoichiometrically complexity that is truly impressive. It is only in very recent years that computational algorithms and computer hardware have existed which place such systems within reach. The application of ab initio quantum mechanical methods to this class of materials provides a new approach to understanding and predicting the interfacial chemistry of oxides, silicates, and carbonates.

## **Technical Accomplishments**

During past years, we have demonstrated the use of two ab initio techniques, periodic Hartree-Fock and full potential linearized augmented plane wave (FLAPW), on a range of materials including several  $\text{SiO}_2$  phases,  $\text{CaO}$ ,  $\text{CaSiO}_3$  and  $\text{MgSiO}_3$  perovskites, iron oxide ( $\text{FeO}$ ), and iron sulphides ( $\text{FeS}$ ). Some of the highlights of this work included the determination of the electronic structure, equations of state, and pressure-induced phase transitions of stishovite. We have also predicted that  $\text{CaSiO}_3$  perovskite is stable relative to the free oxides to pressures found at the core-mantle boundary. In  $\text{FeO}$ , a determination of the static free energies and equations of state of  $\text{FeO}$  in the B1 (ideal NaCl), rhombohedrally distorted antiferromagnetic B1, ferromagnetic B2 (CsCl), and ferromagnetic B8 (NiAs) structures were also investigated.

As a result of such studies it was determined that although periodic Hartree-Fock and FLAPW are accurate and reliable methods, the overall cost of the calculations prohibited their application to lower symmetry or more complex materials and interfaces. Periodic Hartree-Fock theory, for example, has been used extensively for the study of solid-gas interfaces but its ability to treat more general cases (low dispersion overlayers and liquids) is somewhat limited due to the extreme computational cost. Current generations of FLAPW theory are simply too costly in this context.

## *High Pressure Phase Transitions of FeO II*

Shock-wave compression experiments on  $\text{FeO}$  show a phase transition near 70 GPa and  $T > 1200\text{K}$ . The nature of this phase transition has been unknown but has inspired

much speculation in the geophysical literature. We determined the static free energies and equations of state of  $\text{FeO}$  in the B1 (ideal NaCl), rhombohedrally distorted antiferromagnetic B1, ferromagnetic B2 (CsCl), and ferromagnetic B8 (NiAs) structures. We used the FLAPW method beyond the local density approximation. The generalized gradient approximation for the exchange-correlation functional appears to give an accurate description of  $\text{FeO}$  as the equation of state and ground state structure are predicted correctly. The static ground state of  $\text{FeO}$  is predicted to be antiferromagnetic with a rhombohedrally distorted NaCl structure. The rhombohedral distortion increases with pressure. The B8 (NiAs structure) phase is stable relative to the B2 (CsCl) structure for all pressures below 200 GPa\*. The high-pressure, high temperature phase of  $\text{FeO}$ , therefore, is argued to be  $\text{FeO}$  with the B8 (NiAs) structure. The structure differs from the ideal NiAs in that the  $c/a$  ratio is 1.9 (0 GPa) and increases to 2.2 (150 GPa). The static transition pressure from the rhombohedral  $\text{FeO}$  phase to the B8 (NiAs) structure is predicted to be near 125 GPa. If this transition is that occurring near 70 GPa and  $T > 1200\text{K}$  under shock compression then the Clapeyron slope must be at least  $-0.046 \text{ GPa/K}$ . From the 70 GPa volume change of  $-0.1 \text{ Å}^3/\text{mol FeO}$ , we predict that the entropy change is  $2.7 \text{ J/mol-K}$ .

## *High Pressure Phase Transitions of FeS II*

$\text{FeS}$  undergoes a high pressure phase transition to a paramagnetic phase near 16 GPa. The nature of the electronic structure change and the high pressure structure of  $\text{FeS}$  have been unknown. FLAPW calculations on  $\text{FeS}$  give the correct ground state structure (NiAs). Of great theoretical interest is that the magnetic moment of  $\text{FeS}$  disappears under small compression. In the traditional ligand field theory view, this would be interpreted as a spin-pairing transition. This would cause  $\text{FeS}$  to become a diamagnetic insulator. However, the high pressure electronic structure corresponds to a metallic Pauli paramagnet. The high pressure structure of  $\text{FeS}$  is a distorted B2 (CsCl structure).

The final year of this project has focused on testing local basis density functional theories on aluminosilicates and in obtaining experimental data concerning the behavior of mixed metal oxide thin films in Dr. Wayne Goodman's laboratory at Texas A&M University. Several studies designed to establish the accuracy with which density



functional theories methods can describe the structure and energetics of zeolites (aluminosilicates) have been carried out. As noted above, our work has indicated that the use of periodic Hartree-Fock methods for the study of large, low-symmetry systems is prohibitively expensive. Periodic density functional theories methods, which are currently under development by our group, have a potentially significant computational advantage over periodic Hartree-Fock techniques. Thus, the verification of the accuracy of the results of these methods for environmental materials is needed.

In this regard, we have studied the structure and energetics of a series of clusters that represent key features of the aluminosilicate ZSM-5. The calculations were done using the LDA and the Vosko-Wilk-Nosair exchange-correlation functional. Considering that the results of cluster calculations have a well-known dependence on the size of the cluster, we tested clusters of four different sizes. Although the results from the two smallest size clusters were somewhat erratic, the optimized structures of the two largest clusters agreed very well with the reported crystal structure. We also tested the changes in properties associated with the incorporation of Al, Ga, B, and Fe into the lattice. The trend in the theoretically predicted deprotonation energies agreed well with the acidity trend indicated by the experimentally measured infrared stretch frequencies of O-H bonds in the substituted silicates. In addition, the absolute deprotonation energies predicted by density functional theories were within the range of experimentally determined values. Overall, the results suggest that density functional theories methods can give

structures and energetics that are in good agreement with experimental data, with substantially less cost than traditional ab initio techniques. Other work in aluminosilicates studied the adsorption of small basic molecules on acidic sites and began the exploration of reaction mechanisms on the same materials.

## Publications

M.S. Stave and J.B. Nicholas. "Density Functional Studies of Zeolites II. Structure and Acidity of [T]-ZSM-5 Models, T = B, Al, Ga, and Fe." *J. Phys. Chem.* (in press).

J.B. Nicholas et al. "Unified NMR and Density Functional Theory Study of Hammett Bases in Acidic Zeolites." *J. Am. Chem. Soc.* (in press).

R. Nada et al. "An ab Initio Periodic Hartree-Fock Study of Basis Set Effects on the Interaction Energy of He, Ne, and Ar in Silica Sodalite." *International Journal of Quantum Chemistry* (in press).

J.F. Haw et al. "A Physical-Organic Chemistry of Solid Acids: Lessons from In Situ NMR and Theoretical Chemistry." *Accounts of Chemical Research* (submitted).

L.W. Beck et al. "Kinetic NMR and Density Functional Study of Benzene H/D Exchange in Zeolites, the Most Simple Aromatic Substitution." *J. Am. Chem. Soc.* (in press).

# Environmental Catalysis

Anthony C. Hess (Theory, Modeling, and Simulation)

---

## Project Description

This project was designed to provide a better understanding of the role played by surface geometry and electronic structure on the reactivity and selectivity of environmentally important heterogeneous catalysts. Special emphasis has been placed on identifying and subsequently understanding the surface chemistry of environmentally important catalysts capable of remediating chemical waste. The ability of ab initio periodic Hartree-Fock theory to accurately and reliably treat such systems has also been assessed by the activities of this project.

## Technical Accomplishments

During the past several years, we have carried out investigations into the surface properties of metal oxides and microporous aluminosilicates. Many of the materials studied are important industrial catalysts with several being widely used to reduce chemical waste (often in the context of emission abatement). Understanding the detailed interactions of a reactant with a catalyst surface is an enormously complex problem which has proven to require both sophisticated experimental and theoretical techniques. Neither approach can provide all of the required information on the system of interest. The most powerful approach involves the combined use of accurate experimental measurements and reliable high level theoretical tools. Of course, in order to adopt a joint theoretical and experimental approach, the appropriate tools must be available and an assessment of their respective strength and weaknesses must be made. In this context, this project has focused on understanding the ability of ab initio periodic Hartree-Fock theory to provide accurate and reliable information on complex systems relevant to heterogeneous catalysis. Using this method, we have investigated the ground state structural and electronic properties (including interactions with molecular adsorbates) with the surfaces of such metal oxide as ZnO, MgO, and  $\alpha$ -Al<sub>2</sub>O<sub>3</sub>.

The above materials were chosen for study due to the fact that reliable experimental data exists for several quantities of interest and the materials are known to function either as catalysts or as supports for metal promoters. Our work on  $\alpha$ -Al<sub>2</sub>O<sub>3</sub>, for example, has resulted in an increased understanding of the surface structure of this compound and has stimulated work related to the synthesis of ultra-thin films of this material. As a result of this work we have found the periodic Hartree-Fock approach to be a valuable tool for the study of gas/solid interfaces although the cost of this approach can be prohibitively expensive for systems containing more than approximately 50 independent (non-symmetry) related atom centers. The work supported by this project has contributed to the body of work required to establish the behavior (and value) of this theoretical method.

## Publications

- J.B. Nicholas and A.C. Hess. 1994. "Ab Initio Periodic Hartree-Fock Investigation of a Zeolite Acid Site." *J. Am. Chem. Soc.*, 116, 5428.
- R. Nada, A.C. Hess, and C. Pisani. 1995. "Topological Defectes at the (001) Surface of MgO: Energetics and Reactivity." *Surf. Sci.*, 336, 353.
- J.E. Jaffe and A.C. Hess. 1994. "Ab Initio Investigation of the ZnO (10-10) Surface Relaxation." *Phys. Rev. B*, 49, 11153.
- J. Anchell and A.C. Hess. "The dissociation kinetics of H<sub>2</sub>O on stepped MgO (001) surfaces." *JPC* (submitted).

# Flow Injection Analysis

Jay W. Grate (Materials and Interfaces)

---

## Project Description

Flow injection analysis constitutes a combination between wet analytical chemistry and instrumentation that automates analyses and processes in miniature form. Flow injection techniques are extremely flexible and analyses have been developed for a great variety of inorganic and organic chemicals on samples ranging from soils, waste water, and industrial process streams. The purpose of this project was to enhance the flow injection analysis technique and conduct proof of principle experiments that will demonstrate the usefulness of these methods in addressing a variety of problems at Hanford and other DOE sites. Specific areas of interest include radiochemical analysis, soil and groundwater analysis, and process simulation.

## Technical Accomplishments

A rapid, automated, microanalytical procedure for the determination of  $^{90}\text{Sr}$  in aged nuclear waste has been developed. It is based on a sequential injection analysis (SIA) system which rapidly separates  $^{90}\text{Sr}$  from  $^{90}\text{Y}$ ,  $^{137}\text{Cs}$ , and other radionuclides. This automated separation system is coupled to a flow-through scintillation counter for on-line detection. We have characterized this new method in detail and demonstrated its effectiveness in the analysis of aged tank waste samples from the Hanford Site.

The separation is achieved using a sorbent extraction minicolumn containing a resin (EiChrom, Sr-Spec) that selectively binds  $^{90}\text{Sr}$  as a crown ether complex under acidic conditions. The  $^{90}\text{Sr}$  is eluted with water, mixed with liquid scintillation cocktail, and detected in the flow cell of the counter. Sample  $^{90}\text{Sr}$  activity can be quantified from peak areas, giving linear calibration curves. The instrument can also be operated in a stopped-flow mode for longer counting times. Analyses of aged nuclear waste samples from the Hanford site by the sequential injection analysis method and a manual method were in excellent agreement: correlation coefficient  $R = 0.994$ .

Our automated sequential injection method offers several important advantages over manual analysis. All solution handling operations are fully automated and contained, reducing the handling of open sources of radioactivity, reducing generation of associated solid low-level waste (gloves, pipettes, vials, etc.), minimizing the likelihood of

spills, and minimizing potential exposure of personnel. Even if performed in batches, the manual method of separation is labor intensive and time-consuming. The radioactivity detection steps in the manual method (requiring both beta and gamma counting and calibration of two detectors) limit the overall sample throughput, such that two working days are required to complete the analysis of a set of 12 samples. The sequential injection method combines sample separation and detection in one automated procedure making the analysis data available in less than 40 minutes and allowing complete analysis of up to 15 samples in one working day.

Our sequential injection method is also simpler and faster than reported automated or semiautomated ion chromatographic methods in the literature. These ion chromatographic methods are difficult to optimize and require careful pH control. The separation systems involve multiple columns and pumps, and the components are expensive. In the most recent published example, the time required to separate Sr from Y and Cs is 4 hours.

A method for extracting hexavalent chromium from soil samples on line, and analyzing the extract, has been developed. This extended our initial work on hexavalent chromium analysis on aqueous standards to analysis on heterogeneous samples. Several issues with regard to extraction conditions had to be worked out to achieve this. Special attention was devoted to the redox instability of hexavalent chromium under acidic conditions. The work demonstrated the need for rapid onsite analysis of samples, because chromium speciation is easily changed with time and handling conditions.

Initial experiments have been conducted demonstrating that cesium ion exchange unit operations can be automated using a flow injection analysis system. Breakthrough and elution curves under various conditions have been determined. Issues remain with regard to demonstrating that results on small-scale separations can be used to model larger-scale separations.

## Publications

J.W. Grate, R. Strebin, J. Janata, O. Egorov, and J. Ruzicka. "Automated Analysis of Radionuclides in Nuclear Waste: Rapid Determination of  $^{90}\text{Sr}$  by Sequential Injection Analysis." *Analytical Chemistry* (accepted).



R.H. Taylor and J. W. Grate. 1995. "A Flow Injection Technique for the Determination of Chloride using Reflectance Detection." *Talanta* 42, 257-261.

#### Presentations

J.W. Grate, J. Janata, R. Strebin, O. Egorov, and J. Ruzicka. 1995. "Rapid Microscale Determination of Sr-90 in Nuclear Waste by Sequential Injection Analysis." 188th Meeting of the Electrochemical Society, October 8-13, Chicago, Illinois.

J.W. Grate, R. Strebin, J. Janata, O. Egorov, and J. Ruzicka. 1995. "Separation and ON-Line Detection of Sr-90 in Nuclear Waste Samples by Sequential Injection Analysis." Seventh International Conference on Flow Injection Analysis - ICFIA 95, August 13-17, Seattle, Washington.

R. Taylor and J.W. Grate. 1995. "Sequential Injection Method for the Determination of Hexavalent Chromium in Water and Soil." Seventh International Conference on Flow Injection Analysis - ICFIA 95, August 13-17, Seattle, Washington.

R.H. Taylor and J.W. Grate. 1995. "Sequential Injection Method for the Determination of Hexavalent Chromium in Soils and Groundwater." American Chemical Society National Meeting, April 2-7, Anaheim, California.

O. Egorov, J. Ruzicka, J.W. Grate, J. Janata, and R.S. Strebin. 1995. "Application of Flow Injection Methodology in Radiochemical Analysis: Sequential Injection Analyzer for Sr-90 in High Level Tank Waste." American Chemical Society National Meeting, April 2-7, Anaheim, California.

R.H. Taylor, and J.W. Grate. 1994. "Flow Injection Method for the Determination Hexavalent Chromium in Soils and Groundwater." Pacific Northwest International Section Air and Waste Management Association 1994 Annual Convention, November 16-18, Eugene, Oregon.

# High Field NMR and NMR Imaging

Gary P. Drobny (University of Washington)

## Project Description

The objective of this project was to determine the three-dimensional solution-state structure of a synthetic deoxyoligonucleotide,  $d(C1-A2-T3-A4-C5-G6-T7-A8-T9-G10)_2-d(C11-A12-T13-A14-C15-G16-T17-A18-T19-G20)_2$ , which contains a covalent cross-link, reductively activated FR66979, between G6 and G16. FR66979 is a member of a family of antitumor and antibiotic agents similar in structure to mitomycin C. Like mitomycin C, activated FR66979 bonds exclusively to the exocyclic amino groups of two deoxyguanosine residues, forming an interstrand cross-link which is positioned in the minor groove of the DNA (Figure 1). The ability to cross-link may be responsible for the biological activity of this compound. Two-dimensional solution-state  $^1H$  nuclear magnetic resonance is being used in conjunction with molecular mechanics, restrained molecular dynamics, and two-dimensional NOESY back-calculation to generate three-dimensional structures for the sythetic deoxyoligonucleotide,  $[d(CATACGTATG)]_2$ , and the cross-linked FR66979- $[d(CATACGTATG)]_2$  adduct.

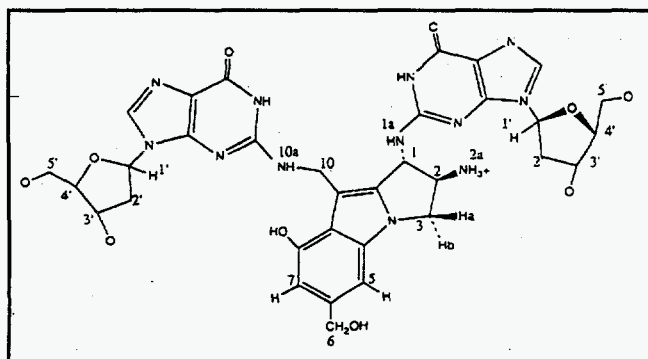
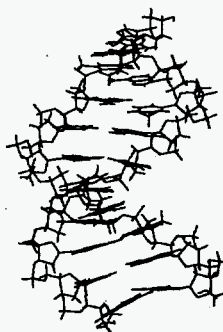


Figure 1. FR66979 Cross-Link Site.

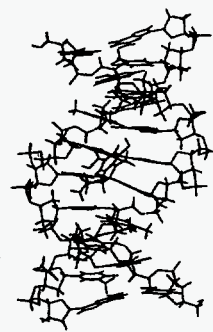
## Technical Accomplishments

Two-dimensional  $^1H$  NOSEY, DQF-COSY, TOCSY, and  $^1H$ - $^{31}P$  COSY spectra have been collected and processed for both the decamer and the FR66979 complex in  $D_2O$  and  $H_2O$  to identify the scalar and dipolar connectivities between non-exchangeable and exchangeable protons. The assignment of NO inter-proton distance connectivities indicates a B-DNA conformation for the deoxyoligonucleotide in both the native decamer and the adduct. However, several aspects of the assignment of the complex are noteworthy. The symmetry of the self-complementary sequence has been broken. This is shown by the presence of two sequential assignment pathways for aromatic H6/H8 to sugar H1' protons, one for each strand of the duplex (Figure 2a). The symmetry is essentially maintained near the ends of the duplex and is dramatically broken near the cross-link site. Unusually weak cross-peaks between T17 H6 and T17H1' and between T17H1' and A18H8 indicate a distortion in the geometry of the native decamer. This perturbation is further evidenced by the presence of an exceptionally broad resonance between T17H6 and the 2'/2'' sugar protons of T17 or G16 (Figure 2b). Structure refinement is still under way for both the decamer and the drug-DNA complex. Interim structures to date are given below.

$[d(CATACGTATG)]_2$



FR66979- $[d(CATACGTATG)]_2$



# Sequential Assignment Pathways for FR66979 Complex

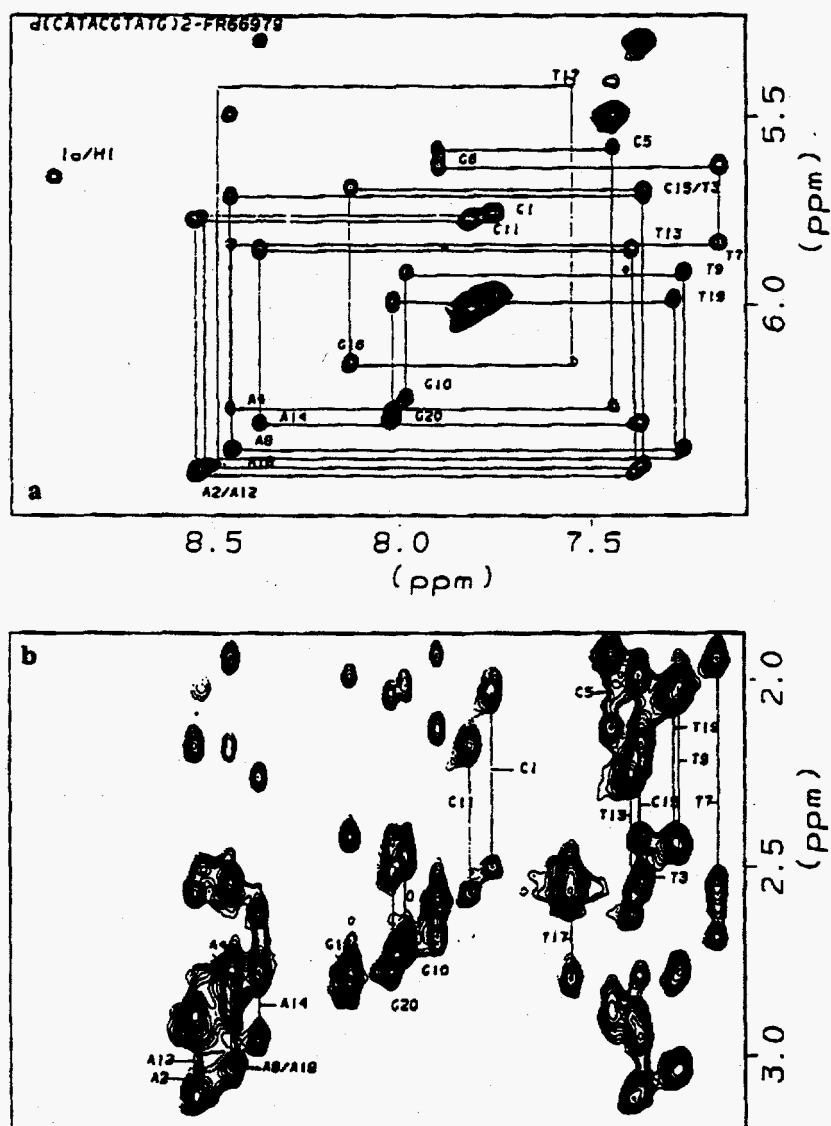


Figure 2. The sequential assignment of the expanded (a) H6/H8-H1' and (b) H6/H8-H2'/2'' regions of NOESY spectrum at 150 ms for d(CATACGTATG)2-

# High Resolution and Solid State NMR Studies of Proteins and DNA-Adducts

Gary P. Drobny (University of Washington)

---

## Project Description

The objective of this project was to determine the local structural and dynamical impact accompanying the introduction of cross-linking adducts into DNA oligomers of defined sequence. Nuclear magnetic resonance quantities of DNAs with cross-linking lesions have been synthesized in collaboration with Professor Paul Hopkins (Chemistry, University of Washington) and studied by high resolution nuclear magnetic resonance. One such lesion, *cis*-diamminedichloroplatinum(II) (*cis*-DDP) has been introduced into the DNA decamer [d(CATAGCTATG)]<sub>2</sub> where it forms an interstrand cross-link between the N7s of 5G and 5G'.

## Technical Accomplishments

We have obtained a high resolution structure of the DNA dodecamer containing the interstrand cross-linked *cis*-DDP (Figure 1A). The resulting structure is, to our knowledge, without precedent, reversing the double helix locally to a left-hand form and placing the platinum-containing bridge in the minor groove rather than the major groove where theoretical models have placed it.

Figure 1A shows the DNA sequence studied, with the cross-linking bridge between the purine rings of G5 and G5' indicated by a solid line. Several lines of evidence suggested that the cross-linked deoxyguanosine residues of 5G and 5'G were not base-paired to deoxycytidines 6C and 6'C, which were themselves not stacked in the duplex. For instance, even at long NOESY mixing times, the NOEs 5GH1'-6CH6 and 6CH1'-7TH6 were undetectable (designated "a" and "b" in Figure 1B). Similarly, the NOEs 5GH2'/2"-6CH6 and 6CH2'/2"-7TH6 were undetectable ("e" and "f" in Figure 1C). Instead, two unexpected NOEs were observed indicating an unusually close proximity of 5G to 7T, namely 5GH8-7TH1' ("d" in Figure 1B) and 5GH4'-7TH6 (not shown).

In addition, the weakness of the intra-residue NOEs 5GH2'/2"-5GH8 indicated an unusual glycosidic angle for the cross-linked deoxyguanosines. Particularly striking, however, were NOE cross-peaks indicating the proximity of the 5GH2'/2" protons to the preceding 4AH8 ("g" in Figure 1C) and to the preceding sugar 4AH1' (not shown), suggesting that 5G was not in an orientation typical of B-DNA.

The refined structure reflected the unusual features deduced from qualitative inspection of the NOEs, including lack of a hydrogen bonding partner for 5G and extrahelicity of 6C. More surprising was the finding that the *cis*-diammineplatinum(II) was in the minor, rather than the major, groove and there as an attendant, highly localized change of the double helix from right-handed to left-handed at 5G. This structure neatly accounts for the conclusion, drawn from gel electrophoresis measurements, that this lesion unwinds DNA by some 80 degrees; this unwinding cannot be rationalized using major groove models of the lesion. The DNA oligomer is bent toward the minor groove at its effective center.

We have corroborated these results by an electrophoretic experiment of the type pioneered by Crothers, which shows that the lesion bends DNA toward the minor groove, rather than the major groove.

This structure raises mechanistic questions as to the relative ordering of the bond-making steps and conformational organizational steps and may be relevant to the slow rate at which monoadducts progress to cross links. The structure will likely have implications concerning the locations at which this lesion is formed in chromatin as well as how and by which proteins (including repair enzymes) it is recognized. The very novel structure induced by this lesion motivates further study of interstrand cross-linking.

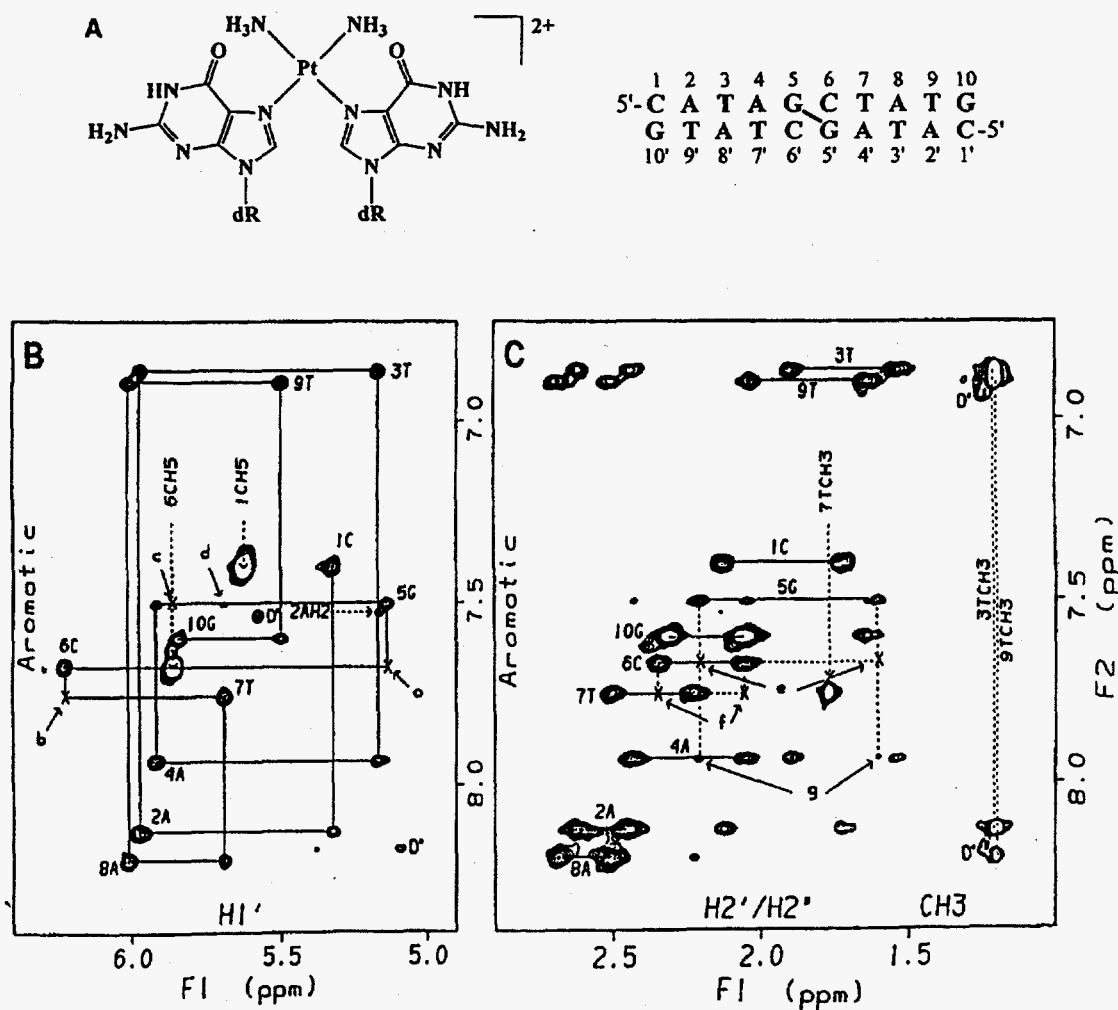


Figure 1. Covalent Structure of  $\text{cis}-(\text{NH}_3)_2\text{Pt}:[\text{d}(\text{CATAGCTATG})]_2$  and  $^1\text{H}$  NOESY NMR spectra. (A) Left: covalent structure of cis-DDP cross-link; right: sequence and cross-link location of cis-DDP cross-linked DNA. (B) The base-H1' region and (C) the base-H2'/2'' region of the NOESY spectrum at mixing times of 450 ms.

## Publications

H. Huang, L. Zhu, B.R. Reid, G.P. Drobny, and P. B. Hopkins. "Solution Structure of a Cisplatin-Induced DNA Interstrand Cross-Link." *Science* (in press).

L. Zhu, B.R. Reid, and G.P. Drobny. 1995. "Errors in Measuring and Interpreting Values of J Coupling Constants from P.E. COSY Experiments." *J. Magn. Reson. A* 115, 206-212.

## Presentations

G. Drobny. 1995. "New Solid State NMR Techniques for the Study of Structure/Dynamics in Biopolymers." Chemistry Department, Yale, February, New Haven, Connecticut.

G. Drobny. 1995. "New Solid State NMR Techniques for the Study of Structure/Dynamics in Biopolymers." Chemistry Department, University of Nebraska, March, Lincoln, Nebraska.

G.P. Drobny. 1995. "Solid State NMR Studies of Nucleic Acids." Invited lecture, *Gordon Conference for Magnetic Resonance*, Brewster Academy, June, Wolboro, New Hampshire.

# *Identification and Structural Determination of Paramagnetic Species Using Pulsed EPR*

Michael K. Bowman (Macromolecular Structure and Dynamics)

---

## **Project Description**

The goal of this project was to develop and demonstrate magnetic resonance techniques for the characterization of reactive species on the surface of potential catalysts, biodegradative enzymes with some potential for bioremediation, and biomolecules sensitive to chemicals or radiation.

## **Technical Accomplishments**

The key intermediates in many chemical reactions, especially those catalyzed by enzymes or oxide surfaces are free radicals. The identification and characterization of these free radicals is a key step in understanding the mechanism and mode of action. Magnetic resonance, particularly electron paramagnetic resonance, is an excellent spectroscopic method for the study of these free radical intermediates because it is uniquely selective for and sensitive to free radicals. During the last year, we have achieved considerable success in all three areas of this project.

We have started a study of Lewis acid sites on the surface of  $\gamma$ -alumina. These are the catalytic sites of many industrially important catalysts and can, in fact, destroy chlorinated hydrocarbons. However, there appear to be a number of different Lewis acid sites on alumina surfaces. Some are quite reactive and are responsible for the complete destruction of molecules and the formation of coke on the surface of the catalysts which limits the operating lifetime of the catalyst. Consequently, catalysts are often modified to remove the most reactive sites and leave behind sites with reduced activity but better selectivity. Two of these surface modifications react boric or phosphoric acid with the surface. We have studied the active Lewis acid sites on surface modified alumina to determine the structural characteristics of the highly

selective catalytic sites. We introduced a diamagnetic molecule onto the activated, surface-modified catalyst. Those molecules that reached a catalytically active site underwent a reaction to form a free radical which then bound to that site. Thus, we selectively introduced our probe free radicals into those Lewis acid sites which retained catalytic activity. The pulsed electron paramagnetic resonance spectra, Figure 1, show interactions between the free radicals and phosphorus or boron atoms that modify the surface. In addition, three different types of surface aluminum ions are seen. Phosphoric acid modified surfaces show evidence of coordinatively unsaturated octahedral and tetrahedral sites while the boric acid modified catalysts show only the later. In addition, the relative amounts of the two sites in the phosphorus modified catalyst changes with the degree of surface modification.

We have studied the iron-sulfur center, Figure 2, in an enzyme of interest to bioremediation, 2,4,5-T monooxygenase. We have identified the center as a Rieske-type cluster. It transfers electrons to the catalytic site in the enzyme. Unlike some other Rieske-type centers, we find no evidence of interactions with protein peptide nitrogens, which may indicate that the redox potential of the Rieske-type center is tuned through hydrogen bonding involving the sulfurs and peptide nitrogens of the protein. We have also studied the active site of xylose isomerase using the oxovanadium ion as a spin probe and were able to assign the histidine ligands to a particular metal site. The radiolysis of frozen solutions is a powerful method that we have started to use for the reduction of metal centers in proteins with minimal structural rearrangement. In particular, the Rieske-center mentioned above was found to have exactly the same structure whether reduced and allowed to structurally relax at room temperature or if it was reduced radiolytically at cryogenic temperatures where the structure of the oxidized form was frozen in.



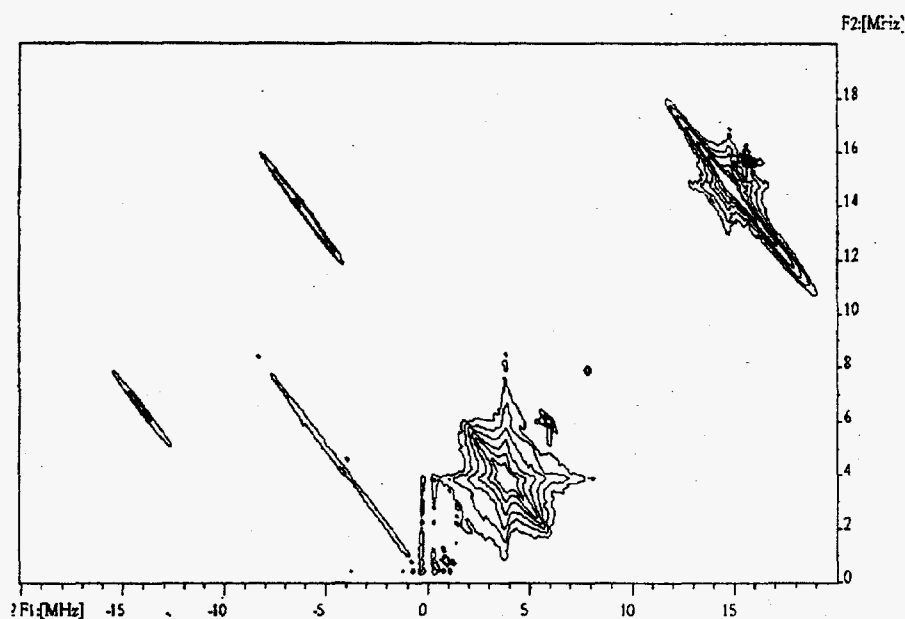


**Figure 1.** The HYSCORE spectrum of a quinone free radical reporter molecule prepared at a catalytic site on a phosphorus-modified alumina surface. The pair of long ridges on the upper left of the spectrum are from a strongly interacting aluminum atom at the catalytic site, while the large, star-shaped peak near the center is from aluminum atoms on the surface near the catalytic site. The long ridge on the upper right is from protons on the reporter molecule and on the alumina surface. A narrow, intense peak at +6,+6 MHz is from the phosphorus atoms modifying the surface.

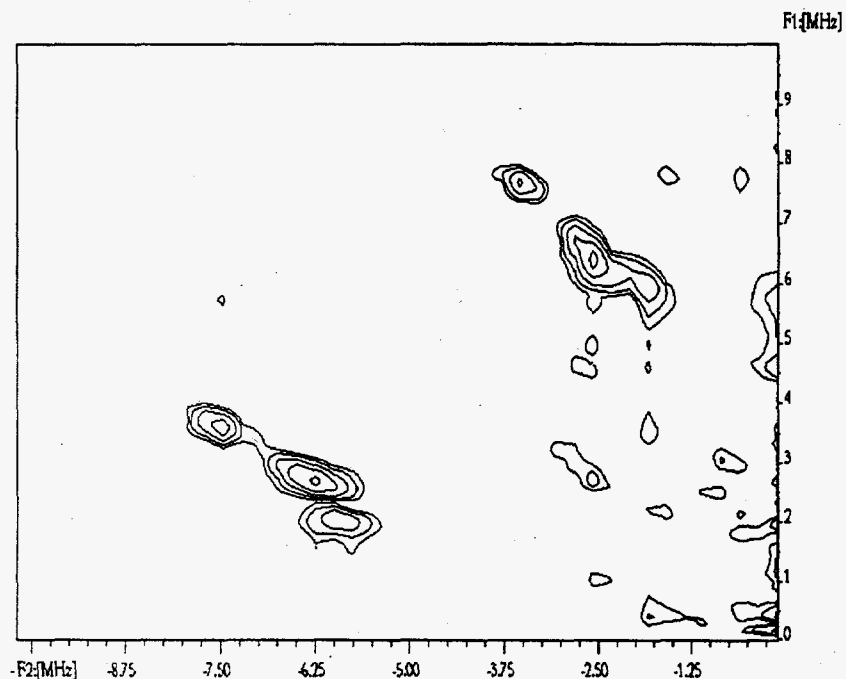


**Figure 2.** Portion of a contour plot of a 2-dimensional pulsed EPR spectrum known as HYSCORE that shows peaks correlating double-quantum nitrogen ENDOR frequencies in the Rieske-type center of 2,4,5-T monooxygenase. These peaks allowed us to determine that this is indeed a Rieske-type center and that there are small, but real, structural differences between Rieske-type centers in this and other enzymes which may be responsible for fine tuning of its electron transfer properties in different enzymes.

## Publications

S.A. Dikanov and M.K. Bowman. 1995. "The Contour Lineshape of Cross-Peaks in Two-Dimensional ESEEM Spectra of Orientationally-Disordered Spin Systems  $S=1/2$  and  $I=1/2$ ." *Journal of Magnetic Resonance*, Ser. A, 116, 125-128.

S.A. Dikanov, A.M. Tyryshkin, J. Huttermann, R. Bogumil, and H. Witzel. 1995. "Characterization of Histidine Coordination in  $VO^{+2}$  Substituted D-Xylose Isomerase by Orientationally-Selected Electron Spin Echo Envelope Modulation Spectroscopy." *Journal of the American Chemical Society*, 117, 4976-4986.

S.A. Dikanov, A.M. Tyryshkin, I. Felli, E.J. Reijerse, and T. Hüttermann. 1995. "C-Band ESEEM of Strongly Coupled Peptide Nitrogens in Reduced Two-Iron Ferredoxin." *Journal of Magnetic Resonance*, Ser. B, 108, 99-102



# Magnetic Resonance Spectroscopy

Herman M. Cho (Macromolecular Structure and Dynamics)

---

## Project Description

This project combined the development of new magnetic resonance methods with the application of established nuclear magnetic resonance techniques to the scientific study of solid materials relevant to toxic waste treatment and environmental restoration and remediation problems.

## Technical Accomplishments

### *Studies of Water in Single Crystal Minerals*

A proton nuclear magnetic resonance investigation of water dynamics in single crystals of the mineral milarite have revealed a unique macroscopic ordering of water molecules in the crystal lattice, with complicated, and as yet, poorly understood motional dynamics involving rotations around well-defined axes of the water molecule. Natural milarite, because it is highly crystalline and available as relatively large single crystals, represents an attractive model system for determining the dynamics of water molecules in inorganic crystal lattices. Theoretical simulations demonstrate that naïve models of the dynamics of the water molecules do not account for the experimental observations.

### *Methodological Advances*

Much of the work in this project involved proton nuclear magnetic resonance measurements of samples containing low amounts of hydrogen. A novel variable-temperature, high-power, proton nuclear magnetic resonance probe with a low hydrogen background was designed to facilitate these measurements and initial fabrication of a prototype was completed. A design for a deuterium probe suitable for variable temperature studies of solid materials has also been initiated. Probes of this type will be valuable for isotopically labeled synthetic samples, where deuterons may be substituted for protons during the synthesis.

In addition, theoretical work is being performed on relaxation pathways in condensed phases, particularly external-field assisted relaxation, and on novel time-domain experiments in electron paramagnetic resonance

and electron-nuclear double resonance spectroscopies, in an effort to expand sensitivity, resolution, and information content of magnetic resonance experiments.

## Publications

J.M. Koons, E. Hughes, H.M. Cho, and P.D. Ellis. 1995. *J. Magn. Reson. A* 114, 12.

H. Cho. *J. Magn. Reson. A* (submitted).

## Presentations

H.M. Cho. 1995. "NMR of Catalysts, Glasses, and Minerals." Pacific Northwest Laboratory Symposium on Magnetic Resonance and the Environment, April, Richland, Washington.

H.M. Cho. 1995. "Solid State Proton NMR: Simulations Elucidating Experiments." Varian Solid State NMR Users' Conference, July, Denver, Colorado.

H.M. Cho. 1995. "NMR Determination of Hydrogen Coordinates and Dynamics in Inorganic Solids." 37th Rocky Mountain Conference on Analytical Chemistry, July, Denver, Colorado.

H.M. Cho and R.S. Maxwell. 1995. "Variable Temperature  $^1\text{H}$  and  $^2\text{H}$  NMR Studies of Proton Dynamics in Boehmite and Pseudo-Boehmite." Thirty-sixth Experimental Nuclear Magnetic Resonance Conference, March, Boston, Massachusetts.

H.M. Cho, D.F. Stec, R.S. Maxwell, T.D. Brewer, and P.D. Ellis. 1995. "A NMR Investigation of Sulfur Promoted Sn and Zr Solid Acid Catalysts." Thirty-sixth Experimental Nuclear Magnetic Resonance Conference, March, Boston, Massachusetts.

# Magnetic Resonance Spectroscopy Studies of Glasses, Minerals and Catalysts

Herman M. Cho (Macromolecular Structure and Dynamics)

## Project Description

The elucidation of the link between structure, dynamics, and macroscopic properties of inorganic materials was the focus of this project. The inorganic materials we chose to study included metal-supported catalysts, multi-component glasses, and natural and synthetic minerals. Spectroscopy, primarily magnetic resonance and infrared, combined with a host of analytical techniques such as inductively coupled plasma (ICP) spectrometry, thermal analyses (thermal gravimetric analysis [TGA], and differential thermal analysis [DTA]), and x-ray crystallography, are the principal methods we used to probe these samples.

## Technical Accomplishments

### Metal Supported Catalysts

We are endeavoring to identify and study the active sites of a number of metal-supported catalysts, among them, sulfate-promoted zirconia and  $\gamma$ -alumina. The goal was to determine the properties of these materials that are responsible for their ability to catalyze a number of organic reactions of commercial significance, and to elucidate the reaction mechanisms that occur at the active sites.

For the sulfate-promoted zirconia catalyst, the focus of our early attention has been on surface Brønsted and Lewis acid sites. The belief that these sites play some role in determining catalytic activity is supported by studies showing that these materials are highly acidic, as measured by a number of pH indicators, and that high activity appears correlated with low  $pK_a$ .

Initial nuclear magnetic resonance and infrared experiments aimed at quantifying the number of Brønsted acid sites suggest that the majority of protons in the active catalyst is confined to the surface in the form of mobile hydroxyl groups. To assess the contribution of Brønsted sites to overall catalytic activity, the synthesis of samples with varying concentrations of Brønsted acid sites was attempted and the activity of the different samples quantified in a laboratory scale reactor.

Figure 1 shows the percent yield of three different samples for the conversion of butane to isobutane. The surface hydroxyl concentration was controlled by varying

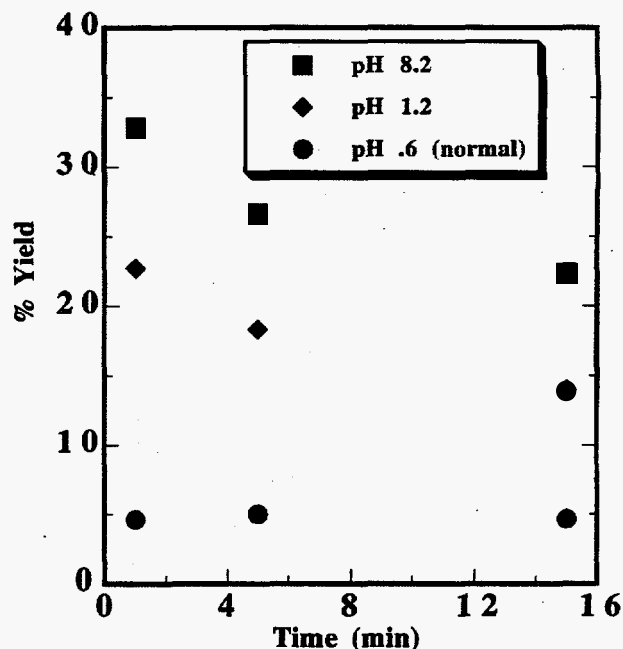


Figure 1. Percent yield of the n-butane to isobutane conversion vs. time, as catalyzed by sulfate-promoted zirconia prepared under different pH conditions.

the pH of the sulfuric acid soaking solution during the sulfation step of the synthesis. While the actual surface hydrogen concentrations for these samples have not yet been measured, our attempts to manipulate the concentrations have resulted in a fivefold enhancement of catalytic activity, as compared to materials prepared using conventional procedures. A spectroscopic investigation into the origin of this phenomenon is in progress.

The number and mobility of Brønsted and Lewis acid sites are also the subjects of our studies of  $\gamma$ -alumina. As for the zirconia case, most of the hydrogen in  $\gamma$ -alumina appears to be on the surface. Moreover, the temperature dependence of the hydrogen nuclear magnetic resonance lineshape indicates that the protons on the surface are highly mobile, even down to temperatures as low as 150K. Surface Al-27 nuclear magnetic resonance studies provide some indirect evidence that the same is true of Lewis acid sites on the surface. Variable temperature multinuclear nuclear magnetic resonance work and experiments involving the adsorption of strong Lewis bases to the alumina surface (e.g., pyridine) are currently being attempted in order to elucidate the dynamics and structure of both types of acid sites.

## Multicomponent Glasses

We are exploiting the natural isotopic selectivity of nuclear magnetic resonance to probe the microscopic environment of elements, such as phosphorus and fluorine, that exist in relatively small concentrations in certain multicomponent oxide glasses. The goal of this work was to improve understanding of the factors affecting the undesirably low solubility of mixed wastes containing these elements. Spectroscopy, particularly nuclear magnetic resonance, infrared, and Raman, represents a particularly attractive method for investigating modes of incorporation in cases where such elements are embedded in a bulk matrix.

Figure 2 displays a preliminary set of P-31 magic-angle spinning (MAS) nuclear magnetic resonance spectra on a series of glass samples, each containing approximately 1.187 wt%  $P_2O_5$ . The glasses differ in calcium, boron, and aluminum concentrations, but contain equal amounts of other elements, the main component being silicon, which is present at a concentration of 56.78 wt%  $SiO_2$ . A qualitative interpretation of electron micrographs of these samples suggests that these glasses separate into amorphous and clearly crystalline phases. The spectra in

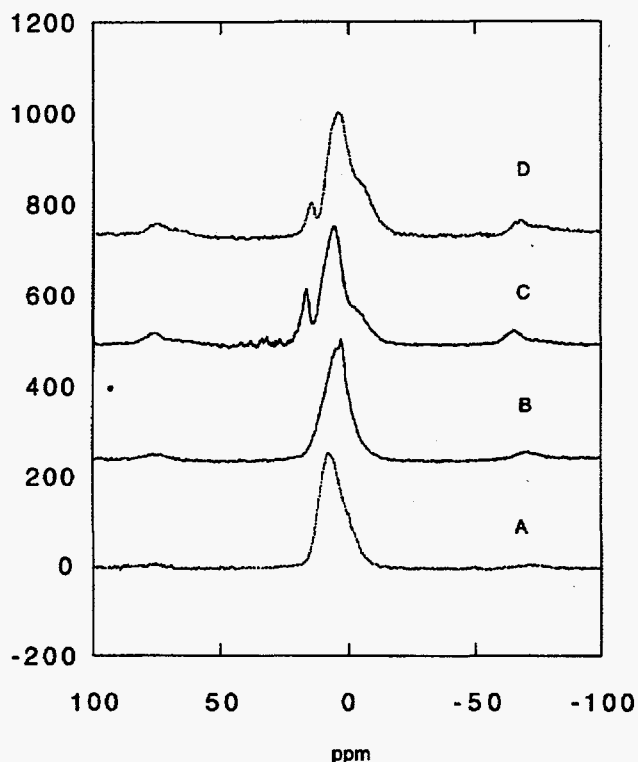


Figure 2. 300 MHz P-31 MAS NMR spectra of phase-separated phosphorus-loaded low-level waste glasses.

Figure 2 are ordered according to estimated degree of phase separation, with spectra of the most homogeneous and amorphous specimens at top. Nuclear magnetic resonance, Raman, and infrared experiments that will enable us to assign the nuclear magnetic resonance lines to specific phosphorus-containing species are currently under way. From the intensity of the nuclear magnetic resonance lines, quantitative data on the proportions of each species may also be derived.

## Minerals

Nuclear magnetic resonance measurements of hydrogen positions and dynamics in synthetic and natural minerals is the focus of our work in this area. Our approach is to combine infrared spectra with published x-ray coordinates of the heavy atoms to construct plausible models of hydrogen dynamics and positions, which we then use to generate simulations of proton nuclear magnetic resonance spectra. The experimental results enable us to compare and refine our models.

We have completed the hydrothermal synthesis of two crystalline proton-containing minerals (boehmite and kaolinite), and are proceeding with the synthesis of others. Preliminary infrared and nuclear magnetic resonance results show the presence of both rigid and mobile protons, and proton network geometries that deviate significantly from arrangements predicted on the basis of heavy atom positions and electron structure calculations.

## Publications

J.M. Koons, E. Hughes, H.M. Cho, and P.D. Ellis. 1995. *J. Magn. Reson. A* 114, 12.

H. Cho. *J. Magn. Reson. A* (submitted).

## Presentations

H.M. Cho. 1995. "NMR of Catalysts, Glasses, and Minerals." Pacific Northwest Laboratory Symposium on Magnetic Resonance and the Environment, April, Richland, Washington.

H.M. Cho. 1995. "Solid State Proton NMR: Simulations Elucidating Experiments." Varian Solid State NMR Users' Conference, July, Denver, Colorado.

H.M. Cho. 1995. "NMR Determination of Hydrogen Coordinates and Dynamics in Inorganic Solids." 37th Rocky Mountain Conference on Analytical Chemistry, July, Denver Colorado.

H.M. Cho and R.S. Maxwell. 1995. "Variable Temperature  $^1\text{H}$  and  $^2\text{H}$  NMR Studies of Proton Dynamics in Boehmite and Pseudo-Boehmite." Thirty-sixth Experimental Nuclear Magnetic Resonance Conference, March, Boston, Massachusetts. Poster presentation.

H.M. Cho, D.F. Stec, R.S. Maxwell, T.D. Brewer, and P.D. Ellis. 1995. "A NMR Investigation of Sulfur Promoted Sn and Zr Solid Acid Catalysts." Thirty-sixth Experimental Nuclear Magnetic Resonance Conference, March, Boston, Massachusetts. Poster presentation.

# Materials Surface and Interface Chemistry

Charles H.F. Peden (Materials and Interfaces)

---

## Project Description

The objective of this project was to develop a molecular level understanding of the surface structure and chemical reactivity of environmentally relevant materials. We focused our efforts on correlating the acid-base properties of different titanium dioxide single crystal surfaces (using water as a probe molecule) with the geometrical arrangement of cation and anion sites on each surface.

## Technical Accomplishments

Our research activities over the past fiscal year have yielded a much clearer picture of the relationship between oxide surface structure and adsorbate surface chemistry for the titanium dioxide system. We have been able to show, using water as an adsorbate, that the structural arrangement of cation and anions sites on  $\text{TiO}_2$  single crystal surfaces dictates whether or not water dissociation occurs. Since water dissociation is the proto-typical acid-base probe of oxide surfaces, the dissociation of water probes the correlated acid-base properties of an oxide. That is, water probes both the ability of acid sites to bind a molecular base to the surface, and the ability of anion sites to abstract a proton from an adsorbed molecular acid. Using isotopic labeling studies in conjunction with temperature programmed desorption, we have demonstrated that oxygen atoms on water adsorbed on the  $\text{TiO}_2(100)$  surface extensively scramble with lattice oxygen anions. This, however, does not occur on the  $\text{TiO}_2(110)$  surface. The observation of scrambling is definitive proof that water dissociates on the (100) surface, but is not proof that dissociation does not occur on the (110) surface. The latter point, however, was confirmed using vibrational spectroscopy (high resolution electron energy loss spectroscopy). We estimate that less than 10 percent of the water adsorbed on the (110) surface dissociate, whereas greater than 30 percent dissociate on the (100) surface. Studies on structurally damaged  $\text{TiO}_2(110)$  indicate that dissociation of water on the (110) probably occurs at defect sites such as steps and kinks, but not at stoichiometric defects, such as  $\text{Ti}^{3+}$  sites. The differentiating structural property responsible for water dissociation on the (100) but not on the (110) surface is the close proximity of anion sites to cations sites on the (100) surface which permits abstraction of the water proton.

In a separate series of experiments, we have investigated the mechanism by which charge (that is, charged species such as ions) is funneled between the surface and the bulk of titanium dioxide surfaces. For example, when  $\text{TiO}_2$  surfaces are ion sputtered in vacuum, the surfaces become reduced (Ti cations in lower oxidation states) due to preferential removal of oxygen. When sputtered  $\text{TiO}_2$  is heated in vacuum the surface is reoxidized to its pre-sputtered state at the expense of the bulk of the material. We have dubbed this phenomena "bulk-assisted reoxidation." To date, the surface science community has viewed this bulk-assisted reoxidation process to involve the diffusion of bulk oxygen anions to the surface. By incorporating oxygen-18 into the sputtered film and using static secondary ion mass spectrometry we have shown that the reoxidation does not involve oxygen diffusion, but the diffusion of reduced titanium cations from the surface to the bulk. We expect that this result will significantly affect the way researchers view charge transport phenomena in titanium dioxide materials.

## Publications

M.A. Henderson. "An HREELS and TPD Study of Water on  $\text{TiO}_2(110)$ : The Extent of Molecular Versus Dissociative Adsorption." *Surface Sci.* (submitted).

M.A. Henderson. "Formic Acid Decomposition on the  $\{110\}$ -Microfaceted Surface of  $\text{TiO}_2(100)$ : Insights Derived from  $^{18}\text{O}$  Labeling Studies." *J. Phys. Chem.* (in press).

M.A. Henderson. "Mechanism for the Bulk-Assisted Reoxidation of Ion Sputtered  $\text{TiO}_2$  Surfaces: Diffusion of Oxygen to the Surface or Titanium to the Bulk?" *Surface Sci.* (in press).

M.A. Henderson. 1994. "The Influence of Oxide Surface Structure on Adsorbate Chemistry: Desorption of Water from the Smooth, the Microfaceted and the Ion Sputtered Surfaces of  $\text{TiO}_2(100)$ ." *Surface Sci.* 319, 315.

M.A. Henderson. 1995. "The Influence of Surface Structure on the Interaction of Water with  $\text{TiO}_2(100)$ ." *Mater. Res. Soc. Proc.* 357, 91.

G.S. Herman, M.C. Gallagher, S.A. Joyce, and C.H.F. Peden. "The Structure of Epitaxial Thin  $\text{TiO}_x$  Films on W(110) as Studied by Low Energy Electron Diffraction and Scanning Tunneling Microscopy." *J. Vac. Sci. Technol. A* (in press).

## Presentations

M.A. Henderson. 1994. "The Influence of Surface Structure on the Interaction Water with  $\text{TiO}_2(100)$ ." Fall Meeting of the Materials Research Society, November 28-December 2, Boston, Massachusetts.

M.A. Henderson. 1995. "Decomposition of Formic Acid on the {110}-Microfaceted Surface of  $\text{TiO}_2(100)$ : The Role of  $\text{Ti}^{3+}$  Sites." Gordon Research Conference (Chemical Reactions at Surfaces), Ventura, California.

M.A. Henderson. 1995. "Mechanism for the Bulk-Assisted Reoxidation of Ion-Sputtered  $\text{TiO}_2$  Surfaces: Diffusion of Oxygen to the Surface or Titanium to the Bulk?" 7th Annual Pacific Northwest Symposium of the American Vacuum Society, September 20-21, Troutdale, Oregon.

M.A. Henderson. 1995. "Decomposition of Formic Acid on the {110}-Microfaceted Surface of  $\text{TiO}_2(100)$ : Competing Processes and the Role of  $\text{Ti}^{3+}$  Sites." 209th American Chemical Society National Meeting, April 2-7, Anaheim, California.

C.H.F. Peden, G.S. Herman, M.C. Gallagher, and S.A. Joyce. 1995. "Structure and Growth of Ultrathin  $\text{TiO}_x$  Films on W(110)." 7th Annual Pacific Northwest Symposium of the American Vacuum Society, September 20-21, Troutdale, Oregon.

G.S. Herman, M.C. Gallagher, S.A. Joyce, and C.H.F. Peden. 1995. "Interaction of  $\text{D}_2\text{O}$  with Model Oxide Surfaces: Clean and Oxidized W(110)." 7th Annual Pacific Northwest Symposium of the American Vacuum Society, September 20-21, Troutdale, Oregon.

G.S. Herman and C.H.F. Peden. 1994. "Growth and Reactivity of Thin  $\text{TiO}_x$  Films on W(110)." American Vacuum Society, October 24-28, Denver, Colorado.

T.A. Jurgens, G.S. Herman, C.H.F. Peden, J.W. Rogers, Jr., T.T. Tran, and S.A. Chambers. 1994. "Reactions of Tetraethoxysilane (TEAS) Vapor on Titanium Dioxide Surfaces." American Vacuum Society, October 24-28, Denver, Colorado.

M.C. Gallagher, G.S. Herman, C.H.F. Peden and S.A. Joyce. 1995. "Structure of Ultrathin  $\text{TiO}_x$  Films Grown on W(110)." American Physical Society, March 20-24, San Jose, California.

S.A. Joyce, M.C. Gallagher, G.S. Herman, and C.H.F. Peden. 1995. "Structure and Growth of Ultrathin Films Grown on W(110)." American Vacuum Society, July 23-28, Aspen, Colorado.

G.S. Herman. 1995. "Interaction of  $\text{D}_2\text{O}$  with Metal Oxides: Clean and Oxidized W(110)." American Chemical Society, August 20-25, Chicago, Illinois.

# Mechanisms of Radiolytic Decomposition of Complex Nuclear Waste Forms

Thomas M. Orlando and Wayne P. Hess (Chemical Structure and Dynamics)  
Keith D Keefer (Advanced Processing)

---

## Project Description

Nuclear waste glasses are subject to large radiation doses such as those due to the beta and gamma decay of the embedded  $^{137}\text{Cs}$  and  $^{90}\text{Sr}$ . For a glass containing 1.25 wt%  $^{137}\text{Cs}$ , the energy released is on the order of 20 W/L which translates to a self dose rate of about 800 rad/second or about  $10^9$  rad/year. This large rate of irradiation could produce a significant steady-state concentration of highly reactive albeit, short-lived species, that could react with water, air, or container materials, both during processing of the glass as well as in storage. Though there seems to be no "official" long-term performance criteria established for the glass waste forms, fundamental research on the mechanisms of radiolytic degradation of complex nuclear waste forms is clearly needed to ensure that this "storage option" is implemented in a safe manner. Borosilicate glasses are imagined to be the final waste form and tritium immobilization via the use of phosphate glasses is currently under consideration.

The objective of this project was to probe the effects of radiation and ionization driven chemistry on/in composite solids (i.e., ionic materials, glasses, and ceramics) which may be used in the long-term storage and/or processing of low/high-level nuclear wastes. An emphasis will be on understanding the underlying physical and chemical mechanisms responsible for radiation damage and loss of composite integrity. The production of charge carriers and bulk and/or surface defects will be probed using electron-stimulated desorption, transient conductivity, and time-resolved luminescence techniques. Detailed measurements of energy thresholds, desorption cross sections, and charge-trapping probabilities will be made to determine what electronic processes are involved in surface degradation and bulk damage. In addition, material removal, surface pitting, and possible bubble formation will be analyzed using atomic-force surface microscopy in conjunction with laser ablation.

## Technical Accomplishments

To date, we have demonstrated large electron-induced degradation cross sections ( $\sim 10^{-15}$  -  $10^{-16}$  cm<sup>2</sup>) in  $\text{NaNO}_3$ ; a wide band-gap material typically found in Hanford wastes. The degradation primarily involves dissociation of the nitrate group via intermolecular auger decay of Na

excitons and/or holes in the Na 2p band. In addition, intramolecular auger decay of holes in the nitrate valence band, shallow valence excitations, and dissociative electron attachment processes also result in efficient destruction of the nitrate group. These energetic processes lead to efficient energy localization at the interface/surface and are expected to contribute significantly to the production of hazardous byproducts typically observed in underground waste storage tanks.

Though we expect smaller cross sections ( $10^{-18}$  to  $10^{-20}$  cm<sup>2</sup>) for the radiolytic degradation of soda glass, iron phosphate glasses, and silicotitanates, we fully expect the general mechanisms to be similar to those leading to the degradation of ionic materials such as  $\text{NaNO}_3$ . It has been pointed out (Dunlap et al. 1981) that material susceptibility to radiation degradation scales with the strength of the effective hole correlation energies. Thus, damage cross sections are expected to decrease as one progresses from salts to glasses to ceramics. We intend to study the trends in degradation cross sections quantitatively and have begun detailed studies on electron-beam induced damage of glass samples. Since it is likely that the glasses used for the storage or immobilization of wastes will contain high concentrations of Na, we have begun studies on glasses which contain varying amounts of Na.

To date we have measured, using atomic force microscopy (AFM), the surface damage induced by irradiating a 5 x 5 x 5 mm sample of soda glass (20 percent Na) with a 3 keV electron beam. The samples were prepared at Pacific Northwest National Laboratory (by Drs. Y. Su and K. Keefer) and the surfaces were imaged in room air. The unirradiated surface of one sample is fairly "smooth" with several 200-nm high columns. The sample was placed in a high-vacuum chamber and irradiated with a fairly low-flux 3 keV auger-electron beam for approximately 10 minutes. The resulting surface damage was then probed in air by atomic force microscopy. The surface damage was rather severe with pits and canyons more than a micron deep. Stress release and damage was observed several minutes after irradiation which suggests the build-up of charge, exciton transport, and possibly some local heating. These preliminary results clearly indicate that soda glass is susceptible to electron-induced degradation. Current work involves measuring the electron- and

laser-stimulated desorption yields and thresholds of O<sup>+</sup>, O<sup>-</sup>, O(<sup>3</sup>P<sub>j</sub>), Si<sup>+</sup>, Si, and SiO from soda and borosilicate glasses. In the case of soda glass, samples with controlled amounts of Na will be studied in an effort to discern if direct excitation of the Na 2p to 3s exciton results in high desorption yields.

Laser ablation will be also used in conjunction with atomic force microscopy studies to probe the surface roughness under pre- and postirradiation conditions. These two approaches can be combined to determine quantitatively the material removal rates and cross sections.

## References

B.I. Dunlap, F.L. Hutson, and D.E. Ramaker. 1981. "Auger Lineshapes of Solid Surfaces-Atomic, Bandlike or Something Else?" *J. Vac. Sci. Tech. A*, 18, 556.

J.F. DeNatale, and D.G. Howitt. 1984. "A Mechanism for Radiation Damage of Silicate Glasses." *Nucl. Instr. and Meth. B1*, 489.

W.J. Weber. 1991. "The Effect of Radiation on Nuclear Waste Forms." *J. of Min., Metals, and Mat. Soc.* 43, 35.

## Publication

K. Knutsen, and T.M. Orlando. "Low-Energy (5-80 eV) Electron-Stimulated Desorption of H<sup>+</sup>, (D<sup>+</sup>), OH<sup>+</sup>, (OD<sup>+</sup>), O<sup>+</sup>, and NO<sup>+</sup> from Solution Grown NaNO<sub>3</sub> Crystals." *Surf. Sci.* (in press).

## Presentations

K. Knutsen and T.M. Orlando. 1995. "Low-Energy (0-80 eV) Electron-Stimulated Desorption of H<sup>+</sup>, (D<sup>+</sup>), OH<sup>+</sup>, (OD<sup>+</sup>), O<sup>+</sup>, and NO<sup>+</sup> from Solution Grown NaNO<sub>3</sub> Crystals." National American Physical Society Meeting, March 20-24, San Jose, California.

T.M. Orlando. 1995. "Low-Energy Electron-Stimulated Interactions at Wet Interfaces." May 16, Argonne National Laboratory, Argonne, Illinois.

T.M. Orlando. 1995. "Low-Energy Electron-Stimulated Interactions at Wet Interfaces." May 17, Northwestern University, Evanston, Illinois.

T.M. Orlando. 1995. "Low-Energy Electron-Stimulated Interactions at Wet Interfaces." May 18, Radiation Laboratory, University of Notre Dame, Notre Dame, Indiana.

K. Knutsen, and T.M. Orlando. 1995. "Low-Energy (0-80 eV) Electron-Stimulated Desorption of H<sup>+</sup>, (D<sup>+</sup>), OH<sup>+</sup>, (OD<sup>+</sup>), O<sup>+</sup>, and NO<sup>+</sup> from Solution Grown NaNO<sub>3</sub> Crystals." July 16-22, Gordon Research Conference on Dynamics at Surfaces.



# Multinuclear Solid State NMR Characterization of Early Forms of Mineralization

Paul D. Ellis (Macromolecular Structure and Dynamics)

## Project Description

The aim of this project was to investigate the process of biological mineralization and determine the sequence of events that leads to the formation of mature bone. Such an understanding would aid in the diagnosis and possible treatment of diseases of the skeletal system and may play a role in the development of more natural prosthetic devices.

## Technical Accomplishments

The process of biological mineralization is complex and requires further clarification. Much of the controversy has focused on the initial phases present. Mature bone is composed of the calcium-phosphate hydroxyapatite (HA), the general form of which is  $\text{Ca}_{10}(\text{PO}_4)_3(\text{OH})_2$ . However these biological apatites incorporate numerous vacancies and ion substitutions in the crystal lattice. These imperfections play an important role in how bone functions in the body. Bone formation has been mimicked in an attempt to determine the exact components and the sequence of events that leads to the final hydroxyapatite product. Chemical modeling studies have shown that in aqueous solutions, the formation of hydroxyapatite is preceded by one or more precursor phases. Based on a variety of studies, the precursor(s) have been thought to be various solid phases, including brushite,  $\text{CaHPO}_4 \cdot 2\text{H}_2\text{O}$ , amorphous calcium phosphate (ACP),  $\text{Ca}_3(\text{PO}_4)_2(\text{H}_2\text{O})_n$ , and octacalcium phosphate (OCP)  $\text{Ca}_8(\text{PO}_4)_4(\text{HPO}_4)_2 \cdot 5\text{H}_2\text{O}$ , depending on the conditions used during the precipitation reaction. Certain complexes composed of the acidic phospholipids and calcium-phosphate have also been shown to demonstrate nucleational capabilities in calcifying tissue. Phosphatidylserine has been shown to be active in this process. Thus, it becomes important to establish the nature of the first mineral phase, since this finding will provide an important clue to the conditions present during the initial precipitation reaction and eventual formation of bone. Using mineral extracted from matrix vesicles we have attempted to characterize these phases.

During FY 1995, we have developed a two-pronged methodology to examine these phases using a combination of multinuclear nuclear magnetic resonance and factor analysis. In brief, with factor analysis the experimental observations are converted into a covariance matrix,

which is diagonalized and the eigen vectors and eigen values are then employed to reproduce the original data in terms of abstract "factors" and "weights." The number of factors required to reproduce the data were also determined. The factors were converted into physically meaningful parameters by target transformation using model compounds. Recombination regenerated the experimental observations in terms of the reproduced factors and their relative concentrations. Using this approach, we have been successful in identifying the mineral content in the matrix vesicles. Figure 1 shows the cross polarization spectrum of the MV sample and its three component factors that have been identified through factor analysis. These are hydroxyapatite, an amorphous calcium phosphate-like phase, and a phosphatidylserine-calcium-phosphate complex (PS-Ca-P). This work represents the first study performed on mineral at such an initial stage in the mineralization process and is the first physical characterization of the PS-Ca-P complex.

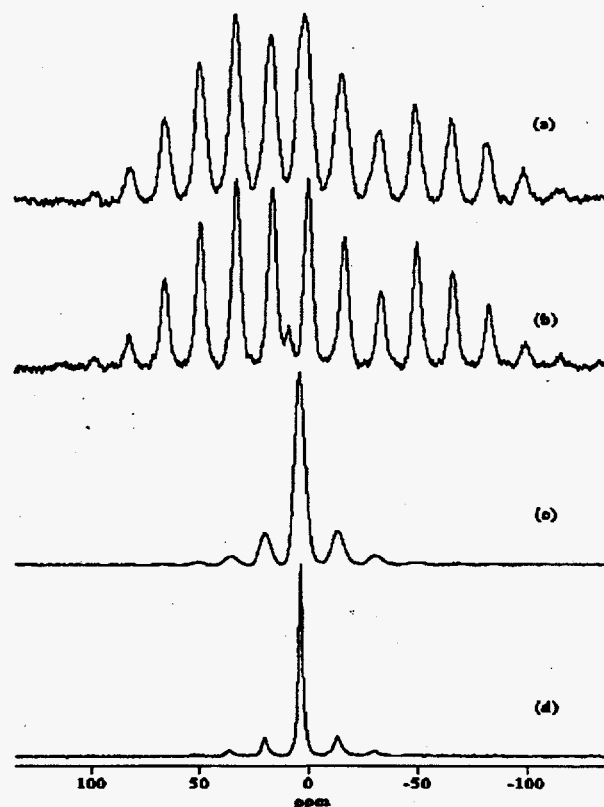


Figure 1. MV Samples and the Three Factor Components. (a) MV, (b) PS-Ca-P, (c) ACP, (d) HA.

Figure 2 illustrates the evolution of each of the three mineral phases. As time progresses the hydroxyapatite species grows while the amorphous calcium phosphate-like

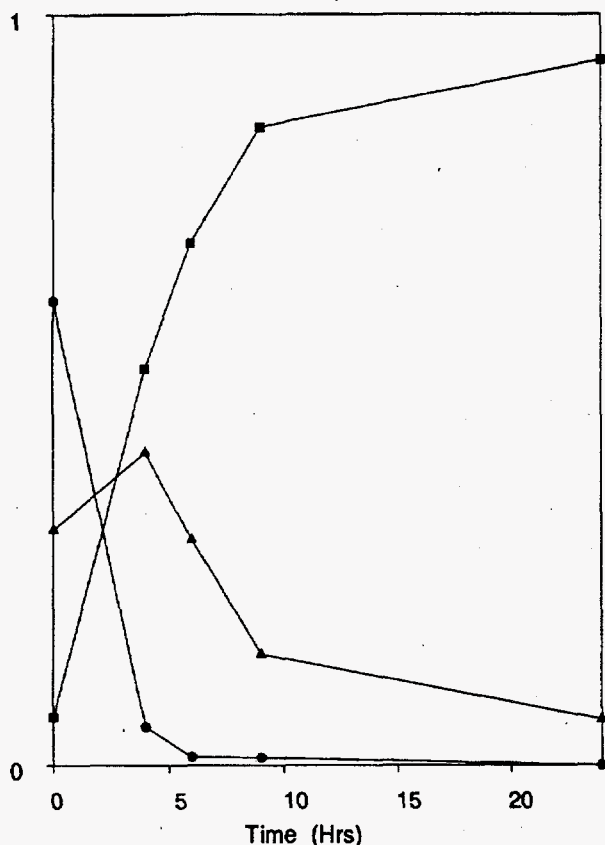


Figure 2. Temporal Evolution. (•) PS-Ca-P, (Δ) ACP, (■) HA.

phase and PS-Ca-P complex become less dominant. This evolution follows formation of mature hydroxyapatite found in bone and allows for the first time the visualization of the sequence of events in biological calcification. The PS-Ca-P complex acts as an anchor point for the calcium and phosphate ions, causing their accumulation and eventual precipitation as an amorphous calcium phosphate-like phase. As time progresses this ACP-like phase matures into hydroxyapatite. Hence, this spectroscopic analysis has led to the determination of the initial phases present during mineralization. These data also facilitate an understanding of other data in the literature.

### Presentations

1995. "Multi-Nuclear NMR Studies on Biominerals." Rocky Mountain Conference.

1995. "Multi-Nuclear NMR Studies on Biominerals." Experimental NMR Conference.

# NMR Studies of Altered-DNA/Protein Complexes

Michael A. Kennedy (Macromolecular Structure and Dynamics)

## Project Description

During FY 1995, we focused on studies of the human DNA repair protein XPAC. XPAC is thought to be the first protein involved in the recognition of DNA damage. Previous studies on the sequence and cloning of XPAC have reported it to consist of 273 amino acid residues with a corresponding molecular weight of 31 kD. XPAC has also been shown to contain a zinc finger DNA binding domain which falls into a class which has been identified in the chick erythroid transcription factor GATA-1. This class of zinc finger is unique in that only a single copy of the zinc finger is necessary for specific binding to DNA. This binding is accomplished by a core zinc finger which contains an alpha helix that interacts in the major groove of DNA and an "arm" that interacts in the minor groove of DNA. Our goals in studying this protein include using nuclear magnetic resonance spectroscopy to determine the structure of XPAC, complexes of XPAC with damaged DNA, and complexes of fragments of XPAC with damaged DNA.

## Technical Accomplishments

Our initial studies focused on folding and determining the structure of a synthetic 40-residue fragment of XPAC which contains the core of the zinc finger domain. We have successfully folded the synthetic fragment monitoring the folding by both circular dichroism spectroscopy and by nuclear magnetic resonance spectroscopy. Figure 1 shows a comparison of the unfolded (Figure 1a) and folded (Figure 1b) peptide in the amide and aromatic proton region of the spectrum. The increased dispersion of the proton resonances is an indication that the protein is structured. Preliminary two-dimensional nuclear magnetic resonance data have been collected. Figure 2 shows the amide to alpha proton and amide to side-chain proton regions of a TOCSY spectrum. This experiment contains crosspeaks for protons that are coupled significantly through bonds. These data will help provide assignments of crosspeaks to corresponding protons in the peptide fragment. Our immediate goal is to determine the structure of this 40 residue fragment of XPAC and to compare its structure to the known structure of the analogous GATA-1 structure.

Based on the similarity of the zinc finger classes for the GATA-1 DNA binding domain and the zinc finger DNA binding domain of XPAC, we are considering the

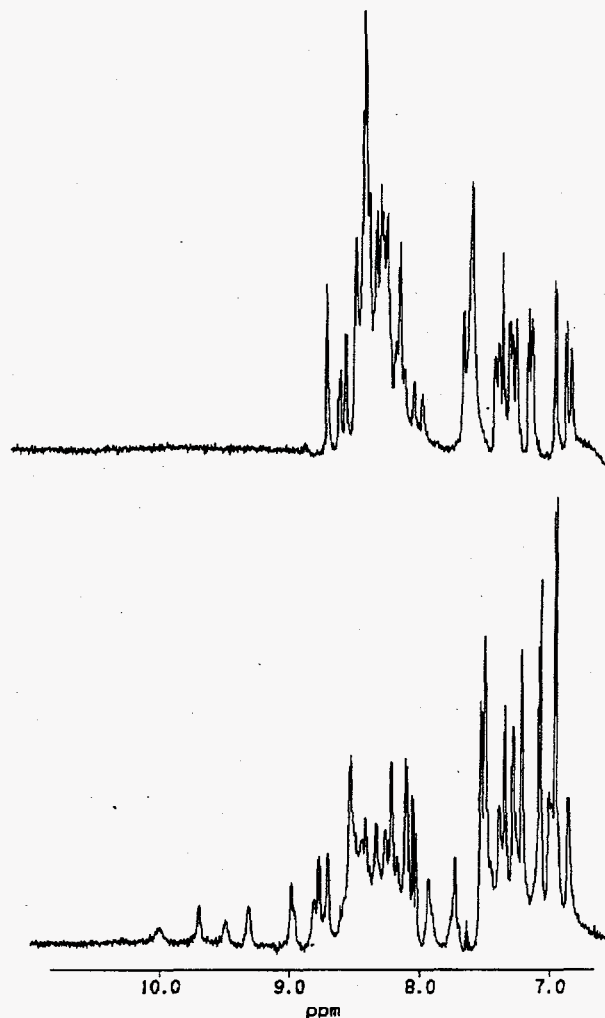


Figure 1. The 750 MHz  $^1\text{H}$  spectrum of 40 residue synthetic peptide fragment of XPAC without zinc (top) and with zinc added (bottom) collected at 25°C.

possibility that an extended fragment of XPAC that contains the "arm" of the domain will bind to damaged DNA with some specificity. Whereas the structure of the 40 residue fragment described above can potentially be determined by nuclear magnetic resonance spectroscopy without the incorporation of isotopic labels, and the feasibility of synthesis of a fragment of such a length is not overwhelming, synthesis of a 60-residue peptide is much more challenging and expensive. Nuclear magnetic resonance studies would be greatly complicated without the use of isotopic labels. Furthermore, structure determination of complexes of the 60-residue fragment

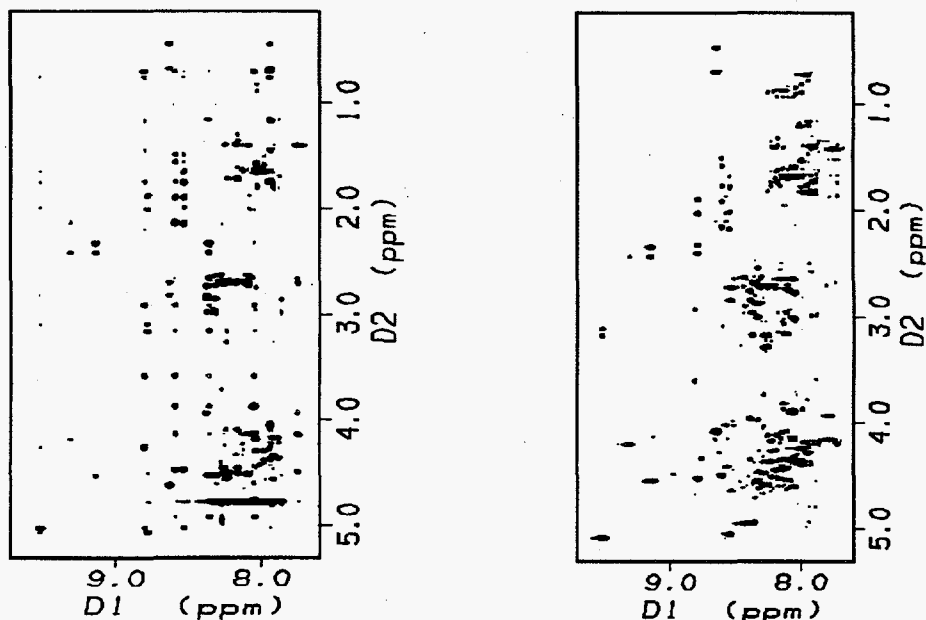


Figure 2. The 750 MHz  $^1\text{H}$  NOESY (left) and TOCSY (right) spectra of the 40-residue synthetic peptide fragment of XPAC.

with a short segment of DNA would likely be impossible or impractical. Therefore, we have pursued cloning the cDNA coding for the peptide fragment into a bacterial expression system.

The cDNA was PCR-amplified using a template derived from reverse transcript of human RNA. Primers were designed to facilitate ligation of the cDNA fragment into the pGEX-4T2 expression vector. Ligation of the cDNA was accomplished and the new plasmid was used to transform XL1 Blu bacterial cells. The cloning was successful and the protein has been expressed as a glutathione S-transferase fusion protein. The fusion protein has been successfully isolated by affinity chromatography using a glutathione bound column and the recombinant protein subsequently isolated after cleavage from the fusion protein following cutting with the specific protease, thrombin.

Our research will continue with assays to determine if the XPAC-60 fragment binds to damaged DNA using traditional gel shift assays. If the outcome is positive, the expression will be optimized and scaled up in order to produce milligram quantities needed for nuclear magnetic resonance structural studies. If the binding assays are negative, larger fragments will be subcloned and expressed so that the minimal XPAC fragment required for binding to damaged DNA can be determined.

#### Publication

J.R. Tolman, J.M. Flanagan, M.A. Kennedy, and J.H. Prestegard. 1995. "Nuclear Magnetic Dipole Interactions in Field-Oriented Proteins: Information for Structure Determination in Solution." In *Proceedings of the National Academy of Science*, Vol. 92, 9279-9283.

# NMR Studies of Proteins

David F. Lowry (Molecular Structure and Dynamics)

## Project Description

This project is directed toward understanding the structure and function of replication protein A which is involved in most aspects of DNA metabolism (replication, recombination, recombination repair, and nucleotide excision repair). The protein is a heterotrimer with 70 kD, 32 kD, and 14 kD subunits. The initial goals of this project are to express and purify these subunits in various combinations, express fragments of these subunits that retain their respective functions, and explore their feasibility for high-resolution nuclear magnetic resonance studies on the assembly of holoprotein, as well as interaction with other proteins and DNA.

## Technical Accomplishments

In July 1995, David Lowry conducted a literature search on nucleotide excision repair. As a result of this literature search, a collaboration on replication protein A with Marc Wold from the University of Iowa was vigorously pursued. Dr. Wold is an expert on replication and has made several constructs that express replication protein A holoprotein, subunits, and fragments. Dr. Wold was also the first to publish that replication protein A interacts with XPAC as the recognition event in nucleotide excision repair.

In September, sufficient supplies for protein expression and purification arrived and two of the three constructs that Dr. Wold sent were successfully electrotransformed. Test inductions to optimize expression were performed as were two separate successful purifications of replication protein A 32/14. Production of 20 mg of protein from a 500 mL culture was accomplished. This was a significant improvement over Dr. Wold's published results (2.5 mg/500 mL). Such optimization is important because stable isotopes are expensive and culture volumes should be minimized.

The 20 mg of protein from purification two was about 80 percent pure. A fraction was given to Richard D. Smith for analysis, and the correct sizes of replication protein A 32/14 were measured. A fraction was given to

Brian D. Thrall and David L. Springer to test for binding to XPAC. Results are pending. The remainder was tested for amenability to nuclear magnetic resonance studies. The spectrum of the sample was quite encouraging, with many downfield amides and upfield methyls which indicate a folded complex (Figure 1). Furthermore, replication protein A 32/14 does not aggregate and is stable at high temperature. Isotope labeling will therefore be pursued. After the nuclear magnetic resonance characterization, replication protein A 32/14 was spin labeled with maleimide and passed on to Michael K. Bowman for ESR studies. Results are pending.

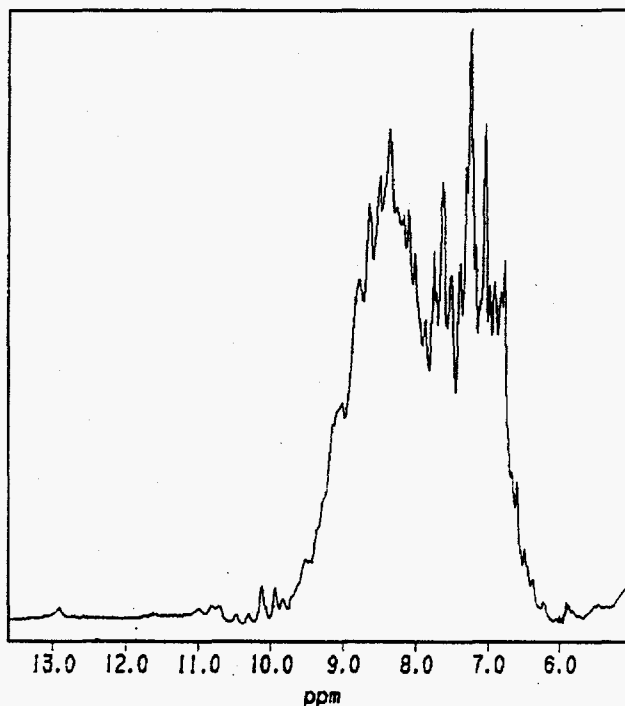


Figure 1. The amide/aromatic region of the  $^1\text{H}$  spectrum of 0.5 mM RPA 32/14 at pH 7.6, 25°C. The resonances above 10 ppm are from strongly hydrogen bonded amides. The resonance at 13 ppm is from a hydrogen bonded histidine imidazole NH. Random coil amides give a sharp intense resonance at 8.8 ppm, which is not seen here, indicating a fully folded heterodimer.

# Novel Synthesis of Metal Cluster/Polymer Composites

Mira A. Josowicz and Scott A. Chambers (Materials and Chemical Sciences)

---

## Project Description

The objective of this project was to develop a detailed understanding of the mechanism(s) of spontaneous, in situ formation of metal clusters and their size distributions in electroactive polymers. The understanding of this process will impact the rational design of conducting polymer/metal cluster composite materials for specific gas/solid interactions that are important to the fabrication of chemical sensors. Furthermore, the knowledge of the novel concept of preparation of modified electrodes is needed to realize fabrication of an environmentally friendly lightweight battery and supercapacitor and development of electrocatalytic conversion processes for use in new environmental processing technologies.

## Technical Accomplishments

An immersion of conducting polymer, immediately after its synthesis, in solution containing a low concentration of metal salt and a background electrolyte of the same concentration as used for the electrochemical synthesis of a conducting polymer, introduces three effects 1) change in the protonic doping, 2) change in the redox state of the conducting polymer and consequently, 3) leads to incorporation of metallic species into the matrix of the polymer. In that process, the polymer matrix can be seen as a macromolecular host and the metal species inserted into the film as guest molecules. The rate of inclusion of the metal particles is governed by the diffusion of metal ions into the host matrix and by the kinetics of the relaxation process which determines the rate of release of electrons from the polymer matrix. The nucleation and growth of the cluster depends on the mixed equilibrium potential between the reactants and products. In that context, electrons released during relaxation of the conducting polymer film, as well as the metal ions in the solution are acting as reactants. The products of the relaxation process depend on the final deposition potential of polymer from which the relaxation was carried out. This observation suggests that the nucleation and growth of the clusters is in general, a nonrandom process.

During FY 1995, we investigated the kinetic aspects of the palladium cluster formation in polyaniline film, PANi, the catalytic function of the composite, PANi-Pd, and the sensitivity to hydrogen and ammonia gas. The PANi films were always synthesized under the same conditions. It was proved that the most important parameter is the thickness of the polymer, which controls the porosity of the polymer matrix. It was observed that in thicker PANi films (50 nm), the palladium clusters grow to approximately 80 nm in diameter. In thinner PANi films (3 nm) the palladium clusters are limited to approximately 20 nm. We felt that the thinner PANi film would be preferable for investigation of the nucleation process. The description of equilibrium between the PANi semiconductor film and the electrolyte solution containing the  $\text{Pd}^{2+}$  ions is achieved by equating electrochemical potentials of electrons in the two phases. The chemical equilibration in such a system will mirror the charge exchange between the matrix and the guest species.

The time dependence of the equilibration of PANi film in the background electrolyte was monitored by recording changes in the open cell potential, ultraviolet-visible (UV/VIS) and x-ray photoelectron spectroscopy. The open cell potentials indicate that the PANi films equilibrate within 2 to 3 hours until they reach the mix potential of +0.45 V versus SCE. The recorded UV/VIS absorption spectra suggest strongly a structural transition of the PANi film synthesized with the final potential of +0.75 V from its more oxidized form, a bipolaron type to the less oxidized form of a polaron type. The indications are the two absorption bands near 420 nm and 800 nm. In the case of the final potential being -0.1 V the PANi reaches its quasi-undoped state while the relaxation facilitates the doping of the polymer with the counter-anion and protons. The conducting state shows again the appearance of the typical two absorption bands of the polaron state. The x-ray photoelectron spectroscopy spectra of the N (1s) core-level of PANi as a  $\text{N}^+/\text{N}$  ratio confirm that the same final redox state of PANi film after relaxation in 1 M  $\text{H}_2\text{SO}_4$  is reached.



The changes in the density of the Pd-cluster obtained for the PANi film relaxed from the negative potential with relaxation time in a solution of 0.01 M PdSO<sub>4</sub> in 1 M H<sub>2</sub>SO<sub>4</sub> were elaborated from the auger electron map distribution as obtained from the scanning electron microscope image of the surface of the PANi-Pd particles. The density of clusters of almost the same size evaluated after 3, 17, and 24 hours of relaxation of PANi film were estimated to be 15 to 17/μm<sup>2</sup>, 20 to 22/μm<sup>2</sup>, and 18 to 20/μm<sup>2</sup>, respectively. Besides the larger cluster, there are a lot of very small clusters with distribution density higher than that of the larger clusters.

Spectra recorded using ultraviolet photoelectron spectrometer (UPS), show that the relaxation time in solution governs the change in work function of PANi-Pd composite films. The difference in energy of the cut-off of the secondary electron spectrum in ultraviolet photoelectron spectrometer gives a measure of the work function difference, Δφ. The most significant change of Δφ of approximately 0.3 V ± 0.1 V which was measured after 0.5 hour immersion of PANi film in the Pd<sup>2+</sup> containing electrolyte. That result was also confirmed by the work function measurements using the Kelvin probe.

The x-ray photoelectron spectroscopy core level spectra of the Pd 3d5/2 of metallic Pd, which correspond to peak 335.5 eV and Pd 3d5/2 of Pd<sup>2+</sup>, which corresponds to peak 337.8 eV are also governed by the relaxation time of PANi film in the sulfuric acid solution containing PdSO<sub>4</sub> salt. The data obtained from integration of the area of the Pd<sup>0</sup> and Pd<sup>2+</sup> peaks show that the ratio of Pd<sup>0</sup>/Pd<sup>2+</sup> is changing within the relaxation period of up to 75 hours in the range from 2.4 to 0.8. The N(1s) core-level spectrum of the PANi-Pd film shows a dominant peak at 399.1 eV which can be related to the N-amine binding energy state. The significant difference between the relaxation process carried out from the positive and the negative potential, respectively, is observed on the peaks of the positively charged nitrogen at binding energies higher than 400 eV. The N<sup>+</sup>/N ratio obtained for the PANi relaxed from the positive potential is 0.50, and that for the PANi relaxed from the negative potential is only 0.16. The S/N ratio is at the same level for both of the PANi-Pd samples. That result leads us to assume that the smaller ratio of the N<sup>+</sup>/N for the PANi relaxed from the positive potential could be related to the greater involvement of the N<sup>+</sup> binding site in the N-Pd bond. Furthermore, a binding energy band at 398.2 eV is observed only for the relaxation from the negative potential. This band probably corresponds to the N-H imine bond. Since that band is not seen for the PANi which was terminated at +0.75 V, its presence can be the sign of a proton gain on nitrogen core. That result could

be seen as supplementary evidence that the positive stopping potential results in the formation of a nitrogen-Pd complex.

The PANi film as synthesized shows a high sensitivity to ammonia gas but no response to hydrogen. All the synthesized PANi-Pd films are losing the ammonia sensitivity but gaining the hydrogen sensitivity. It was observed that the sensitivity to hydrogen is governed by the relaxation process. The highest sensitivity of 100 mV/decade concentration was obtained for films where the cluster formation procedure was applied only for 0.5 hour. With increased relaxation time to 17 hours, the sensitivity is changing to approximately 60 mV and with 75 hours of relaxation is down to 2.5 mV/decade.

The combined experimental approach has provided detailed information about the metal cluster formation in the PANi matrix. The formation of the clusters is governed by the simultaneous process of formation and dissolution which is affected by the final potential applied to the polymer, and by the composition of the solution in which the relaxation takes place. So far we have not been able to identify parameters that would produce the composite with predicted size and amount of metal clusters. Similar, cross-disciplinary combined studies will be necessary to quantify the formation of other metallic clusters such as nickel, iron, etc., and to find out the influence of electrophilic substituents present on the polyaniline chains on the cluster formation process during relaxation of polyaniline.

## Publications

Hong-Shi Li, M. Josowicz, D.R. Baer, M.H. Engelhard, and J. Janata. 1995. "Preparation and Characterization of Polyaniline-Palladium Composite Films." *J. Electrochem. Soc.* 42, 798.

M. Josowicz. 1995. "Applications of Conducting Polymers in Potentiometric Sensors." *Analyst* 120, 1019.

D. Chinn, J. DuBow, M. Liess, M. Josowicz, and J. Janata. 1995. "Comparison of Chemically and Electrochemically Prepared Polyaniline. 1. Electrical Properties." *Chem. Mater.* 7, 1504.

D. Chinn, J. DuBow, Jing Li, M. Josowicz, and J. Janata. 1995. "Comparison of Chemically and Electrochemically Prepared Polyaniline. 2. Optical Properties." *Chem. Mater.* 7, 1510.

## **Presentations**

M. Josowicz. 1995. "Chemical Modulation of Work Function of Organic Semiconductors." Lecture at the Nagatsuda Campus of the Tokyo Institute of Technology, February, Tokyo.

M. Josowicz. 1995. "Organic Semiconductors as Sensing Layers." Lecture at the National Agricultural University, February, Tokyo.

M. Josowicz. 1995. "Organic Semiconductors as Sensing Layers." Lecture at the EE Department of the Tokyo Institute of Technology, February, Tokyo.

D. Chinn, M. Josowicz and J. Janata. 1995. "Relaxation Phenomena in Polyaniline." 187th Electrochemical Society Conference, May, Reno, Nevada.

K. Domansky, H. Li, A. Kane and J. Janata. 1995. "Field-Effect Transistor Based Work Function Sensor with Polyaniline Sensing Layer." 188th Electrochemical Society Conference, October, Chicago.



# Numerical Solution of the Schrödinger Equation

Robert J. Harrison (Theory, Modeling, and Simulation)

---

## Project Description

We have been working toward a fully numerical solution of the electronic Schrödinger equation. Mainstream *ab initio* methods adopt the algebraic approximation by using basis sets at all levels of theory to turn the numerical problem of solving Schrödinger's equation into a large, sparse, eigenvalue problem. At the lowest level of theory, molecular orbitals are expanded in a finite 1-particle basis set, usually chosen as atomic centered orbitals. The underlying 1-particle basis has recently emerged as the main source of error in conventional *ab initio* calculations. Yet more recently, it has become apparent that the algebraic approximation leads to inferior scaling of computational expense with respect to both required accuracy and system size, when compared to possible numerical alternatives. Thus, numerical solution of effective one- and two-electron approximations to the many-electron Schrödinger equation promises both greater accuracy and significantly decreased computational expense.

## Technical Accomplishments

During FY 1994, we identified the free-space Poisson equation as a prototypical problem. Initial efforts in FY 1995 focused on FEM methods, attempting to generate compact and accurate representations of molecular charge distributions in the KASKADE package. We adopted a quintic polynomial basis and a modified adaptive grid generation and modified the program to prove the feasibility of solving the free-space Poisson equation in this framework. The wavelet approach was investigated in order to be able to make a meaningful comparison of the two schemes.

Initial work in one dimension indicated that standard bases were inappropriate for the largely smooth molecular wavefunctions, and after some investigation, we adopted the multi-wavelet basis (due to Alpert). This basis is derived from a piecewise linear combination of polynomials and in contrast to other orthonormal wavelet bases has a closed form and is readily computed permitting direct quadrature and straightforward analytic manipulation.

Extensive formal and algorithmic work then ensued in order to detail how the Green's function to the Poisson equation could be applied in a rapid [i.e.,  $O(N)$ ] fashion.

Code to compute the necessary matrix elements was implemented and verified to be internally consistent and also have the correct long-range values and symmetries. This required use of very-high order ( $L=42$ ) multipolar expansions, special adaptive quadrature routines, recursive expressions to circumvent the solution of large linear equations, and extensive use of symmetry properties to reduce the required number of matrix elements by several orders of magnitude. However, even given these matrix elements, much work remains to realize an efficient implementation of the Green's function. Another major component of the three-dimensional wavelets code is compression, i.e., transferring functions from another representation. We have implemented a tree-based code to perform this operation, and this is enabling quantitative determination of the compressibility of three-dimensional molecular wavefunctions.

We are also able to conclude from this study that wavelet-based algorithms indeed provide a very powerful and general framework for formulating efficient solutions to many linear problems, and our work also lays the foundation for successful application of this technology to three-dimensional molecular quantum problems. However, much fundamental mathematical and algorithmic work remains to be done before wavelets are easily adopted. Another major problem is that the tensor-product basis leads to poor behavior as the dimensionality increases and the fast wavelet algorithms do not lend themselves to using mixed representations such as are natural with FEM.

## Presentations

M.E. Brewster. 1995. "Introduction to wavelets." Pacific Northwest National Laboratory seminar, Richland, Washington.

M.E. Brewster, G.I. Fann, and R.J. Harrison. 1995. "Numerical Solution of the Electronic Schrödinger Equation." Albuquerque High Performance Computing Workshop, Albuquerque, New Mexico.

# Protein-DNA Complexes: Dynamics and Design

Rick L. Ornstein (Theory, Modeling, and Simulation)

---

## Project Description

The primary objective of this work was to validate the best available computational methods and develop new strategies for understanding the dynamic recognition process underlying protein-DNA complex formation. The function of proteins that complex with DNA include gene activators, gene repressors, DNase, RNase, polymerase components, developmental regulators, topoisomerase, AIDS, endonuclease, recombination, and repair. Understanding gene regulation is a critical factor in developing in situ microbial environmental bioremediation strategies. Understanding gene regulation will also play an essential role in making use of microbial, human, and other genomic and structural databases. It is now recognized that important but poorly understood transient structural/ dynamic pathways are significantly contributing to protein-DNA complex formation and ensuing functionality. In the first year of this project, we studied the interactions involved in the initial step of gene transcription involving the complex between the TATA-box binding protein (TBP) and DNA.

## Technical Accomplishments

Structural studies of proteins that bind DNA have accelerated in recent years due to advances in molecular genetics, DNA synthesis, protein crystallography, and nuclear magnetic resonance. Unraveling inherent structure-function-dynamics relationships is necessary in order to obtain a fundamental mechanistic understanding of the processes of biomacromolecular recognition such as occurs during protein-DNA recognition. While many experimental three-dimensional structures of such complexes are available, and many more will be forthcoming, the essential dynamic motions are poorly understood.

During FY 1995, we studied the nature of the molecular structure, dynamics, and energetics of the TBP-DNA complex and the constituent domains by computational simulations. Simulations have been performed on the isolated protein, isolated DNAs, and their complexes. Formation of this complex is the first step in formation of a polymerase preinitiation complex. These studies are being performed in collaboration with Professor Stephen Burley from The Rockefeller University, New York. The main goal is to understand the basis for the very high affinity of TBP toward its consensus DNA sequence and

the directionality of DNA binding to TBP. Crystal structures of TBP-2 from *Arabidopsis thaliana* and the C-terminal region of yeast TBP have been previously reported in the literature. In both cases, homodimers of TBP were observed in the crystals and in several different solution studies. However, in spite of the observed strong tendency to homodimerize, TBP binds to DNA as a monomer. We do not know in what form TBP exists in living cells, although the experimental results described above indicate that dimerization or even higher multimerization can occur. TBP binding to DNA may occur by interactions involving a monomeric form of TBP. Since this form of TBP has not yet been observed experimentally, we used molecular dynamics simulations to answer the question, "how stable is the monomeric structure of TBP in solution?". The simulations were performed using AMBER 4.0 and included explicit counterions and water. Three similar trajectories were computed, each leading to essentially the same results. Large amplitude hinge-bending is observed that brings the two domains of TBP close to each other and results in closure of the DNA binding site (Figure 1-top). The resulting 'closed' structure of monomeric TBP appears to be a stable conformation with relatively small atomic motions (Figure 1-bottom).

Such large interdomain motions are quite often seen in the proteins built from domains. The hinge-bending seen here for TBP is similar to the motion described for lactoferrin which is a transport protein that uses domain closure to recognize and sequester iron. The rather large amplitude of motion observed here for TBP is similar to that seen in other substrate-binding proteins, like for example maltodextrin-binding protein and histidine-binding protein. Thus, the hinge-bending motion as presented here in TBP is not unexpected, but it could be anticipated based on similarities of its spatial structure with other proteins where hinge bending has previously been detected. Binding to the substrate DNA, or another TBP molecule, stabilizes an open form of TBP. Motions of the two TBP domains have also been found in our simulations on the TBP-DNA complex.

The pattern of interactions between protein and DNA observed in the crystal structures is well retained during the simulations performed on the complex between TBP and DNA. However, some interesting modifications to this pattern can be seen. In the crystal structures, interactions only with the eight-base pair TATAAAG region of DNA are detected. In our simulations, we also

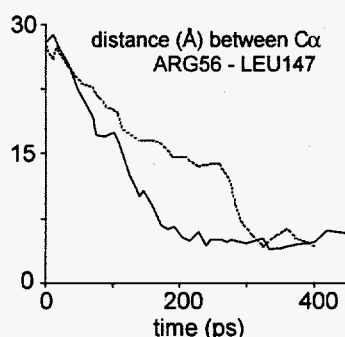
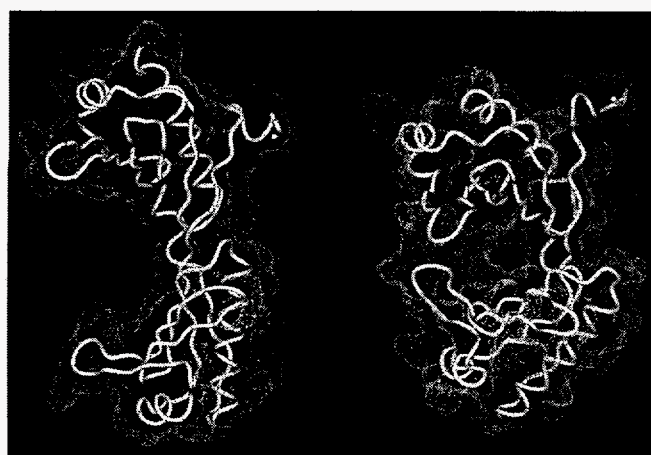


**Figure 1.** TOP: Two snapshots taken from the simulation. Proteins are represented by ribbons with solvent accessible surfaces displayed. The structure on the left is the x-ray crystal protein structure from the complex after energy minimization. Notice the arrows pointing to the C $\alpha$  atoms of the amino acids forming the out boundary of the open DNA binding surface. The structure on the right is the last snapshot after 300 ps of dynamics simulation. BOTTOM: Plot quantifying the inter-domain hinge bending motion for two simulations. The black solid and gray dashed lines were from two simulations with different equilibration procedures.

see hydrogen bond formation with the guanine base which is adjacent to the 3' end of the TATA element. This interaction is not seen in the crystal structures and is formed gradually during the simulation through small structural rearrangements on both protein and DNA. Since the 2-amino group is specific for a guanine base, our observation correlates well with the preference for guanine bases observed experimentally at the flanking position on both ends of the TATA element, which preference was difficult to explain based solely on experimental crystal structures. Our simulations indicate that the binding interface between TBP and DNA, while stable, is not rigid and should be considered as a dynamical system. Figure 2 illustrates this point. In the crystal structure ASN117 is seen hydrogen bonded to N3 of ADE6. However, in the simulation ASN117 interacts interchangeably with N3 of both ADE6 and ADE7, and in addition, is also found in van der Waals contacts with the sugar parts of these nucleotides. As pointed out by Arndt

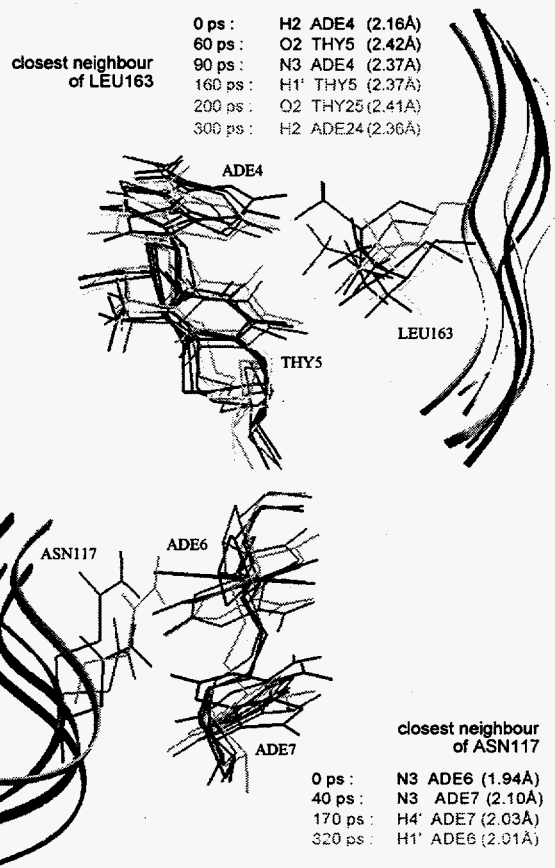


**Figure 2.** Two examples of the dynamics of the protein side chains on the DNA binding interface. See text for explanation.

and coworkers, LEU163 contacts the second base of the TATA sequence (i.e., ADE4 here) in the *A. thaliana* TBP crystal complex, while the same leucine contacts rather the third base (i.e., THY5 here) in the yeast TBP complex. Our simulations offer an explanation to this paradox: the side chain of LEU163 is quite flexible and flip-flops between ADE4 and THY5. These observations illustrate the important contribution of dynamic flexibility in protein-DNA complexation.

DNA bending as in the complex, appears to be induced by the inherent tendency of TBP to undergo hinge-bending that brings the domains in close contact, as observed in the present study. The resulting conformation of the complex may be a compromise between two forces: hinge-bending in TBP and the rigidity of the bound DNA. Thus, interdomain motions and regional flexibility appear to play an important functional role in TBP-DNA binding and recognition. To better understand the role of DNA rigidity, we have recently completed some simulations on TATA-DNA sequences that tightly or weakly bind to TBP; this data is currently being analyzed and additional simulations are continuing.

## **Publications**

K. Miaskiewicz and R.L. Ornstein. "DNA Binding by TATA-Box Binding Protein (TBP): A Molecular Dynamics Theoretical Study." *J. Biomolec. Struct. Dyn.* (in press).

K. Miaskiewicz and R.L. Ornstein. "Structure of a Monomeric Form of TBP (TATA-Box Binding Protein): Insights Based on Molecular Dynamics Simulations." *Proteins* (submitted).

## **Presentations**

K. Miaskiewicz and R.L. Ornstein. 1995. "Recognition of a TATA Element by TBP (TATA-box binding protein): a Molecular Dynamics Theoretical Studies." Ninth Conversation in Biomolecular Stereodynamics, June 20-24, University at Albany, Albany, New York.

K. Miaskiewicz and R.L. Ornstein. 1995. "DNA Binding by TATA-Box Binding Protein (TBP): A Molecular Dynamics Theoretical Study." Ninth Conversation in Biomolecular Stereodynamics, June 20-24, University at Albany, Albany, New York

K. Miaskiewicz and R.L. Ornstein. 1995. "DNA Binding by TATA-Box Binding Protein (TBP): A Molecular Dynamics Theoretical Study." The Fidelity of DNA Replication conference, September 10-14, Wrightsville Beach, North Carolina.

O. Norberto de Souza, K. Miaskiewicz, and R.L. Ornstein. 1995. "Structural and Dynamical Variations in a TATA-Promoter and Its Mutants." The Fidelity of DNA Replication conference, September 10-14, Wrightsville Beach, North Carolina.

# Solid State Multisensor Array

Karel Domansky (Materials and Interfaces)

---

## Project Description

The objective of this project was to develop a second-order solid-state multisensor array for detection of gases in complex environments. The multisensor will be based on the suspended gate field-effect transistor (SGFET) microfabricated in silicon. Individual gates with sensing layers of varying composition will be kept at different temperatures yielding second order data (a matrix with response as a function of two controllable parameters) for each gas sample analyzed. The data matrix will be processed by chemometric methods developed specifically for second order data. Since SGFET sensors have a dynamic range from sub-ppm levels to several percent, this approach will be useful for monitoring a gas concentration with severe fluctuations even in the presence of other interfering species. We will specifically demonstrate that the SGFET array in combination with advanced chemometric techniques can detect and quantify hydrogen, ammonia, and nitrous oxide with high sensitivity and selectivity, singly and in mixtures. The sensor technology is expected to find a wide application in monitoring gases generated in waste tank headspaces and in other applications such as waste processing, occupational safety, and environmental protection.

## Technical Accomplishments

Chemically sensitive layers, previously developed on the Kelvin probe, have been electrodeposited on the SGFETs. Both catalytic and noncatalytic films (palladium and polyaniline) have been applied. Operating temperature of the sensing layer was controlled either by heating the whole sensor or by passing a small electric current through the suspended gate. The sensors have been tested against hydrogen, ammonia, nitrous oxide, methane, and hydrogen/ammonia mixtures. For evaluating the sensor performance against these gas mixtures, a fully automated gas handling system has been developed. A wide dynamic range of the sensor spanning from 200 ppb up to 3 percent has been demonstrated. The ammonia sensor has shown high selectivity and linear response with the logarithm of concentration regardless of hydrogen concentration. The ammonia sensor exhibits negligible sensitivity to methane

and nitrous oxide. The sensitivity of the hydrogen sensor toward nitrous oxide has been shown to be highly dependent on the presence of oxygen. The presence of oxygen virtually eliminates sensitivity of the palladium film to nitrous oxide while the sensitivity to hydrogen is reduced only by a few percent. These results achieved with SGFET sensors illustrate the potential of these sensors and the array approach for quantifying hydrogen/ammonia gas mixtures. Hardware capable of controlling and processing signals from eight SGFET sensors has been developed. The multifunctionality of the SGFET device has been demonstrated by operating it both as a chemical sensor and gas flowmeter. The hot-wire principle used for controlling the operating temperature of the sensing layer has been used to operate the device as a flowmeter. The SGFET flowmeter has a sensitivity higher than  $0.1 \mu\text{A}/\text{sccm}$  in the investigated range from 100 to 1800 sccm.

## Publication

K. Domansky and J. Janata. 1995. "Combined Gas Microflowmeter and Potentiometric Sensor." *Japanese Journal of Applied Physics*, Vol. 34, No. 9A, p. 5054.

## Presentations

K. Domansky, H.S. Li, A. Kane, and J. Janata. 1995. "FET-Based Work Function Sensors with Polyaniline Sensing Layer." Presented at 188th Meeting of the Electrochemical Society, October, Chicago.

K. Domansky, H.S. Li, and J. Janata. 1995. "Polyaniline Thin Films for Chemically Sensitive Field-Effect Transistors." Presented at the 42nd National Symposium of the American Vacuum Society, October, Minneapolis.

K. Domansky, H.S. Li, M. Josowicz, and J. Janata. 1995. "Evaluation of Hydrogen and Ammonia Gas Mixtures with the Suspended-Gate Field-Effect Transistor Sensor Array." Presented at the International Chemical Congress of Pacific Basin Societies, December, Honolulu.

# Spectroelectrochemistry

John L. Daschbach (Materials and Interfaces)

---

## Project Description

The purpose of this project was to study important electrified interfaces, using a combination of electrochemical and optical techniques, in an effort to understand solid/liquid and liquid/liquid interfaces, especially those relevant to waste and remediation problems.

## Technical Accomplishments

There were three principal accomplishments from this project during FY 1995. The first was instrument installation and development of a spectroelectrochemical laboratory. The second and third were electrochemical studies designed to provide a framework for possible future optical experiments. The first of these was a study of well-defined and defected  $\text{TiO}_2$  (110) surfaces and the second was a study of surface films at the mercury-electrolyte interface.

Equipment was obtained and installed to perform in situ Second Harmonic Generation (SHG), Raman spectroscopy, ultraviolet-visible (UV-VIS) reflectance spectroscopy, photoluminescence, and intensity modulated photocurrent spectroscopy. Initial studies performed include Raman spectra of electrochemical polymer precursors and second harmonic generation of ex situ electrodes.

Electrochemical and photoelectrochemical studies were initiated on  $\text{TiO}_2$  single crystal electrodes and niobium-doped epitaxially grown  $\text{TiO}_2$  electrodes. The  $\text{TiO}_2$  single crystal work investigated the role of surface defects in the observed electrical properties of these electrodes. Samples with well-defined surfaces, as determined by x-ray photoelectron spectroscopy, were prepared by sputtering with  $\text{Ar}^+$  and annealing in  $\text{O}_2$ . Defected surfaces were prepared in a similar manner but without the  $\text{O}_2$  anneal, leaving the defected surface. Electrochemical impedance measurements were performed on these samples immediately after preparation and after aging in an  $\text{N}_2$  ambient for >100 hours. All samples

exhibited some potential dependent hysteresis in the electrochemical impedance measurements upon initial transfer to electrolyte after vacuum preparation.

This hysteresis was considerably greater in the defected samples than the well-defined surface samples. Samples of either type, aged at atmosphere after vacuum preparation and electrochemical cycling, were observed to have no hysteresis upon subsequent electrochemical impedance measurements performed without further vacuum treatment. These effects are attributed to subsurface defects which are generated by the vacuum doping or sputtering treatments and which have slow overall kinetics (kinetics plus mass transport) for reoxidation or healing. The potential dependent hysteresis is likely the result of migration of these defects in the space charge field as the potential is varied.

Octadecanethiol and octanethiol films at the mercury-electrolyte interface are examined using cyclic voltammetry and differential capacitance measurements at a single frequency. A mercury flow-system is used to alter the volume, and therefore, the surface area and surface pressure of the mercury electrode. Manipulation of the mercury electrode's volume enables the introduction and removal of defects in the insulating thiol films. Octanethiol and octadecanethiol film behavior are contrasted under conditions of expansion and contraction. Octadecanethiol forms extremely impermeable layers that allow 1000 times less redox probe current than seen on uncoated drops. Expansion of the mercury electrode to increase the electrode surface area produces defects and pinholes in the thiol film. These defects are almost completely removed when the drop is compressed back to its initial surface area. Octanethiol also forms insulating films on mercury sessile drops, however these films contain more defects than octadecanethiol films. While expansion of an octanethiol-coated mercury drop increases redox probe current, recompression of the drop does not return the film to its initial condition. Pinholes and defects in the octanethiol and octadecanethiol films can also be produced by cycling to negative potentials, which produce abrupt stripping peaks.



These experiments show that by changing the size of a mercury sessile drop electrode, it is possible to control the packing of alkanethiols on the drop surface. Increasing the drop surface area results in the formation of pinholes and defects in the thiol coating which allow electron transfer between the mercury electrode and ruthenium hexamine ions. For mercury drops, these defects are almost completely removed when the drop is compressed to its original volume. Thus, octadecanethiol could serve as a suitable clamping molecule for stabilizing molecules for study at a mercury electrode. While expansion increases the permeability of octanethiol films, compression does not decrease the film permeability to its initial value, indicating that octanethiol would not serve as a suitable molecular vise clamping molecule.

The permeability of the initial film was also affected by the thiol chain length. The longer octadecanethiol produced extremely well-ordered defect-free films on the mercury electrode that decrease faradaic currents by about 1000 times compared to an uncoated mercury drop. Octanethiol also produced insulating films, however these films were 10 to 50 times more permeable to the redox probe than the octadecanethiol. Thus, the longer C-18 thiols would be useful for insulating the electrode surface to allow kinetic studies of electroactive species dispersed within the thiol film.

## Publications

C. Bruckner-Lea, R.J. Kimmel, J. Janata, J.F.T. Conroy, and K. Caldwell. "Electrochemical Studies of Octadecanethiol and Octanethiol Films on Variable Surface Area Mercury Sessile Drops." *Electrochimica Acta* (in press).

D.R. Baer, L.Q. Wang, A.S. Shultz, J.L. Daschbach, M.H. Engelhard, and W.M. Hetherington III. "Defect Generation and Interactions with Small Molecules on the TiO<sub>2</sub> (11) Surface in Vacuum and Solution." In *New Techniques for Characterizing Corrosion and Stress Corrosion* by The Metallurgical Society (submitted).

## Presentations

C. Bruckner-Lea, R. Kimmel, and J. Janata. 1995. "Electrochemical Characterization of n-Alkanethiol Films on Surface Area Manipulated Hg-Aqueous Interfaces." ECS Meeting; May 22-26, Reno, Nevada.

J.L. Daschbach, L.Q. Wang, D.R. Baer, and A.S. Shultz. 1995. "Electrochemical Interactions with Well Defined and Defected TiO<sub>2</sub> (110) Surfaces." American Vacuum Society, National Meeting, October 16-20, Minneapolis, Minnesota.

# *Structural and Kinetic Studies at Model Oxide Surfaces*

Bruce D. Kay and Stephen A. Joyce (Chemical Structure and Dynamics)

---

## **Project Description**

The objective of this project was to examine phenomena occurring on model oxide surfaces in an effort to unravel the mechanistic details of the complex interfacial chemistry occurring in the subsurface environment. Scanning probe microscopies (scanning tunneling and atomic force microscopy) were employed to study the growth and structure of model thin film oxide surfaces. Molecular beam scattering and surface analytical techniques were utilized to explore the dynamics and kinetics of adsorbates interacting with both thin film and bulk oxide materials.

## **Technical Accomplishments**

Many aspects of environmental problems, from soil contamination and transport through the groundwater to catalytic remediation schemes, involve the adsorption of molecules on a surface. The scanning tunneling microscope (STM) is capable of imaging solid surfaces and molecular adsorbates with atomic-scale resolution. As a real space probe, the scanning tunneling microscope can directly determine the role of surface structure, especially at defects such as steps, vacancies, etc., in the adsorption and heterogeneous chemistry of molecules on surfaces. Unfortunately, many surfaces of relevance to environmental chemistry are unsuitable for detailed studies due to the insulating nature of many oxides, the lack of large, single-phase crystals, and/or difficulties associated with surface preparation. These problems can be obviated by using ultrathin films grown epitaxially on well-characterized, single crystal, conducting substrates.

The growth of microscopically thin films on conducting substrates overcomes the electrical charging problems associated with bulk insulators. To this end we have used in situ scanning tunneling microscope to investigate the growth and electronic properties of MgO thin films deposited on Mo(001). We have chosen the growth of magnesium oxide on molybdenum to study for a number of reasons: MgO, with a bandgap of 8 eV, is a prototypical ionic solid insulator, the epitaxial growth on Mo(100) has been demonstrated, and several groups at Pacific Northwest National Laboratory, both experimental and theoretical, have extensively studied the structure, growth, and chemistry of MgO. The films were grown by evaporating Mg metal in a background pressure of oxygen. We have successfully imaged films as thick as 25 Å, clearly demonstrating the feasibility of this method.

Films were grown at substrate temperatures between 300 and 1050K. Low temperature growth produced smooth, uniform films with small MgO islands of between 20 Å to 100 Å. Based on the domain size, we estimate the edge defect densities to be about 40 percent of the exposed surface area. Annealing these films at 1100K results in domain coalescence and a higher degree of crystalline orientation of the domain edges. Annealing, therefore, significantly reduces the number of edge defects in the films. Images of films grown at high temperature reveal nonwetting behavior with large three-dimensional islands indicating a Volmer-Weber growth mode. In contrast to films deposited in a background pressure of oxygen, growth of Mg metal on Mo(001) was pseudomorphic at low coverage. At higher coverage a transition to three-dimensional Mg hexagonal islands was observed, which is consistent with a Stranski-Krastanov growth mode.

Macroscopic single crystals of the rocksalt oxide,  $\text{TiO}_{x-1}$ , are not available. G. Herman and C.H.F. Peden from the Materials and Interfaces group have shown that long-range, periodic structures of ultrathin film  $\text{TiO}_x$ , however, can be grown on the surface of W(110) substrates. Films were produced by depositing Ti metal on a room temperature substrate, dosing with molecular oxygen, and then annealing. Scanning tunneling microscope and low-energy electron diffraction studies reveal a rich structural "phase diagram" for this system which is sensitive to the amount of Ti deposited and to the final annealing temperature. Most of the observed diffraction patterns are quite complex and can only be reasonably interpreted as multiple scattering from both the  $\text{TiO}_x$  overlayer and the W(110) substrate.

The molecular beam scattering studies employ variable-energy supersonic molecular beams to determine energy, angle, and coverage dependent trapping and/or dissociation probabilities. In addition to using bulk single crystal samples, the chemisorption of water was compared on ordered single crystal, sputtered damaged single crystal and vapor deposited thin film samples. We developed a novel sample mount that enables us to rapidly heat and cool bulk single crystal samples of oxide surfaces. Figure 1 displays TPD spectra for  $\text{D}_2\text{O}$  desorption from bulk single crystal MgO(100) (upper panel) and a vapor deposited thin MgO film. The sputter damaged, bulk crystal yields results that are similar to the thin film. There are qualitative similarities between  $\text{D}_2\text{O}$  adsorption onto and desorption from the single crystal and thin film



substrates. On both substrates  $D_2O$  adsorbs via precursor mediated kinetics with a sticking coefficient near unity and largely independent of coverage and surface temperature up to 200K. On all substrates the desorption spectra exhibit two prominent features: a high temperature peak ( $\sim 235K$ ) that saturates at a coverage corresponding to approximately one water molecule per surface metal ion and a non-saturable low temperature peak ( $\sim 160K$ ) indicative of the formation of an ice-like multilayer. Careful examination of the high temperature TPD feature reveals that the sub-monolayer water desorption kinetics are strongly substrate dependent. Water desorption from the single crystal substrate results in a TPD feature that increases with increasing exposure and has a peak at 235K for all coverages above 0.1 monolayers. Water desorption from the thin film and sputter damaged substrates result in a TPD feature that increases with increasing exposure and has a peak that shifts smoothly from 290K at low coverage to 235K at saturation coverage.

The lineshape of the TPD spectrum and how the peak temperature shifts with increasing coverage are often used to infer the molecular nature of the adsorbate. TPD peaks yielding coverage independent maxima are indicative of

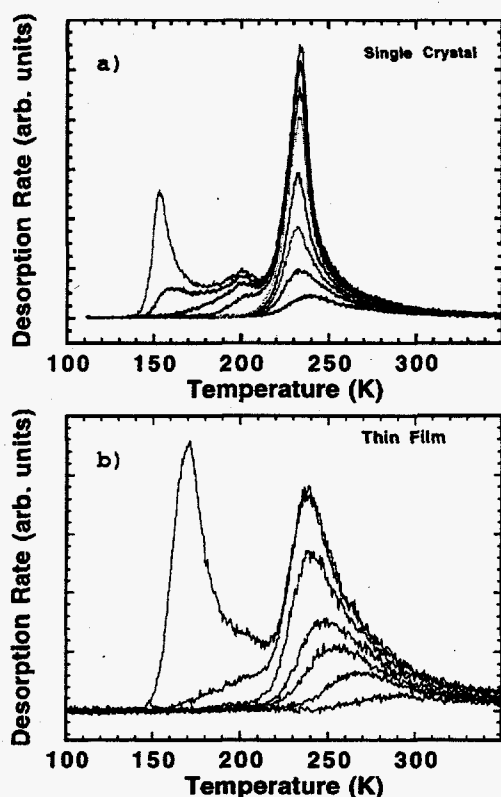


Figure 1. TPD spectra for  $D_2O$  desorption from bulk single crystal  $MgO(100)$  (upper panel) and thin film  $MgO$  grown on  $Ru(0001)$  (lower panel). The high temperature monolayer desorption feature is substrate dependent.

first order kinetics and suggest molecular adsorption. TPD peaks that shift to lower temperature with increasing coverage are indicative of second order kinetics and suggest dissociative chemisorption. Based on this, we hypothesize that water adsorbed on the bulk single crystal is largely molecular in nature while water adsorbed on the thin film and defected surfaces is predominately dissociated. The hydroxylation of  $MgO$  by water to form  $Mg(OH)_2$  is exothermic by  $\sim 15$  kcal/mole but may not occur at a measurable rate on the basal plane of  $MgO(100)$ . Hydroxylation of the thin film and sputter damaged substrates may be more facile due to the presence of coordinatively unsaturated surface defects that catalyze the hydrolysis. Since the sticking coefficient is determined to be unity, there is no kinetic barrier to adsorption. From the desorption data alone, we are unable to determine definitively whether the adsorption is molecular or dissociative.

## Publications

M.C. Gallagher, M.S. Fyfield, J.P. Cowin, and S.A. Joyce. 1995. "Imaging Insulating Oxides: Scanning Tunneling Microscopy of Ultrathin  $MgO$  Films on  $Mo(001)$ ." *Surf. Sci.* 339, L909.

G.S. Herman, M.C. Gallagher, S.A. Joyce and C.H.F. Peden. "The Structure of Epitaxial Thin  $TiO_x$  Films on  $W(110)$  as Studied by Low Energy Electron Diffraction and Scanning Tunneling Microscopy." *J. Vac. Sci. Technol.* (in press).

## Presentations

M.C. Gallagher, G.S. Herman, C.H.F. Peden, S.A. Joyce. 1995. "Structure of Ultrathin  $TiO_x$  Films Grown on  $W(110)$ ," American Physical Society, March, San Jose, California.

S.A. Joyce, M.C. Gallagher, M.S. Fyfield, J.P. Cowin. 1995. "Growth of Ultrathin Films of  $MgO$  on  $Mo(001)$ ." American Physical Society, March, San Jose, California.

M.C. Gallagher, G.S. Herman, C.H.F. Peden, and S.A. Joyce. 1995. "Structure and Growth of Ultrathin  $TiO_x$  Films Grown on  $W(110)$ ." *STM'95*, July, Snowmass, Colorado.

M.C. Gallagher, M. Fyfield, J.P. Cowin, and S.A. Joyce. 1995. "STM of Thin Film  $MgO$  Grown on  $Mo(001)$ ." *STM'95*, July, Snowmass, Colorado.

M.J. Stirniman, C. Huang, R.S. Smith, S.A. Joyce and B.D. Kay. 1995. "The Kinetics of H<sub>2</sub>O Adsorption, Desorption, and Reactions on MgO(100)." Pacific Northwest American Vacuum Society Meeting, September, Troutdale, Oregon.

M.J. Stirniman, S.C. Huang, R.S. Smith, S.A. Joyce and B.D. Kay. 1995. "The Kinetics of H<sub>2</sub>O Adsorption, Desorption, and Reactions on MgO(100)." National American Vacuum Society Meeting, October, Minneapolis, Minnesota.

S.A. Joyce and M.C. Gallagher. 1995. "A Model for Scanning Tunneling Microscopy of Ultrathin Film Insulators." National American Vacuum Society Meeting, October, Minneapolis, Minnesota.

M.C. Gallagher, S.A. Joyce, C.H.F. Peden. 1995. "Structural Characterization of Ultrathin Films of Titanium Oxide on Tungsten." National American Vacuum Society Meeting, October, Minneapolis, Minnesota.

# Theoretical and Computational Molecular Science Research

Anthony C. Hess (Theory, Modeling, and Simulation)

---

## Project Description

The objective of this project was to conduct initial investigations into biogeodynamics and structure-function-dynamics relationships and redesign of ferredoxin NADP reductase.

## Technical Accomplishments

The activities of this very brief project focused on literature investigations into the two subject topical areas.

### *Biogeodynamics*

An important but very poorly understood component of in situ bioremediation strategies concerns the interplay of geochemical, geological, and biological (microbial) processes. For the purpose of designing more accurate and robust bioremediation strategies, it is desirable to understand how molecular and interfacial events influence contaminant and nutrient availability as well as microbial activity and mobility. Research has historically focused on obtaining an atomic-level understanding of the structure and reactivity of mineral surfaces with respect to abiotic reactants. A task of this project involved literature searches designed to uncover previous experimental or theoretical studies that had investigated molecular processes at the bio-inorganic interface. Of particular interest to us was any evidence that such systems had been studied using state-of-the-art molecular level experimental techniques. As atomic level theorists, it is not possible for us to easily become involved in a field of research unless an accurate statement of the physical system can be obtained. The results of these preliminary investigations revealed that although there were a considerable number of macroscopic and microscopic investigations of bio-inorganic interface, we were unable to locate sufficient

amounts of high atomic level information for us to initiate a study on any system. Due to the very short duration of this project, we acknowledge the possibility that crucial data was overlooked.

Had a satisfactory amount of information been located, preliminary work would have been performed to determine if a scientifically reasonable response could have been made to examine the biogeochemical dynamics of intrinsic and enhanced bioremediation.

### *Structure-Function-Dynamics Relationships and Redesign of Ferredoxin NADP Reductase*

The motivation for this work was based upon recent scientific discovery that the enzyme ferredoxin NADP reductase (FNR) (from spinach) was able to reduce 2,4,6-trinitrotoluene (TNT) and 2,4,6-trinitrophenyl-methylnitramine (tetryl). This is the first demonstration of the removal of a nitramine nitro group via an enzymatic process and suggests that modified redox enzymes, and/or conditions, may lead to enzyme processes with far-reaching degradation potential for explosives. In addition, staff have targeted ferredoxin NADP reductase and redox enzymes for developing environmentally sound and cost-effective enzymatic processes for the synthesis of a range of nitroaromatic speciality chemicals. Initial concepts were developed to employ state-of-the-art computational simulation methods to ferredoxin NADP reductase to obtain a molecular based understanding of the inherent structure-function-dynamics relationships in aqueous solution, as well as a comparative study of such relationships in a range of solution conditions. This knowledge would then be applied to the development of specific enzyme mutants to be made and tested by staff at the Laboratory.

# *Tumor Formation in Cells and Tissues Studied by Means of Liquid-State and Solid-State NMR*

Robert A. Wind (Macromolecular Structure and Dynamics)

---

## **Project Description**

The main objectives of the project were to improve the characterization of mammary tumors and to discriminate between preneoplastic and neoplastic mammary lesions by means of nuclear magnetic resonance (NMR) spectroscopy. The investigations will be carried out by in vitro liquid-state and solid-state nuclear magnetic resonance and localized in vivo nuclear magnetic resonance spectroscopy on live animals. The in vitro experiments will be performed on healthy mammary tissues obtained from female Fischer rats, on R3230AC mammary tumors implanted in the animals, and on normal epithelial cells and malignant cells extracted from the tissues. The in vivo investigations will be carried out on mice bearing mammary tumors. If successful, the outcome of this research will assist in an improved understanding of the carcinogenic process and an improved characterization of mammary lesions.

## **Technical Accomplishments**

The importance of both in vivo and in vitro nuclear magnetic resonance imaging and spectroscopy for the detection and characterization of tumors has long been recognized. It has been found that several parameters that can be determined by nuclear magnetic resonance, are different in healthy and tumorous tissues. Examples are the water proton  $T_1$  and  $T_2$  values and the intensities of the water-soluble metabolites. These results are often used in in vivo nuclear magnetic resonance to enhance the contrast in an image between a lesion and the surrounding tissue. However, the results are often ambiguous, as many different types of tumors and other lesions give similar results, and as a large scatter in the results often makes the differentiation between healthy and tumorous tissues difficult. Several approaches were taken to improve this situation significantly

- Extend the existing in vivo and in vitro liquid-state nuclear magnetic resonance methodologies to higher fields than currently used.
- Investigate whether the composition of the organic compounds in the cells and tissues become different after transformation.

- Perform high-resolution solid-state experiments on frozen samples. This makes it possible to investigate structures and dynamics of large-molecular weight molecules such as phospholipids, proteins, and nucleic acids, which form a significant fraction of the total amount of biological material, but which cannot be observed with 'standard' liquid-state nuclear magnetic resonance techniques. Moreover, solid-state nuclear magnetic resonance makes it possible to study the tissues for a long time without degrading the samples, and to obtain information about slow motions in the samples, normally overshadowed by fast overall molecular tumblings.
- It is generally accepted that cancers in epithelial organs arise via one or more intermediate stages called preneoplastic stages. Therefore, our investigations were extended to preneoplastic lesions as well.
- Investigate under which experimental conditions the differentiation between healthy and tumorous cells and tissues become maximal, and whether a combination of liquid-state and solid-state nuclear magnetic resonance parameters will lead to an improved tumor detection and characterization.
- Perform our experiments on cells and tissues obtained from model inbred rodent lines.

During FY 1994 we started an in vitro liquid-state  $^1\text{H}$  and  $^{13}\text{C}$  nuclear magnetic resonance study and a solid-state high-resolution  $^{13}\text{C}$  study of healthy mammary tissues obtained from female Fischer rats, and of R3230AC mammary tumor tissues implanted in the animals. The liquid-state nuclear magnetic resonance experiments were performed at  $4^\circ\text{C}$  in magnetic fields of 11.7 and 17.6 tesla. The solid-state experiments were carried out on frozen samples at  $-100^\circ\text{C}$  in a field of 7 tesla. The liquid-state experiment results are very similar in both magnetic fields. Moreover, it was found that the  $T_1$  values of the water protons are very similar in healthy and tumor tissues, and that the  $T_2$  values are significantly different. The liquid-state  $^{13}\text{C}$  spectrum of the healthy adipose tissue is different from that of the tumor tissue. The solid-state  $^{13}\text{C}$  spectrum of the tumor tissue can be obtained in a much shorter time than the liquid-state spectrum, and provides new information.

In FY 1995, the experiments were focused on the healthy mammary epithelial cells and the tumor cells, extracted from the healthy and tumorous tissues, respectively. It has been shown that the R3230AC tumor derives from epithelial cells, so that a comparison of the nuclear magnetic resonance results of both types of cells provides relevant information about the changes in the structures and dynamics occurring in the cells after transformation.

#### Liquid-State Nuclear Magnetic Resonance

Significant differences were found between the normal and malignant cells in both the  $^1\text{H}$  and  $^{13}\text{C}$  spectra. This is illustrated in Figure 1, where the  $^{13}\text{C}$  spectra are shown of both compounds. It can be concluded from the measurements that the tumor cells contain increased amounts of mobile lipids with relatively long chain lengths. Both saturated lipids and unsaturated lipids are present. The results are consistent with literature findings in other tumors.

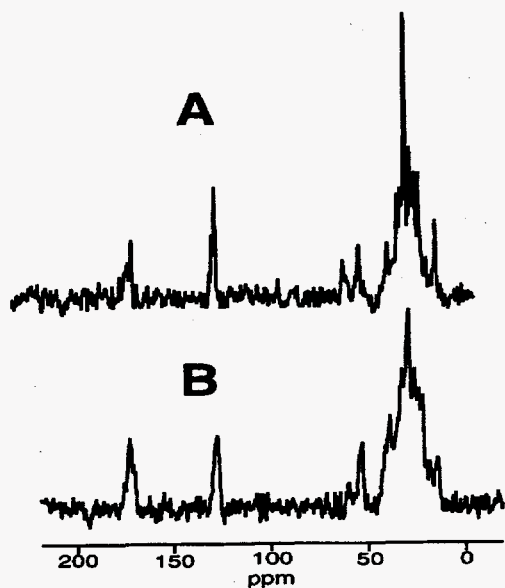


Figure 1. Liquid-state  $^{13}\text{C}$  spectra of malignant (A) and normal (B) cells observed at  $4^\circ\text{C}$ .

#### Solid-State Nuclear Magnetic Resonance

It is found that at  $-100^\circ\text{C}$  the proton rotating-frame relaxation time of the lipids is larger than that of the proteins, so that proton-carbon cross polarization with a prolonged contact time can be used to obtain the lipid spectrum separately. Moreover, it was observed that at both  $-100$  and  $-40^\circ\text{C}$  the tumor spectra, which is the same for the tumor tissue and tumor cells, differ from that of the normal epithelial cells. This is illustrated in Figure 2, where the solid-state  $^{13}\text{C}$  spectra are shown of the normal cells (A) and the tumor cells (B), observed at  $-100^\circ\text{C}$ .

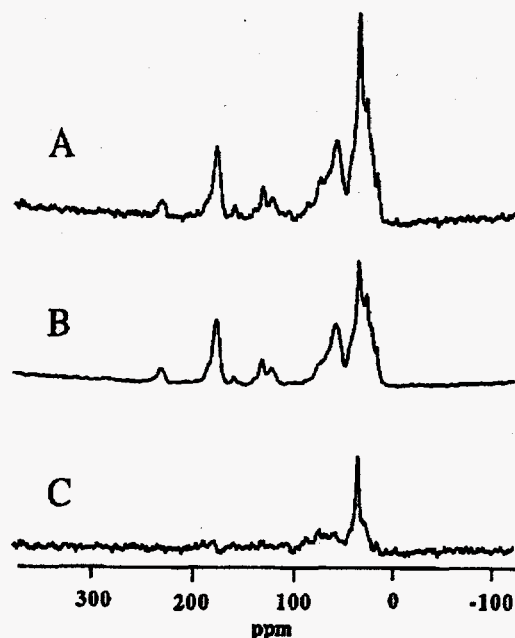


Figure 2. Solid-state  $^{13}\text{C}$  spectra of normal (A) and malignant (B) cells observed at  $-100^\circ\text{C}$ . (C) denotes the difference spectrum.

The main differences are a decreased intensity of the spectral line due to the lipid methylene groups in the tumor spectrum at  $-100^\circ\text{C}$ , and a minor difference in the protein composition. This is illustrated in Figure 2 (C), where the difference spectrum is given. At  $-40^\circ\text{C}$  in tumors part of these methylene groups become mobile, a phenomenon which was not observed in the normal cells. This result is consistent with the observation obtained with liquid-state nuclear magnetic resonance that tumor cells contain an increased amount of mobile lipids. It was concluded that both liquid-state and solid-state nuclear magnetic resonance are capable of discriminating between healthy mammary tissue, normal epithelial cells, and tumors, and may provide valuable contributions to an improved understanding of the cellular changes after transformation, and to the diagnosis of mammary cancer.

#### Publication

R.A. Wind, B.A. Concannon, K.M. Groch, D.N. Rommereim, and R.A. Santos. "An Investigation of Rat Mammary Healthy and R3230AC Tumor Tissues and Cells by means of Solid State  $^{13}\text{C}$  NMR." *Solid State NMR* (submitted).

## **Presentations**

R.A. Wind, B.A. Concannon, K.M. Groch, D.N. Rommereim, and R.A. Santos. 1995. "Solid State NMR and Cancer Research." 36th ENC, Boston (invited presentation).

R.A. Wind. 1995. "Studies of the Effects of Exposure on Cells and Tissues." Conference on Magnetic Resonance and the Environment, Richland, Washington.

B.A. Concannon, K.M. Groch, D.N. Rommereim, R.A. Santos, and R.A. Wind. 1995. "High Resolution High Field NMR of Normal and Malignant Mammary Tissues and Cells." 36th ENC, Boston.

R.A. Santos, B.A. Concannon, K.M. Groch, D.N. Rommereim, and R.A. Wind. 1995. "Solid and Liquid State NMR Studies of the R3230AC Mammary Adenocarcinoma in Model Fischer Rats." 37th RMC, Denver.

# X-Ray Absorption Fine Structure

Steven M. Heald (Molecular and Environmental Sciences Research)

## Project Description

This project is focused on the creation of an advanced x-ray microprobe, and other advanced x-ray absorption fine structure (XAFS) capabilities. The intent of this research was to push x-ray methods to new realms of spatial resolution, and to establish new x-ray methods for research on environmentally related problems. The effort is being conducted in collaboration with the Pacific Northwest Consortium Collaborative Access Team (PNC-CAT) which is developing these capabilities at the Advanced Photon Source (APS).

## Technical Accomplishments

The new generation of synchrotron radiation sources such as the Advanced Photon Source at Argonne National Laboratory, offer x-ray beams of unprecedented brilliance. These beams are well suited to applications such as an x-ray microprobe. If suitable optics are developed, submicron x-ray beams can be developed with intensities similar to the millimeter sized beams at current x-ray sources. Such microbeams allow advanced x-ray methods to be applied to complex and fine-grained materials and provide imaging capabilities complementary to standard optical and electron based methods. To develop this unique resource, a group of Pacific Northwest and Canadian institutions formed the PNC-CAT. During FY 1995, the PNC-CAT beamline effort has been moved forward significantly. Detailed effort has resulted in an insertion device beamline design which has passed the preliminary design review of the advanced photon source.

In FY 1995 we began producing and testing tapered capillary x-ray concentrators which will be the primary optic used in our microprobe. A fiber optics tower at the Laboratory has been modified to produce capillaries of varying diameter, and has been used to produce capillaries with linear taper. The results of x-ray tests performed at the NSLS are shown in Table 1. These results show that long capillaries can be produced to provide micron sized beams with efficiencies close to calculated values. This indicates that the inner wall of the capillary is a good x-ray reflector. These capillaries are already good enough to provide x-ray flux approaching 1010 photons/s/micron<sub>2</sub> when used at the advanced photon source. Work is ongoing to produce capillaries with non-linear tapers. These promise to increase the throughput by another factor of ten.

The intensity gain is the measured increase in the flux per unit area. We have continued to work with staff in carrying out x-ray experiments at the NSLS and elsewhere. Supercritical fluids are believed to have important technology applications, from extracting fat from eggs to environmental cleanup. In collaboration with John Fulton, Dave Pfund, S. Wallan, and C. Yonker, we continue to pursue x-ray absorption fine structure studies of supercritical fluids. In addition to XAFS experiments, we have experimented with sample cells with different windows, cells for supercritical CO<sub>2</sub>, and perform XAFS experiments on energy dispersive beamlines at the NSLS. In the future it is planned to use the focusing properties of the tapered capillaries to make novel sample holders for supercritical CO<sub>2</sub> and other high pressure fluids. Measurements at the Aladdin storage ring in Madison were made to assess the usefulness of Si and Al K-edge measurements for such areas as glass forming and tank wastes.

Table 1. Summary of measurements and calculations for three capillaries. Note: The measured inlet of capillary #19 was 156 mm but an effective size equal to the entrance pinhole diameter (150 mm) was used in the ray-tracing calculations of efficiency, and the calculation of intensity gain.

Capillary	Length	Inlet/Outlet Diameters	Intensity Gain	Measured Efficiency	Calculated Efficiency
#17	875mm	106/12.4 $\mu$ m	32	99.7%	99.7%
#19	548mm	105/1.3 $\mu$ m	274	3.6%	3.6%
#12	360mm	145/1.4 $\mu$ m	239	2.5%	2.5%

Work continued on developing x-ray resonant inelastic scattering spectroscopy. This should be an important technique with many applications to environmental problems. The technique can be used for structural determination and for studying electronic structures of complex materials.

#### Publications

S.M. Heald, J.E. Amonette, G.D. Turner, and A.D. Scott. 1995. "An XAFS Study of the Oxidation of Structural Iron in Biotite Mica by Solutions Containing Br<sub>2</sub> or H<sub>2</sub>O<sub>2</sub>." *Physica B* 209, 604.

D.T. Jiang, Z.Q. Gui, S.M. Heald, T.K. Sham and M.J. Stillman. 1995. "XAFS of Silver(I) Metallothionein." *Physica B* 209, 729.

Y. Ma, K. Miyano, P. Cowan, Y. Aglitzkiy, B. Karlin. 1995. "Anisotropy of Silicon K $\alpha$  Emission: Interference of Fluorescence X-rays." *Phys. Rev. Lett.* 74, 478.

Y. Ma and M. Blume. 1995. "Interference of Fluorescence X-rays and Coherent Excitation of Core Levels." *Rev. Sci. Instrum.* 66, 1543.

Y. Ma. 1995. "Soft X-ray Emission and Resonant Inelastic Scattering." *Synchrotron Radiation News* 8, 26 (a brief review).

#### Presentations

Y. Ma. 1995. "X-ray Resonant Inelastic Scattering: Wave-Particle Duality in X-ray Spectroscopy." International Workshop on X-ray Spectroscopy, Uppsala University, March 24-25, Sweden.

Y. Ma. 1995. "X-ray Resonant Inelastic Scattering: Wave-Particle Duality in X-ray Spectroscopy." University of Helsinki, March 26, Helsinki, Finland.

Y. Ma. 1995. "Young's Experiment, Wave-particle Duality and Coherence in Inelastic X-ray Processes." Workshop on x-ray absorption fine structure, May 7, NSLS, Brookhaven National Laboratory.

Y. Ma. 1995. "X-ray Resonant Inelastic Scattering." International Symposium on Synchrotron Radiation and Applications, Institute of High Energy Physics, Academic Sinica, July 11-15.

Y. Ma. 1995. "Young's Experiment, Wave-particle Duality, and Coherence Effects in Inelastic X-ray Processes." International Workshop on New Opportunities in Soft X-ray Emission Spectroscopy, August 26, Osaka Electro-optical Communications University.

Y. Ma. 1995. "X-ray Resonant Inelastic Scattering: Wave-Particle Duality in X-ray Spectroscopy." The 11th International Conference on Vacuum Ultraviolet Radiation Physics, University of Tokyo, August 28-September 1, Tokyo.



## **Nuclear Science and Engineering**



# *Boiling Water Reactor Advanced Fuels*

Bruce D. Reid, Edward F. Love, Andrew W. Prichard, and Sandra L. Harms (Safety and Performance Analysis)

---

## **Project Description**

The objective of this project was to develop the reactor physics capabilities needed to evaluate advanced boiling water reactor fuel concepts. The capabilities developed under this project are necessary to fully assess the benefits of advanced fuel concepts that have potential energy-efficiency improvements. Such improvements in energy efficiency would result in cost savings to nuclear utilities.

## **Technical Summary**

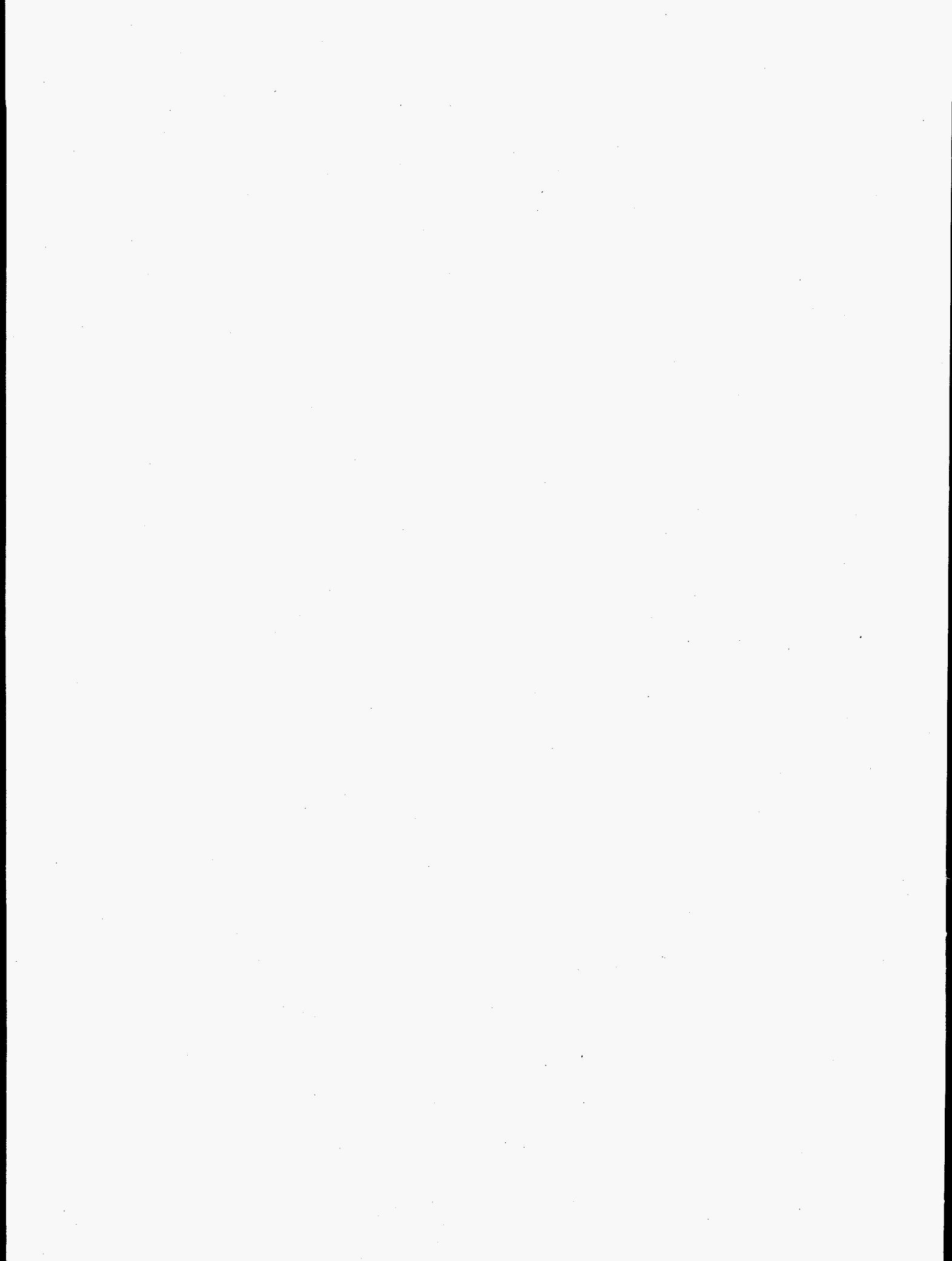
Three separate concepts were identified as having the potential to provide benefit to existing boiling water reactor fuel assemblies. Each of the three concepts were assessed as having the potential to provide improved neutronic efficiency and fuel performance capability. Reactor physics capabilities were developed to determine the technical feasibility of each of these concepts. A brief description of the three advanced boiling water reactor fuel product concepts follows.

- To improve fuel use in the upper regions of a boiling water reactor core, a spectral shift insert component that could be inserted into the lower region of a boiling water reactor bundle was devised. A reactor physics model was developed so that the capability now exists to specifically evaluate this advanced fuel concept.

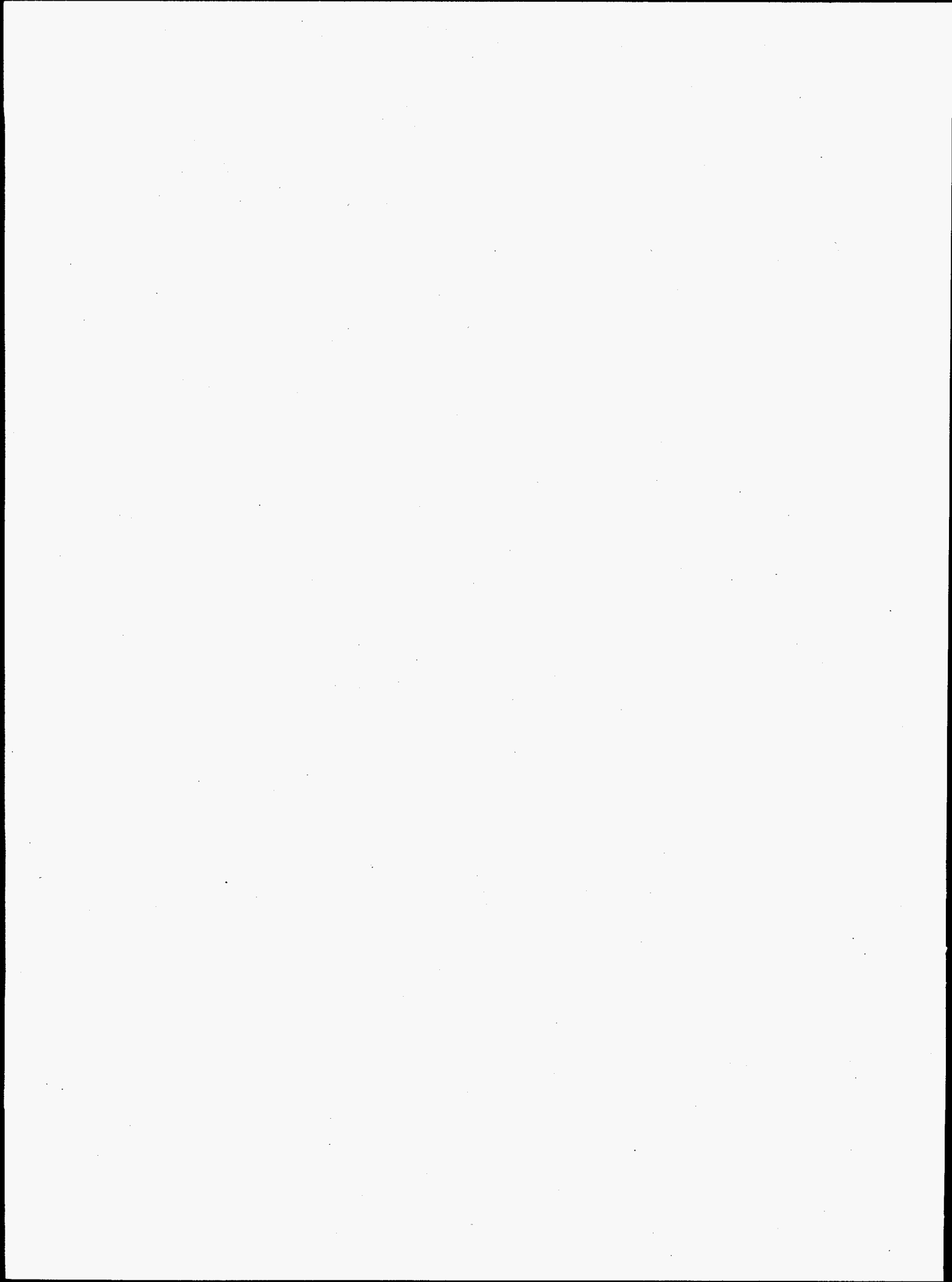
- A boiling water reactor solid moderator concept was devised to improve fuel use in the upper regions of a boiling water reactor core. Modifications to existing neutron cross-section libraries were made so that the capability now exists to evaluate the solid moderator concept.
- A burnable absorber coating concept was explored in an effort to remove lumped burnable poisons from boiling water reactor fuel assemblies. Reactor physics analysis capabilities were developed which will now permit the detailed evaluation of advanced fuel concepts such as this.

## **Publications**

Technical white papers were prepared that describe in detail the resulting evaluations of the three advanced fuel concepts that were enabled by the development of the new reactor physics capabilities. In each of the white papers, a description is provided of the new reactor physics capabilities that were developed and employed in the evaluation. These white papers, however, are not yet available for unlimited distribution.



## **Process Science and Engineering**



# ***Advanced Instrumentation Real-Time Acoustic Planar Imaging of Dense Slurries - RAPIDS***

Alireza Shekarritz (Analytic Sciences and Engineering)

---

## **Project Description**

For flow of rheologically complex fluids, such as the fluids commonly encountered in oil and gas, pharmaceutical, pulp and paper, polymer, and food processing, it is essential to monitor the mixture rheology in real-time. The mixtures are often optically opaque and exhibit pseudoplastic or shear-thinning behavior. Intrusive measurement techniques can lead to degradation in morphology of the material. Furthermore, off-line measurements are often too slow, may require stopping the process, and often do not represent the conditions encountered in the process lines.

The objective of this task is to demonstrate how an ultrasonic imaging system can be used to determine the local rheology of the process mixture in real-time. Two different set of parameters are important for rheological measurements 1) local viscosity and 2) local strain rate (shear and extension). The ultrasonic energy transmitted through a fluid is damped/attenuated by viscosity of the fluid. In general, for high Prandtl number Newtonian fluids, this attenuation is directly a function of the viscosity. Most polymers, for example, are very high Prandtl number fluids, in that viscous diffusion takes place much faster than thermal diffusion in these materials. Thus, from local attenuation measurements using this technique one should be able to measure local viscosity in a fluid. The local strain rate will be measured by locally measuring the velocity profile in the flow. The velocity profile is determined from following the motion of tracers in the flow as has commonly been done in particle image velocimetry (PIV).

## **Technical Accomplishments**

During FY 1995, we investigated the feasibility of using a novel approach for measuring the fluid velocity profile in a circular pipe. This approach was based on using the ultrasonic imager to capture frame-by-frame images of the flow field. When consecutive images are cross-correlated, the local displacement of tracers in the flow stream is obtained.

In an acoustic field, in order for a tracer element to be "visible," the acoustic energy would have to be scattered or absorbed by this tracer. This scattering commonly occurs as a result of a difference between the acoustic impedance of the tracer and its surrounding fluid. It has previously been demonstrated that if local heterogeneities as a result of concentration of solid particulate in a solid-liquid mixture exist in the flow stream, one may be able to obtain the flow velocity.

A uniformly mixed slurry or a polymer melt may not have local variations in the concentration that could be used to trace the flow. Introduction of foreign particles or bubbles as tracers may not be desirable in a production environment. In this task, it was shown that tracer elements could be produced without foreign particles, and the velocity profile can be obtained fairly accurately.

For demonstration of this technique, an existing ultrasonic imager called RTUIS (real-time ultrasonic imaging system) was used. An image was obtained using RTUIS. The flow was from the top to bottom and a bright line across the pipe section was caused by scattering of the acoustic energy by the fluid tracer element. The motion of the tracer element was followed in the downstream direction and the velocity across the pipe section was determined. The velocity profile is shown on Figure 1. The discrepancy between the measured and calculated velocities are caused by the flow not being fully axisymmetric or fully developed. But integration of the curves shows that the continuity or conservation of mass is satisfied.

In summary, this approach is clearly feasible for velocity measurement in pipes and will be adopted as an essential component of in-line acoustic rheometry of non-Newtonian slurries.

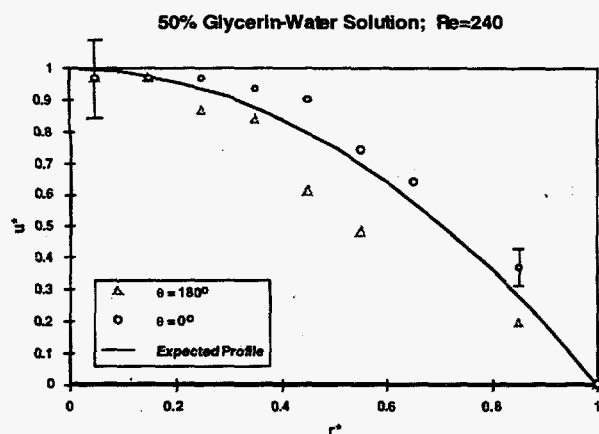


Figure 1. The velocity profile across the pipe obtained using the acoustic imaging technique compared to a fully developed velocity profile.

## Publications

A. Shekarriz and B.B. Brenden. 1995. "Planar Ultrasonic Imaging of a Two-Phase Mixture." *Journal of Fluids Engineering*, Vol. 117, No. 2, pp. 317-319.

A. Shekarriz, B.B. Brenden, and H.K. Kytömaa. "Planar Ultrasonic Technique for Visualization and Concentration Measurement in Dense Slurries." *Powder Technology* (submitted).



# Analytical and Reaction Chemistry

Donald M. Camaioni, Steven C. Goheen, and Amit K. Sharma (Chemical Sciences)

## Project Description

The objective of this project was to perform the analytical chemistry required to determine the overall chemical reaction mechanisms of low temperature plasma for treating organic contaminants. Over 90 percent removal of pentachlorophenol, an acutely hazardous chlorinated compound, was achieved in the corona reactor under a variety of conditions. High pressure liquid chromatography (HPLC), ion chromatography, and ultraviolet-visible (UV-VIS) spectroscopy were used to continuously follow the removal of pentachlorophenol, and to determine the total chloride content. Destruction of volatile chlorinated compounds such as perchloroethylene was also achieved in the corona reactor.

## Technical Accomplishments

It was determined in FY 1994 that ozone is the most abundant, neutral, reactive oxidant produced in a corona reactor. Ozone is formed in the head space of the corona reactor, which is largely air, by the corona-induced reactions. Previous work on glow discharge electrolysis by Hickling and Lincare (1954) indicated that the mechanism and rate of contaminant removal might depend on gas pressure. Hickling's work showed that production of hydrogen peroxide occurs at 50 torr, while we have shown that ozone is produced at atmospheric pressure. Hydroxyl radicals are extremely reactive, and therefore, react rapidly with aqueous pollutants.

In FY 1995, the corona onset voltage was found to reduce from 15 to 20 KeV at atmospheric pressure to 1 to 2 KeV at 50 torr, thus reducing the cost of power input to the reactor. The yields of oxidants were determined by using KI oxidation, in terms of oxidation events per electron discharged for a constant current at different pressures. It was found that as the pressure is varied from 50 to 300 torr, the yields vary from 9 to 33 events per electron for a constant current of 150  $\mu\text{A}$ . The yields are lower at lower pressure because the mole fraction of ozone produced at lower pressure decreases. Ozone reacts under a stoichiometry of 1:2 with KI.

Destruction of pentachlorophenol was investigated under atmospheric pressure conditions as well as at 50 torr. It was found that the rate of pentachlorophenol removal increases with increasing current (shown in Figure 1). The rate of pentachlorophenol removal using corona

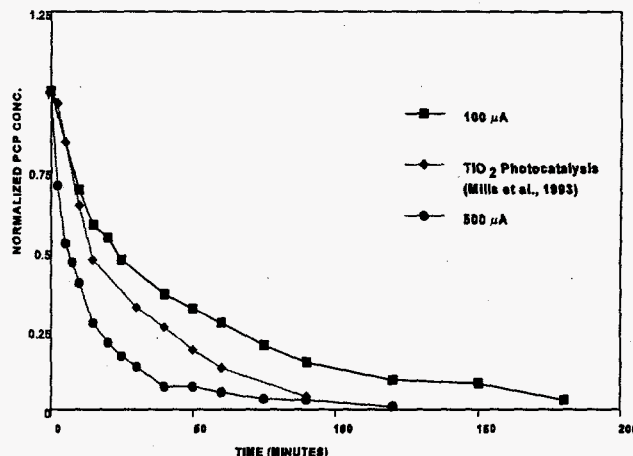


Figure 1. PCP Destruction Rate: Corona versus Photocatalysis

discharge has also been compared with that of pentachlorophenol removal by photocatalysis. A Kratos 450-W Xe arc lamp was used by Mills and Hoffmann (1993) for  $\text{TiO}_2$  assisted photochemical destruction of pentachlorophenol. Several different types of filters ( $\text{CuSO}_4$ , IR, etc.) were used to prevent heating and direct photolysis of the sample. Thus a large amount of power was wasted during the  $\text{TiO}_2$  assisted photocatalysis of pentachlorophenol. Whereas, the average power consumed by corona reactor for pentachlorophenol removal was between 1 to 3 W, therefore, corona discharge is significantly more efficient in removing pentachlorophenols from aqueous systems than  $\text{TiO}_2$  assisted photocatalysis.

The rate of pentachlorophenol removal in the corona reactor was found to be faster at 500  $\mu\text{A}$  than that by photocatalysis. Furthermore, the rate law for pentachlorophenol destruction by corona discharge as well as by photocatalysis was found to follow a mixed-order kinetic dependence on pentachlorophenol. An initial zero order decay with respect to pentachlorophenol concentration was followed by a first order decay by both corona discharge and photocatalysis in either photocatalysis or corona discharge systems, oxidants are produced at a constant rate. In the initial stages of destruction, oxidant generation is rate limiting. As the reaction progresses, the oxidants consume the organic pollutants such that the pollutant becomes the limiting reagent and therefore a first order decay is observed after 15 to 20 minutes.

Effect of variation in other parameters including stirring and pH upon rate of pentachlorophenol removal was also investigated. The rate of pentachlorophenol removal in the corona reactor was enhanced when the rate of stirring was increased. In addition, removal of pentachlorophenol at neutral pH (pH=7) was found to be faster than that under basic conditions (pH =11).

## References

A. Hickling and J.K. Lincare. 1954. "Glow Discharge Electrolysis Part II, The Anodic Oxidation of Ferrous Sulphate." *J. of Chemical Society* 711.

G. Mills and M.R. Hoffmann. 1993. "Photocatalytic Degradation of Pentachlorophenol on TiO<sub>2</sub> Particles: Identification of Intermediates and Mechanism of Reaction." *Environ. Sci. Technol.* 27, 1681-1689.

## Publication

A.K. Sharma, D.M. Camaioni, G.B. Josephson, S.C. Goheen, and G.M. Mong. "Formation and Measurement of Ozone and Nitric Acid in a High Voltage d.c. Negative Point-to-Plane Continuous Corona Reactor." *Journal of Environmental Health* (submitted).

## Presentations

A.K. Sharma, D.M. Camaioni, G.B. Josephson, S.C. Goheen, and G.M. Mong. 1995. "Formation and Measurement of Ozone and Nitric Acid in a High Voltage d.c. Negative Point-to-Plane Continuous Corona Reactor." Presented at AIChE 1995 summer national meeting, July 31, Boston, Massachusetts.

A.K. Sharma, D.M. Camaioni, G.B. Josephson, and S.C. Goheen. 1995. "Destruction of Chlorinated Phenols Using a Point-to-Plane Continuous Corona Process." Presented at Emerging Technology in Hazardous Waste Management VII: American Chemical Society, September 17-20, Atlanta, Georgia.

# Catalyst Development and Testing

Thomas D. Brewer and Charles H.F. Peden (Materials Sciences)

William J. Thomson (Washington State University, Department of Chemical Engineering)

---

## Project Description

This project developed and evaluated new catalytic materials for industrially important chemical reactions. The catalysts were novel metal oxides synthesized by unique methods including Rapid Thermal Decomposition of precursors in Solution (RTDS), nonaqueous synthesis of mesoporous materials, and direct intercalation of oligomeric cations between clay layers. The catalysts were evaluated for activity and selectivity for isomerization and alkylation. This project also developed the foundation for understanding the structural properties of the solid superacids which gave rise to the unique and interesting chemistry observed in these systems.

Catalytic reforming is the second most important process for converting hydrocarbons in petroleum refining after catalytic cracking. Alkylation and transalkylation of aromatic compounds are processes well known for their ability to produce products such as ethylbenzene, cumene, and linear alkylbenzenes, that are, in turn, important chemical precursors in the production of detergents and polymers. Alkylation catalysts that are known to produce alkylaromatic compounds include the commonly used Friedel-Crafts catalysts: sulfuric acid, phosphoric acid, hydrofluoric acid, and aluminum chloride. However, these catalysts typically produce undesirable byproducts such as oligomers and heavy polyaromatic compounds, as well as an extremely corrosive sludge byproduct.

There have been recent literature reports that amorphous zirconium, titanium, hafnium, iron, and tin oxides become superacidic after sulfation and subsequent thermal crystallization. Such superacidic catalysts hold great promise as replacements for the conventional Friedel-Crafts catalysts. Besides this application, sulfated superacidic oxides have shown great promise for a number of air-pollution control catalytic processes; notably, the removal of NO<sub>x</sub> from both stationary (power plants) and mobile (automobiles operating under "lean-burn" conditions) sources. As such, there is an opportunity to have a significant impact on the economy of a number of catalytic processes by the development of these materials.

## Technical Accomplishments

This project builds on the following previous efforts: 1) the Advanced Catalysts project for development of solid superacid catalysts, and 2) the project for nuclear magnetic resonance analysis of solid superacids. The parameters affecting solid superacid synthesis have been identified, catalytic materials have been screened for catalytic activity, and the existence of multiple types of acid sites have been identified.

Hammett acidity of sulfated zirconyl hydroxides was measured. The acidity of the acid-treated zirconium oxides is much higher than that of 100 percent H<sub>2</sub>SO<sub>4</sub> (pK<sub>a</sub> = -12) when the precursor hydroxide is dried below 400°C. The superacidity results from the presence of hydroxyl groups for sulfate condensation.

TGA data for the acid-treated zirconyl hydroxide samples was taken. An initial weight loss of each sample is observed and results from the desorption of adsorbed water. A second weight loss results from dehydroxylation. The third observed weight loss results from the decomposition of the acid and liberation of SO<sub>3</sub>. Sulfate loading decreases when the hydroxide precursor drying temperature is increased and is a direct result of the decreasing hydroxyl content of the heat treated hydroxide precursor.

The BET surface area and the sulfur content of sulfated zirconyl hydroxides were measured. BET surface areas are maximized, and S content remains relatively constant, when the hydroxide precursor is dehydrated but not dehydroxylated before sulfation. The catalytic activity of sulfated zirconia depends on the BET surface area and the sulfur content. Conversion of n-butane to i-butane is highest when the BET surface area is at its maximum.

# Ceramic Permeation Membranes

Glenn W. Hollenberg (Process Technology and Engineered System)

## Project Description

The objective of this project was to determine the ability of ceramic sodium-ion conductors for the separation of sodium metal from radiological impurities, specifically cesium, and the ability of alumina to select on the basis the molecular signature of sodium metal ions in comparison to cesium ions was assessed. Large quantities of alkaline-metal, mixed waste exist in the DOE complex and must be treated for recycling or disposal. The scope of this effort was to conduct nonradioactive tests on sodium-cesium mixtures in which it was anticipated that sodium was transported and cesium was not.

## Technical Accomplishments

Three activities have been completed with respect to this project 1) established a glovebox for handling sodium metal, 2) fabricated a sodium separation cell and demonstrated sodium separation, and 3) contacted sodium reactor representatives to better understand the problem.

Approximately 300,000 gallons of contaminated sodium metal has been used in primary loops, secondary loops, and other piping at FFTF, EBR-II, and FERMI reactors. Many approaches to stabilizing this material have included the construction of a facility which would decontaminate, react with water to form sodium hydroxide, and finally react with carbon dioxide to dispose of the material as sodium carbonate. The primary concept for decontamination in the past has been to distill the sodium by heating to greater than 1100°C and condense the purified sodium. In the approach pursued under this LDRD project, an electrochemical cell using a ceramic membrane ( $\beta$  alumina) would be used to separate sodium from radionuclides. The anticipated advantages were that 1) the technology was mature as a result of the sodium/sulfur battery activities, 2) the equipment is small and portable, hence avoiding costly facility construction and permitting cleanup at the point of extraction, and 3) the membrane was expected to be highly selective to sodium. It was the purpose of this project to initially evaluate the selectivity of the membrane with respect to one of the more troublesome isotopes, cesium.

The sodium separation experiments were conducted by mixing sodium metal and nonradioactive cesium metal in order to achieve 1900  $\mu\text{g/gm}$  of cesium in the sodium. A  $\beta$  alumina tube was purchased and inserted into the sodium mixture at temperatures between 258°C and 350°C. A small amount of "clean" sodium was placed on the inside of the tube to provide a conduction path. Upon application of up to 0.1 volt, a current of up to 1 ampere was achieved. Essentially all of the conductivity in beta alumina is due to sodium ion conduction. Hence, sodium metal filled the inside of the tube as electrochemical transport of the sodium occurred (i.e., electrorefining). Samples were taken after sodium transport at 258°C and again after transport at 350°C. The concentration of cesium in the anolyte sodium remained at 1900  $\mu\text{g/gm}$ . The concentration of cesium in the catholyte remained at the 4  $\mu\text{g/gm}$  which is near the detection limit under these conditions. Hence, no cesium transport could be measured in this experiment. On the basis of volume transported and uncertainty in the data a "separation factor" of greater than 500 was derived from this data, but the measurements are at the detection limit of sodium. Hence, it is recommended that separation experiments with radioactive cesium would be far more accurate in order to identify decontamination factors that may be as high as  $10^5$ . The cost of these experiments is anticipated to be much greater than the present investment.

Discussions with FFTF (WHC) and EBR-II (ANL-W) staff were conducted in order to assess the practicality of applying this technology. At FFTF most of the sodium has much lower radioactivities than initial predictions. At EBR-II, a visit to the sodium processing facility revealed that if primary sodium is to be processed for waste disposal prior to the year 2000, then sodium-22 will be the dominant radionuclide and addition of shielding to all phases of the process will be required. Obviously, this or other processes will not separate out a sodium isotope. If processing is done after the year 2000, then removal of cesium and other radionuclides would be valuable and personal dose would be reduced below 25 mR/hr. At EBR-II however, there are small volumes of sodium with very high cesium levels and this electrochemical approach could be very useful in those applications. The small size of these units means that processing could be done in existing hot cells. Discussions are continuing.

# Characterization of Rapid Dechlorinators: Remediation of DNAPL

Brian S. Hooker (Process Technology and Engineered Systems)

## Project Description

The primary objectives of this project were to identify and characterize rapid dechlorination metabolic activity in subsurface sediments taken from chlorinated ethenes contaminated sites as well as previously reported isolates and consortia obtained from other researchers. Characterization activities include batch kinetic and bottle studies necessary to acquire data to evaluate the efficacy of applying these organisms to chlorinated solvent non-aqueous phase liquid (NAPL) remediation.

## Technical Accomplishments

Anaerobic microcosms of subsurface soils from three chlorinated ethylene contaminated sites were used to investigate the separated effects of several substrates on tetrachloroethylene (PCE) dechlorination activity. The objective of these tests was to determine the prevalence of rapid dechlorination activity as well as the environmental conditions that stimulate this type of metabolism. Two of the sediments studied were obtained from a jet fuel and chlorinated ethylene contaminated region of Tinker Air Force Base, one (Tinker VZ) from the vadose zone at a depth of 15 feet BGS and the other (Tinker PA) from a sandy-silty perched aquifer at 37 feet BGS. The third sediment material (Victoria) was collected from a chlorinated ethylene contaminated aquifer that underlies the former DuPont Plant West Landfill near Victoria, Texas. Substrates tested in separate microcosms for each sediment included methanol, lactate, acetate, formate, and sucrose.

Sulfate reducing, acetogenic, fermentative, and methanogenic activity were stimulated in all three sediments. Microcosms using the Victoria sediment exhibited the most robust anaerobic activity as each of the five substrates tested were completely converted to methane with no volatile organic acids (VOAs) remaining in the cultures after 174 days.

The general metabolic responses of the two Tinker sediments to the added substrates were similar to the Victoria sediment, except that the cultures were less able to convert acetate to methane. This is evident since acetate-fed Tinker VZ samples did not generate any methane and only one of the acetate-fed Tinker PA samples converted the substrate to methane. In addition,

all the sucrose-fed Tinker VZ and Tinker PA microcosms fermented the substrate to acetate and propionate which were not further metabolized to methane. No hydrogen was measured in the headspace of the Tinker cultures. Some acetotrophic methanogenesis was exhibited by both Tinker sediments since all but one methanol-fed culture (Tinker VZ) produced acetate and subsequently converted it to methane. Acetate was also converted to methane in the lactate-fed Tinker VZ cultures.

Sulfate was typically consumed in both Tinker sediments during the first 130 days for cultures fed methanol, lactate, and sucrose. However, the acetate-fed cultures required much longer times before sulfate was eliminated from the media. The acetate-fed Tinker VZ samples never depleted sulfate while the acetate-fed Tinker PA sediments required 190 days before all sulfate was consumed.

PCE dechlorination products were detected in all microcosms. However, there was a large difference in the amount of dehalogenation activity among both the different substrates and sediments tested. Figure 1 shows the cumulative dehalogenation products measured at the end of the incubation period for each microcosm. Duplicate bottles for each condition are shown separately as bottles a and b. The average initial PCE level for all tests was  $0.76 \pm 0.09$   $\mu$ mole/bottle (aqueous concentration of  $1.42 \pm 0.17$  mg/L). The final mass balance for chlorinated ethenes in all bottles was between 87 percent and 114 percent (average of  $102 \pm 8$  percent). The primary dehalogenation product detected in all bottles was TCE. Small amounts of cis-DCE, 1,1-DCE, and VC were also measured at the end of the tests in both the methanol-fed and lactate-fed Tinker VZ cultures. In each case, these materials were present at levels less than 0.5 percent of that for TCE. cis-DCE, 1,1-DCE, and VC were also detected in the lactate-fed Victoria sediments after a second addition of substrate (data not shown). For all sediments, dehalogenation was associated with biotic activity since no dehalogenation products were detected in any of the autoclaved controls.

It is evident from Figure 1 that lactate was the most robust substrate for stimulating dechlorination since it was the only carbon source to create significant dechlorination products in more than one sediment. In contrast, sucrose and acetate gave little activity in any of the sediments and methanol generated significant dehalogenation only for Tinker VZ sediments. Also, although lactate could not



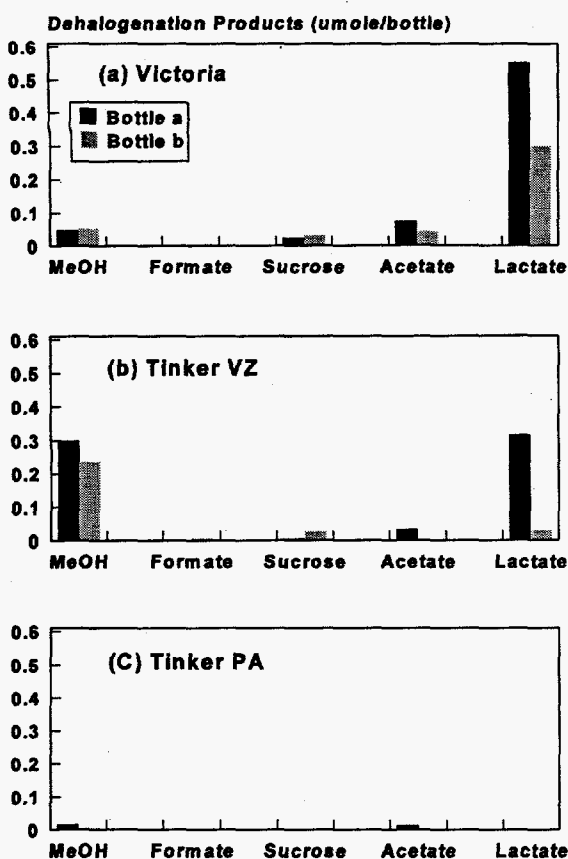


Figure 1. Endpoint results for dehalogenation products for the three sediments.

stimulate large amounts of dehalogenation activity in all bottles tested, as one of the two Tinker VZ bottles and neither of lactate-fed Tinker PA microcosms produced large amounts of dehalogenation products.

Examining the transient response of measured components for all cultures that gave large amounts of dehalogenation shows no consistent trend during the period when dehalogenation is occurring. In all cases, dehalogenation ensued after the added substrate was converted to organic acids. In addition, sulfate was always depleted prior to detecting less chlorinated daughter products. However, not all cultures which produced organic acids, or depleted sulfate showed large amount of dehalogenation.

For lactate-fed Victoria sediments and methanol-fed Tinker VZ sediments most dehalogenation occurred during a period when acetotrophic methanogenesis was occurring. However, acetate conversion to methane was not related to high dehalogenation activity since none of the acetate-fed, or sucrose-fed cultures produced large amounts of dechlorination products. In addition, the lactate-fed Tinker VZ sediment showed high levels of dechlorination after the bulk of the acetate had been converted to methane.

To compare the efficiency of the PCE dechlorination process in these experiments with those previously reported, the electron yield for each substrate was calculated based on measured amounts of dechlorination products at the final time point. All electron yields were adjusted to exclude reducing equivalents remaining in substrate, acetate, and propionate. Table 1 shows the highest electron yield for three sediment tested in this work compared to values shown from previously published data. Both the lactate-fed Victoria and Tinker VZ sediments have electron yields several orders of magnitude higher than those of methanogenic organisms, but lower than those of highly enriched dechlorinating cultures. It is unlikely that sulfate reducing or acetogenic organisms could account for the increased electron yields in these microcosm studies since others have shown that pure cultures of these organisms facilitate little PCE dechlorination (Ballapragada et al. 1995). In addition, there was no measurable dechlorination during periods of sulfate reduction in any culture and also no correlation between acetate production and dechlorination. Hence, these sediments are using more reducing equivalents for dehalogenation than can be accounted for by methanogenesis, sulfate reduction, or acetogenesis and it appears that these materials may contain organisms that facilitate highly efficient dehalogenation.

Table 1. Dechlorination Electron Yields

Source	Substrate	Electron Yield
Victoria	Lactate	$4.4 \times 10^{-4}$
Tinker VZ	Lactate	$1.6 \times 10^{-4}$
Tinker PA	Lactate	$8 \times 10^{-6}$
Methanol-enriched, anaerobic sediment <sup>(a)</sup>	Methanol	$2.4 \times 10^{-6}$
Methanosarcina mazei <sup>(b)</sup>	Methanol	$2.8 \times 10^{-6}$
Anaerobic digester sludge enrichment (DiStephano et al. 1991)	Methanol	0.31
Amended Rhine river sediment <sup>(c)</sup>	Lactate	0.38
Anaerobic digester sludge enrichment (Ballapragada et al. 1995)	Lactate	0.03
Anaerobic soil microcosm <sup>(d)</sup>	Mixed VOAs	0.05

(a) Yield value represents the overall yield for PCE dechlorination to ethylene calculated from the individual dechlorination yields for each step (Skeen et al. 1995).

(b) Yield value calculated from data shown in Table 1 of Fathepure et al. (1987).

(c) Yield value based on data reported in Figure 4 (DiStephano et al. 1992) and the assumption that all added substrate is consumed.

(d) Yield value calculated from the low substrate data in Figures 1 and 2 of Gibson et al. (1994) and assuming all the added VOAs were consumed.

Additional microcosm studies were completed on an anerobic sediment culture enriched for direct PCE dechlorination obtained from J. Gossett of Cornell University, Ithaca, New York (DiStefano et al. 1992). These studies focused on the effect of inhibition of methanogenesis on direct PCE dehalogenation activity. Methanogenesis was inhibited in separate microcosms through raising initial PCE concentrations to a maximum of 100 mg/L or through the addition of increasing levels of 2-bromoethanesulfonic acid (BES), a known inhibitor of methanogenic activity. BES-containing cultures were maintained at initial PCE levels of 2 mg/L. All microcosms were initially fed 50 mg/L methanol as the electron donor.

Sediments cultivated in the presence of increased PCE concentrations (10 and 100 mg/L) demonstrated greater rates of dehalogenation as well as inhibition of methanogenesis. Microcosms cultivated at 2 mg/L PCE in the presence of BES, at all concentrations tested, also showed little or no methane production. However, dechlorination activity in these sediments was significantly lower, as rates of PCE degradation were similar to those observed without methanogenesis inhibition.

From these studies, it was clear that the dechlorination rate was directly related to initial PCE concentration. However, it remains to be determined whether the increase in activity is due to either greater availability of electron acceptor (PCE) driving direct dechlorination or the absence of methanogenesis. An additional set of ongoing microcosm studies are focused on this determination.

## References

B.S. Ballapragada, J.A. Puhakka, H.D. Stensel, and J.F. Ferguson. 1995. In R.E. Hinchey, A. Leeson, and L. Semprini (eds.), *Bioremediation of Chlorinated Solvents*, Battelle Press, Columbus.

T.D. DiStefano, J.M. Gossett, and S.H. Zinder. 1992. *Appl. Environ. Micro.* 58:2287-2292.

T.D. DiStefano, J.M. Gossett, and S.H. Zinder. 1991. *Appl. Environ. Microbiol.* 57:2287-2292.

B.Z. Fathepure, J.P. Nengu, and S.A. Boyd. 1987. *Appl. Environ. Microbiol.* 53:2671-2674.

S.A. Gibson, D.S. Roberson, H.H. Russell, and G.W. Sewell. 1994. *Environ. Tox. Chem.* 13:453-460.

R.S. Skeen, J. Gao, and B.S. Hooker. *Biotechnol. Bioeng* (in press).

## Publications

J. Gao, R.S. Skeen, B.S. Hooker, and R.D. Quesenberry. 1995. "Effects of Several Substrates on Tetrachloroethylene Dechlorination in Anaerobic Soil Microcosms." *Appl. Environ. Microb.* (submitted).

J. Gao, R.S. Skeen, B.S. Hooker, and R.D. Quesenberry. "Tetrachloroethylene Dechlorination Process Evaluation by Subsurface Field Sediment Cultures with Various Substrates and Additives." (in preparation).

M.M. Shah, J. Gao, R.S. Skeen, and B.S. Hooker. "Characterization of Anaerobic Perchloroethylene Dehalogenation Activity at Varying Substrate and Perchloroethylene Concentrations." (in preparation).

## Presentations

B.S. Hooker, R.S. Skeen, J. Gao, M.M. Shah. 1995. "Kinetic Characterization of a Tetrachloroethylene Utilizing Microbial Consortium." Presented at the 34th Hanford Symposium on Health and the Environment, October, Pasco, Washington.

M.M. Shah, J. Gao, R.S. Skeen, and B.S. Hooker. 1995. "Characterization of Anaerobic Perchloroethylene Dehalogenation Activity at Varying Substrate and Perchloroethylene Concentrations." Presented at the 1995 ACS National Meeting, September.

J. Gao, M.M. Shah, R.S. Skeen, and B.S. Hooker. 1995. "Treatability Tests for Biodegradation of Perchloroethylene by Different Contaminated Site Sediments in Microcosm Cultures with Various Substrates." Presented at the 1995 ACS National Meeting, September.

# Colloidal Waste Science

Jeffrey E. Surma and Wesley E. Lawrence (Chemical Technology)

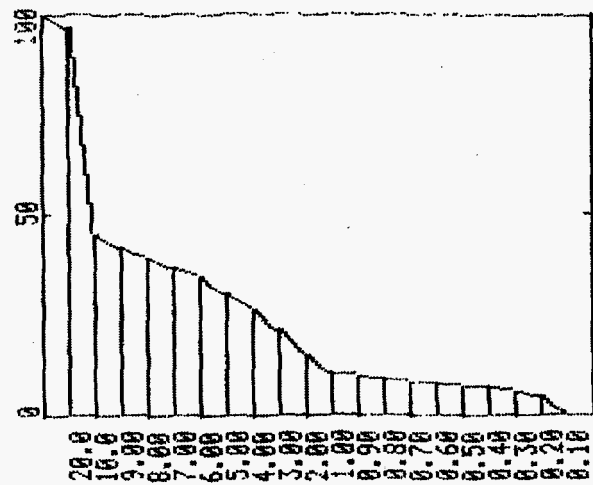
## Project Description

The objective of this project was to evaluate electrocoagulation as a possible enhancement to traditional solid-liquid separations. The problem of separating small colloidal particles poses problems for traditional separations methods across the DOE complex. At Hanford, the Tank Waste Remediation System (TWRS) and spent fuel storage basins require solid-liquid separations of fine particulate matter. The TWRS baseline involves retrieval of waste to filtration and ion exchange processes. Ultrafine particles are known to decrease the efficiency of filtration and potentially interfere with subsequent ion exchange processes. Therefore, electrocoagulation proof-of-concept with Hanford tank waste simulants will be conducted.

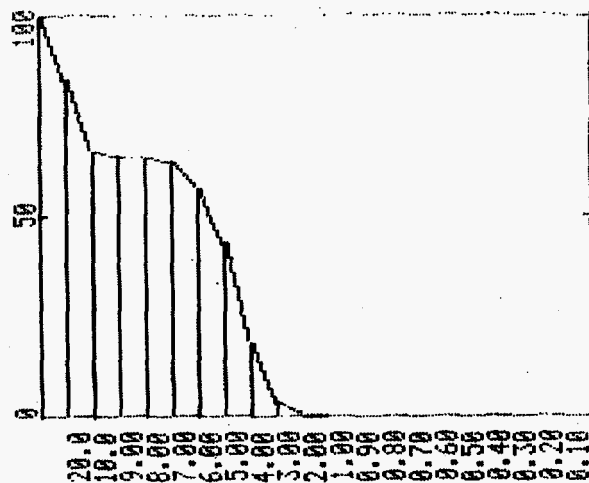
In addition, activities will involve evaluation of electrocoagulation for spent fuel storage basin simulants, as well as the development of a prototype flow cell for conducting a small scale demonstration. If successful this activity will demonstrate the applicability of this technology for enhancing solid-liquid separations involving ultrafine particles.

## Technical Accomplishments

Batch and flow cell experiments were conducted to evaluate the effectiveness of electroflocculation for Hanford tank wastes and fuel storage basin wastes. The Hanford tank waste simulant, 241-SY-101, and a simplified aluminum oxyhydroxide and sodium salt based solution were used for the electrocoagulation tests. A spent fuel basin simulant was developed based on data from the Hanford 200 Area East K-basin. Batch testing electrocoagulation experiments were carried out with each of the simulant types. An anodic current was applied to a sacrificial iron electrode. The iron (III) ion serves to agglomerate or flocculate the suspended ultrafine particles. These agglomerates will settle and/or filter more readily than their smaller counterparts. Figure 1 shows the change in the particle size distribution before and after electroflocculation treatment.



Particle Size (microns) Before Treatment



Particle Size (microns) After Treatment

Figure 1. Cumulative particle size distribution showing the change in size distribution for tank waste simulant before and after treatment.

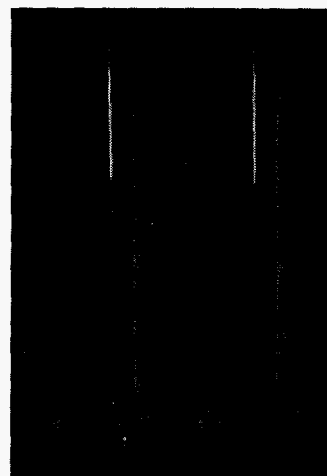


In the particle size range of interest (i.e., below 5 microns), the particles before treatment are distributed to the lower measurement bound of 0.1 microns. After treatment the distribution shifts showing fewer particles in the 0.1 to 1-micron range. Settling experiments support these results indicating the formation of larger agglomerates. Figure 2 shows the untreated and treated simulants side by side. The two solutions are shown for settling times at time zero, after 30 minutes, and after 180 minutes. These experiments show that the treated solution settles approximately three times faster than the untreated simulant.

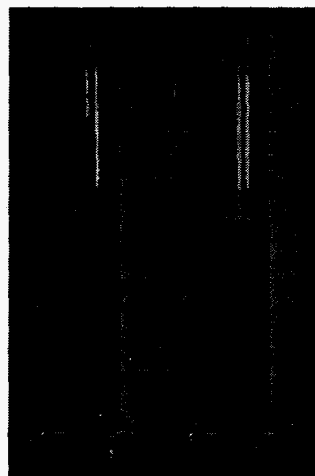
The batch electrocoagulation experiments were observed to be most effective for the low conductivity spent fuel basin waste. The higher conductivity present in the tank wastes simulants resulted in lower anode dissolution efficiencies as the oxidation of other species competed with the electrode dissolution. In an attempt to increase the iron dissolution rate, a high surface area flow cell design was implemented. Other investigators have had difficulties with standard plate and frame type designs as the cell design produces dead spots where solids would accumulate leading to decreased anode dissolution rates. Therefore, a semi-fluidized bed design using steel shot as the sacrificial anode was investigated.

The flow cell apparatus was evaluated using the boehmite tank waste simulant. Testing showed an increased rate of anode dissolution, though visual inspection of sampling settling rates showed that the treated material had an increased settling time over the untreated samples. The longer settling time in the treated simulant was attributed to mechanical pumping shear forces that destroy agglomerates and even further reduce particulate size. Lower pump flow rates were observed to increase the settling rates, by reducing the mechanical degradation of particulates, but the lower flow velocity within the cell reduced the efficiency of anode dissolution. Higher operating currents were used to increase the oxidation rate of the steel shot; though, operating costs in a practical process would be prohibitive as a significant portion of the power supplied was going toward side reactions and resistive heating.

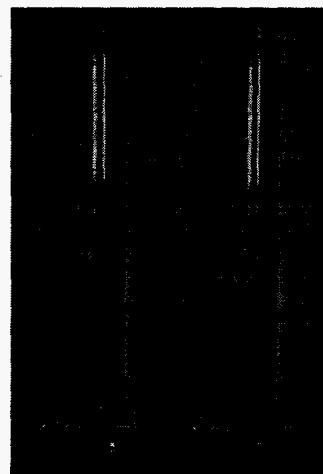
These activities showed that electroflocculation enhanced simulant settling rates for batch experiments. However, issues with flow cell design and agglomerate mechanical stability were observed during flow cell testing. Higher process throughput and efficiency will require improved cell designs that take advantage of high surface area electrodes and minimize mechanical forces on the particles.



Zero Minutes



30 Minutes



180 Minutes

Figure 2. Settling experiments with treated and untreated K-basin simulant solution. The treated solution is on the right.

# *Development of Carbonate Barriers for In Situ Containment<sup>(a)</sup>*

Rahul R. Shah (Process Technology and Engineered Systems)

---

## **Project Description**

The objective of this project was to investigate the feasibility of emplacing a vadose zone barrier of calcium carbonate (limestone) via the reaction of an aqueous solution of calcium hydroxide with carbon dioxide gas. This reaction would take place in the soil beneath a contaminated area such that the calcium hydroxide would precipitate within the pores of the soil beneath the waste site, thus sealing the pores to form a barrier. Ideally, this barrier would be similar to natural calcareous formations which are relatively impermeable to water flow and are especially resilient or self-healing in alkaline environments. The original concept for barrier formation entailed introducing the calcium hydroxide solution into the soil, possibly through the use of horizontal wells located below the waste site. Carbon dioxide would be bubbled upward from horizontal wells located below the calcium hydroxide wells, such that a calcium carbonate barrier could be formed in between the two groups of wells. Recent efforts have explored the iterative addition of two aqueous reagents for the formation of the barrier material.

## **Technical Accomplishments**

In FY 1994, carbonate barrier formation tests were performed in an unsaturated column of 90  $\mu\text{m}$  glass beads, using countercurrent streams of carbon dioxide gas and calcium hydroxide solution under alkaline conditions ( $\text{pH} > 12$ ). Different reactant injection techniques were tried, using both countercurrent and co-current flow. Calcite, which is the predominant crystalline form of calcium carbonate, was most successfully precipitated (70 to 80 percent conversion) when carbon dioxide was bubbled in from approximately one inch above the bottom of the packed bed while calcium hydroxide solution was dripped from the top. The permeability of the column was measured using a falling head technique, and no change in permeability was seen.

During the initial phase of FY 1995, it was determined that using calcium hydroxide solution and carbon dioxide gas would be technically infeasible for forming a calcium carbonate barrier in situ. Calcium hydroxide is relatively insoluble in water (0.17 g per 100  $\text{cm}^3$  water), which

would entail injecting over 1300 pore volumes of solution to completely fill the soil pore space. Also, the solubility of calcium carbonate increases with increasing acidity. Thus, the addition of carbon dioxide must be quite precise, as any excess will result in the formation of  $\text{HCO}_3^-$ , which lowers the pH of solution and subsequently solubilizes the barrier material.

The next approach for barrier emplacement involved an iterative addition of reagents to the soil column. The reagents chosen were calcium chloride and sodium carbonate, as the byproduct of reaction would be sodium chloride solution (besides the precipitated calcium carbonate) which, compared to other byproducts, is quite innocuous. These solutions were also chosen due to their higher solubilities, enabling a barrier to be emplaced with less pore volumes of solution. These reagents were added to both 90  $\mu\text{m}$  glass beads and Hanford McGee Ranch silt. The addition of 2.5 pore volumes of reagent to the soil resulted in a 75 percent reduction in permeability as measured by the falling head technique. However, a control test utilizing only sodium carbonate solution resulted in a 66 percent reduction in permeability after 2.5 pore volumes of solution were added. The precipitate was washed out of the soil column very quickly with little pressure or superficial fluid velocity. Two potential reasons for the precipitate washing out were the fine size of the precipitate, and the surface charge of the precipitate. The zero point charge of calcite occurs at a  $8.0 < \text{pH} < 9.5$  in most natural waters, and above this pH the surface charge of calcite is negative. As most soils have a negative surface charge, there would be an electric repulsion between the soil particles and the precipitate.

The next approach involved choosing an additive that would result in a larger precipitate, or one that would induce the precipitate to "stick" to the soil medium. Iron (III) chloride was chosen, due to its historical use as a coagulant aid and its low pH in solution. The low pH was desired as it could induce an electric attraction between the precipitate (which tends to be positive in neutral to lower pH solutions) and the surface of the soil particles. Compared to other potential coagulants (such as aluminum sulfate, sodium silicate, and sodium aluminate) iron chloride was determined to be the least environmentally disruptive additive. A ferric chloride and calcium chloride solution was added to McGee Ranch silt and

---

(a) This project is another task related to the project entitled, "In Situ Containment Using Heat Enhanced and Carbonate Barriers."

followed with sodium carbonate solution. A total of 0.45 pore volumes of reagent was added, and resulted in an 83 percent decrease in permeability.

Although adding ferric chloride to the reagents resulted in a larger decrease in permeability than resulted from the sole addition of the reagents, it was decided that further exploration of additional coagulation aids or cationic

surfactants would not be pursued. Due to the large array of materials available for subsurface barriers, pursuing calcium carbonate as a material would not be further recommended, unless a technically feasible and unique emplacement method can be employed in conjunction with the formation of a calcium carbonate barrier.

# *Electric Field and Current Modeling of Electrical Discharge Processing*

Delbert L. Lessor (Analytic Sciences and Engineering)

---

## **Project Description**

Electrical discharges and the resulting cold plasmas offer potential benefits in environmental cleanup, waste treatment, energy utilization, and chemical synthesis. Chemicals successfully destroyed in electrical discharges include aliphatic hydrocarbons, benzene, toluene, methylene chloride, trichlorotrifluoroethane, and phosgene.

The goals of this project were to develop a fundamental understanding of the electric field and electrical discharge conditions and electron-induced chemistry in advanced electrical discharge reactors and novel reactor configurations. Specifically, a voltage-current model for a coaxial cylinder geometry packed bed corona reactor driven at power line frequency is being developed to predict voltage/current relationships in this device, and this model is being linked to a computation of the plasma electron energy distribution and a computation of the electron-impact induced chemical reaction rate constants. These effective reaction rate constants will be used in a computation of the chemical evolution of the gas as it flows in the axial direction. The result of this model development work should be a capability to predict performance of such a packed bed corona reactor for candidate mixtures and chemical processes, provided cross section information is available.

## **Technical Accomplishments**

An electric field program identified as EI has been written to compute the transient electric field over a few cycles of

the power line frequency alternating voltage applied to the packed bed corona reactor. Program EI assumes charge carriers of three types with their corresponding mobilities: electrons, negative ions, and positive ions. Processes modeled include: field-induced charge transport, electron impact ionization, electron attachment, emission of electrons at electrode surfaces, volumetric production of free electrons by ultraviolet processes, and microdischarges between beads. The ultraviolet and microdischarge models are simple parameterizations. Transient deposition and dissipation of charge on the dielectric barrier is modeled. Typical calculated current waveforms with a harmonic driving voltage are shown in Figure 1. Calculated radial distributions of currents associated with each of the three charge carrier species is shown in Figure 2 at the negative half-cycle peak.

The electric field and electron current distributions in space and time are used in the calculation of direct electron-induced chemical reactions, such as O<sub>2</sub> breakup. An electron energy distribution, calculated by Boltzmann equation solver ELENDF, was used in this process. Integrations of the product of cross section and flux over electron energy, radial position, and time within a cycle are performed to obtain rate constants for the electron impact-induced processes.

The rate constants for electron impact-induced processes are used in the CHEMKIN chemical kinetics code for a calculation of chemical evolution in the flowstream direction.

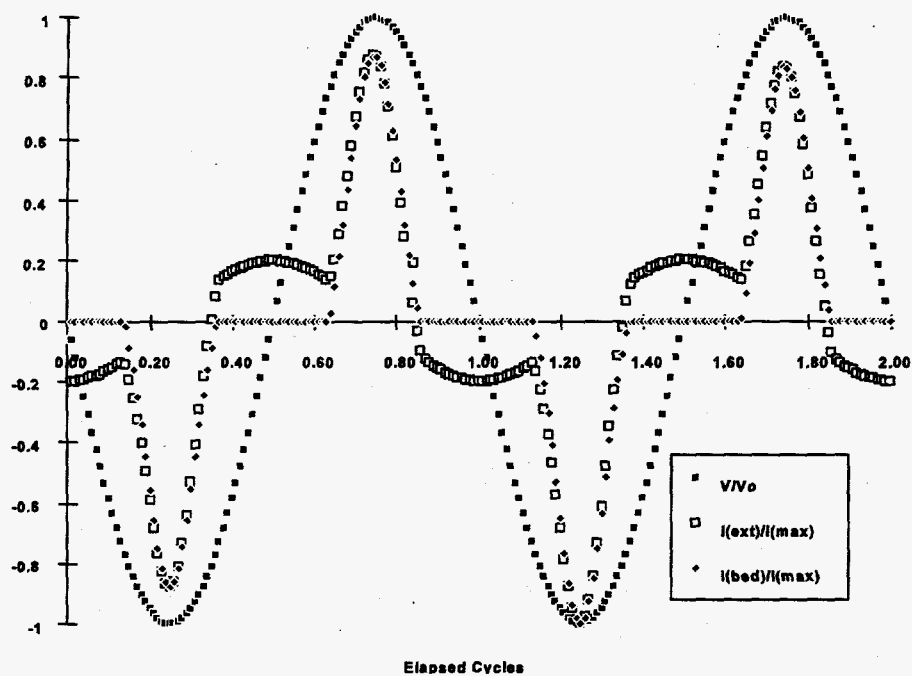


Figure 1. Calculated Current Waveforms

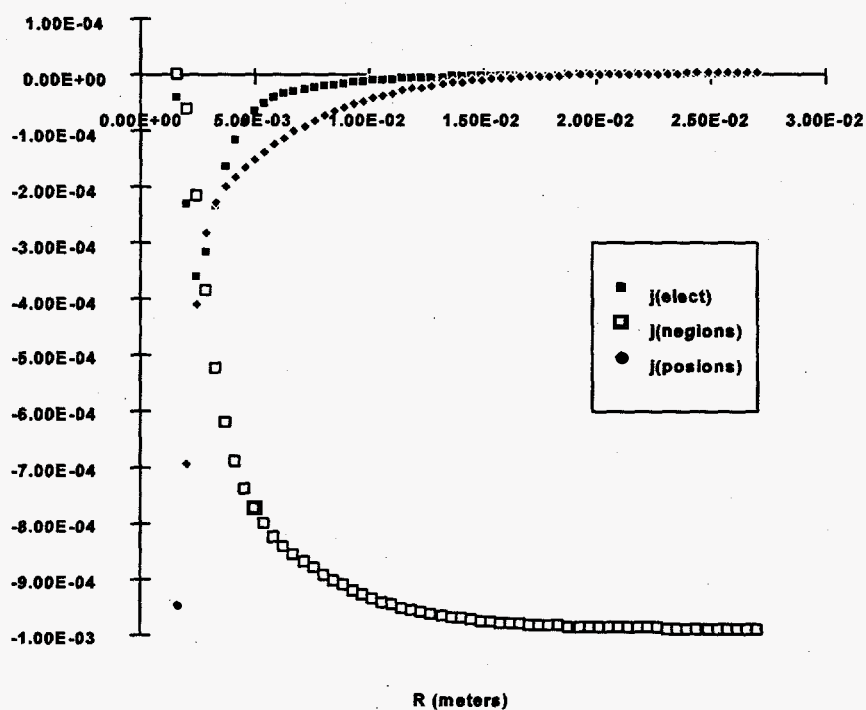


Figure 2. Calculated Radial Distributions of Currents for Three Charge Carrier Species

# Electroactive Materials

Jeffrey E. Surma, Mark F. Buehler, and Johannes H. Sukamto (Chemical Technology)

## Project Description

The objective of this project was to develop a capability in electrochemical processing—specifically, using an electric potential to control the ion exchange capacity of a material. This new approach, is termed electroactive ion exchange. The work will develop the electroactive ion exchange technology with an emphasis on providing experimental data for a large-scale process design and developing a portable, disposable sensor that operates using the technique. Although the approach will be verified by studying a system for cesium removal relevant to the Hanford site cleanup, the selectivity of the exchange can be readily altered to address industrial separation needs such as toxic metal ions.

The scope of this activity involved the development of new electroactive surfaces, characterization of the surfaces, and design and fabrication of laboratory-scale working models implementing the new electroactive materials. Initially, the work focused on Hanford problems (i.e., cesium removal from Hanford tank waste), and initial demonstrations were limited to cesium removal. Ultimately, it is anticipated that other surfaces will be developed for the removal of ions, such as heavy metals, from waste water. If successful, this activity will demonstrate a new efficient ion exchange process in a laboratory-scale system for the removal of cesium from Hanford tank waste.

## Technical Accomplishments

Nickel ferricyanide films were deposited onto industrially available porous nickel electrodes. In this system, the oxidation state of the Fe (+2 or +3) is easily controlled by relatively small changes in the applied voltage (100 to 300 mV). When a cathodic potential is applied to the film,  $\text{Fe}^{+3}$  is reduced to the  $\text{Fe}^{+2}$  state, and a cation must be intercalated into the film to maintain charge neutrality (i.e.,  $\text{Cs}^+$  is uptaken). Conversely, if an anodic potential is applied to the film, the  $\text{Fe}^{+2}$  is oxidized to the  $\text{Fe}^{+3}$  state, a cation must be released from the film (i.e.,  $\text{Cs}^+$  is desorbed or eluted). Therefore, to uptake Cs, the film is simply reduced; to elute Cs, the film is oxidized.

Several proof-of-principle experiments were performed with the nickel ferricyanide system to validate the approach. Nickel electrodes, with surface areas up to  $100 \text{ cm}^2$ , were coated with a ferricyanide ion exchange film, and the Fe oxidation state was modulated electrochemically. The experiments showed that the Fe oxidation state (+2 or +3) can be easily changed without water electrolysis. The redox reaction of Fe (+2 and +3) in a nickel ferricyanide film was cycled several times in sodium sulfate solution. The film is extremely reversible with little capacity loss (i.e., decrease in peak current) after several uptake/elution cycles. The film stability is substantially higher than the baseline ion exchange technology which is estimated to be economical for only 20 to 30 cycles. We have also shown qualitatively that the deposited nickel ferricyanide films are selective for Cs.

Figure 1 shows three cyclic voltammograms for a nickel ferricyanide film in solutions of: 0.66 mM  $\text{CsNO}_3$ , 0.5 M  $\text{Na}_2\text{SO}_4$ , and a mixture of 0.66 mM  $\text{CsNO}_3$ /0.5 M  $\text{Na}_2\text{SO}_4$ . The peak current for the pure 0.66 mM  $\text{CsNO}_3$  solution is significantly lower than that of the pure 0.5 M  $\text{Na}_2\text{SO}_4$  solution. This is primarily due to the lower Cs concentration. The peak current in the mixture was also found to be lower than that measured in the pure  $\text{Na}_2\text{SO}_4$ . This strongly suggests that the deposited film preferentially uptakes and elutes Cs even in the presence of a high Na concentration.

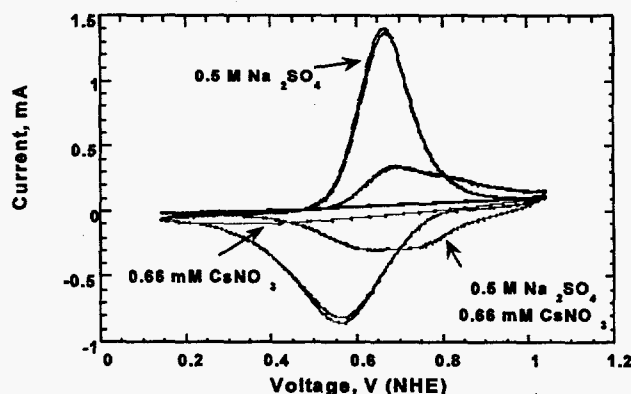


Figure 1. Cyclic voltammograms of a nickel ferricyanide film in 0.5 M  $\text{Na}_2\text{SO}_4$ , 0.66 mM  $\text{CsNO}_3$ , and a mixture of 0.5 M  $\text{Na}_2\text{SO}_4$ /0.66 mM  $\text{CsNO}_3$  showing Fe oxidation and reduction reactions.

For scale-up demonstration there are several relevant engineering issues to address. Some of these will be similar to those that have been investigated for traditional IX applications using ferricyanides, such as capacity, stability (physical and chemical) of the ferricyanides, and process flowrates. Additional issues to consider include electrochemical Cs uptake and elution rates, film lifetime, and ease of film regeneration. It should be noted that although this work is targeted on  $^{137}\text{Cs}$ , the ferricyanide films can also be used to separate other alkali metals, alkaline earth metals, rare earth metals, and transition metals.

#### Publication

M.F. Buehler and J.E. Surma. 1995. "Electrochemical Processes." In *Separation Techniques in Nuclear Waste Management*, Eds. T.E. Carleson, N.A. Chipman, and C.M. Wai, Chapter 6, CRC Press Inc., pp. 91 - 107.

#### Presentations

M.F. Buehler, J.P.H. Sukamto, J.E. Surma, J. Bontha, W.E. Lawrence, and G. Pillay. 1995. "Electrically-Enhanced Separations for DOE Tank Waste." Electrochemical Society Meeting, Reno, Nevada.

M.F. Buehler. 1995. "Environmental Electrochemistry: Prospects, Issues, and Applications for the Hanford Site." PNW Electrochemical Society Meeting, Seattle, Washington.

# Electroconversion

Jeff E. Surma, Mark F. Buehler, and Wesley E. Lawrence (Chemical Technology)

## Project Description

The objective of this project was to develop new, safe electrochemical techniques for the conversion of hazardous waste materials, such as energetics, to innocuous species or into useful products. The aim was to develop and demonstrate the electrochemical conversion process with an emphasis on providing process operating information and scaling data, as well as development of a safe controlled solubility limited dissolution of solid energetic material. This work focused on conversion of high explosive (HE) materials that have been identified as a safety and disposal need at DOE facilities such as Pantex.

The scope of this activity involved the evaluation of process chemistry, the development of electrochemical methods to drive the desired chemistry, and the demonstration of the developed methods on actual waste materials. The anticipated outcome of this effort is a working laboratory-scale process in which energetic waste materials can be processed to either useful product chemicals or are rendered safe for disposal. If successful, this activity will demonstrate the applicability of this technology for conversion of energetic materials and as a viable alternative to thermal processes.

## Technical Accomplishments

Direct electrochemical reductive destruction of a high explosive; specifically, HMX was demonstrated. Destruction of the HMX was demonstrated in both water and water/cosolvent systems. In Figure 1 the destruction of HMX is shown by comparison of the HPLC chromatograms before and after electrochemical treatment.

Figure 2 shows HMX destruction in water and cosolvent systems. At 100 percent water and 100 percent cosolvent (dimethyl sulfoxide, DMSO), concentrations the applied potential was 0 V versus saturated calomel electrode (SCE) for the first 60 minutes, followed by -1.0 V (saturated calomel electrode) for 60 to 120 minutes,

(saturated calomel electrode) was significant destruction. In comparison, no destruction of the high explosive was observed at a concentration of 100 percent cosolvent. The high explosive material is strongly solvated and difficult to reduce. However, at intermediate cosolvent concentration in water (50:50) the rate of destruction was approximately

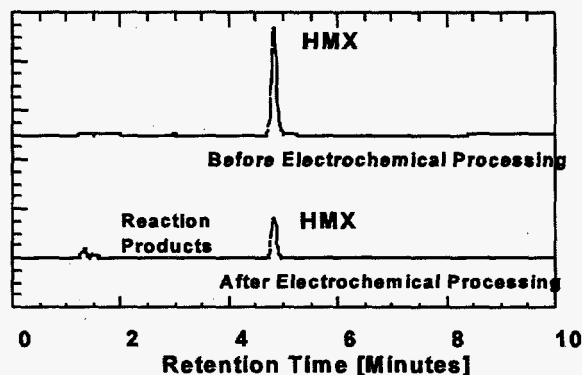


Figure 1. HPLC chromatograms showing destruction of HMX as a result of electrochemical processing (-2.0 V versus SCE for 60 minutes). Top chromatogram is before processing, bottom chromatogram after processing.

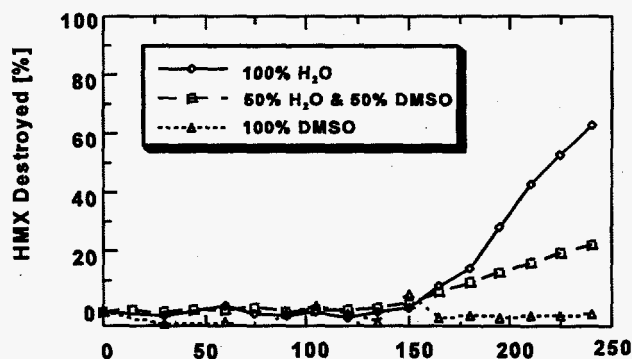


Figure 2. HMX destruction extent as a function of time for electrochemical reduction in 100% H<sub>2</sub>O, 100% DMSO, and 50:50 H<sub>2</sub>O and DMSO. Applied potential vs. SCE for 100 H<sub>2</sub>O and 100% DMSO: 0 to 60 minutes, no current; 60 to 120 minutes, -1.0 V; 120 to 180 minutes, -1.5 V; 180 to 240 minutes, -2.0 V. Applied potential vs. SCE for 50% water and 50% DMSO by volume: 0 to 120 minutes, -1.5 V; 120 to 240 minutes, -2.0 V.

-1.5 V (SCE) for 120 to 180 minutes, and -2.0 V (saturated calomel electrode) for 180 to 240 minutes. Only at values greater than -1.5 V (saturated calomel electrode) was significant destruction observed in the 100 percent water system. The rate of destruction was 0.06 ppm/min in water at -2.0 V (greater than -1.5 V) 0.04 ppm/min showing that electrochemical reduction of the high explosive in cosolvent is feasible. The role of the cosolvent is to enhance the high explosive solubility over water alone.



Dimethyl sulfoxide was selected as the primary cosolvent because of its excellent solvating properties, ability to swell the fluoroelastomer binder material, and excellent oxidative and reductive stability. Through communications with Pantex, DMSO was identified as a primary solvent for high explosive recovery. The stability of the cosolvent was investigated under both oxidative and reductive conditions. Under reductive potentials up to -2.0 V, the DMSO did not degrade. In an oxidative environment, 4 M HNO<sub>3</sub> and 1.5 M cerium electrogenerated to the cerium(IV) state, the DMSO was observed to be stable. These results indicate that DMSO would be stable under nominal process operating conditions.

Based on these activities a preconceptual process flowsheet was developed to take advantage of the benefits offered by electrochemical processes over traditional

methods of treating high explosive. Issues to consider include reducing personnel exposure through decreased handling of high explosive, emissions of toxic gases, and the generation of secondary waste streams.

#### **Presentations**

G. Pillay, W.E. Lawrence, J.P.H. Sukanto, J.E. Surma, and M.F. Buehler. 1995. "Electrochemical Destruction of Explosives." AIChE National Meeting, Boston, Massachusetts.

N. Nelson, G.A. Steward, and W.E. Lawrence. 1995. "Mediated Electrochemical Destruction." Workshop on Advances in Alternative Demilitarization Technologies, September, Reston, Virginia.

# *Enhanced Mixing for Supercritical Fluid Oxidation—Phase Separations*

Fadel F. Erian and David M. Pfund (Analytic Sciences and Engineering)

---

## **Project Description**

The supercritical water oxidation process has great potential for use in the pretreatment of mixed wastes. The solubilities of organic compounds in supercritical water are enhanced, and those of inorganics are reduced relative to ambient water. Thus, the use of this solvent offers the possibility of simultaneously oxidizing organic and separating inorganic wastes. In addition, aggregation of solute and solvent molecules occurs which causes solubilities, and sometimes reaction rates, to be strong functions of pressure as well as temperature. Thus, control of pressure provides an additional way of manipulating the reaction. In a process which utilizes this chemistry, three conditions need to be fulfilled:

1. Contaminants must be desorbed from the solid matrix into the supercritical solvent.
2. Oxidant and contaminant loaded solvent must be combined.
3. Fine, uniform suspension of solids must be maintained.

The last condition is necessary to allow the development of a continuous, steady-state process which allows no build-up of solids or reaction products. A continuous process is more desirable than a batch process in most cases involving large throughput because of the lower equipment cost and/or higher stream factor of the continuous process. A technology of mixing in supercritical fluid systems needs to be developed to meet these conditions. A cylindrical vessel with several concentric baffles is capable of mixing the fluid and suspending the solids using only the over-and-under motion of the fluid around the baffles without any mechanical mixing. We proposed to investigate mixing in such a vessel using a two-dimensional analogue. The flat, multi-pass vessel represented a vertical section of a cylindrical, baffled vessel. The moving fluid was examined through a series of vertical windows in the face of the vessel. Initial studies were made using supercritical carbon dioxide instead of water to avoid corrosion problems.

The extent of mixing of contaminant and oxidant streams was determined using fluorescence spectroscopy. A fluorescent probe molecule was dissolved in the carbon dioxide - a probe whose fluorescence is quenched by

oxygen. A vertical sheet of light from an ultraviolet-enhanced argon ion laser was used to excite the probe, thus providing a luminous cross section of the fluid. The cross section of the fluid was viewed at a right angle to the laser beam with a CCD-based camera. The second stream containing oxygen was mixed with the carbon dioxide stream so that the oxygen could react with the probe and quench its fluorescence. Uniform, low fluorescence across the flow path indicates good mixing between the carbon dioxide and oxygen streams.

## **Technical Accomplishments**

In FY 1994 the requirements for the laser optics and carbon dioxide flow loop systems were determined. A carbon dioxide pump, laser optics, and optical mounts were acquired. Estimates were made of the luminescence from the experiment. From these estimates specifications for the laser and camera were determined. Several candidate probe species were selected for batch tests and the necessary chemicals and equipment for such tests were acquired. Flow rates, temperatures, and pressures of oxygen and carbon dioxide were determined and equipment sizing began. Preliminary contacts were made with laboratory safety personnel to begin the development of procedures for safe operation of the laser and of the high pressure oxygen system.

In FY 1995 we were able to acquire some laboratory space in the PDL-W high bay building. Utilities such as water, compressed air, and electrical power had to be brought to the location of the planned experimental facilities. The laser equipment which had been specified and defined during FY 1994 was purchased using non-LDRD funds. Based on the planned experimental program, a process design was completed for the pipe loop. An engineering firm was contracted to produce mechanical and electrical designs based on the supplied process design. Most process instrumentation and control equipment have been procured except for two relatively small pressure vessels and two pressure sensors.

Partial fabrication of the pipe loop facility has been carried out. This includes the structural fabrication of the support skids and most of the CO<sub>2</sub> system piping assembly. The control system software (Labview) is nearly 75 percent complete.

# *Evaluation and Selection of In Well Separations*

Thomas M. Brouns and Ward E. TeGrotenhuis (Process Technology and Engineered Systems)

---

## **Project Description**

In-well treatment of groundwater contaminant plumes offers several advantages over conventional pump and treat scenarios, including reduced operating and equipment costs, as well as ALARA and regulatory benefits. Currently, the technology is being applied to remediate groundwater that is contaminated with volatile organics using vapor stripping and bioremediation techniques. The intent of this project was to extend the base of in-well technologies to treatment of metals and radionuclides. One objective was to develop a prototype process by determining functional requirements for a test apparatus and producing a detailed design with specifications and costs. A second objective was to extend flow modeling that was performed to include transport modeling, in order to estimate remediation time-scales and to facilitate development of remedial strategies.

## **Technical Accomplishments**

A serious problem throughout the DOE complex, as well as private industry, is groundwater plumes contaminated with heavy metals and radionuclides. The conventional strategy for treating groundwater plumes is pump and treat with multiple extraction wells or the combination of extraction and reinjection wells. Sorption of contaminants onto the aquifer matrix and migration into pore space not accessible by moving water causes long remediation times and multiple flushing to achieve cleanup. An innovative alternative to pump and treat is the use of multi-screened, recirculating wells. In these wells, groundwater is withdrawn from the aquifer into the well through a lower screened interval and reinjected at or above the water table through a second interval, thereby generating a recirculating flow through the aquifer. The combination of extraction and reinjection within the same well provides the opportunity for treatment within the well bore, and avoids costly pumping of groundwater to the surface and extensive ex situ treatment facilities. In addition, the same water is used to repeatedly flush a given region, and prevents water from being drawn from uncontaminated regions into the contaminated zone. Other benefits include ALARA advantages and avoiding regulatory permitting for reinjecting treated groundwater.

Efforts in FY 1994 focused on surveying conventional and innovative inorganic treatment technologies that are potentially implementable as in-well processes for treating

metals and radionuclides. Innovative super-adsorbent technology was selected as the most promising for in-well metals treatment of groundwater, because of high selectivities, compactness, and low secondary waste volumes. In addition, an apparatus was conceptualized for the selected technology. The second focus area in FY 1994 was performing flow field calculations to characterize the importance of system parameters on range-of-influence and flushing times. The calculations indicated that the most important parameter in dictating range-of-influence of recirculating wells is the spacing of the injection and extraction screens. For an isotropic media, 50 percent of the flow stays within a cylinder that is centered on the well bore and has a radius equal to the screen spacing distance.

A primary objective in FY 1995 was to design a prototype system that could be used to demonstrate in-well treatment of metals and radionuclides. In order to translate functional requirements into a prototype design, system specifications were developed for a fictitious but representative application. Depth to the water table was assumed to be 30 m, and the aquifer depth was assumed to be at least 20 m with a hydraulic conductivity of 0.0001 m/s. A 0.2 m well casing and 2 m screens were used in the design, and a 150 mm Hg pressure drop through the formation at a flow rate of 20 L/minute was assumed. Figure 1 is an engineering drawing to scale of the prototype. All equipment are catalogue items, with the exception of the ion exchange column, which will be tailored to the super-adsorbent resin used in a specific application. The design is fully instrumented for use in a technology demonstration, and allows for regeneration of the adsorbent in place without having to recover the device from the well bore. Aboveground equipment not shown includes a power source, regeneration equipment, and analytical equipment to support data acquisition. Flow modeling with mass transport was accomplished in FY 1995 using two techniques. The purpose was to determine zero order estimates for treatment times and for the extent of cleanup. First, an analytical model was developed that incorporates only convection and retardation while neglecting dispersion. Retardation was based on an equilibrium model for adsorption-desorption, neglecting effects of kinetics. Although the model is over-simplified for accurate prediction, it does provide initial estimates. The solution predicts a moving front that travels at a velocity equal to fluid velocity divided by the retardation factor. Figure 2 illustrates a moving remediation front in an isotropic aquifer of infinite extent.

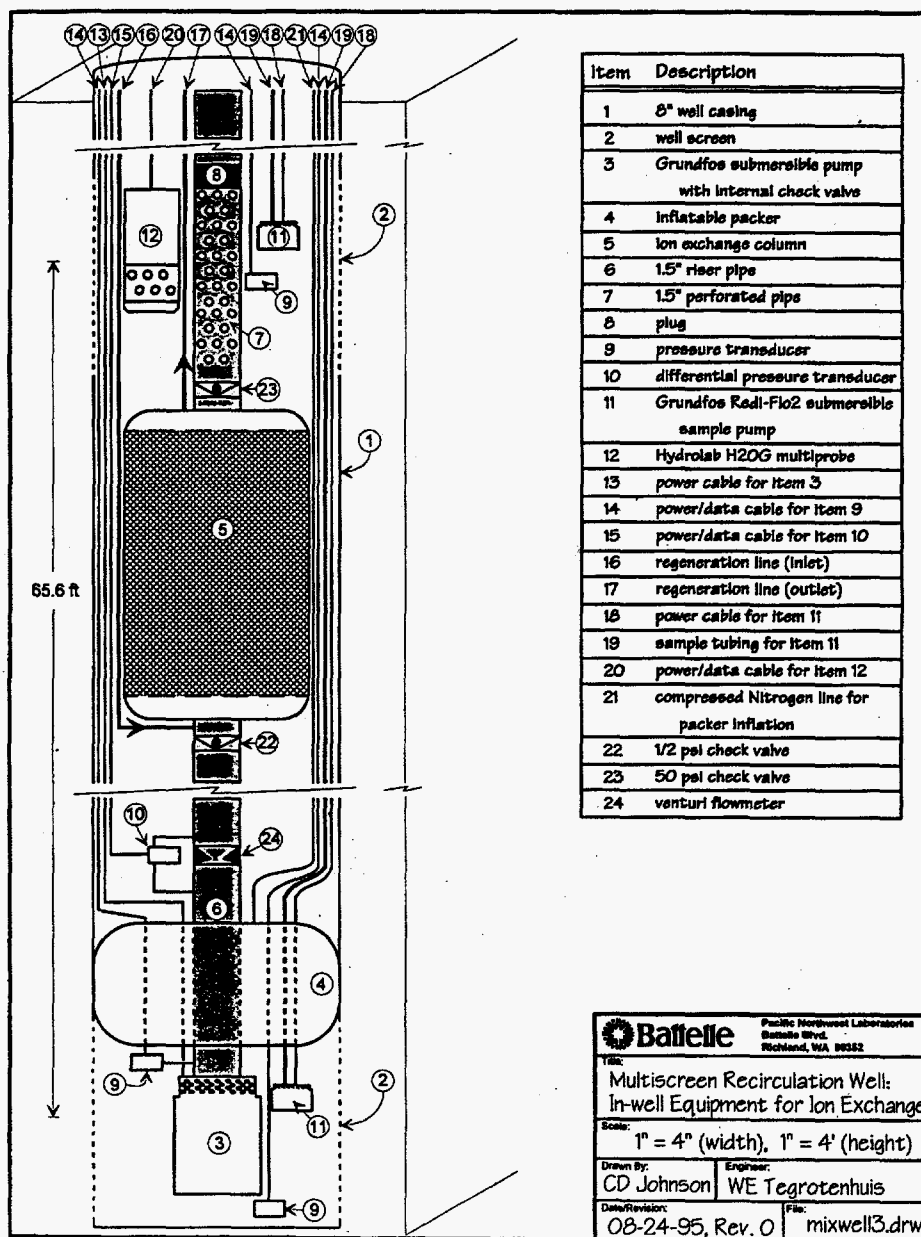


Figure 1. Prototype design of an in-well system for treating groundwater plumes contaminated with metals and radionuclides utilizing emerging super-adsorbent technologies.

The front initially moves relatively quickly and cleans the region immediately around the well, but then slows dramatically as it moves out as seen by the relative time spacing of the contours. The analytical solution was complemented by three-dimensional simulations of a recirculating well using the MODFLOW and MT3D commercial software packages. The model includes convection, dispersion, and retardation, while the equilibrium retardation model was retained. Results are qualitatively similar to results from the analytical solution. With retardation factors that are typically observed for metals and radionuclides sorbed in aquifer matrices,

remediations times are typically found to be on the order of tens of years or higher and are relatively insensitive to the well placement strategy. This indicates that operating costs are the predominant factor in the economics of remediating metal contaminated groundwater plumes. Therefore, the reduced operating costs of in-well treatment over traditional pump and treat make it economically attractive, despite the higher capital costs associated with having more wells because of the limited range-of-influence of recirculating wells.

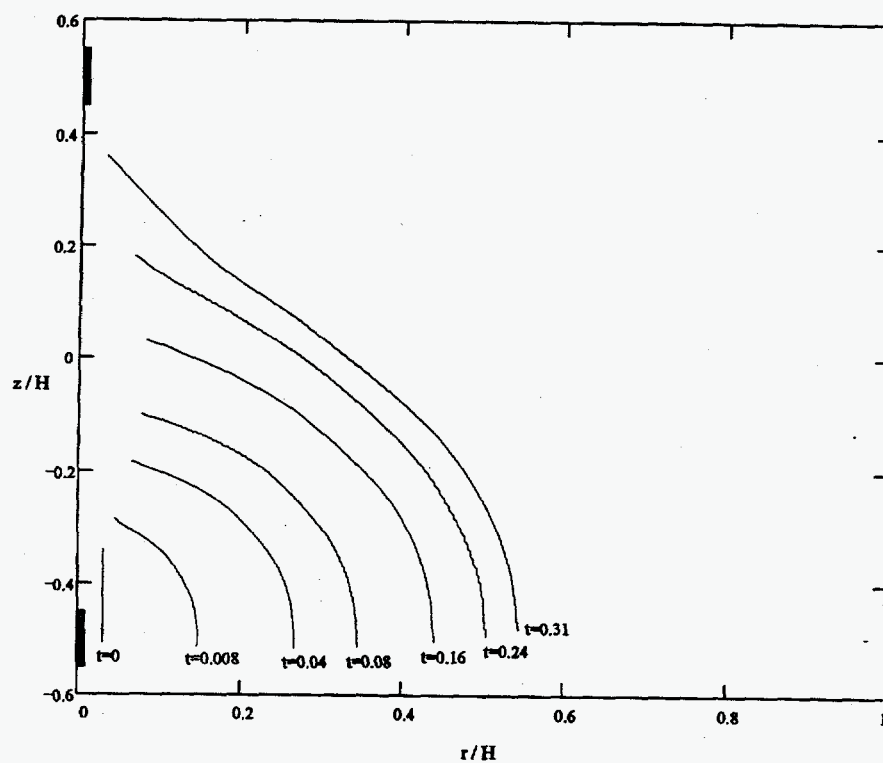


Figure 2. Simulated movement of a remediation front for a flow field generated by a two-screened recirculating well; lower injection screen and upper extraction screen are shown as shaded rectangles and distances are nondimensionalized by the screen spacing. Front is initiated along a straight line near the injection screen, and is shown at nondimensionalized time increments.



# Experimental Investigation of Pipe Flows of Complex Fluids

John D. Hudson and Jon R. Phillips (Analytic Sciences and Engineering)

## Project Description

The behavior of a concentrated suspension of solid particles flowing near a boundary is a poorly understood problem in solid-liquid two-phase flow. Since the rheology and turbulence characteristics of the suspension are a sensitive function of the distribution of particles and their mutual interactions, an understanding of suspension behavior in a boundary layer has important consequences in many industrial processes. Examples of some of these processes are the transport of concentrated radioactive and chemical waste slurries, paper pulp slurries, pharmaceutical suspensions, and food products.

A boundary layer flow of a concentrated suspension can exhibit fractionation effects near the wall since particle-liquid and particle-particle interactions may cause the particles to either migrate away from the surface or congregate near the surface. If the wall layer becomes particle depleted when compared to the bulk suspension, the result may be a drag reduction. In the opposite case where particles congregate near the wall, apparent viscous effects may increase. Since two-fluid continuum models will likely be the practical engineering approach to simulating this important problem, we proposed to convert the solid-liquid micro structure effects into boundary conditions for these simplified numerical models.

## Technical Accomplishments

In FY 1993, an extensive review was conducted to clarify key technical issues in solid-liquid slurry flows. This review led to the initiation of fundamental experiments that consider the boundary interactions in turbulent slurry flows. In FY 1993 and 1994 a facility was designed and constructed which allows the study of laminar, transitional, and turbulent flows of slurries and other complex fluid mixtures. In FY 1995, this work focused on obtaining detailed turbulence measurements near the pipe wall under several conditions to provide a basis for wall turbulence and boundary condition model development.

### *Non-Newtonian Fluid Measurements*

In an effort to understand homogeneous suspensions of fine particulate matter that display non-Newtonian rheologies, the flow of Carbopol (hydroxymethylcellulose) water mixtures were studied with particular attention

given to the near wall behavior. Rheological measurements of these mixtures indicated that dramatic changes in behavior are observed between 0.05 and 0.10 weight percent Carbopol, with the 0.05 percent case behaving nearly Newtonian and the 0.10 percent mixture having significant shear-thinning behavior.

Velocity data were obtained in the pipe flows using a conventional LDV system using silvered, hollow glass spheres of approximately 12  $\mu\text{m}$  diameter as seed particles. For reference, data were also obtained with pure water at a Reynolds number of 270,000 which has a similar bulk velocity to the data obtained with the Carbopol mixtures. Pressure drop measurements were also obtained. A pressure drop increase of approximately 50 percent was observed for the 0.07 percent Carbopol mixture relative to the 0.05 percent Carbopol and pure water cases.

The mean velocity profile of each flow is given in Figure 1a, with the velocities scaled by the bulk velocity of each flow. The radial distance from the pipe wall,  $y$ , is made dimensionless with the friction velocity and kinematic viscosity of the water data to emphasize the wall scaling regions. The data for the Carbopol mixtures collapses onto the water data from the upper end of the log-law region to the pipe center. At the lower velocities, the profiles depart with a dramatic deceleration near the wall for the 0.07 percent mixture. To emphasize this point, the mean velocity of the 0.07 percent mixture at the location where  $y^+ = 90$  for the water case gives  $u^+ = 3$  when scaled by the water friction velocity.

The turbulence intensities for these flows are presented in Figure 1b. Once again, the three data sets collapse onto one curve for points distant from the pipe wall. The 0.05 percent mixture data are quite similar to the water data both near the wall and near the pipe center, with a small increase observed near the position where  $y^+ = 1000$  for the water case. The turbulence intensities of the 0.07 percent mixture are quite large near the pipe wall, with the maximum value exceeding 0.4. The largest standard deviation of the velocity measurements is 1.2 m/s (not shown) and occurs at approximately 0.3 mm from the pipe wall (approximately where  $y^+ = 200$  for the water case).

While the rheology of the 0.07 percent Carbopol solution differs significantly from the more Newtonian fluids, the first and second moments demonstrate effects of this only

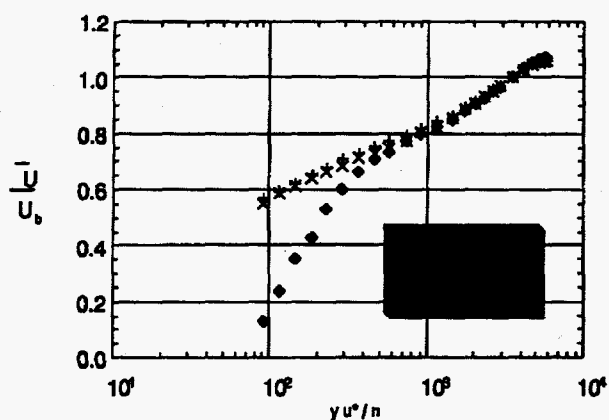


Figure 1. Mean velocities (above) and turbulence intensities (below) of water, 0.05 wt% and 0.07 wt% Carbopol 980 resin solutions. In each case, the velocities are scaled by the bulk velocity of each flow. Distances are scaled by the friction velocity and kinematic viscosity of the water data.

in the near wall region. In this region, the mean velocities are smaller than the water case while the turbulent fluctuations are larger. From this, it appears that the majority of the increase in drag is contained within this region.

#### Solid-Liquid Slurry Measurements

For large-scale particulate matter (above 10  $\mu\text{m}$ ), it is often unreasonable to assume that the slurry particles are homogeneously distributed, particularly near the pipe wall. In addition, because of their relatively large size, the particles have a macroscopic effect on the turbulence, again, particularly in the near wall region. In this case, it is important to adequately model the particulate phase boundary condition in order to accurately describe the slurry drag (or the associated pressure drop) for transport equipment design, or to describe the concentration distribution for the design of separations and solid-liquid contacting devices.

For this reason, measurements of the particle velocity were obtained near the pipe wall at a wide range of bulk Reynolds numbers ( $2700 < \text{Re}_b = D U_b / \nu < 270,000$ ). The slurries studied were 0.7 volume percent mixtures of approximately 90  $\mu\text{m}$  diameter PMMA (acrylic) beads in water or Triton XL-80N (a surfactant with viscosity approximately 25 times greater than water). The 0.7 percent volume concentration was chosen for simplification in applying initial models and for experimental convenience. At this concentration particle collisions and volume effects become important, but do not dominate the fluid-particle motions.

While a variety of parameters affect the particle boundary condition, it is evident from these measurements that a dimensionless particle stopping distance (a measure of

particle inertia describing how well the particle follows turbulent fluctuations) has a significant impact on the complexity of the required particle boundary condition model. For very small stopping distances, the particle follows the turbulent fluctuations very well. For larger stopping distances, the particle velocities near the wall deviate significantly from what is predicted for a single phase system. This effect is demonstrated in Figure 2.

The data obtained in FY 1995 provide detailed measurements unlike those available previously in the literature. These measurements will be useful in developing and testing near wall turbulence and boundary condition models.

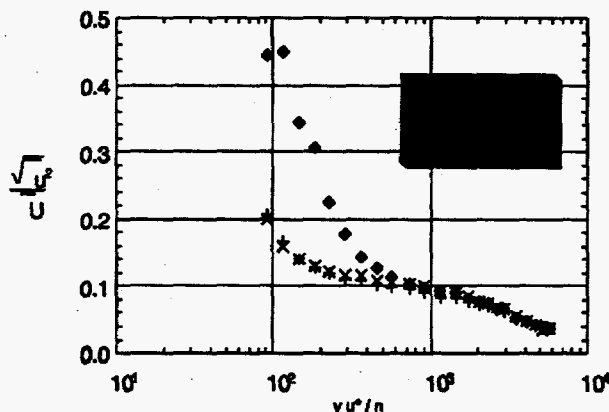


Figure 2. Mean particle velocity distributions in the near wall region for slurry with a small stopping distance ( $\lambda^+ = 2$ , above) and for a larger stopping distance ( $\lambda^+ = 2200$ , below). Lines indicate universal velocity profiles for a single-phase (Newtonian) liquid.

#### Publication

J.D. Hudson, L.A. Dykhno, and T.J. Hanratty. "Turbulence Production in Flow Near a Wavy Wall." *Experiments in Fluids* (accepted for publication).

#### Presentations

J.D. Hudson, J.R. Phillips, and S. Arthanari. 1995. "The Transport of Defense-related Wastes." Invited lecture, Chemical Engineering Department, Clarkson University, September, Potsdam, New York.

J.R. Phillips, and J.D. Hudson. 1995. "High Reynolds Number Pipe Flows of a Shear Thinning Fluid." Presented at the AIChE Annual Meeting, November.

J.D. Hudson, J.R. Phillips, S. Arthanari, and J.B. McLaughlin. "Toward a Near-Wall Boundary Condition Model for Dense Slurry Flows." Accepted for presentation at the ANS/ASME/AIChE National Heat Transfer Meeting, August 1996.

# Fundamental Reaction Diagnostics/Kinetics

Stephan E. Barlow, Russell G. Tonkyn, and Thomas M. Orlando (Chemical Structure and Dynamics)

## Project Description

Over the past several years, the utility of atmospheric pressure packed bed corona reactors in the treatment of gaseous waste streams containing  $\leq 1000$  ppm of various contaminants has been demonstrated. A main goal of this project was to improve our understanding of various fundamental chemical and physical processes important in low temperature plasma destruction techniques. Such an understanding is critical to improving the efficiency of the process technologies in a time- and cost-effective manner. We have developed an innovative atmospheric pressure sampling mass spectrometer that was used to study the dielectric barrier packed bed corona reactor. In particular, we have studied how the efficiency depends on various parameters, e.g., carrier gas composition, humidity, packing material, input power, etc. We directly monitor, in real time, the gas delivered to and coming from the reactor, as well as the power input to the reactor. We provide enough control to give reproducible measurements that can be reliably compared with other work both at the Laboratory and elsewhere. Our investigations have given us insight into the characteristics of these types of reactors, chemical mechanisms in the discharge, information vital to accurate modeling of the discharge, and the scaling parameters.

## Technical Accomplishments

We have developed a phenomenological model that incorporates the known, broad features of discharge chemistry. This model provides a consistent way of reporting results. This modeling activity also allows us to express destruction efficiencies in "universal terms" that can be quantitatively compared to competing technologies.

This model led to experiments that gave us the first measurements of electron (and by extension) ion densities in the discharge. (Standard techniques of plasma diagnostics are not suitable here.) We find that the mean electron density averaged over the length of the discharge tube and over many cycles of the discharge (@60 Hz) is  $\approx 2$  to  $10 \times (10)^6 \text{ cm}^{-3}$ . Estimating the electron energy  $\approx 3 \text{ eV}$ , we find the Debye shielding length to be on the order of 1 mm. This means that the concentration of charged species is too low to provide effective shielding

anywhere in the system. These results also place limits on the extent that ion (or electron)-molecule chemistry plays in the observed chemistry.

Experiments with pure  $\text{N}_2$  as the carrier gas allowed us to investigate the role of the surface oxide as a possible chemical catalyst. We studied several packing materials such as glass,  $\text{Cr}_2\text{O}_3$ ,  $\text{ZrO}_2$ , etc., and did not observe incorporation of surface oxygen into the gas phase products. However, other quasi- or nontraditional catalytic effects, e.g., enhanced secondary electron emission may be important.

## Destruction of TCE and $\text{CCl}_4$

We have investigated a test matrix by examining the destruction of trichloroethylene (TCE) and carbon tetrachloride ( $\text{CCl}_4$ ) as functions of power, flow rate, carrier gas composition, humidity, and packing material. Figure 1 shows a portion of the results for trichloroethylene and Figure 2 shows similar results for  $\text{CCl}_4$  ( $\beta$  is the energy per liter required to reduce a concentration to  $1/e$  of its initial value). Several trends are apparent from these figures. First, trichloroethylene is far easier to destroy than  $\text{CCl}_4$ . The rate of  $\text{CCl}_4$  loss is proportional to the electron density, while TCE can be attacked by a variety of ions and radicals.

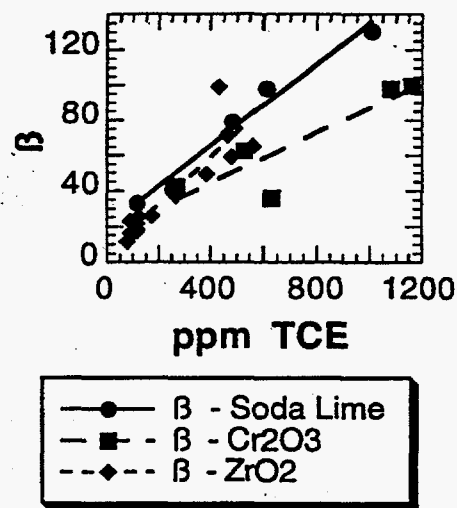


Figure 1. TCE Destruction in Dry  $\text{N}_2$  as a function of packing material



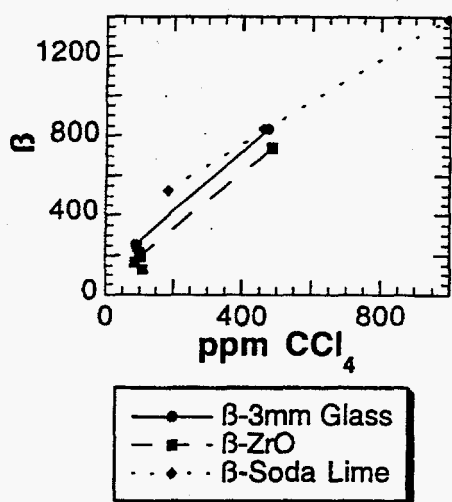


Figure 2. CCl<sub>4</sub> Destruction in Dry N<sub>2</sub> as a function of packing material

### Publications

M.M. Hsaio, B. Merrit, B. Penetrante, G. Vogtlin, P. Wallmam, R. Tonkyn, R. Shah, and T. Orlando, "Plasma Assisted Oxidation of Propene." *J. Oxidation Tech.* (in press).

R.G. Tonkyn, S.E. Badrlow, and T.M. Orlando. "Decomposition of Carbon Tetrachloride Using a Packed Bed Corona Reactor." *J. Appl. Phys.* (submitted).

### Presentations

B. Lerner, J. Birmingham, R. Tonkyn, S. Barlow, and T. Orlando. 1995. "Decomposition of Trichloroethylene by a Large Scale, High-Flow Packed Bed Gas Phase Corona Reactor." 12th Int. Symp. on Plasma Chemistry, August 12-15, Minneapolis, Minnesota.

R. Tonkyn, S. Barlow, and T. Orlando. 1995. "Destruction of Chlorinated Hydrocarbons in a Packed Bed Corona Reactor." 1995 World Env. Congress, September 17-22, London, Ontario.

T.M. Orlando, R.G. Tonkyn, and S.E. Barlow. 1995. "The Destruction of Chlorinated Hydrocarbons in Packed Bed Coronas." Symposium on the Environmental Applications of Plasmas, Gaseous Electronic Conf., October 9-13, Berkeley, California (invited talk).

# Homogeneous Isotropic Turbulence

Lucia M. Liljegren (Analytic Sciences and Engineering)

---

## Project Description

The objectives of this research are to improve the understanding of turbulence in solid-liquid multiphase mixtures. Multiphase flows are frequently encountered at the Hanford Site and in many industrial applications. At Hanford, mixing, retrieval, transport, and separation of solid-liquid suspensions can benefit from this research. In industry, significant improvements in energy and chemical process efficiencies can be achieved by using more accurate and experimentally verified physical models. Also, process equipment that handle multiphase turbulent flows can benefit from physically based design rules.

Improved understanding is achieved through two linked activities. The first is deriving rigorous transport models to predict fluctuating kinetic energy and the rate at which it is dissipated by viscous actions. The second is to obtain data which describes turbulence in a simple, well-described flow field. Grid generated turbulence fits these conditions. Data from this flow field permits testing of models for the creation and dissipation of turbulence due to particle-fluid interactions. The data will then be used to verify existing turbulence models and assist in formulating new ones. Successful models will then be implemented in computational fluid dynamic codes such as TEMPEST.

## Technical Accomplishments

The three major accomplishments of the project in FY 1995 were as follows: the fluctuating kinetic energy of the particle phase in free fall was collected for one particle concentration and a theory describing the correct source term for fluctuating kinetic energy in a mixture was developed and accepted for publication (Liljegren and Foslein, in press) and a paper describing the method used

to measure the dissipation rate in a particulate flow was published (Liljegren 1995). In addition, a new method to derive transport equations was proposed, documented, and submitted for publication (Liljegren 1995). Third, an analysis describing the inadequacies of the frequently used point force models in particulate flows was performed, documented, and submitted to the International Journal of Multiphase Flow.

The measurements were performed in a unique test facility to provide a homogeneous isotropic turbulence in particulate mixtures. This facility was completed and became operational at the end of FY 1994. This data was analyzed to determine the fluctuating kinetic energy and dissipation rate during free settling.

Details of the completed phases have been documented and submitted to peer reviewed publications.

## Publications

L.M. Liljegren. "A Comment on Modeling Particles as Point Forces in Gas-Particle Flows with Two-Way Coupling." *Int. J. Multiphase Flow* (submitted).

L.M. Liljegren. "A Discussion of Some Advantages of Higher Order Closures for Two-Fluid Models." *J. Fluid Engineering* (submitted).

## Presentation

L.M. Liljegren and W. Foslein. "The Transport Equations for Turbulent Kinetic Energy and Turbulent Dissipation Is a Gas-Solid Flow." To be presented at Particle-Fluid Interaction IV in Davos Switzerland (in preparation).

# Hydrogen Separation Technology Using the CHASP Process

Jagannadha R. Bontha and Jeffrey E. Surma (Process Technology and Engineered Systems)

## Project Description

CHASP is a separation process developed by researchers at the Laboratory for the treatment of enriched water. The process exploits the physical properties of enriched and proton water to achieve the desired separation. Although research is required to establish the cost-effectiveness of the CHASP process, initial estimates indicate that this process has several potential applications in the field of waste water treatment.

The overall objective of this work was to demonstrate the effectiveness of the CHASP process for the removal/recovery of enriched water from mixtures of enriched and normal water. The scope of the work is to conduct proof-of-principle tests to establish the capabilities of the CHASP process.

## Technical Accomplishments

In FY 1995, experiments were conducted to determine the thermodynamic equilibrium conditions using enriched water. The phase diagram results along with the thermodynamic data for normal water are shown in Figure 1. The results indicate that the conditions for the phase transformation using enriched water are completely different from those of normal water. The results suggest that for mixtures of normal and enriched water, the later could be separated by operating at conditions in which a phase change can be introduced with enriched water but not with normal water.

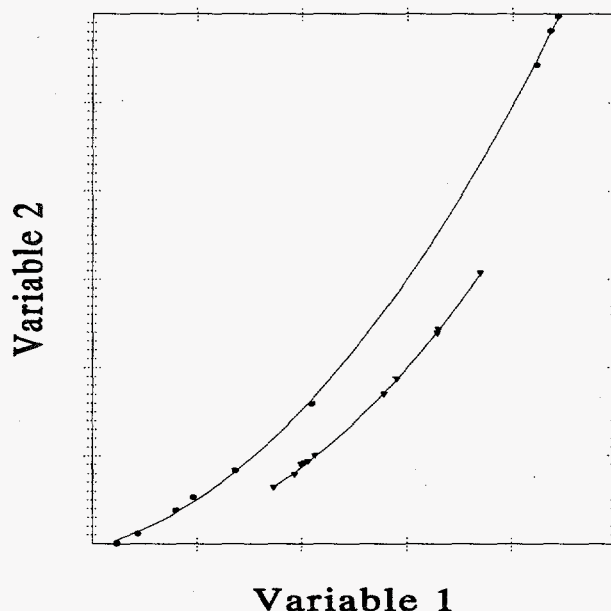


Figure 1. Equilibrium phase diagram data of normal (●) and enriched (▼) water

Using the thermodynamic data, experiments were conducted using normal and enriched water to determine the achievable separation factors. The results using mixtures indicated that due to the dissociation of the enriched water when combined with normal water, the thermodynamic operation conditions are shifted to conditions much different from those of normal water and enriched water.

# *In Situ Containment Using Heat-Enhanced and Carbonate Barriers*

Gautam Pillay, Phillip A. Gauglitz, Rahul R. Shah, and Steven R. Billingsley (Process Technology and Engineered Systems)

---

## **Project Description**

A pressing need exists in the DOE community for reliable methods to install subsurface barriers that function as secondary containment to landfills or underground storage tanks. It is also necessary to develop methods for verification of the integrity of barriers that are installed at these waste storage sites. The barrier materials used at these sites must be able to be induced to flow readily in soil, possess low permeability once they are solidified, possess durability in the presence of radioactivity and potential chemical attack, and be nontoxic to the environment. DOE, with concurrence from Ecology and EPA, will evaluate barrier technology as a means to minimize risks to the environment due to tank waste remediation. They will also study vendor capabilities to deploy and test barriers in Hanford soils. This will be accomplished by 1) estimating the potential environmental impact of waste storage and retrieval activities without the application of barriers, 2) establishing functional requirements of barriers to minimize the impact associated with the waste storage and retrieval activities, and 3) evaluating the application of subsurface barrier technologies to meet functional requirements of barriers and the potential reduction in environmental impacts from the application. Therefore, the study of novel barrier materials and emplacement methods can greatly impact the DOE mission to remediate tank wastes and to minimize environmental impact.

The concept of the heat-enhanced subsurface barrier uses a proven technology known as Six-Phase Soil Heating (SPSH) to ensure the distribution of barrier material around a tank. Originally developed for the heating of soil to remove volatile and semivolatile organics from soil, SPSH slowly heats the soil within an array of electrodes to a predetermined, controlled temperature. As the heating process ensues, the soil around each of the cylindrical electrodes inserted into the ground begins to dry. During conventional SPSH operation, water is then metered into the soil at the electrode to ensure that electrical conductivity is maintained and that the heating process is continued. For application as a barrier, instead of introducing water, an electrically conductive material will be added. This material, either a thermoplastic polymer, microemulsion, or electrorheological fluid, will follow the heated area around and beneath the tank, permeating the soil pores. When the electrical heat source

is removed, the barrier material is expected to solidify and bond to the outside of the tank forming an impenetrable, structurally sound seal.

The overall objective of this work was to study the ability of electrical soil heating to emplace in situ barriers selectively in a laboratory-scale soil tank using unique materials. Parallel studies will also be conducted of emplacement methodologies and power requirements for multiple-phase electrical heating of soil surrounding a large-scale containment zone. This information provides important economic data that will be used to assess the feasibility of continued study of this barrier emplacement method.

## **Technical Accomplishments**

The first objective of this work was to determine the appropriate level of a conductive dopant, such as carbon black, that will make melted paraffin electrically conductive. After selecting a suitable level of dopant, the second objective was to inject the selected mixture into soil columns to determine the ability of the mixture to propagate through sands and to measure the reduction in permeability caused by the solidified barrier. For these experiments, Cabot Black Pearls 2000 was chosen as an electrically conductive dopant. This colloidal carbon black was added to melted paraffin and dispersed in a ball mill. While the resulting mixture would settle slowly over time, it was suitable for testing electrical conductivity and for injecting into columns containing fine sand. The soil column experiments were conducted in 15 cm and 30 cm long clear plastic columns containing 40/60 mesh Ottawa sand. The clear columns allowed visual observation of the barrier material as it propagated through the sand, and the permeability reduction due to solidified barrier was determined by measuring the permeability of the sand before and after barrier emplacement.

Conductivity experiments were conducted with Cabot Black Pearls 2000 carbon black added in various concentrations to paraffin. Results show that this barrier material was electrically conductive when carbon black was present in concentrations greater than 0.5 wt%. A 1.0 wt% mixture was injected into heated soil columns and was observed to propagate readily, although a paraffin front moved ahead of the paraffin/carbon black

mixture. The solidified barriers were found to be very impermeable to the flow of water, and a reduction in permeability between 500- and 1000-fold was measured for three separate tests.

After successfully forming a solid barrier in the soil columns, the same barrier material was injected into a 1-cubic foot container of sand that was heated with a

single-phase AC power source. The barrier material was successfully injected into the heated soil, both during and after electrical heating. The injected barrier did not travel completely between the electrodes placed in the soil, however. Temperature data suggests that the sand between the electrodes was not sufficiently warm, causing the paraffin to solidify.

# ***Ionizing Radiation Assisted Processing of Hazardous Wastes***

Charles H.F. Peden (Materials and Interfaces)

---

## **Project Description**

Recent research at the Laboratory has uncovered the possibility of using common photochemical oxidation catalysts, such as  $\text{TiO}_2$ , as a gamma radiation catalysts for the oxidation of organics, or reduction of metal species present in the Hanford tanks. Ionizing radiation (gamma, beta, alpha) generates electron-hole pairs in inorganic semiconductors which should lead to similar surface mediated redox chemistry as that for optically excited samples. The most common metal oxide substrate for photoelectrochemical reactions is  $\text{TiO}_2$ , an environmentally benign material. Initial work focused on studying gamma catalyzed chemistry on  $\text{TiO}_2$ . Future efforts will extend this study to include wider bandgap oxides, such as zirconium dioxide which is known to be stable in high radiation fields.

## **Technical Accomplishments**

In FY 1995, we performed additional proof-of-principle experiments using EDTA as a model compound. Destruction of EDTA, a major component of tank wastes, has been accomplished over  $\text{TiO}_2$  catalysts using gamma irradiation. The experiments have focused on issues related to the dependence of reaction on catalyst composition, continuous air supply, solution pH, and the presence of impurities such as Sr. In addition, we completed an engineering bounding study of a conceptual use of ionizing radiation-assisted processing.

### *Engineering Bounding Study*

Based on preliminary engineering data obtained in the first (partial) year of funding, this year we were able to estimate the effectiveness of a potential process that uses this technology.

We envision that treatment of tank waste could be performed in reactors using the existing  $^{137}\text{Cs}$  capsules stored at the Hanford Site. A reactor could use 20 to 50  $^{137}\text{Cs}$  capsules. Assuming each capsule still contains about 45,000 curies we have  $1.67 \times 10^{15}$  disintegrations per second per capsule. A single  $^{137}\text{Cs}$  capsule will yield  $1.42 \times 10^{15}$  0.66 MeV gamma particles per second. This is equivalent to  $2.97 \times 10^{20}$ , 3.2 eV photons per second

(where 3.2 eV is the bandgap of  $\text{TiO}_2$ ). Assuming the reactor is constructed such that we absorb 50 percent of the energy in the reaction volume, and that we have 10 percent conversion into useful chemical events, we have  $1.48 \times 10^{19}$  reactions per second per capsule or  $2.47 \times 10^{-5}$  mol/s/capsule. This is an effective G value of about 1.5, while our initial experimental G value has been a factor of 2 to 3 times better. Tank AW106 is 3.8 mM in EDTA and has a volume of  $2.6 \times 10^6$  liters. Using the lower calculated efficiency, it would take 4450 days to process the supernate of Tank AW106 for a reactor that used a single  $^{137}\text{Cs}$  capsule. Therefore, a 20-capsule reactor will process this tank's supernate in 222 days while a 50-capsule reactor will only require 89 days.

### *Radiocatalysis of EDTA by $\text{TiO}_2$*

A significant accomplishment during FY 1995 was the standardization of our analytical procedure for EDTA quantification. Previous methods used included nuclear magnetic resonance and Cu complexation followed by ultraviolet analysis, both of which gave irreproducible results. For example, reactions were performed in  $\text{D}_2\text{O}$  for the nuclear magnetic resonance experiments, and we found that homogeneous (uncatalyzed) proton exchange was initiated by gamma irradiation. This resulted in a large background "destruction" rate in the absence of  $\text{TiO}_2$  catalyst. Our current method involves the use of ion chromatography that was very recently developed by Scott Clauss and coworkers at the Laboratory.

Studies of the dependence of reaction on catalyst composition, the continuous supply of air, solution pH, and the presence of Sr were performed this year. While these studies are not yet complete, a number of preliminary conclusions can be drawn from the data.

The presence of a small amount of Pd in the  $\text{TiO}_2$  catalyst formulation appears to enhance the performance of the material by at least a factor of 4. This is shown in Figure 1 where we plot a comparison EDTA destruction efficiency over  $\text{TiO}_2$  (anatase) and Pd/ $\text{TiO}_2$  (EHC) catalysts. The percent EDTA destroyed in the "blank" experiments shows the rates in the absence of catalyst. The differences in the blanks are the result of varying gamma-flux in the reactor and these numbers have been subtracted from the data obtained with catalyst present.

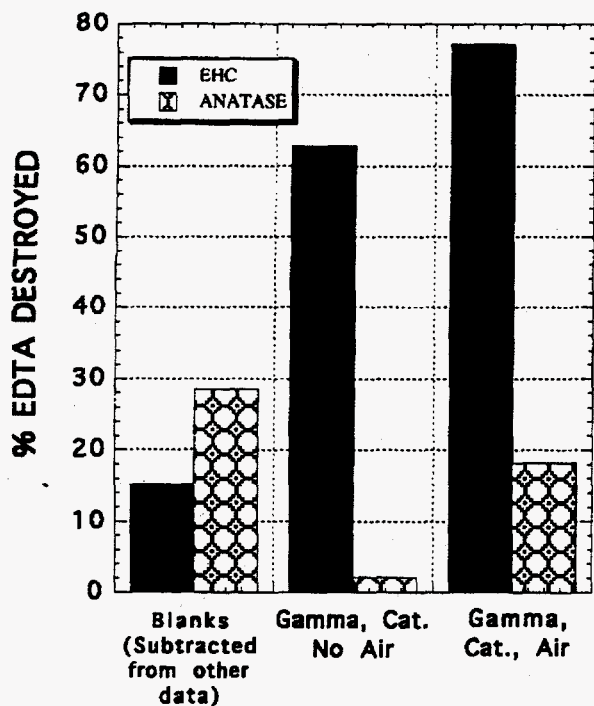


Figure 1. Reaction Rates Show a Strong Dependence on Catalyst Composition

This behavior is commonly observed in  $\text{TiO}_2$  photocatalysts because the precious metal serves to promote the separation of charge (electron/hole pairs) of the semiconductor. This is due, in part, to enhanced electron transfer reaction rates on the precious metal relative to pure  $\text{TiO}_2$ . Note also in the figure that a continuous supply of air, bubbled through the reaction mixture, led to increased EDTA destruction efficiencies. We believe that this is due to the need to maintain the concentration of dissolved oxygen in the reaction mixture.

Studies of the effect of solution pH, and the presence of Sr on EDTA destruction efficiencies were also initiated. These preliminary experiments were performed with ultraviolet irradiation rather than in the gamma-reactor because they can be performed more readily. Reactivity dropped monotonically with increasing pH by a total factor of about 3 between a pH of 4 and 14. Based on a recently proposed reaction mechanism, this behavior is expected for photocatalytic organic oxidations in aqueous solution. The effect of Sr was also assessed because it is possible that complexation of EDTA might reduce its reactivity. While no effects of Sr were observed, the ultraviolet-irradiation experiments were performed at a solution pH likely to be too low for there to be appreciable complexation with Sr. Both of these studies will be continued in this next fiscal year in the gamma-reactor.



# *Isolation and Use of Extremophilic Bacteria for the Treatment of High Nitrate and Sulfate Containing Wastes*

Brent M. Peyton, Michael J. Truex, and Melanie Mormile (Bioprocessing)  
Margaret F. Romine (Environmental Microbiology)

## Project Description

The objective of this study was to develop a bioprocess based on extremophilic microorganisms for treating and reducing high nitrate and/or sulfate concentrations in industrial wastes. Within this project, a matrix of extremophile organisms and their capabilities were developed through enrichment, purification, and identification of extremophiles and characterization of their growth and metabolic capabilities. Reaction kinetics and operational parameters for bioprocesses using extremophiles was also be developed.

## Technical Accomplishments

The development of a bioprocess for nitrate and sulfate degradation under harsh conditions includes isolating extremophilic microorganisms, determining bioprocessing parameters, and demonstrating the bioprocess.

Two approaches were employed to obtain cultures of nitrate- and sulfate-reducing bacteria that can function under conditions of extreme temperature, pH, and/or salinity. Bacteria having the desired properties were obtained from culture collections, and through local, national, and international collaborative relationships. For example, environmental samples from evaporation ponds in Australia were obtained through contacts made in the Internet group of halophile researchers. Isolation of specific consortia and/or microorganisms is scheduled to begin soon. Denitrifying consortia from local sources were obtained and tested for their nitrate reducing abilities under high pH and salt conditions. In addition, enrichments from select environments are being undertaken to isolate consortia with the desired traits, for instance, denitrification at pH=9 and NaCl = 20 g/L. Microbial consortia from the above sources were challenged to determine the range of pH and salinity over which they can grow. The collection of cultures has been based on functional capability as opposed to along species or other commonality. For example, Figure 1 shows the range of conditions for denitrifying bacteria that have been added to our collection. We plan to expand the range of conditions covered by our culture collection. We can then select the most appropriate cultures for specific bioprocessing applications.

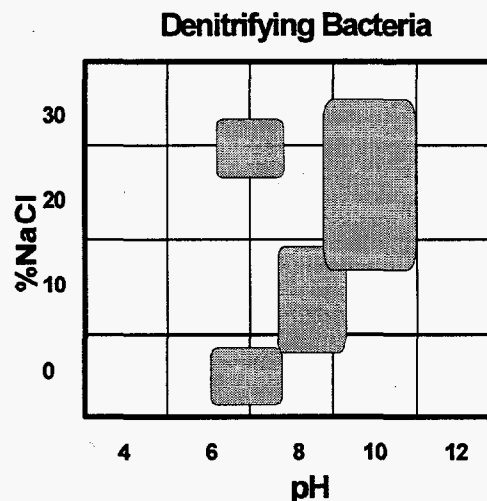


Figure 1. Pure cultures and consortia have been collected that can reduce nitrate in the ranges shown. In this manner, cultures can be targeted to waste conditions.

Biological treatment of model ion exchange regeneration fluids and tank wastes using microbes has served as an initial target to help drive the research toward useful application and develop capabilities in this technical area of research. Ion exchange regeneration produces a brine containing high concentrations of nitrate and sulfate that is difficult to dispose or causes problems in downstream processing. These same constituents are found in DOE tank wastes. Table 1 compares industrial ion exchange regeneration fluids and a reference and concentrated reference Hanford tank waste.

Bioprocess demonstration tests are being conducted on promising nitrate and sulfate reducing cultures to quantify important parameters, such as the maximum specific growth rate, half-saturation coefficient, and biomass yield, for use in engineering design for the construction and operation of a bench-scale bioreactor process. Tests are run in batch or continuous culture depending on the parameter of interest.

These target waste characteristics indicate that the microbial consortia that we collect, identify, and characterize should be both halophilic and alkalophilic in addition to containing nitrate and sulfate reducing bacteria. The advantages of using more extreme



Table 1. Ionic species of interest in ion exchange regeneration fluids and reference tank waste.

Ionic Species	Typical Anion Exchange Regeneration Fluid (g/L)	Reference <sup>(a)</sup> Tank Waste (g/L)	Reference Tank Waste Concentrate (g/L)
Na <sup>+</sup>	18 - 61	1.45	8.3
Cl <sup>-</sup>	12 - 39	.048	0.32
NO <sub>3</sub> <sup>-</sup>	1	1.99	10.9
SO <sub>4</sub> <sup>-</sup>	2	0.37	2.21
pH	8 - 9	NR	11.3

(a) Hanford Waste Vitrification Program reference feed supernatant  
NR - Not reported.

bioprocessing conditions are twofold: 1) treatment will be more cost-effective by treating these wastes with little or no dilution and requiring no physicochemical pretreatment before bioprocessing, and 2) the more extreme conditions will reduce substrate competition from unwanted microorganisms that tend to destabilize microbial process reactors.

A number of microorganisms/consortia have been identified that could potentially be used in nitrate bioprocessing including 1) alkalophilic halophilic denitrifiers isolated from the Great Salt Lake; 2) halophilic denitrifiers found at the WIPP site by A.J. Francis at Brookhaven National Laboratory, and 3) thermophilic denitrifiers from the DOE subsurface microbial culture collection. To demonstrate that these wastes can be treated in a continuous and efficient manner, a 12 liter bioreactor has been built and operated

continuously for the removal of nitrate using a culture obtained from Siemens Power Corporation. The same reactor will be used for demonstration of a sulfate reduction bioprocess. The goal in building this reactor is to develop a portable reactor capability that can be used for bioprocess parameter development and taken to client sites for field demonstrations.

Denitrification data from the initial laboratory testing is given in Figure 2. At a pH of 8.5 and at 10 percent salinity (100 g/L NaCl) the denitrifying consortia was able to reduce 520 mg/L nitrate to nitrogen gas continuously. Effluent concentrations of nitrate and nitrite were 10 and 17 mg/L, respectively. The reactor has been operated at a residence time that is longer than would be optimal in an industrial setting because of limitations in media preparation and waste disposal. However, culture growth parameters suggest that much shorter residence times should be possible. A shorter residence time will be sought for industrial processing applications. We believe that residence-time related costs will not be significant in the application of this technology for treatment of ion exchange wastes and/or tank wastes.

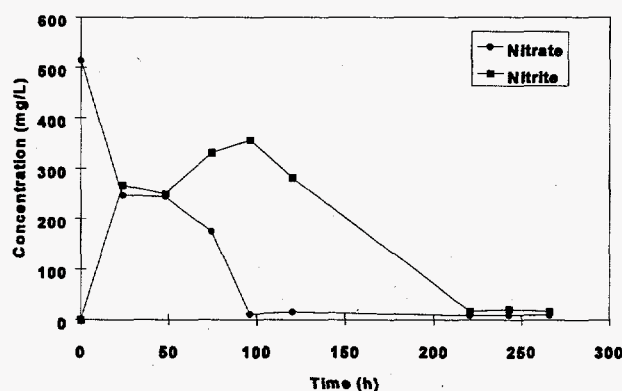


Figure 2. Continuous denitrification from an initial concentration of 520 mg/L to ~10 mg/L at pH 8.5 and 100g/L NaCl. The drinking water standard for nitrate is 44 mg/L.

# Kinetics, Scale-up and Demonstration of Uranium Bioprecipitation Technology

Michael J. Truex and Brent M. Peyton (Process Technology and Engineered Systems)  
Yuri A. Gorby (Earth and Environmental Sciences)

---

## Project Description

The primary objectives of this project were to determine the reaction kinetics and operating conditions needed for uranium bioprecipitation. This information is being used for examining scale-up of the process, for selection of appropriate reactor designs for flow-through operation, and for undertaking treatability studies with industry and at DOE sites.

## Technical Accomplishments

The facultative Fe(III)-reducing bacterium *Shewanella alga* strain BrY (hereafter referred to as BrY) uses oxygen, iron, manganese, and uranium as terminal electron acceptors. This organism, originally isolated from estuary sediments, is of interest because it is facultatively anaerobic, performs dissimilatory metal reduction, can grow very rapidly under aerobic conditions, is halotolerant, and reduces metals under non-growth conditions in a minimal medium. Additionally, BrY produces active metal reductase under some non-metal-reducing conditions. Because of these characteristics, BrY may be effective in bioprocesses to separate uranium from aqueous streams by enzymatically reducing U(VI) to U(IV) forming the insoluble compound uraninite.

BrY is applied in a bioprecipitation process to enzymatically reduce soluble U(VI) to insoluble U(IV), which readily precipitates from solution resulting in a very large reduction in waste volume. For most applications, the process operates by supplying uranium-reducing bacteria and lactate, an energy source, to the aqueous stream. The bacteria reduce uranium under nongrowth conditions without affecting other constituents in the stream. Thus, the resulting insoluble U(IV) can be separated in a relatively pure form.

Fundamental microbial data and engineering kinetic results to date indicate that bioprecipitation can be a competitive process for selective uranium removal from aqueous streams. The following paragraphs summarize our research to quantify the kinetic parameters required for a successful pilot-scale demonstration of the process.

The nonlinear regression of U(VI) reduction data to the Monod-based kinetic expression yields a maximum

specific U(VI) reduction rate,  $V_{max}$ , of 0.563 mg-U(VI)/(mg-biomass/hr) with a 95 percent confidence interval of 0.508 to 0.619 mg-U(VI)/(mg-biomass/hr). The half-saturation coefficient,  $K_s$ , is 31.5 mg-U(VI)/L with a 95 percent confidence interval of 20 to 43 mg-U(VI)/L. The correlation coefficient,  $r^2$ , is 0.874.

To demonstrate that the reduction process under non-growth conditions is catalytic and to determine U(VI) reduction activity under more realistic processing conditions, the change in the specific reduction rate over a longer period of time was measured. In an extended-activity test where U(VI) was respiked into treatments on four successive days, the specific reduction rate dropped to 60 percent of the initial specific reduction rate between 8 and 24 hours after the start of the experiment. The specific reduction rate then stayed constant through the remainder of the 80-hour test. Therefore, reactors that have a mean cell residence time of greater than 8 hours will be designed with a  $V_{max}$  that is 60 percent of the  $V_{max}$  calculated from the initial activity ( $t < 8$  hours). It appears that the loss of activity is related to the experiment duration rather than the amount of U(VI) processed by the cells, because in the four successive spikes over the duration of this experiment, a total of 38 mg/L of U(VI) was reduced. This is less U(VI) than was reduced in 8-hour tests where the initial U(VI) concentration exceeded 200 mg-uranium/L.

In addition to kinetic studies, other tests have been performed in preparation for larger scale bioprocessing. Operating parameters for continuous production of active uranium-reducing bacteria have been determined for the bacterium BrY. It is possible to efficiently grow high concentrations of the organisms since aerobic growth conditions can be utilized. Reactor conditions are manipulated to provide the oxidation/reduction potential needed for inducing the metal reductase system in the bacteria while maintaining aerobic growth.

This technology can be used in combination with soil/tailings leaching operations, for treatment of groundwater, and/or for treating process streams as a component of larger processing systems. CERCLA Superfund sites associated with uranium mining and nuclear materials processing include United Nuclear Corp., Uravan Uranium Project, Fremont National Forest Uranium Mines, Midnight Mine, and Dawn Mining Company Mill

Ponds. Uranium-contaminated DOE sites include Paducah Gas Diffusion Plant, Feed Materials Production Center (Fernald), Hanford Site, Rocky Flats Plant, Oak Ridge Reservation, and the Savannah River Site. There are also 16 active, 25 inactive, and 11 shutdown uranium mining/processing sites in the U.S. Many of the above sites would benefit from this technology because 1) it greatly reduces the volume of uranium contamination, 2) the uranium is selectively removed so that the resulting waste is not a mixed waste, and 3) downstream processes to remove other waste constituents are not affected.

#### **Publications**

M.J. Truex, B.M. Peyton, N.B. Valentine, and Y.A. Gorby. 1995. "Uranium Reduction Kinetics of a Dissimilatory Fe(III)-Reducing Bacterium Under Non-Growth Conditions." *Environ. Sci. Technol.* (submitted).

M.J. Truex, B.M. Peyton, Y.A. Gorby, and N.B. Valentine. 1994. "Initial Process Development for Uranium Bioprecipitation. In: *Proceedings of the 9th Annual Conference on Hazardous Waste Remediation*, Great Plains-Rocky Mountain Hazardous Substance Research Center, Kansas City University, Manhattan, Kansas.

#### **Presentations**

M.J. Truex, B.M. Peyton, Y.A. Gorby, and N.B. Valentine. 1995. "Kinetics of Uranium Bioprecipitation." In *Situ and On Site Bioreclamation Conference*, April 24-27, San Diego, California.

M.J. Truex, B.M. Peyton, N.B. Valentine, and Y.A. Gorby. 1995. "Selective Separation of Uranium From Aqueous Wastes Using Bioprecipitation." *Fifth International Conference on Radioactive Waste Management and Environmental Remediation*, September 7-9, Berlin, Germany.

M.J. Truex, B.M. Peyton, Y.A. Gorby, and N.B. Valentine. 1995. "Uranium Reduction Mediated by a Dissimilatory Metal-Reducing Bacterium." *American Chemical Society, Emerging Technologies in Hazardous Waste Management*, September 17-20, Atlanta, Georgia.

# Membrane Materials

Annalee Y. Tonkovich and John L. Cox (Chemical Technology)

---

## Project Description

The objective of this project was to develop and evaluate new membranes in novel chemical reactors. Thin nickel membranes were evaluated for hydrogen separation in FY 1994, and thin palladium films were investigated in FY 1995. Novel high temperature sorbents (molten salts impregnated in porous alumina) for eventual use in facilitated transport membranes were also investigated in FY 1994.

Full utilization of membrane reactor technology requires the ability to selectively separate products from reactants as they are formed. In the high temperature environment of most reactions of interest to the chemical industry, only inorganic membranes and materials will survive. Palladium is available as a dense membrane for permselective hydrogen separation, but other materials are desired. Molecular sieving for selective separation could be realized in the limit of microporous membranes (3 to 10 Å). However, the smallest pores currently available are 50 Å. Chemical modification of existing membranes is required to facilitate separation of gaseous reactants and products.

Porous ceramic membranes modified with molten salts are sought if suitable salt compositions are found that exhibit chemical specificity between alkanes and alkenes at elevated temperatures. The incorporation of molten salts inside membrane pores will allow for selective adsorption and trans-membrane transport of reaction products at elevated temperatures. The selective removal of intermediate reaction products as they are formed will improve product selectivities by inhibiting further side reactions.

## Technical Accomplishments

In FY 1994, proof-of-principle experiments were conducted with ammonia sorption on a molten zinc chloride salt. The zinc chloride was impregnated in

porous alumina pellets, and the sorption capacity at elevated temperatures was investigated. Selective ammonia complexation between 250°C and 350°C was observed. However, this material does not readily desorb ammonia, and required temperatures up to 500°C at 50 psig to desorb ammonia.

In FY 1995, proof-of-principle experiments were conducted with ethane and ethylene sorption on molten salt materials. Several compositions of silver chloride, cadmium chloride, zinc chloride, and cuprous chloride were evaluated and found to exhibit slight preferential sorption of ethylene from ethane in the 400°C to 600°C temperature range. The difference was not great enough to warrant additional study for high temperature ethane/ethylene separation.

Palladium alloy membranes are an important material for hydrogen separation. An existing membrane (0.01 inch thickness) was tested for regenerability after carbon deposition. At a temperature of 550°C, a hydrogen flux of 20 cm<sup>3</sup>/min-cm<sup>2</sup> was measured on the unsupported membrane. After surface poisoning with carbon, the flux dropped by 60 percent. Pure hydrogen gasified the carbonaceous deposits to methane, and the flux returned to 80 percent of its original value. Further regeneration in air returned the permeability to its original value.

## Publications

J.L. Cox, A.Y. Tonkovich, D.C. Elliott, and E.G. Baker. 1995. "Indirect Liquefaction of Biomass: A Fresh Approach." Preprints, Div. of Fuel Chem., 40(3), 719.

J.L. Cox, A.Y. Tonkovich, D.C. Elliott, and E.G. Baker. 1995. "Hydrogen from Biomass: A Fresh Approach." In *Proceedings of the Second Biomass Conference of the Americas*, 657.

# Membrane Separations

Mark F. Buehler (Chemical Technology)

---

## Project Description

In this project efforts were concentrated on the development of bench- and pilot-scale membrane research capabilities. The capabilities will be used for testing and evaluating new membranes being developed at the Laboratory, such as the polyphosphazine membranes project.

## Technical Accomplishments

Electrochemical separation techniques are becoming more popular for industrial and hazardous waste applications because of the low operating temperature, minimal secondary waste, and high selectively controlled by the applied potential. Here, a membrane based electrochemical method, electrodialysis, was evaluated for the separation of aqueous ions from industrial waste streams.

Electrodialysis was used to separate both cations and anions using a continuous laboratory-scale flow-cell. Waste streams from water-based nuclear power plants were examined because they require stringent control of water chemistry to avoid high-temperature corrosion and transport of radioactive colloidal dispersions. For example, ion exchange separations within a typical reactor system will remove borate from process water while maintaining a pH of  $7.9 \pm 0.2$ . A three-compartment cell was used with a Nafion™ 450 cationic membrane and a Neosepta™ AMH anionic membrane. Borate concentration in the anolyte, lithium concentration in the catholyte, and pH of the process stream are monitored at limiting current density of cell. The borate and lithium were successfully removed to discharge limits with approximately a 0.5 pH unit change.

In addition, anionic separation of phosphate and nitrate was evaluated using an Neosepta AMH anionic membrane. The equilibrium characteristics of the

membrane allowed for separation factors greater than 10 to be obtained. A pulsed-mode method was investigated to take advantage of the membrane characteristics for continuous operation.

## Publications

M.F. Buehler, J.E. Surma, and J.W. Virden. 1994. "In Situ Soil Remediation Using Electrokinetics." *In-Situ Remediation: Scientific Basis for Current and Future Technologies.*, Eds. G.W. Gee and N.R. Wing, Battelle Press, Vol. 2, pp. 991-1010.

M.F. Buehler, J.E. Surma, and J.W. Virden. 1994. "Transport of Radioactive Ions in Soil by Electrokinetics." *Metals and Materials Waste Reduction, Recovery, and Remediation.* Eds., K.C. Liddell, R.G. Bautista, R.J. Orth, pp. 111-126.

L.J. Silva, L.A. Bray, J.G. Frye, and M.F. Buehler. 1994. "Spent Catalyst Processing with Electrochemistry." *Metals and Materials Waste Reduction, Recovery, and Remediation*, Eds., K.C. Liddell, R.G. Bautista, R.J. Orth, pp. 61-64.

## Presentations

M.F. Buehler, D.W. Campbell, and G. Hollenberg. 1995. "Anionic Separation Using Electrodialysis." National AIChE Meeting, Boston, Massachusetts.

M.F. Buehler, D.W. Campbell, and G. Hollenberg. 1995. "Borate Separation Using Electrodialysis." North American Membrane Society, Portland, Oregon.

M.F. Buehler, L.J. Silva, and J.G. Frye. 1994. "Electrochemical Regeneration of Spent Catalyst." National AIChE Meeting, San Francisco, California.

# Microplasma Reactor

Joseph G. Birmingham (Environmental Technologies)

## Project Description

This project developed and demonstrated a miniature plasma (or ionized gas) reactor that uses micromachining fabrication techniques. The prototype microreactor produced a plasma that was revealed by experimental data and visual observations. The use for the micromachined plasma reactor (MPR) is expected to be validated with additional testing. It is expected that the synthesis of temperature-sensitive and -reactive compounds and the decomposition of toxic or hazardous gases will be accomplished by a micromachined plasma reactor.

Mass production of microscale components and systems, using fabrication techniques developed for microelectronics, has the potential to make small-scale, distributed chemical processes economically attractive relative to centralized processes normally used today. Microtechnology has matured to the point where initial applications of microsensors are reaching commercialization, and powerful microactuators (that can be used as prime movers for pumps, valves, and other mechanical components) are under development within the U.S. and abroad. The development of the microchannel heat exchanger has demonstrated successful operation of high heat fluxes during FY 1995. The design of the microreactor will be similar to a microchannel heat exchanger with two additional masking steps to deposit materials needed for the initiation of the plasma (or ionized gas). All of the fabrication work was performed in the RTL facilities at the Laboratory.

## Technical Accomplishments

The design of the micromachined plasma reactor involved the deposition of metals by vacuum deposition techniques into ceramic channels. A machinable ceramic MACOR had channels cut with a slitting saw using conventional carbide tools. These microtechnology fabrication techniques were used to deposit 5 microns of aluminum metal and 5 microns of alumina (defect-free dielectric) in the MACOR structure. The overall reactor length was about four centimeters in length. The swagelock fittings served as both the electrical feed through and the conduit for the gas flows. In addition, a membrane imprint was milled into the micromachined plasma reactor to hold a polymeric material in the middle of the plasma as seen in the schematic diagram of Figure 1. Teflon tape was used

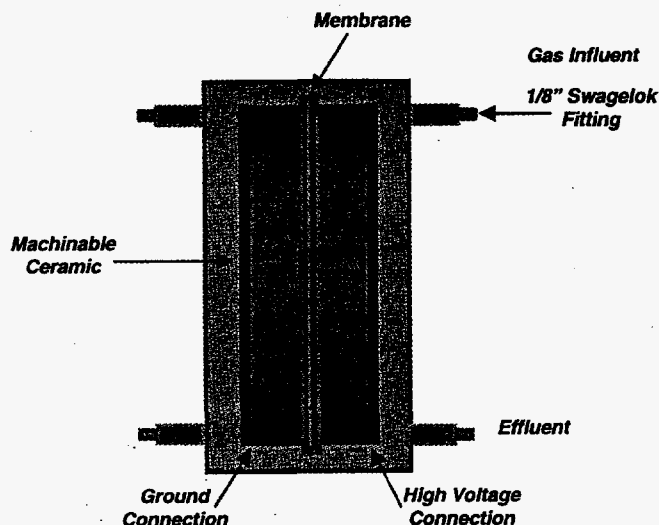


Figure 1. Membrane/Plasma Microreactor

to seal this reactor and worked adequately since the operating temperatures were close to ambient.

Proof-of-principle experiments were conducted on a micromachined plasma reactor micromachined plasma reactor and the experimental data is shown in Figures 2 and 3. The electrical data in Figures 2 and 3 illustrate different characteristics of the plasma created within the micromachined plasma reactor when argon gas is flowing. The plasma was initiated at 1 kilovolt as seen on Figure 3. The small wavy noise at the crests of the sine-wave are indicative of microarcs. These microarcs reveal the presence of an active corona. These micromachined plasma reactor systems were designed to operate at lower voltages due to the "defect-free" dielectrics and Figure 2 corroborates this hypothesis. The current diagram in Figure 3 shows that the 17 milliamps of current have induced a typical waveform for corona initiation. The total power deposited in the micromachined plasma reactor was measured to be close to 17 watts of power in a reactor space that was small. The high energy density plasma was so intense as to be seen glowing through the ceramic MACOR walls of the micromachined plasma V reactor. Although several technical issues need to be resolved, the micromachined plasma reactor testing provided encouraging results in miniaturizing chemical reaction systems to create unique synthesis and decomposition environments.

28-Aug-95  
15:04:08

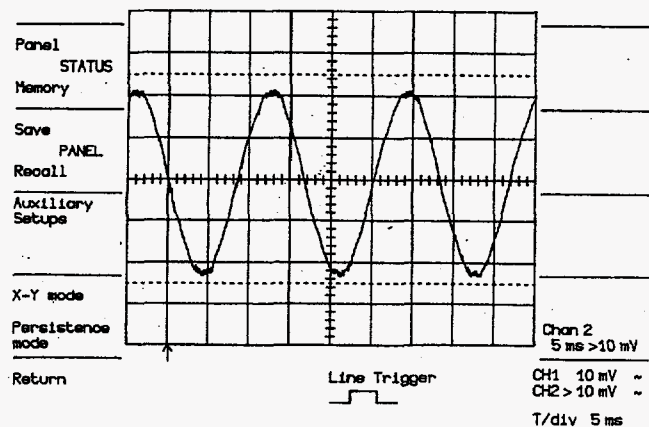


Figure 2. Secondary Voltage Waveform of a MPR

28-Aug-95  
15:15:24

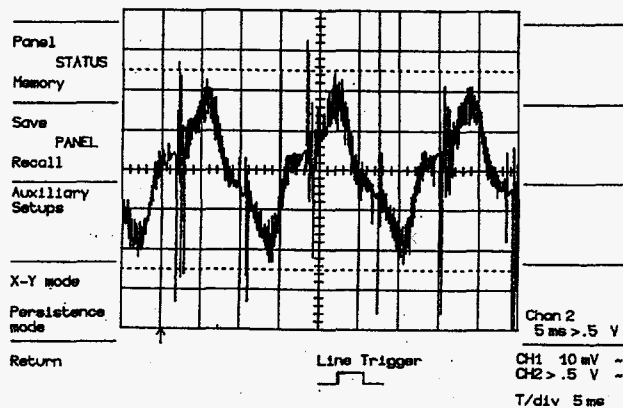


Figure 3. Current Waveform within a MPR

# Modeling of Colloidal Systems

David R. Rector (Environmental Technologies)

## Project Description

The goal of the project was the development of models that provide a microscopic description of the formation of microporous inorganic materials in the presence of surfactant aggregates. Using surfactant molecules it is possible to mediate and direct the synthesis of inorganic materials with well-defined microstructures and morphologies. Novel zeolite-like mesoporous molecular sieves have been synthesized based on hexagonal and cubic surfactant aggregates. These materials are characterized by ordered porosity, narrow pore size distribution, and adjustable pore size (from 1.5 nm to 20 nm). Experimental investigations into the synthesis and properties of these materials are already under way at Pacific Northwest National Laboratory. This project was aimed at supplying theoretical support for these experiments.

## Technical Accomplishments

The primary objective of this project was the development of a molecular dynamics code capable of simulating model surfactant solutions in the presence of solute at constant temperature-constant pressure conditions. The model surfactant solutions are composed of simplified surfactants and solvents that interact via Lennard-Jones potentials. The interactions between different sites can be individually specified, as well as details such as the length of the surfactant chains and the bending and stretching potentials along the surfactant. This code has been written and tested to verify that it is working correctly.

The initial simulations were aimed at identifying parameters and conditions under which the surfactant models would actually form micelles and other ordered structures. For a parameter set with energy scale ordering analogous to those in aqueous surfactant systems, it was found that at high surfactant concentrations the simulations spontaneously formed micelles. An example of a cylindrical micelle formed in one of the simulations is shown in Figure 1. The view is down the axis of the cylinder with the solvent particles removed. The figure clearly shows a ring of head sites surrounding an inner core of tail sites.

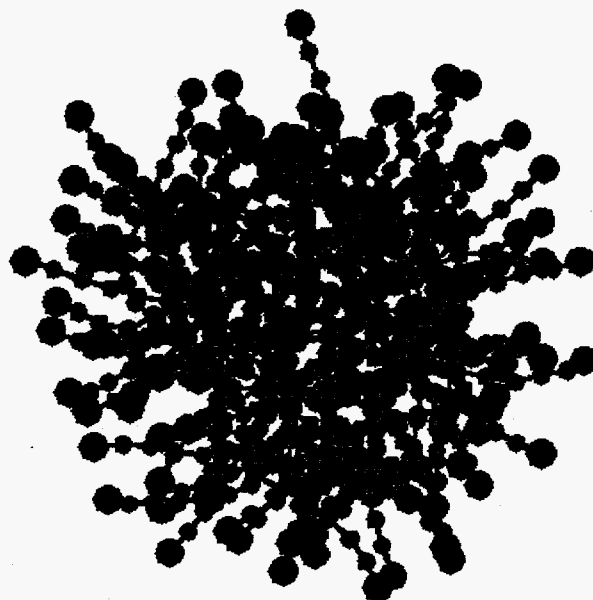


Figure 1. Example of a cylindrical micelle formed in one of the simulations.

Although not shown, the solvent is almost completely excluded from the micelle core.

Recent work focused on examining the behavior of the surfactant solutions when a solute has been added to the system. The parameters on the solute are generally chosen so that the pure solute would form a solid phase under the conditions of the simulation. Initially, a solute that interacted with other solute sites via a simple Lennard-Jones interaction was examined but more recent work has focused on including multi-body interactions in the solute potential. The multi-body terms can be used to alter the coordination number and change the nature of the solid material formed by the solute. The simulations indicate that the presence of the solute can profoundly alter the behavior of the micelles and that this may, in turn, influence the formation of the solid phase.

## Publication

B.J. Palmer and J. Liu. "Simulations of Self-Assembly in Surfactant Systems." *Langmuir* (submitted).



# Plasma Engineering and Prototype Development

Theresa M. Bergsman (Process Technology and Engineered Systems)

## Project Description

The goal of this project was to investigate innovative reactor designs for use with nonequilibrium plasma processes. A nonequilibrium (low temperature) plasma is created when electrons are accelerated in an electric field to the point where they ionize gas molecules. This creates very reactive conditions which can be used to destroy undesirable compounds such as organic contaminants or  $\text{NO}_x$ , or synthesize valuable chemicals. A nonequilibrium plasma is characterized by high electron energies and low ion or molecular energies. This makes it a potentially very energy-efficient means of conversion.

## Technical Accomplishments

In FY 1995, this project investigated both a coaxial reactor design for  $\text{NO}_x$  formation and destruction and a point-to-plane design for liquid treatment.

### *$\text{NO}_x$ Formation/Destruction*

$\text{NO}_x$  formation and destruction was investigated on a 12-cm coaxial corona reactor.  $\text{NO}_x$  formation/destruction was studied as a function of electron density and energy, gas composition, and packing material. It was found that lower electron energies and densities prevent formation of  $\text{NO}_x$  (however, some  $\text{N}_2\text{O}$  is formed). At lower power densities, without the presence of contaminants, ozone is formed. Higher electron energies and densities favor efficient  $\text{NO}_x$  destruction in low  $\text{O}_2$  atmosphere. This creates greater destruction, with less energy loss in  $\text{N}_2$  vibrational mode. Microdischarges may be important because of higher electron energies in the "heads" of streamers. Packing type appears to be important and packing performs three functions:

1. "refraction" of electric field
2. sorption
3. surface catalysis.

It is unclear the degree to which each of these affects the overall reaction. Additional work is necessary to confirm relative effects of each variable.

### *Liquid Corona*

The liquid corona task investigated methods for treating liquids using a point-to-plane configuration. Earlier work on liquid corona had characterized liquid corona as

- essentially an in situ ozone generator
- operating in the regime of glow discharge with a current limitation of approximately 100 uamps/discharge point or 1mA/plane. To make a practical unit, either the apparatus had to have tens of thousands of points or thousands of planes.

Operating as an ozone generator, the liquid corona operated under an inherent disadvantage. Ozone generation is severely hampered by the presence of  $\text{H}_2\text{O}$  in the gas. This disadvantage would make liquid corona impossible to compete directly as an ozone generator. Power costs were at least 10 times too high for oxidant generation.

The focus areas for FY 1995 development were fourfold:

1. Discover a method of generating highly reactive oxidants other than ozone so that liquid corona could treat materials which ozone could not effectively treat.
2. Deliver the oxidants directly to the liquid (reactive oxidants would not survive the transfer from the glow tip to the liquid, approximately 1 cm).
3. Reduce power costs to generate and deliver oxidants.
4. Design a system to deliver commercial quantities of oxidants in a reactor system.

An unexpected discovery this year accomplished steps 2 and 3 above. By operating the reactor at low pressure, it was discovered that it was possible to use higher currents and extend the corona discharge completely to the liquid surface. The very surface of the liquid itself indeed glowed. Instead of the reactants being formed at the tip and transporting across 1 cm of gap, at least some of the reactants were being generated at the liquid surface.

Goal 3 was a more expected result of reducing pressure. Reducing the pressure inversely increases the mean free path of the electrons emitting from the electrode. The electric field accelerates the electrons and adds energy approximately equal to  $Vxd$ .  $V$  is the voltage gradient in the locality and  $d$  is the distance before the electron collides with another body (i.e., mean-free path). When the electrons have sufficient energy to dislodge other electrons from the gas molecules, then a few electrons generate more electrons (cascade) and a plasma is formed. It is apparent from  $Vxd$  that it will take  $\frac{1}{2}$  the voltage to reach a critical ionization energy if the distance " $d$ " is doubled. By operating at 50 mm Hg absolute pressure, the voltage required to create ionized particles dropped from approximately 15 kV to less than 1 kV.

Other researchers operating in this regime (Kankazi et al. and Cserfalvi et al.) identified emission spectra  $H^*$ ,  $OH^*$ , and  $O^*$  radicals in the plasma. The  $OH^*$  and  $O^*$  radicals are especially strong oxidants. These identifications were not verified as part of this research. However, these results are consistent with one another and consistent with mechanistic theories. It is expected at this time that goal 1 is also accomplished by operating at low pressure with the plasma contacting the surface.

Model studies on pentachlorophenol indicated that to accomplish a 99 percent destruction treatment it would require approximately 1 electron for every 4 pentachlorophenol molecules destroyed. For a 10 gpm stream at 100 ppm contamination this would require about 8 amps of current. The glow discharge corona would require 80,000 points or 8,000 edges for discharge. At low pressure it was discovered that currents up to about 50 mA were possible from a single point. This greatly reduced the number of points required.

Use of dielectrics and high frequency alternating current offers opportunities to get significant discharge currents with just a few discharge electrodes. These experiments were delayed due to power supply failures and will continue pending equipment repair and time allowance.

### **Presentations**

Two papers were presented on this effort, one to the AIChE Summer conference in Boston and one to the Emerging Technologies in Hazardous Waste Management ACS conference in Atlanta. Two papers will be published in the Journal of Environmental Science and Health.

# Reaction Engineering

Annalee Y. Tonkovich and John L. Cox (Chemical Technology)

---

## Project Description

The objective of this project was to develop and deploy a membrane reactor as an energy-efficient industrial chemical reactor. Membrane reactors are a new class of reactors which improve per pass yields for partial oxidation reactions. A porous, but non-permselective, membrane controls the in situ oxygen feed rate to preferentially promote the desired reaction. In industrial practice, a large hydrocarbon to oxygen ratio is used in a traditional tubular reactor design to achieve high product selectivities. Low hydrocarbon conversions per pass result and a large separation and recycle load of the unreacted material is required.

The membrane reactor employs the synergistic combination of simultaneous reaction and separation to improve product yields. The breadth of the work presented in the literature focuses on dehydrogenation reactions using palladium membranes and selective oxidation reactions using dense zirconia or silver membranes. These technologies have not been commercialized in large part because of a lack of materials in engineered forms.

A tube and shell membrane reactor configuration is used, where the hydrocarbon is fed tube-side and the air is fed shell-side. Distributing the air feed along the length of the reactor reduces local oxygen concentrations and thus inhibits undesired side reactions. Both higher yields and selectivities per pass are observed over traditional fixed-bed reactors.

## Technical Accomplishments

In FY 1993, a membrane reactor for partial oxidation reactions was designed, constructed, and proof-of-principle experiments were conducted for a simple test reaction (ethane oxidative dehydrogenation). In FY 1994, the membrane reactor was redesigned to improve the performance and the operating parameters (temperature, feed ratio, and residence time) were characterized experimentally.

In FY 1995, reactions of importance were evaluated in the membrane reactor with varying degrees of success. The oxidative coupling of methane (OCM) and the oxidative dehydrogenation of propane (OXDP) were evaluated using doped metal oxide catalysts in the membrane reactor.

Incremental yield increases over an analogous fixed-bed reactor were observed for oxidative coupling of methane. Greater yield increases were observed for OXDP, but not as large as those observed for the oxidative dehydrogenation of ethane. For all reactions, radial and axial temperature profiles are measured as the reaction proceeds. Hot spots begin to form only for oxidative coupling of methane.

A one-dimensional isothermal model was developed to investigate the effect of reaction kinetics on the magnitude of the observed MBR yield increase. The model qualitatively validates the experimental trends and requires inclusion of other process variables (temperature) to quantitatively predict performance.

## Publications

A.L.Y. Tonkovich, J.L. Zilka, D.M. Jimenez, G.L. Roberts, and J.L. Cox. "Experimental Investigations of Inorganic Membrane Reactors: a Distributed Feed Approach for Partial Oxidation Reactions." *Chemical Engineering Science* (in press).

A.L.Y. Tonkovich, D.M. Jimenez, J.L. Zilka, and G.L. Roberts. "Inorganic Membrane Reactors: Applicability Regions for Membrane Reactor." *Chemical Engineering Science* (accepted for publication).

## Presentations

A.L.Y. Tonkovich. 1995. "Membrane Reactors for Partial Oxidation Reactions." AIChE Fall Meeting, Miami, Florida.

A.L.Y. Tonkovich, J.L. Zilka, D.M. Jimenez, G.L. Roberts, and J.L. Cox. 1995. "Pollution Prevention Through Novel Chemical Reactor Designs." AIChE Summer Meeting in the Waste Minimization and Waste Management session, Boston, Massachusetts.

A.L.Y. Tonkovich. 1995. "Novel Separative Reactors for Pollution Prevention." AIChE Summer Meeting in the Fast Tracking Pollution Prevention session, Boston, Massachusetts.

A.L.Y. Tonkovich, J.L. Zilka, D.M. Jimenez, G.L. Roberts, and J.L. Cox. 1995. "Inorganic Membrane Reactors: Applications for Partial Oxidation Reactions." North American Catalysis Society Conference, Snowbird, Utah.

A.L.Y. Tonkovich, D.M. Jimenez, G.L. Roberts, and J.L. Cox. 1995. "Inorganic Membrane Reactors for Partial Oxidation Reactions." North American Membrane Society Conference, Portland, Oregon.

A.L.Y. Tonkovich, J.L. Zilka, D.M. Jimenez, G.L. Roberts, and J.L. Cox. 1995. "Inorganic Membrane Reactors: a Distributed Feed Approach for Partial Oxidation Reactions." ACS Conference, Anaheim, California.

# Structure Function Analysis

Richard T. Hallen and Timothy L. Hubler (Chemical Technology)

## Project Description

The objective of this project was to provide an understanding of the fundamental structure/function relationships for organic phenolic ion-exchange materials and processes by synthesizing and characterizing derivatives of resorcinol-formaldehyde (R-F) and phenol-formaldehyde (P-F) resin. Resorcinol-formaldehyde resin is a regenerable ion-exchange material which may have application for removal of radioactive cesium from alkaline waste tank supernates.

Previous studies showed that the chemical stability of resorcinol-formaldehyde resin is an important issue. Part of our examination into this issue has been directed toward preparation of resins that contain fluorine and carboxylic acid functionality to examine the effect on the chemical stability of the phenolic resins and to explore the result of such structural modification on cesium selectivity.

## Technical Accomplishments

Resorcinol-formaldehyde and phenol-formaldehyde resins were prepared according to procedures developed by Wallace and Bibler at Savannah River Technology Center. The phenolic polymers were modified by addition of 5 percent and 10 percent of the following compounds: 2-fluorophenol; 3-fluorophenol; 4-fluorophenol; 2,5-difluorophenol; 3,4-difluorophenol; 3,5-difluorophenol; salicylic acid; and 3-hydroxybenzoic acid.

The distribution coefficients ( $K_d$ s) for all the modified resins were equal to or less than the values for underivatized resorcinol-formaldehyde or phenol-formaldehyde resin. The phenol-formaldehyde resins gave lower  $K_d$ s when more (10 percent versus 5 percent) of the polymer modifier was present. The opposite trend was generally observed for the resorcinol-formaldehyde resin, but the magnitude of the difference was smaller. Both resorcinol-formaldehyde and phenol-formaldehyde monofluorophenol derivatives had higher  $K_d$ s compared to the difluorophenol derivatives, indicating that the strongly electron-withdrawing fluorine groups remove electron density from the phenoxide ion-exchange sites. For phenol-formaldehyde resins, the hydroxybenzoic acid derivatives produced higher average  $K_d$ s because the hydroxybenzoic acid derivatives have two ionogenic groups that enhance the capacity of the phenol-formaldehyde resin.

The resins were structurally characterized using solid-state  $^{13}\text{C}$  and  $^{19}\text{F}$  nuclear magnetic resonance techniques. The  $^{13}\text{C}$  nuclear magnetic resonance spectra for the fluorophenol derivatives were obtained as normal double-decoupled CP-MAS spectra and compared with their respective  $^1\text{H}$  and  $^{19}\text{F}$  dipolar-dephased spectra for assessment of the structure of the copolymer.

Information regarding the extent and nature of crosslinking for the fluoropolymer resins was obtained by examination of their  $^{19}\text{F}$  nuclear magnetic resonance spectra. For example, the  $^{19}\text{F}$  nuclear magnetic resonance data obtained for the resorcinol-formaldehyde polymer prepared using 90 percent resorcinol and 10 percent 3,4-difluorophenol indicated that the 3,4-difluorophenol moiety occurred mainly as "end-cap" groups on the polymer chain, with a much smaller percentage cross-linked into the polymer matrix. The absence of spinning sidebands indicated enhanced motion of the fluorophenol units and end-capping. The  $K_d$  for this resin was 3420 mL/g. For the resin prepared from 90 percent resorcinol and 10 percent 3-fluorophenol, large spinning sidebands were observed in the  $^{19}\text{F}$  nuclear magnetic resonance spectra at comparable sample spinning speeds. The  $K_d$  for this resin was 5334 mL/g, about the same as resorcinol-formaldehyde resin. The nuclear magnetic resonance results show that a reduction in crosslinking drastically reduces the selectivity of the polymer resin (there is a smaller change in capacity).

Oxygen uptake experiments monitored in tandem with  $^{13}\text{C}$  nuclear magnetic resonance clearly show that phenol-formaldehyde resin and its derivatives are chemically oxidized at a much slower rate than resorcinol-formaldehyde resin. The observed  $K_d$ s for phenol-formaldehyde resin are generally 5 to 25 percent of that observed for resorcinol-formaldehyde resin under the same experimental conditions.

Characterization of the new derivatives has clarified the observed differences in performance for resorcinol-formaldehyde and phenol-formaldehyde resin. Cross-linking for phenol-formaldehyde and resorcinol-formaldehyde resins are essentially the same with cross-links occurring at the 2 and 4 positions of the phenolic ring. The primary structural difference between phenol-formaldehyde and resorcinol-formaldehyde resin is that a substantial fraction (> 50 percent) of the hydroxy groups of the phenol ring form ether groups during synthesis of the polymer with consequent loss of ion-exchange sites

(Figure 1). Thus, the observed  $K_d$ s for phenol-formaldehyde resin are at best 25 percent of that observed for resorcinol-formaldehyde resin.

The greater chemical stability of phenol-formaldehyde resin occurs not because of greater cross-linking, but because resorcinol-formaldehyde resin has a ring position that is para to a hydroxyl group and is easily oxidized; formation of para-bisquinones and loss of ion-exchange sites is facile for resorcinol-formaldehyde resin (Figure 2). The same process does not occur as readily for phenol-formaldehyde resin because the position para to the hydroxyl group is alkylated.

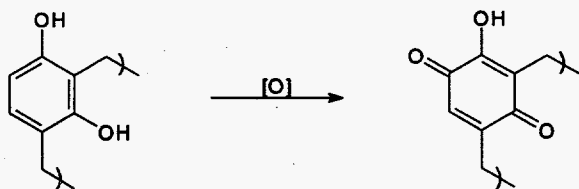


Figure 1. Etherification of Phenol-Formaldehyde Resin and Loss of Ion-Exchange Sites

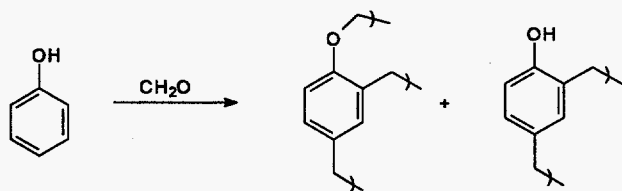


Figure 2. Facile Oxidation of Resorcinol-Formaldehyde Resin

## Publication

T.L. Hubler, J.A. Franz, W.J. Shaw, S.A. Bryan, R.T. Hallen, G.N. Brown, L.A. Bray, and J.C. Linehan. 1995. *Synthesis, Structural Characterization, and Performance Evaluation of Resorcinol-Formaldehyde (R-F) Ion-Exchange Resin*. PNL-10744, Pacific Northwest Laboratory, Richland, Washington.

## Presentations

T.L. Hubler and R.T. Hallen. 1995. "Cesium-Selective Modified Phenol-Formaldehyde (P-F) and Resorcinol-Formaldehyde (R-F) Ion-Exchange Resins." Presented at the 50<sup>th</sup> American Chemical Society Northwest/Rocky Mountain Regional Meeting, June, Park City, Utah.

T.L. Hubler, J.A. Franz, and R.T. Hallen. 1995. "Structure-Function Investigations of Modified Phenol-Formaldehyde and Resorcinol-Formaldehyde Ion-Exchange Resins that are Selective for Cesium." 210<sup>th</sup> American Chemical Society National Meeting, August, Chicago, Illinois.

# Supercritical Fluid Separations

Clement R. Yonker (Chemical Sciences)

---

## Project Description

This project studied the effects of pressure and temperature on the conformation, chelation equilibria, kinetics of chelate formation, and inorganic chemistries in supercritical fluids. The project specifically focused on investigations using supercritical carbon dioxide, which shows promise as a "green" solvent of the future. Operation at pressures and temperatures near the critical point may provide fine control of solubility and enhanced extraction kinetics. The resulting developed capabilities and investigations provided a fundamental background for the development of new separation and extraction technologies based upon supercritical fluids.

## Technical Accomplishments

The separations and extraction of metal ions and radionuclides are important in the environmental remediation of hazardous waste sites throughout the nation and DOE's complex. The need to accomplish these extractions in a cost-effective, environmentally benign manner has driven the investigation of novel complexing agents and new solvents. Using supercritical fluids, one can continuously vary density, dielectric constant, viscosity, and mass transport properties between that of a gas and liquid by manipulating pressure. The compressibility of a supercritical fluid is large just above its critical point, where small changes in pressure result in large changes in the solvent strength of the fluid. As a consequence, molecular interactions can be varied over a considerable range. As pressure is increased, the solubility of a metal complex will often increase by many orders of magnitude. These increased intermolecular interactions between the fluid and the metal complex will affect the kinetics and thermodynamics of complex formation and can be used to advantage in extraction schemes.

In FY 1994, studies were undertaken investigating the solution dynamics of pure supercritical fluids as a function of pressure and temperature. Ligand displacement reactions using supercritical fluid solvents were also investigated, where the fluid solvent reversibly displaced a complex's organic ligand as a function of pressure and time. This was the first time this behavior was observed using high pressure nuclear magnetic resonance.

During FY 1995, continuing high pressure nuclear magnetic resonance investigations built upon the efforts from FY 1994 and extended the project into structure/function determination of organic ligands as a function of pressure and temperature. The specific systems investigated were acetylacetonate, trifluoroacetylacetonate, and hexafluoroacetylacetonate. These organic ligands are becoming important in metal extractions using supercritical CO<sub>2</sub>. They have the capacity to undergo a keto/enol tautomeric equilibria which will effect their ability to complex with a metal ion. The enol form of the ligand is the structure which can complex with the metal ion. The investigation of the effect of fluorination and structure was accomplished using high pressure nuclear magnetic resonance for these ligands. These studies demonstrated that the degree of fluorination not only enhanced the solubility of the ligand in supercritical CO<sub>2</sub>, but the tautomeric equilibrium was driven toward the enol form due to fluorine stabilization of the enol structure. Increasing temperature was seen to increase the keto tautomer population for both acetylacetonate and trifluoroacetylacetonate, while increasing pressure had a small effect on the keto/enol equilibrium population. This study demonstrated that fluorination enhanced ligand solubility in supercritical CO<sub>2</sub> and metal complexation. Temperature increases at constant pressure will decrease the ability to form the complex with these ligands as the keto tautomeric form does not complex with the metal ion. Higher pressure slightly favored the keto tautomeric form too.

This information is important in the application of these ligands to metal extractions using supercritical CO<sub>2</sub>, as fluorination favors the complexation of metal ions, but one needs to use extraction temperatures as low as possible due to the formation of the less favorable keto form of the tautomer as temperature increases.

## Publications

C.R. Yonker, S.L. Wallen, and J.C. Linehan. "High Pressure NMR Study of Metal Complexes in Supercritical Fluids." *J. Supercrit. Fluids* (in press).

C.R. Yonker, S.L. Wallen, and J.C. Linehan. "Application of Supercritical Fluids to Inorganic Extractions." *AIChE, J.* (submitted).

S.L. Wallen, C.R. Yonker, C.L. Phelps, and C.M. Wai. "Effect of Fluorine Substitution, Pressure and Temperature on the Tautomeric Equilibria and Hydrogen Bonding of  $\beta$ -diketones." *J. Phys. Chem.* (submitted).

#### **Presentations**

S.L. Wallen, D.M. Pfund, J.C. Linehan, and C.R. Yonker. 1995. "Molecular Clustering in Supercritical Ethylene Studied by Nuclear Magnetic Resonance Spectroscopy." Presented at the 36th ENC - Experimental Nuclear Magnetic Resonance Conference, Boston, Massachusetts.

C.R. Yonker, S.L. Wallen, and J.C. Linehan. 1995. "Application of Supercritical Fluids to Inorganic Extractions." Presented at the Summer AIChE meeting, Boston, Massachusetts.

S.L. Wallen, and C.R. Yonker. 1995. "High Pressure NMR study of Solvation Dynamics in 1,1,1,2-Tetrafluoroethane and Metal Chelating Agents." Presented at the 12th Winter Fluorine Conference, St. Petersburg, Florida.



# *Synthesis Reaction in a High Energy Corona*

Joseph G. Birmingham (Waste Treatment Technology)

---

## **Project Description**

The primary focus of this effort was to investigate innovative processing methods to reduce energy consumption and impact to the environment. One such processing method utilizes a "low temperature" or non-equilibrium plasma. A low temperature plasma is produced when a strong electric field is established in a gas, causing the gas to partially ionize. This generates electrically excited chemical species that react to produce the desired product. A major advantage of this method is that these reactions can be initiated at low temperatures resulting in an energy-efficient, low-cost processing system. In addition, the unique ability of a low temperature plasma to produce reactive species at low temperatures may result in the ability to significantly increase conversion to high-value products without creating undesirable byproducts.

The goals of this project were to investigate low temperature plasma processing to synthesize chemical products. The initial focus of this effort was on conversion reactions with methane and synthesis of hydrogen peroxide.

## **Technical Accomplishments**

Preliminary screening experiments were performed during FY 1995 to determine the feasibility of converting methane to higher molecular weight compounds. A 2.5 percent methane in argon carrier gas was passed through a small-scale corona reactor at a flow rate of approximately 1 SCFM. Argon was chosen as the carrier

gas because of its ability to readily ionize and create secondary electrons. Gas concentrations into and out of the reactor were measured using a Hewlett Packard gas chromatograph/mass spectrometer and a Fourier transform infrared spectrometer. In addition, a scanning monochromator was used to help identify radical species produced in the plasma. Power was measured using a Lecroy oscilloscope to calculate cycle average powers both on the primary and secondary of the transformer. Fluoroptic temperature probes were used for on-line temperature measurement.

For initial experimentation, the reactor was run at a relatively low power density. At these low power densities, data indicated that 5 to 10 percent of the methane was converted to primarily ethylene (approximately 85 percent), acetylene (approximately 15 percent), and a ring-structure hydrocarbon. Additional analysis of the compounds formed is continuing. A total power of approximately 7 watts was applied. Additional experiments will be performed at higher power density and higher methane concentrations to improve overall conversion.

Hydrogen peroxide production was also a focus of experimental work. The first method tested for producing hydrogen peroxide was the direct oxidation of water. A plasma was initiated in an air stream containing 20 percent, 40 percent, 60 percent, and 80 percent relative humidity to determine if any peroxide was produced. These experiments did not produce hydrogen peroxide of significant concentrations. Therefore, hydrogen addition will be investigated as a next step to optimize the conversion process for hydrogen peroxide.

# Ultra High Rate Sputter Deposition of Highly Reflective Metal Films

John D. Affinito (Materials Sciences)

## Project Description

The objective of this study was to develop improved magnetron sputtering cathodes and processes capable of rates high enough to run simultaneously, in-line in a vacuum web coating process, with the PML flash evaporation process. Many multilayer film applications of interest require metal, oxide, nitride, and other types of layers deposited sequentially, one atop the other. We have developed a process for vacuum deposition of polymer layers, the PML process, that in a roll-to-roll web coater, can deposit polymer layers at line speeds up to 600 m/min. In many instances the PML layer can replace an oxide or nitride in a traditional application. Often times the PML layer can replace a polymer layer that, traditionally, is deposited in a separate atmospheric step - requiring moving the substrate in and out of vacuum multiple times. In still other instances, new applications are under development that use PML layers along with oxides, metals, or both in a multilayer structure. In all of these cases, the production costs are determined by the overall deposition rate which is determined by the slowest of the deposition processes involved. Traditionally, metals have been faster than oxides or nitrides while polymers, which are often fast, require the substrate to be shuttled between air and vacuum which is very slow. The PML process not only makes the polymer layer vacuum compatible, it makes it the fastest of the processes. To maximize the manufacturing benefit of the ultrahigh rate of the PML process, when it is used with sputtered metal and/or oxide layers, we are working to increase the rate of the metal and oxide processes by increasing the magnetron sputtering rate.

## Technical Accomplishments

### The Sputtering Process

Figure 1 depicts the basic sputtering processes in a schematic form. A target material that is to be sputtered to produce a thin film is placed in a vacuum chamber. After the base pressure is reached, with the pumps still operating, a steady flow of gas, usually Ar, is allowed into the chamber and an equilibrium Ar partial pressure is reached. A negative voltage is applied to the target and, if the Ar partial pressure is appropriate, a glow discharge is produced with the target acting as the cathode. Positive

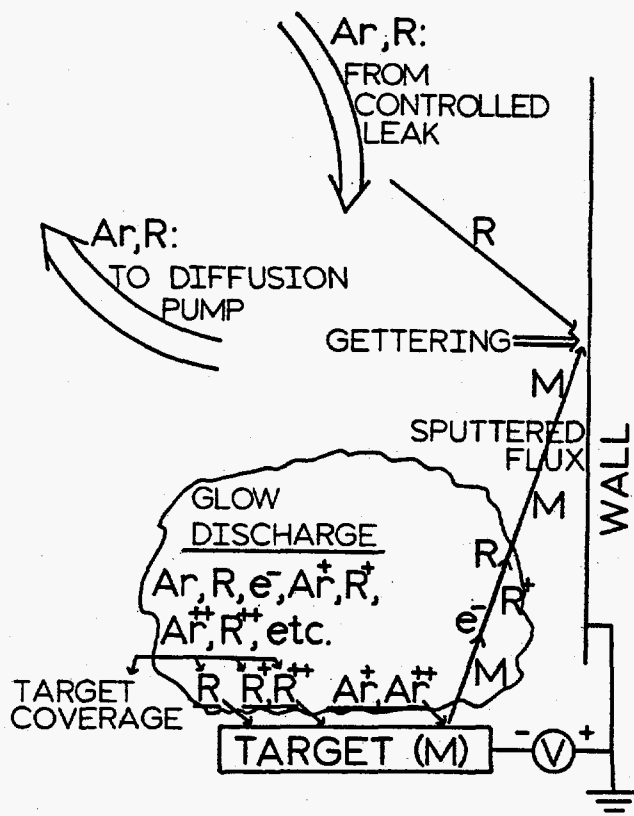


Figure 1. Schematic representation of the various processes that occur during the operation of a basic diode sputtering cathode. (Ar=Argon atom, R=reactive gas atom/molecule, e=electron, M=target material atom)

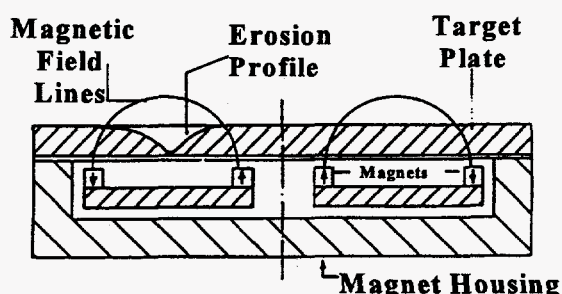
Ar ions in the glow are accelerated toward, and strike, the cathode. When the  $Ar^+$  ions strike the cathode/target, electrons and target atoms are ejected through momentum and energy transfer mechanisms. The ejected electrons help to sustain the glow discharge, by causing further ionization of the Ar, and the ejected atoms land on surfaces and form films. If reactive gas atoms (R) are mixed in with the Ar then they may combine with the target material atoms (M) to form compounds ( $M_xR_y$ ). This latter process is called reactive sputtering.

The basic diode sputtering process has the drawback of extremely low deposition rates per unit of power input to the glow discharge. This inefficiency is largely due to the diffuse nature of the glow discharge. The ions in the glow discharge plasma form a very diffuse cloud with many of the  $Ar^+$  species being produced so far from the

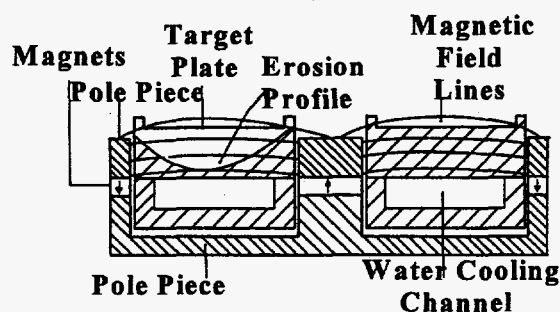
target that they cannot contribute to the sputtering process. Therefore, several strategies have been developed to confine the plasma near the target surface in order to increase the sputtering efficiency.

### Magnetron Sputtering

One strategy used to improve the sputtering efficiency is to place magnets behind the target so that the plasma is confined by the magnetic fields. This technique is called magnetron sputtering and the top portion of Figure 2 is a schematic representation of a conventional magnetron cathode. Magnetron cathodes show dramatic improvement in sputtering rate over diode cathodes. The two biggest drawbacks to the magnetron are that the target erosion is highly nonuniform due to the plasma distribution and that the technique is not very effective for magnetic target materials. This latter problem arises because the field from the magnets is shunted through the magnetic target material, which acts like a pole piece for the magnet, and there is not sufficient field in front of the target to confine the plasma. For efficient plasma confinement the magnetic field strength above, and parallel to, the target surface must be at least 100 Gauss, and 300 to 500 Gauss is preferable.



**Conventional Magnetron**



**Cross-Field Magnetron**

Figure 2. Comparison of magnet and target geometry for a conventional and a cross-field magnetron sputtering cathode.

### Cross-Field Magnetron Cathodes

To get sufficient magnetic confinement, with highly magnetic target materials, the geometry shown in the

bottom portion of Figure 2 was developed. This geometry, called the cross-field magnetron geometry, brings the magnet pole pieces up through the center of the target and up along the sides of the target. Thus the pole pieces direct the field across the target surface. In this geometry some field is still shunted into the magnetic target material, however, sufficient field remains above the target to provide efficient plasma confinement. The small vertical walls extending from the top of the target, in Figure 2, serve to provide a degree of electrostatic plasma confinement in addition to the magnetic field confinement.

This geometry affords two other advantages in addition to enabling magnetron sputtering of highly magnetic materials. First, as the field lines tend to be more uniform across the target surface than for a conventional magnetron, the target erosion is more uniform. This permits higher utilization of the target material. Second, the sputtering rate is much higher for nonmagnetic materials, as well as for magnetic materials, again for two reasons. First the higher magnetic field strengths provide better confinement and, thus, permit operation at higher power densities. Second, because the field is more uniform, sputtering occurs over a larger area of the target surface. Rates, for Cu, have been reported as high as 2000 Å/s above cross-field magnetrons. These rates are 5 to 10 times higher than for conventional magnetrons. With this type of cathode, the secondary electron emission, sputter rate, and plasma confinement efficiency can even be high enough to permit the target to sputter without any sputtering gas. This is called self-sputtering since it is ionized target atoms being turned around in the plasma and impinging on the target again that produce the sputtering effect.

### Sputter Cathode Development

The vacuum web coater system is set up to allow multiple vacuum deposition processes to be employed, simultaneously, during a single pass of the substrate material through the system. Currently there are two cross-field sputtering stations, two PML flash evaporation (with e-beam and ultraviolet cure) stations, one monomer extrusion die (with e-beam and ultraviolet cure) station, one e-beam (or thermal) evaporation station, and two parallel plate glow discharge stations that can serve either for substrate pre-treatment or for Plasma Enhanced Chemical Vapor Deposition.

We have developed a new variation on the cross-field magnetron design as part of a program to raise sputter deposition rates high enough to take better advantage of simultaneous operation with the PML process. For instance, with conventional magnetrons a PML/Ag(1000 Å)/PML solar reflector might run at 5 to 10 m/min—gated by the Ag sputter deposition rate. Note

that, while Ag has the highest sputter rate of any material, the PML process may deposit any thickness, from zero to several  $\mu\text{m}$ , at any speed from about 1 to 600 m/min. Also note that sputter deposition line speeds are not speed independent as is the PML process. Sputter line speeds are inversely proportional to the desired thickness, for a given power. All other, conventional, vacuum deposition processes have this same speed-thickness-power limitation. If we use cross-field magnetrons we can push this rate to 25 to 50 m/min.

Figure 3 shows the type of modifications we have implemented on the target plate of a cross-field magnetron. The bottom portion of Figure 3 shows the copper backing plate, which is in direct contact with the water cooling. The target plate, shown in the center portion of Figure 3, is usually bonded to the backing plate. For reasonably machineable and inexpensive materials, the target and backing plate are machined from a single piece of metal. For nonmagnetic materials, the magnetic field in our design is high enough that targets up to 2.75 cm thick may be sputtered.

**All components are 5"ID by 8"OD**

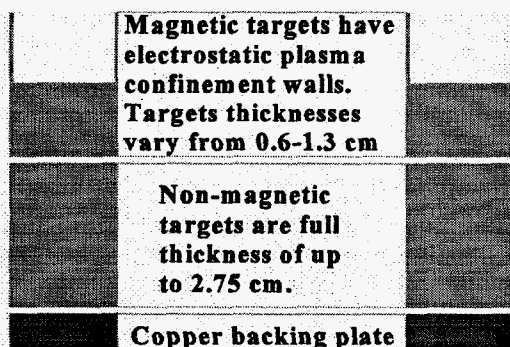


Figure 3. View of target backing plate, full size target, and electrostatic confinement target for magnetic materials. Target geometries, with our cross-field magnet configuration, support 40 kilowatts of power and have been shown to enter self-sputtering mode for Ag and Cu targets.

For highly magnetic materials, the target thickness must be reduced to counter the shunting of the field into the target material. In order to keep the same magnet assembly/cathode housing/form factor in our machine, we have employed the strategy depicted in the top portion of Figure 3. We machine the target plate surface down to a thickness at which it will sputter. However, we do not machine the entire surface down but, instead, leave thin

walls ( $\sim 0.1$  cm thick) standing around the inner and outer diameter of the target plate. As these walls are perpendicular to the magnetic field lines they contribute minimal shunting. The top and sides of the walls are the surfaces closest to the ground shield, and the target wall-to-ground shield spacing (the dark space) must remain relatively constant. The walls do provide electrostatic confinement for the plasma, thus permitting the thickness of the magnetic target plate to remain greater than if the walls were not present. A much greater advantage, in regards to ease of operation and maintenance, is afforded by these walls however. Varying the wall-to-bulk target height allows all of the other cathode assembly/ground shield components to remain the same while still permitting sputtering of materials with all levels of permeability and coercivity.

In some cases the copper backing plate and walls are machined as a single, solid piece out of a copper block and an annular disk of the magnetic target material is bonded in the cavity. During the sputtering process, both the horizontal target plate, and the vertical walls, are sputtered. However, the rate of deposition of the material from the horizontal surface onto the vertical walls is greater than the rate at which it is re-sputtered from the vertical surface. Therefore, there is no contamination of the deposited film due to sputtering of the copper walls.

With these cathodes we have successfully sputtered the nonmagnetic metals Ag, Al, Cu, Mo, Ta, Zr, and Zn. We have also reactively sputtered AlN,  $\text{Al}_2\text{O}_3$ ,  $\text{Ta}_2\text{O}_5$ , and ZnO. The nonmagnetic target material utilization is about 50 percent. The magnetic materials we have attempted are Fe, Ni, and several permalloy (NiFe) compositions. All sputtered well with target thicknesses of about 1 cm. Target use for the magnetic materials is in the 20 to 30 percent range.

In our initial work, we used a 10 kW, Advanced Energy MDX10, power supply. With this source we could supply an average power of about  $50 \text{ W/cm}^2$  to the target surface. This provided sufficient power to self-sputter Ag—at about  $45 \text{ W/cm}^2$  Ag will sputter without gas. Recently, we had our existing MDX10 modified, and have obtained three additional, modified, MDX10 supplies. These modified supplies can operate as independent 10 kW supplies or they can be assembled in parallel to act as 20 kW, 30 kW, or 40 kW supplies. With the 40 kW combination, we can now apply greater than  $200 \text{ W/cm}^2$  to our cathodes. At 15-kW ( $\sim 85 \text{ W/cm}^2$ ) we have self-sputtered Cu. Ag, Al, and Cu targets have each been sputtered at the 40 kW level.

Follow-on work will undertake three tasks. The first is to perform detailed sputter rate measurements on the various target geometries discussed above. Second is a straightforward use of our cathodes to reactively sputter oxides and nitrides at the 40 kW levels already demonstrated with the simple metal targets. Last, we will look at a design modification to allow the cathodes to maintain a more constant operating voltage over the lifetime of the target. With Al targets, for example, the voltage for a new, flat target is greater than 900 volts. Near the end of the target lifetime, with an erosion groove more than 2.5 cm deep, the operating voltage is nearer to 400 volts. This voltage variation has two causes. One is that the walls of the erosion groove are providing a high degree of electrostatic confinement. The second is that the sputter rate, and secondary electron emission coefficient, are each increased due to oblique incidence sputtering of the sloped walls of the highly eroded target.

The voltage variation is not a fundamental processing problem. However, to operate at full power, the transformer taps on the power supply must be changed three times (1000, 800, 600) over the life of an Al target—this is, at least for Advanced Energy power supplies, an extremely tedious, delicate, and labor intensive operation. To enable use of a single transformer tap setting, over the entire life of the target, we will redesign the cathode assembly. We will make the magnet assembly a completely separate entity from the target/ground shield assembly. We will mount the target/ground shield assembly on an adjustable platform that allows the relative positions of the target surface and the magnetic field lines to be varied. This should allow operation over a much narrower voltage range over the entire life of the target. As well, it may permit even thicker target plates to be used for both magnetic and nonmagnetic materials.

## Conclusions

The use of a variable wall height as an electrostatic plasma confinement tool built into a cross-field magnetron target plate has been successfully demonstrated. This design permits a single cathode/magnet/ground shield assembly to sputter the entire range of magnetic and nonmagnetic target materials at very high rates. Power densities in excess of 200 W/cm<sup>2</sup> were achieved with this geometry. As well, these cathodes permit self-sputtering of Ag and Cu at power densities above 45 W/cm<sup>2</sup> and 85 W/cm<sup>2</sup>, respectively.

## Publications and Presentations

J.D. Affinito, P.M. Martin, M.E. Gross, C.A. Coronado, and E.N. Greenwell. 1995. "Vacuum Deposited Polymer/Metal Films for Optical Applications." *Thin Solid Films* (in press). Presented at the International Conference of Metallurgical Coatings and Thin Films, April, San Diego, California.

P.M. Martin, J.D. Affinito, M.E. Gross, C.A. Coronado, W.D. Bennett, and D.C. Stewart. 1995. "Multilayer Coatings on Flexible Substrates." Presented at and in *Proceedings of the 38th Annual Technical Conference of the Society of Vacuum Coaters*, April, Chicago, Illinois.

P.M. Martin, J.D. Affinito, M.E. Gross, and W.D. Bennett. 1995. "Reflective Coatings for Large Area Solar Concentrators." Presented at and to appear in the *Proceedings of 42nd Annual National Symposium of the American Vacuum Society*.



# Vacuum Extruded Polymer Films

John D. Affinito (Materials Sciences)

---

## Project Description

The objective of this study was to develop a new vacuum deposition technology capable of depositing polymer, polymer electrolyte, and polymer composite films at very high rate. A research and development/prototype production vacuum roll coater designed for multilayer thin film deposition onto flexible substrates in a roll-to-roll configuration was adapted for use in this work. The process is capable of simultaneous deposition of polymer, metal, semiconductor, oxide, nitride, or carbide thin film multilayer structures. This work will continue to develop the process for application to the in-line, fully vacuum fabrication of electrochromic windows, mirrors, and switches.

## Technical Accomplishments

Interdigitated, large area, metal/polymer electrolyte/metal structures were vacuum fabricated by several variations involving PML, flash evaporated, electrolyte material or LML, extruded, electrolyte material. In all cases a flexible web substrate was used and deposition was on a moving web in a roll-to-roll geometry. Variations of the web substrate that we employed included nickel foil, polyester, or polyester with aluminum foil patches taped to the surface. Bottom electrode variations included the nickel foil web, the aluminum foil patch, or sputtered aluminum. Top electrodes were aluminum deposited by either sputtering or e-beam evaporation. The electrolyte layers were deposited by both PML flash evaporation of monomer electrolyte mixtures followed by either e-beam or ultraviolet curing or by LML vacuum extrusion of monomer electrolyte mixtures that were ultraviolet cured. The lateral position of the deposition zones for each electrode were controlled by positioning the apertures of each source to form the desired interdigitated structure. The structures were sometimes deposited in a single, roll-to-roll, pass through the system and sometimes in multiple passes. As part of the in-line processing, the substrate was always pretreated with an O<sub>2</sub> plasma prior to electrolyte deposition. The plasma pre-treatment improved both wetting by the monomer electrolyte and adhesion of the cured polymer electrolyte.

Three different types of electrolyte mixtures were employed. One was a proprietary formulation. The other two consisted of a salt mixed in a mixture of poly[ethylene glycol] diacrylate (PEGDA, at 55 percent

by volume), poly[ethylene glycol] methyl ether (PEGME, 35 percent by volume), acrylic acid (5 percent by volume), and Darocure 4265 (5 percent by volume). The acrylic acid is added to promote adhesion to the substrates and the metal layers while Darocure 4265 is a commercial photoinitiator (a trimethylbenzophenone blend) supplied by Ciba Geigy. The salts used were lithium trifluoromethanesulfonate (LiCF<sub>3</sub>SO<sub>3</sub>) and lithium hexafluorophosphate (LiPF<sub>6</sub>) at concentrations ranging from 0.1 moles per liter through 0.33 moles per liter. These two electrolyte mixtures were chosen for baseline tests of the process since Morita et al. published conductivity measurements for very similar materials when they were mixed and cured under atmospheric conditions in a beaker. In this way the results of the vacuum deposition process could be compared to those obtained when fabricating the same materials in air.

As mentioned earlier, two of the electrolyte formulations were selected specifically to attempt to relate the conductivity obtained by these vacuum deposition techniques to what is obtained when the material is mixed and polymerized in air. Morita made AC impedance measurements at 10 kHz with four salts (LiCF<sub>3</sub>SO<sub>3</sub> and LiPF<sub>6</sub> among them) at several concentrations, with six variations of monomer-to-ether volume ratio. At 30°C, for all but the LiCF<sub>3</sub>SO<sub>3</sub> salt, Morita found conductivities in the 10<sup>-4</sup>-to-10<sup>-5</sup> S/cm range. The conductivities for LiCF<sub>3</sub>SO<sub>3</sub> mixtures were found to be about 10 times lower. At 10 kHz, we found substantially the same results with measurements at 22°C as Morita et al. found at 30°C. To examine effects of the organic constituents independently of the salt, we used a proprietary electrolyte mixture but substituted LiCF<sub>3</sub>SO<sub>3</sub> instead of their standard salt. Figure 1 shows conductivity measurements for three extruded, and one flash evaporated, monomer electrolytes containing LiCF<sub>3</sub>SO<sub>3</sub>. All four of these formulations were identical, though one was flash evaporated and the other three were extruded under identical process conditions. For the three extruded formulations, the conductivity variations are due to experimental process control fluctuations and measurement uncertainties. Also shown is a representative measurement of the a formulation with LiCF<sub>3</sub>SO<sub>3</sub> as the salt measured only at 1 kHz.

Like Morita et al., we measured roughly 10 times higher conductivity for the LiPF<sub>6</sub> mixtures compared to the LiCF<sub>3</sub>SO<sub>3</sub> mixtures. However, the depth of cure was poor for these LiPF<sub>6</sub> mixtures. This gave rise to uncured

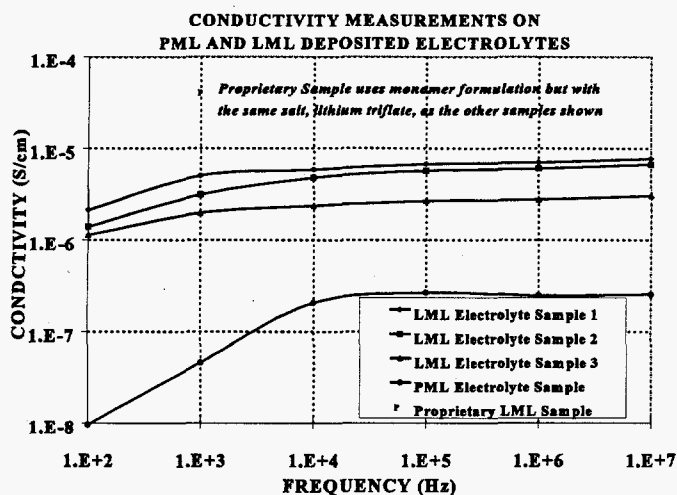


Figure 1. Either the LML (extruded) or PML (flash evaporated) process can be used to vacuum deposited polymer electrolytes.

interfaces at the bottom electrode when  $\text{LiPF}_6$  salts were used. Future work will examine the  $\text{LiPF}_6$  mixtures with different photoinitiators and higher ultraviolet exposures. It is common to need different line speeds and photoinitiators to optimize cure for different monomer formulations in atmospheric roll coating. Therefore, this result is not surprising and is likely not indicative of any inherent inadequacy of  $\text{LiPF}_6$  as a salt for use in these processes.

Note that the PML flash evaporated electrolyte has conductivity about 10 times lower than for the same monomer electrolyte solution deposited by the LML process. This is because not all of the salt gets carried over with the flash evaporated monomer. At the temperature of  $245^\circ\text{C}$ , at which we were operating the evaporator, the  $\text{LiCF}_3\text{SO}_3$  would not be expected to evaporate at all on its own. We suspect that the  $\text{Li}^+$  and  $\text{CF}_3\text{SO}_3$  ions may be carried over as part of an evaporated complex of monomer and ether solvating the ions. The main advantages of being able to deposit the electrolytes with the PML process, as opposed to the LML process, would be better thickness uniformity (down to  $\pm 1$  percent or less compared to a few percent) and much thinner films ( $100 \text{ \AA}$  compared with  $10 \text{ }\mu\text{m}$ ). Whether or not these benefits offset the disadvantage of conductivities that are lower by more than a factor of ten will need to be determined for each individual application.

All of the polymer electrolytes deposited in this work were completely transparent in the visible range of the spectrum. This makes them viable for the electrolyte layer in electrochromic, switchable, windows and mirrors. Several years ago at the Laboratory, we fabricated  $35 \text{ cm} \times 35 \text{ cm}$  electrochromic windows by sputter deposition of the electrochromic layer on glass, followed by an

atmospheric application of a polymer electrolyte, with a further vacuum deposition of the counter electrode. Currently, we are in the process of integrating our older electrochromic oxide vacuum deposition technology with this new vacuum deposition technology for polymer electrolytes. We hope to demonstrate single pumpdown, in-line, deposition of a complete 5-layer electrochromic device on a flexible substrate in the near future. Such an integrated process would eliminate the need for the three step, vacuum-air-vacuum, manufacturing technique required without the LML or PML technology.

## Conclusions

The LML and PML processes have been demonstrated to produce polymer electrolyte layers in a vacuum deposition process that is compatible with simultaneous, in-line, vacuum deposition by sputtering and e-beam evaporation. Based on our results, the conductivity to be expected from the LML process should be close to what one would measure if the same starting monomer electrolyte/salt mixture is polymerized in air. The conductivity for the PML flash evaporated electrolytes will be dependent upon the degree to which the salt, or solvated cation/anion complex, is carried over in the flash evaporation process. Thus, conductivities for PML deposited polymer electrolyte layers will need to be determined experimentally on a case by case basis. The ability to integrate these two polymer processes, with or without the added salts, into a single step, multilayer, vacuum deposition process with conventional vacuum deposition sources opens the way for lower cost production of a variety of products currently fabricated in multiple steps.

## Publications

- J.D. Affinito, P.M. Martin, M.E. Gross, C.A. Coronado, and E.N. Greenwell. 1995. "Vacuum Deposited Polymer/Metal Films for Optical Applications." *Thin Solid Films* (in press). Also presented at International Conference of Metallurgical Coatings and Thin Films, April, San Diego, California.
- C.A. Coronado, and G.C. Dunham. 1995. "High Rate Vacuum Deposition of Polymer Electrolytes," *Proceedings of 42nd Annual National Symposium of the American Vacuum Society*.

## Presentation

- J.D. Affinito, M.E. Gross, C.A. Coronado, and P.M. Martin. 1995. "Vacuum Deposition Of Polymer Electrolytes On Flexible Substrates." Plenary talk given at the *Ninth International Conference on Vacuum Web Coating*, November 13, Tucson, Arizona.

# Vining Plant Control

Dominic A. Cataldo and David F. Lowry (Environmental Toxicology and Risk Assessment)

## Project Description

The objective of the study was to develop a prototypical slow-release technology for long-term control of aggressive vining plant species. The initial goal was control of vining plants on power and utility poles. The prototype can then be adapted to protect a wide array of artificial or natural structures from various vining and rhizomatal plant species. Development of a slow-release control method will mitigate the economic and ecological damage caused by invasive vining plants. Alien vining plants, such as the air potato (*Dioscorea bulbifera* L.) and kudzu (*Pueraria lobata*) considered among the most harmful of all nonindigenous organisms in America, have become hazardous pests that cause severe economic and ecological losses to invaded areas. The aggressive climbing habit of these species results in virtually total coverage of utility poles and power lines resulting not only in interruption of power supply and slowed repair, but also in real safety hazards for utility workers. Native trees and plants are also choked out by the alien plants. These climbers are particularly aggressive in disturbed areas making poles and lines along utility line right-of-ways even more vulnerable. A corridor of dense kudzu vines reaching as high as the tallest trees or poles is common site along highways in southern states. Traditional control methods (herbicides) fail because they must be applied so often that it is logistically impossible or environmentally unsafe to maintain an effective application schedule. The expense of repeated applications over hundreds of miles of powerlines is also prohibitive. Other methods (mechanical) actually result in spread of the vining plants.

## Technical Accomplishments

No control method for aggressive vining on power and utility poles exist that is low maintenance, long-term in effect, and environmentally safe. During FY 1995, the matrix of slow-release substrates and substrate release characteristics established by D.A. Cataldo et al. were used to isolate a matrix suitable for slow-release of a meristem growth inhibitor. Because native weed species such as morning glory (*Ipomoea purpurea*) can also be pernicious climbers, morning glory was used as the test species for the efficacy tests. Plants were grown in eight-inch pots in a growth chamber and trained to a wood dowel for climbing. The substrate was added to the poles at a height of at least 24 inches above the pot. Several

release rates were tested with the selected herbicide/substrate. A second substrate was used as a coating in an attempt to refine the release rate. Although an effective release rate was roughly estimated, there was not sufficient time to finalize the most efficacious release rate. In addition, three structural configurations of the herbicide-amended-substrate were produced. These prototype devices were designed to be both amenable to the climbing habit of the plants and to ease of pole application. The devices tested included a solid surface that wrapped around the pole (singly or with two separated devices), a spiral design that coiled around the dowel, and a flexible mesh. The most efficacious design was the solid surface wrap. Unexpectedly the herbicide used not only controlled tendril growth (Figure 1), but ultimately killed the entire plant (Figure 2) once contact with the device was made.

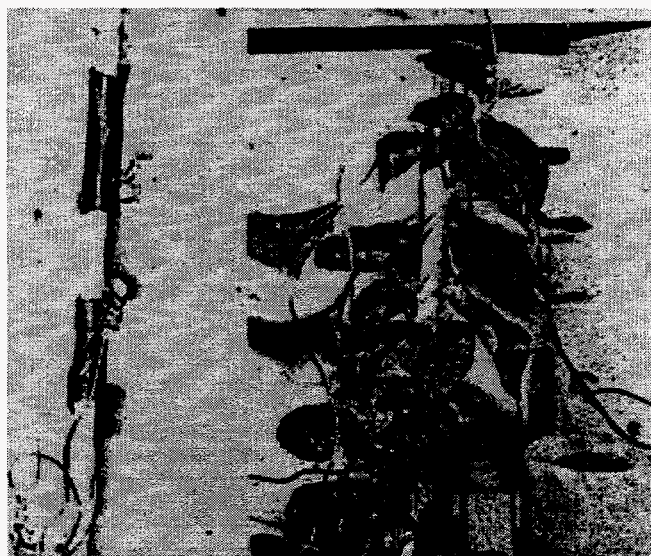
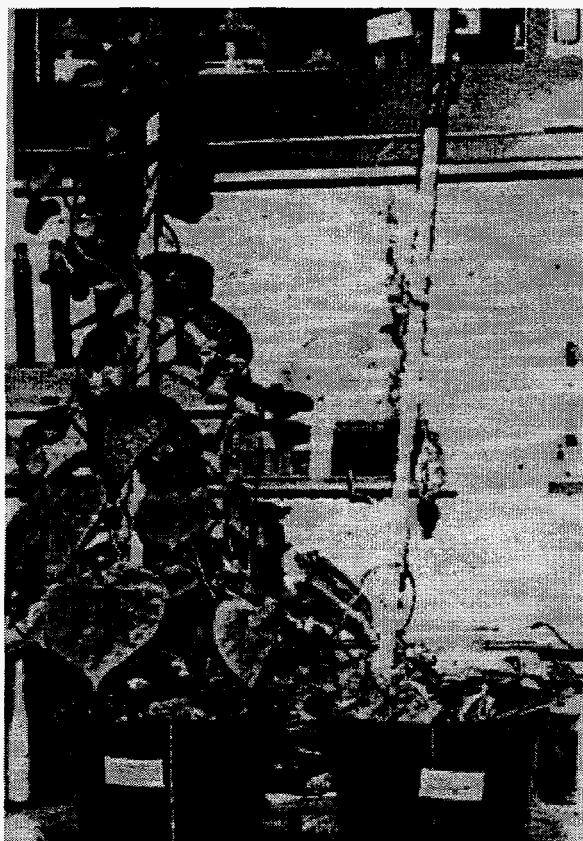


Figure 1. Control of vining by use of slow-release substrate placed above the growing tendrils of climbing weeds. Vining aspect of a control plant is shown on the right.

A small number of kudzu plants were grown under APHIS control conditions to test the efficacy of the solid substrate on this nonindigenous pest species. Although the effective release rate for the kudzu could not be established due to time and budget constraints, an interesting avoidance response was observed. Tendrils coiled over 6 times around the dowel poles would unwind in the presence of the substrate and move to and coil around adjacent control poles. When a slower-release

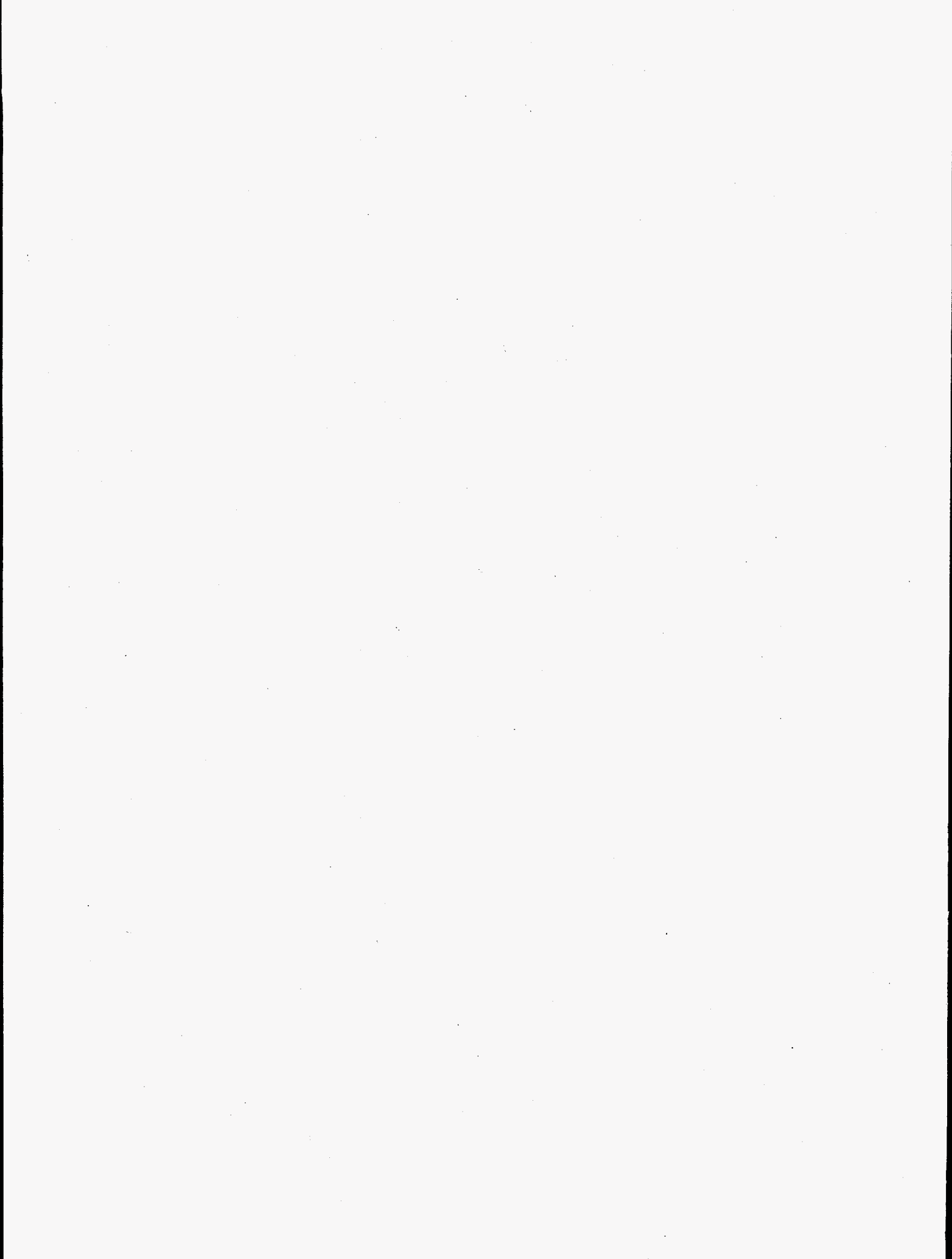




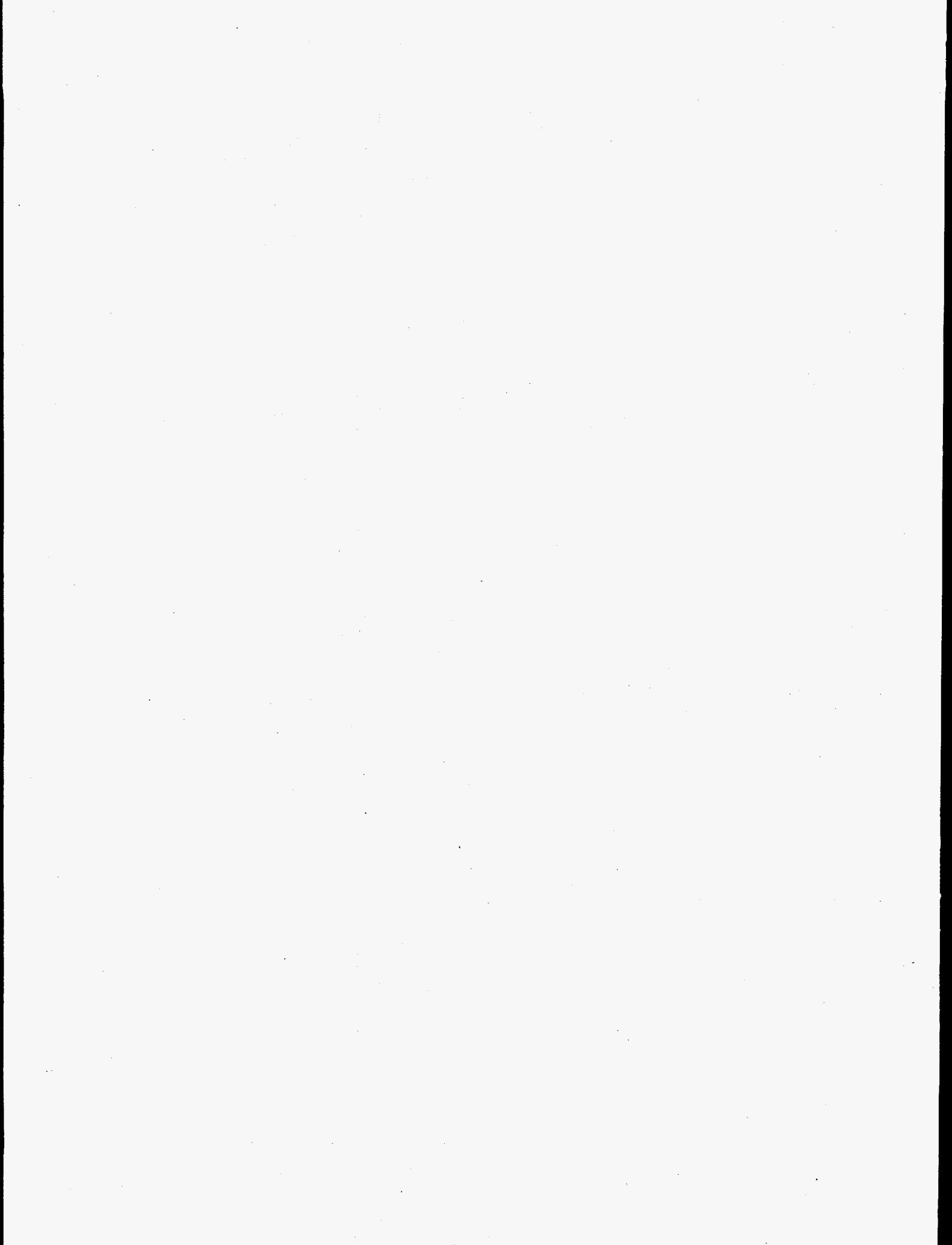
**Figure 2.** The effect of slow-release herbicide device on vining plants following contact with the substrate (death occurred 2 weeks after tendril inhibition). Note the necrotic and absent foliage of the affected plant on the right. One of two slow-release substrate devices (the black patch) is visible towards the top of the dowel pole. A control plant is at the left.

substrate formulation was tested, the tendrils remained in contact with the substrate longer, but eventually unwound from the pole and moved to adjacent climbing surfaces. The leaves on the parent tendril that had contacted the substrate became necrotic, but the plant survived. Although not as direct a control measure as killing the vining plant, the redirection of tendrils away from the pole containing the slow-release device holds considerable promise for reducing the overgrowth of power and hydroelectric poles and cables.

In summary, a prototypical slow-release system was designed that inhibited tendril adherence or growth on pole structures and had the ability to cause plant death in some species. Further work on various vining rhizomatal species and substrate parameters should provide a long-term, low maintenance, and environmentally safe control device that is applicable to the protection of numerous natural and man-made structures.



## **Risk and Safety Analysis**



# A Tribal Risk Model

Barbara L. Harper (Health Risk Assessment)

---

## Project Description

This project developed background material for a general tribal risk model suitable for evaluating impacts to the health and culture resulting from Hanford-related stressors. The utility of this model to Hanford risk management and decision making as also outlined, and initial descriptions of practical applications described. These products are based on tribal letters, reports, conversations, and comments.

## Technical Accomplishments

At complex DOE sites, decisions are frequently made in such small increments that an outcome may be determined without ever consciously setting values-based goals or making formal decisions about the target end state. For example, decisions based solely on reducing human exposure frequently do not protect much of what is really "at risk," especially from holistic tribal perspectives. If decisions are not supported by an information base which includes the full range of potential impacts to health, resources, culture, and tribal identity, decisions may be "unstable" and budgets harder to justify.

Ways to visualize the overall Hanford mission, set performance goals, describe stressors (chemical, physical, institutional, and so on), develop an adequate yet not data-intensive information base about risks and impacts, and select decision principles have been described. If each of these processes matches in scale and precision level, it is easier to describe program interfaces and remediation and restoration goals.

Tribal risk policies regarding Hanford are beginning to focus at this higher holistic level, so it will be increasingly important to understand how to incorporate this into conventional risk-based decision processes. Two practical applications have been described as straw-models for trial decisions.

The first application, lifeways-based health impact assessment, begins with tribal-specific exposure considerations, and then considers additional ecological and cultural impacts. This approach is typically used in remediation contexts where human exposure is a primary concern. It is patterned after CERCLA methods and expanded to include comparative risk measures.

The second application (Figure 1) landscape-level comparative risk, is more useful in prospective land use planning contexts, and shifts the scale of analysis from short and local to hierarchical and long-term. It also shifts from thinking probabilistically to thinking geographically, and from measuring individual variables to measuring functions provided by multiple embedded landscapes.

Decision principles were also developed from various tribal documents. Because they match the scope of the proposed Hanford integrated environmental management goal and also the breadth of information collected under comparative and tribal risk models, they will likely result in improved Hanford decisions.

## Presentations and Publications

D.L. Powauke, D. Conrad, and B.L. Harper. "Environmental Management, Land Use Planning, and Nez Perce Reality." Presentation and (to be) published paper, Waste Management 96.

D.L. Powauke, D. Conrad, and B.L. Harper. 1995. "The Earth and Myself Are of One Mind: Achieving Equity in Risk Based Decision Making and Land Use Planning." Poster and (to be) published paper, State and Tribal Risk Forum, St. Louis.

B.L. Harper. *Technical Guidance for Preparing a Risk Assessment for Storage, Handling, Processing and Incineration of RCRA Hazardous Waste*. Report prepared for the Confederated Tribes of the Umatilla Indian Reservation.

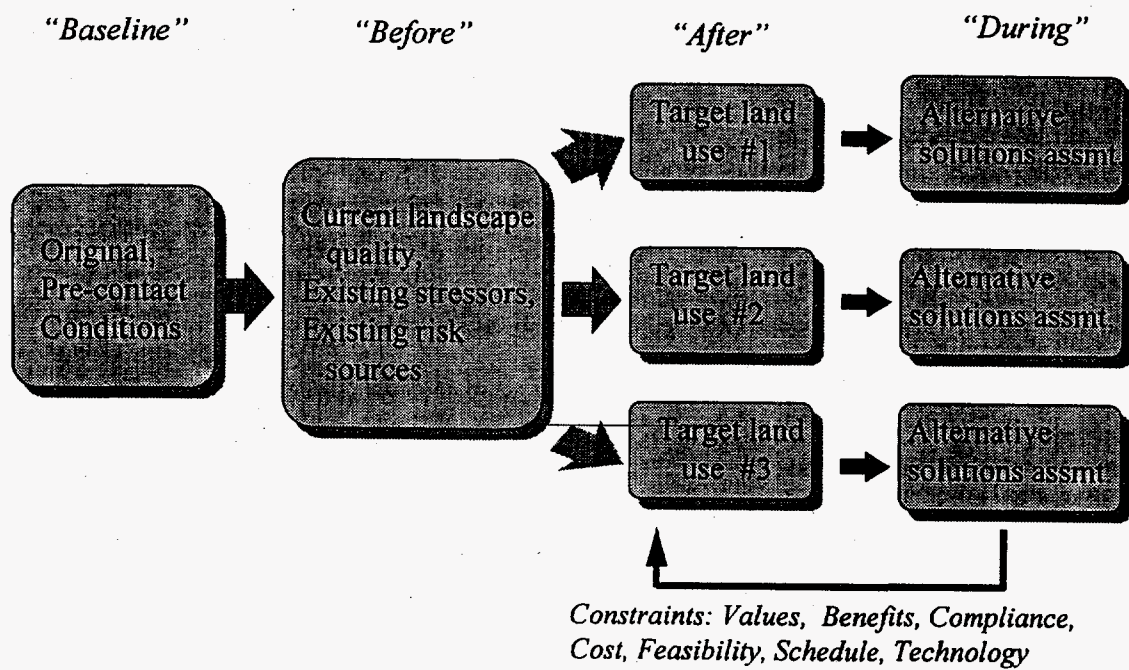


Figure 1. Landscape-Level Comparative Risk

# Cell and Tumor Growth Kinetics

Lyle B. Sasser (Biology and Chemistry)

Robert A. Wind (Molecular Structure and Dynamics)

## Project Description

The purpose of this project was to develop experimental data that will allow descriptions of changes in cell division and tumor growth induced by active metabolites of chlorinated hydrocarbon solvents widely distributed in DOE sites. Recent data indicate that these metabolites act by four distinct modes of action. Obtaining quantitative data on how each of these modes of action influences tumor growth and progression is critical to the development of alternative methods for estimating cancer risk at low exposures found in the environment.

## Background

This project focused on hydrocarbons, such as carbon tetrachloride, that selectively kill normal cells and provide a growth advantage to intermediate cells. Selective stimulation of the growth of intermediate cell populations is a property of dichloroacetate (DCA). Suppressed apoptosis appears to be the mode of action represented by trichloroacetate (TCA). These two acids are metabolites of several chlorinated solvents that produce liver tumors in mice and drive risk assessments. The fourth mode of action is direct increases in mutation frequency by chemicals that have genotoxic properties.

Rates of cell division and the phenotype of tumors are being characterized at appropriate intervals of treatment in mice. In parallel with this work, magnetic resonance imaging techniques are being developed to study the progression of initiated cells into hepatic tumors in mice in a noninvasive, nondestructive way. This approach will be validated by following the sequential induction of benign nodules, adenomas, and hepatocellular carcinomas that are induced by dichloroacetate or trichloroacetate in mice. These treatments produce a large number of benign tumors within 6 to 9 months and the progression of these tumors appears to depend solely on continued stimulation of division of cells expressing a particular phenotype.

## Technical Accomplishments

During FY 1995, parallel efforts conducted at Washington State University have shown that dichloroacetate selectively stimulates division of cells expressing elevated levels of c-Jun and c-Fos within tumors while suppressing division within normal hepatocytes (Figure 1).

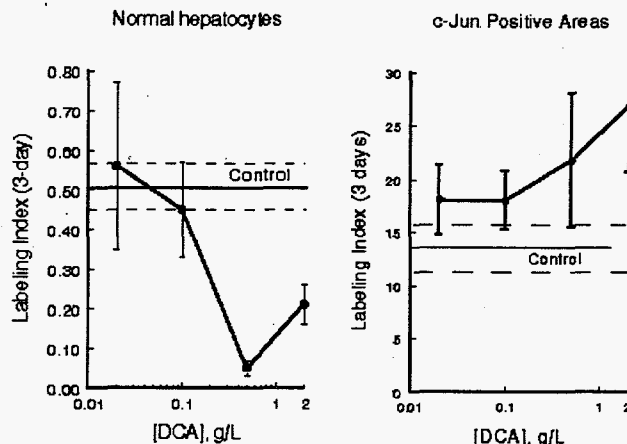


Figure 1. The effect of dichloroacetate on replication rates within normal liver and preneoplastic lesions of  $B_6C_3F_1$  mice. DCA strongly depresses replication of normal hepatocytes, but stimulates replication within portions of lesions that express c-Jun. Note the differences in scale.

These findings provide a good model of one of the modes of action for which a biologically based model is needed. Furthermore, work done at Pacific Northwest National Laboratory has shown that the relative potency of carbon tetrachloride for selectively killing normal hepatocytes in mice and rats closely parallels the relative sensitivities of these two species to the hepatocarcinogenic effects of this chemical. Other work at Washington State University has shown that cell replication within tumors induced by trichloroacetate is independent of continued treatment with trichloroacetate. This indirectly supports our hypothesis that its principal mode of action is suppressing apoptosis, an effect associated with other peroxisome proliferators. Collectively, the data with these three compounds have provided examples of chemicals within the chlorinated solvent group that display three of the four distinct modes of action which we are interested in for exploring alternates to the linearized multistage model for cancer risk assessment. The fourth mode of action (mutagenesis) is the conceptual basis for the linearized multistage model that is the default methodology used by regulatory agencies. Therefore, the project can now focus on obtaining the empirical data that will allow the construction and validation of models for nongenotoxic carcinogens that can be used as alternatives to the conservative linearized multistage model.

In parallel with this work, magnetic resonance imaging methodologies are being developed to allow us to follow growth rates of individual tumors in vivo. Magnetic resonance imaging has been widely applied to determine the spatial location and the size of tumors in animals and humans. Its application to measurement of growth and progression of preneoplastic lesions to malignant tumors will greatly simplify the collection of data for other chemicals in the future. Magnetic resonance imaging is noninvasive and nondestructive, therefore, animals do not have to be periodically sacrificed to obtain these data, and a specific animal can be followed over time. This means that relatively few animals need to be examined in order to get statistically valid results. Such data can be used for acquiring the desired kinetic data needed for developing models developed upon the toxicodynamics of each chemical.

The in vivo magnetic resonance imaging experiments will be performed in a large external magnetic field of 11.7 tesla. This field is larger than that used in any commercial imaging instrument. High-field imaging increases the spatial resolution achievable in an image, and this in turn makes it possible to detect smaller lesions at an earlier stage. However, in order to fully realize this capability, methods have to be developed to overcome problems specifically occurring at high-field strengths.

Therefore, during FY 1995, the emphasis of our magnetic resonance imaging research has been on evaluating and calibrating the magnetic resonance imaging instrumentation by in vitro magnetic resonance imaging on excised tissues and sacrificed animals. These evaluations included the use of special magnetic resonance imaging techniques to enhance contrast between normal tissues and regions of hyperplasia. These techniques utilize possible differences in the motional properties of the tissue water in lesions and in the surrounding healthy tissues. When these differences occur, they give rise to alterations in several magnetic resonance imaging parameters such as the spin-lattice and spin-spin relaxation times,  $T_1$  and  $T_2$ , respectively, and the translational diffusion coefficient of tissue water. Because no mice with sizable hepatic lesions are yet available, we have investigated the effects of contrast-enhanced imaging techniques in mice bearing urethane-induced lung tumors.

Figure 2 shows images of the same slice through an excised lung obtained with different magnetic resonance imaging methods. It follows that especially the  $T_1$ - and diffusion-weighting techniques increase contrast between the tumors and the surrounding lung tissue. Enhanced image contrast like that shown will improve the detection of small lesions and measurements of their volume and growth rates.

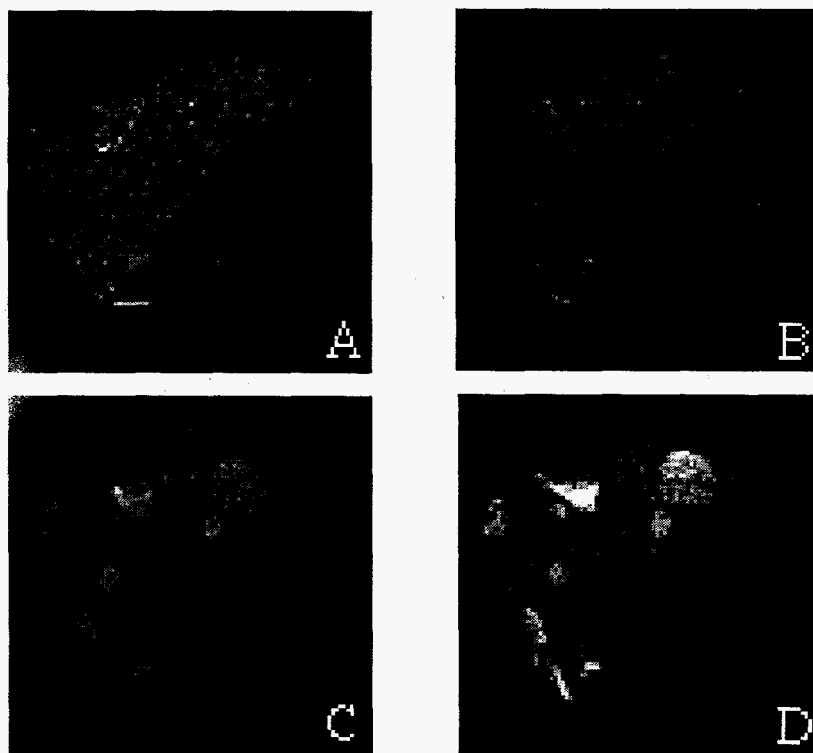


Figure 2. MR images of a tumor-bearing excised mouse lung obtained with different magnetic resonance imaging methods. A: Spin Density; B:  $T_2$  Weighted; C:  $T_1$  Weighted; D: Diffusion Weighted.



Finally, in Figure 3 an image is shown of a slice near the diaphragm of a sacrificed healthy mouse. This image illustrates the spatial resolution that can be obtained with the high-field magnetic resonance imaging instrumentation.

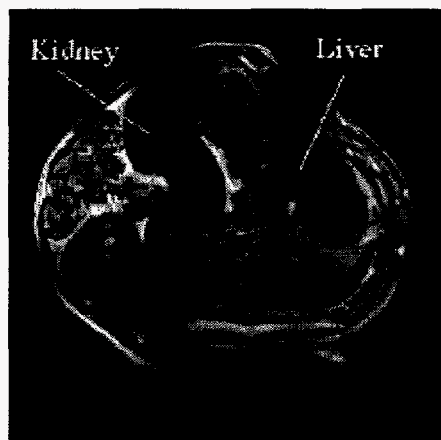


Figure 3. MR transverse image of a sacrificed healthy mouse showing the different lobes of the liver, the two kidneys, the spinal column, the pancreas, and the gall bladder.

This coupling of the empirical data on tumor growth and progression using traditional methods with parallel experiments with magnetic resonance imaging provides a unique opportunity to validate the latter approach for other applications in diagnostic medicine as well. In turn, this work will provide direction to research at the cellular and molecular level in the cell signaling and direct and indirect genotoxicity projects. This final step is important to the conceptualization of how data should be extended to doses in which tumor responses cannot be practically studied. Acceptance of these concepts will provide a firm foundation for exploring alternative risk assessment models for "nongenotoxic" carcinogens.

#### **Presentations**

R.A. Wind. 1995. "NMR and MRI Studies of the Effects of Exposure on Cells and Tissues." Workshop on Magnetic Resonance and the Environment, April, Richland, Washington.

A.J. Stauber, M.E. Bull, and R.J. Bull. 1995. "Different Modes of Action of Dichloroacetate and Trichloroacetate in Hepatocarcinogenesis." Presented at the Pacific Northwest Association of Toxicologists Meeting, September 16, Moscow, Idaho.

# Cell Signaling Mechanisms

Brian D. Thrall and Richard J. Bull (Biology and Chemistry)

## Project Description

Halogenated solvents are the most common contaminants of hazardous waste sites in the country. They are found on virtually every major DOE and DOD site. The induction of liver cancer in mice is the effect that drives the cleanup levels, and in most cases this response is attributable to two metabolites of these solvents, trichloroacetic acid (TCA) and dichloroacetic acid (DCA). Since neither trichloroacetic acid nor dichloroacetic acid are mutagenic, it is likely that the mode of action for these chemicals involves selection of genetically altered (initiated) cell populations, either by direct deregulation of the cell cycle in initiated cell populations and/or altering programmed cell death. Mechanistically, these modes of action must be accomplished by altering the cellular signaling pathways which regulate cell division and programmed cell death. It is estimated that one in three proteins in cells are regulated by changes in phosphorylation via both phosphatase and kinase enzymes. These cell signaling pathways are both tissue- and species-specific. The goal of this project was to identify the major cell signaling pathways that are altered during trichloroacetic acid- and dichloroacetic acid-induced carcinogenesis. An understanding of the critical molecular pathways involved in rodents will ultimately allow us to determine the relevance of these pathways in humans, and the potential for trichloroacetic acid and dichloroacetic acid to induce similar pathologies at dose regimens which involve human exposure.

## Technical Accomplishments

Trichloroacetic acid and dichloroacetic acid are the principal hepatocarcinogenic metabolites of trichloroethylene, tetrachloroethylene, 1,1,1-trichloroethane, 1,2-dichloroethylene, 1,1-dichloroethane, and 1,1,1,2-tetrachloroethane; solvents that have been improperly disposed of on DOE sites. These metabolites are also significant byproducts of the chlorination of drinking water. Although these metabolites are not genotoxic, they are both complete carcinogens in mouse liver. However, the relevance of the hepatocarcinogenic effects of trichloroacetic acid and dichloroacetic acid in humans is unclear. In rodents, trichloroacetic acid-induced hepatocarcinogenesis is associated with activation of the peroxisomal fatty acid beta-oxidation pathway and proliferation of liver peroxisomes. Peroxisome proliferation is now known to

be mediated via a family of nuclear receptors (PPARs) which form heterodimers with a variety of nuclear transcription factors from the retinoic acid, vitamin D, glucocorticoid, and thyroid hormone receptor families. In mouse hepatoma cells, we find that treatment with trichloroacetic acid activates the PPAR. The effect with trichloroacetic acid is greater than that of dichloroacetic acid but less than a more potent peroxisome proliferator (clofibric acid), consistent with the proposed mechanism of peroxisome proliferation. Since the tissue- and species-specificity of trichloroacetic acid may depend on the heterodimer nuclear receptors which are predominantly activated, we are conducting studies to identify the heterodimers involved in mouse and human cells.

Although the carcinogenic effects of trichloroacetic acid are associated with peroxisome proliferation and PPAR activation in rodents, it is not clear that this is a causal relationship. In addition, the ability of peroxisome proliferators to induce this response in humans has been questioned, although a human PPAR has been identified. To understand which cell signaling pathways might be altered during trichloroacetic acid-mediated carcinogenesis, we have examined the expression of several key proteins in normal liver and tumor tissue of mice chronically fed trichloroacetic acid in drinking water. In this experiment, male B6C3F1 mice were fed 2.0 g/L trichloroacetic acid in drinking water for 50 weeks to induce tumors. The mice were then switched to 0, 0.02, 0.5, 1.0, or 2 g/L for 2 weeks. Normal liver and tumors were removed, and immunoblot analysis was used to determine the expression patterns of p34<sup>cdc2</sup> (a kinase which regulates entry into mitosis), PPAR $\alpha$ , and ERK1/2 (a mitogen activated protein kinase which regulates differentiation and cell division). As shown in Figure 1, tumors induced by trichloroacetic acid express very high levels of p34<sup>cdc2</sup> compared to normal liver, consistent with a rapid rate of cell division within the tumor. The presence of trichloroacetic acid in drinking water also appears to induce PPAR expression, although a clear dose dependence was not observed. However, expression of the ERK1/2 MAP kinase was significantly reduced in tumors from trichloroacetic acid-treated animals, and there appears to be a dose-dependence on ERK1/2 expression in normal liver as well. These results indicate that the ERK1/2 kinase pathway may be downregulated in trichloroacetic acid-induced tumors. We are currently investigating whether this involves changes in the phosphorylation status of ERK1/2, and whether this is a direct effect of trichloroacetic acid treatment.

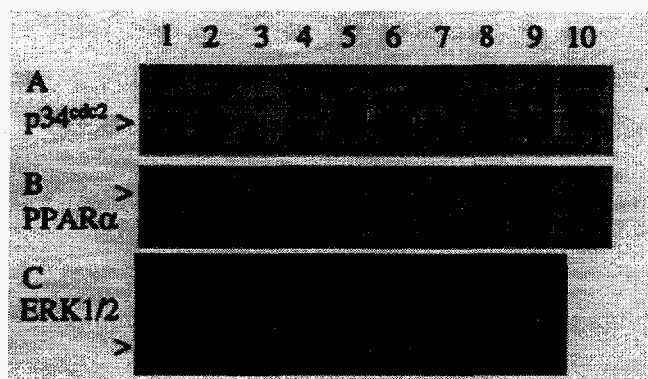


**Figure 1.** Alterations in cell signaling proteins in normal and tumor tissue of TCA-treated mice. Levels of p34<sup>cdc2</sup> (A), mouse PPAR $\alpha$  (B), and the MAP kinases ERK1/2 (C) were measured by immunoblotting. In blots A and B, lanes 1, 2, 4, 6, 8, and 10 contain normal tissue from animals treated with 2 g/L TCA for 52 weeks, then were switched to 0, 0.02, 0.5, 1, 2, and 0 g/L (respectively). Lanes 5, 7, and 9 contain tumor tissue from the same livers as lanes 4, 6, and 8 (respectively). In blot C, lanes 1 and 2 contain 50 ng of a GST-p44 MAP kinase fusion protein. Lanes 3-7 contain normal liver tissue from mice treated with 2 g/L TCA for 52 weeks, then switched to 0, 0.02, 0.5, 1, or 2 g/L TCA for 2 weeks. Lanes 8 and 9 contain tumor tissue from animals treated with 2 g/L TCA for 54 weeks. The > indicates the protein of interest.

Dichloroacetic acid also induces peroxisome proliferation, but at higher doses than required to induce liver tumors in mice. The induction of tumors by dichloroacetic acid is, however, associated with altered regulation of glycogen in liver. Consistent with this finding, our results indicate that dichloroacetic acid also suppresses serum insulin. Alteration of glycogen levels and suppression of serum insulin may play a pivotal role in the deregulation cell division during dichloroacetic acid-induced carcinogenesis. For example, the cellular pathways which regulate glycogen synthesis overlap with kinases which are involved in the regulation of the transcription factor c-Jun (see Figure 2). In a study funded through Washington State University, it was determined that tumors induced by dichloroacetic acid express high levels of c-Jun and c-Fos in rapidly dividing cells. It is hypothesized that dichloroacetic acid interacts with pathways involving mitogen activated protein kinases (MAPK) resulting in both alterations in glycogen metabolism and control of c-Jun activity. In particular, the ERK1/2 members of the MAPK family are known to activate the insulin-stimulated protein kinase (ISPK), which in turn plays a role in glycogen regulation. Alterations in serum insulin levels induced by dichloroacetic acid may be a compensatory feedback mechanism due to changes induced in the ERK1/2-ISPK pathway. In addition, an upstream activator of the ERK1/2 pathway is the *ras* oncogene product. Spontaneous liver tumors from B6C3F1 mice have a high incidence of *ras* mutations, thus, it is plausible that dichloroacetic acid treatment allows the selective outgrowth of spontaneously initiated cells. The

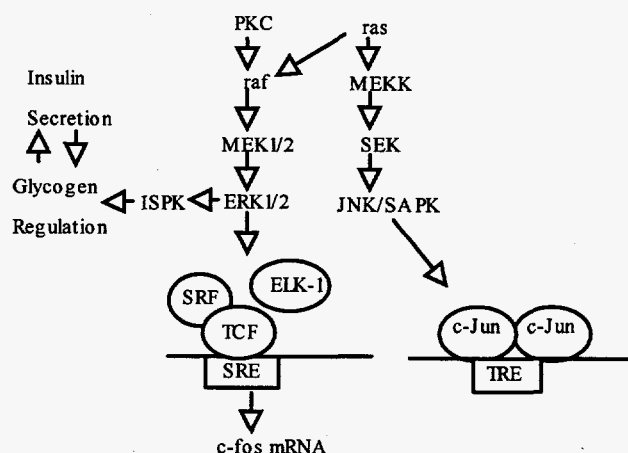


**Figure 2.** Cell signaling pathways altered during TCA and DCA hepatocarcinogenesis. Mitogen Activated Protein Kinase (MAPK) cascades from the ERK1/2 (extracellular stimulus receptor kinase) family and JNK (Jun N-terminal kinase) family contribute to the regulation of a variety of essential cell functions, including stress responses and cell cycle control. Tumors induced by DCA have characteristics consistent with alterations in both the JNK and ERK1/2 pathways, whereas TCA-induced tumors show alterations in expression of ERK1/2.

*ras* protein also activates a separate pathway involving a related MAPK, called the JUN N-terminal kinase (JNK), which phosphorylates c-Jun. Therefore, chronic deregulation of c-Jun by dichloroacetic acid may be accounted for by crosstalk between more than one signaling pathway.

Cell signaling pathways such as those involving MAPK are complex and nonlinear (reviewed in Johnson and Vaillancourt 1994; Cohen 1993). Although the pathways hypothesized to be involved with trichloroacetic acid and dichloroacetic acid hepatocarcinogenesis involve a great deal of crosstalk, the distinct pathology of trichloroacetic acid- and dichloroacetic acid-induced tumors suggest there are also clear divisions between the cell signaling pathways involved. Our initial studies have focused on two related, but physiologically distinct signaling pathways involving the ERK1/2 and JNK families of MAPK. An abbreviated form of these pathways is outlined in Figure 2.

Both pathways act as upstream regulators of either the expression or regulation of the transcription factors such as c-Fos and c-Jun. In dichloroacetic acid-induced tumors, changes in c-Jun and c-Fos expression as well as glycogen regulation are observed. In trichloroacetic acid-induced tumors, expression of ERK1/2 is lower than in normal liver, and there is not a significant induction of either c-Fos or c-Jun protein. Previous reports suggest that acute treatment of cells with peroxisome proliferators can induce c-Fos mRNA, and that this effect is abrogated

by inhibitors of protein kinase C (PKC) (Ledwith et al. 1993; Bieri 1993). Since protein kinase C is an upstream activator of the ERK1/2 pathway, it is possible that the decreased expression of ERK1/2 in trichloroacetic acid-induced tumors is a result of chronic treatment and down regulation of PKC and ERK1/2 pathways, although further studies are needed to confirm this hypothesis. Identifying the doses required to alter these cell signaling pathways, as well as the relevance of these effects in human liver will play a significant role in our understanding of the carcinogenic effects and risks associated with trichloroacetic acid and dichloroacetic acid. This, in turn will clarify the human risk of liver cancer from several halogenated solvents.

## References

- F. Bieri. 1993. "Peroxisome Proliferators and Cellular Signaling Pathways." A review. *Biol Cell* 77:43-46.
- P. Cohen. 1993. "Dissection of the Protein Phosphorylation Cascades Involved in Insulin and Growth Factor Action." *Biochem Soc Transact* 21:555-567.
- G.L. Johnson and R.R. Vaillancourt. 1994. "Sequential Protein Kinase Reactions Controlling Cell Growth and Differentiation." *Current Opinion Cell Biol* 6:230-238.

B.J. Ledwith, S. Manam, P. Troilo, D.J. Joslyn, S.M. Galloway, and W.W. Nichols. 1993. "Activation of Immediate-Early Gene Expression by Peroxisome Proliferators *in vitro*." *Mol Carcinogenesis* 8:20-27.

B.D. Thrall, L.K. Fritz, G.A. Orner, and M.Y. Laurino. 1995. "Novobiocin Induced Apoptosis in HL-60 Cells." *PANWAT Proc.* 12(1): 26.

J. Kato, A.J. Stauber, and R.J. Bull. 1995. "Effects of Hepatocarcinogenic Dose of Haloacetates on Control of Glycogen Metabolism in Male B6C3F1 Mice." *PANWAT Proc.* 12(1):20.

M.K. Smith and R.J. Bull. 1995. "Influence of Dichloroacetate Treatment on Serum Insulin Levels in Male B6C3F1 Mice." *PANWAT Proc.* 12(1):18.

## Presentation

B.D. Thrall, R.C. Horan, M.S. Weir-Lipton, and C.G. Edmonds. 1995. "Inhibition of Excision Repair and Induction of Apoptosis by Novobiocin." Presented at the Seventh International Congress of Toxicology, July 2-6, Seattle, Washington.

# Comparative Metabolism and Pharmacokinetics

Richard J. Bull (Biology and Chemistry)

## Project Description

The objective of this project was to investigate metabolism and pharmacokinetics of hazardous chemicals, including the identification of those metabolites or intermediates that are actually responsible for the adverse effect.

Chlorinated ethane and ethylene solvents are widespread contaminants found on DOE, DOD, and CERCLA sites throughout the country. They are regulated primarily because of their induction of liver cancer in mice. The intent of this project is to develop a linkage between the metabolism of trichloroethylene in rodents, and the identification of dichloroacetate (DCA) and trichloroacetate (TCA) as the principal causes of liver cancer in mice. This work will form the basis for developing models for normalizing dose of these two carcinogenic metabolites in humans relative to the sensitive test species.

This work will ultimately apply to a whole class of the solvents that give rise to these same two carcinogenic metabolites. A critical issue is the rates and pathways for further metabolism of dichloroacetic and trichloroacetic in humans and the mouse where they have been shown to be very effective carcinogens. Prior work has demonstrated that there are major interspecies differences in their clearance and that prior exposure to the chemicals can drastically inhibit metabolism of subsequent doses. The other halogenated hydrocarbons that give rise to these metabolites are listed in Table 1 in order of their frequency of occurrence on DOE sites. Therefore, the approach developed under this project should be applicable to the development of physiologically-based pharmacokinetic models that can be extended to humans for a large group of chemicals.

## Technical Accomplishments

Three important findings were made with respect to the oxidative metabolites of trichloroethylene in FY 1995. First, the metabolism of trihaloacetates to dichloroacetate differs significantly between mice and rats. This is primarily reflected in substantially different changes in rates of metabolism and urinary products that are found as dose is increased in the two species. Second, subsequent metabolism of dichloroacetate is subject to strong inhibition by prior exposure to dichloroacetic in rats, but not in mice. This effect also becomes apparent when

Table 1. Contribution of haloacetates to risks at DOE sites

Solvent	Freq.	Trichloroacetate	Dichloroacetate
Trichloroethylene	14	Major	Measurable
1,1,1-Trichloroethane	11	Major	Minor
1,2-Dichloroethylene	11	None	Measurable
Tetrachloroethylene	10	Major	Minor
1,1-Dichloroethane	10	None	Major
Chloroform	10	None	None
Carbon Tetrachloride	7	None	None
1,2-Dichloroethane	7	None	None
Dichloromethane	7	None	None
Chloroethylene	5	None	None
1,1,2-Trichloroethane	4	None	None
1,1,1,2-Tetrachloroethane	4	Major	Major

dichloroacetic is produced as a result of metabolism of trihaloacetates. Humans more closely resemble rats in this case. Third, metabolism of the trihaloacetates appears to be initiated in the endoplasmic reticulum. However, metabolism of the dichloroacetic appears to occur largely, if not entirely, within cytosolic fractions. The nature of the reactions responsible for this metabolism and the reason why it is so easily and completely inhibited by prior treatment are very important to assessing human risk resulting from exposure to these solvents.

Pursuit of the haloacetates has broader public health implications than simply being metabolites of chemicals commonly found in hazardous waste. Both chlorinated and brominated haloacetates are produced in the disinfection of drinking water. Conventional risk assessments on dichloroacetate utilizing the linearized multistage model indicate an average risk from this compound alone as being in excess of one additional cancer case per 10,000 population in the U.S. This has been recognized by the Environmental Protection Agency when they developed a negotiated rulemaking with drinking water industry and environmental groups. Risk from haloacetates are the most critical of the byproducts of chlorination identified to date. On the other hand, it is clear that abandonment of drinking water disinfection would not be in the best interests of the public health without much clearer demonstration of the risks.



The present results strongly suggest the possibility of interactions between the myriad of haloacetates that are produced in drinking water and those produced in the metabolism of solvents. Because of the nonlinear behavior of the kinetics of this class of compounds in the dose ranges that induce tumors, neurotoxicity and developmental effects of the extrapolation of these risks between species cannot be done without an understanding of the metabolism of these chemicals and how it relates to the induction of toxic effects. This will mean developing a quantitative physiological model of the kinetics of the active metabolite to allow dose to be normalized between species and knowing how co-exposures to several members of the class modifies the concentrations of each active metabolite at its target site.

Another accomplishment was the publication of papers on glutathione-conjugate pathway of trichloroethylene metabolism. This pathway results in formation of the mutagenic metabolite, dichlorovinylcysteine, which has been held responsible for renal tumors induced by trichloroethylene in the male rat. Our work demonstrated that the simplistic view that the rat was more sensitive to this metabolite was not true, as cell replication was

increased in the kidney of mice at about 1/25th the dose required in rats. Moreover, this sensitivity could be correlated with formation of specific protein adducts. Formation of these adducts and cytotoxic responses to trichloroethylene in the two species correlated were consistent with one another. Resolution of risk issues with trichloroethylene will require resolution of how activation of this pathway induces cancer because N-acetyl-dichlorovinylcysteine has been measured in the urine of humans exposed to trichloroethylene.

### Publications

M.V. Templin, D.K. Stevens, R.D. Stenner, P.L. Bonate, D. Tuman, and R.J. Bull. 1995. "Factors Affecting Species Differences in the Kinetics of Metabolites of Trichloroethylene." *J. Toxicol. Environ. Health.* 44:433-445.

G. Xu, D.K. Stevens, and R.J. Bull. "Metabolism of Bromodichloroacetate in B6C3F1 Mice." *Drug Metabolism and Disposition* (in press).

# ***Development of Environmental Dosimetry Modeling Parameter Database Editor***

Bruce A. Napier, Dennis L. Streng, N. Corrie Batishko (Health Risk Assessment)  
Brad R. Warren (Multimedia Exposure Assessment)

---

## **Project Description**

This project involved the development of a database of probability distributions of parameters required for radiological dose and risk assessment, along with a Windows-compatible, interactive computer program to aid maintenance and traceability of the individual values. The goal of this development effort was to improve the quality, traceability, and defensibility of radiological dose and risk assessments by providing a robust database with an interactive database manager.

## **Technical Accomplishments**

A functional database editor named Radiological Parameter Database Editor was prepared using Visual

Basic programming. The editor allows the user to view or modify parameters in separate files for agricultural databases, radiological parameter databases, individual exposure databases, and site-specific databases. An unlimited number of individual databases in each of these categories are supported, and each is allowed its own associated list of references. The editor currently allows data to be in formats supporting either the GENII Environmental Dosimetry Software System or the Multimedia Environmental Pollutant Assessment System (MEPAS).

Databases were established in each category with default information from existing files. An extensive effort was begun to update and reference all parameters.

# *Direct and Indirect Genotoxic Mechanisms*

David L. Springer (Biology and Chemistry)

---

## **Project Description**

A key determinant for the choice of the mathematical model to be used for low-dose extrapolation of carcinogenic risk is whether the chemical is mutagenic. If a carcinogen acts through a mutagenic mechanism, its effects are thought to be linear at low dose. If not, it becomes important to establish the mechanism by which it produces cancer, as the carcinogenic response may have a threshold. This would translate into cleanup levels that may be 1 to 4 orders of magnitude less restrictive to achieve the same target risk level for a mutagenic carcinogen.

One of the major contaminants at Hanford is carbon tetrachloride which is well recognized as a liver carcinogen. Carbon tetrachloride is known to selectively kill normal hepatocytes because cells that have been initiated generally lack the metabolic capacity to activate it to a toxic form. The reparative hyperplasia that results from this killing of normal cells provides a very strong stimulus to the tumors cells that are not killed by carbon tetrachloride. This process is generally believed to be responsible for tumor development.

Carbon tetrachloride is also known to induce oxidative stress that could damage DNA through the generation of reactive oxygen species. Such damage is likely to occur only at high doses and may be in large part secondary to inflammatory responses initiated by necrosis. If it occurs at low doses, however, it could contribute to a mutagenic mechanism and to carbon tetrachloride's tumorigenic effects. On the other hand, oxidant stress is also known to modify cell signaling mechanisms that control the cell cycle. It is predicted that effects mediated through these pathways will occur at much lower doses than DNA damage. The present project is aimed at distinguishing these two mechanisms and estimating their relative contribution to liver cancer at low doses. Results from these studies will be integrated with data obtained from other projects that evaluate altered gene expression and altered cell cycle control in mice and rats treated with carbon tetrachloride. Finally, the ability to predict the effects for carbon tetrachloride based on these data will be tested using a biologically based dose-response model.

## **Technical Accomplishments**

Our technical approach during the first year was designed to identify the mode of action of halogenated hydrocarbons and focuses on the selective cytotoxicity of the normal cell population. For this work we are testing the hypothesis that carbon tetrachloride induced tumors are generally due to reparative hyperplasia. Currently we are conducting a study with several purposes including 1) obtaining dose response information for oxidative stress induced damage to DNA which will clarify the role of oxidative DNA damage in tumors produced by carbon tetrachloride, 2) determining the dose response relationship for killing of hepatocytes and compare this with the doses that cause oxidative stress, and 3) determining the role that oxidative stress induced activation of transcription factors plays in altering the expression of several important genes.

Exposure to high doses of carbon tetrachloride produces significant increases in reactive oxygen species. Since these reactive oxygen species produce DNA damage products such as 8-hydroxydeoxy-guanosine (8-OHdG), thymine glycol, and other modified nucleobases, our approach is to determine the doses of halogenated solvents required to produce detectable (significantly greater than background levels) oxidative base damage products in hepatic DNA taken from treated animals. For this we isolate nuclear and mitochondrial DNA, enzymatically digest the DNA to nucleosides, separate the modified bases by HPLC, and quantitate the level of 8-OHdG using electrochemical detection. Although analysis of samples from this study are not yet complete, these results will help determine whether oxidative DNA damage occurs at doses that produce hepatic liver tumors. If the DNA damage is observed at doses above those that increase cell replication, this will strongly suggest that oxidative DNA damage has minimal involvement in the carcinogenesis process; however, if DNA damage occurs at doses at or below those that produce tumors, then the contribution of this pathway will require further consideration.

Another intermediate dose effect is cell killing. For our studies it is essential that information on cell killing is obtained from animals that are used for biochemical and



molecular endpoints so that direct comparisons can be made. Cell killing is usually determined by measuring the amount of hepatic enzyme leaked into the serum by cells that are severely damaged; the amount of serum activity of these enzymes is related to the number of cells killed. For these studies we exposed rats to carbon tetrachloride at a dose of 100 mg/kg and determined the activity of serum alanine aminotransferase (ALT). A time course study demonstrated that alanine aminotransferase activity reached a maximum (approximately twice control levels) at 6 hours after carbon tetrachloride treatment and then returned to control levels by 24 hours. These results suggest that carbon tetrachloride at 100 mg/kg, a dose that did not cause tumors in rats when administered by gavage in corn oil, produced measurable levels of cell killing. Currently, we are in the process of confirming the cell killing by histopathological techniques.

Interestingly, concentrations of glutathione were not altered by the carbon tetrachloride treatment. Since GSH acts as a scavenger of reactive intermediates, these results demonstrate that this protective mechanism was not overwhelmed at this dose of carbon tetrachloride. Similarly there was no difference in lipid peroxidation as measured by the thiobarbituric acid reactive substances (TBARS) assay. This assay provides an estimate of the amount of malondialdehyde present in the tissue and is a measure of lipid damage and degradation. In addition, these lipid breakdown products are reactive and may covalently bind to DNA producing damage to nucleobases. Lack of measurable changes in these biochemical parameters suggests that other cellular processes must be

responsible for the tumor response. Oxidative stress induced changes in transcription factors is a likely candidate. Activation of transcription factors may occur at doses below those that induce DNA damage and cytotoxicity. The transcription factor AP-1 is a heterodimer of Fos and Jun. Even though exposure of rats to carcinogenic doses results in significant increases in expression of both c-Fos and c-Jun, the activity of AP-1 is controlled by additional mechanisms including phosphorylation and dephosphorylation reactions. While there is evidence that carbon tetrachloride induces changes in these pathways at relatively high doses, the responses at lower doses and the shape of the dose response curves have not been determined. Similar arguments apply to another transcription factor, NF- $\kappa$ B, which also may be activated by oxidative stress. To determine the role of these factors, we will isolate mRNA and prepare nuclear extracts from liver tissue obtained from rats exposed to different doses of carbon tetrachloride for short periods of time (1 to 4 weeks). DNA probes on the order of 500 bases in length will be prepared by PCR amplification and used to probe and quantify c-Jun and c-Fos; other DNA sequences will be synthesized for gel shift assays for AP-1 and NF- $\kappa$ B. Our work will provide quantitative dose response information for expression of c-Fos and c-Jun by Northern blotting, and DNA binding activity of these transcription factors by gel shift assay. Induction of glutathione S-transferase- $\pi$  will be also measured as an indicator of AP-1 activation since glutathione S-transferase- $\pi$  has an AP-1 like site in its promoter region.

# ***Ethical, Legal, and Social Implications of the Human Genome Project for Screening, Monitoring and Health Surveillance of Department of Energy Workers***

Lowell E. Sever and Rebekah Harty (Health Risk Assessment)

---

## **Project Description**

The objective of this study was to identify ethical, legal, and social issues that may be raised by the U.S. Department of Energy's Human Genome Project as it expands our ability to identify workers with increased susceptibility for adverse health effects from exposure to hazardous substances as a consequence of their genetic makeup (genetic screening). The scope of this study was limited to investigating issues that may be raised by the rapidly developing Human Genome Project with respect to genetic screening of DOE workers and to assessing potential solutions to the ethical, legal, and social issues as they related to DOE's operations. By reviewing relevant literature to obtain information regarding approaches taken by other investigators, it was possible to begin targeting these activities to DOE workers to define the issues and begin to work on potential solutions. The work resulted in a white paper, as discussed below.

## **Technical Accomplishments**

The accomplishments in prior years included the development and review of bibliographies relevant to legal and ethical aspects of genetic screening and monitoring programs. In addition, staff participated in a DOE workshop related to worker surveillance and monitoring and a DOE conference related to privacy issues. Extensive references were obtained, reviewed, and abstracted. Particular attention was paid to literature in the areas of worker screening, the Human Genome Project, genetic sensitivity to environmental agents, and social, legal, and ethical issues related to genetic programs and policies. The literature review focused on

exclusionary policies, legal implications of fetal protection policies, and ethical and legal aspects of privacy and discrimination, as well as relevant policy paradigms related to genetic screening.

During FY 1995, a white paper entitled, "Screening Workers for Genetic Hypersusceptibility: Potential Ethical, Legal, and Social Implications Arising from the Human Genome Project" was written and submitted to the *Milbank Quarterly* for publication. The emphasis of the white paper was to explore a range of issues that surround the use of genetic screening in the workplace. Specifically, five topics that surround the use of genetic screening in the workplace were examined

- issues of risk
- the rationale and legal basis for screening
- privacy concerns of the workers
- the confidentiality of test results
- potential discrimination.

The white paper concluded with a discussion of some possible parameters for how screening programs might be formulated. Two parameters, public safety and the protection of worker's health and safety appear to have considerable merit as a rationale for testing.

## **Publication**

A.C. Wicks, L.E. Sever, R. Harty, and S.W. Gajewski. "Screening Workers from Genetic Hypersusceptibility: Potential Ethical, Legal, and Social Implications Arising from the Human Genome Project." *Milbank Quarterly* (submitted).

# Health Protection and Standards for Hazardous Chemicals

Barbara L. Harper (Health Risk Assessment)

---

## Project Description

This project focused on examining the regulatory aspects and actual application of health protection standards in general, and on Hanford human health risk assessment and risk management in particular. Regulatory aspects include the quality of the experimental evidence, the way it is used in setting health standards, and the additional management factors used in setting standards. In actual practice, risk-based standards are intended to apply to high-risk subpopulations as well as to the average population. Identifying higher-risk segments of the population surrounding or impacted by Hanford has two parts: identifying high exposure situations and identifying populations with potential high sensitivity.

## Technical Accomplishments

A report summarizing the toxicology of over 100 of the most common Hanford chemical and radiological contaminants was published for use in site risk assessments.

During FY 1995, some of the primary culture-specific variances in Hanford-related exposures were identified. Due to the unique location of Hanford within the ceded lands of four Indian nations or bands, this effort focused on identifying exposure situations with potentially different (nonsuburban) exposure pathways to members of tribal communities as they exercise treaty-reserved rights on- and offsite. These exposures are related to traditional dietary and cultural practices. Both types of exposure were included in total human exposure estimates.

These human exposure concerns exist within a larger arena of risk-related concerns having to do with risks posed by contaminants and other Hanford-derived stressors to the ability of tribal members to safely follow traditional practices and to adhere to traditional values, both of which require a clean environment. Initial considerations of these concerns suggest that values-based impact analysis or comparative risk might be a better way to anticipate how Hanford remediation and waste management decisions will actually be negotiated.

Methods for extending the conventional risk methodological paradigm are being compared to more holistic concepts that start with an indigenous perspective on health and drawing on conventional metrics where appropriate.

## Publications

B.L. Harper, D.L. Strenge, R.D. Stenner, A.D. Maughan, and M.K. Jarvis. 1995. *Toxicology Profiles of Chemical and Radiological Contaminants at Hanford.* PNL-10601, Pacific Northwest National Laboratory, Richland, Washington.

B.L. Harper. "Risk Assessment, Risk Management and Risk-Based Land Use Planning Incorporating Tribal Cultural Interests." In: V. Molak (ed.) *Fundamentals of Risk Assessment and Risk Management*, CRC/Lewis Publishers (in press).

# Light at Night

Richard G. Stevens and Bary W. Wilson (Biology and Chemistry)

---

## Project Description

DOE-sponsored work to develop building standards is carried out with two primary considerations in mind:

1) energy efficiency and 2) environmentally sound design, construction, and operation. An ancillary goal is to optimize energy efficiency while maintaining an environment (e.g., light levels and ventilation) that does not impede worker productivity. Productivity is related to ergonomics and job satisfaction issues. Worker safety and indoor air quality are important to building standards development, however, other health issues are not currently emphasized. Because recent research suggests that there may be increased risk of disease resulting from chronic disruption of hormone balance, another crucial aspect of building standards and subsequent building operation should be long-term health. An important aspect of long-term health is maintenance of circadian hormonal rhythms, particularly melatonin. Melatonin is normally high at night and low during the day, and its production by the pineal gland is strongly influenced by light intensity and wavelength. The goal of this project was to clearly define issues related to building standards and operations as they impact long-term health, and to determine what specific research needs to be carried out.

## Technical Accomplishments

The characterization laboratory, is located in room 105 of the Annex, consists of a PVC frame ~8 feet in height, 4 feet in depth, and 8 feet in width. Wall material is affixed to the back and two sides, and ceiling typical of offices is hung from the top. Light fixtures are accommodated in the ceiling, and there is an adjustable platform to serve as a simulated desk. Using a spectrophotometer, and electromagnetic frequency measurement instruments, the spectral and intensity characteristics of different luminaires can be examined in a controlled environment and compared with the light and electromagnetic frequency found in real offices. The long-range purpose of this laboratory is to evaluate various luminaires with regard to the scotopic response curve for pineal melatonin production. Electromagnetic frequency measurements were evaluated for their potential to affect pineal function.

To date we have performed spectrum/intensity measurements on approximately 20 different light sources in the laboratory, and are now making extremely low frequency and transient measurements as well. Light and extremely low frequency profiles will be compared with the known response curves of the pineal to light, and form the basis of a paper.

A portion of the data generated under this project is depicted in Figures 1 through 7. Spectral and irradiance data were collected using a spectrophotometer model PR 650 from PhotoResearch. There were two different measurement situations:

- individual luminaires were assessed in our characterization laboratory in the Annex building
- actual lighting was characterized in a series of offices in the 2400 Stevens building.

In the characterization laboratory it is possible to examine specific light sources one at a time. The offices represent real-life combinations of lighting.

Life in modern societies differs in many ways from life in the environment before industrialization. One change has been in exposure to light. We have come from an environment with dark nights and bright, full spectrum days to an environment with lighted nights in homes during sleep and dim, spectrum-restricted "days" inside buildings where most people now work. The long-term basis for our research is that human health will be optimized by exposure to dark nights and bright days; in particular, bright days that have a strong component of light in the scotopic range. This should yield a strong melatonin rhythm. In each of the figures, both the photopic and scotopic response curves are shown (these are relative response curves and the scales are not meaningful). The pineal gland's production of melatonin is suppressed according to the scotopic curve (rod dominated), whereas photopic lux (cone dominated) is the quantity uniformly utilized by the lighting community. The normal nocturnal melatonin rise in humans can be lowered by light of ambient intensities ranging from approximately 200 to 3,000 lux. Exposure to 509 nm monochromatic light as low as 30 scotopic lux

(1.6 RW/cm<sup>2</sup>) as measured at the level of the cornea can also partially lower melatonin in a laboratory setting. Electric lighting at night that is low intensity and minimal in the scotopic range and lighting during the day that is high intensity particularly in the scotopic range may best encourage a strong rhythm.

There is mounting evidence to suggest that disruption of the melatonin rhythm may lead to chronic fatigue, depression, reproductive anomalies, and perhaps even hormone-related cancers such as of breast in women and prostate in men. The competing needs in indoor lighting are energy efficiency and performance optimization for work which includes subjective preferences.

Figure 1 shows the very bright, broad spectrum of outdoor sunlight. As seen in the figure, intensity during this particular measurement was 117,496 photopic lux and 110,390 scotopic lux. Figure 2 shows the spectrum of a commonly used fluorescent bulb as determined in our characterization laboratory. Figure 3 is an office using the same model of fluorescent light and that also has a window. The measurement was taken at the position of the head of the occupant when in usual working position (sitting at the desk). This spectrum shows the spikes of the fluorescent source with contributions from the sun particularly apparent over 650 nm. The sun also boosted

scotopic exposure relative to other wavelengths. Figure 4 is the spectrum of a computer monitor, and Figure 5 is a standard 75 watt light bulb. These two sources are combined in an inner office (no window and fluorescent bulbs off) in Figure 6. Finally, Figure 7 shows the spectrum of an inner electronics laboratory that uses both incandescent and fluorescent lights.

From Figure 1, it is apparent that sunlight produces light with about equal photopic and scotopic lux. From Figure 2 it is apparent that a commonly used fluorescent light produces approximately 60 percent greater photopic than scotopic lux and from Figure 5 a standard incandescent bulb produces approximately 90 percent more photopic than scotopic lux. If photopic lux is also a measure reflecting light quality as perceived by the occupant, and is needed for optimum performance, and if scotopic lux is important to hormone rhythms, then the balance of the two in daytime luminaires becomes a central part of the issue.

#### Publication

J. Bullough, M.S. Rea, and R.G. Stevens. "Light and Magnetic Fields in a Neonatal Intensive Care Unit." *Bioelectromagnetics* (in press).

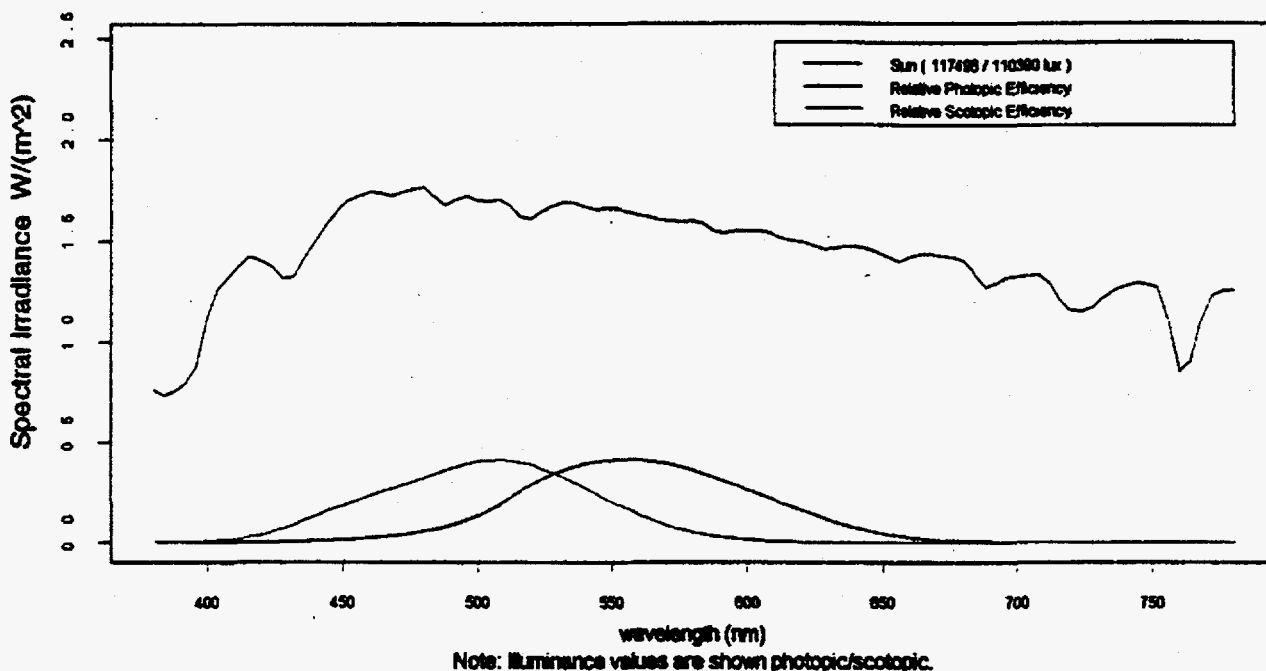


Figure 1. Outdoor - Sunny Day

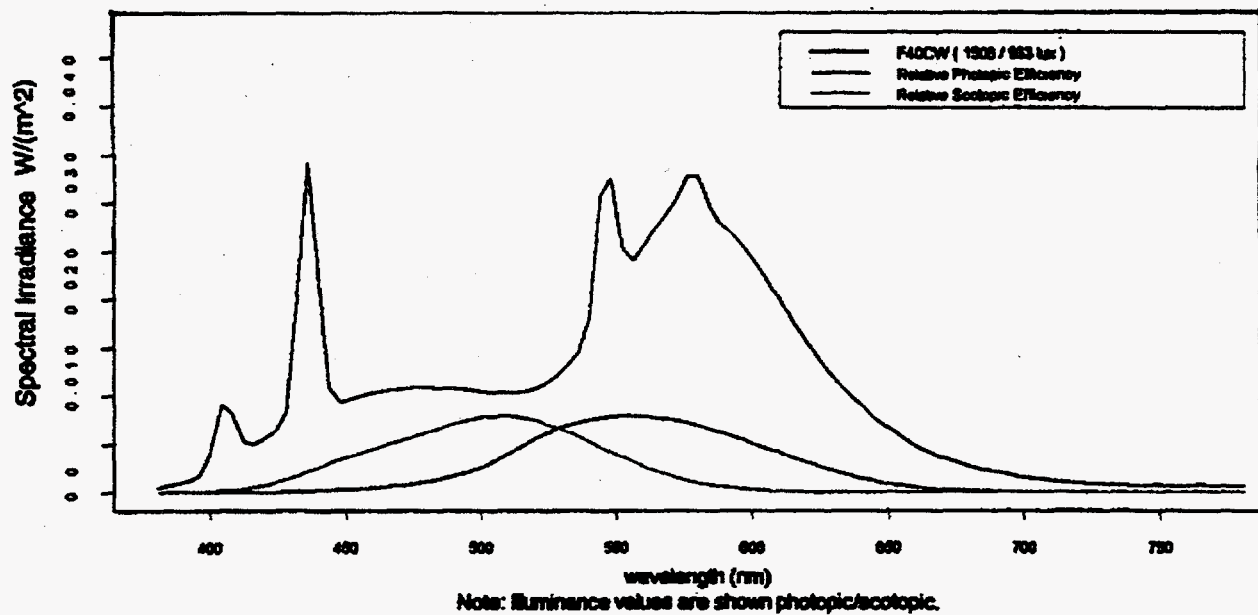


Figure 2. F40CW Cool White Fluorescent

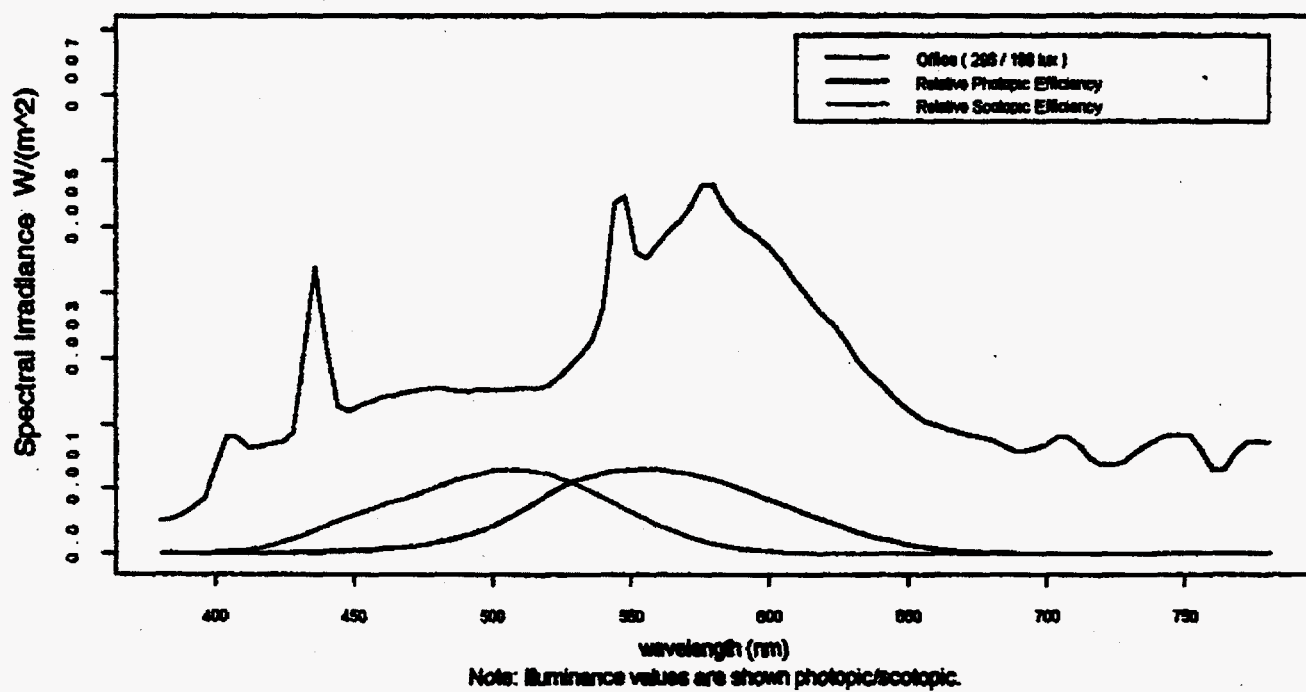


Figure 3. Window Office

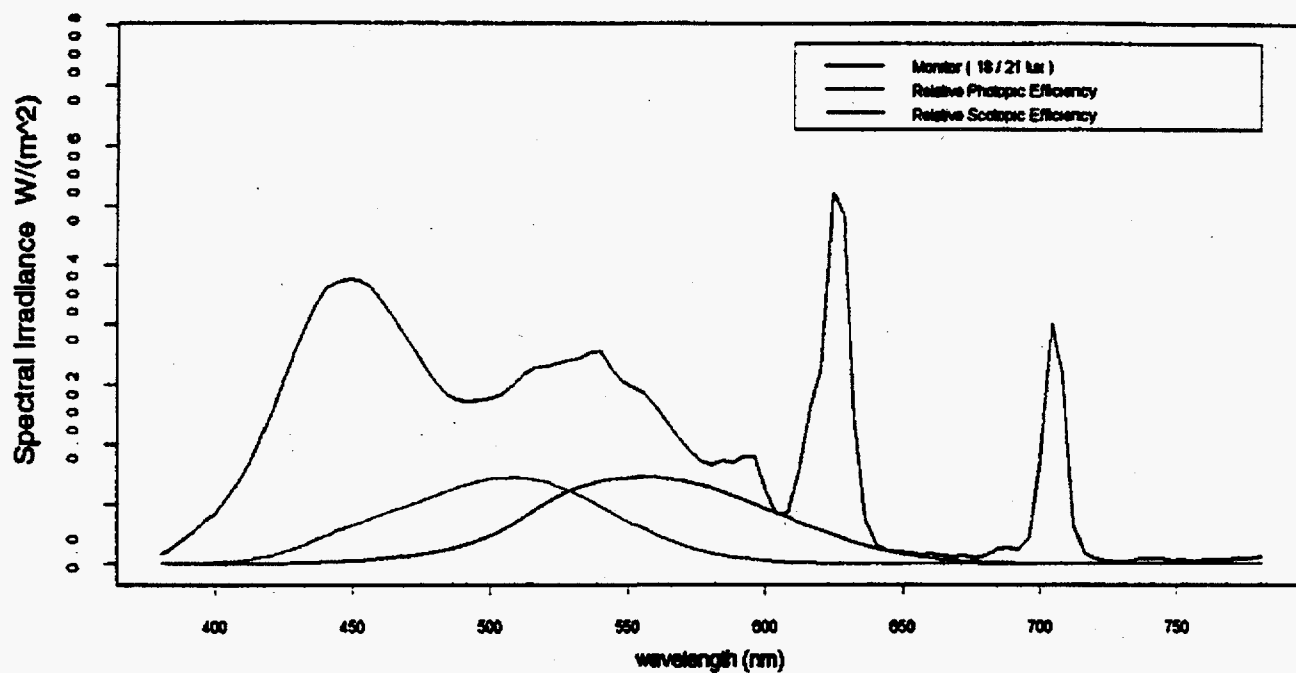


Figure 4. Computer Monitor - Default Colors

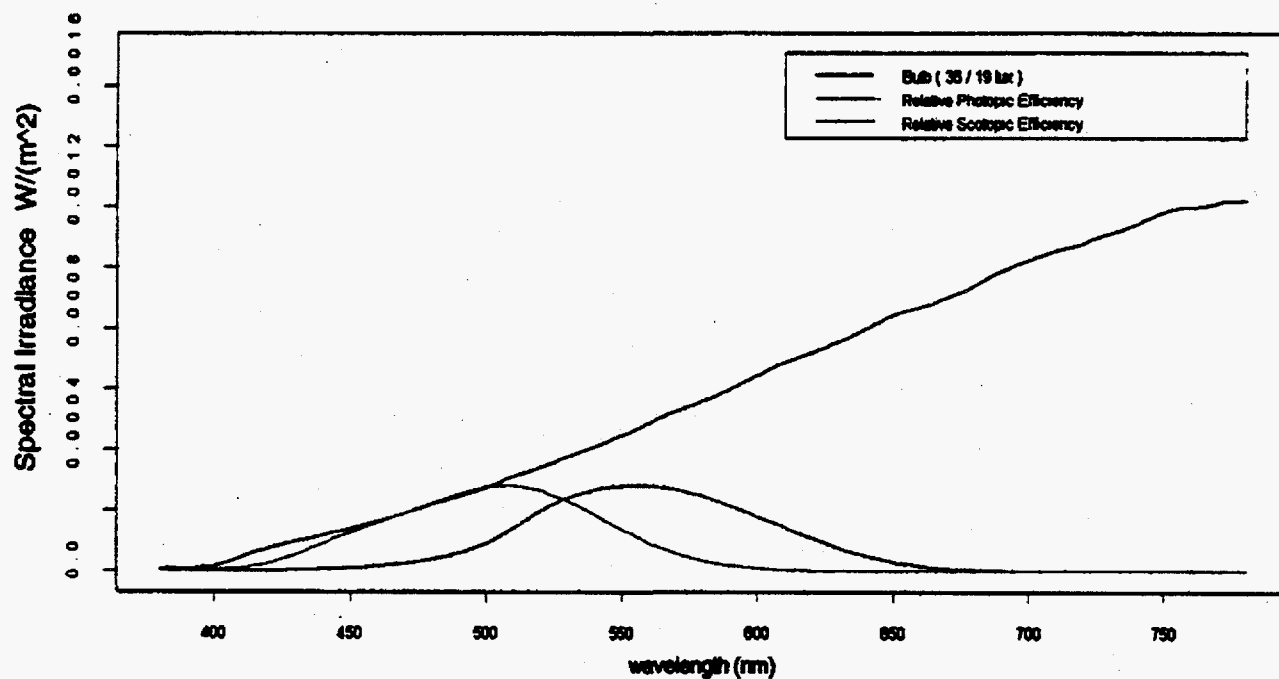


Figure 5. Standard 75 W Light Bulb

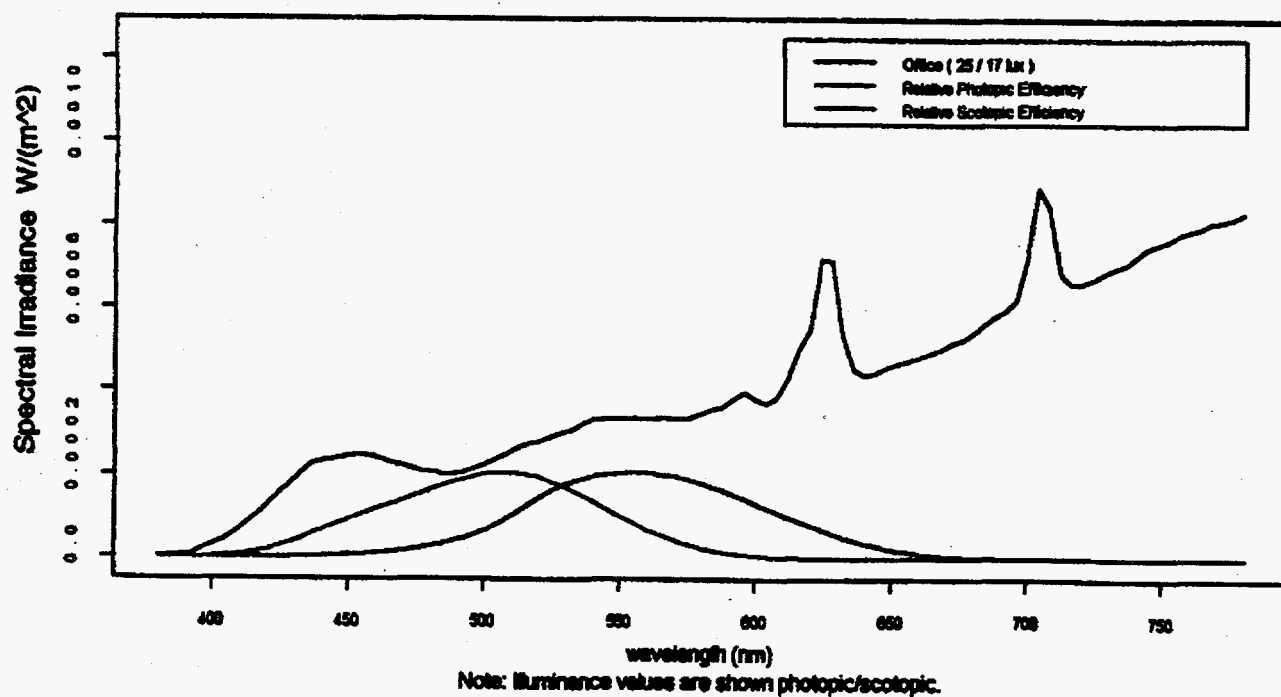


Figure 6. Inner Office

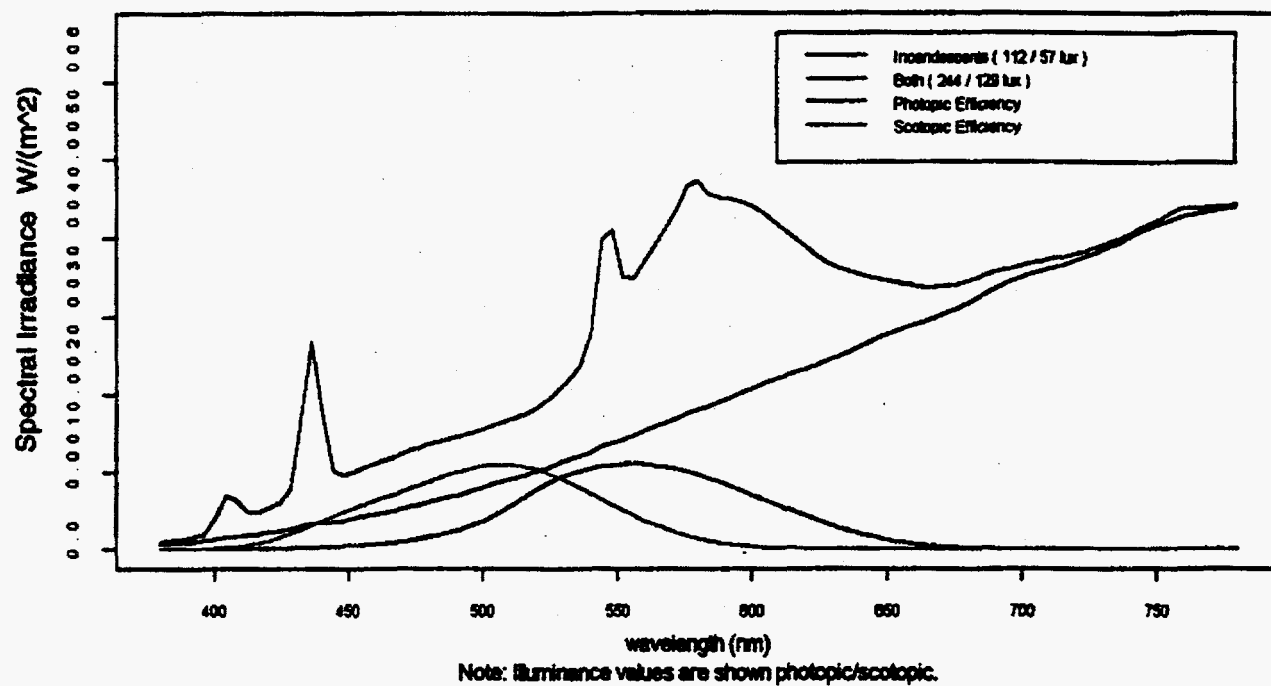


Figure 7. Inner Electronics Lab



# Technical Analysis and Integration of Health Effects Data

Richard J. Bull (Biology and Chemistry)

---

## Project Description

Diverse sets of data result from individual studies of health effects. Much of this data requires rapid interpretation and reintegration into an overall integrated assessment. The major thrust of this project is to develop general principles for assessing risks from all classes of physical and chemical carcinogens. The project will ensure that data which impacts the overall approach are recognized early and used to redesign efforts within other health effects studies.

## Technical Accomplishments

A technical approach to cancer risk assessment that has developed in the first year of effort is to conceptually categorize potential mechanisms into four modes of action. These modes of action (see Figure 1) include

1. increased mutation frequency
2. selective killing of normal hepatocytes
3. selective stimulation of clones of cells initiated for cancer
4. prevention of apoptosis, or programmed cell death.

Increased mutation frequency would come from DNA damaging activity of a chemical that leads directly to mutation. Selective killing or cytotoxicity would provide a selective advantage to intermediate cells causing the lesion to grow out more rapidly. The third and fourth modes involve receptor-mediated effects and essentially provide a positive selection for intermediate and/or malignant cells. It should be recognized that these four modes of action are general to chemical carcinogenesis and are not specific to chlorinated hydrocarbons.

These concepts were developed based upon data developed within a cell and tumor growth kinetics project that demonstrated that dichloroacetate (DCA) induces cell division within initiated cells and confirmation of prior data indicating that carbon tetrachloride acts primarily by selective killing of normal hepatocytes. Trichloroacetate (TCA) was found not to affect the rate of cell replication within initiated cell populations, but work under the cell signaling mechanisms project support the view that it may

be suppressing the normal rates of programmed cell death. Prior data has demonstrated that other halogenated solvents can modify the mutation frequency.

These findings demonstrate that all four modes of action can be identified within the chlorinated solvent class of chemicals. This indicates that our approach to gathering data to improve cancer risk assessment can be appropriately tested within this single group of chemicals. Practically, this is important because it allows pursuit of metabolism and pharmacokinetics of the class utilizing similar analytical methods, greatly simplifying the proof of principle.

The four modes of action immediately suggest how alternate risk assessment models should be constructed. Based on these concepts we project a minimum of four models will be needed for cancer risk assessment in general. With examples within the class we can proceed with some confidence on the basic structure of these models while we proceed to collect data that will improve and validate these models.

The four modes of action also provide a focus for mechanistic research with this particular class of chemicals in the project on cell signaling. For example, the finding that dichloroacetic stimulates cell division is associated with a modified phenotype in the initiated cells that involves elevated expression of c-Jun and c-Fos (see the cell and tumor growth kinetics project). This suggests that the dependence of cell replication within these areas on dichloroacetic may be related to a dichloroacetic-induced modification of the functional state of the of c-Jun or c-Fos. Dichloroacetic is known to be a kinase inhibitor in other systems. It is also known that binding of the AP-1 transcription factor (a heterodimers of c-Jun and c-Fos) depends upon the level and sites of phosphorylation. Modification of phosphorylation would as a result modify expression of other genes. If the carcinogenic effects of dichloroacetic can be shown to be entirely dependent upon this type of activity, the use of a nonlinear risk assessment model can be justified for estimating risks at the low doses that would be expected from metabolism of environmental levels of trichloroethylene and related chlorinated hydrocarbon solvents. Similar approaches can be applied to the modes of action represented by carbon tetrachloride and trichloroacetate. This approach should apply directly to other carcinogens.

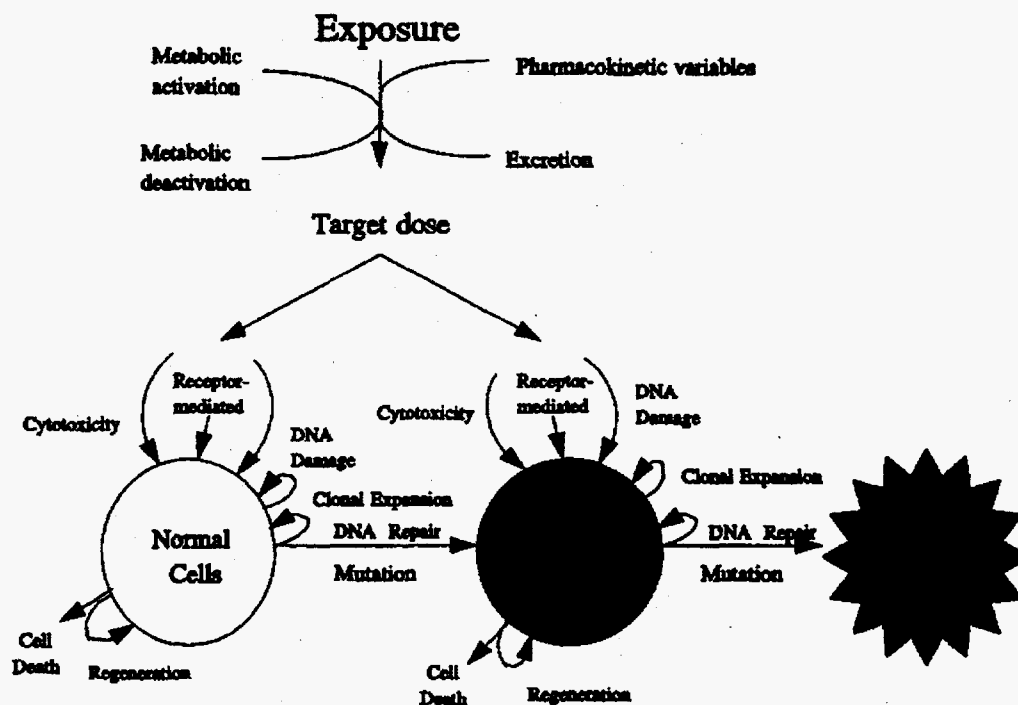


Figure 1. Modes of Action

Increasing mutation frequency is a recognized contributor to the development of cancer. It is also reasonably well accepted that this activity contributes a linear term to most risk assessment models. However, the actual quantitative contribution of mutagenesis to a tumor response at the doses used in cancer bioassays in experimental animals is not clear even with highly mutagenic carcinogens. For reasons of sensitivity these tests are conducted at such high doses that other modes of action invariably contribute to the response. Therefore, to assess the real impact of chemically induced mutation, experiments have to be designed to essentially correct for these other effects of high doses. Consequently, once chemicals are identified that express rather pure modes of action, the interaction of effective doses of chemicals that modify cell replication can be combined with low doses of mutagenic chemicals to explore their actual contribution to the response.

The second major problem in risk assessment is comparative dosimetry. To make full use of the toxicodynamic data described above, a biologically based dose response model must also deal with issues of dose. While a variety of dose surrogates may have to be used, accurate scaling of the effective dose between species must utilize physiologically based pharmacokinetic models. There are generally two technical limitations to the application of such models: 1) the identity of the metabolite responsible for the effect is not known and 2) lack of human data. A study conducted at Washington State University on chloral hydrate metabolism in human

volunteers provides a way to estimate effective doses of Trichloroacetic from external exposure of humans to trichloroethylene. Chloral hydrate is a sedative-hypnotic which can be safely administered to humans. Chloral hydrate is the intermediate in the metabolism of trichloroethylene that also yields Trichloroacetic and trichloroethanol as metabolites. Thus, we can obtain kinetic parameters for these metabolites in humans from this study.

The chloral hydrate study was designed to examine the effects of both increasing dose and repeated doses. The time course of changes in trichloroacetic concentrations under each of these experimental conditions is provided in Figure 2. Four significant findings are apparent in these data: 1) the half-life of trichloroacetic is much longer in humans than in rodents, 2) the kinetics of trichloroacetic are quite complex, reflecting the enterohepatic circulation of the trichloroethanol glucuronide, 3) the initial conversion of chloral hydrate to trichloroacetic becomes saturated at the 1500 mg dose (marked depression of initial peak), and 4) blood levels achieved by three doses of 500 mg/kg given every other day are significantly greater than that observed with a single bolus dose of 1500 mg. Therefore, these data provide use with critical information for estimating human doses of trichloroacetic obtained from trichloroethylene and will allow us to scale that dose with those that resulted in tumors when mice were administered either chloral hydrate or trichloroethylene.

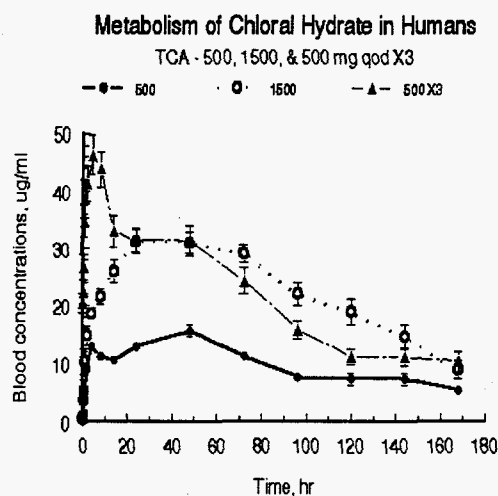


**Figure 2.** Time course of trichloroacetate concentrations in blood after administering single doses of 500 or 1500 mg or three doses of 500 mg each every other day. Time course reflects blood levels only after the last dose. Data set reflects results from 8 healthy male volunteers and the vertical bars represent +SEM.

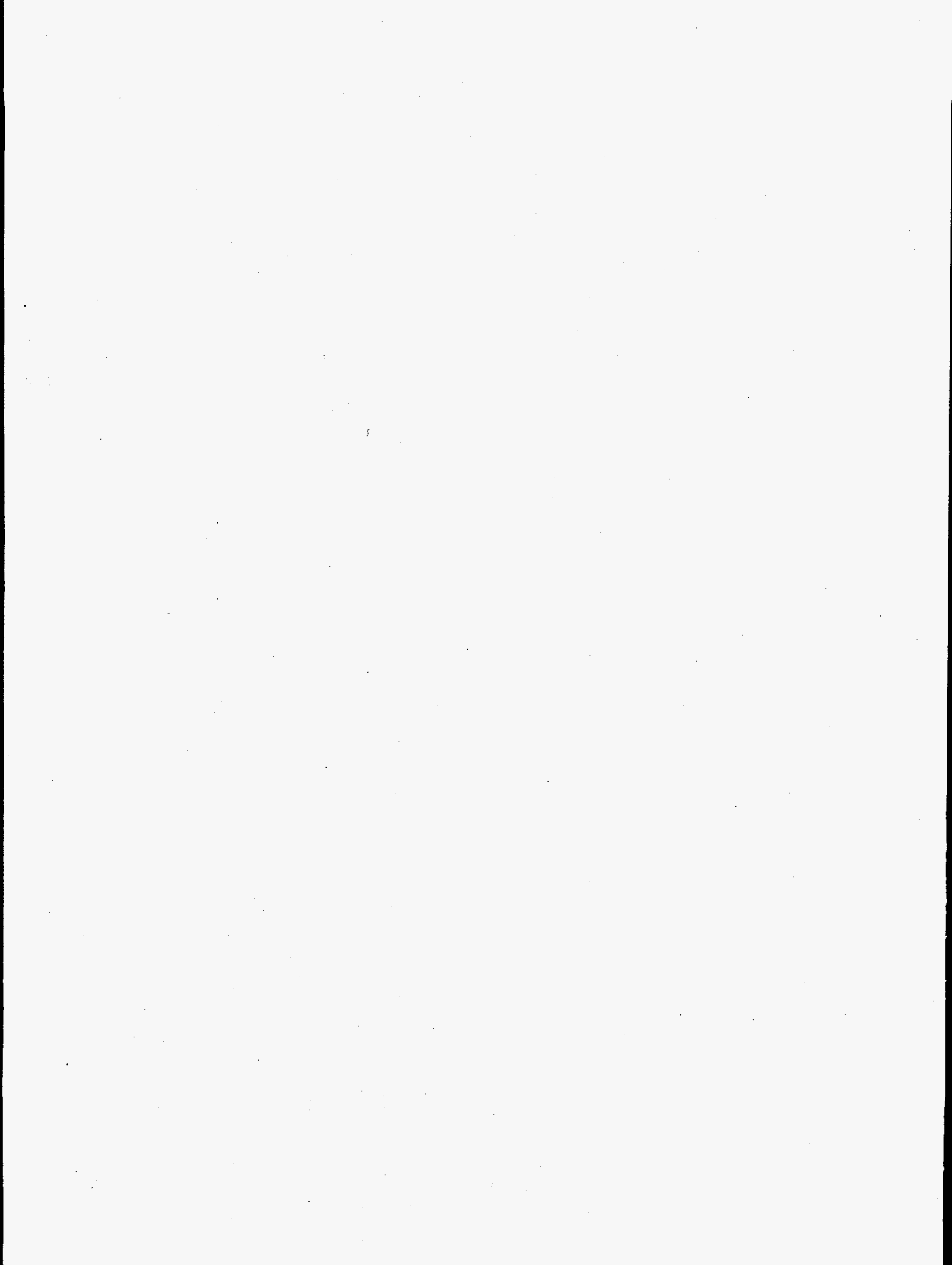
## Publication

R.J. Bull, L.S. Birnbaum, K. Cantor, J.B. Rose, B.E. Butterworth, R. Pegram, and J. Tuomisto. "Symposium Overview: Water Chlorination: Essential Process or Cancer Hazard?" *Fundam. Appl. Toxicol* (in press).

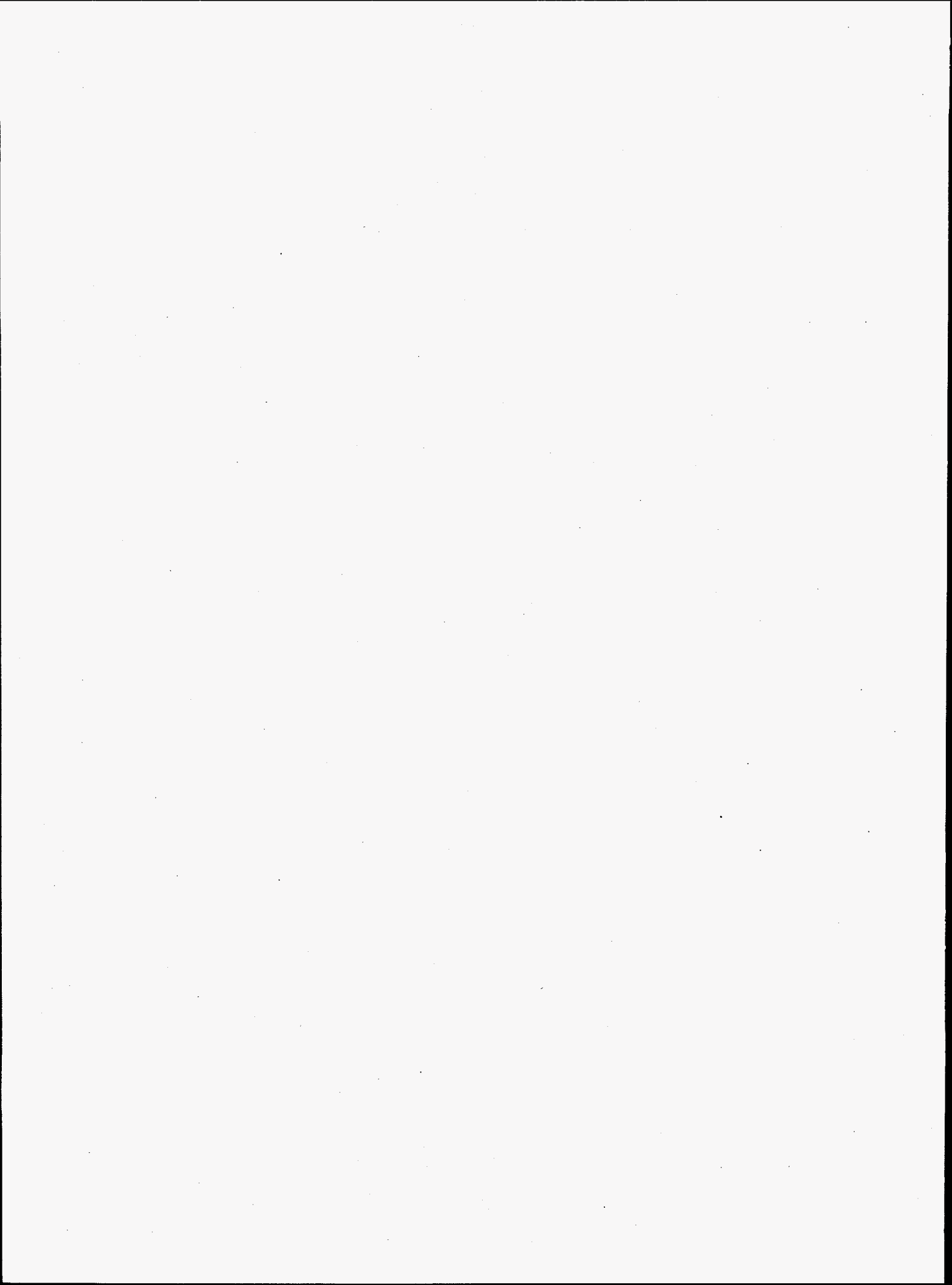
## Presentations

R.J. Bull and L.S. Birnbaum. 1995. (co-chaired a symposium) "Chlorination: Essential Process of Cancer Hazard?" Annual Meeting of the Society of Toxicology, March 8, Baltimore, Maryland.

R.J. Bull. 1995. "Across Species and Low Dose Extrapolation of Health Effects Data." Jason's Meeting, June 27-29, LaJolla, California.



## **Statistics and Applied Mathematics**



# *The Development of Adjoint Sensitivity Methods for Complex Physical and Chemical Simulation Models*

Margaret K. Brown (Applied Mathematics)

---

## **Project Description**

This project focused on developing and demonstrating an adjoint modeling capability. Adjoint models are a state-of-the-art computationally efficient technique for calculating the sensitivity of the final state, with respect to input parameters, for time-dependent systems of partial and ordinary differential equations. This will facilitate sensitivity analyses and optimization problems that are currently beyond reach. Target applications include the modeling of transport and chemistry in the atmosphere, in constrained fluids (e.g. tanks), and in groundwater flows.

The goal of this project was to evaluate available tools and techniques for constructing adjoint models, to explore their applicability to a variety of computational models to actually construct an adjoint model for Pacific Northwest National Laboratory's in-house global chemical transport model GChM, and to demonstrate the utility of that model by using it to address a scientific problem of current interest.

## **Technical Accomplishments**

The approach that was taken includes the following. First, a simple yet physically meaningful problem is formulated, for which the results of a sensitivity study will be of interest to the scientific community. The formulation and solution to this problem will serve as verification and proof of principle as well as a means to obtain publishable results. The complexity of model will gradually be enhanced, ultimately leading to the adjoint model to the already existing, state-of-the art, in-house global chemical transport model, GChM.

Specifically, the order of the tasks are outlined as follows.

1. Investigate the feasibility of implementing tools already available for adjoint modeling. These tools include

ADGEN, a FORTRAN code developed at Oak Ridge National Laboratory; SWAT, a FORTRAN code developed at Pacific Northwest National Laboratory; and automatic differentiation, an algorithm that when run backward is equivalent to the formulated adjoint model.

2. Applications to various models will be investigated, including the chemical kinetics code AREST.
3. Formulate and solve the adjoint to a one-box gas-phase chemical kinetics model with specific application to the atmosphere. Use this problem to study the efficiency of the various computational methods available. After a solution to the adjoint model is obtained, this solution will be verified by comparing forward modeled responses with those predicted by the adjoint method.
4. Use this adjoint model to calculate the sensitivity of tropospheric ozone production to modeled reaction rate coefficients. The coefficients to which this production is most sensitive will be identified.
5. Formulate and solve the adjoint to a global Eulerian transport simulation model of the atmosphere using an inert tracer. This model will be used to formulate the inverse source problem, applying this inversion to observations of the anthropogenic species CFC 11, CFC 12, and methylchloroform for verification tests.
6. The adjoint to the transport model will be combined with the adjoint to the chemical kinetics model. This model will be used to produce objective estimates of CO emissions and to determine the data collection policy that would be most effective in defining these emissions.

The principal investigator left the Laboratory before the project was complete. As such, the results of this project are unavailable.

# *Uncertainty Analysis for Computer Models*

Albert M. Liebetrau (Analytic Sciences and Engineering)

---

## **Project Description**

The purpose of this project was to develop practical methods of sensitivity and uncertainty analysis for complex computer codes. In this context, a complex code is one that has either a large number of input variables or extremely long run times. The methods are especially intended for system codes that involve the linking of several sub-models (codes) that are complex in their own right. Our approach to uncertainty analysis is to rely on approximations to the codes in question to reduce the computational burden associated with uncertainty analysis. Essential properties of the approximation are that it preserve the essential features of the underlying code, and that it run much faster than its complex counterpart.

The three major aspects of this approach to uncertainty analysis involve sampling design, response surface approximation, and updating. Efficient input designs reduce computing times by minimizing the number of runs required. Response surface approximations are used to perform simulations that would otherwise be prohibitive because of the long run times involved. Updating algorithms help to select the most informative points in the design (input) space points at which to make additional runs of the underlying codes.

In this work, we have concentrated on finding computationally fast approximations to the response surfaces of the underlying codes. We have done this for several reasons. First, good sampling designs, such as Latin hypercube sampling, already exist. But more importantly, the greatest reduction in computer time can be achieved by using efficient approximations for the majority of the simulations required for uncertainty analysis. Keeping in mind that no approximation can capture all the features of its complex counterpart, we have identified several methods of approximation that perform reasonably well and significantly reduce the computational burden of uncertainty analysis for complex systems of computer models.

## **Background**

Human and earth systems are extremely complex processes. The modeling of these systems to assess the effects of climate change, for example, is an activity fraught with uncertainty. System models typically involve the linking of a series of computer codes, each of which

may be a detailed model of some physical or social process in its own right. In such system models, the output from one process model is the input to another. Traditional methods of uncertainty analysis involving Monte Carlo simulation fail because of the sheer complexity of the modeling effort and the heavy computational burden. The objective of this project was to develop more efficient methods for learning about and performing uncertainty analyses with system models that are constructed from a collection of computer codes.

## **Technical Accomplishments**

Under this project, we have developed a conceptual framework for uncertainty analysis for systems of computer-intensive codes that is hierarchical in nature. The basic idea was to develop computationally less demanding approximations to the underlying codes that can be used for most uncertainty calculations. The three major elements of this strategy include

- selection of an initial set of inputs at which to run the underlying code (the design step)
- development of a suitable approximation to the response surface of the underlying code (the approximation step)
- the use of information from existing runs to determine the optimal locations for additional runs of the underlying code (the updating step).

Our research has shown that acceptable procedures exist for designing the set of initial runs of the underlying codes. Latin hypercube sampling (LHS) is one widely used design strategy that has proved very effective for sensitivity and uncertainty analysis. Consequently, we have used Latin hypercube sampling to select initial runs and have concentrated our efforts on the approximation step.

A first step was to identify potentially useful strategies for approximating the response surface of the underlying code. We have identified several potentially useful methods of approximation. These are MARS, which involves the use of multivariate adaptive regression, TREES, which involves the regression trees, and GAM, which involves generalized additive models. All procedures are similar in the sense that they can be



classified as constrained linear optimization procedures. We also investigated the use of wavelets, but we did not find representations that reduced the computational burden enough to be practical for problems of the complexity encountered in practice.

All approximation methods were applied to two codes, the EPIC code and the AREST code. The two codes are quite different, yet each has characteristics typical of codes used to simulate some system or process. The EPIC code was used in the MINK study to simulate crop production for a variety of climate scenarios. The AREST code was developed to simulate the containment and release performance of a geologic repository for radioactive wastes. The response of the EPIC code is quite linear over regions of interest, but the output is truly stochastic. On the other hand, the AREST code is highly nonlinear but it can be run in a deterministic mode. The AREST code estimates releases of radionuclides, which of course must be non-negative.

The MARS approximation procedure is attractive because it yields an approximation of minimal complexity (under specified constraints) for a given set of runs of the underlying code. A second desirable feature is that variance estimates computed from the MARS approximating surface were not significantly different than those computed directly from the underlying model. We discovered, however, that the MARS procedure did not work well when the response surface of the underlying model was constrained. Regression trees worked better for dealing with the "hard" zeros which are a unique feature of the AREST code (but typical of many physical or chemical processes). The GAM procedure provides a very flexible way to approximate the response surface of the computer model when the main effects and interactions are approximately additive. The flexibility comes from the fact that component functions of the approximator may be functions of one or several variables, and they may represent main effects or interactions. Moreover, the functional forms of the

additive components can be fairly general; for example, smoothing splines and nonparametric functions can be used. A disadvantage of the GAM approach is that determining which main effects and interactions to include is not easy. Substantial knowledge of the model is required, together with considerable experimentation to determine which combinations of terms to include in the approximation.

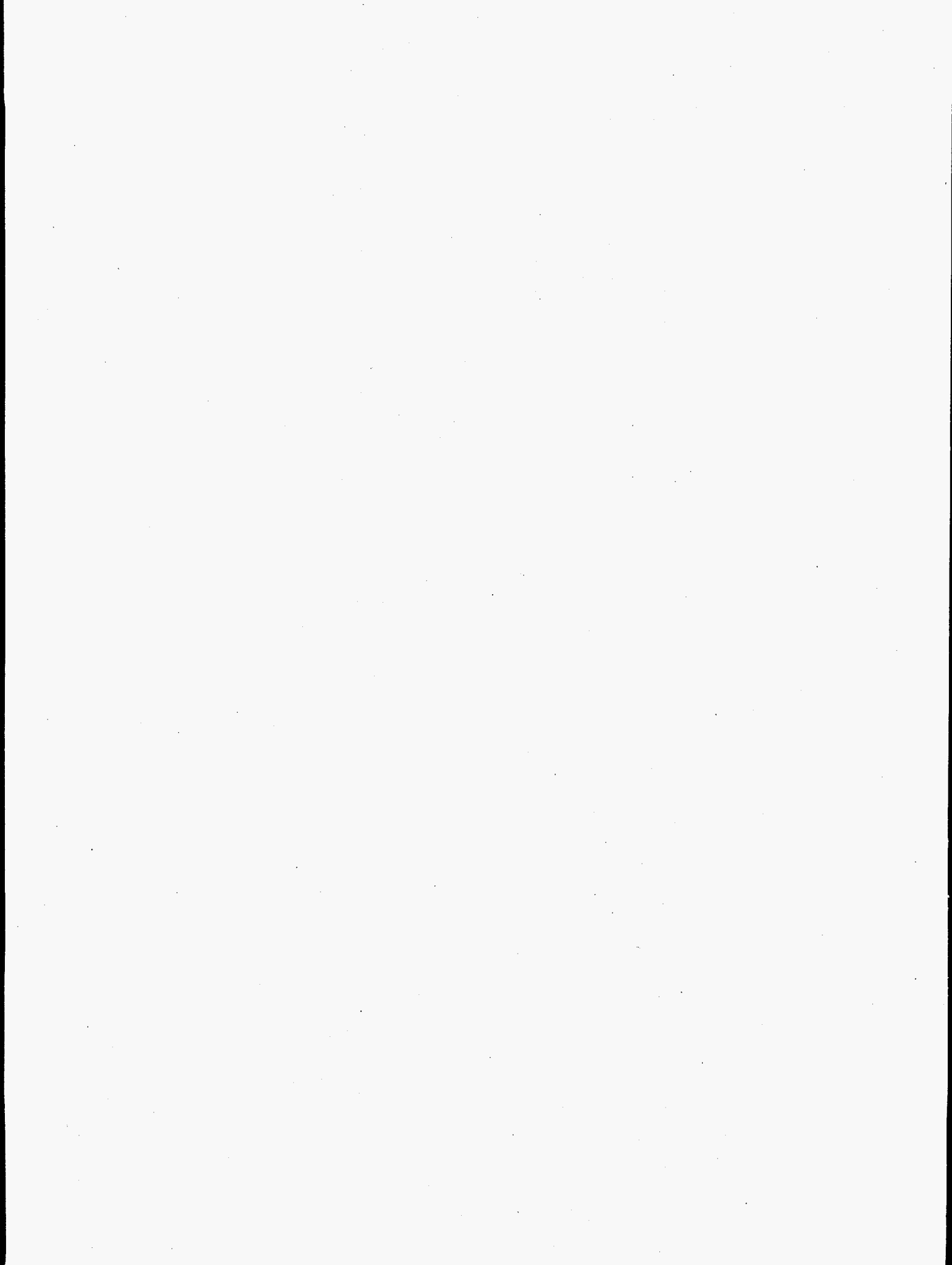
No method clearly outperformed all others in the applications we have studied to date. Moreover, given the natural variability in the outputs of the underlying models, all the methods performed about as well as one could expect. This suggests that approximation methods can be useful for uncertainty analysis. However, the results of this work also suggest that a variety of approximation methods will be required to obtain suitable approximations to the many different codes that are likely to be encountered in practice.

Considerable experience was gained in the use of response surface approximation methods through this project. Moreover, an extensive set of software has been assembled for implementing the approximation methods investigated in this work.

### **Presentations**

A.M. Liebetrau, N.K. Neerchal, and F. Gao. 1995. "On Optimal Design of Computer Experiments." Invited paper presented at MODSIM 95, University of Newcastle, Newcastle, November 27-30, NSW, Australia.

A.M. Liebetrau, F. Gao, and N.K. Neerchal. 1995. "Uncertainty Analysis for Systems of Linked Computer Models." Invited paper presented at the Sixth International Conference on Statistical Methods for the Environmental Sciences, December 6-9, Selangor, Malaysia.



## **Thermal and Energy Systems**



# *Advanced Numerics and Visualization for Power Systems*

Jeffery E. Dagle (Analytic Sciences and Engineering)

---

## **Project Description**

The progress that some electrical utilities have made in developing more comprehensive access to power system operating data has outstripped their means for extracting and distributing the imbedded information. Thus system control centers are progressively inundated by data that they are not yet able to use effectively. Utility restructuring and other factors promise to sharply increase the need for measurement-based information, while contracting the time frame in which it must be produced and incorporated into decision processes. They also dictate that cost recovery for the requisite technology investments be prompt and low risk.

The primary focus of this project is to develop and demonstrate the application of visualization tools to represent power system analysis and simulation results, with the overall objective of improving effectiveness of these tools with improved interpretation of data using scientific visualization techniques. In addition, advanced numerics play an important role in communicating complex data in a manner that can be easily comprehended, augmenting man-machine interfaces for power system analysis tools. These technologies are also applicable to other areas of power system operations, related to the DOE initiative in real-time power system control.

## **Technical Accomplishments**

The first year of the project (FY 1994) was primarily a scoping period to evaluate visualization tools and compare issues associated with the various tools available. Several visualization tools were acquired and evaluated with temporary software licenses in order to determine which packages would be suitable for use for prototype demonstration. Issues, such as cost and functionality, were compared and presented in the first-year deliverable. Another part of the first year scoping effort was to quantify the long-term marketability of visualization tools and how the Laboratory might best serve the needs of the industry in this arena. As a result of these deliberations, a focus on methods for displaying eigenanalysis simulation results for power system operations (particularly as they relate to future real-time power system control architectures) was selected.

Activities in FY 1995 included the following:

### *Prototype Visualization Package for Eigenvalue Analysis Software*

A prototype demonstration of a visualization package for displaying eigenvalue results of power system operation was developed. The challenge was developing a context in which complex eigenvalue analysis results could be displayed in an intuitive manner, which could be eventually applied in an operational arena. This area of research is unique to the industry, and combines distinctive competence the Laboratory has in power system eigenvalue analysis with resident expertise in scientific visualization methods. The deliverable after this phase included a prototype visualization package for conveying eigenvalue simulation results in a manner suitable for future applications in power system control.

### *Interactive Visual User Interface for Portable Dynamic Analysis and Design System*

A graphical-based visual user interface was developed for the MATLAB version of the portable dynamic analysis and design system, developed under the auspices of another LDRD project in the ETDI T&D initiative. The user interface was designed to increase the effectiveness of interactive Prony analysis tools, the cornerstone of these dynamic analysis tools. This development augments future commercialization activities. The user-interface was constructed from MATLAB-resident routines and open-architecture software.

### *Numerical Methods for Ambient Mode Identification*

Research on signal analysis methods to identify the electric power system dynamic characteristic from measured ambient data was performed. This research was conducted by Dr. John Pierre, an electrical engineering professor from the University of Wyoming. One of the approaches studied uses a high order finite impulse response whitening filter on ambient data where the models can be identified as the dominate polynomial roots in the frequency band of interest. Other analysis was performed, including coherency and spectral analysis, using traditional Welch type periodograms and higher resolution algorithms such as minimum variance distortionless response spectral estimation. Results of this

research indicate that system identification using ambient data can approach the accuracy of perturbed system-response identification as would be performed with Prony analysis software tools.

#### *Dynamics in Time-Domain Simulation Analysis Tools*

An investigation was performed researching numerical stability issues associated with combining two widely-used simulation software tools. The Electromagnetic Transients Program (EMTP), a simulation program used in the electric power industry to study transient phenomena and high-speed switching events in the power system, and transient stability programs, such as the Electric Power Research Institute's Extended Transient/Midterm Stability Package (ETMSP), which simulate slower electro-mechanical oscillatory behavior, use dramatically different approaches and assumptions in the formulation of their respective simulations. However, both programs analyze the same physical system, and the different modeling approaches could lead to divergent results if overlapping analysis domains occur. The recent trend toward numerous high-speed switching devices in the electric power system (devices such as static-var compensators or thyristor-controlled series capacitors) result in situations where capabilities of both programs are needed simultaneously.

#### *Automatic Generator Control Simulation Software*

Automatic generator control (AGC) is a strategy to provide sufficient generation to meet total load on a system in an economically optimum fashion. This goal of this task was to understand the basis for this software, gain experience using it, and demonstrate competency with its application.

Third-year efforts will complete the advanced numerics tasks begun in FY 1995, as well as explore other advanced numerics technologies which could be used to create an intelligent man-machine interface for complex engineering analysis tools. In parallel with this effort will be evaluations as to how these technologies can be incorporated into a real-time operational environment. Recent results in mathematical theory and tools for time- and frequency-domain analysis will be assessed, drawing upon Laboratory expertise in wavelets and Prony analysis plus the perspective of leading university experts associated with the Laboratory. Archive disturbance records will be analyzed to determine appropriate descriptors for event summaries and signature recognition. Related model studies will be used to identify context factors for event recognition and ranking, and minimum signal and descriptor set will ensure recognition.

# *Advanced Power System Dynamic Stability Assessment*

Matthew K. Donnelly (Analytic Sciences and Engineering)

---

## **Project Description**

The scope of this project included the development of an enhanced understanding of the distributed utility concept as it applies to the future power system, an assessment of the analytical tools and models that will be required to study the distributed utility, and a set of studies indicating how the distributed utility will impact certain aspects of future power system operation.

The electric power system is being stressed by delamination, increased competition, and societal pressure to pursue paths that are more economically and environmentally acceptable. At present, utility investment in transmission and distribution is over twice the investment in new generation. Emerging small modular technologies, such as photovoltaics, small gas-fired generators, and energy storage are becoming economic options, when considered as an alternative to transmission and distribution system upgrades.

The topics addressed under this project are key elements in a technologic response to the challenges described above. The distributed utility incorporates the idea that generation, using modular and renewable technologies, modular storage facilities, and specially designed customer efficiency programs can be distributed throughout the distribution system and serve as alternatives to planned central generation investment and transmission and distribution expansion. The assessment of the dynamic stability of a modern power system requires the use of complex simulation and analysis computer tools. With the emergence of the distributed utility, the power system will become even more complex and decisions will require methods to solve more challenging technical problems.

## **Technical Accomplishments**

In FY 1994, a preliminary assessment of the potential impacts of a distributed utility architecture on electric power bulk transmission system stability was performed.

Using a reduced-order system and the gas turbine models developed under this project, the project team produced results that indicate an improvement in small signal stability (and therefore increased transmission system capacity) under a distributed utility scenario. We found that these results held for the large base cases which we began running in early FY 1995. In general, we also see an improvement in transient stability, but excitation system and protection assumptions play a large role in those studies.

Also in FY 1995, dynamic models for various distributed resources were constructed and tested. These models will prove to be important in future planning for utilities incorporating distributed utility feeders into their resource mix. As a result of this exercise, a project team member was elected to chair a CIGRÉ task force on modeling small generators.

## **Publication**

M.K. Donnelly, J.E. Dagle, D.J. Trudnowski, and G.J. Rogers. "Impacts of the Distributed Utility on Transmission System Stability." IEEE Power Engineering Society Paper # SM95-064, IEEE PES 1995 Summer Power Meeting, Portland, Oregon, July 1995. (Pending publication in IEEE Transactions on Energy Systems).

## **Presentation**

M.K. Donnelly. 1995. "Modeling Distributed Generation." IEEE Power Engineering Society: Summer Meeting, July, Portland, Oregon.

# *Artificial Intelligence for Power System Control*

Rex C. Stratton (Information Sciences and Engineering)

---

## **Project Description**

The goal of this work was to develop automated intelligence methods for planning and operations in transmission and distribution activities. The targeted artificial intelligence technology elements include, but are not limited to, neural networks, fuzzy logic, machine learning, and model-based reasoning. It is recognized that different elements of this technology are more suited for solving specific problems than other elements, and that the appropriate match between technology element and need is a fundamental part of the capability development. Additionally, in some situations, multiple artificial intelligence technology elements will be required to develop solutions. The identification and effective integration of these elements will also be conducted.

Research was performed in the following areas:

- Distribution Short-Term Load Forecaster Technology
- Intelligent Configuration Management (ICM)
- Semantic Based Information Navigation
- Expert Systems for Diagnosis of Hydroelectric Generation Equipment.

## **Technical Accomplishments**

### *Distribution Short-Term Load Forecaster Technology*

Accurate predictions of hourly distribution loads is a fundamental requirement for many distribution automation (DA) and distributed utilities (DU) activities and critical to a number of real-time control requirements (e.g., economic generating capacity scheduling, fuel purchase scheduling, security analysis, transaction evaluation, power flow and switching cycle optimization, and distribution reconfiguration). Such a capability, characterized as distribution short-term load forecasting (DSTLF), is necessary to ensure power system stability under high load demands, to perform demand-side management load management activities, to optimally configure the system for current/near-term conditions, and to economically optimize system operation with respect to power flow/generation.

Our long-term objective is to develop an artificial neural network (ANN), fuzzy logic, and model-based reasoning (MBR) based DSTLF technology to predict electrical feeder, line section, and endpoint loads an hour, a day, and a week in advance. The DSTLF will consist of three major components: the monitored endpoint load forecaster (MELF), the nonmonitored endpoint load forecaster (NELF), and the topological integration forecaster (TIF). In FY 1994 a DSTLF methodology was developed and a MELF component was built using artificial neural network technology.

Development of the artificial neural network MELF technology was continued in FY 1995. The MELF data preparation code was tested and enhanced to include peak and holiday analysis, and MELFs were designed for these data types. In addition, the artificial neural network MELFs were used as part of an analysis to compare artificial neural network, building engineering, and loss load forecasting techniques. Analysis of the results of this comparison is ongoing.

The primary FY 1995 objective was to establish proof of concept of the NELF technology. NELF technology allows a utility to estimate endpoint, line section, and/or feeder loads without the installation of additional (and costly) monitoring equipment. NELF research was designed as a proof-of-concept experiment to test the notion that a distribution short-term load forecaster for a utility's distribution system can be constructed from available metered customer loads. Such data are available for a sample of all utilities' customers as required by the Public Utilities Regulatory Policy Act and typically take the form of hourly or half-hourly building-total load measurements.

Our approach was to use the ELCAP/REMP dataset as a test platform for a DSTLF system that uses representative load shapes from clusters of statistically similar customers to represent expected loads from all customers that would fall into the respective clusters. Membership in a cluster is predicted by various characteristics of a customer such as building type, vintage, and size, and various consumption indicators constructed from typical monthly billing information. ELCAP/REMP provides hourly data for slightly more than 100 commercial buildings for use in this test.



Development of the NELF is essentially a three-stage process. The first stage is to characterize each building load in a concise form amenable to cluster analysis. This load characterization must embody several important features of a building's consumption behavior, the most important of which are response to weather and operating schedule. The second stage is a cluster analysis that groups buildings with similar load characterizations together, and identifies a load characterization representative of all buildings in that group. The final stage is to construct a model by which group membership can be predicted from building characteristics typically available for all utility customers (e.g., SIC classification, consumption patterns from billing records).

1. Load Characterization - We tried two approaches to building load characterization. The first, and primary, approach involves conducting a nonparametric regression of building loads against outdoor temperature for each hour of the day. This results in 24 response curves for each of two day types, weekday and weekend. These curves embody information about both temperature sensitivity and schedule. Take-offs from these curves at selected values of outdoor temperature provide "variables" from each building from which a distance matrix can be constructed as input to a clustering algorithm.

The second approach attempts to segregate the weather response of a building from its schedule. We divide each building's measured loads into "bins" defined by various outdoor temperature ranges. Within each temperature bin, a representative 24-hour load shape (for each of weekdays and weekends) is identified for each site. The 24 hourly loads provide the variables for constructing a clustering distance matrix.

2. Clustering - We used the simple hierarchical clustering algorithm available in the Splus statistical package to cluster the buildings. The most difficult part of any clustering exercise is deciding how many clusters to keep. One needs to choose enough clusters that the within-cluster variability is reasonably small, but few enough that data storage efficiency is maintained and prediction of cluster membership from known building characteristics is reasonably precise. We found that the 117-building ELCAP/REMP sample is too small to allow construction of a reasonable set of commercial clusters. Nonetheless, to allow continued testing of the third stage of DSTLF construction, we subjectively determined that 10 clusters gave the best compromise between within-cluster homogeneity and between-cluster distinction.
3. Prediction of Cluster Membership - Our approach to prediction of cluster membership was to use a simple classification tree methodology to regress cluster

membership against the following variables: building type; building vintage; building size (floor area); primary heating fuel; ratio of January peak load to January mean load; ratio of July peak load to July mean load; difference between January and July mean loads divided by annual mean load. In spite of the rather large within-cluster variances (resulting from our too-small test sample) our regression tree predicts cluster membership correctly about 50 percent of the time.

The methodology of using nonparametric curve fits to characters building loads is problematic. Doing temperature take-offs at 11 points results in 264 (11 x 24) variables on which clustering is computed. This huge number of inputs makes construction of meaningful clusters difficult. It is unknown whether a larger sample would alleviate this problem. However, it should be noted that this difficulty reflects the power of the nonparametric curve fits to characterize a lot of information about a building's loads in a relatively simple construct. More research is needed to learn to adequately cluster such information-laden structures.

The temperature-bin methodology resulted in considerably better clusters. Clustering on only 24 variables at a time resulted in clusters that are visibly distinct from one another yet internally homogenous.

### *Intelligent Configuration Management (ICM)*

This task concerns the development of a prototype system that determines one or more possible configurations of a multi-source power generation from a base configuration subject to constraint rules. The goal of the task was to perform a proof of concept of an intelligent configuration management system.

A configuration management system consists of two separate components 1) network topology and attribute data visualization, maintenance, and storage and 2) a suite of analytical tools. An intelligent configuration management system, on the other hand, is a configuration management system in which the data representation and analytical tools share a common approach to the knowledge contained in the system. The analytical tools can be thought of as different views of the same data.

Because of its simplicity, low cost, controllable environmental impacts, photovoltaic generation was selected for the prototype demonstration. The prototype is to be composed of 5 foot x 5 foot platform which holds 64 individual photovoltaic arrays which is used to produce four separate power sources with varying voltage and power requirements. Each array is fully switchable with its adjacent arrays, allowing maximum flexibility in developing alternative configurations.

The heart of the ICM for this system is composed of two fuzzy logic based technologies: 1) an evaluation module that continuously monitors and assesses the performance of each array as an individual entity, and the performance of each of the four power source circuit configurations which are composed of the individual arrays; 2) a construction module that develops the preferred configuration for each of the four power source requirements for the current operating environment. The output of the evaluation module is a directive to either remain in the current state or to reconfigure. The output of the construction module are directions on where (to what circuit) and how (whether in series or parallel) to place each of the 64 photovoltaic elements.

The ICM software has been completed and tested. The hardware has been acquired and is to be constructed in the near term. Integration of the two elements will occur following the completion of the construction of the hardware. The hardware/software demonstration tool provides an effective means for communicating how a responsive change in the configuration of generating units to a change in operating conditions can improve a power source's operating efficiency and flexibility.

#### *Semantic Based Information Navigation*

The objective of this task was to develop semantic based navigation technology. The scope was to enhance an existing data collection, indexing, and query tool by adding components that make it semantic oriented and by coupling our new semantic navigation tool to a visual information data browser. We will use the "Galaxies," "Spires," and "ThemeScapes" technology that has been developed in the Pacific Northwest National Laboratory Information Technology Department. Also, this technology will be evaluated on a test bed simulating the information diversity on an energy utility. The results of this project will be a prototype semantic navigation tool, an evaluation of how this technology works, an indication of applicability to energy utilities, and directions for further development.

This task began in the latter half of FY 1995. So far the ideas behind semantic based information navigation have been formulated, a Harvest World Wide Web server has been implemented and some testbed indexes of the electric power industry have been developed. The next step is to develop some semantic components to couple into Harvest. They will include a synonym manager and a personality module. The synonym manager examines queries made by an individual and adds synonyms to the list of queried items. The personality module adapts to the query behavior of a user so that new queries can be done more efficiently as the personality module learns the types of information of interest to the user and the way the user prefers to view the data.

#### *Expert Systems for Diagnosis of Hydroelectric Generation Equipment*

The goal of this task is to create an expert system which will allow workers in the hydroelectric generation industry to diagnose problems with their generation equipment by using expert knowledge stored on a computer. The expert system was designed to incorporate uncertainty within expert testimony to allow it to make better decisions.

There are several phases in creating a workable expert system:

- The expert system shell must be built.
- An appropriate problem must be determined for which expert knowledge is available.
- The knowledge engineer should research the topic for which the system is to be built.
- The knowledge engineer should conduct several interview sessions with the expert to create a functioning expert system.
- The expert system must be validated (tested).

The knowledge base in the expert system being developed is currently stored in two text files one of which consists of rules and the other data which the rules use. The processing (inference) is done within a program written in C++, and the results are displayed to the screen. The results are a combination of several tests and give an indication based on expert testimony of how likely possible faults are.

Areas that the system uses to model uncertainty include fuzzy set theory and Dempster-Shafer evidence theory. The system incorporates fuzzy set theory to allow an expert to give a vague linguistic statement such as the temperature is high, and allow that information to be processed. Dempster-Shafer evidence theory is used to allow experts to assign incomplete evidence to an event yet allow the information to be used to make a decision; for example, if an expert is only partially convinced that a high temperature causes a problem, the partial certainty can be expressed and used to make a decision.

Recently, work has focused on designing the user interface portion of the expert system. One method for building interfaces on IBM PC compatible computers is Visual Basic. Another feature of Visual Basic is that it has the ability to link to previously compiled computer programs in the form of DLLs (dynamic linked libraries).

Time was spent learning Visual Basic, creating dynamic linked libraries, and coordinating the programs. Eventually a simple Visual Basic program was written that took a number as input, sent it to the dynamic linked libraries which added another number to it, and returned a new value to the Visual Basic interface. This is a start on an actual interface to the expert system shell.

It is expected that enough expert knowledge will be gathered to validate the expert system, and a usable graphic interface for accessing the expert system shell as a dynamic linked libraries will be completed.

# ***Biodegradable Electrostatic Filter Development***

Delbert L. Lessor (Analytic Sciences and Engineering)

---

## **Project Description**

In this project, we proposed to develop a biodegradable form of the Postma-Winegardner electrostatic filter, a method for fertilizer recovery in an  $\text{SO}_2$ - $\text{NO}_x$  gas cleanup concept. Gas-borne ammonium nitrate and ammonium sulfate particulates can be produced from nitrogen oxide ( $\text{NO}_x$ ) and sulfur dioxide ( $\text{SO}_2$ ) contaminants in a flue gas stream by injecting ammonia ( $\text{NH}_3$ ) and catalyzing chemical reaction with electrons. The small sizes of the resulting gas-borne particulates of these materials, which are valuable for fertilizer, makes their collection difficult. The Postma-Winegardner electrostatic filter can collect charged particulates of sizes down to tenths of a micron. If a biodegradable Postma-Winegardner filter of acceptable performance can be developed for this application, the used nitrogen-laden filter can be used to enhance soil fertility and structure directly, with minimal further processing. Deployment of such a system for flue gas cleanup in coal-fired power plants would produce a byproduct valued at \$200/ton instead of \$5/ton for gypsum or a negative value because of disposal requirements characteristic of some other systems.

A Postma-Winegardner electrostatic filter is a filter device in which retention of electrostatic charge actually enhances filtration.

## **Technical Accomplishments**

Experiments using ammonium sulfate particles and a number of filter materials were performed at the Northwest Laboratory Aerosol Wind Tunnel Test Facility. A corona discharge system charged the airborne particles prior to passage of the flowstream through the test filters. The ammonium sulfate particles deposited on the corona charger plates and within the filter. Filter materials tested included straw, grass hay, wood fibers (excelsior), and a highly resistive polymer pad. Deposition of particles in the filter bed was observed with all these materials, but only the non-biodegradable polymer pad gave the Postma-Winegardner filtration enhancement.

It was concluded that a more resistive biodegradable material is needed for this concept, in order to retain sufficient electrostatic charge.

# Compact Spiral Composite Evaporative Cooler

Glenn W. Hollenberg and Gita R. Golcar (Process Technology and Engineered Systems)

## Project Description

The fundamental concept of the compact spiral composite evaporative cooler (CSCEC) is to integrate the conventional adiabatic air humidification with convective heat transfer concept.

The objective of this project is to demonstrate that a compact spiral composite evaporative cooler will successfully cool hot air between (90 to 120°F) and maintain an efficient low relative humidity. The included performance aspect of the CSCEC: 1) the qualitative energy exchange efficiency between hot air at low humidity and the adjacent chilled heat exchanger wall accomplished by the evaporative cooler in a spiral design, and 2) water mist geometry to achieve and maintain an efficient hot air humidification and evaporative cooling ability of CSCEC.

## Technical Accomplishments

The schematic of the experimental apparatus is shown in Figure 1. A CSCEC was fabricated for the purpose of cooling dry air. The experimental setup consisted of a compressed air source of low relative humidity, an air flow meter that controlled inlet air flow rate, heating coils to preheat the air to selected temperatures, thermocouples to measure the inlet and the outlet air temperature from the CSCEC unit, and the CSCEC unit.

The compressed air source was connected to an air flow meter, which regulated the air flow at the rate of 1.15 SCFM. The air was at relatively low humidity, and was heated by circulating through the heating coils. When the CSCEC was heated with hot and dry air and the exit air temperature reached steady state conditions, water was injected to the CSCEC's evaporative-cooler layer. The temperature of air on the evaporative/humidifier side of CSCEC decreased due to latent heat of vaporization. As the temperature of air on the evaporative cooler side dropped, the energy exchange between the cooled humidified air and the low humidity side caused the dry air temperature to decrease.

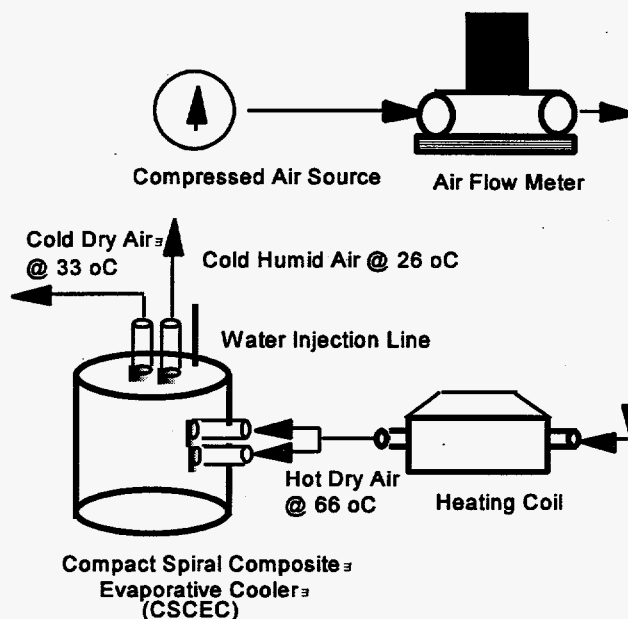


Figure 1. Experimental Apparatus

The stream of air at a low relative humidity entered the system at 1.15 SCFM at 66°C. Approximately 130 cubic centimeters of water was sprayed into the air during the testing, which dropped the outlet air temperature to 26°C of steady state condition at the evaporative cooler side of CSCEC. The high humidity content of this air stream was qualitatively verified by water vapor condensation on room temperature glass. At steady state, the exit air temperature in the dry air outlet of the CSCEC unit was decreased to 33°C.

In conclusion a scoping test program was completed on the use of the CSCEC for production of cool dry air. The successful ability of CSCEC unit to cool a hot air stream containing low relative humidity was verified.

# *Exhaust System Thermal Management*

Mark T. Smith (Materials Sciences)

---

## **Project Description**

This project consisted of two major tasks: thermal energy storage (TES) preheated catalyst and development of an engine test system.

The engine test system task involved the development of the design specifications for an automotive engine test system. Installation of the test cell into the Process Development Laboratory-West (PDLW) building. The completed engine test system provides Pacific Northwest National Laboratory with a state-of-the-art laboratory test capability for evaluation of powertrain materials, engine management technologies, and advanced emission control systems.

The objective of the thermal energy storage preheated catalyst task was to determine the feasibility for a catalytic converter preheater that uses thermal energy storage to reduce automobile emissions during vehicle startup. The thermal energy storage material retains waste heat generated during vehicle operation, then keeps the converter warm for extended "cold-soak" periods (i.e., the time elapsed between engine shutoff and startup). A design concept was devised and evaluated.

Most hydrocarbon emissions from vehicles equipped with catalytic converters occur during the first minute after startup, before the converter reaches the "light-off" temperature (approximately 350°C). One study has shown that 95 percent of commuter vehicles experience cold-soak periods of less than 16 hours. Much of the information used for developing the conceptual design came from published studies by the National Renewable Energy Laboratory (NREL). The NREL design uses thermal energy storage in conjunction with a special variable-conductance vacuum insulation that provides much higher insulating effectiveness than conventional insulation, but is also more expensive and is prone to failure. We chose to use conventional insulation in our design with the emphasis on the design of the thermal energy storage material.

## **Technical Accomplishments**

Accomplishments for the Engine Test System task included the design and specification of an advanced engine dynamometer test cell capable of testing new automotive powertrain materials and emission control systems.

Technical accomplishments for the thermal energy storage Preheated Catalyst task included a series of experiments conducted to determine the lumped-parameter RC time constant for cooling of a typical catalytic converter. This was determined by heating a generic aftermarket converter up to full operating temperature (650°C), then measuring the time to cool down to the light-off temperature. This parameter was also determined for the converter insulated with a 1 inch thick layer of Kaowool ceramic wool insulation and the ends plugged with thin (0.015 inch) steel plates to minimize air movement through the converter.

Analyses were performed using the RC time constant to determine the amount of insulation and thermal energy storage material needed to keep the converter above light-off temperature for the goal 16-hour cold-soak period. For the insulation used in the experiments, the amount of one thermal energy storage material needed was calculated to be 1.3 kg (assuming that the thermal energy storage is fully charged initially), which would occupy only 20 percent of the converter volume. This indicates that using thermal energy storage to retain heat for extended cold-soak periods may be feasible even with conventional insulation.

Some of the issues that will need to be addressed in the design phase include devising a way to thermally isolate the converter without significantly increasing exhaust backpressure, providing enough insulation without exceeding size constraints, keeping the converter from overheating during operation, keeping projected production costs low, keeping the thermal mass low to allow rapid heatup when the thermal energy storage is discharged after an extended cold-soak. A trade-off study will need to be conducted to optimize the design prior to fabrication of a prototype for testing.



# *Heating Plant Maintenance Training System*

Marc C. Pottier, Michael G. Ivanovich, and Michael Perkins (Information Technologies)

---

## **Project Description**

This project was focused on the development of multimedia and advanced three-dimensional modeling techniques for training applications. Specifically, the system was developed for heating plant operators who had little to no understanding of hidden physical phenomena taking place within their work environment. This project strived to expose these hidden phenomena which normally could not be visualized in an effort to educate plant operators and provide recommendations on how to fix these problems.

The phenomena that was selected for the base prototype was cavitation. This phenomena takes place when bubbles begin to form within a circulation pump, causing sub-optimal performance, and eventually costly maintenance due to pump failure. This particular effect was chosen because of its common occurrence in heating plants, and the fact that most operators are unable to properly diagnose and fix this problem.

The key goal of the system was to provide a realistic environment in which operators could safely learn about phenomena, and experiment with approaches to fixing problems without actually shutting down the plant for lengthy maintenance.

## **Technical Accomplishments**

Initial research for this project was performed on three fronts: 1) research into cavitation, 2) research into a specific energy production plant (at 29 Palms), and 3) research into multimedia interaction techniques.

1. The cavitation research was oriented at gaining a thorough understanding of cavitation and its effects in a heating plant. Pump manufacturers were contacted, and members of the DSOM team were brought on the project to provide technical feedback and expertise. The goal of this research was to develop the necessary materials to produce the training modules used in the system.
2. The 29 Palms plant research was geared toward providing the user with realistic visuals of the heating plant. Videos of the plant were obtained, as well as schematics and descriptions of all the various plant functions. Critical components within the plant were identified and modeled based on the videos of the plant. The models were then rendered to provide the capability of walking through the plant.
3. The interaction research focused on developing a software framework which could easily be tailored for new training modules and new areas of the heating plant. The primary development platform was selected as the Macintosh, and Macromedia director was used to integrate all the components generated in the previous two research areas.

The outcome of these three tasks was a fully integrated training system which could be run on a Macintosh powerbook.

## **Conclusion**

The core technology which was developed in this project demonstrated the ability to quickly develop a photo-realistic training environment, and deliver it on a low-cost platform.

# *High Performance Micro Heat Engine Development*

Robert S. Wegeng (Process Technology and Engineered Systems)

---

## **Project Description**

This project built upon Pacific Northwest National Laboratory's recent demonstration of microevaporators and condensers for use in a radically new compact heat engine that may be relevant to a wide range of building, industrial, and transportation energy applications. The project includes development and demonstration of a microtechnology-based combustor/evaporator unit, as a heat exchanger, for use in a sheet heat engine using liquid metal as the working fluid.

## **Technical Accomplishments**

FY 1995 research focused on evaluating options for a high efficiency microscale heat engine and on a more focused

evaluation of the technical feasibility of the most attractive concept. Options included 1) microscale hydrogen production coupled with a microscale fuel cell, 2) thermionic devices, and 3) microscale heat engines.

The microscale heat engine was selected for further study. A review of the concept suggested that the microscale generator was the key technical challenge. A computer model was developed to predict the performance of an electromagnetic micro generator. Results indicated that a micro or miniature high temperature heat engine has the potential to have a 20 percent conversion efficiency and a high energy density. It is planned to experimentally validate the computer model in FY 1996.



# Micro Heat Exchanger Development

Monte K. Drost (Analytic Sciences and Engineering)

Robert S. Wegeng (Process Technology and Engineered Systems)

---

## Project Description

Many applications of microtechnology involve components or devices that use microchannel fluid flow. A limited amount of research has been conducted on single-phase microscale flow, but it has been over limited ranges, and very little work has been done to develop fundamental design models of general applicability. Two-phase flow in microscale geometries is poorly understood and has been given very little attention. There is the potential for significant gains in thermal performance for devices utilizing two-phase flow, but the phase-change process is not well characterized for microscale flows. A fundamental understanding of flow and heat transfer behavior at this scale is essential to the ability to analyze and predict such flows for use in the design, analysis, and validation of systems and devices utilizing this technology. The FY 1995 heat exchanger project was focused on understanding the performance of microchannel two-phase flow devices such as evaporators.

## Technical Accomplishments

Isothermal tests with water as the working fluid were conducted using both the silicon and copper test articles, as part of test loop check-out and instrumentation evaluation. The results obtained were consistent with those reported by other investigators, and showed that the microchannel geometry has a large effect on friction/drag losses in the device. Tests were run with three test articles; two with diamond patterns ion-etched in silicon substrate, and one parallel-channel pattern, cut in copper substrate with a slitting saw.

Results show that relatively high flow rates at low pressure drop can be achieved in microchannels. The channels cut in the copper substrate were considerably larger than those etched in the silicon substrate, but the channels are still very small. The channels in the copper substrate are 1000  $\mu\text{m}$  deep and 270  $\mu\text{m}$  wide, giving these devices a flow area that is two orders of magnitude larger than that in the diamond-pattern silicon-substrate devices. Direct comparison of the performance of the two types of test articles is difficult, since the test conditions do not overlap substantially. However, the lowest test point for the metal device coincides with one test point from each of the silicon test articles. At a flow rate of approximately 20 mL/min, the pressure drop in the silicon

test articles is about 20 psi. In the metal test article, it is less than 1.0 psi.

The silicon-substrate test articles as initially designed and fabricated proved too fragile to withstand the thermal stresses in heated testing. The devices failed due to cracking of the silicon substrate, or separation of the Pyrex cover from the stainless steel end pieces. Subsequent redesign and modification of the fabrication process has resulted in a design that appears able to withstand the pressures and temperatures expected in testing. Tests have been performed on a single experimental device, and additional test articles will be built in FY 1996.

The small amount of data obtained before the test articles failed gave encouraging hints that the heat transfer coefficients were relatively high for the flow rate. The heat transfer coefficients ranged from 2.0 to 2.7  $\text{W}/\text{cm}^2\text{-C}$ .

Single-phase heated tests with water were also performed using the copper substrate devices. In these tests, heat fluxes up to approximately 100  $\text{W}/\text{cm}^2$  were achieved. The estimated heat transfer coefficient ranged from 1.3 to 1.9  $\text{W}/\text{cm}^2\text{-C}$ . In all of these tests, the pressure drop in the test article was on the order of 2 psi or less. These results show a relatively high heat transfer coefficient for single phase forced convection in the microchannels. It also appears that the parallel channel geometry was slightly more efficient than the diamond-pattern, but the difference between the two is not great.

Two-phase flow testing with R-124 was not so nicely characterized with similarity parameters as is single-phase thermal-hydraulic behavior, so the significance of the results is harder to assess. It appears that there are two distinct regimes in these tests. The first occurs at qualities below about 20 percent, in which the heat transfer coefficient is quite high. The second regime occurs for qualities around 20 percent and above, with the heat transfer coefficient in the range from about 0.8 to 2.0  $\text{W}/\text{cm}^2\text{-C}$ . These results indicate that if nucleate boiling occurs at all, it doesn't last long. It was not possible to reliably obtain data in this range for this test series. In addition, flow visualization studies to investigate how vapor forms in the microchannels, and the subsequent two-phase flow patterns are necessary if a complete understanding of what is occurring is to be obtained.

It is interesting to note, however, that even for the test points that appear to be in film boiling, the heat transfer coefficient is generally substantially greater than for the same flow rate in single-phase heat transfer. The average heat transfer coefficient in single-phase conditions appeared to be about  $0.5 \text{ W/cm}^2\text{-C}$  for R-124, while in two-phase flow, the average appears to be about  $1.1 \text{ W/cm}^2\text{-C}$ .

In summary, results show that the two-phase heat transfer coefficient is generally higher than that for single-phase conditions in the microchannels. In applications where the higher temperatures encountered in what appears to be film boiling, two-phase flow can remove more heat than the same single-phase flow rate, without a significant

increase in pressure drop. The data also show that there is some difference in heat transfer performance between the diamond-pattern and parallel channel test articles. In general, the parallel-channel data shows a slightly higher heat transfer coefficient for a given set of conditions.

#### **Presentation**

J.M. Cuta, W.B Bennett, C.E. McDonald, and T.S. Ravigururajan. 1995. "Fabrication and Testing of Micro-Channel Heat Exchangers." Presented at Micromachining and Microfabrication Conference, Austin, Texas.

# Microcompressor Development

Monte K. Drost (Analytic Sciences and Engineering)

Robert S. Wegeng (Process Technology and Engineered Systems)

---

## Project Description

Mass production of microscale components and systems, using fabrication techniques developed for microelectronics has the potential to make small-scale, distributed energy processes economically attractive relative to centralized processes normally used today. Microtechnology has matured to the point where initial applications of microsensors are reaching commercialization. The development of microscale components such as motors, pumps, and actuators is also progressing but the combination of components into systems such as microscale heat pumps and heat engines has not yet been reported in the literature.

The ability to design and fabricate micro-systems out of mechanical and thermal microscale components does not currently exist. This effort is focused on developing the technology and methodologies required to fabricate complete microscale systems relevant to energy applications. This project is consistent with Pacific Northwest National Laboratory's energy and environmental missions and will contribute to the Laboratory's strategic objectives in these areas.

FY 1995 activities involved six experimental investigations focused on understanding microscale phenomena relevant to the electromagnetic compressor concept. Results of these investigations were evaluated and a second proof-of-principle demonstration was developed based on the results of the phenomenological investigations. The fabrication of the second proof-of-principle test was completed in FY 1995 and it will be tested in FY 1996.

## Technical Accomplishments

A microcompressor concept composed of a liquid metal piston (LMP) driven by an oscillating electromagnetic (EM) field was identified as a promising concept late in FY 1994. A mercury oscillator was built and tested in a successful proof-of-principle experimental program. Several embodiments of this oscillator were used to demonstrate its potential to pump liquid against a small pressure gradient. The actuator required considerably higher electrical current than predicted, however, so an experimental research program was embarked upon in FY 1995 to identify and examine basic effects which

governed the actuator performance. A description and summary of findings for each of these separate effects tasks follows:

### *Investigation of Liquid Metal Working Fluids*

Because of the health hazards associated with mercury inhalation, the potential use of other liquid metals was investigated. Selection criteria included: liquid at room temperature, high surface tension, and low hazard. NaK eutectic alloy was obtained from Stirling Technology Co. for experimentation. The NaK was found to be very difficult to work with, reacting rapidly with trace amounts of moisture/air and plugged small tubing used in experiments. Gallium and indium, and alloys thereof, were obtained internally and tested. A GaSn eutectic has attractive properties but was not investigated because no pure tin was readily available on site. Cesium and rubidium were considered very unlikely candidate metals given their reactivity in air.

### *Measurement of Liquid Piston "Stiction"*

The magnitude of electrical and surface tension static forces in a liquid piston was measured in a simple device which used compressed gas to dislodge stationary pistons. The effects of piston geometry (diameter and length) and surface tension were considered. The experimental results showed that the stiction force was independent of piston length and was proportional to both surface tension and diameter. This confirmed that the stiction force is due entirely to the piston end-cap menisci. The non-dimensional stiction force was postulated to be a function only of the contact angle which the meniscus makes with the cylinder wall. For non-wetting combinations, this is a small effect since the contact angle approaches a constant 180 degrees. Empirical formulas for piston stiction force were determined.

### *Measurement of Liquid Piston Viscous Drag*

Viscous drag strongly effects the efficiency of a liquid metal piston working cycle. Quantification of viscous drag was important in order to design powerful and efficient systems. An experimental apparatus was designed and built which measured steady liquid metal piston drag as a function of piston geometry (diameter and length), piston working fluid (viscosity and surface tension), piston velocity, and cylinder material. Results were obtained for a wide range of conditions. The

experimental data was correlated to give liquid metal piston steady drag coefficient as a function of Reynolds number and Capillary number. In order to quantify the nonsteady effects of piston oscillation on drag, additional tests were designed and performed with mercury. It was difficult to obtain absolute drag data due to experimental limitations, however the general observed trend was that nonsteady drag amplification was found to increase with increasing oscillation frequency and decrease with piston length. Drag amplification factors in the range of 2 to 3 are expected for typical oscillating pump operations.

#### *Measurement of Liquid Piston Failure*

One of the significant advantages of a liquid metal piston is that the menisci at the piston ends can support a pressure gradient. This task attempted to experimentally determine the pressure gradient which can be supported by a liquid metal piston without failure. Experiments were conducted with mercury, gallium, indium, a GaIn eutectic, and NaK. All but the NaK tests proved successful. The liquid metal piston failure pressure was found to agree with the theoretically derived bubble burst pressure. Therefore, a simple formula exist for predicting the piston failure pressure which can be used in system design.

#### *Investigation of Micro-Magnet Induction Magnitudes*

A magnetic flux must be sustained across the liquid metal gap for energy transfer to occur. Acceptable liquid metal piston efficiencies and actuation forces can not be attained without magnetic inductions approaching 0.75. This task

focused on determining whether or not large magnetic inductions are achievable on the microscale. The research determined that it is indeed reasonable to attain a 0.75 tesla magnetic induction within a microscale air gap using new rare earth permanent magnetic materials and clever magnetic circuit design. Electromagnets were ruled out early due to large ohmic power losses, which can be fully avoided by use of permanent magnets. Flat sheets of magnetized rare earth magnets are becoming readily available. These prepared sheets are a viable alternative to micro-manufacturing and better match the needs of the channel cross sections presently envisioned for micro-channel pump systems (10 to 1000 microns).

#### *Investigation of Interfacial Issues*

The degree of wettedness between the liquid metal piston and solid surfaces affects both resistive forces and interfacial electrical resistance. This task attempted to measure electrical resistance at an interface as a function of liquid and solid properties, and degree of wettedness. The degree of wettedness was not measured directly due to the location of necessary equipment and safety considerations. The electrical resistance was measured for mercury in combination with copper, gold, silver, palladium, platinum, and steel. The effect of surface roughness was also considered. The results suggested an additional resistance is present which has not been definitively explained at this time. It is speculated that liquid metal purity may have a larger effect on electrical resistance and/or interfacial contact resistance than previously thought.

# *Microscale Sheet Architecture Prototype Development*

Monte K. Drost (Analytic Sciences and Engineering)

Robert S. Wegeng (Process Technology and Engineered Systems)

---

## **Project Description**

Activities related to the FY 1995 scope of work for this project involved investigations of extensions of the sheet architecture concept to two new applications, power electronics and absorption cycle heat pumps.

Results on a microtechnology experts workshop held in 1994 indicated that power electronics could be an attractive application. FY 1995 activities focused on identifying attractive microscale power electronics concepts followed by preliminary screening studies.

The evaluation of the absorption cycle sheet heat pump concept was motivated by the concepts use of heat driven chemical compression in place of the electrically driven mechanical compressor. In addition, the absorption cycle system can use waste heat to drive the device, it uses no CFCs or HCFCs, and the overall energy efficiency (based on primary energy consumed) of an absorption heat pump is higher than that of a vapor-compression heat pump.

The chemical compressor in an absorption cycle heat pump consists of three main components: 1) a gas absorber, 2) a regenerative liquid to liquid heat exchanger, and 3) a gas generator. FY 1995 activities focused on demonstrating a microscale gas absorber. Other research at Pacific Northwest National Laboratory has previously demonstrated the liquid to liquid heat exchanger.

## **Technical Accomplishments**

Investigations of power electronics applications of the sheet architecture concept results in the identification of a novel concept for a ultra thin flat light source and a microscale distributed transformer.

The investigation of the microscale absorption cycle heat pump started with a literature review to obtain information on absorption cycles, microscale chemical component research and development and on materials compatibility.

The two most common absorption cycles used in industry today are lithium bromide (LiBr, absorbent) - water (refrigerant) and water (absorbent) - ammonia (refrigerant). Thermodynamic data was collected on these two cycles to identify typical operating temperatures, pressures, solution strengths, coefficient of performances (COP), and operational constraints. Materials compatibility information was collected for silicon, metals and metallic alloys, bonding and gasket materials, and plastics. The results were used to identify the materials that were most compatible with the two working fluid combinations.

A decision was made to construct an absorber in which ammonia gas was absorbed into water. This pair was chosen because the absorption process occurs at close to atmospheric pressures as compared to LiBr-water where absorption typically occurs at below atmospheric pressure. Analysis was conducted to identify optimal design parameters and to calculate flow rates for the test case. The absorber was designed and several prototypes fabricated. The absorber was designed and constructed to allow integration with existing microscale heat exchangers previously demonstrated at the Laboratory. The absorbers were designed to allow testing over a range of operating parameters. In the absorber demonstration, ammonia gas from a pressurized cylinder was supplied to the test article and absorbed in deionized filtered water. The test apparatus was used to determine important performance characteristics including the rate of absorption of ammonia in water and the resulting temperature rise. The goal was to identify design parameters that optimized the absorption process. The resulting data was analyzed and performance maps were prepared.

Results showed that absorption rates and the resulting heat release were very high when compared to macroscale devices. Heat generation rates in excess of  $7 \text{ W/cm}^2$  were measured and theoretical calculation suggested that isothermal absorption rates could exceed  $40 \text{ W/cm}^2$ . The integration of a microscale heat exchanger with a microscale absorber is straightforward and should result in near isothermal absorption.

# Off-Peak Cooling by Direct-Contact, Open- or Closed-Cycle Ice-Making

Peter R. Armstrong and Michele Freidrich (Analytical Sciences and Engineering)

## Project Description

Thermal storage technologies have had a long, established history of DOE support and diurnal storage has been a high priority for utilities during the past decade. In the past 5 years, energy-efficient, peak-shifting technologies have received the particular attentions of DOE and the utility industry. Another important research and development area is the development of CFC-free cooling and refrigeration technologies. These technology issues spawned the thesis that efficient, environmentally benign, cost-effective air conditioning could be achieved by using water as a refrigerant and ice, made directly from the water, as a storage medium.

Elimination of the temperature drop associated with an evaporator covered with a layer of ice typical in conventional ice-based, off-peak cooling systems results in system cost reduction and energy efficiency. In addition, water has potentially superior performance as a refrigerant. This was shown in FY 1994 by comparing ideal-cycle performance of water, ammonia, and R-12 in ten variations on the basic saturation cycle. Vapor-compression, absorption, and hybrid cycles all appear to be technically feasible. A novel compressor design and new absorption and hybrid-cycle based concepts were also developed.

In FY 1995, the performance sensitivity of a lithium bromide (LiBr) absorption cycle to evaporator temperature was explored by simulation. The ice-making LiBr absorption cycle was then demonstrated using a modified 3-ton absorption chiller to 1) operate continuously at evaporator temperatures of 0°C, and 2) demonstrate batch ice production.

## Technical Accomplishments

Ideal cycle analysis of single and double-effect LiBr-water absorption cycles were completed for ice-making conditions, i.e., the evaporator is at the triple-point pressure and temperature. For ideal cycle analysis the condenser, absorber, generator, and solution heat exchangers are all modeled as infinite NTU devices. For realistic cycle analysis the heat exchanger parameters for a commercial absorption chiller were used. The simulation results show that the performance penalty is less than 10 percent in a modestly (20 percent) derated chiller. This penalty is counterbalanced, in most climates, by lower night cooling tower temperatures. It is expected that reduced chiller and air-handler costs will more than compensate for the cost of the ice-storage vessel.

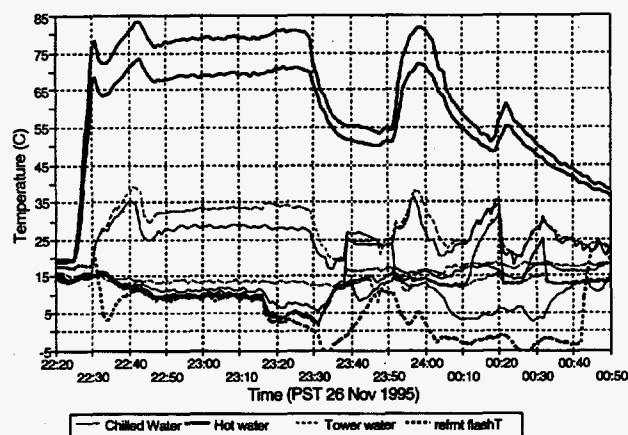


Figure 1. Data from Steady 0°C and Ice Production Test



# *Portable Dynamic Analysis and Design System*

Daniel J. Trudnowski (Analytic Sciences and Engineering)

---

## **Project Description**

To reliably implement real-time control into power transmission systems will require significant technology advancements in many areas. Critical-path areas include engineering analysis and modeling of power system dynamics, design and tuning of advanced control systems, and real-time monitoring of the power system behavior. For the last several years Pacific Northwest National Laboratory has been very active in developing advanced techniques for analyzing both measured and simulated power system response data. Early work focused on development of fundamental mathematical algorithms. These algorithms provide fundamental advances in power system dynamic modeling and analysis. These enabled advances in other areas, including design and commissioning tests for advanced control systems, tuning of generator controls, fault response studies to determine system dynamic characteristics, small-signal stability studies, and subsynchronous resonance analysis.

The purpose of this project was to use mathematical algorithms to conduct advanced field tests related to large power system dynamics. Three objectives have been addressed.

FY 1995 activities included 1) continued development of the Portable Dynamic Analysis and Design System (PDADS) workstation and concept; and 2) continuing demonstration and refinement of PDADS capability. PDADS prototype development included continued work on analysis software interfaces, plus development of a hardware data collection and probing capability. A new demonstration of PDADS capability initiated in FY 1995 includes development of power system load models from measured data. A number of publications and presentations resulted from the PDADS or PDADS-related activities, many of them derived from the demonstration activities of 1994.

## **Technical Accomplishments**

In FY 1995, efforts continued in the refinement of hardware and software. LabVIEW and Matlab development packages were used to extend analysis methods. The hardware development component has

focused on evaluation of methods to conduct coordinated data collection and probing. Of several commercial tools evaluated, the product DSPT SigLab was selected as a portable A/D-D/A system compatible with Matlab. A prototype custom interface for this product was developed, and a portable computer was purchased and configured for use in the field.

Two new application areas were selected for demonstrating PDADS capability in FY 1995. The first was to extend the FY 1994 work in generator controller design to include excitation system tuning. Again this work was coordinated with the USBR. Initial data was collected at the Grand Coulee plant, but the application calls for more data collected under a wider range of operating conditions.

A second problem investigated was development of power system load models from measured response. Accurate load models are necessary for conducting power system analysis and simulation studies. Initial phases of this work were coordinated with the Bonneville Power Administration and the University of Portland.

## **Conclusions**

PDADS is emerging as the unifying framework for an integrated Bonneville Power Administration/Pacific Northwest National Laboratory Dynamic Information Technology Package, called DITPak. This package, which includes the portable power system monitor, contributes the core technology elements for the DOE/BPA/WAPA Wide Area Measurement System Project.

## **Publications and Presentations**

J.F. Hauer, D.C. Erickson, T. Wilkinson, J.D. Eden, M.K. Donnelly, D.J. Trudnowski, R.J. Piwko, and C. Bowler. 1994. "Test Results and Initial Operating Experience for the BPA 500 kV Thyristor Controlled Series Capacitor Unit at Slatt Substation: Part II—Modulation, SSR, and Performance Monitoring." Presented at Flexible AC Transmission System Conference III, October 4-6, Baltimore, Maryland.

J.F. Hauer, W.A. Mittelstadt, R.J. Piwko, B.L. Damsky, and J.D. Eden. 1994. "Modulation and SSR Tests Performed on the BPA 500 kV Thyristor Controlled Series Capacitor Unit at Slatt Substation." IEEE/PES 1995 Summer Meeting, Portland, Oregon. Paper 95 SM 532-2 PWRs. For later publication in *IEEE Trans. Power Systems*.

J.F. Hauer, W.A. Mittelstadt, R.J. Piwko, B.L. Damsky, and J.D. Eden. 1995. "Modulation and SSR Tests Performed on the BPA 500 kV Thyristor Controlled Series Capacitor Unit at Slatt Substation." IEEE Technical Applications Conference-NorthCon '95, October 10-12, Portland, Oregon.

S.J. Kinney, M.A. Reynolds, J.F. Hauer, R.J. Piwko, B.L. Damsky, and J.D. Eden. 1995. "Slatt Thyristor Controlled Series Capacitor System Test Results." Tokyo Symposium on Power Electronics, May, Tokyo.

D.J. Trudnowski, M.K. Donnelly, and J.F. Hauer. 1995. "Estimating Damping Effectiveness of BPA's Thyristor Controlled Series Capacitor by Applying Time and Frequency Domain Methods to Measured Response," IEEE/PES 1995 Summer Meeting, Portland, Oregon. Paper 95 SM 519-9 PWRs. For later publication in *IEEE Trans. Power Systems*.

D.J. Trudnowski and J.C. Agee. 1995. "Identifying a Hydraulic-Turbine Model from Measured Field Data." IEEE/PES 1995 Summer Meeting, Portland, Oregon. Paper 95 SM 454-9-EC. For later publication in *IEEE Trans. Energy Conversion*.

J.F. Hauer, D.C. Erickson, D.J. Trudnowski, and M.K. Donnelly. 1995. "Value Engineering A Dynamic Information Technology Package For Power System Applications." 1995 Fault and Disturbance Analysis/Precise Measurements in Power Systems Conference, November 8-10, Arlington, Virginia.

W.A. Mittelstadt, P.E. Krause, P.N. Overholt, J.F. Hauer, R.E. Wilson, and D.T. Rizy. "The DOE Wide Area Measurement System (WAMS) Project - Demonstration of Dynamic Information Technology for the Future Power System." 1995 Fault and Disturbance Analysis/Precise Measurements in Power Systems Conference, November 8-10, Arlington, Virginia.



# *Pulsed Amplitude Synthesis and Control Development Converter System*

Matthew K. Donnelly (Analytic Sciences and Engineering)

---

## **Project Description**

The Pulse Amplitude Synthesis and Control (PASC) converter is a novel converter topology proposed to interface new generation and consumption technologies with the existing electric power network. In prior research, the converter has shown promise in the consolidation of diverse electrical sources into a single coherent alternating current waveform. The objectives of this project were to demonstrate the applicability of a novel static converter technology to contemporary power system problems and to build a prototype converter for testing and evaluation.

## **Technical Accomplishments**

Fiscal year 1995 was the last year of funding on the PASC project. In FY 1993, researchers laid the theoretical framework for a PASC converter that could operate as a bidirectional interface between the utility electric power grid and isolated electrical devices. This work centered around computer studies using the Electromagnetic Transients Program.

With FY 1993 as a foundation, researchers targeted two efforts for FY 1994. The first effort was the design and construction of a benchtop prototype. Dr. Donald Hammerstrom, a power electronics specialist, was hired as a member of the project team and contributed substantially to the prototype development. Converter components were ordered in FY 1994. The bidirectional converter design used MOS-Controlled Thyristors (MCT) and MCT driver chips newly available from Harris semiconductor company. This project used some of the very first MCT driver chips on the market. Minor project delays resulted from slow delivery of the novel MCT drivers and some of the first deliveries were beta test versions.

In FY 1995, the benchtop prototype converter was completed and was tested in March. The benchtop converter was a three-phase, 10 kW bidirectional converter that used 36 MCT switch modules and four banks of transformers. The output voltage waveform consisted of four-level approximations to a sinusoid. The test bench setup consisted of a high power dc voltage

source, the benchtop PASC converter, a load rack, and the laboratory three-phase ac power supply. Converter timing signals were controlled by the converter's Harris RTX2001 controller board, which detected voltage zero crossings. Real and reactive power were exchanged through the laboratory 120 volt, three-phase ac supply for durations exceeding 40 minutes.

In early FY 1995, an opportunity developed for installing a prototype PASC unit at the existing 6.8 kW photovoltaic site at Tinker Air Force Base (TAFB) in Oklahoma. The experimental PASC converter was configured to parallel to the existing commercial pulse width modulation (PWM) Omnion inverter. The photovoltaic arrays were readily rearranged into four sets of 250 volt arrays for PASC power consolidation. A solid-state relay enclosure was designed and installed at the base of the photovoltaic array to transfer photovoltaic power either to the existing pulse width modulation inverter or to the PASC prototype. The benchtop PASC converter was modified for single-phase operation and installed at the Tinker Air Force Base site in May 1995.

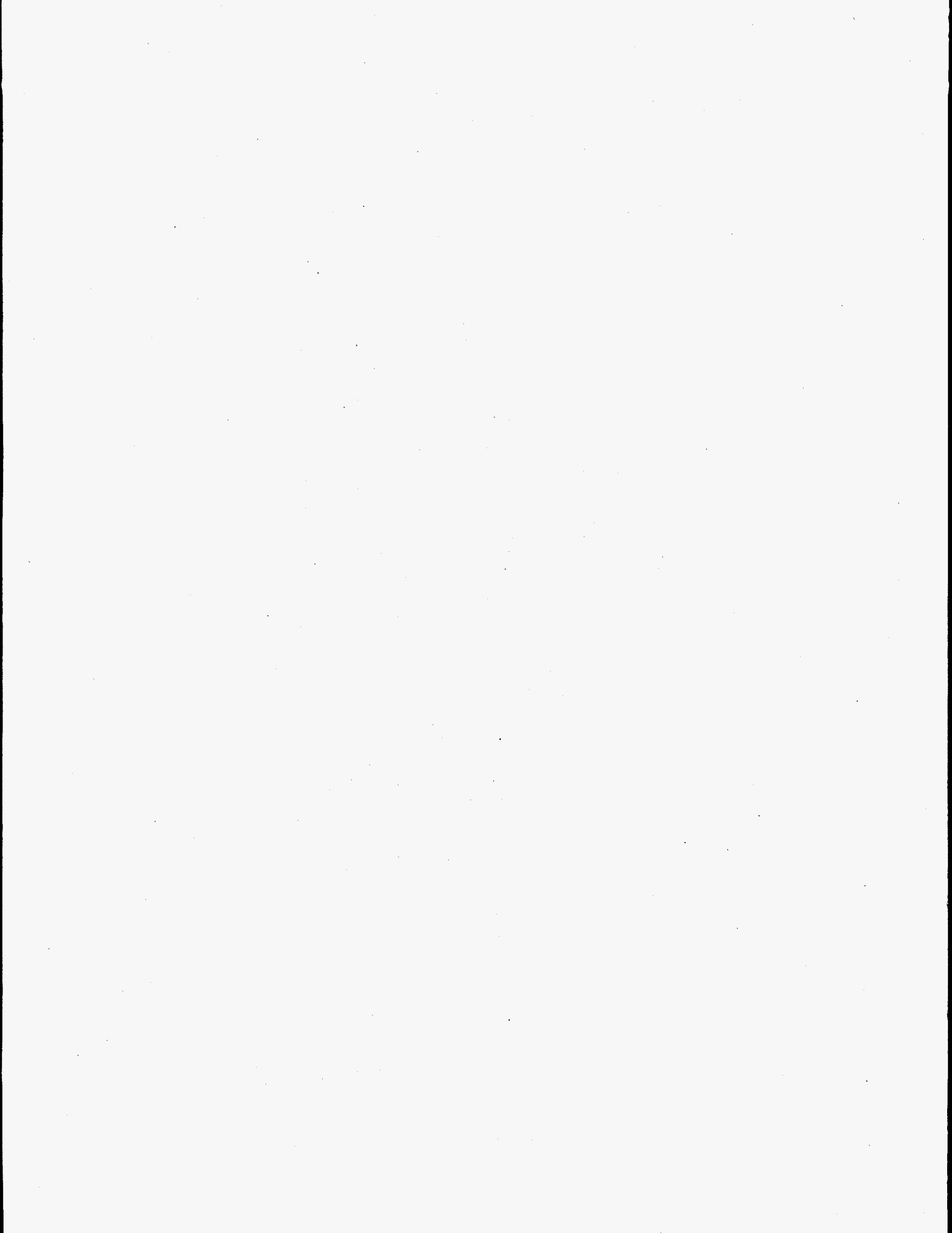
Persistent high voltage transients have limited the success of the Tinker Air Force Base PASC prototype. At the time of this report, long-term operation of the Tinker Air Force Base PASC prototype had not been achieved. Each of three attempts to initiate inversion of photovoltaic power into the single-phase power grid resulted in component failures.

## **Publication**

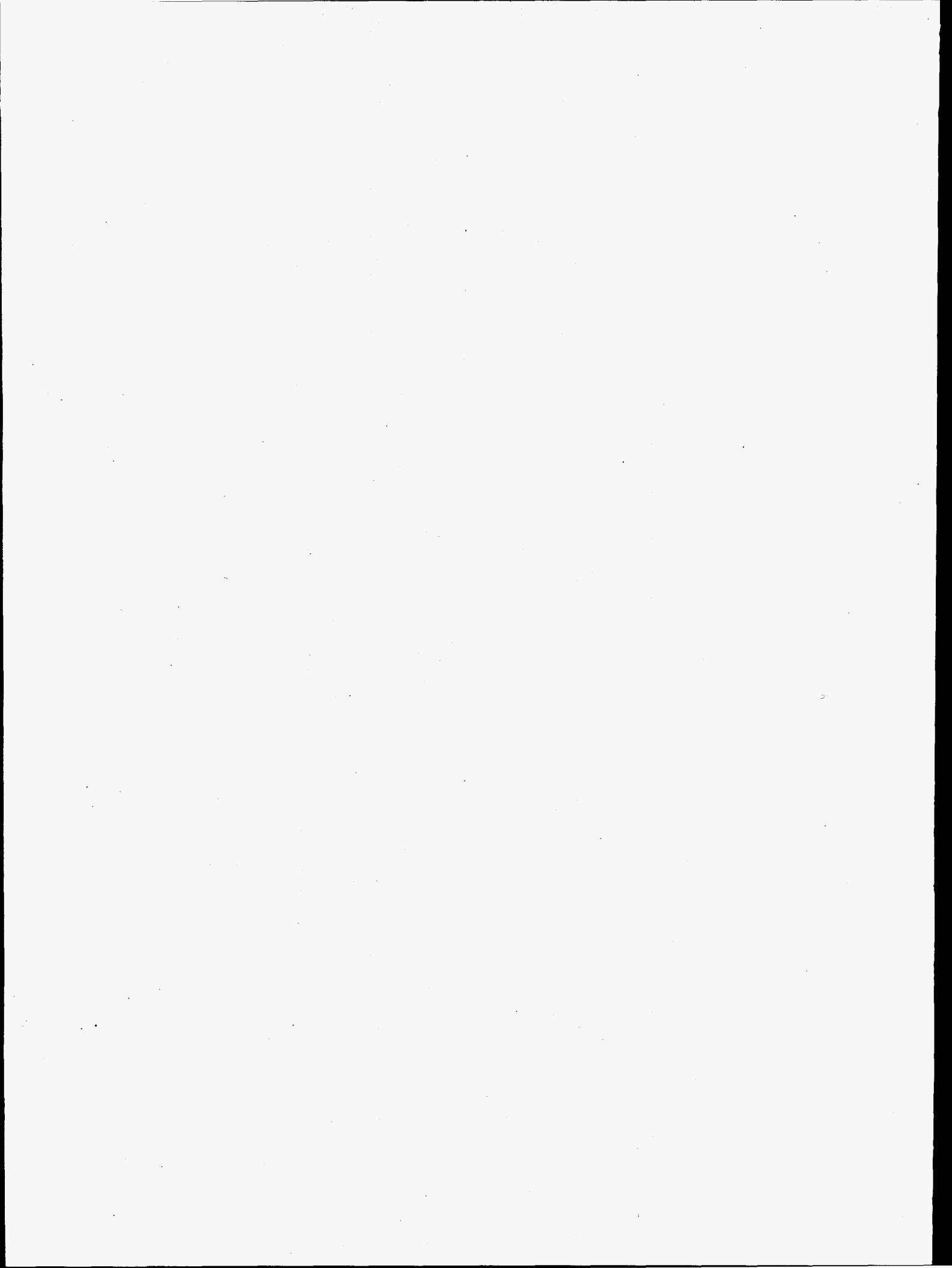
M.K. Donnelly and R.J. Johnson. 1994. "Power System Applications for PASC Converter Systems." In *Proceedings of the 1994 IEEE T&D Conference*, Chicago, Illinois.

## **Presentation**

D.J. Hammerstrom, L.A. Schienbein and M.K. Donnelly. 1995. "Step Waveform Electrical Power Converter for Electrically Isolated Generators," 1995 Innovative Concepts Technology & Business Opportunities Fair, April 20-21, Denver, Colorado.



## **Acronyms and Abbreviations**



# Acronyms and Abbreviations

ANNs	artificial neural networks
ATES	aquifer thermal energy storage
BNCT	boron neutron capture therapy
CSCEC	compact spiral composite evaporative cooler
DGPS	differential global positioning system
DHN	dihydroxynaphthalene
DMSO	dimethyl sulfoxide
DNAPLs	dense nonaqueous phase liquids
DOE	U.S. Department of Energy
DSTLF	distribution short-term load forecasting
ECMWF	European Centre for Medium Range Weather Forecasting
EDTA	ethylenediaminetetraacetic acid
EMAT	electromagnetic acoustic transducer
EPA	U.S. Environmental Protection Agency
EPIC	Erosion Productivity Impact Calculator
ESI-MS	electrospray ionization mass spectrometry
FLAPW	full potential linearized augmented plane wave
FTICR	Fourier transform ion cyclotron resonance
FTICR-MS	Fourier transform ion cyclotron resonance mass spectrometry
GCAM	Global Change Assessment Model
GChM	Global Chemistry Model
ISTUM	Industrial Sector Technology Use Model
ITEMS	Industrial Technology and Energy Modeling System
LDRD	Laboratory Directed Research and Development
m/z	mass-to-charge ratio
MALDI	matrix assisted laser desorption ionization
MAPK	mitogen activated protein kinases
MAPS	measurement of air pollution from satellites
MAS-NMR	magic-angle spinning nuclear magnetic resonance
MCT	MOS-controlled thyristors
MELF	monitored endpoint load forecaster
NA3E	North American economic-energy-environmental
NAFTA	North American Free Trade Agreement
NAPLs	nonaqueous phase liquids
NELF	nonmonitored endpoint load forecaster
NOAA	National Oceanic and Atmospheric Administration
NRC	Nuclear Regulatory Commission
NREL	National Renewable Energy Laboratory
NURBS	non-uniform rational b-splines
OLAM	optimal linear associative memory
OXDP	oxidative dehydrogenation of propane

PASC	pulse amplitude synthesis and control
PBPK	physiologically based pharmacokinetic
PDADS	Portable Dynamic Analysis and Design System
PG&E	Pacific Gas and Electric Co.
PNC-CAT	Pacific Northwest Consortium Collaborative Access Team
RF/MW	radio frequency and microwave
RTDS	Rapid Thermal Decomposition of precursors in Solution
RTUIS	real-time ultrasonic imaging system
SEDOR	spin echo double resonance
SGFET	suspended gate field-effect transistor
SPC/E	extended single point charge
SPSH	six-phase soil heating
TBP	TATA-box binding protein
TeCH-RD	tetrachloro- <i>p</i> -hydroquinone reductive dehalogenase
TRIC	time resolved ion correlation
TWRS	Tank Waste Remediation System
UV-VIS	ultraviolet-visible
XAFS	x-ray adsorption fine structure